Jozef A. Helsen
Yannis Missirlis

BIOLOGICAL AND MEDICAL PHYSICS, BIOMEDICAL ENGINEERING

Biomaterials

A Tantalus Experience

Springer

BIOLOGICAL AND MEDICAL PHYSICS, BIOMEDICAL ENGINEERING

For further volumes:
http://www.springer.com/series/3740

BIOLOGICAL AND MEDICAL PHYSICS, BIOMEDICAL ENGINEERING

The fields of biological and medical physics and biomedical engineering are broad, multidisciplinary and dynamic. They lie at the crossroads of frontier research in physics, biology, chemistry, and medicine. The Biological and Medical Physics, Biomedical Engineering Series is intended to be comprehensive, covering a broad range of topics important to the study of the physical, chemical and biological sciences. Its goal is to provide scientists and engineers with textbooks, monographs, and reference works to address the growing need for information.

Books in the series emphasize established and emergent areas of science including molecular, membrane, and mathematical biophysics; photosynthetic energy harvesting and conversion; information processing; physical principles of genetics; sensory communications; automata networks, neural networks, and cellular automata. Equally important will be coverage of applied aspects of biological and medical physics and biomedical engineering such as molecular electronic components and devices, biosensors, medicine, imaging, physical principles of renewable energy production, advanced prostheses, and environmental control and engineering.

Jozef A. Helsen
Yannis Missirlis

Biomaterials

A Tantalus Experience

With 166 Figures

Springer

Professor Dr. Jozef A. Helsen
Katholieke Universiteit Leuven, Department of Metallurgy and Materials Engineering
De Croylaan 2, 3001 Leuven, Belgium
E-mail: jef.helsen@mtm.kuleuven.be

Professor Dr. Yannis Missirlis
University of Patras, Department of Mechanical Engineering and Aeronautics
265 00 Patras, Greece
E-mail: misirlis@mech.upatras.gr

Biological and Medical Physics, Biomedical Engineering ISSN 1618-7210
ISBN 978-3-642-12531-7 e-ISBN 978-3-642-12532-4
DOI 10.1007/978-3-642-12532-4
Springer Heidelberg Dordrecht London New York

Library of Congress Control Number: 2010938119

Cover design: eStudio Calamar Steinen

Printed on acid-free paper

Springer is part of Springer Science+Business Media (www.springer.com)

Foreword

The book written by Prof. Helsen and Prof. Missirlis is different from many books I have read on biomaterials. It shares with the best books on the topic accuracy and clarity. But it goes beyond that. This book has body and soul. The authors, who have been my friends for many years, have engraved their spirit in many parts of the work. In the sense of humor that crops up everywhere, in the critical attitude toward block-busters and dernier cries that function as chemoattractants to scientists looking for funds, when they unveil compelling evidence of failed hopes and promises of "almost-perfect" implant concepts, I recognize Jef and Yannis. They have left their fingerprints everywhere. If, instead of writing a book they were trying to plot a perfect crime, they would be rapidly discovered by an apprentice detective. References made to history – not only of biomaterials, but also of mankind – are abundant, putting science in social and humane context. This is something you do not find while searching databases. Culture has to be deeply embedded in your mind to fill fringes in the discourse so accurately and smoothly. As they say, with remarkable honesty, the book is not comprehensive. They go as far as mentioning important topics that are not covered. Instead of dangling conversation on so-called hot topics, they preferred to draw our attention to biomaterials whose history illustrates the multifaceted and critical perspective that one should take at anything in science. The length with which they discuss dental materials and amalgams is a perfect example of this. Although I have never investigated dental materials, I found this chapter a beautiful example of an evolutionary view on biomaterials, going from amalgams for dental fillings to regenerating teeth. It is also an excellent demonstration of the multidisciplinary approach that Prof. Helsen and Prof. Missiles have adopted throughout the book. Mechanical properties, degradation behavior, design, thermodynamics, kinetics, and a wide range of materials are harmoniously dealt with in the chapter. The way the book opens is extremely creative and provocative. In the first chapter, they refer to the "perfect human machine". I would add wonderful and mysterious human machine. Then, in the second chapter, the topic is "the failing human machine". They could not have chosen a more distressing, but true, title. The homage they make to Prof. Charnley is unquestionably deserved. The quotation of Charnley's sentence on the limitations of technology is remarkable. We should have it at the entrance of every lab. The pairing of corrosion and toxicity of degradation products is very opportune. In many books they are not so

intimately related, although corrosion has a double facet: it is detrimental to the material and to the environment. In case of biomaterials degradation, the environment is the body. In this respect, the authors relieve the anxiety some people may feel about carrying something that is made of potentially toxic elements. Complex formation and precipitation of metal compounds in the vicinity of implants may be the reason for restricted damage caused to tissues. Improvement in manufacturing practices, more stringent quality controls and greater awareness to biomaterials properties have been responsible for increased implant safety and survival. The book has many other aspects that appealed me. I will mention only a couple of them. One was the use of magnesium foams. It goes against mainstream thinking to consider using a metal that is highly reactive in the body. We were brought up in the belief in certain dogmas, and high corrosion resistance is one of them. However, if we take the other side of the coin, which was spotted in the 1970s by polymer chemists, biodegradation comes as a "why not?" approach, even for metals. Finally, I would like to refer to heart valves because they are an excellent example of the dilemmas we face when confronted with natural and artificial biomaterials. The issue of reproducibility of properties crops up in any discussion about the use of natural materials. However, mimicking the natural tissue is a goal of any tissue engineer. Valve-replacement surgery has taught us that there is no such a thing like a single solution to a problem. Life is, fortunately, more complex than choosing between black and white. Daring to think differently is also the only route towards innovative science and technology. This book is an excellent example of this attitude.

Prof. Mário A. Barbosa INEB, Porto (Instituto de Enghenharia Biomedica, Portugal)

Porto *M.A. Barbosa*
June 2010

Preface

New technologies don't simply replace old ones... they just add another layer of complexity to our lives.

David Rooney

Wise words extracted from Rooney's book *Ruth Belville: The Greenwich Time Lady*. This phrase may stand for the mix of facts and figures, historical backgrounds, old and new ground breaking designs, and state-of-the-art and future perspectives in the biomedical world. That is all what this book is intended to be about. Bridging past and present – the highway to the top, the z-axis – is particularly cherished throughout the text. Distinct exits of the highway are taken for roaming through the landscape for an xy-view on the biomedical field.

In the early 1980s, *new materials* were the magical keys, which opened doors when applying for grants with the hope to have a share in the European flesh pots. Ceramics are one of those miracle products: a full ceramic motor block and ceramic ball bearings without lubrication would allow to start the engine with just one click of the contact key even in the middle of a night in Siberia. Just one or two cars with ceramic engines were ordered to be manufactured but thirty years later, few cars with ceramic motors can be found on the road, neither here nor in the arctic. Corrosion and wear were a nightmare for metal implants but inert aluminum oxide solved these problems. In fact, nothing was less true and only in the course of the last decade, the manufacturing of complex composites of aluminum and zirconium oxide emerged as a mature technology for manufacturing heads and cups for hip prostheses. The new magical key is 'nano'. Not mentioning these four letters is begging for problems in grant applications. But, fortunately, capturing part of the flesh pot is not the aim of this book and therefore, the reader will not be flooded with exaggerated promises by innovative proposals.

Research follows odd ways. Another hot research topic three decades ago was the manufacturing of complex metal parts in near net shape using metal powders, an adaptation of a technology practiced by ceramists since ages. In the chapter *Layer by layer*, the reader will find how a variety of *custom-made* metal implants are manufactured today by techniques that are fundamentally different from what was proposed three decades ago. Nickel-free alloys such as iron–manganese–aluminum, glass–fiber composites, porous coatings, and many other proposals to

solve recognized risks or shortcomings of existing materials and implants did not result in the breakthroughs they promised: while conventional stainless steel is still an alloy in use for some (successful) implants, today's porous coatings or porous devices are distinctly different from designs proposed in the 1980s. Fortune-telling is a risky profession!

Myths are vivid reflections on the invincible will of man to lengthen life in a comfortable way, so the eagerness to insert some mythological stories in the text was irresistible. Archaeological biomedical artefacts look less romantic than myths but they are the tangible witnesses of ancient creativity. They instruct us about the biomedical progress, or any other kind of progress. They are never stand-alone acts but are a universal conversation between aspiration, technology and science – xyz-space.

The generic class of materials in this book are not bound to separate chapters. A story or case study at the beginning of a chapter introduces a problem and invites the readers explore solutions: for example, adequate implant design and manufacturing by adequate selection of (bio-)materials or combination of materials. Occasionally, an excursion from the mainframe is made to situate artificial and natural materials in a wider context, trace elements in the body or biominerals in relation to the mineral world...

Science is a sustained effort to arrive at a unifying theory. Efforts are made to point to those characteristic properties of matter and materials that go beyond the typical characteristics of one generic class. To name a few, the austenite–martensite transformation as a physical process common to steel, shape memory alloys as well as to ceramics; grain size and its relation to strength in ceramics and metals alike; the role of grain boundaries and sensitivity to corrosion or chemical degradation; and scaling, similarity of properties at different scale lengths. The driving force for all physical or chemical processes is dictated by the Second Law of Thermodynamics, paraphrased in the text as *Water does not flow uphill* or, viewed from the top of the hill, *All nature's streets are one way and downhill*. The ultimate definition of the law is *that in a closed system* (like the universe), *all irreversible processes lead to an increase of entropy*. An apocalyptic consequence of the Second Law is the inevitability of death. This statement was, unintentionally we guess, nicely illustrated in an otherwise very charming German village: next to a sign post, which mentioned *Zum Friedhof*, we saw another sign post saying *Einbahnstrasse* (to churchyard, one-way street)! But despite these discouraging statements, we do stay alive quite a number of years. In a way, our body succeeds cheating the second law by built-in negative feedback systems or homeostatic mechanisms to keep the increase of entropy under control. These mechanisms have direct consequences for implants as well as for the body. *Homeostasis* (Homeodynamics in reality) will often be referred to in the text.

An inspection of the Table of Contents shows that conventional items such as metals, toxicity, corrosion, ceramics or, in general, materials for hard tissue replacements are, discussed in a number of pages, apparently overrepresented with respect to cellular or physiological response. The counterbalance are the two chapters on heart valve substitutes and tissue engineering. Should it not be the other way round? On the one hand, it is beyond doubt that substantial progress has been

made in understanding tissue response to foreign materials. On the other hand, the long-term success of, say, (even conventional) total hip prostheses is undeniably remarkable, while decades long studies of surface modification to enhance biochemical and physiological compatibility resulted in rather modest successes. Exception might be made for orthopedic hydroxyapatite coatings, but the initial success of hydroxyapatite-coated dental implants is vanishing. Experience taught us that *close fit* seems to be more beneficial than surface modification, selecting of course materials with an otherwise good record of service. The Gallo–Roman dental implant (Chap. 10) is a quite unexpected support for that view. New forming technology permits manufacturing custom-made prostheses fast and at reasonable cost. One chapter is devoted to forming techniques for metals as well as for ceramics and polymers (Chap. 7). The elastomer-coated prosthesis discussed in Chap. 11 is another proposal for meeting, among other requirements, a close fit. But history teaches us that once a technology is nearly perfect – think about steam engines – one no longer needs it. Tissue engineering is lurking at the corner to undermine the world of the materials scientists, from cartilage to heart valves. May not be tomorrow, but somewhere down the line it is bound to happen.

Permanent implants need materials with long-term stability and resistance to corrosion and wear, for example, definitely when considering that even young patients are getting implants. For controlled drug delivery devices, which do not endure high loads, materials that dissolve gradually in the course of time are required. Nonpermanent implants subject to moderate loads, which are currently removed when functional support is no longer needed, are potential candidates for being manufactured out of very corrosive alloys, whose dissolution rates (and production of hydrogen) can be tightly monitored. Chapter 8 is devoted to a discussion of these alloys.

The excellent survival rate of permanent implants demands an updated attention to toxicity. The toxic behavior of the major elements is elaborately studied. No alloy, however, is inert. Many of the minor elements have documented toxic, mutagenic or cancerogenic properties but the effect of sustained exposure over long periods of time is not known.

Understanding macroscopic processes by studying (inter-)reactions at molecular, atomic, or cellular level is a noble goal and the ultimate dream of scientist. The trend is already seen as toxicity testing is carried out on human cells instead of animal cells, to study friction at nanoscale level or similar research in almost every domain of science and technology. The question remains whether it can reflect the behavior of materials at the macroscopic level. For the time being, it is not (yet) true, for example, in friction research. It has long been a concern of physicists and Robert March formulated it already forty years ago in his elegant book *Physics for Poets* ([1], p. 96), when he wrote:

> *Though laws describing the behavior of atoms are, at least in principle, the basis for the behavior of larger objects, it is inconvenient and perhaps even impossible to so use them in practice. On the basis of this, a physicist might well suspect that, for example, even if psychology were to become a perfectly exact science, it would be of little value in understanding society.*

Were March's statements in the 1970s too pessimistic toward an atomistic approach? The theory of complex systems was not as advanced as it is today but the cited text certainly fits the modern line of thought on *emerging properties*: a system is more than the sum of its component parts. It is a warning against oversimplification. Properties cannot (yet?) simply be scaled up from nano- or subnano- to the macroscopic level.

To conclude this introduction, the book is not a revolutionary pamphlet but a trial to offer the reader an integrated view on the field of biomaterials: cherishing the past, discussing robust state-of-the-art materials and opening a prudent, although modest, window to the future. Through this book, the authors hope to attract readers desiring an introduction to the field, not too general and not too specialized, students or beginning scientists in the field, as well as more experienced readers in an engineering and/or medical environment. The incentive to introduce a chapter by a clinical case study was also to emphasize the necessity of the close interaction between clinical practice and engineering, a close interaction that was too often absent in the earlier days of biomaterials research. Or, as Marie Csete (CIRM) expressed it in *Nature* (2 October, 2008) *We've had a crisis finding someone who understands clinical medicine and basic science*.

Bibliography

The bibliography is quite extended, tough, not exhaustive. Our excuses if not always the most representative papers are cited. In many instances, reference is made to older, but not at all, obsolete books. They were selected because of their intrinsic and historical value.

About the Book Title

Read the story on p. 109 (Sect. 5.3).

Illustrations and Italics

When not otherwise stated, photographs and graphical illustrations are produced by the author. When a name is added without affiliation, the person's name is listed in the acknowledgments.

Printed in italics are:

- Terms which are introduced in the text for the first time.
- Latin words or other non-English words.
- Text excerpts from other authors.
- Sentences or part of sentences that need to be emphasized.

Acknowledgements

We are particularly grateful to colleagues, academic and technical, at our own and other universities or from companies for their scientific advice, critical reading, supplying case studies or technical advice.

Colleagues at the Catholic University of Leuven: J. Bellemans, J. Lammens, M. Mulier, J.-P. Simon (Orthopedic Department, Faculty of Medicine), I. Naert, B. Van Meerbeek (Division of Prosthetic Dentistry, University Hospitals), E. Aernoudt, J.-P. Celis, J. Vleugels, Martine Wevers, P. Wollants, Els Naegels, R. De Vos, P. Crabbé (Department of Metallurgy and Materials Engineering, Faculty of Engineering), R. Van Audekercke (Department of Mechanics, Division of Biomechanics).

R. Verdonk (Faculty of Medicine, Division of Orthopedics, University of Ghent, Belgium).

Special thanks to L. Holans, Monique Kumps, C. Nassen and G. Festjens for their sustained competent assistance and helpfulness in answering all questions regarding bibliography.

Contributions by companies are especially acknowledged. A clinically recognized and marketable product is after all the goal of materials research. Let it be clear, however, that the companies that contributed by supplying information on their products or rendered other relevant help were not selected to the detriment of others but for often very simple reasons. F. Gelaude (Mobelife n.v., Leuven, Belgium); P. Mercelis (LayerWise, Leuven, Belgium); Griet Van Wesemael (Materialise NV, Leuven, Belgium); J. Breme (Department of Metallic Materials, University of Saarland, Saarbrücken, Germany); H.F. Hildebrand (INSERM, Lille, France); J. Monbaliu (Johnson-Johnson, Pharmaceutical Research and Development, Beerse, Belgium); B. Gasser (Mathys Ltd, Dr Robert Mathys Foundation, Bettlach, Switzerland); L. Thon (Mathys Ltd, Belgium); L. Labey (Orthopedics Smith & Nephew, Leuven, Belgium); J. Hermans (Zimmer BVBA, Belgium); L. Beckers (Unident nv, Leuven, Belgium).

A few persons deserve our intense gratitude for the many years of intense scientific collaboration: S. Jaecques (Leuven Medical Technology Center, L-MTC); E. Schepers (Division of Prosthetic Dentistry, Faculty of Medicine, KU Leuven); Kirsten Van Landuyt (Dept. Dentistry, Faculty of Medicine, KU Leuven); J.-P. Simon (Department of Orthopedics, Faculty of Medicine, KU Leuven).

The first author wishes to thank his son Stijn Helsen. His invaluable and sustained help through all those years for all computer and imaging problems, without whose help he could hardly have brought this book to a good end. He is also offering apologies to his children and grandchildren, who might have expected him to spend some more time in the past years. And last but not least, his wife Ria Van Boxmeer,

who has borne months and months of computer widowhood and merits his most exquisite love and gratitude. Yannis Misirlis also thanks Ria for her indulgence through the countless hours of intense discussions on so many matters with her and Jef in Leuven, Samos and Peloponese.

Leuven, Patras *Jozef A. Helsen*
September 2010 *Yannis Missirlis*

Contents

Chapter 1
The Perfect Human Machine

Nature provided its genetically engineered living products with considerable built-in self-assembling and, moreover, auto-repair capabilities. The example *par excellence* is the human body and for the reasons just mentioned, we quote it as a *perfect machine*. The excessive efforts by top athletes definitely provoke microfractures in muscles, bone and tendons but these fractures are continuously repaired on condition they remain below the critical level of damage. The same holds for hard tissue, which is constantly remodeled under stress. However, it is not failure free. Main reasons for failure are: accidents provoked by extra-corporeal interventions, genetic accidents, physiological accidents and natural (built-in!) auto-destruction at cellular level, i.e., natural cell death or *apoptosis*. Biomaterials figure as main partners in the production of devices for relieving the inconvenience of the last two reasons of failure and to assist the repair of the first reason of failure. Figure 1.1 is a nice archaeological example of the first: a man's tibia, broken in a nondocumented accident around the turn of the first millennium. The healing is not beautiful but anyway, the fracture healed with at best primitive if any surgical help.

1.1 Biomaterials: Philosophical Background

Thinking and talking about *biomaterials* is to some extent still done in car mechanic terms: what component of the engine failed, how can it be repaired or substituted by the appropriate spare part? This is not merely a caricature of biomedical speech but is rooted in western European philosophy. The herald of speaking about the human body in machine terms is credited to the sixteenth century anatomist Andreas Vesalius; his brilliant book *De humani corporis fabrica* was published in Basel, Switzerland, in 1543 [2]. The human anatomy is described herein with amazing accuracy as an assembly of functional spare parts. Outside its value as a milestone in anatomy, the book is a jewel of printers' skill and the plates are pure art! The mechanistic concept gained gradually official status in western European philosophy through the seventeenth century philosophers, e.g., Descartes [3]. They denied

J.A. Helsen and Y. Missirlis, *Biomaterials*, Biological and Medical Physics, Biomedical Engineering, DOI 10.1007/978-3-642-12532-4_1,

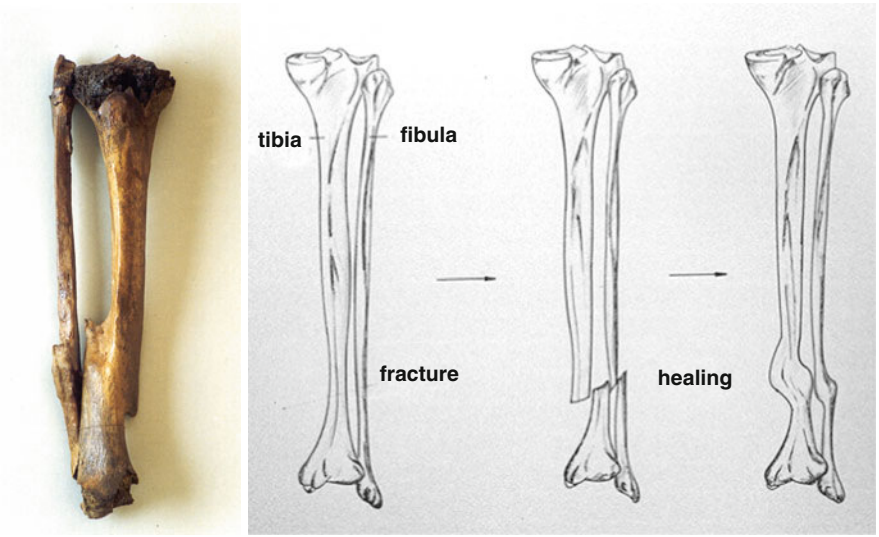

Fig. 1.1 Healed tibia and fibula of a man living around the turn of the first millennium. Courtesy of the *Wetenschappelijk en Cultureel Centrum van de Duinenabdij en de Westhoek, Koksijde, Province of West Flanders, Belgium*

the Aristotelian way of thinking that nature consists of what can be called *conscious dust* and hypothesized that nature, including living matter, was built up from particles of *inert matter*. A logic consequence was that these philosophers asked the question: *are humans machines?* Therefore we "adapted" the famous text in the book *Epidemics* of the Hippocratic Corpus [4, p.165]:

> Declare the past, diagnose the present, foretell the future; practise these acts. As to diseases, make a habit of two things: to help, or at least to do no harm. The art has *four* factors, the disease, the patient, the physician and *the engineer.*

Including the engineer, or be it a materials scientist, chemist or physicist, into the medical business justifies that the development of implants and the materials to make them is all overarched by the term *biomedical engineering*.

The performance of materials of interest to this book is intimately linked to the implant locus and consequently, the generic classes of materials will be discussed, where possible or relevant, starting from a case study. Let us first try to define the term *biomaterials*.

Till half a century ago, a material happened to be a biomaterial by lucky accident or educated guess. A metal, ceramic or polymer could accidentally exhibit an *ensemble* of properties, which made it suitable for covering a broken tooth, because it accidentally happened to have sufficient wear resistance, was not corroded when drinking Coca Cola, was not deformed when biting in a half-ripe apple, was not poisonous, was not giving bad taste in the mouth… Such a material was so-called

biocompatible, was quoted as a biomaterial but, let it be clear, for that particular application. The same alloy, e.g., a gold alloy, is occasionally suited for manufacturing a vascular stent but will definitely not be appropriate for a hip or knee prosthesis. Herewith we wanted to state that *biocompatibility* is somewhat a confusing term: the required performance of a material used is too different from one site in the body to another that a general definition will be either too vague or too restrictive! The same concern was expressed by Jonathan Black, where he preferred the term *biological performance* instead of biocompatibility [5]. A definition we propose is:

> A biomaterial is any material, single member of a generic class or a combination of two or more members out of the same or different classes, which can be used in a living body for a particular implant or group of implants, which does not incite negative response by the body, which is stable or exhibits only controlled and well-assessed breakdown.

It is a definition with all pros and cons of any other definition and many others can be found on the web. Admittedly, it is a definition that biocompatibility restricts to the ability of a material to perform with an appropriate host response in a specific application and meets, to some extent, David Williams' remark that *the adjectival counterpart 'biocompatible' should not be used because there is no such thing as a biocompatible material* [6]. Of course, along the same lines, one could say that there is no such thing as a biomaterial!

An implant, however good it may be, remains a foreign body and triggers a defense reaction, a clear proof of the interaction between body and implant. This interaction may be positive, wanted, if possible stimulating tissue growth or remodeling, or negative with respect to body and/or implant and to be avoided. In between exists a grey zone of indifferent behavior, if indifference exists at all in a living body. Biomedical research tries to grasp the puzzling interaction mechanism between body and implant with the ultimate goal of tailoring materials, optimized with respect to as many requirements as possible for a given *optimized shape*. Different from Vesalius' time is that physicians today are aware that malfunction of an organ has almost always a complex set of causes; beyond doubt, however, remains evident that the animal body is subject for part of its function to purely mechanical constraints and the biological materials are designed to meet these particular constraints. Implants and the materials to make them should, as far as possible, meet these requirements too. The right tailoring of materials and implants remains the goal for at least another two decades. That is how we see it today but what tomorrow will bring us might be another story: computational biologists may be the future rulers in the field. These newcomers apply computer simulations, increasingly paired with experiments, to understand and predict the quantitative behavior of complex biological systems and in the next stage drive new experiments [7]. Do not forget, however, the warning formulated in the Preface on complex systems and emerging properties.

1.2 Staying Alive Despite the Second Law

A living body is not a closed but an open system and through this the body deceives physics. It puts a brake on an uncontrolled increase in entropy ΔS, i.e., the increase of heat content ΔQ per degree Kelvin, heat being the least noble form of energy. A body is a complex biological system that by a self-regulating process maintains a dynamic stability for all vital parameters (temperature, ionic concentration, metabolic rate, energy conversion...). The process is called *homeostasis* or, as some authors prefer, *homeodynamics* because of the dynamic character of the process. *Self-regulating* may be substituted by *negative feedback* which is the basic principle of a branch of science named *cybernetics*. Feedback is a mechanism that reacts to disturbance of conditions through modifications of equal size and opposite direction. The disturbance may concern the global body, for example change of external temperature or humidity of the environment, or local parts, for example a change in ionic concentration at an implant interface. Feedback tries to maintain the internal balance. A sustained disturbance may go beyond the capability of the feedback mechanism to reestablish equilibrium and at that point, the mechanism itself may become destructive for the system it is intended to protect. The overencapsulation by fibrous tissue of the stem of a hip prosthesis, the inhibition of apposition of new bone and the subsequent failure of stability may be understood in these physical terms.

The foregoing paragraph seems not to learn us anything how implants should be improved or manufactured. The intention was to introduce homeostasis as the iron consequence of the physics of complex open systems. Although at first sight it is far away from the prosaic reality of biomaterial business, it is not. In testing the biological performance of a material or a device *in vitro*, the compelling dynamic character of the body site, in which it is intended to function, is often ignored in the concept of experiments.

1.3 Scaling of Plants and Animals

Since the time of Vesalius, the machine concept of the human (or animal) body has continued to develop till today. Seventeenth century masterpieces and milestones in this respect are the studies of blood circulation by William Harvey (1578–1657) *De Motu Cordis et sanguinis in animalibus, Anatomica Exercitatio* [8] and the motion of animals by Giovanni Alfonso Borelli (1608–1679) in *De Motu animalium* [9]. These are descriptions in qualitative mechanical terms of those magnificent running, swimming or flying *machines*. The interplay between geometry, physics and mechanics, be it of rigid bodies, fluids or gases, and biology is obvious, and is translated in a number of mathematical laws.

Leonardo da Vinci was already fully aware of this interplay. He was dreaming that, one day, it would be possible for man to sustain himself in the air by modifying

the structure of the body through the addition of wings. For this purpose, he studied the flight of birds and introduced scaling principles:

> With wings expanded the pelican measures five braccia, and it weighs twenty-five pounds, its measurement thus expanded therefore it to the square root of the measurement of the weight. The man is four hundred pounds and the square root of this figure is twenty: twenty braccia therefore is the necessary expanse of the said wings. [10, pp. 25–26]

Leonardo's scaling law was not to blame for its oversimplification because five centuries later fanatics of maths and biology are still busy refining scaling laws: man cannot fly for a complex set of mechanical and physiological reasons. One of those fanatics was D'Arcy Wentworth Thompson who published in 1916 *On Growth and Form*. Although willingly ignored by many of contemporary colleagues, it is a real masterpiece, still readable as witnessed by the recent reprints of the unaltered republication by Cambridge University Press of 1942 [11]. Kleiber's law (1932) is following the same philosophy; it is an allometric scaling law of which the mechanistic part became theoretically well underpinned during recent years. Max Kleiber (1893–1973), a Swiss agricultural chemist, joined the Animal Husbandry Department at the University of California, Davis, in 1929 to study the energy metabolism of animals [12], [13, Chap. 10]. The conclusion that all biological structures were affected by their size is a result of his studies. The allometric scaling of a biological variable Y with the body mass M is of the form

$$Y = Y_0 M^b, \tag{1.1}$$

where b is a scaling exponent; Y_0 is a constant, characteristic of the kind of organism. The basal metabolic rate scales as $M^{\frac{3}{4}}$. If simple geometric constraints were involved, one would expect multiples of one third for the exponent b. However, many biological phenomena scale as multiples of one fourth with body mass. West and colleagues proposed a mechanism underlying these laws: *living things are sustained by the transport of materials through linear networks that branch to supply all parts of the organism* [14]. The $M^{\frac{3}{4}}$ behavior of branching by space filling fractallike networks can be derived analytically [15, pp. 63–66], [16]. This law is experimentally confirmed over 18 orders of magnitude (unicellular organisms to whales) [12]! Mammalian blood vessels, the bronchial network or vascular systems are examples of such networks. In this paragraph we discussed so far one example of biological scaling. Next, we want to explore what happens to the ratio of mechanical variables like limb length and diameter or, say, the elastic properties, when the size of bodies increases? Let us first see what we can learn from trees!

During growth, the root system of a tree is optimizing its shape in order to account for the load distribution at the top of the tree. Mechanical analysis shows that during growth the geometry of the root system tends to minimize stress concentration. For an unbalanced load distribution, the case for a tree on the edge of the wood, the root system will have an 'optimal' shape different for the tensile and compression side as shown in Fig. 1.2. The same holds for the shape of the implant zone of the branches, bifurcating branches, etc. The subject is treated *in extenso* by,

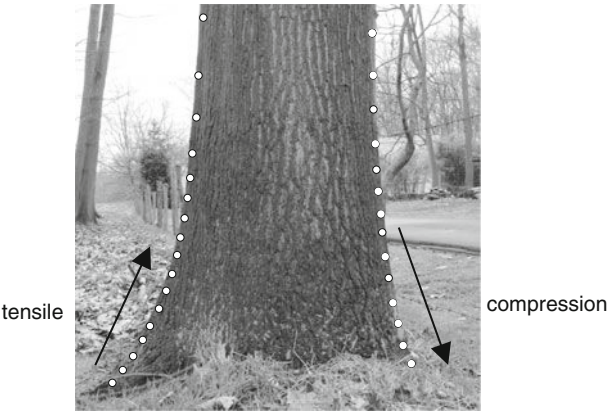

Fig. 1.2 Trunk of an oak. The tree is situated at the edge of the wood. More branches are pointing away from the wood with unbalanced loading as consequence. The root system accommodates its shape to minimize the stress distribution on both sides of the trunk

e.g., Claus Mattheck [17]. It is an example of the ingenious biological minimization of mechanical stress. In the design of implants, sharp edges will be avoided not exclusively but often for reason of stress distribution.

The slender construction of a tree has a length to diameter ratio $\frac{l}{d} > 25$. A column height l and diameter d collapses when its total weight exceeds the maximum compressive stress $\sigma_{\max}$. A small lateral displacement applied on too slender a column will make it collapsing at what is called the critical length l_{crit} for buckling. For a cylinder, the critical length is related to diameter by:

$$l_{\text{crit}} = k \left[\frac{E}{\varrho} \right]^{\frac{1}{3}} d^{\frac{2}{3}} \tag{1.2}$$

with ϱ the mass per unit volume (specific mass) and E the elastic modulus.[1] The constant k is 0.851 for a cylinder but changes with the shape of the column, tapered or any other form, while the exponent $\frac{3}{4}$ remains the same. For bending, an exactly identical equation is valid but the constant is different. The law is verified by a collection of quantitative observations on trees, representing almost every American species. Tree height plotted versus trunk base diameter on a double logarithmic scale fit to a line with slope $\frac{2}{3}$ (Fig. 1.3). Trees are said to maintain *elastic similarity* during growth.

A total of 576 records of tree height vs. trunk diameter are plotted in Fig. 1.3: the dotted line is the best fit through the data points with slope $\frac{2}{3}$. It is parallel to the solid line, calculated according to (1.2) and taking $E = 1.05\,\text{MPa}$ and $\rho = 6180\,\text{Nm}^{-2}$;

[1] Mechanical terms and definitions are collected Sect. 1.4.

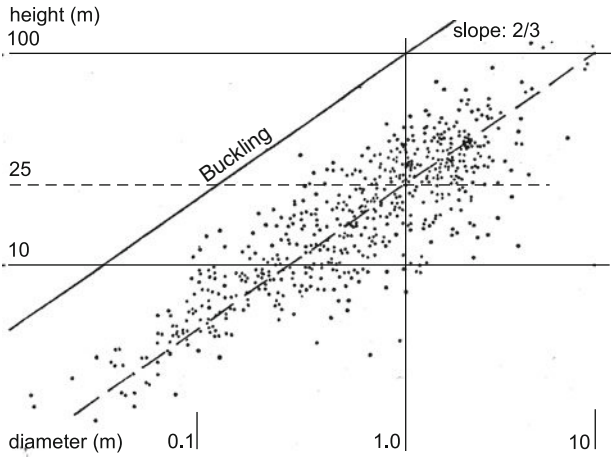

Fig. 1.3 Double logarithmic plot of overall height versus trunk base diameter of trees. The grey zone encloses 576 records representing almost every American species. The best fit is the dotted line with slope 2/3 and parallel to it, the solid line, calculated by (1.2). Adapted from [18]

E/ρ is fairly constant for green woods. This good fit leads to the conclusion that the proportions of trees are limited by elastic criteria (no data points above the calculated solid line). A second conclusion honors nature's prudence: the height of most records is about one fourth of the critical height for buckling, a fair safety factor. A common factor in engineering is 3 but apparently, plants play at the safe side.[2]

An issue of the discussion above is the importance of the elastic modulus, in general and during plant growth in particular. What about animals? How do they adjust their shape to scale? If scaling would be determined only by the strength criterion, animals *would grow no larger than a size which makes the applied stress equal to the yield stress of their materials*. Animals follow the same scaling exponent as trees: limb length, measured parallel to the direction of compression or tension, scales with the $\frac{2}{3}$ power of diameter. If this is true for quasicylindrical elements and simple loading geometry, it remains true independent of the type or combination of gravitational 'self-loading', static or dynamic. Also total body mass, chest circumference or body surface are subject to exponential scaling.

An important scaling law is the relation between metabolic heat production and body weight. The power output of a muscle fiber depends on the flow of energy, which in turn is proportional to its cross-sectional area. The fiber is a fraction of the body mass M and its diameter d is, from geometrical arguments, proportional to $M^{3/8}$. The cross section of the fiber is proportional to d^2 and hence, to $[M^{3/8}]^2$ or simply $M^{3/4}$. That is schematically how the allometric scaling law of Kleiber

[2] In a recent paper Kolokotrones et al. presented an interesting nonlinear model on the logarithmic scale for metabolic scaling. See [Nature 464, 753–756 (2010)].

was deduced with its magic exponent 3/4 in (1.1). The former discussion is based on [18–23].

For the discussion on scaling laws we went far back in history, against the current trend to confine citations to papers of say the last five or ten years, blinded as we are by the achievements of computer-assisted modeling, finite element analysis and the like. The papers we referred to, however, remain readable literature. Speaking about the branching pattern of trees in 1976, McMahon and Kronauer state that it is approximately stationary within any species and *That this means, that the structure is self-similar with respect to the parameters we recorded . . . the elastically similar model provided the best fit* [20, p. 460]. Their statement preceded by many years the hype that the concept of self-similarity as part of the definition of fractals provoked by Mandelbrot's publication in 1983 [24].

Searching universal laws is an integral part of any science. Kleiber's $\frac{3}{4}$ power law is one of these universality attempts in biology. It seems to be mathematically well underpinned (although the discussion is definitely not closed). The scaling laws bring us automatically to the concept of fractals, which by West et al. are beautifully quoted as the *fourth dimension of life*. These authors state that: *Natural selection has tended to maximize both metabolic capacity, by maximizing the scaling of exchange surface areas, and internal efficiency, by minimizing the scaling of transport distances and times. These design principles are independent of detailed dynamics and explicit models and should apply to virtually all organisms* [14].

One example of these principles are the arteries and veins (transport of nutrients and waste!) in the mammalian body. Although arteries, veins and blood represent only about 5% of the weight, blood vessels are found within a distance of a few cells throughout almost the whole body, a rare exception being the vascularity of the cornea required for optical clarity [25]. Nature devised here an utmost efficient bifurcating distribution system, already described by Leonardo da Vinci, although he considered veins and arteries as transporting heat [10, Chap. VIII]. It would last another hundred years before the real function was revealed by Harvey [8].

In Euclidean objects, mass (M) and length (L) scale with integer exponents (3 in this case). Many biological 'objects' show non-Euclidean order and scale with noninteger exponents. The network of blood vessels is an example, the structure of lungs is another, both are scale invariant and self-similar. Detailed definitions on fractality and self-similarity are beyond the scope of this textbook but for this purpose Mandelbrot is the original source [24]. This subject is referred to here because it is intrinsically linked to the discussion on scaling. Moreover, the bifurcating and pervasive vascular network explains why, a couple of decades ago, the intense investigation on ingrowth in porous surfaces for dental and orthopedic implants failed and why currently massive tissue substitutes fail.

Reference to scaling and/or fractality is not common in biomaterials literature. Why then should this relatively long discussion on biological scaling laws be relevant in the context of this book? Does it contribute anything to the discipline? A number of reasons compel us to answer yes.

Universal laws. It is the statuesque beauty of science that it is searching for an ever smaller number of principles from which particular cases can be deduced. Scaling laws belong to that category. Application of this principle finds not only its place in 'big science'! Science starts at the bottom with decently interpreted experiments. Help in seeing the light through the burden of data can be triggered by reduction and/or normalization of data. These simple tools can be basically instructive but inspection of the current literature indicates that they are often neglected, forgotten, or worse, not known anymore. Below we discuss an example. The same holds for statistical data treatment and data reduction [26].

Understanding processes. In Fig. 1.4 (top) are displayed setting curves of brushite cement, monitored by FT-IR absorbance at a given wavenumber; the parameter is retardant concentration (details are not important for the present discussion). 'Macroscopic' difference in rate is easily registered by simple inspection of the graphs but subtle differences between those three curves is not. If the reaction mechanism is independent of retardant concentration, the curves should overlap

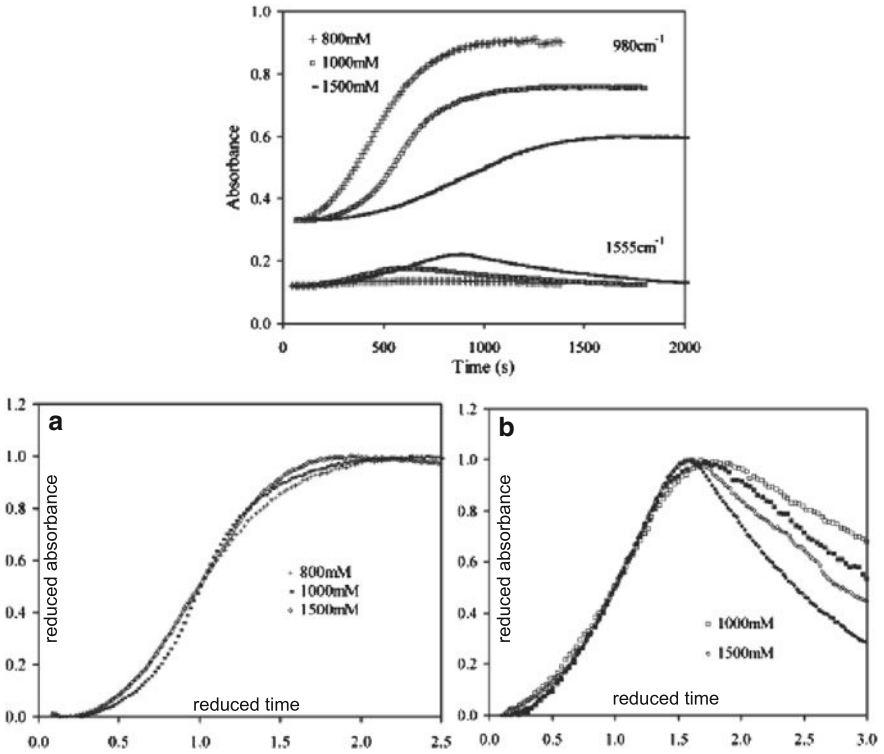

Fig. 1.4 Setting kinetics of brushite cement (FTIR-monitoring). (**a**) IR-absorbance vs. time (*s*) for three concentrations of retardant; (**b**) normalized absorbance vs. reduced time $t/t_{0.5}$, t divided by the time to complete 50% of the reaction. Adapted from [27]. Reproduced by permission of the Royal Society of Chemistry

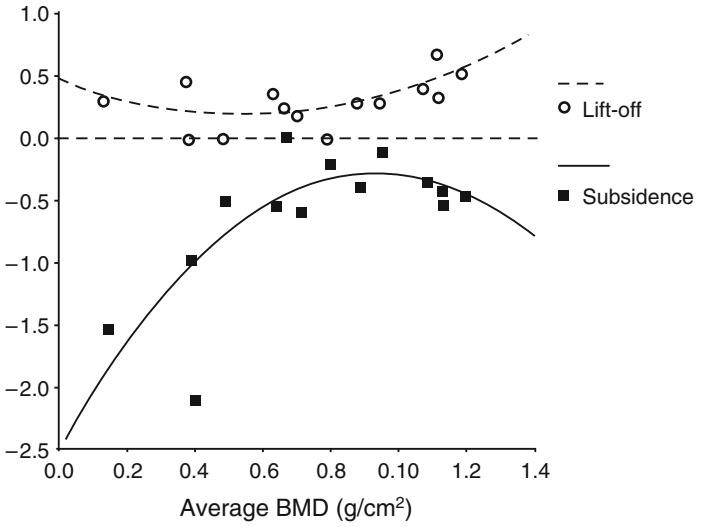

Fig. 1.5 Subsidence and lift-off (mm) of an uncemented total knee tibial plateau versus average bone mineral density. Courtesy Luc Labey [28]

on normalizing. They qualitatively do as seen in (a): the reaction mechanism is probably the same irrespective of the retardant concentration; however, the small differences between the curves point to differing formation rates of the sequence of intermediate compounds and/or to conformation differences, for example diffusion hindrance, in the heterogeneous matrix; in (b), however, clear rate differences exist above $t/t_{1/2}$, not easily observed in the original data. This one example from literature is rather the exception than the rule. On the contrary, curves fitting by more or less sophisticated computer programs is good fashion, can be of help in technological applications, but does not help science to progress: a physical model should underlie the analyzed data. The reference is given to emphasize that 'old-fashioned' techniques are still valid today. Detailed understanding of a process allows more intelligent experiment planning, reduces the number of experiments and is occasionally applicable to similar processes: it is the way up from a particular system to a more universal level. Science?

Understanding functions. In a study of migration of the tibial component in a total knee arthroplasty, Li and colleagues found a relationship between bone mineral density (BMD) and subsidence [28, 29]. An obvious clinical conclusion is that there seems to be an optimal range of BMD, and no doubt, it is a clinically relevant observation. The authors fit a nice curve through the experimental data but do not supply, not even suggest, a biomechanical or physiological explanation. We have no data available for a thorough analysis but, based on insight in the structure of bone we would not be surprised to see the given relationship analyzed in terms of a multifractal response of the solicited bone structure (see for example [15, Chap. 9]).

Self-similarity. In one of the following chapters, we will examine materials for scaffolds. But first this: we selected at random two papers on scaffolds by Schantz et al. and Manjubala et al. [30, 31]: different preparation techniques, different materials, etc. (details not relevant for the present purpose), scaffolds with 3D architecture. The produced product is geometrically regular and thus dimensionally self-similar. The self-similarity we were referring to a few paragraphs back will not fit this geometric model. In a recent paper, drug release is reported from an *ordered* silica material. Order might not be an obstacle here because at the nanoscale the process is going on but who will pretend that a distribution of pores would not result in a more regular drug delivery [32]? Biologic order is non-Euclidean!

By foregoing thoughts biomaterials research was projected on a broad biologic and scientific background. The purpose was to demonstrate that in installing 'biospare parts' here and there in the body, a sound holistic view on the body is unmistakably a safe guide in research. Not that the holistic view helped the individual patient but it could have helped the biomaterials community, when it was investing in bone ingrowth in porous coatings during the 1970s to pay simultaneous attention to vascularization. Only now is appearing an awareness about it in the booming area of scaffolds as was already mentioned, an item on which we will come back later. We could not refrain from ventilating some criticism on current shortcomings in scientific reporting, fully aware of our own sins in the past. Further useful reading on scaling is the book *Fluctuations and scaling in biology* [33].

Statistical analysis. Before walking to the next section a parenthesis on statistics. Statistical data treatment of, say, mechanical properties may look less stringent. In 'Fire of Life' Kleiber paid special attention to statistics: he even summarized the 'The Twelve Commandments of Biostatistics' which still sound unbelievably alive [13, p. 385]. Computer facilities make statistical analysis easy to day, too easy and often applied undiscriminatingly. Many good textbooks exist but as a first aid 'Statistical Rules of Thumb' by Gerald van Belle [26] is warmly recommended. Only a sound application of statistics can be of any really valuable help! Outside the basics, items like sample size (a pertinent question for all investigators in the field), covariation and in particular a critical chapter (pp. 153–173) on 'Words, Tables and Graphs' worth the following illustrative excerpt of van Belle's rules of thumb:

1. Use text and not a table for displaying few numbers (2–5).
2. Limit the number of significant digits in a table and convey crucial information in the heading!
3. When possible always graph the data. The graphs given by van Belle in Fig. 7.1 were taken from a paper by Anscombe [34]. They show how instructive a graph may be for interpreting statistics!
4. Never use a pie chart and always think of an alternative to bar graphs, or worse, stacked bar graphs (they are waste of ink!) or even worse 3D bar graphs (misdirected artistry!).

These are a few points about the use (and abuse) of statistics in a refreshing perspective.

1.4 Definitions

In this chapter, we wanted to stress through biological examples and scaling laws the interplay between pure mechanics and biology. The goal is that the designer should learn from nature. In the past, it was not simple to quantify nature, but today, even more detailed analyses and computer-aided simulations allow to penetrate natural processes with increasing accuracy. These simulations are all part of that learning process.

In this section, we define the current mechanical properties introduced thus far in the text. The meaning of these variables are easily illustrated graphically by the stress–strain curve given in Fig. 1.6. Inserted in the graph are the shapes of a test specimen at three stages during its deformation in a tensile machine. In a first approximation, the stress–strain curve is characterized by the elastic deformation zone, the plastic deformation zone (beginning of necking) and fracture. More complex curves will occasionally be given when materials such as superelastic alloys displaying complex deformation behavior are discussed.

Given are: *the name of the property (occasionally an alternative name): the current symbol, the dimension between [. . .] (with L for length, M for mass, T for time, [-] for dimensionless), basic units or their multiples (m for meter, g for mass,*

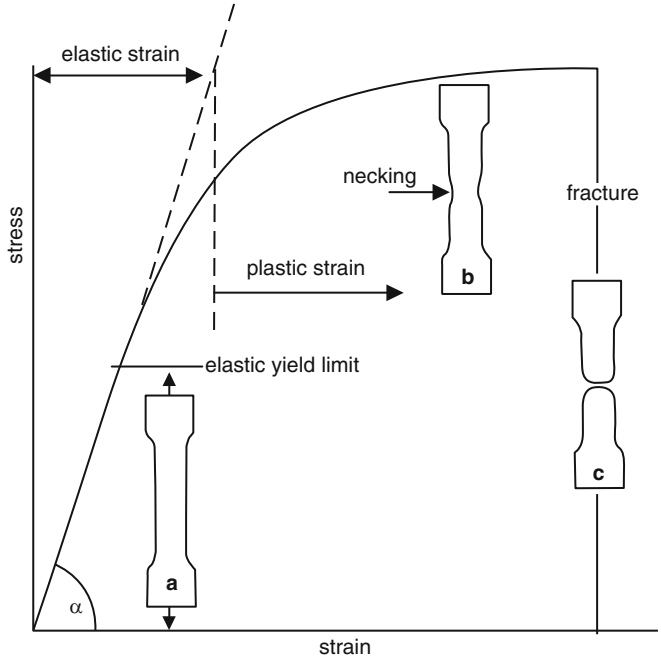

Fig. 1.6 Increase of strain (reduced length) of the specimen as a function of applied stress (load per unit area of cross section). All variables are defined in the text

s for second; the first figure refers to the SI unit); definition. The dimensions are useful to test the consistency of the units in a result of calculation through an equation or to define the units after deduction of an equation. Test specimens for the determination of mechanical properties are normally machined to standardized shapes and by standardized procedures. They can be found in national and international standards for testing materials listed, e.g., by Helsen and Breme [35, pp. 67–71]. The main units used and conversion factors in the text are summarized in Tables A3 and A4 (Appendix A).

Creep: ϵ, [-], %. Creep is a slow continuous deformation or strain under constant stress. It is function of stress, temperature and time. It only represents a problem for metals and ceramics near their melting or softening temperature. For polymers, however, is it sizable at low temperature (<200°C) and as such a major design parameter. Glass transition temperature is a criterion for creep resistance. A special kind of creep to mention is viscous flow and, it is, like diffusion, an exponential function of temperature and a linear function of stress:

$$\frac{d\epsilon}{dt} = C\sigma e^{-\frac{Q}{RT}} \tag{1.3}$$

with t time, C a constant for a given polymer, Q the activation energy for viscous flow, R the universal gas constant and T the temperature in °K. C and Q are supplied by producers.

Density: ϱ, [ML^{-3}], kg m^{-3} or with the same numerical value g dm^{-3}; kg dm^{-3}, g cm^{-3}, g mL. It is a property that depends on the way atoms or molecules are spatially organized. It is measured as mass per unit volume; sometimes expressed as multiples of the density of a standard material (usually water at 4°C).

Ductility: A, [-], %. Ductility or elongation at fracture means strain at fracture, i.e., the strain at the high end of the stress–strain curve in Fig. 1.6. The reduction in area of the specimen at that point is a measure of ductility. It is the ability of a material to undergo large plastic deformation before it is breaking. In some instances, in addition to tensile tests, the reduction in area in the necking zone is given.

Elasticity modulus (Young's modulus): E, [$ML^{-1}T^{-2}$], Pa, kPa (kilo-), MPa (Mega-), GPa (Giga-). The linear part of the curve below the elastic yield point is described by the famous law of the English seventeenth century scientist Robert Hooke (1635–1703): *ut tensio, sic vis* ('as the extension, so the force', published in 1676 in anagram form *ceiiinossttuuv*). The modulus of elasticity is determined by measuring the slope of the stress–strain curve, where strain is effectively proportional to stress. Measurement of sound velocity or vibration frequency are other methods to determine E.

Young's modulus is the macroscopic translation of the magnitude of interatomic forces and the packing of atoms (number of atoms per unit volume) and as such, it represents a fundamental physical property of matter. Atoms are held together either by strong primary bonds, ionic (Na^+Cl^-), covalent (as in diamond or in chains of carbon in polymers: –C–C–) or metallic (Fe–Fe), or by secondary bonds,

Van der Waals forces (gravity attraction) or hydrogen bridging (between proton donor and a proton acceptor in polymers for example). The values of E-moduli may be as low as 0.1 GPa for low-density polyethylene or as high as 1,000 GPa for diamond, which has the highest modulus of any material.

Fatigue strength: σ_f, [$ML^{-1}T^2$], Pa, kPa, MPa. Materials may fail at stresses below the UTS or YS (see below) by exposure to repeated stress cycles. ASTM defines fatigue strength as the limiting value of stress at which failure occurs as N_f, the number of stress cycles, becomes very large. It is the stress level for steel and the like below which fatigue failure never occurs (<endurance limit). More ductile materials such as aluminum do not have such a distinct limit and these are tested on fatigue by subjecting to given stress amplitudes and up to a fixed number of cycles, usually $N = 10^7$. Fatigue strength is an extremely important engineering and design property.

Fracture toughness: K_{Ic},[$ML^{-3/2}T^{-2}$], $N\,m^{-3/2}$ or k- or $MPa\,m^{1/2}$. Fracture toughness is a property which describes the ability of a material containing a crack to resist fracture. It is an important property for all design applications. The subscript "Ic" denotes *mode I* crack opening under a normal tensile stress perpendicular to the crack. Numerically it is always smaller than the yield strength. For a condensed treatment of this property, we may refer for further reading to Ashby and Jones [36, pp. 131–139].

Friction coefficient: μ, [-]. The force that will just cause two materials to slide over each other, is called the static force F_s, and is proportional to the force acting normal to the contact surface; once the sliding started, the frictional force decreases slightly but remains proportional to the normal force acting on the sliding surfaces:

$$F_s = \mu_s P \quad and \quad F_k = \mu_k P, \tag{1.4}$$

where μ is the proportionality or friction coefficient, respectively, for the static and the kinetic case. Numerical values are difficult to give because they depend on the material, surface finishing and lubrication.

Rigidity modulus: see Shear Modulus.

Shear modulus: G, [$ML^{-1}T^{-2}$], MPa, GPa. While Young's modulus describes the response of a material to linear strain, the response to shear strain is described by the shear modulus.

Strain: ϵ for nominal strain or γ for shear strain, [-], fraction or %. Materials respond to stress by straining. The degree of strain depends on the elasticity modulus: a stiff material strains less than a compliant material under a given stress. The change of length l and radius r of a cylinder of a material is measured as function of the applied stress. Strain is calculated by taking the ratio of change in length to original length l_0 and of change in radius to original radius r_0, called, respectively, tensile strain or lateral strain:

$$\epsilon_{\text{tensile}} = \frac{l - l_0}{l_0} \quad and \quad \epsilon_{\text{lateral}} = \frac{r - r_0}{r_0}. \tag{1.5}$$

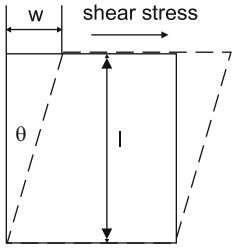

Fig. 1.7 Induction of shear strain by shear stress

The negative ratio of lateral strain to tensile strain at a given stress is called the *Poisson ratio* ν. Its value is ∼0.3 for most metals (steel, Ti, Cu, ...) in the elastic range, for glass ∼0.2 and for rubber, an upper extreme, ∼0.5.

Shear strain: When the sample is not subjected to tensile or compressive stresses but to shear stress, the deformation is defined as shear strain. If a given shape, say, a cube shears sideways by an amount w as shown in Fig. 1.7, the shear strain is:

$$\gamma = \frac{w}{l} = \tan\theta \simeq \theta \tag{1.6}$$

If the deformation is small, $\tan\theta \simeq \theta$.

Stress: σ, [$ML^{-1}T^{-2}$], Pa, kPa, MPa. When a force (F) is applied to a cylinder of material in tension or compression, it is said to be in a state of stress. It is calculated by the force applied to the cylinder divided by the area (A) of a section perpendicular to the direction of the force at any moment of the deformation. Why is this said? Where the stress–strain curve starts leveling off (ductility zone), one is seeing a reduction of section somewhere halfway between both ends, the so-called *necking* as shown in Fig. 1.6. If the actual section at any moment of the curve is not taken into account, the stress is called *engineering stress*. In that case the curve will go through a maximum before fracture.

Thermal expansion coefficient: α, [T^{-1}], °C^{-1} (usually $\times 10^6$). The linear expansion coefficient is the ratio of the change of length per degree C to the length. It is only approximately linear in function of temperature range. The volume expansion coefficient is roughly three times the linear coefficient.

Yield strength: YS, [$ML^{-1}T^{-2}$], Pa, kPa, MPa, Nmm^{-2}. Tensile yield is a given value of stress where the stress–strain curve departs from linearity. From this value on a permanent set or deformation remains after removal of stress. For practical reasons, the stress inducing a plastic deformation of 0.2% is generally taken as the yield strength.

Ultimate tensile strength: UTS, [$ML^{-1}T^{-2}$], Pa, kPa, MPa, Nmm^{-2}. It is the highest endurable stress at which the test specimen begins to neck in tensile or to fracture (mainly for brittle materials) in compression.

Viscosity (dynamic): η or μ, [$ML^{-1}T^{-1}$], Pa s or kg/s m. It is a measure of the resistance of a fluid which is being deformed by either shear stress or extensional stress (see Sect. 2.3.1).

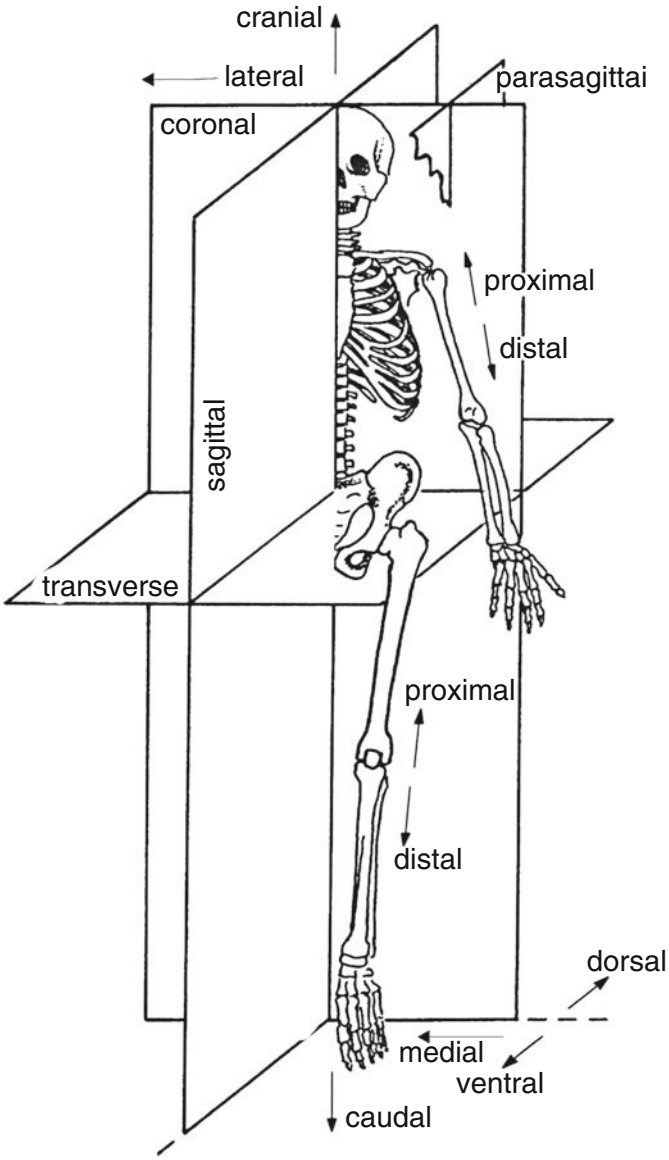

Fig. 1.8 Most common terms relative to skeletal anatomy. Adapted from [40], Fig. 1.1. Reproduced by permission of Springer Verlag

For a more in-depth treatment of mechanical properties, the reader is advised to consult current textbooks (Ashby, Timoshenko, Allen and Thomas or French [36–39]).

Anatomical terms: the most common terms are relative to the skeletal anatomy and are illustrated in Fig. 1.8.

In this chapter, the content of the book is introduced projected against a philosophical background. Prior to human implantation, implants are developed and tested in smaller animals and are subsequently upscaled for human use. Therefore, a discussion was devoted in Sect. 1.2 to scaling laws because upscaling is not a linear process, supplemented with some thoughts on data handling and data reduction. In Sect. 1.3, definitions are given of common mechanical properties figuring throughout the book.

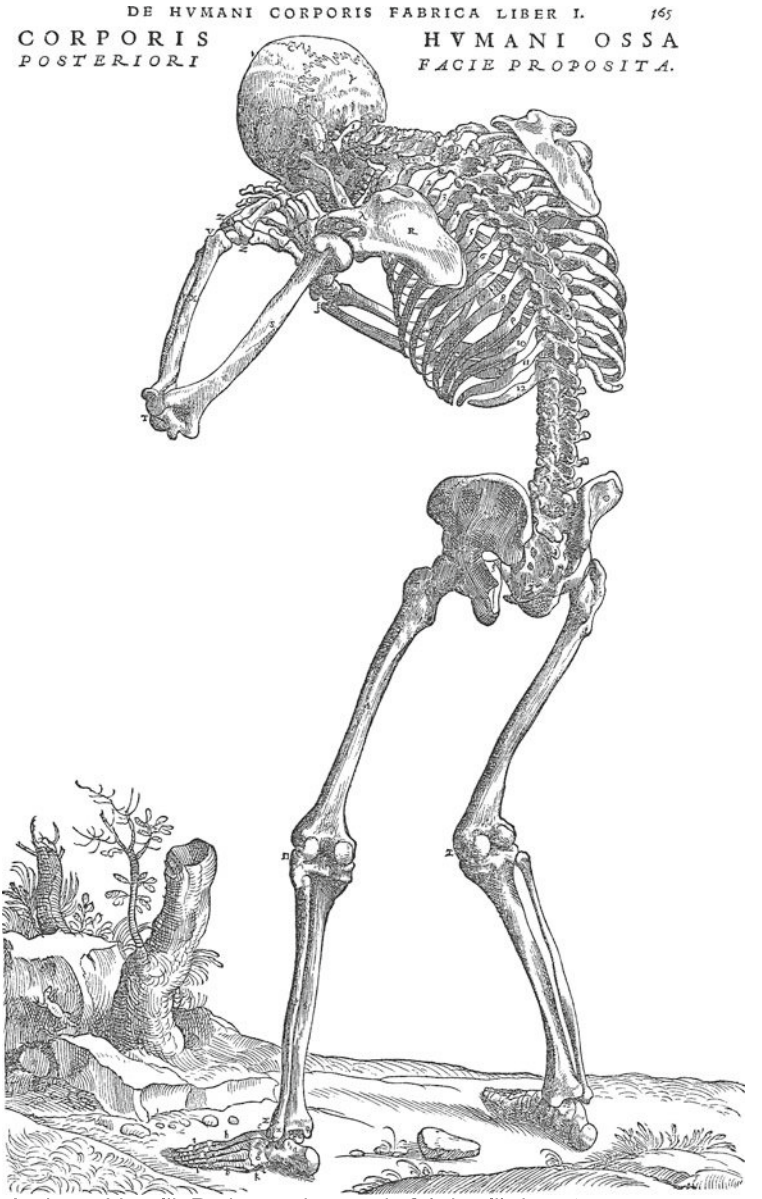

Andreae Vesalii: De humani corporis fabrica libri septem
Basileae: ex officina Joannis Oporini, 1543

Failing, no doubt about!

Chapter 2
The Failing Human Machine

Unification of principles is a fundamental goal of science. Four centuries of intense experimental and theoretical research in physics culminated through the work of Kepler, Newton, ... Einstein in laws applicable from subatomic to cosmological scale. Scaling laws in biology serve the same unification purpose. In Chap. 1, a flavor of these laws was discussed to gain some insight in the engineering constraints that developing living organisms were facing during growth, be it oligocellular organisms or animals as big as an elephant. Nature provides the right materials on the right place (but failures were legio, Darwin already knew!). If, however, it goes wrong somewhere in our body, we want to remedy it: without surgery if possible, with if unavoidable and even then, it can go wrong! In this chapter, we start from a case study of a broken hip prosthesis: where and why did it go wrong and by what should it be replaced. A total hip replacement is an example of a heavy duty application beleaguered by many predators! We will explore the most plausible causes of failure, mechanical and/or chemical, and discuss each of these aspects in some detail. In Chap. 1, the *perfect* side of natural machines was discussed, here we will look at the *failing* human machine and in particular at human failures in design and materials' selection for the production of *spare parts*.

2.1 A Total Hip Replacement

A patient suffering from bilateral coxarthrosis had a total hip replacement or arthroplasty (THR or THA) in two successive surgical interventions in 1973 (left hip) and 1974 (right hip).[1] With a length of 1.72 m and weight of 96 kg, he was a rather obese person, moderately active and was for almost 27 years after surgery without problems. At the end of 1999, the patient fell and experienced pain in his left leg and had reduced mobility. Radiographic examination revealed a broken stem of the left hip (Fig. 2.1) and a revision was indicated. The stem broke roughly at the junction of proximal one third and distal two third of the stem length (*proximal* or *apical*: near

[1] Courtesy of Prof. J.-P. Simon.

J.A. Helsen and Y. Missirlis, *Biomaterials*, Biological and Medical Physics, Biomedical Engineering, DOI 10.1007/978-3-642-12532-4_2,

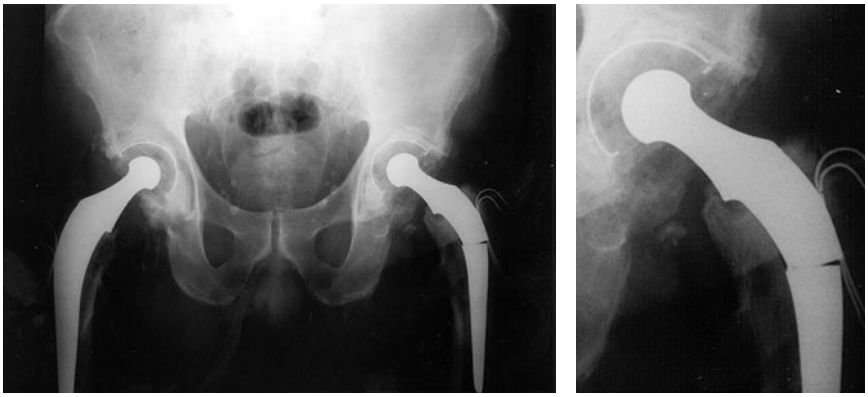

Fig. 2.1 Radiograph of a bilateral total hip replacement. The left prosthesis was broken after 27 years of successful functioning. *Right*: detail of cup, head and broken part

the upper end; *distal*: near lower end). Both stems were of the same very successful type, designed by Sir John Charnley in the beginning of the 1960s. In the last section of this chapter, we will give a brief biography of this surgeon and pioneer of the field of biomedical engineering. The *monobloc* prosthesis was cemented in the femoral canal by inserting a complex low viscosity mixture of partially polymerized methylmethacrylate and other components (more details in Chaps. 10 and 11), ultimately solidifying to polymethylmethacrylate (PMMA). *Monobloc* means a prosthesis design in which head and stem form one solidary unit, as opposed to *modular* where head and stem are separate units, consisting of various combinations of materials (stainless steel + stainless steel, titanium alloy stem + cobalt–chromium or ceramic head, stainless steel head + cobalt–chromium stem, ...). The cup was made of polyethylene (PE), the femoral part of stainless steel which seems to belong to a type 304 (or may be ENJ58?), as we determined by energy dispersive X-ray spectrometry (EDS): chromium ∼17%, nickel ∼13%, manganese <1.5%, silicon <0.6% and no molybdenum. This type of steel is not a top choice for this purpose because its corrosion resistance in media containing sulfur (proteins) is not excellent (high nickel, no molybdenum). The ultimate tensile strength (UTS) is 550–750 MPa, the E-modulus about 193 GPa [35]. The section at the fracture site was 156 mm^2. Why was it broken? Was the weight of the patient with his 96 kg overload and/or insufficient material strength the cause of fracture? Let us explore a number of possible causes.

Load versus strength: The deflection δ of a cantilever beam of square section with thickness t of 12.5 mm, a length l of 65 mm and loaded as shown in Fig. 2.2 by a force of 4,000 N is calculated by the formula

$$\delta = \frac{4l^3F}{Et^4} \tag{2.1}$$

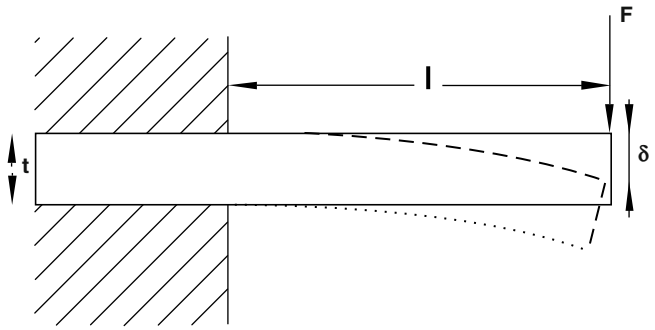

Fig. 2.2 A bar with square section clamped on one side and loaded at the free end

ignoring the beam's own weight. Inserting the numerical values in (2.1) gives a deflection δ of 1.03 mm. The strain at the clamp site is <0.2% or comfortably within the elastic deformation region of the stress–strain behavior and far below the strain at fracture! The numerical values l and t were realistic and measured on the explanted prosthesis: $t = 12.5$ mm corresponds to the section of 156 mm^2 at the fracture site of the prosthesis; $l = 65$ mm is the distance of the fracture site to the center of the head; a load F of 4,000 N corresponds to more than 400% of the patient's body weight, which is an estimation of the force acting on the THR head when standing on one leg. This is the static approximation of maximum loading which occurs during level walking. Clamping on one end as in Fig. 2.2 is less favorable than in reality because a hip prosthesis stem is supported at least partly along its whole length. The example shows that overload is not a plausible cause of the fracture of the prosthesis.

The applied 400% body weight is a realistic value. Thorough analysis of the complex load distribution on the hip joint (and other joints) has been performed in the past years (see references under heading of Table 2.1). It is a typical research item in the field of biomechanics. A set of data for loads on joints of knee and hip measured by an instrumented prosthesis are juxtaposed in Table 2.1. Built-in strain gauges, electronics for telemetric communication and mathematics allow for analyzing forces along the femur-based axes $-F_X$, $-F_Y$ and $-F_Z$ as shown in Fig. 2.3. The magnitude of the resultant $-F$ of these forces is given by $\sqrt{X^2 + Y^2 + Z^2}$ and is expressed as % body weight (%BW).

The bending and torsional moments are expressed as %BWm. Where available, the last two columns contain the estimated number of cycles/year N_y for a particular activity and the total number of cycles N_{tot} performed during the expected life span of a prosthesis. The mathematical model used is described by Bergmann et al. [41]. A complete set of updated gait patterns, muscle forces, activity frequencies and hip contact forces from instrumented hip prostheses were published in papers by Bergmann and colleagues [42–44]. A recently developed and very advanced example of an instrumented implant will be presented in Chap. 10. They also produced a CD, HIP98, freely available on the Internet. Implants are always subject to complex load patterns and these patterns should be taken into account when designing

Table 2.1 The resultant force, bending and torsion moments expressed in % body weight respectively % body weight meter [46–49]

Joint	Activity	F[%BW]	N_y	N_{tot}
Hip	Walking (1–6 km h^{-1})	280–430		
	Jogging (5–8 km h^{-1})	490–540	6.10^5	3.10^7
	Stairs up	345–552		
	Stairs down	390–509		
Knee	Level walking	340	3.10^6	1.10^8
	Stairs up	425	8.10^4	3.10^6
	Stairs down	383		
	Jumping	2,400		
Joint	Activity	M_{bend}[%BWm]	M_{tors}[%BWm]	
Hip	Walking (1–6 km h^{-1})	4.8–5.8	1.6–3.1	
	Jogging (5–8 km h^{-1})	7.2–8.7	4.0–4.7	
	Stairs up	4.0–6.0	3.4–4.5	
	Stairs down	6.8–7.8	2.7–3.1	

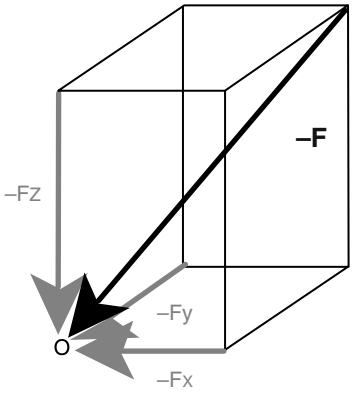

Fig. 2.3 Acting forces on the femur and resultant

a prosthesis. The instrumented prosthesis developed by Bergmann contributes to this quantification by supplying realistic load values to improve the knowledge of the boundary conditions as well as knowledge-based postoperative revalidation programs for patients. Moreover, based on such sets of data, instruments were developed for in vitro mimicking these load patterns to predict realistically the in vivo behavior of a prosthesis.[2] The detailed biomechanical story can be read in the cited references.

The commercialized prostheses have at least nowadays sufficient mechanical strength but this has not always been the case in the past. The Vandeputte

[2] Examples: *AMTI-Boston 12 Station Hip Simulator* or the *Endolab hip simulator*; references can be found on Internet.

endoprosthesis was an example of a poor mechanical design. This prosthesis was designed for complex peri- and fractures. The proximal bulky part was developed for substituting defect bone. Fracture sometimes occurred in the proximal part of the slender stem just below the bulky cubic part. The section of the stem was in this case probably not sufficient to withstand the bending moment at that particular side of the stem [45]. More historic cases of this kind are known but all documentation has disappeared.

Inclusion: Another reason for fracture could be a material defect, something like an inclusion or an impurity just at the surface which acts as a notch for the onset of fracture. An aluminum oxide particle could, for example, have penetrated the surface during sand blasting. Inspection by optical microscopy and scanning electron microscopy, preferentially equipped with an energy dispersive X-ray fluorescence spectrometer (SEM-EDX) of the fracture surfaces are the indicated detection tools here. Analysis of the case of Fig. 2.1 learned us, however, that it was not the case here. An example of an inclusion that caused a fracture initiation is discussed by Helsen and Breme in their book *Metals as Biomaterials* [35, Chap. 15].

Fracture occurs when a critical stress is exceeded but a notch can lower this critical stress. A notch can have many origins: careless manufacturing, an inclusion at or just underneath the surface... Rapid loading of notched pieces (a fall of a patient) can provoke progress of the notch into catastrophic fracture. More about rapid loading in [50].

Fatigue: Joints of hip or knee and their replacements are typically all cyclically loaded structures. Consequently, the materials concerned were all subject to *fatigue*. The stress–strain curve of Fig. 1.6 ends at a stress by which a crack propagates catastrophically and results in fast fracture of the test specimen. Cracks, however, can grow gradually at stresses much lower than the UTS, the stress at the catastrophic end of stress–strain curve! In Fig. 2.4, the explanted prosthesis is shown and the fractured surface in Fig. 2.5.

Fig. 2.4 The explanted broken Charnley prosthesis of Fig. 2.1. The lower part of the stem is heavily corroded. On the fracture surface, the progressing crack (*lower left*) and the ductile fracture (*upper right* on the fracture surface) can be clearly distinguished

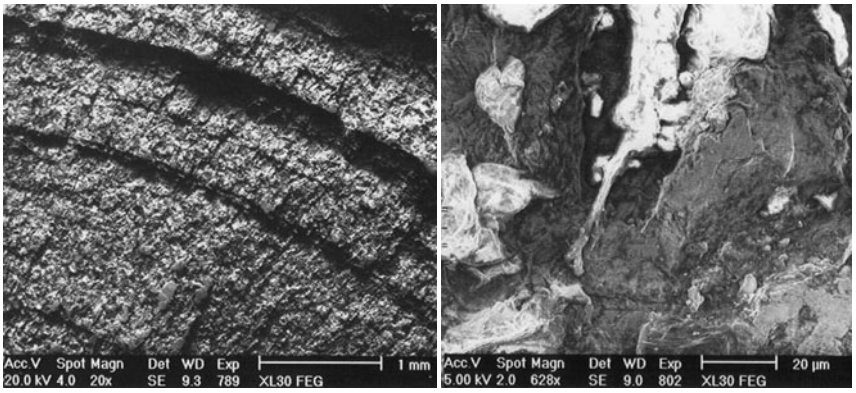

Fig. 2.5 *Left*: one striation represents a progress of the crack by one step (bar = 1 mm); *Right*: the fast fractured surface (bar = 20 µm). The surface at this stage is normally rough but was smoothed by wear after the fracture occurred

Each striation in the left side of the latter figure stands for one step forward in progressing fracture of the stem of Fig. 2.1. At the right side is the situation where the progressing fracture weakened the prosthesis to an extent where it could no longer bear the imposed load and was breaking catastrophically. This surface is normally very rough and without striations but in this case, the patient did continue to walk after the stem was broken, which smoothed the surface.

With an assumed load of 4,000 N (>400% of the patients BW) and a section of the 165 mm^2, the applied stress was of the order of magnitude of 26 MPa. Calculating the number of cycles the patients' prosthesis performed by summing the activity cycles/year as given by Black, jogging excluded, and multiplying by 27, the number of years of service the total of cycles must be something like 10^8 cycles [51]. This is below the expected fatigue limit for a stainless steel type 304 (see Sect. 2.2.1). As shown in Fig. 2.5, fatigue is definitely at least part of the reason for failure, although the applied stress remained below the fatigue threshold.[3]

Corrosion: Still a number of other things can go wrong. On the medial part of the prosthesis (Fig. 2.4), some surface deterioration either by *wear* (rubbing against the PMMA cement) or by *corrosion* or by synergy of both phenomena is visible. Medial means facing the median or sagittal plane of the body (Fig. 1.8) or more detailed in any book of anatomy, e.g., Gray's Anatomy [52, p.13]. Wear and corrosion as in Fig. 2.4 is no longer seen in modern prostheses.

Corrosion is a potential onset of fracture, particularly for stainless steels. Close inspection of the fracture site (metallography, microanalysis by X-ray spectrometry in the scanning electron microscope (SEM)) could not prove that corrosion was the cause here. However, the alloy of this prosthesis is sensitive to attack by chlorides

[3] An important research center on fatigue is located in the *Graduate School of Engineering of Osaka University (Japan)*, headed by Prof. Masary Zako. Coordinates are easily found on Internet.

and sulfides and it is known that at the tip of a crack sulfur is often detected and suspected to promote the progress of the crack.

Wear: In an artificial hip joint, the head (in stainless steel in this case study but can be either in other alloys or in ceramics; see following chapters) is often articulating in a plastic (polyethylene) socket replacing the acetabulum. Wear produces wear debris: metal and polymer particles. Debris can contribute to wear, when it remains trapped between the articulating surfaces, it is called *third body wear*, or to immunologic response by the host body if diffusing into the surrounding tissue. Wear rate is very variable from one case to another: in the present case, the surgeon did not have to replace the cup after 27 years, which is quite exceptional! In other cases, it can go wrong after a few months. It is evident that wear also promotes corrosion.

Although the evidence is not conclusive, the failure is most probably explained by a combination of fatigue and corrosion. All questions raised in the preceding paragraphs will be discussed systematically in the following sections and chapters.

2.2 Strength and Response to Load

Resistance, which we experience when trying to lengthen a metal or polymer rod by a tensile force or to deform it by torsion or bending, is the translation at the macroscopic length scale of interatomic and/or intermolecular forces and kind and degree of ordering at this atomic length scale. However, speaking in terms of *materials' properties*, interatomic forces are only experienced in a direct way when measuring the tensile strength of a simple linear chain of atoms or, in the limit, of a perfect crystal. In this very hypothetical case, it would be found that the maximum force between atoms is reached at separation of their centers by $1.25r_0$, r_0 representing the atomic radius. These forces are responsible for the elasticity modulus (Table 2.2). Bond rupture takes place for a tensile force exceeding the bond force. Knowing the real interatomic potentials, the ideal(?) strength of a material should be predictable from first principles. Unfortunately, real life is more complicated: the result would be grossly overestimated. Therefore, let us examine real crystals. Crystalline materials are important because metals dealt with in this chapter are all polycrystalline.[4] Molecular materials will be dealt with when discussing polymers.

By definition a perfect crystal is one in which *the atoms are arranged in a pattern that repeats itself periodically in a self-similar infinite way in three dimensions.* In real life, crystals are never infinite and even those consisting of one atomic species, deviate from perfect periodicity.[5] Imperfections in crystals can be classified

[4] In a later chapter amorphous materials (glasses) will be dealt with. For the time being we are not aware of any bioapplication of monocrystalline materials, except indirectly silicon as a substrate for bioelectronic devices.

[5] The term *perfect crystal* is to some extent a misnomer because it refers only to geometric perfection. In Chap. 1, the structure of trees is so well adapted to fulfill its function that it can be

Table 2.2 Range of E-moduli per bond type [36, p. 60]

Bond type	Example	E(GPa)
Covalent	–C–C–	200–1,000
Metallic	Fe–Fe	60–300
Ionic	Li–Cl	32–96
Hydrogen bond	H_2O–H–OH	8–12
Van der Waals	Between polymer chains	2–4

as: point, line ($1D$) or surface ($2D$) defects.[6] They have fundamental implications for the mechanical behavior of a metal. Some properties of single crystals are highly anisotropic but a polycrystalline sample, consisting of many randomly organized grains, will exhibit isotropic properties. When, however, those microcrystals exhibit some preferred orientation, the properties will become anisotropic and such a microstructure is called *texture*. Texture can be the result of production processes as solidification, annealing by thermal treatment or deformation by, for example, drawing. It is a kind of structure or ordering at a higher length scale than the atomic length scale, which dominates crystal structure.

For a theoretical treatment of structure the book by Allen and Thomas can be recommended [38], for thermomechanical treatment a new comprehensive book on the subject by Verlinden [53].

Both defects in crystals and texture are responsible for the particular properties of metal alloys and for all other materials as well. Let us return to the stress–strain curve shown in Chap. 1. In its *engineering form*, it is slightly different and mostly the stress passes through a maximum before fracture. While in Fig. 1.6, the applied force was divided at each point by the effective section of the specimen, i.e., the *true stress*, the applied force is in the engineering convention only divided by the initial section of the specimen, the so-called *nominal stress*, $\sigma_n = \frac{F}{A_0}$ plotted against the nominal strain $\epsilon_n = \Delta l$. No permanent strain remains after applying stresses within the elastic region: that means that the material follows simply Hooke's law for the ideal spring: $\sigma = E\epsilon_n$. The upper boundary of the elastic region is called the *elastic limit*. The 0.2% proof stress is commonly used as yield strength (YS) for materials yielding gradually (without distinct yield point). Any stress exceeding this value induces permanent strain. Deformation beyond the maximum of the (engineering) curve leads to fracture at the ultimate tensile strength (*UTS*). The strain after fracture ϵ_f is calculated by the sum of the lengths of the broken pieces minus l_0 divided by l_0. These parameters are characterizing strength, are extensively tabulated and are experimentally measured by tensile/compression testing machines, standard equipment in all engineering laboratories.

called perfect, although without any geometrically definable structure. When glasses are discussed in later chapters, we will come back on this issue; perfection in the geometric sense is not meeting real-life requirements. This statement can be quoted as one of the *benefits of chaos*.

[6] *Defect* has a pejorative meaning and therefore substituted by some authors by imperfection; see former footnote.

Table 2.3 Concentration ranges for the main and minor (but important) elements of the three generic classes of medically used alloys. The balance element for stainless steel is always Fe, for cobalt-chrome: Co and for titanium: Ti

			Stainless steels[a]			
	Cr	Ni	Mo	C		
420	13		0.2			
304	17–20	8–11		0.08		
316L[b]	17–20	11–14	2–3	<0.03		
			Cobalt-chrome[c]			
	Cr	Ni	Mo	W	C	
F75, F799	27–30	<2.5	5–7		<0.35	
F90	19–21	9–11		14–16	<0.15	
F562	19–21	33–37	9–11			
			Titanium[d]			
	Al	V	Nb	Zr	Ta	O
α						
CP(4)						0.40
β						
Ti-13-13			12–13	12–13		
Ti30Ta					31.4–32.3	
Ti30Nb			29.4			
$\alpha + \beta$						
Ti-6-4	5.5–6.5	3.5–4.5				<0.13
Ti-6-7	5.5–6.5		6.5–7.5		<0.50	<0.20

[a] Minor elements: Mn, Si, P, S
[b] 316L is the only one used for endoprosthetic purposes
[c] Minor elements: Mn, Si, Fe, P, S, Ti
[d] Minor elements: C, Fe, N. $H \leq 0.01\%$

The prosthesis shown in Fig. 2.4 was made of Fe-Cr-Ni steel of type 304. The calculated strength of the said prosthesis stem proved that its strength had to be sufficient but practice proved that it was not! The use of type 316L would have been a better choice and in the 1970s better performing alloys made their entrance. In Table 2.3 are collected the main constituting elements of the three generic classes of alloys used for implants, stainless steel, cobalt-chrome and titanium alloys, and in Tables 2.4 and 2.6 typical values for their mechanical properties. The properties of the most important surgical alloys were collected.

2.2.1 Stainless Steel

Many of the constituting elements of stainless steel (SS) and the following two generic classes of alloys are apt to be corroded. In powder form, iron, aluminum or titanium can burn explosively: the reducing agent in the boosters of the Space

Shuttle is iron powder; in bulk or after alloying high resistance to corrosion can develop. The main elements in stainless steel are iron (balance), chromium, ∼18%, and nickel, ∼10%. Chromium forms, simply by contact with air, an adherent layer of chromium oxide Cr_2O_3 on the surface, protecting the bulk against access of deleterious reactants as acids, chlorides or sulfur compounds. Superior protection can be obtained by conditioned oxidation, for example with nitric acid, a treatment for which standardized procedures exist. The condition for a decent oxide layer is that the carbon content of the steel should be lower than 0.03%, designated by adding L to 316L. Higher carbon concentrations tend to form carbides such as the common $Cr_{23}C_6$, which precipitates at the grain boundaries. It forms at the expense of chromium near the grain boundary, which in turn limits the availability of chromium for the formation of the oxide layer. Such a steel is called *sensitized* and these sites acts as onsets for cracks and finally fracture (corrosion fatigue). More on the basics of corrosion processes in the next chapter.

The structure of an alloy, of any material after all, is the end-result of a hierarchy of structures at different length scales. Its skin endowed the SS 316L with a peculiar property making it suitable for applications in a 'hostile' environment. The century-long path toward reliable implant materials proved that the body is indeed an environment extremely hostile to materials. Much effort in biomaterials research has been invested in 'compatibilizing' bulk and tissue through manipulation of the 'skin' of the material, the bridge between bulk and tissue, but the feasibility for doing so is born at the very early stages in the hierarchical level.

Composition and crystallography: Both these facets represent the bottom of the hierarchical column, the *nanoscale*. The iron-chromium system is the basis of a wide range of stainless steels. But before returning to our familiar 316L, a few words about other species like 420 (see Tables 2.3 and 2.4). For concentrations ≥13%, the steel becomes corrosion resistant because, from that concentration on, a compact film of Cr_2O_3 will form. Its structure is body-centered cubic.[7] If carbon is added, say to something like 0.1–0.5%, the phase diagram Fe–Cr is thoroughly changed and these steels can be quenched to give martensite, and the latter can be tempered to give a fine dispersion of carbides.[8] These steels are not used for implants but serve

[7] Hard spheres tend to pack into structures either face-centered cubic (f.c.c.), body-centered cubic (b.c.c.) or hexagonal close-packed (h.c.p.). The highest packing density is given by f.c.c. and h.c.p. with 74% of the volume taken up by the spheres, while only 68% for a b.c.c. packing. In a first approximation, we may exchange the spheres by metal atoms. Important? The f.c.c. structure of stainless steel is, for example responsible for its ductility and a toughness by far superior to ordinary carbon steel. Dislocations move most easily on slip planes, occurring in particular on crystal planes with higher spacing and with large densities of atoms per unit area as is the case in f.c.c. crystals. For further reading on this subject, the book of Allen and Thomas is advised [38]. In Appendix B a 3D view of a dislocation is given.

[8] Quenching: rapid cooling from high to room temperature by immersion in water or oil. It is undertaken to 'freeze' mechanical properties associated with crystalline phases otherwise lost by slow cooling. Tempering: subtle heat treatment for alloys, provoking complex structural changes, to adapt strength, ductility or brittleness to specific needs. It is one of the oldest heat treatments applied to steel. The mechanism is only recently well understood.

for medical instruments such as pincettes, forceps, suture hooks, curettes, drills, or with carbon content up to 0.5%, for scissors and scalpels.

316L should be a single-phase *austenitic* steel, and the conditions to cast and to cool the alloy are read from *phase diagrams* displaying the relationship between temperature, crystallographic phase and composition; a fourth parameter is time for castings, what means relatively larger volumes and consequently dominated by large temperature gradients, almost the rule and not the exception. Concentration ranges of the main alloys are summarized in Table 2.3. An austenitic crystallographic structure is the stacking of the composing elements into a face-centered cubic (f.c.c.) crystal. Chromium and the minor elements molybdenum and silicon, however, tends to 'freeze' the weaker ferritic phase which has body-centered cubic symmetry (b.c.c.). This effect can be countered by the addition of nickel, which freezes austenite. The presence of chromium, nickel and manganese slows down the diffusive transition of f.c.c. to b.c.c. with orders of magnitude. The effect is that SS 316 and the like can be cooled from 800°C down to room temperature without transforming to b.c.c., of utmost importance when heat treatments are needed for finishing a piece of work (welding, coating, annealing). Inclusions (lowering strength) or impurities such as sulfides (MnS, causing pitting corrosion) should be absent. We will encounter again austenite and another member of the crystallographic families *martensite*, when talking about shape memory alloys. Strong mechanical deformation favors the formation of the ferritic phase, which makes SS magnetic while austenite is nonmagnetic. A 3D representation of the crystallographic structures is given in Appendix B.

Grains, texture, strength and the mesoscale: The casting is not one big single austenitic crystal but an aggregate of small polyhedral crystals called grains. The adjacent grains display different crystallographic orientation and are separated by *grain boundaries*. The size should be uniform and according to the specification of ASTM 100 μm or less.[9]

Grain size is not a matter of beauty but is intimately linked with strength: higher yield strengths can be achieved by finer grains, all other things being equal. An inverse relationship exists between yield stress (σ_y) and grain size d, the so-called Hall–Petch equation:

$$\sigma_y = \sigma_0 + \frac{k}{\sqrt{d}} \tag{2.2}$$

where σ_0 and k are constants and d the grain size; k is the *strengthening coefficient*, unique to each material. That means for mild steel that the yield stress rises from 100 to 500 MPa when d is decreasing from 0.25 mm to 2.5 μm. The underpinning theory of this equation handles the propagation of dislocations, which is impeded by grain boundaries.[10] Equation (2.2) is the quasi embryonal form of the

[9] ASTM: American Society for Testing and Materials.

[10] Silicon can be crystallized as an almost perfect monocrystal, the exception in the material world. Those imperfections localized along a space curve passing through a crystal are called *line imperfections* or *dislocations* (for an in-depth treatment of this important issue [38].)

relationship between *YS* and d, a more detailed treatment being far beyond the scope of this book. Another complication is the size d, determined from the number of grains per mm^2 visible at a magnification of 1X (ASTM standards E 112, E 1382 or others). The procedures have been developed for rating the grain size of equiaxial structures with a normal distribution. Mostly, however, multimodal distributions will be the case. The law breaks down at grain sizes of $\sim$10 nm (only possible in thin foils), if not, a metal could be made infinitely strong! Grain refinement is mainly a manufacturing dependent phenomenon.

Other strengthening processes are solid-solution hardening precipitation hardening, cold deformation like forging or rolling and texturing (for further reading, we refer to [35,36,54]). The effect of forging or rolling on YS, UTS and fatigue strength is clearly demonstrated for stainless steel in Table 2.4: cold forging multiplies YS by a factor of about three!

By directional deformation of the metal, for example by drawing into wire or bar, the grains become elongated and the alloy is no longer isotropic and the alloy develops a texture. A good example is shown in the section on titanium alloys below where equiaxial and textured grain structures are displayed. In the table displaying the mechanical properties of titanium alloys, the effect of anisotropy is documented for extruded Ti6Al4V: parallel with the extrusion direction $YS_{\parallel} = 871$ MPa and perpendicular to it $YS_{\perp} = 934$ MPa (see Table 2.6).

All this illustrates the *micro- to mesoscale*: a few μm to a mm.

Forging and rolling, cold or warm, are used not only for mastering the mechanical properties but also dominates the *macroscale* when giving the metal its final or semifinal shape. Hip implants in 316L used to be produced by casting or forging and screws are shaped from drawn bars. Steel, however, has been widely substituted in implants by alloys of cobalt or titanium. Zirconium seems to be a productive newcomer and more about it in Chap. 5, where also the merits of other candidate metals as Ta will be evaluated.

2.2.2 Cobalt–Chrome alloys

Castable cobalt–chrome alloys have been in use since the late 1920s for oral implants and since the 1970s for orthopedic purposes (knee, hip, screws, osteosynthesis plates). The main element is cobalt which is responsible for the f.c.c. matrix, the other components being chromium, molybdenum, and nickel or tungsten and in particular carbon. High strength, high wear, fatigue and corrosion resistance are the superior characteristics of these alloys. In Table 2.3, the composition of representative members of the family are given, mechanical characteristics are summarized in Table 2.4. A synoptic table in an appendix is devoted to the jumble of trade names and designations.

Different ‘brands’ are commercially available. F75 is the godfather of the family. It is shaped by conventional casting techniques. The high chromium content, 50% more than 316L, imparts its high corrosion resistance. The high carbon content

Table 2.4 Stainless steel and Cobalt-chrome alloys: typical values of mechanical properties. Fatigue strength is expressed as the stress below which the material will not fail at specified conditions for R and number of cycles

Alloy	Condition[a]	Design. ASTM	E GPa	YS MPa	UTS MPa	Fatigue[b] MPa
420	an.				> 720	
	h+t			1,420	>1,720	
304	an		193	205	515	250
316L	an	F138	200	330	590	250
316L	cw	F138	190	790	930	390
	CF	F138	190	1,210	1,350	820
Co29Cr5Mo	c+an	F75	210	480	770	260
Co29Cr5Mo	hf	F799	210	1,050	1,500	750
Co20Cr15W10Ni	cw 44%	F90	230	1,600	1,940	590
Co20Cr35Ni10Mo	cw+a	F562	230	1,500	1,800	740

[a] Condition: *a*:aged; *f*:forged; *an*:annealed; *ca*:as cast; *cw*:cold worked; *CF*:cold forged; *h+t*:hardened+tempered

[b] At 10^7 cycles with $R = -1$. R is the ratio of min.stress to max.stress

gives rise to the formation of carbides with Co, Cr or Mo ($M_{23}C_6$) and these carbides enhance the wear resistance. The intrinsic limitations of this cast alloy were the millimeter-sized grains and the development of Cr, Mo and C rich domains (with carbides) and dendrites depleted in Cr and rich in Co. The large grain size is unfavorable for its fatigue characteristics while the domains of different composition are unfavorable for its corrosion resistance (galvanic differences between the segregated domains; see next chapter). Figure 2.6a is a metallographic section through an orthopedic screw: oddly shaped large grains and carbides along the grain boundaries are the main feature, the latter also shown into more detail in Fig. 2.6b. The finer grains at the surface of the material are already produced during solidification. Because of a higher cooling rate at the surface as compared to the inner part and because of imperfections at the mould walls, more nuclei are formed producing finer grain size (screw of unknown manufacturer).

Another metallographic feature is the smaller grains at the surface, a result of thermal treatment after machining and probably performed to improve the torque strength.

An alternative alloy is F799. It has about the same composition but is forged. It lifts important shortcomings of F75: smaller grain size and fine more homogeneously distributed carbide precipitates. Superior fatigue and wear resistance compared to F75 made it for many years the alloy of preference for hip prostheses.

Another respected member of the family is a CoNiCrMo alloy, called originally MP35N. High corrosion resistance, UTS and fatigue strength and excellent abrasive wear properties are the strong points and made it a suitable candidate for hip stems

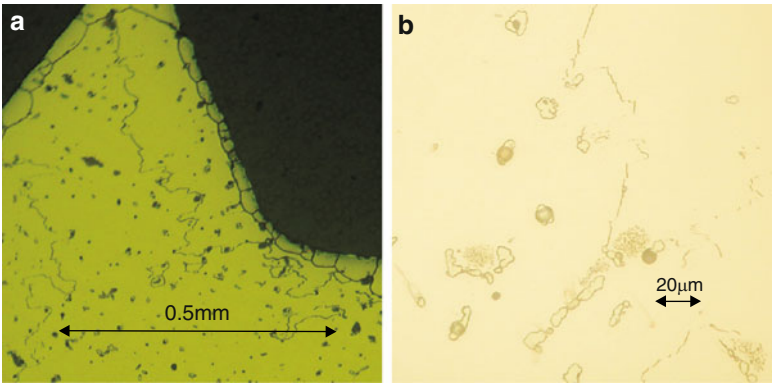

Fig. 2.6 Metallographic section of an orthopedic screw (CoCrMo). (**a**) large grain size in the bulk, smaller ones at the surface. (**b**) carbide precipitates in the grains and at the grain boundaries. Photo by P. Crabbé

but not recommended for joint surfaces. It exhibits poor frictional properties with itself and other materials.

Machined, cast or wrought, the production conditions already pointed to deeply influence the quality of the final product, convincingly demonstrated by a quick look at the Table 2.4: the YS of F75 annealed is 480 MPa, for forged it increases to 1,050 MPa. We discussed thus far stainless steels and CoCr alloys merely to show how experience forced specialists to explore the introduction of new materials. Only members prominent with respect to properties or to historical 'eminence' are listed. The story, however, does not end with these two generic alloy families because perfection was not their fate and throughout the book, the reader will experience that pursuit of perfection is a never-ending story.

The next leap in the story was the introduction of titanium alloys.

2.2.3 Titanium Alloys

We already mentioned that fine titanium powder may oxidize or corrode quite spectacularly, but bulk titanium is fortunately more manageable. The oxide formed at very high speed at the surface has the attractive property of being an unassailable obstacle for aggressors and the oxidation stops after formation of a dense but only submicron thick oxide layer: 8–10 nm for alloyed titanium and 3–4 nm for pure titanium. The oxide layer can be thickened by simple annealing in the temperature range of 350–550°C or by electrochemical techniques [55]. A pretty 'collateral' effect is that these layers give rise to interference colors and are used to give an identifiable color to a given prosthesis or… have been used for artistic purposes.

Table 2.5 Colors of oxide layers on titanium as a function of thickness

d (nm)	Color	d (nm)	Color
10–25	Golden	80–120	Yellow
25–40	Purple	120–150	Orange
40–50	Deep blue	150–180	Purple
50–80	Light blue	180–120	Green

Techniques and theoretical background of this art are exposed with Italian charm by Pietro Pedeferri [56–58]. For the color palette offered by the various thicknesses, see Table 2.5 (taken from Velten et al. [59]).

Titanium alloys are relatively young members of the metal alloy family and not produced in quantity until the late 1940s. Their high melting point (1,678°C), low density and excellent mechanical properties, in particular at high temperature, made them uniquely attractive to the aerospace industry. These properties together with a high resistance to corrosion did not escape the attention of the biomedical world. Moreover, and in this case much like steel, many titanium alloys undergo allotropic transformations, usually between the high-temperature b.c.c. (β) and low-temperature hexagonal (α) phases, so that a wide variety of microstructures and properties can be developed by heat treatments and thermomechanical processing (further reading in Verlinden et al. [53]). Titanium alloys and implants proved to be a happy and, thus far, a stable marriage. The use of stainless steels and cobalt–chromium alloys in implant business in the foregoing sections was based on rather restrained knowledge of the behavior in the biological environment and focused merely on purely mechanical criteria. With so vast a body of materials properties documented now, a selection of a material for a specific use can be made on more solid grounds.

In Fig. 2.7 specific yield strength, YS divided by ρ, and equivalent weight are plotted for a set of common alloys. The equivalent weight was calculated for a bar with square section as represented in Fig. 2.2: constant load of 4,000 N, beam length $l = 100$ mm, thickness t calculated by (2.1) needed to limit the deflection δ to 1 mm. The equivalent weight for Zr 705 is about equal to that of Ti CP4 and Mg CP. Zr and Mg alloys are discussed in later chapters.

Inspection of the figure learns that tantalum is not a good partner (very high density, $\rho = 16.55$, and low YS): a tantalum hip stem would be a cumbersome block. After all a pity because it has a superior corrosion resistance. The other extreme is beryllium: low density, high YS but completely shunted off by its toxicity. Nontoxicity as will be discussed later is an absolute *conditio sine qua non* in implants! For this reason, aluminum alloys such as Alu6063 (about similar to F75) are rejected because of their toxicity, moreover they suffer from various diseases: toxic, mechanically not that excellent and a corrosion behavior biologically below the limit. The others are quite acceptable but Ti4Al6V, or Ti6Al7Nb as preferred today is the best choice, mechanically speaking (similar mechanical properties but vanadium is toxic while niobium is not). A wrought Ti6Al7Nb ($\alpha+\beta$) alloy T67 was developed in the early 1980s [60]. We narrowed the selection by including corrosion

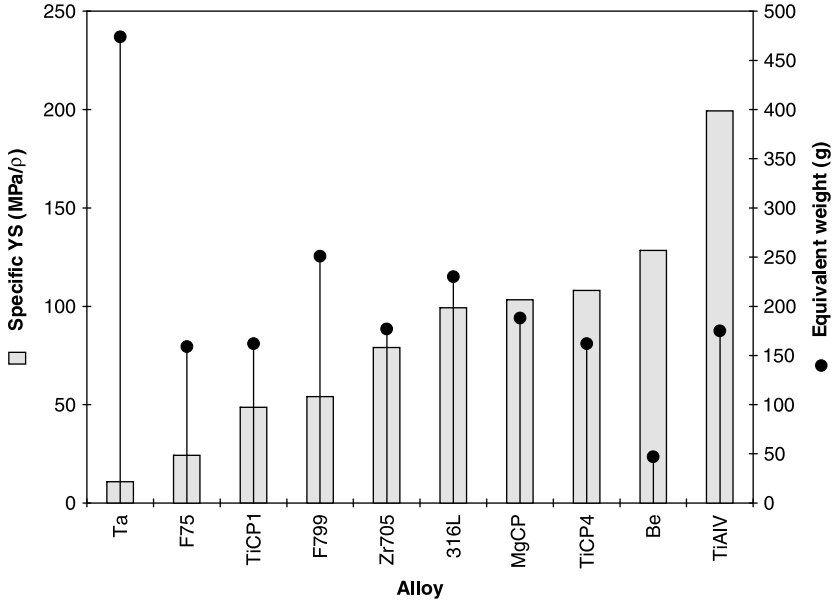

Fig. 2.7 Specific yield strength (MPa/ρ) (*bars*) and equivalent weight (g) (*black dots*) for a series of alloys. The values were calculated for: Ta (Cabot,R05200), CoCr F75 (cast+annealed), Ti-CP1, CoCr F799 (hot forged), Zr 705 (cold worked+annealed, ASTM min.val.), SS 316L (30% cold worked), Mg-CP, Ti-CP4 (30% cold worked), Be, Ti4Al6V F136 (forged+annealed)

and toxicity as criteria, another illustration that selection is a multidimensional process, the graph above was only 1-dimensional.

The foregoing paragraph was an example of an exercise in materials selection. Ashby and Waterman introduced some years ago selection aids in the form of *Materials Properties Charts*. If you want to select a material with a specific combination of fracture toughness and modulus or any other combination, consult the appropriate Property Chart [61, 62].

Microstructure, Composition and Properties

The common differentiation of titanium alloys is according to their microstructures: single-phase α-alloys, near α-alloys, Ti6Al2Sn4Zr2MoO,1Si for example, $(\alpha + \beta)$-alloys, metastable- or near-β-alloys such as Ti13Nb13Zr and Ti30Nb. Pure β-alloys such as Ti35V15Cr or Ti40Mo are of minor interest. When the melt cools down, it is not immediately evident to find at room temperature a solid in one of these three forms. The two extremes, α and β, need their own stimuli: α-stabilizers are Al, B, C, O, N; β-stabilizers are Mo, V, Nb. Zr is in this respect a neutral element. As life is never simple, a number of intermediate forms and mixtures exist. We skip a discussion of phase diagrams because it would lead us inexorably to a lengthy separate

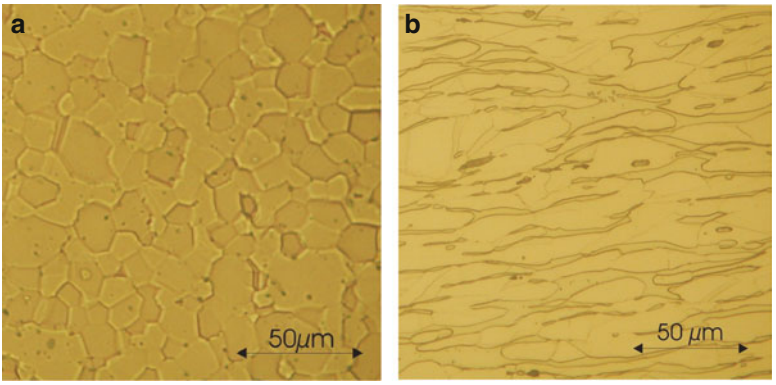

Fig. 2.8 Metallographic section through titanium (F67) (**a**) with nearly equiaxial grains; (**b**) section through a Ti6Al4V wire parallel to the wire axis: the grains are elongated by uniaxial deformation. Photo by P. Crabbé

chapter! A general overview of composition is given in the synoptic Table 2.3 and properties in Table 2.6.

α-alloys: The microstructure is single-phase h.c.p. The attribute 'single-phase' makes it on the one hand easily weldable, because the heating during welding does not change the microstructure, on the other hand it cannot be heat-treated for strengthening. Nearly equiaxial grains is the main feature of the crystallographic section of CP titanium of Fig. 2.8a. The only commonly used alloys are several grades of commercially pure titanium (CP titanium), which are in effect Ti-O alloys. We encounter here oxygen as an explicit alloying element with drastic effect on the properties. Here and there some oxide will be found in the matrix but talking of oxygen as alloying element means that oxygen is present as interstitial element in the crystal lattice with consequences for its properties. Ti CP grade1 for example with 0.18% oxygen has a YS of 221 MPa, while CP grade4 with 0.4% has a YS 559 MPa. The properties are relatively insensitive to grain size. Oxygen is one factor, texture another as shown in Fig. 2.8b. Texture has so its own impact on properties as demonstrated in Fig. 2.9: fatigue properties will be superior in a direction perpendicular to the main orientation of the grains as shown.

β-alloys: The crystallographic structure is b.c.c. The addition of the elements Mo, V, Fe, Mn, Cr or Nb stabilizes the β-phase below the transformation temperature to the h.c.p. phase. Experience in hip implants learns that a modulus too much different from the one of bone should be responsible for stress shielding, a phenomenon we will deal with in Chap. 11. The opportunity offered by β-alloys is the combination of low modulus, closer to bone, with high strength, similar fatigue and good fracture behavior, improved wear resistance, low sensitivity to corrosion, as a matter of fact a favorable mix of mechanical, biological properties and, say, biocompatibility. Numerous slip systems favor dislocation mobility which results in excellent formability. It is evident that this combination opens the possibility to realize a hip stem quasi-isoelastic with bone. A comprehensive set of data was published by Mishra

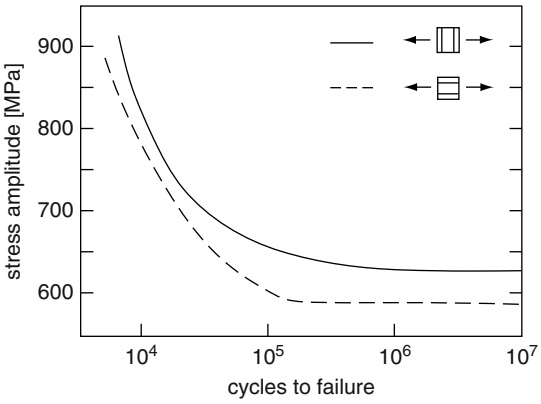

Fig. 2.9 Effect of texture on fatigue strength. Shown are two curves for fatigue strength versus cycles to failure for a direction parallel and perpendicular to deformation. The curves were determined for Ti6Al4V in an aqueous solution of NaCl 0.06 M. Reproduced with permission of ASM [63], Figs. 17–30

Table 2.6 Titanium alloys: mechanical properties, typical (mid range) values

	E	YS	UTS	Fatigue[a]	Fracture[b]
	GPa	MPa	MPa	MPa	MPa$\sqrt{m}$
Ti CP grade1	103	221	345	270[a]	
Ti CP grade2	103	352	483	330[a]	66[a]
Ti CP grade3	103	462	593	350[a]	58[a]
Ti CP grade4 (sheet)	104	640	390	376	54[a]
Ti13Nb13Zr[c] WQ+aged	81	864	994	500	65
Ti13Nb13Zr WQ+DH	83	906	1034	425	
Ti13Nb13Zr WQ+CW	48	599	798		
Ti30Nb	45	500	700[c]		
Ti6Al4V[a] annealed	113	923	992	500	70
Ti6Al4V extruded $\parallel$		871	976		
Ti6Al4V extruded $\perp$		934	1015		

[a] $K_t = 1.0$ MPa (ASTM 466)
[b] Fracture toughness K_{1c} (ASTM E399)
[c] Materials Properties Handbook Titanium Alloys [66]; Mishra et al. [64]; Helsen and Breme [35]

and Colleagues [64] and a few are reproduced in Table 2.6. What more are we looking for? In as far as we are aware, the β Ti-Mo alloy for orthodontic archwires is the main biomedical application.

$(\alpha+\beta)$-alloys: The purpose of the alloying elements is to stabilize both α- and β-phases (Al and V or Nb or Ta, respectively). Ti-6Al-4V was the candidate of choice at least, if high YS and low weight were the soul saving criteria.

Figure 2.10 is a metallographic section of a wire of Ti6Al4V: the light-grey color points to the β-, the darker to the α-phase (the latter rich in Al and depleted in V and *vice versa* for the β-phase) [65]. This is only one example of microstructure because a different thermal and mechanical processing history changes drastically the structure and also the properties. A fine grained structure is a result of a heat

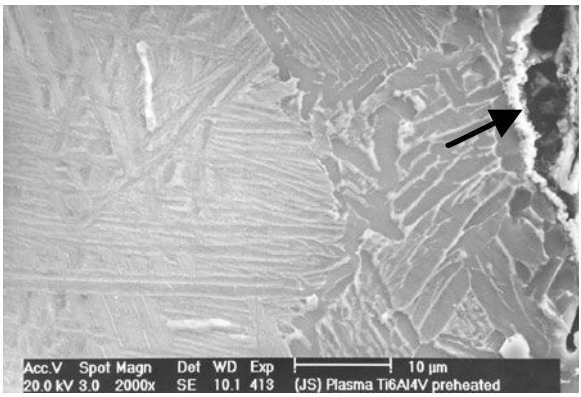

Fig. 2.10 Metallographic section through a Ti6Al4V wire: the light-grey zone is the α-, the darker the β-phase. In the *upper right corner*, a surface layer of bioactive glass is visible

treatment, hot working and annealing. In Table 2.6, typical values for a selection of alloys are collected. To simplify the table, mid-range values of published data are given only. The range can be quite broad and depends on slight changes in composition and thermal history.

2.3 Skeletal Tissue

Thus far we were watching the fate of 'heavy duty' substitutes for bone. Right time to turn our attention to bone itself, not for the pleasure of learning a petty fact more. Understanding how complex a material is, that an implant has to substitute, is vital to design better-performing implants.

Mechanical properties of polycrystalline alloys, and glassy inorganic and organic materials are preponderately isotropic, unless anisotropy was intentionally induced. Composites consist of two or more phases with the intention to generate properties the individual phases do not and cannot have. A carbon fibers filled epoxy resin is substantially different from the pure epoxy with isotropic mechanical properties. When in the composite the fibers are nicely aligned, the bending strength perpendicular to the fiber orientation will be an order or orders of magnitude higher than that of the epoxy matrix. On the contrary, loading parallel to the alignment of the fibers the strength might even be lower than the resin itself: an extreme example of anisotropy.

Bone is a composite but complex and of 'intelligent design': complex because it has much more than two phases, 'intelligent' because it is produced *in situ* in the body with the properties the body imposes at that particular spot, the right stuff at the right place! Skeletal tissues, bone and cartilage, form a class of structural

connective tissues, consisting of cells embedded in a matrix permeated by a system of fibers.

2.3.1 Cartilage

During early fetal life the human skeleton is mostly cartilaginous. Subsequently, it is largely replaced by bone but persists in, for example, synovial joints. It is essentially a type of stiff, load-bearing connective tissue. Its distinctive properties are: a low metabolic rate and a vascular supply confined to its surface or to large, percolating tunnels, a capacity for continued and often rapid interstitial and appositional growth, high resistance to tension, compression and shearing. Articular cartilage, typical *hyaline cartilage*, has neither nerves nor blood vessels. Cartilage is covered by a fibrous *perichondrium* except at the osseous junction; the synovial surfaces are lubricated by the *synovial fluid*, carrying nutrients, secreted at the osseous junction, and from the synovial membrane. The lubrication is absolutely fabulous: the *friction coefficient* of cartilage to cartilage can be as small as 0.002, and moreover, is decreasing as loading increases!

Let us make here a parenthesis on viscosity.

Newtonian Fluids

Consider a thin layer of fluid between two parallel planes a distance dy apart as in Fig. 2.11.

One plate is fixed and a shearing force F is applied to the other. For steady conditions, F will be balanced by an internal force in the fluid due to its *viscosity*. For a laminar flow and a so-called Newtonian fluid, the stress is linearly proportional to the velocity gradient dv/dy and the proportionality constant is the Newtonian viscosity, independent of shear rate and only dependent on temperature and pressure. Water is an example of a Newtonian fluid. More complex fluids with long molecules or dispersions exhibit a complex viscous behavior. Three other generic classes of viscous behavior of fluids will be distinguished (see Fig. 2.12).

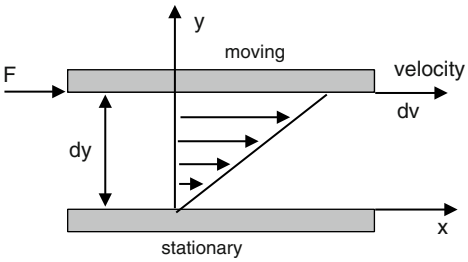

Fig. 2.11 Newtonian fluid between parallel planes

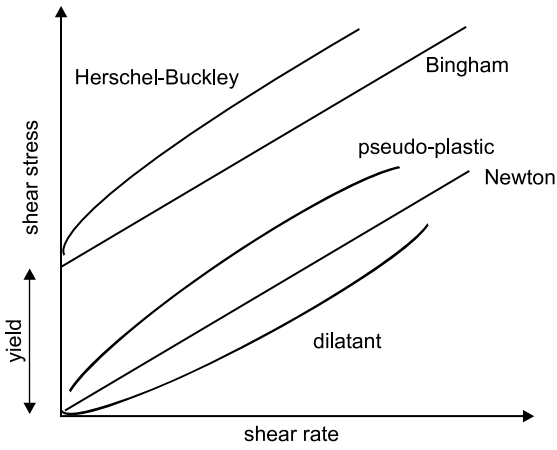

Fig. 2.12 Generalized flow behavior of fluids

Time-Independent Non-Newtonian Fluids

Here too, two subdivisions have to be made:

Bingham: differs only from Newtonian fluids by the *yield stress* i.e., the stress to be exceeded before flow starts. Many common fluids approximate this type. A fluid at rest contains a 3D structure which is sufficiently rigid to resist any stress less than the yield stress (example: oil paints).

Pseudoplasticity: no yield value but the shear stress decreases progressively with shear rate. The molecules of a pseudo-plastic fluid align after starting shear so quickly that the time effect cannot be detected.

Dilatancy: similar to pseudoplasticity, showing no yield stress but the apparent viscosity increases with increasing shear rate. It is observed for highly concentrated suspensions. At rest the voids between the agglomerated particles is at a minimum and the liquid sufficient to fill the voids. When sheared, the agglomerates are broken up and the material 'dilates' because the liquid phase is not sufficient to fill up the voids.

Time-Dependent Non-Newtonian Fluids

For these fluids, the relation shear stress/shear rate depends not only on shear rate but also on the duration of shear. The behavior cannot be described by simple rheological equations. Two classes are distinguished:

thixotropic fluids for which shear stress or apparent viscosity is decreasing with shear duration;

rheopectic fluids for which shear stress is increasing with shear duration.

Many colloidal suspensions are thixotropic and exhibit structural hysteresis [67, 68].

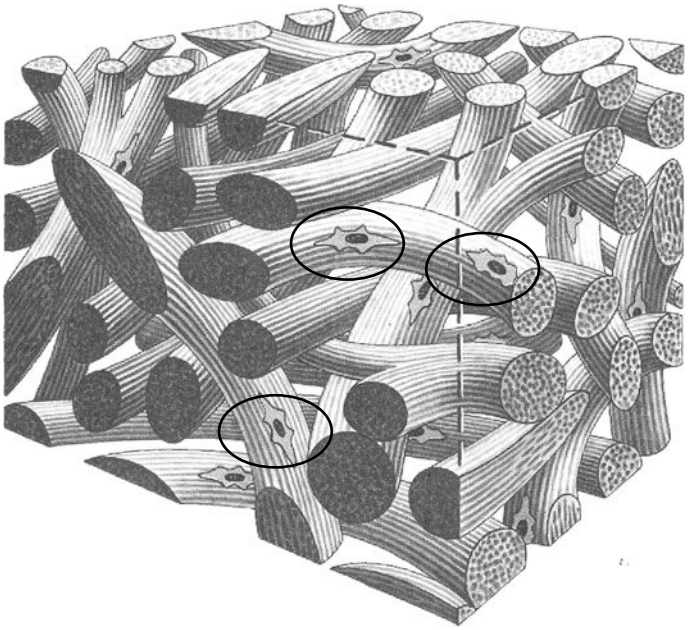

Fig. 2.13 Arrangement of dense but irregularly packed collagen fibers in joint cartilage, sparsely seeded with fibroblasts (*encircled*) responsible for auto-repair. On the contrary, in ligaments or tendons the fibers are highly organized. Reproduced from Gray's Anatomy [52], Fig. 1.77. Copyright Elsevier, 2010

Viscoelastic Fluids

The fourth class are the *viscoelastic* fluids which exhibit partly Newtonian behavior for the viscous component and partly elastic (Hookean) behavior.

In Chap. 11, we will have to come back on this issue when discussing polymers. The purpose of this parenthesis was to make a link between what was said about synovial fluids to the physics and flowing fluid *rheology*. In the human body, almost nothing flows in a Newtonian way: complex viscosity is of basic biological interest.

According to the definition in anatomy, the matrix consists of cells, chondrocytes and chondroblasts, and a complex watery gel with high content of carbohydrates. Collagen fibers mainly of type II are imbedded in the matrix. Figure 2.13 is an example of irregularly stapled collagen as present in joint cartilage. They represent about 50% of its dry weight. The fibers form a 3D network which is interlinked with proteoglycans, long chain carbohydrates bearing sulfate and carboxyl groups and covalently linked to a core protein and, subsequently assembled into filamentous aggregates. For obvious reasons, glucosamine sulfates are popular pharmaceutical products, promising to reduce cartilage wear and regeneration. Is it hype or a miracle drug?

Table 2.7 Dynamic friction coefficients

Materials couple	Lubricant	μ_d
CoCr/CoCr	Dry	0.55
CoCr/UHMWPE	Serum	0.08
Cartilage/cartilage	Synovial fluid	0.002

The synthesis of the building blocks up to procollagen happens intracellularly in the chondrocytes. They secrete procollagen into the extracellular space where the final assembly into collagen fibers takes place.

The growth of cartilage is both interstitial, i.e., from within the cartilage, and appositional, i.e., at the chondrogenic layer of the perichondrium. The interstitial growth must persist for long periods in epiphyseal bone. Regeneration of lost cartilage is known to be poor. It exhibits, however, a low *antigenicity*, what means that defects are prone to be repaired by *homotransplantation* without pronounced immune reaction. We come back on this issue later.

Outside the joint surfaces in general, cartilage survives in: ribs, nasal septum and vertebrae (mainly hyaline), ear, epiglottis, cornea (mainly elastic fibrocartilage) and intervertebral discs (mainly dense fibrocartilage), all with the site-specific composition. The composition is quoted as 'mainly' because there is always a whole set of substances involved. In the larynx and the ear, elastic fibrocartilage plays an important role in sound production (larynx) and detection (ear). Did we not say 'the right stuff on . . .'!

Friction: The low friction coefficient of cartilage in joints was highlighted above. A restraining force is encountered when one is attempting to move one body over another. The frictional force F_f is given by

$$F_f = \mu F_\perp,$$

where $F_\perp$ is the force perpendicular to the interface and μ is a dimensionless number between 0 and 1 (μ is also the symbol for viscosity). In Table 2.7, the dynamic value of μ_d is given. The initial value μ_i at the start of the movement is much closer to 1.

A high friction coefficient means always a higher risk for wear but this will be discussed either in relation to corrosion, to polymers or to ceramics. It is the philosophy of rheumatological pain relief by injection of intraarticular injection of hyaluronic acid. This polymer is naturally concentrated in the surface layer of cartilage and provides the synovial fluid its viscoelastic properties. The therapy is apparently not without controversy but speaking in pure rheological terms its use makes sense.

Improve the viscosity of the (lubricating) fluid; reduce pain, swelling and inflammation within the joint; increase the articular cartilage depth on load bearing surfaces.

Bone

Like cartilage, bone is a complex composite. It is highly vascularized and constantly changing. The matrix, i.e., the extracellular phase, consists of water 10–20%,

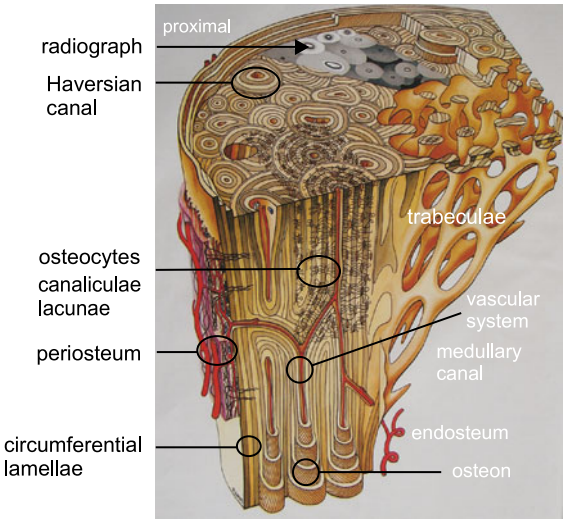

Fig. 2.14 Microstructural features of mature bone: a transverse and longitudinal section. The grey section simulates a microradiograph, the densities reflecting variation in mineralization. Reproduced from Gray's Anatomy [52], Fig. 3.21. Copyright Elsevier, 2010

ordered collagen fibers 30–40% of its dry weight, various inorganic salts as calcium, phosphates 60–70% of its dry weight, and the remaining part various proteins and carbohydrates. The collagen (+glycoproteins) is of type I but strongly cross-linked. Lodged in the gaps between the fibers are the microcrystals of a specific type of calcium phosphate *hydroxyapatite*.

Let us have a look at the internal kitchen of a long mature bone, say, a femur. It is schematically a hollow cylinder, filled with marrow and near the proximal and distal ends gradually filled with trabecular bone. Figure 2.14 is a transverse and longitudinal section through the proximal part just below the neck of the hip joint. The eye-catching feature is its highly organized structure at all scale lengths.

Cortical or compact bone: Circumferential lamellae: consist of a few continuous layers of mineralized matrix and collagen fibers. The greatest part, however, is the Haversian system or *osteons* (for histogenetic reasons called secondary osteons): 6–15 concentric cylinders or lamellae around a neurovascular channel (Haversian canal). As is clearly shown in the picture, the fiber orientation of the adjacent lamellae varies between 0 and 90°. The osteons are 100–400 μm in diameter and the phosphate crystallites 20–40 nm long follow the orientation of the collagen fibers. A cement line consisting mainly of glycoproteins and proteoglycans demarcates the individual osteon sharply from the interosteon space. The maximum diameter of the osteons ensures that the distance of an osteocyte from a blood vessel is no more than 200 μm, a statement that was already made on page 8 when discussing scaling.

Lacunae: Osteoprogenitor cells are stem cells which differentiate into osteoblasts. The activity of the latter is synthesis, deposition and mineralization of the bone matrix. Subsequently, these cells differentiate into *osteocytes*, constituting the preponderate cell type in mature bone. They are lodged in small cavities, lacunae. Numerous dendrites emerge from these lacunae through small tunnels, *canaliculi*, through which nutrients and waste products diffuse. The distal ends of these

dendrites contact those of adjacent osteocytes, thus forming a communicating network throughout bone. The maintenance of bone seems to be their essential function. The nerves penetrate the whole structure.

Medullary canal: It is filled with marrow with different kinds of cells, fat, collagen, and plays the role as biochemical factory but is not a candidate for being substituted by artificial materials.

Trabecular bone: At the proximal and distal ends of long bones, one finds the epiphysis; in between, the long part is called the diaphysis. The epiphysis is filled with trabecular (spongious or cancellous) bone. The orientation is optimally adapted to the stresses in these regions.

Periosteum: For long bones nerves are concentrated near the articular extremities and in a layer enveloping the shaft, the periosteum, and penetrate the bone mass through nutrient vessels and the perivascular spaces of the Haversian canals. It is a fibrovascular layer from where blood vessels enter the medullar canal for centrifugal tissue irrigation as well as direct centripetal irrigation of the peripheral lamellae.

Remodeling: Bone is constantly renovating throughout life and by re-adjustment after fracture. Bone growth is *appositional*: new layers are added to existing surfaces. It is a complex interplay between deposition, removal and an important mechanical component: stress. This was already recognized in 1892 by Wolff, a German surgeon, inspired by the trajectories of the trabeculae in the femoral neck. They follow the stress trajectories and the relation between stress and bone growth is known as *Wolff's law* (J.Wolff, *Das Gesetz der Transformation der Knochen*, A.Hirshwald, Berlin, 1892). The interplay is more complex than described by Wolff. However, the law is till today invoked in explaining at least partially the success or failure of implants such as hip or knee prostheses and the effect of stress-shielding. Although a vast body of research has been devoted in the last decennia to understand the physiological and biochemical implications of arthroplasty, the impact of this research on the development of hard tissue implants remains inferior to mechanical considerations. We come back on this issue in Chap. 11.

The discussion of the peculiar structure of bone was introduced to show how extremely complex implant materials should be before the ideal physiological prosthesis will become a reality.

A stainless steel and a polymer as materials were involved in the case study we started from. Polymers will be the subject of Chap. 11 but a preimpression of polymers was introduced here: collagen. Moreover, the way how it is integrated in connective tissue is an example of the efficiency of nature's composite architecture. The architecture shown in Fig. 2.13 is comparable to a nonwoven tissue but densely packed to do what it has to do. With the same concern, the fibers are in quasiperfect longitudinal alignment in tendons while for ligaments the subsequent layers display different orientations for maximal structural stability. Fibroblasts on the external surfaces take care of self-repair in case of damage.

Collagen: Mammalian collagen is a protein with the amino acid residue -glycine-proline-Y-glycine- (commonly abbreviated as Gly-Pro-Hyp-Gly-) and 100 of the Y positions are 4-hydroxyproline (Hyp). Hydroxyproline is unique to collagen and

by assaying hydroxyproline the collagen content is determined. On polymerization in the intracellular chemical factory, the molecules are twisted into a left-handed helix with 3 residues per turn. Subsequently, three of these helices are wound to a right-handed superhelix to form a rod of 1.4 nm in diameter and about 300 nm long. The three chains are hold together by hydrogen bonding. The superhelix is the molecular basis of the precursor of collagen and is excreted into the intercellular space where it forms tropocollagen molecules with a length of 280 nm. These associate to form collagen fibrils, which in turn aggregate into fibers. The association is such, that between head and tail a free space of some 30 nm is left, space for mineralization, and the adjacent tropocollagen molecule overlaps that space by 67 nm. That is the origin of the banding pattern of collagen fibrils as it appears in transmission microscope images. The fibrils obtain finally the strength of mature collagen by intense cross-linking, a process catalyzed by a specific extracellular copper-containing enzyme lysyl oxidase.

There are at least 15 distinct biochemically and structurally different types. In Table 2.8, the actual designation together with the old terminology and the presence in tissue candidates for artificial substitution by implants. The biochemical differences (type of helix, amino acids outside hydroxyproline and glycine, etc.) were omitted because it demands a more extensive biochemical treatment.

The reader interested in more details about foregoing items is referred to [40, 52, 69–72].

Mechanical Properties

Mechanical properties of bone were fascinating scientists as far back as 1634 by Galileo but became an active field of research in the second half of the nineteenth century (Rauber, Messerer, Hulsen). The topic gained new impetus after the second

Table 2.8 Main types of mammalian collagen of potential candidate tissues for artificial substitution. Selected from Gray's [52] and Wintermantel [40]

Type	Older terminology	Tissue
I	Collagen	Widespread, bone, dentin, tendons, skin, vitreous body
II	Cartilage coll.	Cartilage,nucleus bulbosus,[a] vitreous body[b]
III	Embryonic coll.	Skin, blood vessels
IV		Lens capsule[b]
V	A-B collagen	Widespread in small amounts
VI	Intimal collagen	Cornea,[b] blood vessels
VII	LC collagen	Skin
VIII	EC collagen	Blood vessels
IX-XI		Cartilage
XII		Nerves

[a] Intervertebral
[b] Eye

Table 2.9 Directional differences in compressive strength of compact femoral bone of adult men. Selected from Table XIX, Evans [70]

Compressive strength		Publication
$MPa_{\parallel}$	$MPa_{\perp}$	Year
195	178	1896
208	135	1952
204	153	1965
167		1970

Table 2.10 UTS, strain and E-modulus of wet embalmed femoral cortical bone in different age groups. Modified from Evans, Table LXXIV [70]

Age group	0–19	20–39	40–59	60–79	80–99
$UTS\ (MPa)_{\parallel}$	51	93	87	77	73
Strain(%)	1.7	1.9	1.5	1.3	1.4
$E_{\parallel}$ (GPa)		16	15	15	13

world war and a comprehensive book on the subject *Mechanical Properties of Bone* was published by Evans with an extensive literature list [70].

For obvious reasons, the measurements on bone were performed on *post mortem* specimens. The conditions of preservation as embalming by injection of formaldehyde, fresh-wet or drying influence the results. Bone is not homogeneous and even within-laboratory experiments are substantially scattered. Therefore, all excerpted literature data are rounded in the following tables.

Anisotropy: Figure 2.14 perfectly illustrates this characteristic and Table 2.9 shows it in numbers. Ultimate tensile strength $\parallel$ and $\perp$ indicates measurements made in the direction parallel or perpendicular to the longitudinal axis of long bones. The year of publication demonstrates the remarkable reliability of the historic data.

Age: Incidence of fracture is increasing with age. We go over-the-hill between the age of 20-40 and 40-60 year and the numbers of Table 2.10 do not leave us any illusion. We listed the most pronounced but for fracture the most critical values.

Viscoelasticity: Bone is not a Hookean body meaning that a mix of mechanical properties shows a complex non-Newtonian behavior. Data are shown in Table 2.11 and Fig. 11.13 but we dig deeper into this issue when exploring paths to an ideal prosthesis.

Bone and cartilage are discussed here to stress again how complex a behavior of an artificial material needs to be in order to cope with the behavior of the *site specific living material* it is in contact with.

2.4 Total Hip Replacement Register

The ultimate test is the survival rate of a prosthesis in the human body. The case study at the start of this chapter is only a 'snapshot' of one case. A Pandora's box full of variables is co-determining success or failure of an implanted device entailing, that high numbers of devices should be monitored to get a reliable record

Table 2.11 Embalmed human femur: effect of strain rate on E-modulus and compression strength. Modified from Evans, Table XXXVI [70]

Strain rate s^{-1}	UCS MPa	E GPa	Max. strain to failure (%)
0.1	204	18.3	1.80
1.0	225	225	1.78
300	285	302	1.10
1,500	323	415	0.95

Table 2.12 E-modulus, UTS, UCS and strain of wet human bones at different sites. All values are rounded. Extracted from Park and Lakes, Table 9–5 [72] and, between brackets, from Evans, Table XLI [70]

Property bodyside	E GPa	UTS MPa	UCS MPa	Strain %
Femur	17(15)	121(80)	167	(1.5)
Tibia	18(16)	140(95)	159	(1.8)
Fibula	19(18)	146(94)	123	(1.7)
Humerus	17	130	132	
Radius	19	149	114	
Ulna	18	148	117	
Skull			97	

for survival rate. Sweden initiated in 1979 *The Swedish Total Hip Replacement Register* with the mission to improve the outcome after THR. In their hypothesis, the authors state that *feedback of analyzed data stimulates the individual clinic to reflect and improve according to the principle of good example*. An orthopedic surgeon, Professor Bernhard Bloch, was initiating a smaller scale but otherwise similar project in Australia during the late 1960s but we do not know whether his work was seminal to the Swedish project. Anyway, the latter serves as the *good example* for current initiatives in other countries. The Swedish project covers now something like 300.000 implants, diagnosed by year, age, gender, type of fixation (cemented, uncemented, hybrid, reversed hybrid), primary, revision or re-revision, reason for failure, cost, hospital. Since 1999, a more detailed recording of all implant parts constituting the final implant has been added and the follow-up routine is systematically refined to increase the sensitivity of the Register.

Let us examine the graphs of Fig. 2.15 which display on the left side the number of years before revision for 233.151 cemented and right for 9.170 uncemented implants, all reasons for revision included. The same graphs considering only aseptic loosening would show results about 2% less favorable. Analog graphs exist for hybrid and reversed hybrid implants and the latter type seems to give superior results but they are used hardly longer than 10 years. The data cover only surgery in Swedish hospitals. What do we learn from these graphs?

The survival 10 years postoperatively is for the period 1979–1991, 90% for cemented, 70% for the uncemented implants. Within the next 14 years, the situation

Table 2.13 Market share in % for a selection of implants: evolution of the last 26 years. Data selected from a list of 15 most common implants from the Swedish Hip Arthroplasty Register [73, p. 7]. Values rounded to the nearest integers. The data of 1995–1999 are not listed separately in the Register

Year	1979–2000	2001	2002	2003	2004	2005	Total[a]
			Cemented Cup (Stem)				
Lubinus[b]	17	35	36	37	40	41	34
Charnley	27	13	7	2	<1	–	13[c]
Exeter	5	2	2	1	1	7	11[d]
Numbers	191.458	12.217	12.698	12.686	13.391	13.848	256.298
			Uncemented Cup (Stem)				
Spotorno	8	–	–	–	–	36	12
Allofift	–	–	–	–	–	8	10
All other	–	–	–	–	–	–	≤7
Numbers	6.153	316	427	577	758	1,008	9.239

[a] Refers to the proportion of the total number of primary THR performed during the past 10 years
[b] Lubinus SPII, CLS Spotorno, Allofit (CLS Spotorno)
[c] Total for a combination of 3 different types of Charnley implants
[d] Total for a combination of 2 different types of Exeter implants, share of each type not listed

improved to 93.5 and 84%, respectively, a substantial windfall for patients as well as for the national health care! Detailed analysis learned that patient- and surgery-related reasons decreased constantly during the years 1979–2005 but periprosthetic femoral fractures remained roughly constant. Aseptic loosening, by far the most important reason, is reaching a plateau. Of the 69.462 cemented implants 77.6% survived after a period of 26 years. Analyzed per type, the continuous feedback from the register is narrowing the selection, a consequence of the *good example*, though one side of the coin only. The other side, however, could be that innovative designs get less chance. Is it possible that the slow breakthrough of uncemented designs, at least for Sweden, is due to this feedback? Nothing is perfect on earth. Both effects are clearly demonstrated in Table 2.13. Note that the total percentages are a combination for 3 types of Charnley and two of Exeter, therefore no percentages are given for each period or year. The numbers represent the total number of implants for the period or year and the overall total for 1979–2005. Aseptic loosening remains the major cause for revision. Although cement is space filling and implants are not expected to shrink in volume, the reason for loosening is mainly bone resorption. It can be design-related (stress-shielding) or provoked by wear debris from stem and cup, an item addressed in following chapters. Cements and cementing techniques are not shown to cause major problems but all cement packages are registered since the beginning of 2006 as part of the progressive refinement of the register.

Figure 2.15 should incline surgeons to choose cemented prostheses but the debate *to cement or not to cement* remains open. The evermore detailed statistic material will hopefully learn in the near future how the choice cemented/uncemented influences the outcome for different patient categories, and why the outcome is occasionally different.

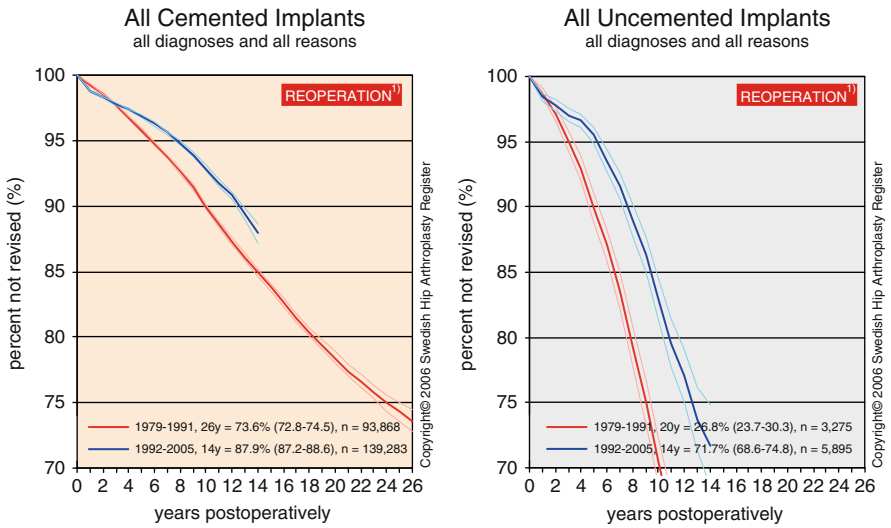

Fig. 2.15 Not revised implants as function of years postop. Copy from the Internet site of the Swedish National Hip Registry [73, p. 28]

And materials, are they not a part of the game? Why bother about further improvements after the apparent absence of a negative story on materials in the Register statistics?

From the register, we learn that most failures are provoked by patient-, design- and surgery-related factors and the superior survival rate of cemented prostheses. Here, however, we come closer to the role of materials in the business. Cements were already mentioned and later on their chemistry and mechanics will receive a closer look. A first class story about materials, however, cannot be skipped here! At the end of 1980s, a new cement Boneloc was introduced: a butylmethacrylate, where the methyl-group of conventional cement had been replaced by a butyl-group. It was said to have a lower setting temperature and thus, potentially less necrotic for bone. In the 1990s, it was commercialized, but soon it became clear it was a full size disaster: in a 5-year period >50% of the stems were loosening, accompanied by dramatic osteolysis [74–76]! Little sparks kindle great fires! Ringing the alarm bell by the Swedish Register confined the disaster.

Further on, we find in the Register that stems perform better than cups and that small changes in surface finish can result in major differences in revision risk. The well-known example is the Exeter implant: the matt finish of the stem gave far poorer results than the polished stem; in later chapters, we will discuss surface modification and encounter other examples for the effect of surface finish. The main properties of the classics stainless steels, cobalt-chrome and titanium alloys were already discussed and polymers and ceramics follow later. A short separate chapter will be devoted to a recently re-introduced metal zirconium (Chap. 5). The cup was mentioned to perform less well. Work is going on to introduce a highly cross-linked

ultra-high-molecular weight polyethylene which should meet the wear problem. In Chap. 11, this subject will be addressed. The body of acquired experience in the last 70 years is enormous but around the corner are lurking the same problems as years ago and Chap. 3 will account for one of these old items. The materials scientists should not worry about the future of their job.

We are not aware of the existence of nationwide registers on other implants. The impact of the Swedish Register in hip arthroplasty may be a stimulus to create analog ones. It is not a trophy-grabbing exercise but a tool. The evaluations of implants published in the current literature cover too low a number of cases to deliver significant and detailed statistics.

This section was stuffed by reading and reflecting on the reports of the Swedish Hip Arthroplasty Register [73, 77–79]. In a recent paper, Wroblewski and colleagues published a follow-up to up to 36 years of Charnley low-frictional torque arthroplasty in young rheumatoid patients. They conclude that the Charnley LFA continues to be an excellent hip replacement for very young arthritis patients, a conclusion slightly differing from the Swedish Register. The paper is, however, worth mentioning in this context because of its specificity, long-term follow-up and interesting data on wear [80].

2.5 Homage to a Pioneer: Sir John Charnley

History is often unfair in attributing the birth of a discipline to one given celebrity, unfair because it generally denies the building blocks laid down by many other persons, whose efforts and creativity for one reason or another dissolved in the mainstream of the past: '*known to God*' as we read on war graves. However, we take the risk and put Professor Sir John Charnley on the podium as the trigger person of biomaterials research. A great variety of hip implants were already designed and implanted in the 1930s but the Charnley prosthesis of the late 1950s was a culminating point in the development and still is considered the gold standard. Its development triggered in many laboratories worldwide an intensive attention to implant design and the study of interaction of materials with the body. The term '*biomaterial*' must have been coined in that period. Charnley was innovative not only in his low friction concept of total hip replacement and its stabilization by acrylic cement but also in his appeal to scientists of other disciplines, e.g., his engineering colleagues, with respect to mechanical design and selection of materials. Moreover, he was very realistic, even modest, in his aims; in his paper in The Lancet of 1961 [81] he writes: *In considering how arthroplasty of the hip can be improved, two facts stand out: 1. . . . Our problem is to make this temporary success permanent. 2. Objectives must be reasonable. Neither surgeons nor engineers will ever make an artificial hip-joint which will last thirty years and at some time in this period enable the patient to play football.*

Professor John Charnley was born in Bury, Lancashire (UK) on 29 August 1911. As son of Arthur Charnley, a local chemist, and Lily, a nurse at Crumpsall Hospital

in Manchester, he grew up in a stimulating environment and entered in 1929, after his grammar school at Bury, the medical school of Victoria Hospital of Manchester. After brilliant studies he graduated in 1935. After World War II, he returned to Manchester in 1946 and specialized in orthopedics. After his marriage to Jill Heaver (1957), he decided in 1958 to focus his efforts on the development of hip replacement research and surgery and moved in his clinical practice in Wrightington. He died in 1982. His work is perpetuated by the John Charnley Research Institute, Wrightington Hospital (Appley Bridge, Lancashire WN6 9EP, UK) [82].

Orthopedic surgeons as well as biomaterials scientists are all tributary to this giant and a reference to his work should not be absent in this book, the paper in The Lancet is just one of his unsurpassed œuvre.

Epitome: Half a century of intense and increasingly integrated research changed the world of biomaterials. The discussion of the fracture of a hip stem was seized to demonstrate the multifactorial character of the interaction between body and implant as well as the intricately multidisciplinary character of the scientific approach. The fracture of a metal is at first glance a mechanic problem and, indeed, it is one but not exclusively a mechanical one. The biomedical community became aware that a successful implant has to meet simultaneously a whole set of requirements to increase the life span of the implants and the patients' comfort. The manufacturers switched progressively from stainless steel over cobalt-chrome to titanium alloys and in the near future may be to β-titanium alloys, all with the aim to increase the overall quality of the implant and to compromise as less as possible the body. *Multifactorial* means that the manufacturers have to reconcile simultaneously properties as tensile or bending strength, fatigue strength, E-modulus close to bone, benign reaction to bone meaning biotolerant, osteoconductive and/or osteoinductive.

A description of the structure of bone was added to show the complexity of the tissue an implant has to substitute and the consequence for the design.

Survival rate of an implant is a great help in evaluating the quality. A decent evaluation, however, requires the follow-up of a great number of cases, exactly because of the very multifactorial character of implant success or failure. Therefore, we included a section on the unique Swedish Total Hip Replacement Register, which meets this requirement.

Chapter 3
Corrosion

Three peculiarities discriminate metals from most other materials:

- Metals are used in a vulnerable oxidation state. It makes them apt to be oxidized or to be corroded.
- Corrosion observed on one spot can simply be the result of a wrong environment at the distant end of a metal object. Metals are highways for electric currents.
- No electrochemical process will occur unless at least two reaction partners are involved.

These statements do not apply to ceramics or polymers. Some authors want to extend the term corrosion to degradation processes of all classes of materials but we prefer to keep it confined to degradation of metals. Atoms of a ceramic are in a higher if not the highest oxidation state. These atoms are held together by a mix of ionic and covalent bonds or by the weaker hydrogen bonds or Van der Waals forces. Except for the special class of highly conducting polymers such as poly-acetylenes, discovered in 1977, and some ceramics such as substoichiometric titanium dioxide, all polymers and ceramics are all electric insulators. In metallic bonds, however, all the atoms share their valence electrons: it is a more or less ordered array of positively charged nuclei bathing in a sea of delocalized electrons. Atoms tied up by a preponderately pure ionic bond, for example *LiCl*, can hardly be called "molecules". In metals no molecules either: long-range collective interactions constitute the bonding forces between the atoms. It is not only for their specific mechanical properties that metals constitute a generic class of materials, but also the statements formulated above drive them together into that specific class.

3.1 It Should not Have Happened

A patient had a primary total hip replacement with the insertion of a prosthesis. Seventy months postoperatively radiographs revealed a fractured prosthetic neck (Fig. 3.1a). A similar case was reported for the same type of prosthesis but 85 months postoperatively. Both were modular PCA prostheses implanted without

J.A. Helsen and Y. Missirlis, *Biomaterials*, Biological and Medical Physics, Biomedical Engineering, DOI 10.1007/978-3-642-12532-4_3,

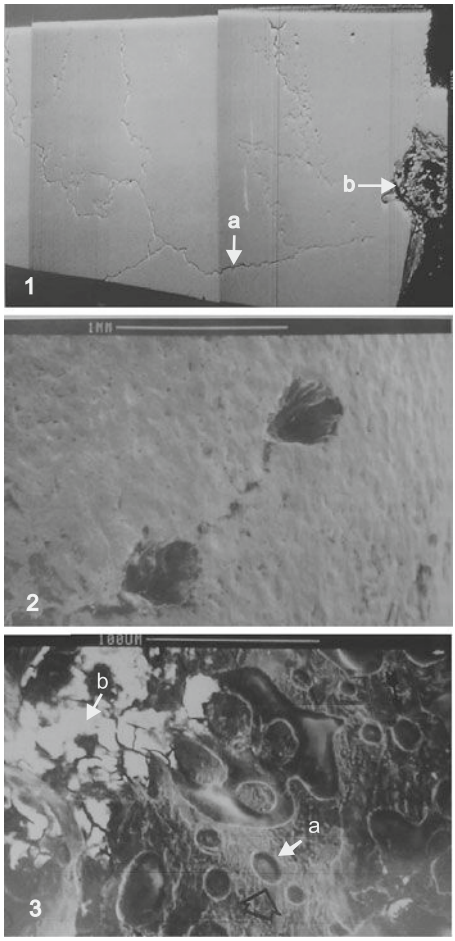

Fig. 3.1 (**1**) The tapered neck of the prosthesis fractured 85 months postop. The cross section clearly shows intergranular cracks (**a**) throughout the neck, while (**b**) points to the onset site of the fracture. (**2**) Micrograph of the free fracture surface, showing pits formed by egression of surface grains (carbides). (**3**) Micrograph of the fracture surfaces: (**a**) pores; (**b**) nonconducting debris, most likely segregated carbides from the grain boundaries. Reproduced with permission of Rockwater and J.Bone & Joint Surgery [83], Figs. 6,4 and 5-b

cement.[1] The parts consisted of a wrought CoCrMo alloy head (ASTM F799) coupled to a CoCrMo stem. The fractures occurred in the neck just distal of the head-neck taper. Both patients were rather obese persons with an active life but, as in the case study of Chap. 2, the mechanical strength of the neck section should have been able to carry the weight of the person. However, something went wrong!

A section through the taper showed the presence of corrosive penetration of fluid along the grain boundaries. It was also observed that the fracture followed the grain boundaries (Fig. 3.1a); (b) points to the onset of the fracture. The free surface outside the taper junction showed pits as large as 500 μm and were connected through intergranular cracks (Fig. 3.12). Analysis of the particles indicated a high chromium

[1] PCA stands for *Porous Contact Anatomic*, How-medica, New Jersey.

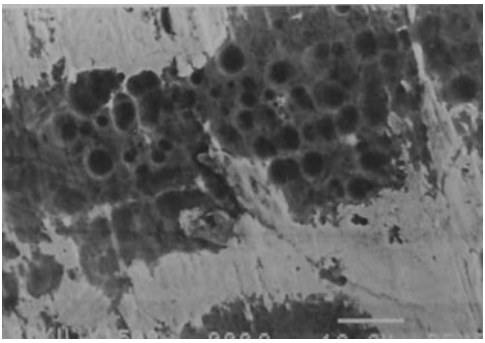

Fig. 3.2 The severely pitted inner taper surface of a CoCr head. The bar (*down right*) corresponds to 10 μm. Reproduced with permission of J. Bone and Joint Surgery [84], Fig. 8

content and consisted most probably of chromium carbide as suggested in Chap. 2. It should be mentioned that the stem had a *porous coating of beads* sintered to the surface. This is an important detail because it indicates that there is a great difference between anode (pits) and cathode (stem) areas (see further in the text). The sintering is performed at temperatures near the melting point, a thermal treatment that possibly provoked diffusional processes resulting in vacancy motion, void formation at grain boundaries and *phase segregations* in the alloy. The voids, the smooth areas present in Fig. 3.13, possibly existed before corrosive attack as a result of the thermal treatment or other manufacturing conditions. The authors mention also that mechanically assisted *crevice corrosion* contributed to the fracture.

Collier and colleagues studied the tapered interface between head and neck of 139 modular femoral components of hip prostheses, removed for a variety of reasons. None of the 91 single-alloy prostheses showed any sign of corrosion, irrespective of they were all CoCr or all titanium alloy. Of the 48 mixed alloy components, 25 had evidence of corrosion, always at the CoCr-alloy head and the titanium alloy neck. These 25 had been implanted for more than 10 months; none showed any sign of corrosion before that residence time in the body. The type of this cohort of retrieved implants was preponderately Harris–Galante Z [84].

The corrosion in the latter cases is different from the former ones: the inner taper surface was pitted as shown in Fig. 3.2 but the CoCr was more severely attacked than its titanium taper counterpart. The corroded inner taper area increased from about 6% after 12–23 months up to more than 80% after 40 months. *Pitting corrosion* was blamed to be the scapegoat of the evil by the authors.

In italics we emphasized terms typical for the corrosion profession. In the following sections, a qualitative insight in the origin of these terms will be given.

3.2 Water Does not Flow Uphill

Corrosion is an electrochemical or galvanic process involving metals. *Galvanic* is a term which pays tribute to Galvani's discovery that a frog's leg contracted when two metals, connected to the nerve and thus to the muscle, were short

circuited.[2] Volta established that the contraction only occurred when two *different* metals were connected.[3] He set up a "potential series" for conductors such as metals (first class conductors he named them).[4] He arranged them in such a way that in a circuit made up of two of them and an aqueous solution (second class conductor, later recognized as ionic conductor) a positive current would pass through the liquid from the higher to the lower one in the series. Hereafter, Ritter discovered that Volta's series was the same as that established from experiments on the power of metals to displace each other from solution.[5] It was here for the first time that a direct connection was recognized between galvanic and chemical processes. Ritter's name is invisible in this scientific discipline, but the link between "electro" and "chemistry" is ultimately due to him and let us gloss over his reported unpleasant character and occultism.

Herewith all systematic development of electrochemistry started. In this short introduction, the very basic players in the electrochemical game are named: metals and electrons on one side and ions in solution on the other side. As we will see further, water is not a passive fluidum but an active player in the game, and moreover, so important a player in biologic systems and a pure brand biomaterial, even fundamental for the origin of life on earth, that it will be granted a separate chapter (Chap. 14). Note that there exists electrochemical life in nonaqueous media but within the context of this book, water is obviously the medium of choice.

The nineteenth century is in science the age of equilibrium thermodynamics. The experiments of Galvani, Volta and Ritter were further developed during that century according to the current thermodynamic concepts. The experiment of Galvani was the far onset of electrophysiology but now, 200 years later, measurement of neuronal activity by electrophysiological techniques is challenged by optical probes [85]. Nothing lasts for ever!

---

[2] Luigi Galvani: an Italian physicist and medical doctor (Bolgona 1727–1798). To be honest, it was his wife who first discovered that a freshly prepared leg of a frog contracted in the neighborhood of an electrostatic generator. Galvani did afterward the more systematic work.

[3] Alessandro Volta: Italian physicist born in Como (Italy) in 1745 and died there in 1827. In honor of the relationship he established between electric charge and potential, the unit of potential was named *volt*. He realized that in Galvani's experiment, the frog's leg acted both as a conductor and detector of electricity. The first battery, the Voltaic Pile, was born by replacing the frog's leg by brine-soaked paper squeezed between two different metals (silver and zinc). A further consequence of these experiments was the discovery of the galvanic series.

[4] Volta made herewith the amazing distinction between electronic and ionic conduction. Only a century later Stoney (1891) could conclude that electricity was indeed "atomic" in nature, an obvious consequence of Faraday's laws. The electric atom was "christened" as *electron* by Stoney.

[5] Johan Wilhelm Ritter: born in Samitz (Silesia) 1776 and died in München (Germany) 1810. He started as an apprentice in a pharmacy, enrolled later at the University of Jena, studied medicine, got a professorship in Jena, then in Gotha and took finally a position at the Bavarian Academy of Science. He is known for his discovery of ultraviolet radiation and for the establishment of the link between galvanism and chemical reactivity. His entrance in occultism destroyed his scientific reputation, reason why historians greatly ignored his scientific work.

Why Iron Corrodes, Why Gold Does not?

Reactions occur spontaneously in a direction where a net release of energy is occurring or, in thermodynamic terms, by a negative change in Gibbs-free energy ΔG. A few examples:

$$\begin{aligned} \mathrm{Mg} + \mathrm{H_2O} + 1/2\mathrm{O_2} &\rightarrow \mathrm{Mg(OH)_2} \quad \Delta G_0 = -596\ (\mathrm{kJ\,mol^{-1}}) \\ \mathrm{Fe} + 3/2\mathrm{H_2O} + 3/4\mathrm{O_2} &\rightarrow \mathrm{Fe(OH)_3} \quad \Delta G_0 = -100\ (\mathrm{kJ\,mol^{-1}}) \\ \mathrm{Au} + 3/2\mathrm{H_2O} + 3/4\mathrm{O_2} &\rightarrow \mathrm{Au(OH)_3} \quad \Delta G_0 = +66\ (\mathrm{kJ\,mol^{-1}}) \end{aligned}$$

ΔG_0 refers to the common thermodynamic standard conditions of concentration, temperature and pressure. From these equations, it is obvious that for gold to corrode we have to add energy, that corroding iron is releasing energy and wires of magnesium burn vigorously in a flash light bulb ... just as for a spontaneous flow of water to occur (change of mechanical free energy), water has to flow downhill. Hence, it will not be different for any other reaction or process occurring spontaneously in the human body.

Made Ritter the link between chemical and galvanic processes, Faraday established the link between thermodynamics and electrochemistry.[6]

The free energy change in an electrochemical cell, for example, a short circuited pair of electrodes of dissimilar metals such as copper and zinc immersed in an acid solution (skipping details) is proportional to the potential difference between the two electrodes:

$$\Delta G = -n_e F \Delta E, \tag{3.1}$$

where n_e is the number of electrons exchanged in the reaction ($\mathrm{Cu^{2+}} + 2\mathrm{e^-} \rightleftharpoons \mathrm{Cu}$ and $\mathrm{Zn^0} - 2\mathrm{e^-} \rightleftharpoons \mathrm{Zn}$), F the amount of electricity for a single electron reaction to go to completion ($F = 96.487$ Coulomb) and ΔE the potential difference between the electrodes. Let us now see what that is all good for. F is a universal constant because it is the product of two other universal constants $N\epsilon$, Avogadro's number N and the charge of the electron (see Appendix A).

3.2.1 Electrochemical Series

Electrochemical potential, potential difference, ... no definition was given so far for these terms. When immersing a titanium rod, let us call it an *electrode*, in an acid solution an electric potential will develop between the rod and the solution. However, it is frustratingly impossible to measure it unless a second electrode is inserted in the solution, which in turn builds up its own potential. Both electrodes

[6] Michael Faraday, English chemist and physicist, Newington, Surrey September 22, 1791-London August 25, 1867. Known for his pioneering experiments in electricity and magnetism.

can be connected by a metal wire to a high input impedance voltmeter to measure the potential difference. The schematic construction of an electrochemical cell, the way electrochemical potentials are determined and the necessary definitions are given into some detail in Appendix C. The equilibrium potential of a metal immersed in a solution with $a_{M^{n+}} \neq 1$ can be calculated by the Nernst equation:

$$E = E_0 + \frac{RT}{nF} ln(a_{M^{n+}}/a_M) \tag{3.2}$$

with a_M, the activity of the metal, accepted to equal one.

The potential E_0 is an equilibrium potential determined under the standard condition $a_{M^{n+}} = 1$ and temperature 25°C. No reaction will occur between two systems, when both are in standard conditions and having hardly differing standard potentials. Any *redox* (oxidation-reduction) system with an E_0 more positive than another one will shift the equilibrium of the latter toward oxidation (to the left as shown in the reactions given in Electrochemical Series of Table C.1, Appendix C.1). In ordinary life, these simple standard and equilibrium conditions are not likely to happen and consequently, not suitable to predict whether one partner in a particular metal couple present in an implant will oxidize the other or will be oxidized by the other. E_0s, however, remain a rough guide for a first approach.

An onset to more realistic potential values was given in the early 1950s by Clarke and colleagues [86]. They determined what was called *anodic back EMF* on single metals but also on alloys. The measurements were done in equine serum, because they realized that corrosion investigations were carried out *in inorganic fluids [were] far simpler than those pervading living tissue*! In Table C.2, a few of their interesting data were collected. Although it was not a particularly well-written paper, it was in the subsequent decades not given the attention it merited.

Another onset to a more realistic approach was given by Pourbaix.[7]

3.2.2 Pourbaix Diagram

Equation (3.2) relates potential clearly to activity of the metal ion. The metal can be oxidized and transformed directly to a hydroxide $M(OH)_n$ or oxide:

$$M + nH_2O \longrightarrow M(OH)_n + ne^- + nH^+ \tag{3.3}$$

$$M + 2nOH^- \longrightarrow MO_n^{n-} + nH_2O + ne^- \tag{3.4}$$

with electron transfer and thus potential and clearly pH dependent. The reaction is generally stimulated to progress to the right by purely chemical reactions:

[7] Marcel Pourbaix (1904–1998) became famous in particular for his E-pH diagrams. He was founder or co-founder of many international and national (Belgian) committees on electrochemistry and one of the important players on the international scene of corrosion science.

$$M^{n+} + n\mathrm{OH}^- \longrightarrow M(\mathrm{OH})_n \tag{3.5}$$

$$MO_n^{n-} + n\mathrm{H}^+ \longrightarrow M(\mathrm{OH})_n \tag{3.6}$$

without electron transfer and thus potential independent, only pH dependent. After a first oxidation as in (3.3), an ion can be oxidized to a higher oxidation state as in:

$$\mathrm{Fe}^{2+} \longrightarrow \mathrm{Fe}^{3+} + \mathrm{e}^-. \tag{3.7}$$

Reactions (3.5) and (3.6) are examples of formation of often insoluble compounds. Complex formation of all kinds is the other general mechanism reducing the effective concentration of the oxidized metal and, even more the rule than the exception in tissues and body fluids. Sulfhydryl groups $-\mathrm{SH}^-$ are eager to react with Ni^{2+} and are abundantly present in all living tissues as amino acids (thioneines, for example), polypeptides and so on; a burden of other biochemical agents offer strong complex forming abilities. The secondary reactions shift the potential of the couple M/M^{n+} to more negative values or, in other words, make the metal less noble. Moreover, the body fluids around implants are dynamic and a continuous disruption of equilibrium concentration happens or may happen, which in turn sustains corrosion. It is a consequence of the extreme tendency to conservatism of biological systems: *be dynamic or perish*.[8]

A Pourbaix diagram is a plot of *redox* potentials as a function of pH for a given metal and standard conditions of pressure and temperature. The criterium assumed for having *protection* (immunity or passivation) is a total equilibrium concentration of the metal $\leq 10^{-6}\,\mathrm{g\,dm^{-3}}$ or, for having *corrosion* $\geq 10^{-6}\,\mathrm{g\,dm^{-3}}$.

Three types of solid lines are distinguished:

Horizontal line: reaction only potential dependent. An example of such a reaction is the equilibrium $\mathrm{Fe}^{2+}/\mathrm{Fe}^{3+}$.
Vertical line: reaction only pH dependent (3.6).
Sloping line: reaction both pH- and potential dependent (3.3 and 3.4).

All features just explained are demonstrated in Fig. 3.3.

The diagonal dotted lines delimit the stability region for water or a region within which no electrolysis of water can occur. They are calculated for the cathodic reactions (3.12) and (3.13) by the Nernst equation. Below the dotted line (a) hydrogen is released; above (b) oxygen is released.

Figure 3.4 is, since many years, the classic example for chromium in contact with an aqueous solution of chloride (0.85N) as given in Black's *Biological Performance of Materials* or, earlier in 1975 by Dumbleton and Black [88]. Superimposed here are typical pH-potential zones for various body fluids. The domain, where chromium

[8] In biology, this conservatism is named *homeostasis*. Finely tuned feedback mechanisms operate at all levels of the body to ensure a relatively constant (micro-)environment. The understanding of this phenomenon steadily progresses [87]. This notion was the greatest contribution to physiological theory by eighteenth century French physiologist and surgeon Claude Bernard (1813–1878).

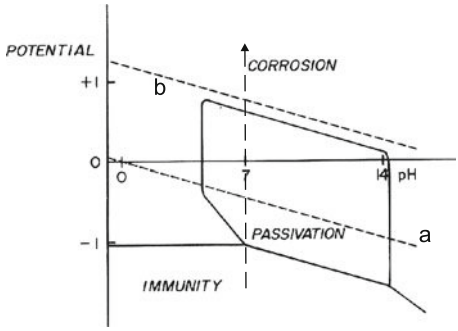

Fig. 3.3 Simplified Pourbaix diagram for chromium, normally given with respect to an equilibrium aqueous concentration of $\leq 10^{-6}\,\mathrm{g\,dm^{-3}}$. For the vertical dotted line, see the end of the next section

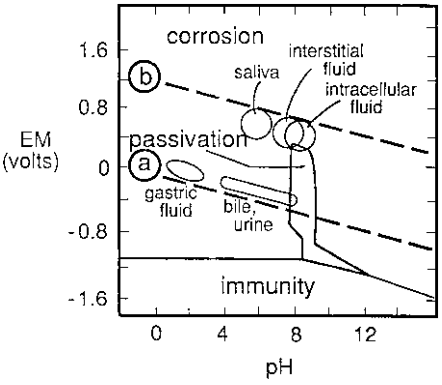

Fig. 3.4 Pourbaix diagram for chromium in a chloride solution of $0.85\,\mathrm{M\,l^{-1}}$. A classic, already displayed by Black [51, p. 43]

is in the zone of passivity, is greatly reduced by the presence of chloride and situated above pH = 8. However, conservative the body is, pHs below that value occur: during the onset of infection, for example in the surrounding of an osteosynthesis plate, pH may go down to 5.5 [89, p. 240] or [90]. Pure chromium is mechanically speaking not suitable, for say a dental implant and indeed, it is always used as alloying element in implants. There too, however, the protective layer is Cr_2O_3 but the practice is, fortunately, somewhat more favorable than the prediction by Fig. 3.4.

The merit of Pourbaixs diagrams is that they are offering the corrosion scientist a perspective on what occasionally can happen, however, not what will. They are purely thermodynamic, composed of pure metals, without accounting for effects of other ions, surface texture, etc. and above all, with which speed it all happens. Let us say that a Pourbaix diagram is like "a room with a view" but, if the room is on the backside, one does not see who is ringing at the front door. The front door is, in modern electrodics, the study of kinetics of corrosion reactions.

3.2.3 Corrosion Rate

In Fig. 3.5 are displayed the basic components of a corrosion cell: two short-circuited dissimilar metals in an aqueous solution. Electrons are flowing from anode

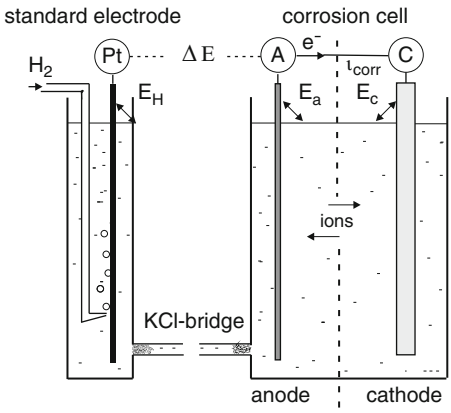

Fig. 3.5 Electrochemical cell. *Left*: standard hydrogen electrode (solution with $a_{H^+} = 1$ and a partial hydrogen pressure of 1 atm (=101.3 kPa; for conversion of units: see Appendix A). *Right*: corrosion cell. The left half cell, if used as a separate unit, is a setup for measuring electrode potentials. In that case, the solution contains a specified activity of the metal ion of the electrode metal

to cathode driven by their potential difference between anode and cathode potential, $E_a < E_c$. No accumulation of charge is happening or even possible, because electrons generated on one electrode are taken up by the other.

Part of the *anode* is consumed by the corrosion reaction. The amount lost is easily calculated by Faraday's law if the corrosion current i_{corr} is known. Faraday's laws for electrolysis can for this application be written as:

$$\Delta w/M = it/nF \tag{3.8}$$

in which Δw is the weight loss at constant current i during a time t for a metal oxidized to an oxidation state n. On the *cathode*, oxygen is reduced or hydrogen formed. In engineering, corrosion rate is expressed as $v_{w,corr}$, loss of weight per year and per unit area (square m, cm or mm):

$$v_{w,corr} = \frac{i_{corr} M t}{nFa} \tag{3.9}$$

with:

i_{corr}: corrosion current in ampere (A, mA, μA).
w: weight of metal.
M: molecular mass of the metal expressed as gram per mole.
t: time in s (31,536,000 s/year).
F: Faraday equivalent: 96,485 Coulomb.
a: electrode area (square m, cm or mm).
n: number of electrons released by the anodic reaction.

Alternatively, corrosion rate is expressed as decrease in thickness per unit of time and per year:

$$v_{\delta,corr} = \frac{v_{M,corr}}{\rho} \tag{3.10}$$

with:

$v_{\delta,\mathrm{corr}}$: loss in thickness (practical units mm or μm).
ρ: density of the metal.

The standard hydrogen electrode of Fig. 3.5 consists of a platina rod immersed in a solution under standard conditions: $a_{\mathrm{H}^+} = 1$, $p_{\mathrm{H}_2} = 1$ atm and $T = 298°\mathrm{K}$.

3.2.3.1 Anodic and Cathodic Currents

The anodic reaction we are interested in can be:

$$M \longrightarrow M^{n+} + n\mathrm{e}^- \tag{3.11}$$

and the cathodic ones:

$$2\mathrm{H}^+ + 2\mathrm{e}^- \longrightarrow \mathrm{H}_2 \tag{3.12}$$

or, in the presence of oxygen:

$$\mathrm{O}_2 + 4\mathrm{H}^+ + 4\mathrm{e}^- \longrightarrow 2\mathrm{H}_2\mathrm{O}. \tag{3.13}$$

The overall driving force for reaction is the cell potential difference $E_{\mathrm{cell}} = E_C - E_A$. The individual polarizations or *overpotentials* η are $\eta_A = E_{\mathrm{corr}} - E_A^0$ relative to (3.11) and, $\eta_C = E_{\mathrm{corr}} - E_C^0$ relative to (3.12) or (3.13). Current and η are linked by the exponential law of Tafel,[9] later theoretically underpinned by the Butler–Volmer theory:

$$\eta = a + b \log i \tag{3.14}$$

with η the overpotential and a and b the Tafel coefficients. It is a very simplified form of the Butler–Volmer equation and holds for $\Delta E \geq 0.1$ V.

A plot of (3.14) is given in Fig. 3.6. In abscissa absolute current i, in ordinate potential E. In case the ordinate is expressed in overpotential, η is equal to zero for E_{corr}. The corrosion cell stabilizes its potential at E_{corr}, where $\mid -i_{\mathrm{c}} \mid = \mid +i_{\mathrm{a}} \mid$. Within a small interval of about 20 mV centered around E_{corr}, the relation current-potential is linear and from its slope the *polarization resistance* R_p can be calculated. Its determination is a method to quantify corrosion rate. It is performed by a constrained modulation of the potential around E_{corr} and recording the resulting current.

$$R_p = \frac{\Delta E}{\Delta i}. \tag{3.15}$$

It is instructive to follow an anodic polarization curve over a wider potential interval at a given pH and measuring the current, as a matter of fact a vertical promenade

[9] Julius Tafel (1862–1918) Swiss chemist. He published his law in Z. phys. Chem. **50**, 641 (1905).

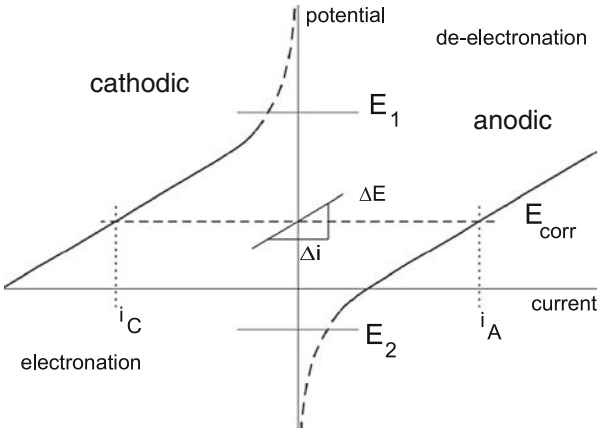

Fig. 3.6 Plot of potential vs. current according to (3.14). For the anodic reactions, see (3.11) for the cathodic (3.12) and (3.13)

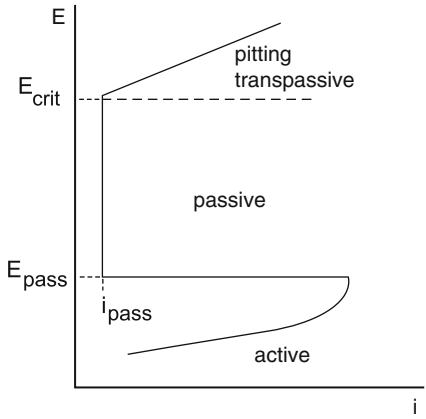

Fig. 3.7 Idealized anodic polarization curve

through the Pourbaix diagram (see vertical dotted line near pH = 7 in Fig. 3.3). The curve in Fig. 3.7 starts at a potential where the metal is unprotected (active region). The current increases steeply till E enters the passive region, where an oxide surface film forms constituting a high resistance barrier. The current roughly stabilizes at i_{pass} and remains there till E_{crit} is reached. From thereon, a breakdown process of passivity leads to localized forms of corrosion (pitting). For conditions $E_{\text{pass}} \geq E_{\text{corr}} \leq E_{\text{crit}}$, corrosion should be minimal. The small current associated with passivity is that required to maintain the passivating film, offsetting its slow dissolution.

A remark about currents: above we used absolute current designated by i. In theoretical treatments, mostly current density is used, i.e., the current normalized to the surface of the electrode. If the global surface of, for instance the cathode is much greater than the anode, the anodic current density will be much greater and roughly

proportional to the ratio of the areas. Practical consequences are demonstrated in the next section. For CoCrMo alloys, the current in the passive region from anodic *overpotential*, potential above E_{corr} of approximately -0.3 V to breakdown potential $E_{crit} \approx +0.7$ V stabilizes around $10\,\mu A\,cm^{-2}$ [91].

About the dynamics of the corrosion process, the reader is referred for further reading to electrochemical impedance spectroscopy, combined occasionally with Raman or other spectroscopic techniques. This technique allows in-depth study of the dynamics of corrosion processes and the nature of the surface layer (for example, porosity). For an introduction to this technique, see Hubrecht on pp. 405–466, or Scharnweber on pp. 101–151 in [35]. An instructive study can be read on the corrosion of chromium by this technique in a paper by Dobbelaar and de Wit [92]. For general reading, the recently updated book *Corrosion and Corrosion Control* is warmly recommended [93].

3.2.4 Styles in Corrosion

We do not like things to corrode but we see it occurring: when an unfortunate potential difference exists as driving force and when the reaction progresses at a detectable rate. The potential difference can be created along very odd ways, giving birth to different "styles" of corrosion.

In the 1960s, the booming days of hip implantology, implant companies were violating basic rules of corrosion prevention by combining noncompatible metals. The next decades, due to some disastrous results, tremendous research efforts were dedicated to the subject and in general to degradation of biomaterials. The monograph of 1991 with texts of a European Course on *Biomaterials Degradation* is not a comprehensive book of this development but it reflects nicely what was all together going on in research centra during these exciting years [89].

General or Uniform Attack and Galvanic Corrosion

Modern architects and sculptors make ample use of Cortensteel because of its uniform reddish color, an excellent demonstration of *uniform corrosion*.[10] It is an omnipresent corrosion style. However, it takes two for corrosion to happen and who is the other partner?

Take two metals with different electrochemical potentials and short circuit them as in Fig. 3.5: the one with the lower potential becomes the anode, the other the cathode. The anodic consumption in such a combination is called *galvanic corrosion*. The partners have a great difference in exposed area. If the partners have exposed

[10] The permanent reddish appearance and nonprogressing attack of this steel is due to an addition of a small amount of copper, which improves substantially adhesion and density of the oxide layer.

Table 3.1 Ratio of the actual concentration in a patient having a THR to the commonly accepted normal levels of Ni, Co and Cr. The ratios were calculated from data in Tables 2 and 1, given by Hildebrand [94]; (–) for values $\leq$10. The original concentrations were expressed for blood in μg/l, for plasma in μg/g creatinine and for urine in μg/g dry weight

	Alloy	Ni	Co	Cr
Total blood	SS	–	–	–
	NiCrMo	*45*	(17)	–
	CoCr	–	(15)	–
	CoCr-wear	–	*376*	–
Plasma	SS	–	–	–
	NiCrMo	30	(15)	–
	CoCr	–	(15)	14
	CoCr-wear	12	*445*	–
Urine	SS	–	–	–
	NiCrMo	13	(15)	15
	CoCr	–	–	–
	CoCr-wear	–	*174*	11

areas equal or below our eye's resolution, the corrosion style falls under the heading of uniform attack. Grains of an alloy with different composition but also adjacent grains in different crystallographic orientation with respect to the exposed area may form corrosive galvanic couples and give rise to an attack macroscopically appearing as uniform. In general, uniform corrosion is defined as *a result of small spatially and temporarily randomly distributed anode and cathode zones on an otherwise macroscopically homogeneous metal substrate* ... say a matter of scale.

Uniform attack is happening for stainless steel, CoCr alloys but also titanium show small but sizeable attack, notwithstanding the dense protecting oxide layer. The process is definitely a combination of a chemical dissolution process of the protecting oxide films, followed by galvanic corrosion of the exposed or nearly exposed alloy substrate. Both chemical and electrochemical reactions are heterogeneous processes: a solid and a liquid phase, with or without dissolved gases O_2 and/or any other agent from the biological *soup* potentially assisting the initiation of attack as explained.

If corroded, the corrosion products have to go somewhere. Table 3.1 ratios for concentration of nickel, cobalt and chromium are given for patients having a total hip replacement with respect to an average person without implant. Only values $\geq$10 are given and values for cobalt slightly higher than 10 are between brackets because of too great a possible error (the normal values for cobalt are sub-ppm; see for more details in Chap. 4). The authors do not specify precisely the type of alloys but we presume that NiCrMo refers to F90 and F562, CoCr to F75 and F799 and SS to 316L. The concentration enhancements are in general not that dramatic. Nickel is somewhat higher with NiCrMo implants. The relative constant but enhanced levels of these elements is partly to be attributed to uniform corrosion of the prosthesis stem, while some percentage originates from a process in between uniform and localized corrosion. Hip prosthesis stems, knee and dental prostheses are not really

fixed but are subjected to small-amplitude sliding (*micro-movements*) as we already pointed out. The movement gives rise to mostly mild wear. The worn areas are many square millimeters if not square centimeters wide and, although present on, mechanically speaking, "logic" sites, it is not what is commonly understood by localized corrosion (matter of scale!). Most cemented hip stems are sandblasted and the said sites are polished accompanied by removal of oxide. One should expect fast progress of corrosion but it does not. We consider concentrations below or less than ten times the normal standard levels as a balance between slow dissolution of the passive metal and evacuation. We come back on evacuation times after removal of the implant and cases of reactions to ions or debris in Chap. 4. The monitoring of highly worn CoCr implants is another story (values in bold). These cases concerned patients having a broken ceramic head, replaced afterward by a metallic one without replacement of the polyethylene acetabulum. Remaining ceramic wear debris provoked high wear and subsequent extraordinary dissolution.

Monitoring patients having a titanium alloy THR showed for at least some time-enhanced but constant blood levels of titanium, vanadium and aluminium without visible localized effect on the stems. This should also attributed to the balance between constant supply of these ions by uniform corrosion and evacuation.

Is the foregoing discussion becoming obsolete after so many years of research and use of successful alloys such as CoCrMo and titanium, as well as progressively more positive implant results? Still today an estimated 20% of human patients require revision surgery for various reasons, aseptic loosening being the most frequent one. The answer is "no" and this statement is refueled by recent studies. One of them is the evaluation of CoCrMo implants by Hodgson and colleagues in sheep and in simulated body fluid: their results are completely aligned with our own experience and with the results of Hildebrand's study 11 years earlier [95, 96]. Metal trace levels in blood and tissues are enhanced but not in the same ratio as in the alloy. From well-fixed to fixed implants, the ratio for cobalt with respect to unimplanted sheep ranges from 10 to 5,000, the loose from 7,000 to 50.000. Cobalt concentrations always exceed largely the reference values, followed by chromium and molybdenum. The results are explained in terms of uniform corrosion combined with tribocorrosion. The nonstoichiometric dissolution of cobalt can be simulated in vitro by cyclic polarization between cathodic and anodic potentials. This observation fits the continuous activation-repassivation cycles in vivo and completes the picture.

Localized Corrosion

We just made reference to dissolved oxygen. Oxygen pressure above a liquid, and consequently its concentration in the liquid, is dominating the equilibrium of the cathodic reaction of (3.13), hence, an important partner in this business. In the second point, at the start of this chapter, we stated that:

> Corrosion observed on one spot can simply be the result of a wrong environment at the distant end of a metal object. Metals are highways for electric currents.

Fig. 3.8 Concentration cell

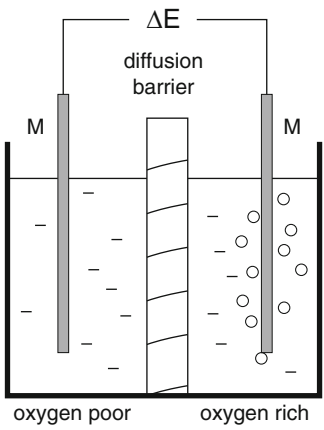

Localized corrosion finds there its origin, but of course the overall process is the combined result of the oxygen concentration gradient, the corroding medium and the type of alloy. Figure 3.8 is a "macro-model" of a corrosion cell with electrodes of the same metal but immersed in solutions of differing oxygen concentration.[11]

The cathodic reaction (3.13) is pH dependent, but assuming in a first approximation a constant pH in both half-cells, the generated potential difference is easily calculated by the Nernst equation. For the oxygen-rich side:

$$E^1 = E^0_{O_2} + \frac{RT}{4F} \ln(p^1_{O_2}) \tag{3.16}$$

and for the oxygen-pour side:

$$E^2 = E^0_{O_2} + \frac{RT}{4F} \ln(p^2_{O_2}) \tag{3.17}$$

Subtracting E^1 from E^2

$$E^2 - E^1 = \Delta E = \frac{0.059}{4} \log\left(\frac{p^2_{O_2}}{p^1_{O_2}}\right) \tag{3.18}$$

shows ΔE to be simply proportional to the logarithm of the oxygen concentration ratio: oxygen concentration is directly related to the oxygen pressures $p^1_{O_2}$ and $p^2_{O_2}$. For an increase of the log-term by 1 what means $p^2_{O_2} \geq 10 p^1_{O_2}$, a potential difference of $+15\,\text{mV}$ is generated. When the electrodes are short-circuited, corrosion may occur for an increase of a few tens of mV above E_{corr} for the given metal. A cell as in Fig. 3.8 is also called a concentration cell, allowing to define the relationship

[11] This set-up can be used to demonstrate the dependence of potential on concentration.

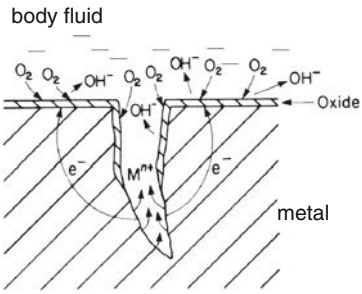

Fig. 3.9 A crevice and reactions occurring in- and outside the crevice. Reprinted with permission of Chapman & Hall; adapted from [99, p. 514]

between pressure and/or diffusion dependent concentration and potential (see for a classical treatment Kortüm and Bockris, p. 240 and ff. [97] or the modern version Bockris and Reddy, p. 1038 and 1052 [98]).

The term *localized corrosion* houses a few family members with eye-catching differences in appearance.

Crevice corrosion. Differential aeration is easily occurring in crevices. The reaction partners produced or consumed at different locations are shown in Fig. 3.9.

Where is oxygen coming from?

The partial pressure in human arterial blood is 12.6 kPa (94.2 mm Hg), in venous 5.1 kPa (38.0 mm Hg), interstitial 0.3–5.3 kPa (2–40 mm Hg) and intramedullary 1.6k Pa (12 mm Hg). The oxygen pressure outside the crevice will be about constant (homeostasis!) and the inflow of oxygen is diffusion controlled. The slower this diffusion, the higher the potential difference. It is no problem as long as the potential remains in between E_{crit} and E_{pass}.

Fretting corrosion. Definition cited by ASM [100]: *A special wear process that occurs at the contact area between two materials under load and subject to minute relative motion by vibration or some other force*. Wear exposes bare metal prone to corrosive attack and is caused by low-amplitude oscillatory displacement of one of the two pieces concerned. It is called fretting when the displacement is ranging from a few tens of nanometer to a few tens of micrometer. A classic biomedical example of fretting is the corrosion between the head of a screw fixing an osteosynthesis plate to bone. Oxygen is in all types the aggressive partner.

Tribocorrosion. This term covers surface transformations resulting from the interaction of mechanical loading and chemical reactions, which occur between elements of a tribosystem exposed to a corrosive environment. It is set apart from *fretting* by the stroke length of the rubbing partners (in real systems or in experimental testing devices) and the emphasis on the modified kinetics of the chemical reactions during sliding. The tribochemical reactions result in oxidative wear of metals, tribochemical wear of ceramics, formation of friction polymer films on surface sliding in the presence of organics and dissolution of, for example, silicon nitride, in water during sliding.

Separating wear and corrosion is clearly not obvious. Degradation where mainly corrosion is involved was the subject of this chapter, but wear became a subject in its own right. For detailed reading, we refer to [101–104].

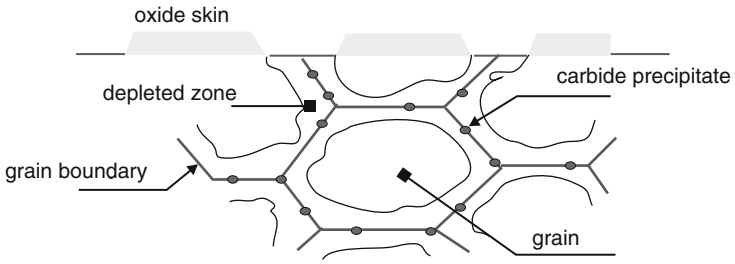

Fig. 3.10 Sensitized stainless steel: carbide precipitates at the grain boundary. The adjacent zone in the grain becomes chromium depleted

Intergranular corrosion. Pure metals or solid solutions can be produced as *single-crystal* metals for high tech applications as silicon for electronic chips or special alloys for turbine blades. Where cost does not balance benefit, all single-phase metals and by definition all multiphase alloys will be polycrystalline and built up by crystals nicely stuck together and separated from each other by grain boundaries. These boundaries display some specific properties: higher surface energy and more open structure, hence a lower bond density. Intruders from outside will find their way along the boundaries, because diffusion is easier along boundaries than diffusion inside the grains. Moreover, also elements from within the grains might find their way to the boundaries. It is self-explaining that this effect lifts up the impurity concentration in the boundary far above the analytical or average concentration of impurities: a few parts per million can end in a local concentration of 10%. Under these conditions, the alloy is said to be *sensitized*. Welding or thermal annealing can sensitize alloys. The phenomenon is visualized in Fig. 3.10.

Precipitated carbide can be distinguished in the micrograph of the CoCrMo screw in Fig. 2.6. When intergranular corrosion occurs, it can give rise to catastrophic structural failure, even though the actual loss of metal in terms of weight may be very small.

Pitting. This member of the family is recognized by the formation of holes or pits on the metal surface. In terms of weight loss, pitting is negligible compared to general corrosion but not negligible in its potential harm. Pitting starts at the critical potential E_c, where the oxide layer is breaking down. The rate of penetration may be 10–100 times the one caused by general corrosion. The pits start modestly small and are in that stage hardly detectable, but they can grow to sizes macroscopically visible and generally in great number. The reason for the excessive fast growth rate is easily explained. The pits are generally anodic and their area is small compared to the rest of the corroding piece, for example the prosthesis stem, which acts as the cathode. The consequence is obvious: the anodic current density, the current per unit area, can be orders of magnitude higher than the cathodic one.

Corrosion fatigue. Fatigue did not get that much attention till the Comet of BOAC, Flight 781, crashed off the Italian island of Elba on 10th January 1954 with the loss of everyone on board. High stresses in the corners of the window,

wrong engineering as we would say now, causing metal fatigue were finally found to be the origin of the catastrophic blow of the fuselage. Fatigue was certainly not unknown as reason for failure, but the dramatic Comet crash (followed by a second one three months later near Naples) made the engineering community extra alert to the phenomenon. Here, only mechanical stresses were involved. The failure of the hip prosthesis of the case study in Chap. 2 was caused by corrosion-assisted fatigue crack growth. In fatigue cracks fresh unprotected metal is an easy prey to biofluids and, as mentioned in the case of stainless steel, sulfur compounds are diffusing into the cracks (and along the grain boundaries as well).

Stress corrosion cracking. The sudden failure of normally ductile metals when subjected to tensile stresses in a corrosive environment is called SCC. It is the result of typically subcritical crack growth, hence under conditions where failure should not occur. Although titanium alloys were recognized for their excellent corrosion resistance, Ti-6Al-4V is also sensitive to this phenomenon. In 0.6 M KCl, the fracture toughness K_{Ic} of Ti-6Al-4V is lowered from 60 to 20 $MNm^{-3/2}$ in 0.6 M KCl solution.[12] It is the α-phase (h.c.p.), which is sensitive in this case [105].

3.3 Does It All Fit the Practice of Implants?

How does it look like in practice?

The chapter was introduced by case studies of retrieved modular hip prostheses. Gilbert and colleagues reported about modular single-alloy prostheses, both parts made of CoCrMo. In terms of simple corrosion potentials, no problem could be expected at all but it was wrong. As shown on Fig. 3.1b inside the taper and just outside the head–neck junction, grain boundary attack happened. The phenomenon is clearly illustrated in Fig. 3.10: in (b) the intergranular paths are seen and in (d) the fractured surface is partly covered with nonconducting debris, whitish in the micrograph, which was identified as carbides deposited in the grain boundaries.

In (c), pits are visible on the free surface of the stem. These pits were formed by *egression of particles* out of the surface. The origin of the pits has a mixed (electro)chemical and mechanical origin. Carbide particles of 2–300 μm were released from the surface. They were nicely located in a grain boundary and the pits would probably deepen in course of time. The egression might have been assisted by corrosion underneath the particle.

The retrieved prostheses had all stems with a porous CoCr coating entailing a few problems. On the electrochemical side, the application of a (porous) coating requires heat treatment close to the melting temperature and provokes phase segregation; moreover, the porosity increased the area of the cathode (the stem) with respect to the area of the pits (anode) with subsequent increase of the anodic current density. On the mechanical side, heat treatment may provoke voids at the grain boundaries.

[12] For more about fracture toughness, see Chap. 9.

Table 3.2 Safety of various alloy couples under passivated-aerated conditions

Couples	Safe/Not Safe
Ti/C, Ti/Co, Co/C	safe
Ti/SS, Co/SS, SS/C	not safe

C: pyrolytic carbon; *Ti*: Ti4Al6V(F136); *Co*: CoCr(F75); *SS*:316L (cold worked)

The case studies by Collier and colleagues showed another pattern. None of the retrieved single-alloy prostheses did show signs of corrosion but all mixed-alloy did after >10 months implantation time... Was the attack of the modular single alloy prosthesis as described by Gilbert a surprise, even so was the failure of the mixed alloy ones!

Electrochemical analyzes on different surgical implant materials, stainless steel 316L, Ti-6Al-4V, carbon and couples of these materials, as well as retrieved modular hip prostheses after 0, 2, 4, and 6 years implantation time were not predicting catastrophies. Pyrolytic carbon was in the 1980s one of the scrutinized partners. Pyrolytic carbon seemed in those days a promising implantation material. The combination of a cold worked SS 316L with carbon was susceptible to pitting ($E_{\text{couple}} > E_{\text{breakdown}}$), which was not the case for Ti4Al6V/C.[13] For a coupling Ti4Al6V/CoCr corrosion potentials of $-0.22\,\text{V}$ and low corrosion rates of $0.02\,\mu\,\text{Acm}^{-2}$ were predicted and verified by in vitro studies. Calculation by (3.9) predicted a loss of about $80\,\mu\text{g}\,\text{cm}^{-2}\,\text{y}^{-1}$ [106–108]. The ranking of couples based on potential are put together in Table 3.2.

A last remark on these case studies. The inner taper space is oxygen depleted and the electrochemical potential may exceed E_c for the cobalt alloy ($\sim+0.4\,\text{V}$) but less probably for the titanium alloy ($\sim+2.0\,\text{V}$). Indeed, although both faces were pitted, the cobalt alloy showed the deepest pits.

3.4 A Conclusion

The history of electrochemistry started by a biological observation on frogs' legs. Two hundred years later, the discipline served biology through its assistance in surgery, something that Volta and Faraday did not have in mind. The brief historical walk highlighted that it is not a shallow waterway that splits analytically thinking chemists or physicists from the practician introducing spare-parts in living bodies.

In the past too, many authors restrained their work to static electrochemical experiments in irrelevant media and it is still partly true today. We tend to attach

[13] The authors of the cited papers base the ranking of couples on the potential difference between the lowest critical potential and corrosion potential for the given system but call it *corrosion resistance*, a misnomer because resistance is calculated according to (3.15), see sub (3.2.3.1). Increasing values of ΔE are indicative for increasing resistance to pitting or general passive film breakdown.

more weight to dynamic measurements as they were already introduced in the late 1970s and now more than in those days feasible [90, 109]. But nobody should be blamed. Corrosion is a multifactorial process and by definition, full understanding both theoretically and experimentally requires all factors to be accounted for, "all factors" of course being the unattainable stochastic limit. The commented cases of this chapter illustrate this statement and justify the paragraph's title *It shouldn't have happened*!

Several trials are published for electrochemical modeling of passivation phenomena in tribocorrosion or by developing methods to measure wear-corrosion synergism [110, 111]. Renner and colleagues used the European Synchrotron light source to reproduce *in situ* at atomic scale the onset of corrosion. The authors studied a gold-copper alloy but their technique is applicable to a better understanding of corrosion in other materials as well [112]. Notice that their study had also an unexpected side effect: a nanostructured porous gold layer was discovered with a potential for technological applications for example for sensors.

It is clear that tailor-made materials come within reach in the near future, but corrosion control will remain a permanent concern, whatever kind of new materials involved. An estimated 3% of the world's gross domestic product is lost through corrosion.

Chapter 4
Intoxicated by Implants?

> Die Furcht vor dem *vermaledeiten Mercurius* und seiner Gefolgschaft trieb ihn auch während des Winters die Abteilungssittzungen bei geöffneten Fenstern abzuhalten.
> ... Wirkungen einer schleichenden Quecksilbervergiftung ohne die er *in jeder Hinsicht viel mehr hätte leisten können*.[1]

The chemistry of the hydrides of boron is indissolubly linked with the name of Alfred Stock. Mentioning Alfred Stock in the context of this book goes back to what happened in his schoolboy laboratory where he experimented with mercury. There probably was planted the seed for his later *hypersensitivity* to mercury. His professional work on hydrides and the development of high vacuum apparatus and other instruments implying the use of mercury in Breslau (now Wroclaw) and Berlin developed further his *erethism* or *chronic mercurialism*. He suffered from headaches, dizzy spells, memory loss and catarrh. After one of his collaborators had a tooth abscess in 1924, a toxicologist finally discovered that his collaborator's as well as Stock's disease was due to mercury poisoning. From that time on, Stock began his research on mercury poisoning and contamination, which were to span the final 20 years of his life. From this work emerged what is called the *second amalgam war*. The first amalgam war took place in the 1840s between the American Association of Dental Surgeons and those dentists who insisted on using the then new techniques of making fillings with dental amalgam. The next war was Stock's one. His fight against amalgam was based on his analytical determinations of mercury content in urine of patients having amalgam fillings.

[1] From a biography by Egon Wiberg [113, XLVI– XLIX]. The text in italics refers to parts of Stock's diary. Alfred E.Stock is born in 1876 in Danzig (now Gdansk in Poland) and died after a brilliant academic career in Breslau, Berlin, Karlsruhe and died in Aken an der Elbe in August 1946 in painful postwar circumstances. For a shortened version in English of this story: see [114].

J.A. Helsen and Y. Missirlis, *Biomaterials*, Biological and Medical Physics, Biomedical Engineering, DOI 10.1007/978-3-642-12532-4_4,

4.1 Trace and Essential Trace Elements

Except for iron, calcium, sodium, potassium and magnesium, all metal ions are present in the body as trace elements. The essential elements are listed in Table 4.1. The second column lists the average total amount of the element present in an adult person. The third column lists the molar concentration in plasma and the fourth column the average daily amount an adult person takes in.

A remark about silicon. This element is not taken up in current tables of essential elements. Its absence in the body should be quite strange as it is the second most abundant element in earth's crust (about 28%). In the context of this book, a paper by Edith Carlisle in *Science* in 1970 cannot be ignored. The author advanced strong evidence that this element is actively involved in bone formation at bone forming sites of the body, particularly in osteoid tissue. At the edge of the trabeculae with Ca contents ranging from 0.1 to 2.0%, the Si content ranges from 0.08 to 1.0%, and similar Si contents are found in periosteal areas for 0.5–15%Ca. At higher Ca contents, Si content vanishes [118]. It was probably not a simple coincidence that we observed increased Si contents on the surface of osteosynthesis plates facing the fracture site with active bone formation while Si was absent elsewhere on the plates' surface.

Table 4.1 Concentration of essential elements in humans [115, p. 12]. The ions are listed as they are expected to occur at pH = 7

Element	Total	Plasma	Daily allowance
Na^+	100 g	141 mM	1–2 g
K^+	140 g	4 mM	2–5 g
Mg^{2+}	19 g	0.9 mM	0.7 g
Ca^{2+}	1000 g	2 mM	0.8 g
$Cr(OH)_2^+$	6 mg	0.5 µM	0.1 mg
MoO_4^{2-}	9 mg	0.05 µM	0.3 mg
Mn^{2+}	12 mg	0.2 µM	4 mg
Fe^{2+}([a])	4.2 g	20 µM	10–20 mg
Co^{2+}	1 mg	0.1 µM	3 µg[b]
Ni^{2+}	1 mg	0.1 µM	170 µg[c]
$CuO\downarrow$([a])	72 mg	18 µM	3 mg
Zn^{2+}	2.3 g	20 µM	15 mg
Si			10–26[d]
HPO_4^{2-}	780 g	2 mM	1 g
SO_4^{2-}	140 g	1 mM	–
$HSeO_3^-$	5 mg	2 µM	0.1 g
F^-	2.6 g	10 µM	2 mg
Cl^-	95 g	103 mM	2–4 g
I^-	30 mg	0.5 µM	0.15 µg

[a] Fe^{3+} and Cu^{2+} are complexed by proteins. [b] Of vitamin B_{12}.
[c] Average daily intake, value taken from [116].
[d] See text.Average daily intake [117].

A second remark concerns nickel. The *Great Oxidation Event*(GOE) 2.7 Gyr ago is marked by decrease in atmospheric methane and increase of oxygen concentration, attributed to the evolution of oxygen photosynthesis within the group of cyanobacteria. According to an alternative theory, the driving mechanism could be the decrease of the oceanic inventory of nickel around that period. The methanogens, with their appetite for nickel to feed their three nickel-containing metalloenzymes, became starving, paving the way for cyanobacterial accumulation of oxygen... a minute trace with a gigantic impact on the course of evolution [119].

A third general remark. The essential elements, both trace and biochemically basic, together with the most common elements used in implants, are highlighted in the Periodic Table of Elements (Table A.2 in Appendix A).

4.2 Toxicity

By definition, essential elements do not have intrinsic toxicity. The supply and subsequent concentration in the body may, however, be *deficient*, *optimal*, *in excess*, or, beyond simple excess, harmful and *toxic*. Intrinsically, toxic elements show a negative response to any concentration, the end of the response curve being possible death. Tables are published for toxicity levels commonly expressed as *Lethal Dose*. LD_{50} is the administered amount of an element in a specified form (e.g., $CoCl_2$) for which 50% of the test animals die. Hercule Poirot, William of Baskerville, Sherlock Holmes and, of course, forensic investigators of today are well acquainted with deliberate administration of lethal doses. Acute poisoning is, however, only reported for accidental ingestion by children, intoxication during industrial accidents or in agriculture (thallium, arsenic, methylmercury). It never happened with implants: thus, the answer to the question mark in the chapter's heading is 'no' but only in as far as *acute toxicity* is concerned and that everything is more complex than it looks like, is once again demonstrated by the alarming concern about hip resurfacing (see Sect. 4.6).

The matter, however, is more complex than just acute cases and specialized tests are more relevant than knowledge of LD_{50}. The level of toxicity of different elements in kidneys is determined by investigating the reaction to salts of these elements with kidney cells of, for example, green African monkeys. In this case, the so-called CCR_{50} is determined, which is defined as the concentration of a substance generating a reduction with 50% of surviving cells in a culture of renal cells. It is just one kind of test out of many described in the literature.

Let us mention again that *homeostasis* is one of the priority articles of the *Constitution of Life*: elemental composition is not less a subject to this law than any other concentration or function:

> *Any element, be it essential or not, becomes toxic when homeostatic mechanisms are overloaded.*

A variety of mechanisms can be mobilized for this purpose.

4.2.1 Complex Formation

Forming stable complexes is a passive action to finish with intruders. The stability of a complex is characterized by its stability constant K_{stab} and calculated from the equilibrium concentrations of the reaction between metal ion M with valence $n+$ and ligand L with valence $m-$:

$$mM + nL = M_m L_n \tag{4.1}$$

and the stability constant is expressed by:

$$K_{\text{stab}} = \frac{[M_m L_n]}{[M]^m [L]^n} \tag{4.2}$$

Equation (4.2) has the same limitation as the equilibrium electrochemical potentials given in Table C.1. It is correct only at infinite dilution. For practical purposes, one should calculate the *conditional constant*, which takes into account activity instead of concentration and all other reactions co-determining the 'naked' concentration of the ion (definition of *activity*: see Appendix C). If the ligand has one or more acid functions, e.g., $-H_4$, [L] becomes pH dependent:

$$H_4L \rightleftharpoons H_3L + H^+ \ldots \rightleftharpoons L + H^+. \tag{4.3}$$

The thermodynamic K_{stab} (infinite dilution) and conditional K'_{stab} at pH $= 7$ for the complex of Ni^{2+} with glutathione are, respectively, $10^{4.0}$ and $10^{2.1}$, not a marginal difference! Workable stability constants should be calculated for the adequate pH and taking into account all other competing reactions as well, easy to say but it was and still is a daunting task. However, there is some light at the end of the tunnel: electronic databases with stability constants are available and computer programs allow to model chemical equilibrium systems (IUPAC database for Stability Constants, modeling programs such as HALTAFALL [120], MINAEQ+ (more info available on Internet); an older but basic comprehensive book on complex formation is written by Ringbom [121, 122], or available in the series on Metal Ions in Biological Systems, edited by Sigel [123]).

The undissociated compound in (4.3) was not merely an unbiased choice. Ethylenediaminetetraacetic acid (EDTA) or its sodium salt has four binding sites and is quoted as a multidentate or chelating ligand.[2] It remains after more than sixty years an extremely versatile molecule.

[2] The term *chelating ligand* comes from the old Greek word $\chi\eta\lambda\acute{\eta}$ meaning a lobster claw (or pincette-like object). A cyanide ion CN^- is an example of a unidentate ligand, having only one binding site. EDTA was developed in the 1940s and was soon introduced in the analytical chemistry lab as a selective titrant for a number of metal ions [124]. It still is the case today and, moreover, it found widespread use in medicine (chelation therapy for coronary artery disease, nephrology, detoxification agent and so on).

4.2.2 Metallothionein

A ligand is present or it is not. In every-day solvent-solute systems however, a ligand is not coming into being by the presence of the metal. Not so for *thionein*. Thionein was discovered in the mid 1950s by Margoshes and Vallée as a cadmium-binding protein responsible for natural cadmium accumulation in tissue [125]. It is a low molecular weight protein (<9 kDa).[3] with a high cysteine content (30%) and binds to both essential and toxic metal ions through thiolate bonds and oligonuclear complexes. In adult mammalian tissues metallothionein (MT) levels are low but their synthesis is inducible by metals, hormones, cytokines, growth factors and stress conditions. It is structurally divided into four distinct subgroups but the major isoforms in mammalian tissues are MT-1 and -2. In adult mammalian tissues MT is found mainly intracellularly in cytoplasm of cells [126].

Research on MT was originally focused on its interaction with zinc and the highly toxic elements as mercury and cadmium, but was later recognized as a pluripotent ligand for other metals. In Table 4.2 the first association constants of the complex with EDTA and cysteine with a selection of metal ions are given. The solubility products (as pK_{sol}) of sulfides were added to illustrate the affinity of these ions for S^{2-} or HS^{-}. The general expression for the solubility product of the simple reaction of sulfide (S^{2-}) with a divalent metal ion:

$$M + \mathrm{S} \rightleftharpoons MS \downarrow \tag{4.4}$$

is in terms of concentration, omitting for a while activities and ignoring competing reactions (H^{+} for sulfide, OH^{-} and other anionic ligands for metal ions):

$$K_{\mathrm{MS}} = \frac{[M][S]}{[\mathrm{MS}]} \tag{4.5}$$

High pK_{sol} ($p = -\log$) means that reaction (4.4) is tending to completion: the value 53 for mercury stands for one metal ion in more than an ocean of water.[4]

In real life reactions are not simple, competing reactions are always present on the party and the activity coefficients are never equal to one. The body contains many candidate and mutually competing ligands, such as transferrin, porphyrins, glycine, diaminoethane and histidine to name but a few, that reactions are going less dramatically to completion than might be expected from their thermodynamic solubility or stability constants. We learn also from Table 4.2 that the magnitude of the solubility product for sulfide and the stability constants for cysteine complexes follow in the same order, illustrating the exquisite affinity of these ions for sulfide bonds wherever the sulfide group is integrated in. The complex formation of MT explains the

[3] A Dalton (abbreviated as Da) is an atomic mass unit and approximately equal to the mass of an hydrogen atom. It is not an IUPAC unit but its use is accepted in biochemistry to express molecular masses of large molecules.

[4] For a trivalent metal ion, (4.5) becomes: $K_{\mathrm{sol}} = [M]^2[S]^3$.

Table 4.2 Stability constants $\log K_{stab}$ of EDTA and Cysteine for a selection of metal ions

Ion	Sulfide pK_{sol}[b]	EDTA $\log K_{stab}$	Cysteine[a] $\log K_{stab}$[b]
Fe^{2+}	17	14.3	
Fe^{3+}		25.1	
Co^{2+}	21	16.3	9
Ni^{2+}	22	18.6	10
Cd^{2+}	26	16.5	10
Ag^{+}	50	7.3	15
Hg^{2+}	53	21.8	14

[a] Values taken from [127]

[b] pK's and logK's are rounded to the nearest integer

accumulation of metal ions in tissues. It is a tool for sequestration, making metal ions unavailable to exert toxic effects and contributes to metal homeostasis of the body.

Studies on MTs remain an active field till today (to name a few papers from Prof. De Ley's laboratory:[128–130]). MTs play an important role in the maintenance of body's immune system. Although the research emphasis is on the role of zinc and copper, other trace elements entering the body are, as already stated, competing partners for the reaction with thionein (homeostasis!). A recent review of metalloproteins has been published in *Nature* (**460**, 813–862, 2009).

4.2.3 Multiple Interactions

Electrochemical potential. The high stability of some complexes encompasses a few consequences. The redox potential of M^{n+}/M is depressed to more negative values and are more eagerly oxidized. The more metal oxidized, the more metal ions dissolved in the body fluids. Part of these ions are evacuated through urine and feces, part travels around, either as ion or as complex, occasionally accumulating in target tissues for some ions. The sensitivity of stainless steel to corrosion by sulfide as discussed in Chap. 2 originates in the affinity of nickel to sulfide.

Rate of excretion and accumulation. The decrease of body concentration c as function of time t can be estimated from pharmacokinetic models but it is not a straightforward business because of the complex interplay between absorption, distribution, biotransformation and excretion. The overall excretion process can be expressed by a general differential equation:

$$-\frac{\mathrm{d}c}{\mathrm{d}t} = bc, \tag{4.6}$$

where b is the elimination constant. Rearranging and integrating between zero and t and c_0 and c_t gives:

$$c_t = c_0 \mathrm{e}^{-bt} \quad or \quad \ln(c_0/c_t) = bt, \tag{4.7}$$

which allows to calculate the biological half-life time $T_{1/2}$, i.e., the time needed to reduce the concentration c_0 (blood, serum, tissue, ...) to half its value; it is also called biological half-life (B.H.L.). Radioactive decay follows the same logarithmic law.[5] Make in (4.7) (logarithmic form) c_0 equal to $2c_t$: $T_{1/2} = \ln 2/b = 0.693/b$ and evidently $T_{1/2}$ is inversely proportional to the constant b.

An obvious and invaluable tool for the study of kinetics and dynamics of administered chemicals, be it oral administration of drugs, inhaled dust from the environment or the steady supply of ions dissolved from implants, is mathematical modeling.

Modern mathematical models exist; good references to these techniques (SAAM/CONSAM computer modeling) are a book edited by Novotny et al.: Mathematical Modeling in Nutrition and the Health Sciences [131], on WinNonlin software (v5.2) commented by Gabrielson and Weiner [132] or [133]. These modelling programs have applications wider than just pharmaceutical drugs (what they were principally developed for) but in general for studies of any other circulating molecules or ions in the body. These programs *digitalize* the concentration-time relationships based on compartmentalized[6] models and try to fit the model to the (experimental) plasma-concentration vs. time function. The result allows to derive parameters as half-life and clearance in single dose applications or in systemic supply by corroding implants. Clearance studies should at least at first sight be simpler. Elimination from the body follows two routes: either metabolism or excretion. A chromium(III) ion, for instance, is not metabolized but just excreted.

Selectivity, interdependence. A complexing anion may reduce the absorption of iron from vegetables or excess of Zn^{2+} may inhibit Cu^{2+} absorption. Complex formation is a *passive process*. We mean by this statement that a cell-mediated mechanism is not necessarily involved. The operating selectivity of the ligands is simply explained by the widely differing stability constants, illustrated for a few ions in Table 4.2. The itai–itai disease, reported in Toyoma (Japan) in 1955, was attributed to high cadmium accumulation in rice, the staple food for the local population. The balanced daily allowance of calcium and other essential elements, which was definitely not the case in Toyoma, explains probably why this disastrous disease (osteomalacia, osteoporosis) is not reported for the population of an industrial area like Balen in Northern Belgium and the adjacent Dutch part [134]. The soil in that region is historically contaminated by cadmium through years of uncontrolled exhaust by the zinc winning and refinery industry. By the same token, the rare cases of toxic effects by implants might be attributed to the same balanced daily allowance of essential elements, counteracting toxic effects and supporting the body's homeostasis. It all does not mean that the subject does not deserve sustained

[5] To calculate the half-life time of radioactive decay, substitute in (4.7) c for N, the number of decaying atoms.

[6] In physiologically based pharmacokinetic modeling (PBPK) *compartments* correspond to discrete tissues or groups of tissues with discrete properties of blood flow, volume, metabolism, etc.

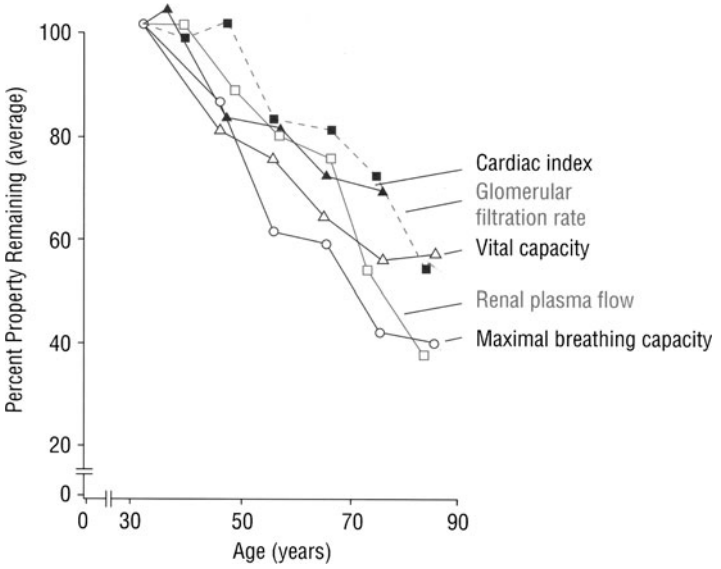

Fig. 4.1 Many physiologic functions diminish with increasing age during adulthood. Reprinted with permission of Williams & Wilkins [135] Fig. 15-4

attention. *The number of people having implants as well as patient's survival rate is steadily increasing which means, that detrimental effects might only become visible in the decades to come.* An example below will illustrate such a potential case.

Age. Time is one of the basic units in science and active on different time scales: subsecond range for most chemical reactions, seconds or less for repair of a protective oxide layer in corrosion, minutes to days for wound healing, years for permanent implants.[7] The latter are by definition intended to remain for long periods of time in the body and thus, time, or *age*, is of particular interest in the context of this book. If the abovementioned multiple interactions are known for an average person of average age, they do not remain necessarily constant with age. Permanent implants are inserted in the body at increasingly young age as is seen for heart valves, stents, hip joints ... The graph of Fig. 4.1 shows convincingly the effect of age on a few parameters.

Let us focus for a while on the glomerular filtration. Homeostasis of the body can only be maintained if it succeeds in one way or another to eliminate excess or noxious concentrations of ions or compounds. One of these exit ways is by *renal clearance*, the term clearance being the most useful concept in pharmacokinetics for the evaluation of elimination mechanisms. Roughly 25% of cardiac output, about $1\,\mathrm{l\,min^{-1}}$ blood, passes along the kidneys. Arterial blood enters the glomerulus, a

[7] The International System of Units defines seven basic units: length, mass, time, ampère, temperature, mole and candela.

capillary knot within Bowman's capsule in the kidney's 'ultrafiltration unit'.[8] Ions and compounds with molecular mass <2,000 pass through this filtration unit. The ultrafiltrate flows through collecting ducts to the ureter. When the rate of renal excretion is directly proportional to the plasma concentration c, most probably the case for ions or low molecular weight complexes (see our remark above on elimination of metal ions), then:

$$-\frac{\mathrm{d}c}{\mathrm{d}t} = CL_R c \tag{4.8}$$

the renal clearance CL_R is constant. From this constancy follows the assumption of proportionality between urinary and plasma concentration data. The data of Table 4.5 might be a good example. Although the data for urine and serum (blood plasma without blood clotting factors and fibrinogen) are expressed in other units, the trend is similar. The data for urine should have been but were not corrected for age, sex and weight, parameters to which creatinine clearance is sensitive; it declines almost linear with age from 30 years on (see [135–137] and the comprehensive book by Brookbank [138]).

Age was selected here as one parameter to keep an eye on in long-term implantation but other parameters as distribution over tissues and body liquids, absorption kinetics and so on will become of growing importance in predicting long-term effects of implantation.

Thus once again, the answer to the chapter's heading should be nuanced: acute toxicity is excluded; systemic toxicity will depend on the balance between sequestration capacity of any kind and rate of metal dissolution (corrosion current, rate of dissolution).

4.3 Immunotoxicology

What follows is a nutshell version of immunologically mediated disorders induced by metal ions in humans. Various metals are known to induce disorders, for example contact dermatitis by nickel and chromium. Phagocytic cells, macrophages, monocytes are part of a battery of mechanisms attempting to degrade, accumulate and/or export all substances not recognized as *autologous*. Metal ions, complexed with low molecular weight proteins, can be considered as a special type of antigens, called *haptens*. Haptens are small molecules which can, although indirectly, elicit immune response by the body. 'Indirectly' because haptens are not recognized as antigens by T lymphocytes (T cells). They need to be digested or processed by antigen processing cells (APC): dendritic or macrophage-monocytes and Langerhans cells. The peptides derived from these antigens are recognized by T cells, which subsequently produce various cytokines, and by B cells.[9] Helper cells are vital to

[8] The branching of the renal arteries exhibits fractal distribution.

[9] B cells are together with T cells the main lymphocyte cells in the body.

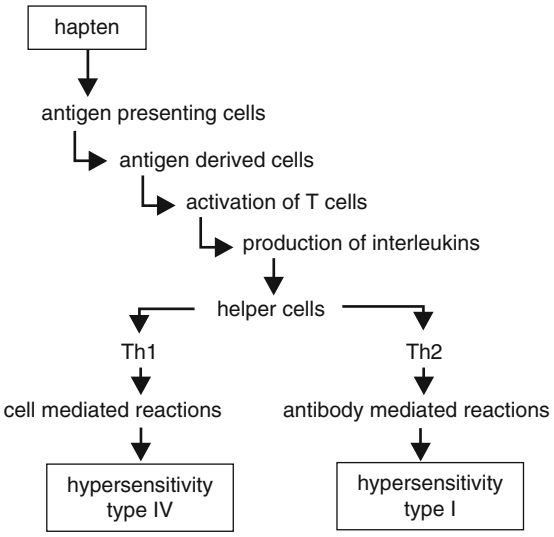

Fig. 4.2 Adaptive immunity: tissue response at contact with a hapten

cell proliferation and secretion of antibodies (immunoglobulins) by mature B cells. Differentiation of T cells leads to two types of helper cells, Th1 and Th2. Th1 cells produce IL-2, gamma-interferon (IFNγ), tumor necrosis factor (TNFβ), angiogenic, fibroblast-activating and transforming growth factors (the latter stimulating the synthesis of extracellular matrix). Th1 cells are responsible for delayed hypersensitivity, called type IV. This type is probably involved in metal-mediated adverse reactions. Th2 leads to type I, II and III hypersensitivity through the production of immunoglobulins(IgE) and interleukins IL-4 and IL-13. These types are responsible for immediate hypersensitivity. The quotation *delayed* means that the sensitivity is manifested after more than 12 h, *immediate* means manifested after minutes to hours following implantation. The immunological pathway is summarized in Fig. 4.2.

The clinical manifestation of immunologic hypersensitivity is *allergy* or *intolerance*. Allergy is determined as an overreaction upon contact with a foreign substance, given a genetic disposition and/or previous exposure. Intolerance is similar except that it is independent of previous exposition. Type I hypersensitivity is an interaction between an allergen and immunoglobulin E (IgE), which stimulates the release of histamine. It is exceptionally occurring with metals. Allergy to proteins, associated with air-dispersed particles released by surgical latex gloves, is an example of type I hypersensitivity, a kind which is in some cases life threatening.

Type IV is cell-mediated allergy. This means that a previous contact with the allergen has activated and specialized T-lymphocytes that are brought into circulation: T cells are the mediators here to macrophage activation. Upon new contact with the allergen, inflammatory mediators are released. These processes are externalized as, for example, eczema. The case of mercurialism, with which we started this chapter, is an example of a type IV hypersensitivity.

Another division of the warfare arsenal against foreign intruders as discussed thus far is the *complement system*. A one-liner saying states that 'antibodies identify targets, but the complement system is destroying them'. It is an intrinsic and important part of the innate immune system. The definition is that the complement system is a biochemical cascade, which helps to clear pathogens from an organism. Inappropriate activation of the complement system by endoprosthetic devices is described for cellulosic Cuprophan membranes used in hemodialysis and for some other extracorporeal devices. The complement system will of course be activated by tissue- or collagen-based materials harvested in insufficiently related species, e.g., porcine heart valves. For further reading, see [139] and [140], pp. 293–354.

4.4 Gulliver and the Lilliputians

The action of macrophages, antibodies and other defense weaponry of foregoing sections can be understood as long as cell-sized objects such as bacteria or metal ions are put on the stage. To be experienced by the poor little tissue cells, however, the giant body of the implant is above their individual abilities: Lilliputians looking at the sleeping Gulliver. When Gulliver woke up on the beach, he found himself tied up by the collective effort of the 15 cm-tall Lilliputians . . . a worst case scenario for an implant: tied up by collagenous ropes.

Bacteria and small foreign bodies can be phagocytized, implants cannot, a matter of scale! Comprehensive treatment of host reactions to the wide variety of biomaterials for soft and hard tissues (cardiovascular, orthopedic, dental, etc.) would be a precarious enterprise. Therefore, the following report is restrained to a diagonal reading through a sequence of events happening to a hip stem implanted in a femur and the response of the injured tissue. The sequence is schematized in Fig. 4.3.

The first minutes to days. The surgical access to the proximal part of the femur through skin and muscles, removal of the head and reaming the femoral canal elicits an immediate tissue response: *acute inflammation*. Extravasation of plasma proteins and fluid causes swelling, ((o)edema). Simultaneously, polymorphonuclear leukocytes (PMNs) are migrating to the site of the trauma.[10] The driving force is said to be a chemical gradient (<*chemotaxis*). The implant surface is recognized through serum factors, called *opsonins*, adsorbed on the surface. As stated above, phagocytosis of the implant is not possible but *frustrated phagocytosis* may occur: release of leukocyte products, which may degrade the material. Thioneins also become immediately part of the emergency battery, secreted at the site by PMN and other cells hurrying to the place of calamity.

[10] It is an alternative term for a category of leukocytes or white blood cells, namely *granulocytes*. They all possess irregular multilobed nuclei, from where the term derived. Another category of leukocytes are the *mononuclear phagocytes* or *monocytes*.

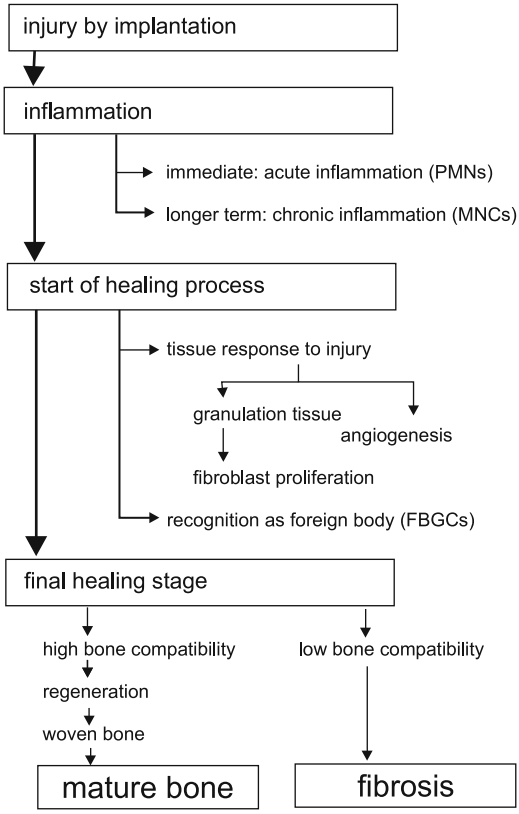

Fig. 4.3 Evolution of tissue response to implant injury and implant

Days to years. Lasting inflammatory stimuli like (micro-)motion lead to the chronic version of inflammation. The presence of mononuclear cells (MNCs) and macrophages at the implant site is the witness of chronic inflammation.

From day one on. Tissue site. Healing is initiated by the proliferation of monocytes, which are turned into macrophages on entering the wound bed. Activated fibroblasts become preponderant at the site and they synthesize and secrete the extracellular tissue, mostly fibers of collagen and elastin. The whole ensemble of cells, blood cloths and so on initiate the formation of granulation tissue 3–5 days postsurgery. The process is accompanied by the formation of small blood vessels (*angiogenesis*), the logistic vehicles for supplying food and energy. Angiogenesis is stimulated through factors secreted by Th1 cells. Tissues gradually remodel and resume their normal strength between 20 and 100 days.

Once the implant is recognized as a foreign body by a complex interaction with factors adsorbed on the surface, a foreign-body reaction starts. It is made visible by the appearance of giant cells (FBGCs) and whatever other cells are present in granulation tissue. The further development of this reaction is determined by the surface properties of the implant.

Days to years: implant site. Distinction should be made here between surfaces with high bone-compatibility and low bone-compatibility; in-between exists a grey zone showing a mixed response. In the scenario of low bone-compatibility, the unwelcome guest is finally sequestered by fibrous capsulation. The latter consists of a layer of an extracellular matrix of collagen fibers, more or less dense, roughly parallel to implant's surface, poorly seeded with cells (Fig. 4.4).

Tissue near the interface is populated with multinuclear foreign-body giant cells (Fig. 4.5).

This reaction is common for polymer implants and for metals with inappropriate surface treatment. Inappropriate stress conditions, as is the case in stress shielding, may lead to necrosis by strong phagocytic activity. For soft-tissue implants, the encapsulation is generally not hindering their function. For orthopedic implants, however, fibrosis severely affects the stability of the implant, leads to loosening and makes revision surgery necessary.

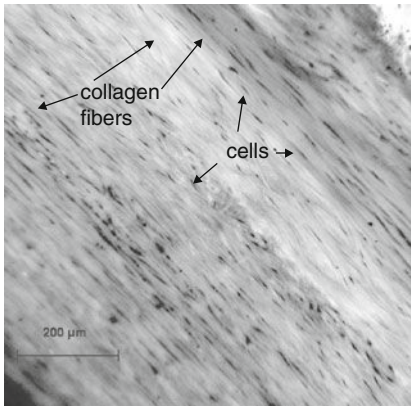

Fig. 4.4 Fibrous tissue: collagen fibers sparsely seeded with fibroblasts. Photo by S.Jaecques

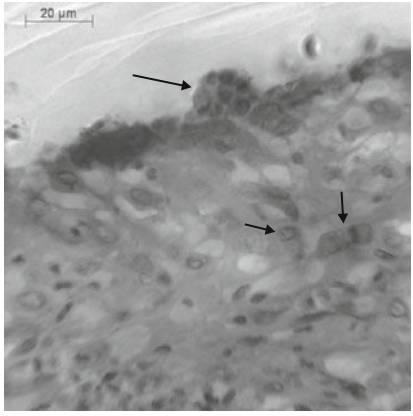

Fig. 4.5 Foreign body giant cells (*arrows*). Photo by S.Jaecques

The better fate is reserved for the first category. High bone-compatibility is obtained for implants coated with hydroxyapatites, bioactive glasses, oxidized titanium alloys, tantalum, some polymer implants. The step, indicated as *regeneration* in Fig. 4.3, might not be the adequate term but it points here to a process of new bone generation, leading to osseointegration. Initially, a kind of lamella-shaped bone is formed, *woven bone*, and is followed by the formation of osteons. Randomly orientated bundles, easily visible under polarized light, are the characteristic microscopic features of woven bone (Fig. 4.6). The bundles are composed of cells, overwhelmingly osteocytes, and an intracellular collagen framework, permeated by mineral salts.[11]

This mix evolves into concentric circles around neurovascular canals to form osteons (Fig. 4.7).

When no adverse reactions are elicited, tissue can either ignore the implant's presence (indifference), or react positively. This is the case when an alloy is,

Fig. 4.6 Cells and interfaces: woven bone (micrograph taken under polarized light). Photo by S. Jaecques

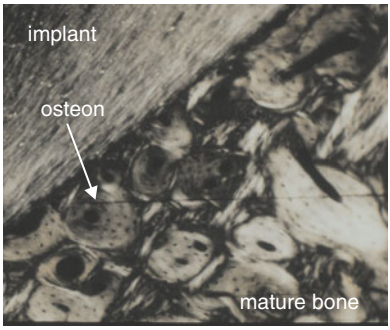

Fig. 4.7 Mature bone: micrograph taken under polarized light. For the structure of osteons, see also Fig. 2.14. Photo by S. Jaecques

[11] Osteocytes are derived from osteoblasts.

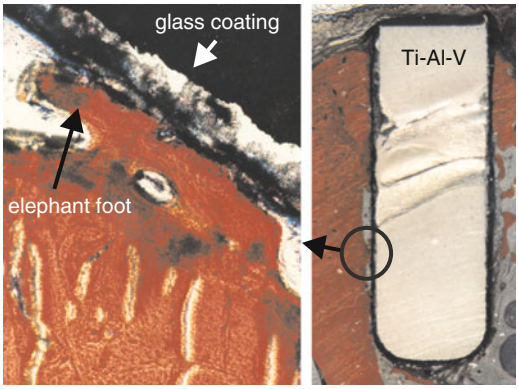

Fig. 4.8 Titanium substrate coated with bioactive glass, which makes the surface osteoconductive. Mature bone is formed along the glass surface. Right: Ti-Al-V rod inserted in a beagle's jaw ($d = 3$ mm); the encircled spot is magnified in the left picture

for example, coated by calcium hydroxyapatite, the main inorganic component of mineralized bone, or bioactive glass. Figure 4.8 illustrates what will happen. Represented is the result of a rod implanted in the jaw of a beagle. Where it is in apposition along the jaw, new bone is growing along the surface, a process called *osteoconductivity*. The shape of the neo-formed bone resembles an elephant foot and is often called as such. This is part of an experimental study on the application of bioactive glasses by plasma-spraying [141, 142].

4.5 Sensitivity to Metal Implants

About 10–15% among the general population is sensitive to nickel, cobalt or chromium but with Ni having the highest sensitivity (>10%). The prevalence of metal sensitivities to one or combinations of Ni, Cr and Co is for patients with well-functioning implants roughly double that of the general population (25 vs. 10%), and four to five times that for patients with poorly functioning implants as reported by 60%. The weighed averages in Table 4.3 are distilled from a paper by Hallab and colleagues who summarized the results cited by a number (N) of authors [143]. Notice, however, that the association of patients to well- or poorly functioning prostheses is not proving causal effect and a number of parameters were not specified (preexisting sensitivity, ...). The outcome is as such not unexpected: wear and corrosion provoke anyway more metal dissolution than well-fixed prostheses. Sensitivity is sex-determined: in a total of 5.3% sensitivity to nickel in the general population the vast majority are women. About 30% of patients with aseptic loosening of metal-to-metal total hip arthroplasties showed sensitivity to cobalt [144]. The diagnosis to metal sensitivity was/is done for most of the data before 2000 by patch testing. Sensitization is frequent in the general population but remains after all limited in orthopedic surgery, definitely with modern prostheses. Moreover, the coincidence of sensitivity and poor implant function is not a prove of causality!

Table 4.3 Estimated (weighed) average percentages of metal sensitivity to nickel, cobalt or chromium or combinations reported for the given periods by N authors on a grand total of n patients: average for general population, for patients having well-functioning prostheses and patients with poorly functioning prostheses

Group	Period (N)	Patients n	Sensitive average %
General population	1993(1)	>500	>10
Well-functioning prosth.	1974–1981(8)	556	∼25
Poorly functioning prosth.	1974–1993(7)	315	∼60

Contact dermatitis, also type IV hypersensitivity, is fortunately more common than implant-related sensitivity: wrist watches, necklaces, earrings. But it can also go the other way round. Tilsley and Rotstein (Australia and Tasmania) reported in 1980 on five cases of patients, where the implant induced contact dermatitis to watches, earrings or bra clips containing nickel, chromium or cobalt [145].

Let us have a look now at a few cases for response to the most common types of alloys.

We conclude this section by citing a recent paper in *Nature*, where the authors stress the key role of metalloproteins in most biological processes and state that:

> Metal ion cofactors afford proteins virtually unlimited catalytic potential, enable electron transfer reactions and have a great impact on protein stability [146].

The cited paper is discussing only microbial metalloproteomes and focuses on metals assimilated by a microorganism (*Pyrococcus furiosus*) and the identification of its cytoplasmic metalloproteins. A great number of protein fractions associated with elements like cobalt, zinc, iron, nickel, zinc, tungsten, molybdenum, and vanadium did not match any known assignation. These observations substantiate our concern about the potential long-term effects and/or toxicity of major and/or minor elements present in currently implanted materials.

4.5.1 Stainless Steels

Nickel. Mid of the 1970s a surgeon had inserted a stainless steel pin in a broken clavicula of an adult female patient (own case study). Two days later, the pin had to be removed because the patient suffered from a severe atopic eczema. The analysis we performed on a freeze-dried biopsy of this clavicula showed extremely high concentrations of nickel and chromium but nickel is proportionately more than its concentration in the alloy: 325 ppm of nickel for 250 ppm of chromium. Average values for freeze-dried tissue (facie lata) near a stainless steel hip stem are for nickel 6.5 and chromium 5.1 ppm, to be compared to 0.2 and 0.3 ppm, respectively, for reference tissue [147]. It illustrates the affinity of tissue for nickel. This extreme case was attributed to highly stimulated production of thioneins by this patient.

Unfortunately, the feasibility of an analytical determination of thionein was in those days beyond the lab's reach.

The high nickel levels just reported forces to a parenthesis on statistics. If a series of samples is analyzed and concentrations, not necessarily as aberrant as those just reported are present in the cohorts, *blind statistics* will remove these values as *outliers*. However, it might be for a serendipitous scientist a fruitful hint!

Hypersensitivity to nickel is not uncommon and clinical aspects are easy to recognize. Nickel subsulfides (αNi_3S_2) are carcinogenic after phagocytosis but soluble Ni(II) in nontoxic concentrations is not (or weakly) carcino- or mutagenic.

Most of the discussion of metals was directly or indirectly referring to load-bearing applications. A more gentle application was the use of stainless steel stents. Coronary stenting is a current practice in cardiology. In-stent restenosis is a complication which impairs the success of stenting. Delayed hypersensitivity to nickel and molybdenum was suspected to be part of the inflammatory process and one of the triggering factors in restenosis, an obvious suspicion. However, despite the intense contact of blood with the device, restenoses were predominantly observed in patients with negative patch test to nickel [148]. Is it simply explained by damage of the stent's surface by wear and/or corrosion?

Chromium. The pure metal is mainly used in the plating industry and in corrosion-resistant alloys. Hypersensitivity to chromium is not frequent. It is mainly known from occupational allergies (cement industry) and the most common source of allergy is the leather of shoes (chromium sulfate is used in the final stage of tanning and increases the average chain length of collagen). Although the sensitivity to this element is not frequent, below we report on one. The radioactive isotope ^{51}Cr has been used extensively in medicine for labeling cells in vivo ($T_{1/2} = 27.7d$) and, at least to our knowledge, no allergic reactions were accompanying this application.

The most stable oxidation states of chromium are Cr(III) or Cr(VI).[12] Under physiological conditions (pH = 7.4), Cr(VI) exists mainly as the tetrahedral chromate ion CrO_4^{2-}. Under physiological conditions, it is a fairly strong oxidant:

$$CrO_4^{2-} + 4H_2O + 3e^- = Cr(OH)_3 + 5OH^- \tag{4.9}$$

with $E_0 = -0.13$ V. Target tissues after intravenous exposure to Cr(VI) and Cr(III) are liver, kidneys and lungs. Cr(VI) is taken up by erythrocytes and becomes bound to hemoglobin. Cr(III) is bound to serum proteins. Cellular uptake of Cr(III) is very poor, whereas Cr(VI) passes the cell membrane by simple diffusion. Chromates were known to be carcinogenic for workers in the plating industry. However, chromium dissolved from alloys, either by oxidation of the metal or by dissolution of the oxide skin of the metal or alloy, is Cr(III). If Cr(VI) is present (oxidized by peroxides?), it is metabolized by substances such as ascorbic acid, thiols, glutathione and many other reducing agents Cr(III) forms thousands of octahedral complexes with O, N, S, C and halides as donor ligands and will travel through

[12] The oxidation state of elements are given in Appendix A.

Fig. 4.9 A patient with severe allergy to cobalt. Courtesy Prof. J.-P. Simon

the body as complex. The most important route of excretion is through the kidneys. Notice, however, that the excretion pattern is complex: whereas nickel and cobalt are mainly excreted in the urine, chromium is only slowly released through both feces and urine [149].

Only a restricted number of malignant tumors at sites of metal implants were reported but the link with chromium or ions such as nickel, manganese or others is not clear [150].

4.5.2 Cobalt–Chromium Alloys

A lady suffered from severe atopic allergy after implantation of a CoCr hip prosthesis (Fig. 4.9). After patch testing, the allergy was attributed to cobalt. In these alloys, chromium ranges from 19 to 30%, nickel 2.5–37% and the balance is cobalt (see Table 2.3).

Another case is shown in Fig. 4.10: a profound skin rash all over the body as a result of chromium allergy two months following implantation of a femoral component made of a CoCr base alloy.

The pits seen in Fig. 3.2 were about 15 μm deep and, calculated from the topography of the corrosion sites, an estimated total amount of material of 500 mg was lost to the body in 5 years or some 270 μg/day. This figure is comparable to the average daily intake for nickel and far more than for cobalt and chromium (see Table 4.1).

Cobalt. Cobalt is an essential element and vitamin B12 is the most important biological cobalt compound. Administered intravenously, the LD_{50} is 10–20 mg/kg body weight. A well-documented story and series of case studies on cobalt toxicity exist but coming from a fairly unexpected corner. The story seems to begin with the advent of automated dish washers and synthetic detergents leaving a film on glass. Tap beer poured in such a glass leaves no foam on the beer, spoiling the

Fig. 4.10 Allergy to chromium two months following implantation of a cobalt–chromium alloy-based femoral component. Courtesy Prof. J.-P. Simon

artistic pleasure of the real beer drinker. The foam could, however, be stabilized by adding cobalt chloride to the beer [151]. Due to fatal cardiomyopathies and thyroid changes (inhibition of iodine uptake by Co^{2+}) in heavy drinkers, the addition to beer stopped in 1966: doses of 10–20 mg ingested daily by heavy drinkers were fatal [145, 152, 153]. Doses of 10–20 mg, however, should not be fatal, so there was more than just dose. The story is probably similar to what was told about cadmium in Sect. 4.2.3. These patients did definitely not have a healthy diet resulting in a deficient intake of potassium, calcium, magnesium, iron, zinc, vitamins, etc. This condition disturbs the balanced competition between ligand molecules. Cobalt, similar to nickel, reacts with $–SH^-$ groups, blocking for example the decarboxylation of pyruvate in the citric acid cycle. The health problem would probably have been attenuated by another way of life.

Contact allergy to cobalt is reported to affect 1% of patch tested individuals in Sweden. An adult person may contain up to 1 mg which means that this element does not accumulate. Daily uptake substantially less than 3 μg leads to vitamin B_{12} deficiency with consequences as pancytopenia (reduction in the number of red and white blood cells and platelets), injury of the peripheral nervous system, etc.

The body's cobalt economy is a perfect example of what was said in the beginning of Sect. 4.2: *elements may be deficient, optimal, in excess or (fatally) toxic*. It is clearly essential that the response to either side of the optimal concentration is harmful, if not fatal. Although cobalt is supposed not to accumulate and the incidence of allergy is low, the case of Fig. 4.9 tells that the element is not always innocent.

Molybdenum. With its average concentration of 10 µg/l (=10 ppb), molybdenum is 20 times more abundant than zinc, 100 times more than copper, 100 times more than tungsten and 3,000 times more than cobalt in modern oceans (in geological terms!) on earth. Of course, we do not drink sea water but it shows that, somewhat unexpected, molybdenum is the most abundant transition element in that huge aqueous reservoir. Its most common oxidation state in aerobic conditions is VI and present in solution as the very soluble alkali molybdate ion MoO_4^{2-}. Two and a half billion years ago, when oxygen started to accumulate in the atmosphere and oceans, MoS_2 got oxidized and solubilized as molybdate, thereby abundantly available to emerging forms of life on Earth and incorporated into metalloenzymes (see also Chap. 6). Nitrogen enters the biological cycle catalyzed by molybdenum enzymes. They are key catalysts in the nitrogen and sulfur cycle but play only a specialized role in the carbon cycle [154]. An adult human body contains around 9 mg molybdenum (Table 4.1).

Molybdenum is a newcomer in the list of essential elements. The enzymes xanthine (1953), aldehyde- (1954) and sulfite-oxidase (1971) have a molybdenum-organic complex as cofactor. In particular, the sulfite-oxidase, critical for human health, established the role of molybdenum as essential element [155]. Molybdenum has a standing and increasing reputation as metal nucleus in many catalysts. It is witnessed by a very recent paper on a highly efficient Mo-based enantioselective catalyst for alkene metathesis and, mentioning *enantioselectivity* is a trigger for ringing the bells for biologists [156]. When solubilized from a Co-Cr-alloy, molybdate is the most probable way to enter tissue and body fluids.

Not enough data are available for establishing a clear picture on the toxicity of Mo. As upper intake level is accepted a value of 2 mg/day (Institute of Medicine, Food and Nutrition board, USA). This value is somewhat in contradiction with observations on workers in parts of Armenia, where daily intakes of 10–15 mg/day resulted in some gout-like symptoms. In a study on molybdenum metabolism, an efficient human homeostatic mechanism was demonstrated in a paper by Thompson and colleagues [157]. The B.H.L. ($T_{1/2}$) in plasma after dietary supply of Mo was 28 min. Notice that for this study the stable isotope ^{100}Mo, the isotope of Mo with atomic mass 100, was used. The application of stable isotopes in biochemical tracing instead of radioactive isotopes became feasible by the easy accessibility of mass spectrometers. The paper of Thompson and colleagues is a nice example of the practice of biokinetic mathematical modeling with a good agreement between observation and simulation [131, 158].

Tungsten. This element was overwhelmed in geological times by molybdenum, in line with the atmospheric changes that allowed the molybdate concentration to increase. Tungsten plays only a specific role in the carbon cycle. Tungstate is also the way it is entering tissues after oxidation. Alkali tungstates, WO_4^{2-}, are soluble, alkaline earth tungstates and most others are not. It is chemically similar to molybdates, as may be expected from its place in the periodic table of elements Table A.1. About 70% of intravenously administered tungstates have a B.H.L. in blood of 35 min, 25% of 70 min and the remainder of 5 h. In tissues accumulation is observed in kidney, liver and spleen, but the major retention site is bone, where

it replaces phosphate. Although similar to molybdenum, W acts antagonistically to Mo, decreasing the sulfite and xanthine oxidase activity. It is also proved to accelerate the development of mammary cancer in rats but is not, in as far as we know, documented for humans [159].

We are not aware of recent epidemiological studies in humans or other studies on tungsten that allow to make assumptions on implant-related adverse effects. Both Mo and W have a quick turn-over in tissue and blood. Problems with these metals when oxidized from an implant alloy are not expected. They were discussed at some length here because, in particular, molybdenum is part of an important enzyme cofactor and tungsten acts antagonistically to molybdenum.

Manganese. This element is in stainless steel as well as in CoCr alloys a minor key element but present in concentration below 2%. It is biologically an essential element and acts as a cofactor in many enzymes. Overt signs of intoxication occur after months to years and it is known and extensively documented for persons who get intoxicated by inhalation of airborne manganese particles.[13] The initial expression of intoxication is not nothing and characterized by psychiatric disorders known as *manganism*, often ending in an irreversible brain damage. Most of the data on levels of tolerance are relative to inhalation. Data on $T_{1/2}$ after intravenous administration are not known. Accumulation in the body or incidence of any deleterious effect attributed to implant-related manganese remains for the time being unclear.

4.5.3 Titanium Alloys

As discussed in Chap. 2, the contact of tissue with titanium implants is with the oxide surface layer. Wear debris is composed mainly of TiO_2. A serious chemical effort is needed to dissolve this oxide but, as already stated, the body is an efficient chemical war machine. The attack is occasionally wear-assisted in load bearing implants and, in case of long-term implants, the body has ample time to act.

Titanium is not an essential element and is considered as biologically neutral. It is the ninth most abundant element in nature and is present everywhere in nature and in our body at low concentration. So, it is not surprising that the daily intake is something like 0.3–1 mg. The tissue concentration of patients bearing titanium implants is enhanced but the element has no intrinsic toxicity. The main if not the only concern is wear debris, but that will be discussed later. So, no intrinsic toxicity problem with implants made of pure titanium.

Aluminum. Aluminum is another history. Till today, the most widely used titanium alloys contain aluminum: Ti6Al4V, Ti6Al7Nb (for composition, see Table 2.3). Ion release in vitro varies strongly with composition of contacting solution. A polished surface of Ti6Al4V is quasi-inert in contact with Hanks', a *simulated body*

[13] Manganese dust in mines, as oxide or hydroxy-oxides, but a recent airborne threat was the use of a manganese containing compound as antiknock agent in gasoline.

Table 4.4 In vitro dissolution of polished discs of Ti6Al4V at pH = 7.6 in (a) Hanks' (H), (b) H + EDTA, (c) H + l-leucine, (d) H + citrate was followed over a period of 12 weeks; exposed surface was 5 mm^2/ml supernatant; concentrations of the supernatant solution at weeks 2 and 12 are given in ppb

Metal	a	b	c	d
Ti	<4	23–234	<4	156–752
Al	<2	79–238	<2	51–339
V	<2	<2	<2	6–357

fluid (SBF).[14] But in an in vitro simulation experiment, addition to Hanks' of a selection of complex forming agents changes the picture completely. EDTA has no biologic roots but is a 'wide spectrum' complex former; l-leucine is an essential amino acid and present in plasma; citrate is an intermediate in the citric acid cycle and a good complex former.[15] The results are summarized in Table 4.4.

Simulated body fluid was and still is today widely used to simulate in vitro the chemical behavior of materials in vivo. It is instructive to analyze the data of Table 4.4: (1) they demonstrate that different dissolution chemistry is provoked by subtle changes in composition of the simulated body fluid, so do not trust too much tests based on too simple simulations; (2) the dissolution rates are very much dependent on the ligands the alloy is in contact with and thus, time is an important parameter. This explains the in vivo observation that the relative concentrations in solution do not reflect the composition of the alloys.

Aluminum is a nonessential element but there are enough question marks about its interactions with the body to remain wary when it circulates in our body. Healthy individuals have formidable barriers toward aluminum absorption. At physiological pH, it exists as the highly insoluble $Al(OH)_3$ and at first sight unavailable for interaction with the body. A characteristic is that, aside from most essential elements, the rate of ligand exchange in and out the coordination sphere is slow, for instance ten times slower than Fe^{3+} or a ten million times slower than Ca^{2+}. Once linked to a ligand it starts circulating in the body. The most likely vehicles are citrate and transferrin. Transferrin has the highest affinity for Al and its ligand sites are only for 30% occupied by iron. This does not preclude that citrate acts as a go-between and presents Al to transferrin. It accumulated, however, in bone tissue of renal failure patients. Already in 1972, neurological disorders in chronic hemodialysis patients, termed *dementia dialysis*, were recognized as a consequence of aluminum accumulation in the dialysate. The elevated occurrence of dementia in England, United States and Scotland were also attributed to aluminum contaminated tapwater [160–164]. The most intriguing aspect of the element's toxicity is the potential implication in the pathogenesis of Alzheimer's disease. However, the active role of aluminum in this pathogenesis is not confirmed though not entirely excluded either.

[14] The composition of Hanks' is tabulated in Appendix D.

[15] The citric acid cycle is the only metabolic pathway that the heart can use for oxidative metabolism.

Table 4.5 Metal ion content in serum (μg/l) and urine (μg/g creatinine) of patients with a total hip prosthesis in Ti6Al4V

Patients	N	Ti		Al		V	
		Serum	Urine	Serum	Urine	Serum	Urine
Control	35	0.20	0.20	0.10	0.15	0.10	0.10
No complications	45	0.30	0.35	0.12	0.20	0.12	0.15
Slight mobility	3	1.05	1.35	0.45	0.51	0.26	0.29
High mobility	4	1.20	1.80	0.56	0.72	0.34	0.47

The excreted concentrations of alloy elements by patients without and with a total hip prosthesis (Atlas) were analyzed after 25 months postsurgery by Hildebrand et al. [165]. The analysis concerned 35 patients without implant, 45 with a successful prosthesis, 3 with moderate mobility due to mechanical failure of the prosthesis and 4 with a strong mobility leading to retrieval. Two from the latter four showed strong wear accompanied by an inflammatory reaction (wear particles!). As shown in Table 4.5, no alarming ion levels were detected, not even for the prostheses with strong wear. It demonstrates the low dissolution rate of the wear particles. The effect of wear debris will be discussed later on.

Vanadium. This element has oxidation states between −I to +V. Biochemically are relevant: the tetravalent form in vanadyl ion VO^{+}, pentavalent in sodium metavanadate $NaVO_3$, orthovanadate $-VO_4^{3-}$ and pentoxide V_2O_5. An interesting point here is that VO^{+} is oxidized spontaneously to VO_3^{-} in vivo or vice versa in blood. When dissolved from the alloy, it is apparently not evident in which oxidation state it will circulate in the body. Toxicity increases with oxidation number but LD_{50} is difficult to determine, may be around 7 mg/kg body weight. Administration of 50 mg twice a week with noninsulin dependent diabetes mellitus is tolerated without toxic manifestation. Excretion happens along feces and urine. It accumulates mainly in kidney, spleen, bone but less in liver of rats but accumulation is less clear for humans. $T_{1/2}$ is estimated to be 20–40 h.

Vanadium is considered to have low toxicity but it is associated with both pathogenesis of some human diseases and might support normal body functions. It interferes in an essential array of enzymatic systems as phosphatases and ribonucleases. Moreover, it is shown to modulate the cellular redox potential and to catalyze the generation of reactive oxygen intermediates. Free radical production and lipid peroxidation are mediators in testicular physiology. Deficiency accounts for malfunctioning of thyroid, glucose and lipid metabolism, regulation of a number of genes and testicular toxicity. Sodium metavanadate provokes pronounced inhibition of spermatogenesis (inhibition of antioxidant and steroidogenic enzymes). Oral supplementation of zinc sulfate resulted in normalization of the perturbed parameters, stressing the particular affinity of zinc to thionein [166, 167]. All these experiments were on rats. But the consequences in humans remain at least partially an open question.

We discussed the importance of relative strengths of (conditional) stability constants of complexes and the stimulated induction of thioneins. With vanadium a

different example of multiple interactions is encountered. Although it seems to be proven that subcutaneous administration of vanadate induces the formation of metallothionein in the liver, the secreted metallothionein is a zinc-thionein and not a vanadium one [168].

So, frustration is the least thing we can say when scanning through the vast literature on the physiological effect of vanadium. It seems till today a peculiar enterprise to piece all the bits of information together into a coherent understanding of its biochemical role. Mukherjee and colleagues conclude a review paper as follows: *The pool of scientific data favors the supplementation with very low dose of this element in fatal diseases like cancer . . . scientific exploration must continue to elucidate the mechanism of action of this element in a varied assortment of biological phenomena; which in turn will define the contribution of this potential element in human benefit* [169].

In the new titanium alloys, vanadium is substituted by niobium but this element will be highlighted in the next chapter.

For the time being, it can be concluded that (1) short- and medium-term toxicity is low and (2) accumulation is low. The multiple biochemical interplay between metal ions and the body should make us alert to potential harm in the long term. The vast number of prostheses, dental and orthopedic, that have been implanted in the last five to six decades stands for a continued systemic presence of vanadium in these patients' bodies. Probably nothing to panic about, but as we said before, time is an important parameter, which is not or cannot be accounted for during in vitro and in vivo testing, say, by nature of the experimental procedures.

4.6 Wear Debris

The extent to which a THP stem can be worn is shown in Fig. 5.1 and uniform corrosion on these large areas considerably increased trace element concentrations, occasionally inciting allergic reactions in metal ion sensitive patients. Debris of polyethylene or methacrylate cements is linked to loosening of femoral and acetabular components but metal ion concentrations in periprosthetic tissue and blood, a hot topic some forty years ago, disappeared for a time from the stage. Reports on hip or knee implant related tumors were rare but suddenly, the situation changed dramatically in the last few years. Some ten years ago, metal-on-metal hip resurfacing (re-)entered the orthopedic practice (Articular Resurfacing Replacement of ASR). Alarming reports on excessive wear debris formation, metallosis and peri-implant solid masses, called *pseudotumors*, are steadily increasing: 23 papers in 2008, 43 in 2009 and already 8 till February 2010 in the *British Journal of Bone and Joint Surgery*. An example of a pseudotumor is shown in Fig. 4.11. The black staining by titanium wear particles around a hip stem is since long a recognized though not alarming feature; however, the pseudotumors are: they may cause soft-tissue destruction, Type IV hypersensitivity (see Sect. 4.3; aseptic lymphocyte dominated vasculitis-associated lesion (ALVAL)) and a poor outcome after revision surgery.

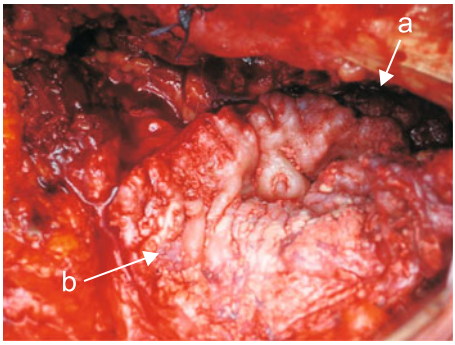

Fig. 4.11 Pseudotumor close to a titanium hip stem: (**a**) black staining by titanium wear particles; (**b**) pseudotumor. Courtesy Prof. J.-P. Simon (UZ-Pellenberg)

Revision rates for tumors for all patients of a follow-up study after 8 years were reported to average 4%, but was 0.5% for men, whereas it was 6% for women over 40 years old and 13% for women under 40 years after six years [170]! Concentrations of Co and Cr are multiples of what was/is common for modern but even for older types of total hip replacements [171].

The causes are not well defined and a review allowing a reasonable conclusion is not obvious yet (see f.i. the recent paper [172]). The difference in intrinsic properties as wear and corrosion resistance of the materials used for metal-on-metal THPs or ASRs cannot account for the present problems. Remains mainly (only?) a biomechanical facet: a small margin of error on orientation, i.e., abduction and anteversion angles, and/or mechanical design constraints may be the cause of excessive wear, producing an amount of debris and, as inescapable consequence, enhanced metal ion concentrations beyond the control capabilities of homeostatic mechanisms. One manufacturer already stopped the production of his ASR. It is reminiscent of another dramatic case, the Prozyr®cups, cited in Chap. 9.

Scanning diagonally through the literature of the last seven years, two different conclusions can be drawn. In as far as the enhanced cobalt levels of serum or whole blood for the second generation of metal-on-metal total hip arthroplasties are concerned, there is reason for concern but no (not yet?) clear proof that it is associated with hypersensitivity or early osteolysis. The situation is, however, worse for resurfacing where accurate acetabular positioning seems to be the main complicating factor [173–179]. So, wait and see how this issue develops in the years to come.

4.7 And the Answer Is?

The answer to the question in the chapter's heading is a *conditional no*.

We often wondered why implants, subjected to a hostile chemical environment, to wear and formation of debris, corrosion, systemic delivery to the body fluids of metal ions intensely interacting with enzymatic systems, ions which are potentially toxic or cancerogenic and so on and so forth, do relatively speaking so little harm.

For that reason, some basics on complex formation, relative stability of complexes, competing reactions, were discussed. It probably looked here and there like a historical retrospection and not relevant to the subject of this book. However, the overview was introduced with the aim to show a road to the why's and how's the noxious effect of dissolving metal is kept within acceptable limits. Complex formation was in the high days of complex chemistry tedious to analyze numerically but this constraint is lifted by modern computing power. From the 'old' physical chemistry of complexes together with the progressing understanding of the biochemical machinery will emerge simulation programs, which hopefully allow to predict short- and long-term behavior of implants... unless of course tissue engineering will make the whole business obsolete if it succeeds in manufacturing new knees, hip joints or arteries!

Talking about vanadium: redox potential, free radical production, reactive oxygen intermediates, etc. was mentioned. This points to the direct or indirect role of metal ions, which means that metal-mediated oxidative DNA damage is one of these roles [180]. Just a few cases of implant-related tumors are reported but the vast body of literature on metal-induced radical formation, as for example •OH, should keep the implant business alert for this potential danger. As implants continuously improve, they survive longer in the body and, as was repeatedly said, time is an important variable, not or only partially accounted for in toxicity assays. The subject is too long a story to be part of this book but it had to be mentioned.

4.8 Postscriptum

The conditional *no* in former section is based on more than just agony of doubt about long-term effects. A visionary article by Andersen and Krewski on the evolution of toxicity testing opens a window on the *not-so-distant future* [181]. These authors assume that all routine toxicity testing will be conducted in human cells or cell lines in vitro: *Dose response modeling of perturbations of (toxicity) pathway function would be organized around computational systems biology models of the circuitry underlying each toxicity pathway. In vitro to in vivo extrapolations would rely on pharmacokinetic models.* The specific tools for these changes in toxicity testing are available or in an advanced state of development which justifies the authors statement on the not-so-distant future, a fair departure of animal-based toxicological tests. This statement is in line with what has been said Sect. 4.2.3.

According to a review published in 2005 by Campaign, to date physiologically based pharmacokinetic models (PBPK) have only been developed for the top five of potentially toxic elements: zinc, arsenic, nickel, lead and chromium [182]. According to this author, issues that are relevant to metals (and different from pharmacokinetics of organic compounds) include:

- Necessity for modeling long-term exposure.
- Impact of diet on metal kinetics and toxicity.
- Impact of changes in oxidation status (*speciation*).

- Metal-specific patterns of tissue accumulation.
- Protein and other ligand binding.
- Metal–metal interactions and interactions between metals and organics.

The list summarizes nicely what has been said in former sections about the potential physiological implications of individual elements. For chromium with its two oxidation states, a PBPK modeling for humans has been published but not for instance for vanadium. For manganese, also an element with complex chemistry, the data gaps were analyzed that will need to be addressed with targeted research prior to successfully modeling the uptake, distribution and elimination. The time has come to collect large epidemiological data sets. The huge number of people carrying implants for a considerable period of time should allow the construction of a statistically powerful tool to develop an accurate PBPK model for all metals used in implants.

Chapter 5
Zirconium and Other Newcomers

At the end of the former chapter, we were wondering why implants and the materials they were made of do behave as they do: not so bad after all. The whole kit and caboodle of strength, fatigue, corrosion, toxicity are all part of the fascinating 'multidimensional coin' called *biocompatibility*, multidimensionality making a satisfactory definition intrinsically difficult (see Sect. 1.1). A few 'dimensions' were put in the limelight in the former chapters but not any of the materials discussed thus far have the ideal combination of properties. Will newcomers or, say, metals that are newly promoted in the last two decades bring relief from persistent problems?

5.1 Excellent But Just not Enough?

The hip stem of the prosthesis shown in Fig. 2.1 was replaced after 27 years. The head was sliding back and forth in the PE cup at an estimated frequency of 2.10^6/year totalling $2.27.2.10^6 = 108$ million sweeps. Assuming a leg sweep of 30° and a head of $r = 22$ mm, a point on the head's surface traveled something like 600 km during that span of time. Notwithstanding this long trip, the head was quite smooth and intact. One would expect no or less wear on the nonarticulating stem's surface. However, nothing is less true. The stem shown in Fig. 5.1 was explanted for loosening after eight years in vivo service and it was wear all over the place. The hip stem in (a) is photographed under visible light. To allow a semiquantitative analysis of the total amount of wear, the prosthesis was wetted by a fluorescein solution; after cleaning with dry tissue, the nonworn surface retained an amount of dye which is fluorescing under UV light with contrast proportional to roughness. The worn area (photograph (b)) was determined by image analysis (described by Simon [183]).

This case seems not to be dramatic unless wear debris was the trigger for loosening. In Fig. 11.5, an example will be shown of a more extreme case: a head made of polyethylene lost millimeters of material already after a couple of years in-patient service!

In Chap. 2, the fracture of a total hip prosthesis stem after 27 years in service was under scrutiny. By metallographic analysis, the history of the fracture was reconstructed and for sure, the fracture did not happen at once. In the limit meticulous

J.A. Helsen and Y. Missirlis, *Biomaterials*, Biological and Medical Physics, Biomedical Engineering, DOI 10.1007/978-3-642-12532-4_5,

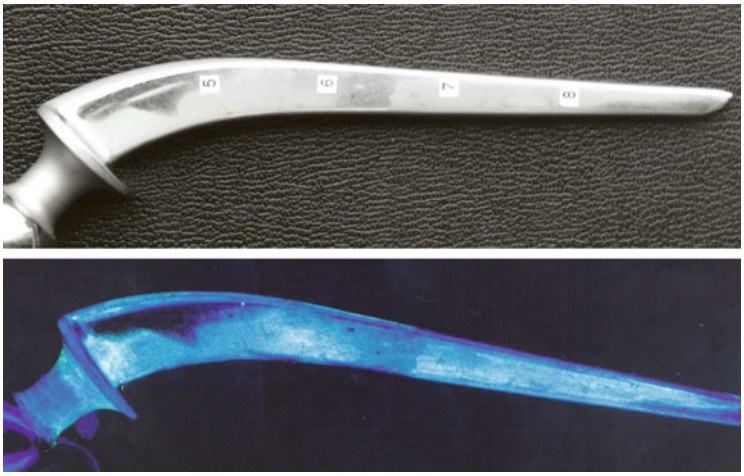

Fig. 5.1 Worn prosthesis stem. (**a**) Normal image. (**b**) Image under UV-light with fluorescein dye retained on the rougher nonworn surface and absent on the worn-polished surface [183]

analysis of metallographic images of the fracture surfaces as shown in Fig. 2.5 would allow the number of critical load cycles to be estimated, say the number of steps climbing the stairs, if not hurrying to the latest bus. Two other cases were analyzed in Chap. 3 and also here catastrophic fracture was excluded. It was demonstrated that the strength of the device by design and materials used far outweighed the in vivo stresses expected from patient's normal or even extravagant activities. Nevertheless, the stem broke.

What then should we look for... extra high strength? A superficial look at a Materials Property Chart offers us an instant solution: ceramics such as Al_2O_3 or ZrO_2. Plotting elasticity modulus E vs. tensile strength one finds the collection of ceramics top right of Fig. 5.2(left). Moreover, ceramics exhibit an extraordinary resistance to corrosion and wear, chemically inert, nontoxic. But remember that we stressed above that the fractures under scrutiny did happen noncatastrophically. Our enthusiasm about ceramics is immediately tempered by inspecting Fig. 5.2(right) where fracture toughness is plotted vs. strength, a plot similar to toughness vs. E.[1] Metals occupy now the top right position of the plot. Moreover, the lower E for metals is mechanically beneficial because it results in less stress shielding.

A stress–strain curve for ceramics does not show the upper end plateau-like behavior before fracture as in Fig. 1.6. This stress–strain behavior tells us the same story as the Materials Properties Charts: ceramics fracture catastrophically; without any warning your ceramic hip prosthesis can fracture descending the stairs on your way to breakfast.

[1] For details, the reader is advised to read the concise paper on philosophy and use of Materials Properties Charts by Ashby [184].

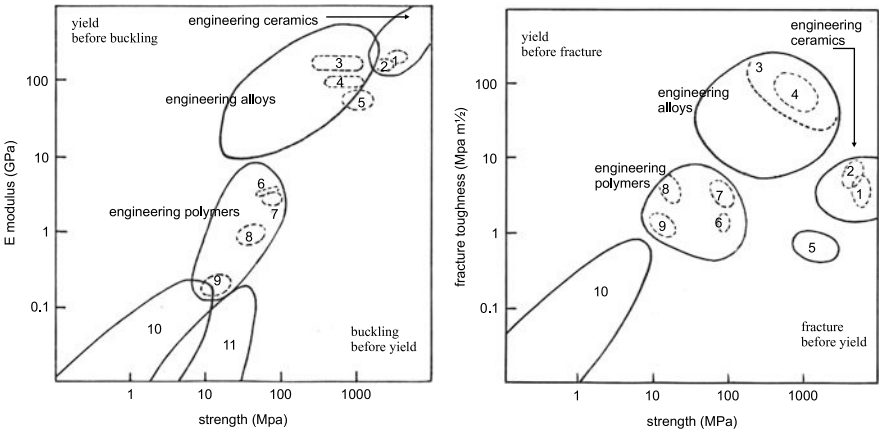

Fig. 5.2 Materials Properties Chart. *E* modulus (*left*) and fracture toughness (*right*) vs. yield strength. (1) Al_2O_3, (2) ZrO_2, (3) steels, (1) Ti alloys, (5) glasses, (6) PMMA, (7) nylons, (8) HDPE, (9) LDPE, (10) polymer foams, (11) elastomers (more on the polymers 6–11 in Chap. 11). Adapted from Ashby [61, 184]

Thus, scratch ceramics from the shopping list?
Yes for use in bending, *no* for example in compression. But read more about ceramics in Chap. 9, because development does not stand still and a new generation of ceramics is arriving. Applicability of materials from other classes in the materials properties chart is either marginal like foams or subject of other chapters. Wood might be another story. Present as a biomaterial in 3000 years Chinese orthopedics and traumatology, it never disappeared completely from the scene: Ezerietis and colleagues used Juniperus communis in fracture healing with considerable success over a period of 55 years [185, 186].

For the time being however, metals still have a future!

5.2 Zirconium, a Newcomer?

Zirconium is not quite a newcomer. In a general paper on oxidized zirconium, Hunter refers to the use of Zircaloy with promising results for orthopedic screws and bone plates by at least one center in England in 1950 [187, 188]. The metal was made unavailable soon after that year due to the priority given in those days to nuclear power programs. When it became available again at the end of the 1950s, the interest in zirconium vanished in favor of the less costly and clinically established titanium alloys. The interest reappeared in the 1990s. For example, Smith & Nephew filed a patent on the use of oxide nitride-coated zirconium prostheses in 1992 (US patent 5152794).

Zirconium is widely distributed in Nature and is the 18th most abundant element in earth's crust with an average concentration of 165 mg/kg, which is more than chromium, nickel, copper or cobalt. Saint John the Divine would be surprised to learn that jacinth, the eleventh gemstone garnishing the foundations of the New Jerusalem (Revelation, **21**:20), was composed of zirconia. We had to wait till 1789 when Klaproth determined zirconia in jargon and later in 1795 in jacinth, another gemstone from Ceylon, now Sri Lanka.[2] Berzelius finally prepared zirconium metal in 1824 [189].[3] The modern production starts with the reduction of zircon sand, a zirconium orthosilicate $(Zr,Hf)SiO_4$. Zirconium is always found in company of hafnium, which is not unexpected through its chemical similarity to zirconium (see Periodic Table of elements in Table A.2 of Appendix A).[4]

We will see whether or not this element is entitled to become a new jewel on the biomaterial's crown.

Physical and Engineering Properties

All metals for prosthetic purposes are recruited from the transition element groups 4 to 11 of the 4th, 5th and 6th periods (see Table A.2). Except for molybdenum and tungsten, the metals discussed thus far belong to the 4th period, which is characterized by an incomplete 3d electron shell structure (10 electrons at completion). Nontransition biomedically interesting metals are aluminum discussed as alloying element for titanium and magnesium which will be looked at in Chap. 8.

Zirconium belongs to the 5th period characterized by a gradually filled 4d electron shell. The theory is outside the scope of this book but the d-shell structure of the transition metals is mentioned because it is basic to the exquisite coordination chemistry of transition elements we already referred to in Chap. 3 (for further reading see the older but standard work on inorganic chemistry by Purcell and Kotz [190] and Sanderson [191]). The crystal structure of the pure metals of the 4th period is h.c.p. (Figs. B.1, 2, 3 and Table B.1 in Appendix B). Why do these atoms pack into a h.c.p. structure and not f.c.c. such as aluminum or nickel? The answer is that they adopt a crystalline framework imposed by the electronic structure of the atoms and by a stapling, which results in the lowest Gibbs free energy state *at a given temperature*. However, the difference in energy between structures is often small. Because of this, the crystal structure with minimum energy at one temperature will not be the most

[2] German analytical chemist (1743–1817). First professor of chemistry at the University of Berlin. It is worth mentioning that the same chemist is the first to study the properties of the for those days new element which he christened as *titanium*!

[3] Berzelius J.J. (1779–1848). Professor of chemistry and medicine at the Stockholm Medical School.

[4] Hafnium, although widely distributed, escaped detection because of its close resemblance to zirconium. It was one of the eleven unfilled spaces in the periodic table at the beginning of the twentieth century. It was finally identified in 1922 in an X-ray spectrum at the wavelength predicted by Moseley's law.

Table 5.1 Chemical composition of zirconium (Zr 702) and zirconium-niobium (Zr2.5Nb, 705)

Grade	Zr702	Zr705	Zr-2.5Nb
UNS designation	R60702	R60705	R60901[a]
Element	wt%	wt%	wt%
Zirconium+Hafnium	99.2	95.5	bal.
Hafnium(max)	4.5	4.5	<0.010
Iron+chromium	<0.20	<0.20	<0.17
Hydrogen	<0.005	<0.005	<0.0025
Nitrogen	<0.025	<0.025	<0.0080
Carbon	<0.05	<0.05	<0.027
Niobium		2.0–3.0	2.40–2.80
Oxygen	<0.16	<0.18	<0.09–0.13

[a] Specification limits of ASTM F2384

favorable at another temperature, the very reason why zirconium is h.c.p. at temperatures <865°C and b.c.c. at >865°C.[5] The h.c.p. structure has one predominant slip system (plus three predominant twin systems) at typical working conditions. The close packed layers lie in only one orientation (basal planes) and therefore Zircadyne alloys are anisotropic at typical forming temperatures and are comparable in this (and other) respects to titanium alloys. How it looks like at the atomic level is shown in Appendix B. Dislocations tend to have the highest mobility on planes with a high density of atoms (number of atoms per unit area) in casu here the basal planes of the h.c.p. structure. Yield strength is determined as the onset of plastic flow, the latter being enabled by migration of dislocations. Dislocations on the intersecting twin planes obstruct each other and accumulate along the intersection. Herein finds the effect *work-hardening* of an alloy its intrinsic explanation. It is a potent and useful strengthening method and all metals and ceramics strengthen by it to greater or lesser degree. Useful yes, but a mixed blessing: if the metal has to be rolled to thin sheets, the yield strength raises so steeply due to work hardening that it has to be annealed, i.e., heated to remove accumulated dislocations, before one can go on to further rolling. In Appendix B are illustrated the hard sphere model of the unit cell and the twin band structure when stressed by a shearing force.

The composition of Zircadyne alloys is given in Table 5.1 (from the Data sheets of Wah Chang, An Allegheny Technology Cy., Albany, Oregon).

The main engineering properties of Zircadynes are summarized in Table 5.2. Extremely pure Zr is very soft as all pure metals but is strengthened by the presence of interstitial oxygen. The difference in YS or UTS between 702 and 705 is due to interstitials but another important strengthening mechanism is also active: the formation of a mixed phase alloy.

[5] The allotropic change of tin below 13.2°C has historical records. It has drastic effects on the mechanical properties: tin coat buttons of Napoleon's army fell apart during the harsh Russian winter. The phenomenon was known as tin plague. It used to be also a plague for organ pipes and tin pottery.

Table 5.2 Zirconium (Zr 702) and zirconium-niobium (Zr2.5Nb, 705). Physical and mechanical properties, juxtaposed with corresponding values for Ti, Ti6Al4V, CoCrMo (F75) and cortical bone (40–59 year old, $E_{\parallel}$)

Property/alloy	702[a]	705[a]	Ti[b]	TiAlV[b]	CoCr[b]	bone[b]
$Alpha$-phase (h.c.p.)	<865°C					
$Beta$-phase (b.c.c.)	>865°C	>920°C				
$Alpha + beta$-phase		<920°C				
ρ (g cm^{-3})	6.51	6.64	4.5	4.4	9.2	∼2
α (10^{-6}K^{-1})	5.8	3.6	9	8.6	14.2	
μ (Wm^{-1}K^{-1})	22	17	17	6.5	14.8	
E^c (GPa, 38°C)	99	94	103	113	210	15
E^c (GPa, 371°C)	64	75				
E (shear) (GPa)	36	34				
YS[d] (MPa, r.t.)	321	506	462	923	480	
UTS (MPa, r.t.)	468	615	593	992	770	87
Fatigue[e] (MPa)	145/55	290/55				

[a] Extracted from Zircadyne 702/705 data sheet (Wah Chang, Allegheny Technology Cy., Albany, Oregon)
[b] Respectively from Tables 2.6, 2.4 and 2.10
[c] For annealed specimens; elastic behavior at 38°C, plastic at 371°C, averages of ∥ and ⊥ values
[d] Annealed and cold worked
[e] Maximum allowed stress (unnotched/notched)

The high temperature b.c.c. or β-phase of zirconium cannot be 'frozen' even by rapid quenching below the allotropic transformation temperature. It needs the addition of niobium, one of the several possible β-stabilizing elements, to obtain an $\alpha + \beta$ alloy.

Fabrication

Zirconium is produced from ore that is found in beach sand containing zircon (Zr and Hf), rutile and ilmenite (Ti). Zircon is separated by standard ore dressing methods. The mineral is first transformed to $ZrCl_4$ ($+HfCl_4$). After a set of purification steps, either by liquid–liquid extraction or distillation and finely reduced by magnesium to form a 'sponge donut'. The last steps of the complex production process is multiple vacuum arc melting, adjusting the composition, adding alloying elements and casting to ingots of about 760 mm diameter.

Next step is the reduction of the ingots to more manageable formats. The ingot is heated to the β-domain temperature (>920°C for the 705) and reduced through a sequence of steps by press forging. The heating contributes to the homogenization of the as-cast structure and the forging stimulates the recrystallization to yield a

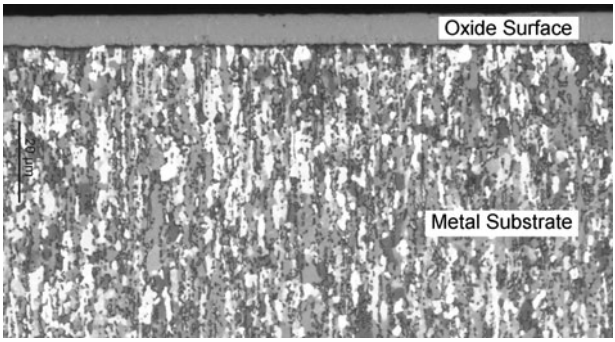

Fig. 5.3 ZrO_2 on top of a medical grade Zr-2.5Nb (UNS R60901) substrate with a refined wrought microstructure. Micrograph produced by Ms.Carolyn Weaver (Smith & Nephew)

product with a uniform and fine grain structure. The alloy is marketed as bars of 65–215 mm diameter.

The forging may receive a β-solution anneal to ensure homogeneous distribution of the solid solution of the elements tabulated in Table 5.1. The forging is followed by water quenching. Why is it? Niobium is soluble in the β- but not in the α-phase. By quenching, fine niobium-rich β-Zr particles precipitate but are inhibited to grow by the rapid cooling and become homogeneously distributed over the bulk. This homogeneity is a must for the formation afterward of a uniform adhering oxide layer in the final component. Figure 5.3 shows the metallographic structure of the wrought alloy with fine but not all equiaxial grains. The long axis is clearly aligned in one direction (*anisotropy*). A bar with this thermomechanical history can be shaped into a component by milling or other machining techniques.

Elaborate descriptions of the production process can be found in papers by Webster or Hunter [187, 192]. Moreover, zirconium and its relation to rare earth elements is an attractive and challenging chemistry for geologists but also an open field for materials scientists, may be a way to tune the properties of the metal or oxide. For a short introductory text, see [193].

Surface Properties

The set of characteristics of zirconium discussed is not superior to other alloys which passed review thus far. It is only in the last step of the production process that the component will be given its exclusive characteristics. Heating in air at a temperature above 500°C of the alloy with the appropriate thermal history allows oxygen to diffuse gradually into the surface turning the metal into zirconium oxide ZrO_2. The growth of the oxide layer is rigorously controlled and continued till a thickness of about 5 μm is reached. Even for complex shapes the process produces a

uniform oxide layer over the entire surface.[6] The component, named further on as OxZr, is finally burnished to produce an articular surface at least as smooth as CoCr components.

By nature of the diffusion process, an oxygen gradient is created inward the substrate. The gradient is functioning as a transition zone in mechanical properties from metal substrate to oxide layer, the latter being a true ceramic. The difference in ductility between ceramic and metal substrate is overcome in the transition zone. The use of a transition zone, although on a more macroscopic scale, is also the basic philosophy of a proposal for the perfect prosthesis, discussed in Chap. 11 and for the development of gradient ceramics (see Chap. 9). A zone between the uniformly grey top layer ZrO_2 in Fig. 5.3 and the metal substrate forms the transition zone. The structure of the oxide is a dense predominantly monoclinic fine-grained (grain size in at least one dimension of $<100\,\mu m$, in the limit qualified as nanostructural zirconia [194].

An oxide layer of a few nanometer is always present on the surface of any metal unless kept under inert atmosphere. To master the oxygen content, the metallurgical processing of zirconium is conducted under vacuum or inert gas. The difference in behavior of the alloys, however, is the velocity of the oxidation reaction and the quality of the oxide as diffusion barrier for ions to or from the substrate. It is bad for iron but improves in the following order: Al_2O_3, Cr_2O_3, TiO_2, ZrO_2 and Ta_2O_5 and/or Nb_2O_5 to name only the oxides of interest in the present context.

Corrosion. From the E-pH diagram we learn that zirconium is not at all a noble metal. On the acid side at pH<1 it dissolves as Zr^{+4}, below 3.5 as ZrO^{+2} and above 13 as $HZrO_3^-$ [195, pp. 226]. Fortunately in between ZrO_2 is stable and screens the bulk from the outside world. At pH = 7, the equilibrium potential Zr/ZrO_2 is about −2 V: contact of the bare metal with an aqueous medium will oxidize the metal with evolution of hydrogen. The diagram is very similar to the one for titanium with stable TiO_2 between pH = 2 and 12 but it has at pH = 7 a higher equilibrium potential (about −1.8 V). The corrosion resistance of zirconium is exuberantly great: it is hardly attacked by concentrated solutions of acetic acid in any combination with reagents as $FeCl_3$, HI, HCl, NH_3, aqua regia, formic acid, H_2O_2, etc. (see Data sheets of Wah Chang, Allegheny Technology Cy, Albany, Oregon). Much work has been done on the electrochemical behavior of oxide films in aqueous media. The results are less relevant here because in the current biomedical applications of OxZr the oxide films are thicker and denser than those studied in most electrochemical work (see [196]).

Biocompatibility. The results of a set of current biocompatibility tests enumerated hereafter were all negative as reported by Davidson et al. [197]:

Cytotoxicity: L929 MEM[7] Mouse Fibroblast Test
Sensitization: Kligman Guinea Pig Maximization Test

[6] Oxidized zirconium components are exclusively produced and marketed under the trade name OXINIUM™ by Smith & Nephew, Inc. (Memphis, TN).

[7] Abbreviations: MEM: Minimal Essential Medium; USP: United States Pharmacopeia.

Intracutaneous Reactivity: USP XXII Class VI Rabbit Injection Test
Systemic Toxicity: USP XXII Class VI Mouse Injection Test
Hemolysis: Autian Method Rabbit Blood Contact Test
Pyrogenicity: USP XXII Class VI Rabbit Injection Test
Intramuscular Implantation: USP XXII Class VI and 90-Day rabbit Tests
Genotoxicity: Ames Mutagenicity and Mouse Bone Marrow Micronucleus

The tests described by USP are used worldwide for biocompatibility testing. Updated versions can be downloaded from Internet.

The daily uptake of zirconium is estimated as high as 125 mg/day which is not unexpected as being an omnipresent element. A relation between Crohn's disease and zirconium was suggested in the 1990s, reminiscent of the relationship of Alzheimer and aluminum. As far as we are aware, the hypothesis is not supported. For the time being, toxicity of zirconium seems not to be an item of concern.

Performance

The goal of all the trouble invested in the production of reliable OxZr components was to marry the advantages of both metals and ceramics. Is it a lucky marriage?

Wear. A back and forth sliding of a spherical tipped bone cement pin on test specimens is a technical control test shown in Fig. 5.4a and described by Hunter et al. [198]. Wear of a specimen of OxZr is different: hardly visible for OxZr, visible for the naked eye for CoCr worn under identical conditions. This remarkable difference is easily demonstrated by our simple qualitative test set-up, which is schematically shown in Fig. 5.4b: a laser beam is pointed on the wear path and the beam is partly reflected or partly diffused, depending on the roughness of the surface. The results shown in (c) do not need further comment. The test can occasionally be made semiquantitative.

In-patient use of a metal/polyethylene (PE) articulation requires more realistic testing. Wear of PE is often cited as responsible for hip and knee replacements by periprosthetic osteolysis and thus an important issue. Mainly two wear mechanisms are operating: adhesive and abrasive wear, the first being caused by frictional shear of PE against a hard counterface, the second by sliding against either hard counterface asperities or by abrasive particles in the PE-metal or ceramic interspace, the latter usually quoted as a separate class of wear: *third body wear*. The wear behavior as shown in Fig. 5.4 is performed under more realistic conditions by wear tests in a four-axis displacement controlled, physiological knee simulator (Fig. 5.5). The applied conditions were: 6 million cycles of 90% walking-gait and 10% stair-climbing activity. In Fig. 5.5(left), the newest guided motion knee prosthesis of Smith & Nephew: Journey BCS prosthesis (bicruciate stabilized). The insert was made of UHMWPE (ultra-high-molecular-weight-PE).

Collectively, the hip and knee simulator tests indicate that OxZr components can reduce wear of the polyethylene counterface by 40–90% (in volume or weight) depending on test conditions. These tests also indicate that the number of wear

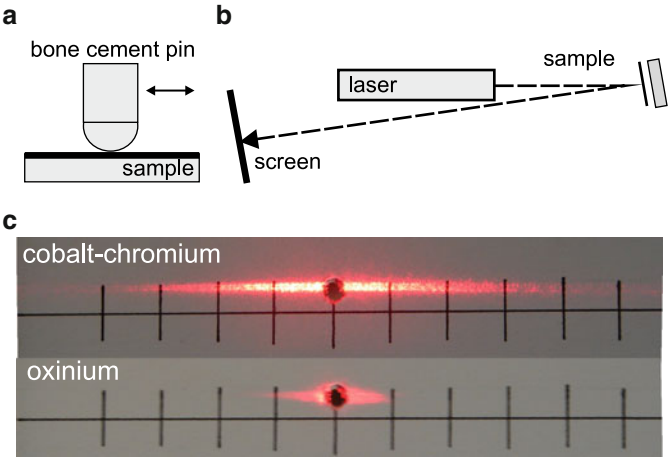

Fig. 5.4 Qualitative optical comparison of wear: (**a**) wear by an oscillating sliding contact of a spherical tipped bone cement pin on a CoCr or oxidized zirconium disc with an initial contact stress of 82 MPa [198]; (**b**) dispersion of a laser beam by the wear track of about 11 mm (design of the experiment by J. Helsen); (**c**) results after 10^7 cycles

Fig. 5.5 In vitro 4-axis testing machine for prostheses. The device simulates the in vivo behavior: on the picture a total knee prosthesis under test. Courtesy Smith & Nephew

particles tends to be less in any size range. It is interesting to note that the surfaces of polished CoCr components roughened during testing even in the absence of intentionally added abrasive particles, while the OxZr surfaces did not [198–203].

Clinical Results

Long-term results are not yet available. The clinical outcome of OxZr heads of THA after two years was found to be equivalent to CoCr heads in an evaluation of a cohort of 100 patients (50 with OxZr heads and 50 with CoCr heads) [204].

A mid-term evaluation is reported of OxZr femoral components of cemented TKA: 50 patients, 51 years of mean age and mean follow-up of 79 months. Radiographic review revealed one nonprogressive tibial radiolucency. There were no femoral radiolucencies or osteolysis and no other negative findings attributable to the oxidized zirconium. Longer clinical use is needed before deciding that the new material results in a longer in vivo performance [205].

An interesting evaluation is reported of experiments on six Oxinium femoral heads retrieved from revision surgery. The heads showed various degrees of abrasive damage but confined to one quadrant of the surface. Subsequently, they were coupled with XLPE (cross-linked polyethylene) liners and compared to new Oxinium and CoCr heads, respectively, coupled to XLPE liners and conventional PE liners. The hip simulator testing was performed using a standard walking gait program (peak load 3,000 N, 1 Hz). The in vivo damaged heads showed enhanced wear of the PE liner, although substantially less than the new heads used for comparison. The authors concluded that the observed wear would not lead to catastrophic damage [206].

Metal hypersensitivity has been identified as possible cause of arthroplasty failure. In these cases, the use of ceramic implants is recommended at revision. Nasser and colleagues report the outcome of a prospective study of patients with recognized hypersensitivity. Neither of the patients developed, after revision knee arthroplasty with either alumina or Oxinium implants, adverse clinical symptoms or changes in antibody profile. The results suggest that Oxinium offers the same hypoallergenic properties as ceramics but a lower cost [207].

To conclude, time as often said, is an important parameter. Long-term assessment, however, is not yet possible. So, mild optimism is probably the best attitude for the time being.

5.3 Tantalum and Niobium

Tantalus, a rich and famous king in Greek mythology, was a son of Zeus. Mortal but honored by the gods, he was allowed to the dinner with the Gods. Dazzled by so much honor he revealed the secrets of the Gods to men. Zeus punished him, forced to stand in the Hades, where the water was receding when he tried to drink, and other kinds of everlasting torments. His daughter Niobe was not less an ambitious person. Niobe had vaunted one day her superiority to the goddess Leto but Apollo and Artemis, Leto's children, punished Niobe by killing her seven sons and seven daughters!

A new metal was discovered by the English chemist Hatchett in 1801 and by the Swedish chemist Ekeberg in 1802 in two different minerals. Ekeberg found it such a *tantalizing* task to trace the element down, that he called it *tantalum*. In 1844, however, it became clear that in fact the discovery concerned two closely related elements: *tantalum* and *niobium*. When in 1844 Heinrich Rose had to name the

other element, the choice of *niobium* was obvious. Werner von Bolton succeeded in 1903 in refining the metal.

But before proceeding to the order of the day… Tantalus offers us, although unwillingly, a truly original link to biomaterials. In his extreme pride, Tantalus wanted to test the gods' omniscience and invited them on a dinner where he served the dead body of his own son Pelops. Demeter ate unconsciously a piece of Pelops shoulder; the other gods, however, realized the truth: they threw the pieces of limbs of the child in a kettle and one of the Fates brought the child back to life. The lacking piece of shoulder was replaced by an implant: a piece of ivory!

Fabrication

The metallurgical processes are very similar to those used for zirconium. Both tantalum and niobium are separated by liquid–liquid extraction, or distillation, precipitated as hydroxide and dehydrated to oxides. Subsequently, the oxides are reduced by sodium, carbon or aluminum, refined and made available as ingots or powder.

As listed in Table 5.3, the melting points of Ta and Nb are fairly high and to improve the mechanical properties of the pure metal they are alloyed mainly with Mo, W or V, all with high melting points and hence, alloying is rather a costly operation. Ta and Nb are both commonly produced as powder and sufficiently ductile so that they can be alloyed at ordinary temperatures by milling in a ball mill under inert atmosphere (*mechanical alloying*). An example of mechanical alloying of Nb with Mo is given by Helsen et al. [208]. Further processing of the alloy powder to near-net shape objects is performed either by annealing at 1,200°C followed by compression and sintering in a vacuum furnace or by hot isostatic compression (HIPping).

Physical Properties

When considering density Table 5.3 learns us that Ta is about twice as heavy as Nb for comparable yield strength. A bulky object like a hip prosthesis would be unpleasantly heavy. For comparison, densities of a series of materials are listed in Table 5.4.

Table 5.3 illustrates also the similarity of Ta and Nb: similar ionic and atomic radii, melting points and the five metals listed have a b.c.c. crystal structure (Appendix B). This crystallographic configuration is responsible for the workability of these metals: mechanical alloying, drawing into wire, rolling into sheet, etc.

Selecting the right alloying metals allows to tailor the mechanical properties as shown in Table 5.5 for Ta or in Fig. 5.6 for Nb.

Table 5.3 Physical data of pure niobium, tantalum, molybdenum and vanadium. Collected from [209–211]. For their place in the periodic system and atomic masses, see Appendix A

	Nb	Ta	Mo	W	V
Atomic radii (nm)	0.143	0.143	0.136	0.137	0.132
Ionic radii[a] (nm)	0.069	0.068	0.062	0.062	0.059
ρ (kg.m^{-3})	8,580	**16,680**	10,280	19,260	6,110
Melting point (°C)	2,468	2,996	2,610	3,410	2,178
α (10^{-6}K^{-1})	7.3	6.5	4.9	4.5	8.3
E[b] (GPa)	110	185	329	405	134
Shear modulus[b] (GPa)	37.5	69			
YS[b] (0.2%)(MPa)	228	207			
E_0 (V)	−0.96	−1.12	−0.2		−1.18

[a] For pentavalent Nb, Ta and V, and hexavalent Mo and W
[b] All data ±10°C because highly composition sensitive

Table 5.4 Intercomparison of density of some materials

Material	Density (kg.m^{-3})
UHMWPE	940
Water	1,000
Soft tissue	∼ 1,050
PMMA	1,200
Compact bone	∼ 2,000
Glass	∼ 2,500
Ti-cp	∼ 4,500
Stainless steel	7,930
Nb	8,580
CoCr (wrought)	9,200
Ta	16,680
Au	19,300

Table 5.5 Tailoring the properties of Ta by alloying. Data collected from data sheets of Cabot Supermetals

	Ta	Ta2.5W	Ta10W	Ta40Nb	R05200[a]
E (GPa)	179	179	207	152	
UTS (MPa)	276	379	620	310	207
YS 0.2% (MPa)	172	241	482	207	138
% elongation	50	30	30	40	20

[a] Sheet 1.5 mm thick, unalloyed, annealed

Corrosion

The standard electrochemical potentials of Nb and Ta are very electronegative telling us that these elements are very 'proletarian' metals were it not, and the story is becoming boring, that the quality of the oxide skin promotes them, in particular Ta, to the noblesse of the most corrosion resistant metals, similar (superior?) to Nb, Ti and Zr. Ta_2O_5 and Nb_2O_5 are stable over the whole pH range in the

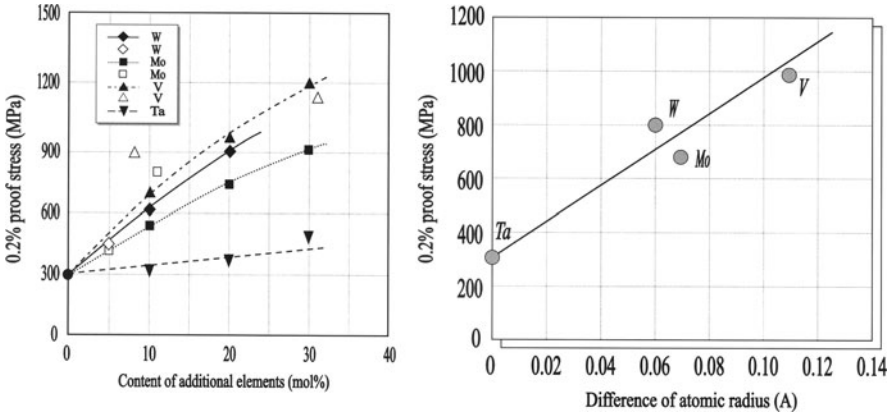

Fig. 5.6 *Left*: the effect of alloying on yield strength. *Right*: relation between the atomic radius and 0.2% yield strength for niobium with additional elements of 20 mol%. Courtesy: Tantalum-Niobium International Study Center

stability region of water (empty Pourbaix diagrams in that region [195]!). The breakdown potentials are high, the polarization resistance for Ta is superior to all other and the passive currents are low. In Fig. 5.7, the passive current densities of SS, CoCr, Ti6Al4V, Ti, Nb and Ta are compared and illustrates very well the exquisite electrochemical properties of Ta with a passive current around 5.10^{-7}A.cm^2 or a dissolution of metal of the order of magnitude of 5 μg cm^{-2} d^{-1}. These curves were recorded according to a procedure described by Rätzer-Scheibe and Buhl [212]. It is worth to mention that the effect of alloying elements on the protective properties of the oxide layer is well studied and understood. With the current alloying elements and the concentrations used, the oxide skin belongs to class I, where the corrosion behavior is determined by the valence of the alloying element in the oxide layer on condition that the concentration of the alloying element in the oxide layer is lower than its solubility in the oxide [213].

Another interesting observation is the determination of the kinetics of repassivation as listed in Table 5.6. Chips of 5–30 μm thick are sliced off by a microtome placed directly in the electrolyte above the test specimen. The potentiostatic measurement of the current as function of time occurs immediately after generating the oxide-free metallic surface. The experimental set-up is described by Rätzer-Scheibe and Buhl [212]. From measurements on the common bioalloys, the behavior of SS is the least favorable but is similar for the others.

Toxicity and Biocompatibility

Ta and Nb are not reported to be toxicologically problematic, Mo on the contrary is moderately toxic but not when incorporated in Nb10Mo. Toxicity was determined by bringing a confluent monolayer of mouse lung fibroblasts (L929) in contact

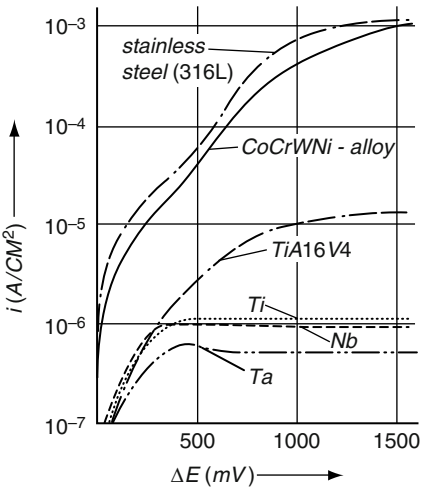

Fig. 5.7 Current density as function of the potential difference between the anodic and cathodic branches of the E-i curves for metals tested in 0.9%NaCl with a stable redox system $Fe(CN)_6^{4-}/Fe(CN)_6^{3-}$. Courtesy of Prof. J. Breme (University of Saarbrücken)

Table 5.6 Illustration of the efficiency of corrosion protection by oxide films. Data collected from [90, 212, 214]

Alloy	E_0	Breakdown potential	Polarization resistance[a]	Repassivation time (ms)	
	V	V	kΩ.cm[b]	−0.5 V	+0.5 V
Au	+1.50	–	0.3	–	–
SS(316L)	–	+0.2–0.3	4.4	**72,000**	35
CoCr[b]	–	+0.42	–	44	36
CoNiCr[b]	–	+0.42	3.3	36	41
Zr[b]	–	+0.32	–	–	
Zr-2.5Nb[c]		+0.53	–	–	–
Ti-50Zr[c]	–	+0.93	–	–	–
Ti6Al4V	–	+2.0	455	37	41
Ti-cp	–	+2.4	714	43	44
Ta	−0.96	+2.25	**1,430**	41	40
Nb	−1.13	+2.5	455	48	43

[a] Determination of polarization resistance see Fig. 3.6. Data from Breme [214]
[b] CoCr: cast; CoNiCr: wrought
[c] Pitting potential, data from Table II in [215]

with solvent extracts of the metal powders. Such extracts were made according to an international standard procedure described in the ISO/EN10993-5 guidelines. An amount of powder is extracted with *minimal essential medium* (MEM) supplemented with calf serum, glutamine and antibiotics. Following a strict time schedule, the cell cultures are evaluated for confluency, degree of cellular lysis, change of morphology and finally a cell count, all compared to a negative (UHMWPE) and a positive cytotoxic control (latex rubber) [216, 217]. MEM is one of the media simulating the body fluids but a more complex one compared to Hanks' (for more

details, see Appendix D). Our experiments were illustrating how subtle compatibility tests in reality are: the fibroblasts in contact with Mo-MEM extracts were all death and showed mayor cell lysis and severe changes in morphology. Cells in direct contact with Nb.cp, Nb10Mo and Nb20Mo 100% confluency was seen, no growth inhibition and no or only slight morphology change. To simulate bone growth, femoral bone marrow cells, collected from young male Wistar rats, were seeded on polished surfaces of the alloys and the results were analyzed microscopically (optical and SEM). The most favorable case was Nb.cp upon which a mineralized matrix was formed. Porosity as well as the alloying elements did not induce mineralization but cell growth was not inhibited. Tantalum is not different in behavior: no adverse effects on tissue, toxicity and good adhesion. It seems to be verified in clinical tests with porous Ta as discussed in next section.

Clinical Use

Nb and Ta are not newcomers in a strict sense. Already in 1940 Burke in Vancouver reported excellent results with Ta wire in skin sutures [218]. Since the 1940s, it was used in nerve repair, cranioplasty, dental implants, pacemaker electrodes, ligation clips, femoral endoprostheses and radiopaque markers. The latter were used in the determination of subsidence of knee and hip prostheses; an extended treatment of this application can be found in the Ph.D. thesis by Labey [28]. A review of the use of Ta in femoral endoprostheses is given by Plenk and collaborators in 1984 [219]. Based on density, however, use of massive Ta is not indicated for bulky prostheses as knee or hip because of their high density. The most successful niche seems to become the use of porous Ta (see Chap. 7).

Manufacturing. Porous Ta is fabricated using a low-density carbon skeleton obtained after pyrolysis of a thermosetting polymer foam. The pores exhibit a rather regular dodecahedral 3D structure with pore size of 400–600 μm. On this skeleton, a Ta coating of 40–60 μm is deposited by chemical vapor deposition. The macrostructure is shown in Fig. 5.8(left). Because of crystallographic growth and orientation during deposition, the resulting surface shows a distinct microtexture (right), a feature that might contribute to ingrowth. The volume porosity is 75–80%.

Mechanical properties. In Table 5.7, we summarized data for the mechanical properties of one marketed product.[8] Compressive fatigue endurance limit is about 23 MPa at 5×10^6 cycles. The interspecimen variability is rather high, say some 10–20%, but the lowest values still are superior to those for cancellous bone.

From mechanical point of view, porous Ta should perform well in bone substitutes or in joint prostheses (e.g., acetabular cups [222]).

Bone ingrowth. During the 1980s, the biomaterial community invested enormous efforts to cover implants with porous coatings and in the determination of ingrowth

[8] Hedrocel™ used to be manufactured by Implex Corp., University of Mississippi Medical Center but is now marketed under the trade name Trabecular Metal.

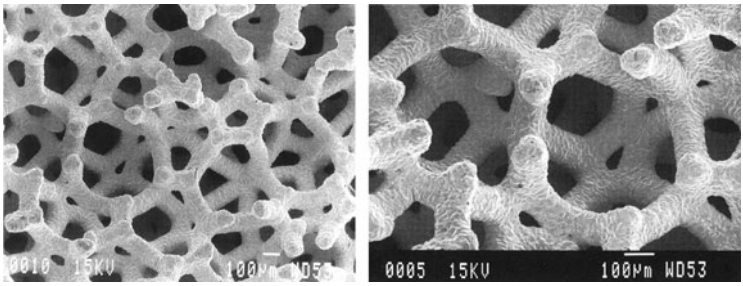

Fig. 5.8 Open cell porous Ta (*left*). At higher magnification a microtexture is visible (*right*). Courtesy: Hacking et al. [220], Figs. 1 and 2

Table 5.7 Mechanical properties of porous Ta. Cancellous bone is added for comparison. Data (rounded) collected from [221]

Test mode	UTS MPa	YS MPa	E GPa	Elongation %	Hardness Vickers
Porous Ta					
Compression	55	37	2–4	317	320
Tensile	63	48	9	5	
Bending	110	74	49[a]		
Cancellous bone					
Compression	10	5	7[a]		

[a] Rigidity MPa/mm

percentages and adhesion strength. With all sympathy to these researchers but the final outcome was rather on the low side, the reason being quite understandable: an error at the conceptual level. Many porous coatings had pore sizes of some tens of µm or less. As mentioned in former chapters, cells are never further away from blood vessels than a few cell layers. A porous substrate with that pore size was not and could not be angiogenic and ingrowth remained necessarily restrained to a few cell layers. Not so here: with pores from 430 to 650 µm the filling with newly formed bone up to 80% after 52 weeks, proving the excellent osteoconductivity of Ta. Close apposition, evidence for vascular supply and cortical remodeling into Haversian systems are suggestive of remodeling associated with increased blood flow (Fig. 5.9). Data collected from [220–224].

The implant shown in Fig. 5.10 is used to intervene in early stage osteonecrosis (femoral neck). It provides a structural support to weak bone and eliminates morbidity associated with autograft and disease potentially associated with allografts. Bone filling similar to natural healing is demonstrated by the thin section b and c after 4 and 8 weeks of implantation.

A second clinical example is shown in Fig. 5.11: a porous Ta backed acetabular cup in a canine model 6 months after implantation. Similar cups as well as porous Ta-coated hip stems are in use for about 10 years.

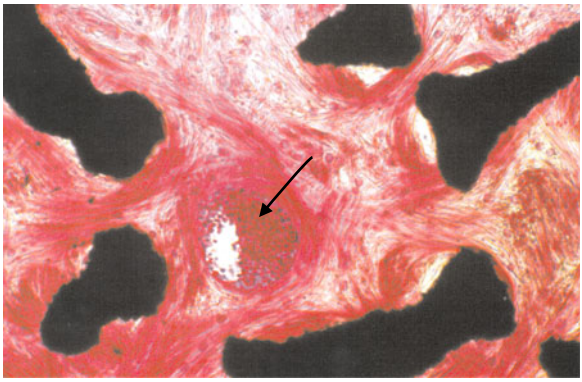

Fig. 5.9 Vascularized ingrowth. Erythrocytes are present in nutrient vessel (*arrow*). Taken from Hacking et al. [220], Fig. 7. Reprinted with permission of John Wiley & Sons, Inc.

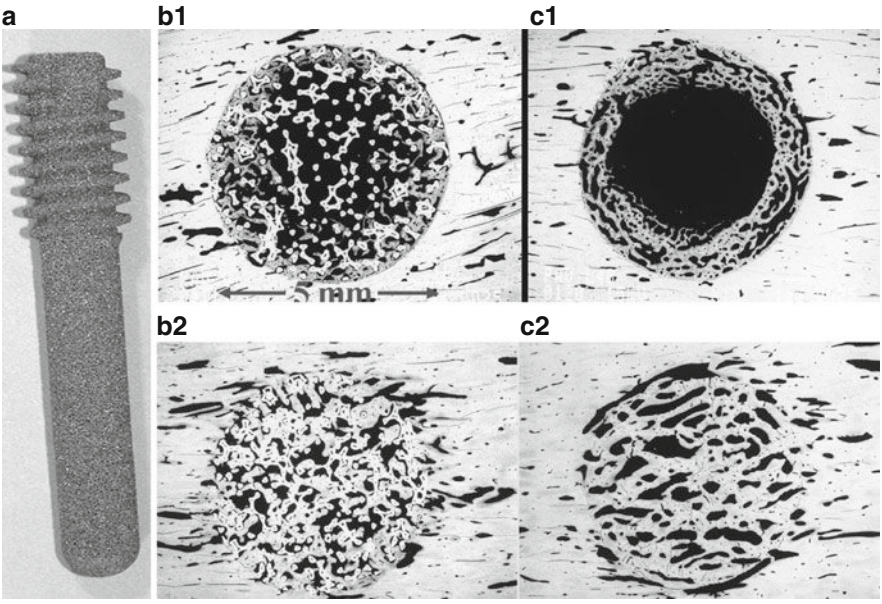

Fig. 5.10 Porous tantalum implant(a). A trabecular metal implant(b1) and void (c1) after 4 weeks. Idem after 8 weeks (b2 and c2). Courtesy: Zimmer

Were the failures in the 1970s with porous coatings to be attributed to a lack of active collaboration between material scientists, biologists and surgeons?

A right place here for an intermezzo on chaotic structures. A successful ingrowth needs building blocks of all sizes: osteoblasts, blood vessels, Haversian canals, etc. This variety of sizes is obviously the most efficient way of filling space. Walls of medieval or older castles, meadow walls in the British countryside and so on are

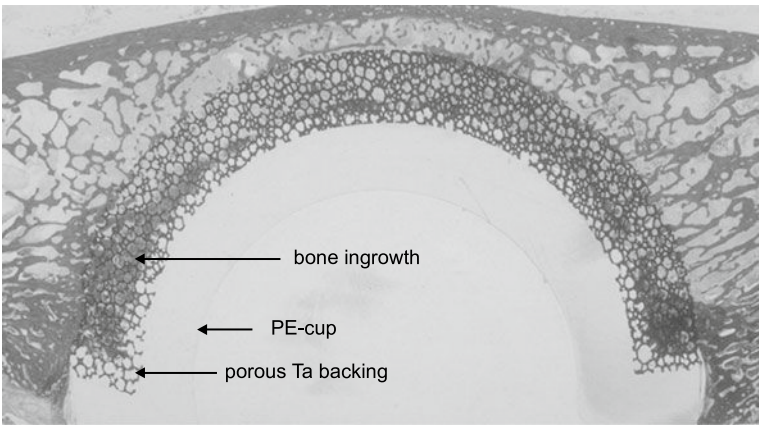

Fig. 5.11 Acetabular cup with porous tantalum backing 6 months after implantation. Courtesy: Zimmer

Fig. 5.12 Wall of the Umayyad Palace in Amman (Jordany)

constructed with large stones whose gaps are filled with a mixture of smaller stones. The result is a strong, efficient, occasionally low cost construction (less cement needed). An example of such a construction is visualized in Fig. 5.12: part of a wall of the Umayyad palace in Amman. We did not analyze the size distribution in this particular case but it can reasonably be assumed on theoretical grounds that a self-similar fractal composition is the most efficient space filler. Herewith we only suggest that the ingrowth in porous Ta and occasionally its fractal nature might be together with pore size co-responsible for the success of this device.

5.4 Alloys with a Future?

Scientists are a strange race of people and always on the run to unexplored corners hoping to discover the ultimate philosopher's stone. Two other classes of materials are introduced hoping that in the future a couple of neonates will emerge from these classes.

Amorphous Zirconium

All biometals and bioalloys scrutinized thus far were polycrystalline, not perfect but with a fair degree of long-range order. A particular class of materials, the atoms of which have less predictable neighbors, are the *glasses*. Metallic glasses are not easy to make but, since a few years, glassy ternary and quaternary alloys are gaining a marketable status. Of interest are the recently developed nickel-free metallic glasses $Zr_{48}Cu_{43}Al_7Ag_2$ and these could be new biomat-candidates. Some can be produced in bulk, meaning here rods of 20 mm diameter, YS of 1.9 GPa, a plasticity of 1.3%, a yield strain of 2% and exhibiting negligible cytotoxicity. The stress–strain curve has a linear part from 0 to ∼1,900 MPa followed by a short curved transit part and ending after ∼1.9% strain in a linear quasihorizontal plastic zone.

Another opening is the design of metallic glass matrix composites as reported by Hofmann et al. [225]. The inhomogeneous microstructure with isolated dentrites in a bulk metallic glass (BMG) seems to stabilize the glass matrix against the catastrophic failure. These authors report on 5 compositions but all contain toxic beryllium and the unwelcome nickel. The list of mechanical properties is stupendous but it is waiting on a similar development for Be- and Ni-free glasses.

The potential biomedical applications are self-expandable stents, blades for surgical instruments and micrometer-sized gear for implanted devices (actuators, pumps, . . . ?) [226–228]. The authors, however, are not generous with information.

Notice that, irrespective of their biomedical use, glasses are an intriguing class of materials (we mentioned in earlier chapters the book of Elliott with the basic principles of the amorphous state [229]). Metallic glasses are most often metastable at ordinary temperatures and difficult to make in 'bulk'. The best known and widespread application is the photoactive cylinder of a photocopy machine coated with a film of amorphous selenium. Amorphous metals are part of an active research community and an emerging field in the biomaterials world. It remains of course an open question what the success niche for applications will be.

Al–Cr–Fe

The alloying elements in this new fabric are old faithful metals throughout the former chapters. We already formulated some reservation with respect to Al but the long experience with Ti6Al7Nb attenuated for the time being the tune of this alarm bell. Al–Cr–Fe alloys belong to the class of *complex metal alloys* (CMAs) with

multifunctional surfaces. Some are indebted with an impressive set of properties: low surface energy (hydrophobe, low friction coefficient), high hardness (wear resistance) and high corrosion resistance. However, the literature data are still too scarce to compose a coherent table on engineering properties or on potential biomedical properties.

Aluminum alloys were intensively studied since many decades to improve their mechanical properties (lighter metals for aircrafts). As already discussed mechanical properties of metals can be improved by precipitating small grains during cooling or grain refining, both pinning down deformations of the lattice. During cooling aluminum+copper copper-rich precipitates are formed reinforcing the aluminum (duralumins). In 1982, Danny Schechtman and coworkers discovered in these alloys Al–Mn crystals with five-fold symmetry, till then unseen in crystallography. One can imagine the delight of the materials scientist when admiring this crystallographic anomaly: *it turned out to be the most sophisticated achievement of Nature in the world of complex intermetallics*. Meanwhile, they can be produced at industrial scale by conventional metallurgical techniques. The set of strange properties are recognized by industry and some are turned into commercial products. Comprehensive texts on this subject are the books of Janot *Quasicrystals, A Primer* [230] and the Dubois's recent book *Useful Quasicrystals* [231].

Penrose, one of the most prominent mathematicians of former century, forced fivefold symmetry into an aperiodic plane filling tiling. It also appeared to be possible to construct a three-dimensional Penrose aperiodic network maintaining five-fold symmetry. Herewith, a fascinating research field was born and a crystallographer's frustration about five-fold symmetry, dodecahedra and icosahedra has been lifted. For the interested reader, the books of Janot and Dubois (under some reserve for his experiments on wear) are recommended literature.

Listed below are the eye-catching properties of these peculiar materials with respect to future biomedical applications. Quasicrystals:

- Exhibit low electrical conductivity $(\sim 300\,\Omega.\mathrm{cm})^{-1}$ at 300°K. This phenomenon is more reminiscent to metallic glasses or amorphous semiconductors than to the constituting metals; the reason for this phenomenon is theoretically not yet cleared out.
- Exhibit low heat conductivity substantially lower than the metallic constituent elements.
- With good lattice perfection and diamagnetic (in contrast to Al and Al-based crystalline intermetallics that are diamagnetic).
- Have low corrosion currents.
- Are hard and brittle and do not show any work hardening like conventional metals.
- Have low friction coefficients.
- Are poorly wetted by polar liquids.

Is it only a dream thinking that the combination of low wettability with high hardness and a low friction coefficient might one day permit to produce more ideal joint prostheses or some other device we are not aware of yet?

5.5 Postscript

A reliable *in situ* oxidation technique of zirconium united the advantages of ceramics and metals, short circuiting their disadvantages and circumventing the problem of coating adhesion to the substrate. Meanwhile, OxZr, marketed under the trade name OXINIUM^{TM}, with an oxide thickness of 5 μm, got its share in joint arthroplasty and is a true technological leap.

Two other leaps in science and technology were briefly reviewed: *glassy metals* and *quasicrystals*. The aim was to open a window on ongoing research on materials hardly present on the biomaterials forum. Coined by two and a half millennium of thinking in terms of Euclidean order, we hardly realize how deeply it determined our vision on structure and physics of matter. All metals discussed thus far were crystalline and the introduction of these new items should stimulate to look behind the present horizon.

Polymer chemists and biologists were already longtime familiar with less ordered or chaotic systems. Silicate glasses are common goods since more than two millennia but glassy metals were not. What do they keep in store for the biomaterialist?

Five-fold rotational symmetry was only common in flowers but unseen or seen as impossible in crystalline matter. But they do exist, can be mass-produced and combine a number of peculiar properties that may one day be exploited by the biomaterialist.

Chapter 6
Long Bones

A middle-aged adventurous man was some years ago on a 10-day motorbike trip through Peru. On his way back from the jungle Madre de Dios to Cuzco, our experienced motorbiker did not see a hole in the jungle track by the dirt blown up by his fellow companions. His vehicle landed upside down off the road while smashing his driver ungently on Peruvian soil. . .end of the Peruvian trip. Half an hour later an aid station, oh wonder, could send a doctor. The supracondylar humerus fracture was immobilized *avec les moyens du bord*: cardboard and belts splinted the fracture in extension. The safety pin on the radiograph is an undeniable witness of the emergency treatment. Hours later the patient arrived in Cuzco on board of an improvised ambulance with paracetamol as the only pain killer. An upper arm plaster immobilized the elbow in extension (this time anesthetized!) allowing the transport of the patient to the academic hospital of the university of Ghent (Belgium). The bits and pieces were adequately hold together by locking plates and screws as shown on the radiographs of Fig. 6.1. The issue was successful and three days later a pleased patient left the hospital. The case was told us by Prof. R.Verdonk (Department of Physical Medicine and Orthopedic Surgery, Ghent University, Belgium).

The first aid in the case of the high impact fracture was offered by splinting using simple materials as cardboard and belts. What is a more advanced materials toolbox offering us for temporary or permanent exo- or endo-support in such cases?

6.1 Plaster of Paris

The splinting of broken legs by a *composite* of bandage and the hemihydrate of calcium sulfate has been invented by the Dutchman Mathijsen in 1851. The hemihydrate is formed by heating the mineral gypsum to 150°C:

$$2CaSO_4.2H_2O \rightleftharpoons 2CaSO_4.\frac{1}{2}H_2O + 3H_2O \nearrow \tag{6.1}$$

In contact with water, the reaction is reversed and the impregnated bandage hardens by hydration to gypsum. A large deposit of gypsum was exploited for the building industry near Montmartre (Paris), explaining the name *plâtre de Paris*. But its use

J.A. Helsen and Y. Missirlis, *Biomaterials*, Biological and Medical Physics, Biomedical Engineering, DOI 10.1007/978-3-642-12532-4_6,

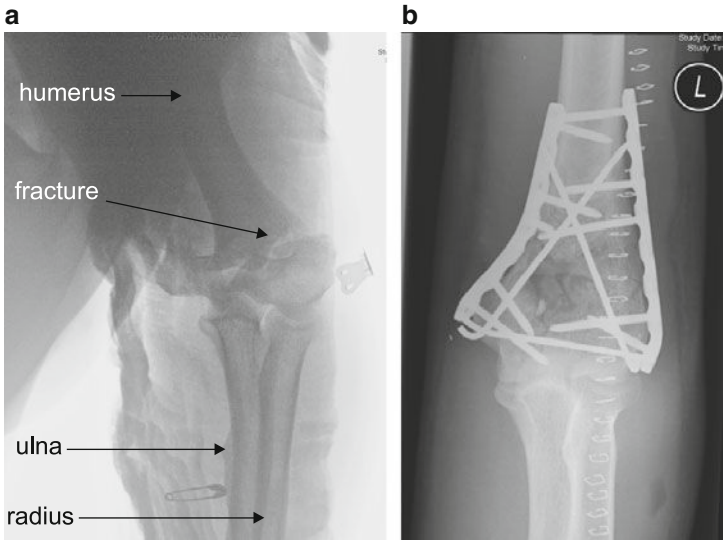

Fig. 6.1 High impact elbow fracture: (*a*) the splinted fracture; (*b*) after stabilizing the fracture by osteosynthesis plates. Courtesy Prof. Dr. R. Verdonk

dates back 2,500 years ago: the Ethiopian soldiers painted their bodies with gypsum and, at least 5,000 years before present by the Egyptians. They covered a dead and dried body with gypsum, adorned it with painting until it was as like the living man as possible, put it in a crystal pillar through which one could see the corpse. The pillar was not crystal but apparently well crystallized pure and transparent gypsum (Herodotus, VII, 69; *Loeb Classical Library* 2006 and III, 24; *Loeb* 2000). Plato uses γύψος, gypsos, to indicate the very pure transparent material used for temple windows (Plato, Phaedo, 110c and 111b; *Loeb* 2001).

Plaster is widely used as a support for broken legs. A bandage impregnated with plaster is moistened, then wrapped around the damaged limb; it sets into a close-fitting. This orthopedic cast, as a matter of fact a *macrocomposite*, is easily removed after healing. The same technique is used for producing long-term external immobilization supports. First, a (negative) cast is made using the same impregnated bandages and setting. After removal, it is filled with plaster to get the positive cast from which a negative impression is made with polymers such as polymethyl methacrylate (PMMA) or thermoplastic polymers such as polyethylene (PE) or polypropylene (PP). An other use still is the mounting cast in dentistry.

6.2 Corollary Between Mineral and Biological Evolution: An Excursion in the Dark Ages

The one-liner 'Water does not flow uphill' we used in a former chapter is a simple declaration of the second law of thermodynamics recognizing the fundamental dissymmetry of nature: hot things cool, cool things do not spontaneously become

hot. The sign of the difference in (electro-)chemical potential determines the sense a physical process will take although it does not say anything about the rate of the reaction (reaction kinetics).

The history of earth's minerals started by accretion of cosmic dust, meteorites and subsequently those formed in earth's magma. That, let us say, happened the *first day* paraphrasing Genesis 1 of the Bible: *the earth was barren with no form of life followed by the command to the light to shine in the first day*. At the typical high temperatures of the magma, a relatively homogeneous mineral soup was produced. Olivine, pyroxene and feldspars were the main minerals in a repertoire containing an estimated number of 250 different minerals at the end of a geological period some 4.55 Gya (i.e., **G**iga **y**ears **a**go).

On cooling, say during *day 2*, the elements of the archean soup became more selective in choosing their reaction partners, not dictated by butterflies in the stomach but by principles of minimizing free energy. Fractional crystallization (conditioned by reaction kinetics, concentration, temperature, pressure, solubility, etc.), the formation of continents, hydrothermal processes, metamorphism, weathering and so on led to further diversification and the repertoire was growing to about 1,500 different minerals. This was the situation at the end of the Neoarchean earth with, as in Genesis 1 the *second day*, *a dome to separate the water above it from the water below*.[1] The atmosphere was anoxic but life (microorganisms) was emerging and had a definite effect (major or minor is not well established) on the mineral composition of sedimentary rocks. Anyway, two things seem to be clear: (1) according to some origin-of-life scenarios the *second day* of chemical processing was a prerequisite for life and (2) once life started it co-conditioned the earth's mineral evolution. We will come back on this issue in Chap. 14.

The dawn of *day 3* (<2.5 Gya) is characterized by the *The Great Oxidation Event*. As just said, for the past 2.5 billion years earth's minerals co-evolved with life. In Genesis1:11 God said *I command the earth to produce all kinds of plants, including fruit trees and grain* and so it was. The oxygenation of the atmosphere was principally a consequence of oxygenic photosynthesis (cyanobacteria). Living organisms found it worthwhile to frustrate thermodynamics. They expended part of their energy reservoir to synthesize minerals that otherwise would not form under the given conditions of temperature and pressure. Gypsum is here the obvious example. Sulfate is at present ocean's second most abundant anion. $CaSO_4$ was formed by the presence of SO_4^{2-}, partly provided through oxidation of sulfur by bacterial activity, the companion source being photooxidation of sulfur. Another example of bioactivated mineral formation are the highly organized aragonite crystals, a polymorph of $CaCO_3$, in the pearl shells of some mollusks [233, 234]. The iridescent

[1] The inspiring review by Hazen and colleagues was the trigger to refer to Genesis [232]. The sequence of geological happenings as elaborated in the Modern Era parallels the logic thinking of Genesis authors some two and a half millennia ago. Realistic time scales, however, are a nineteenth century performance when geology emerged as a new scientific discipline. An indirect product of this emerging science was Darwin (born 1809) and its masterpiece *On the Origin of Species* (published 1859).

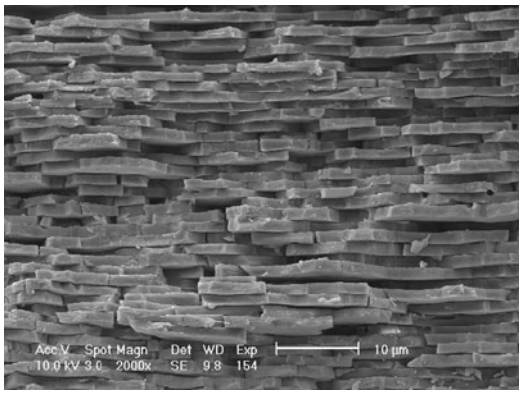

Fig. 6.2 Fracture surface of the iridescent layer inside an ordinary mussel shell (Mytilus edulis). Photo R. De Vos

inner layer of an ordinary mussel shell is composed of a stapling of platelets of aragonite. This wonderful layering is characterized by a micrometer-sized periodicity which is at the origin of its iridescence. It is nicely illustrated by Fig. 6.2.

Glycoproteins control the precipitation of aragonite vs. calcite. Not to forget mentioning here are the otoliths, the minuscule calcite and/or aragonite stones in the saccule or urticle of the inner ear and their relation to fluid dynamics for proper growth and patterning [235]. They are of capital importance for our balance.

Both in invertebrates and in vertebrates phosphates such as hydroxyapatite and whitlockite serve as skeletal minerals for shells, bone and teeth. A series of minerals are continuously synthesized in our body to support its functions such as that of our skeleton, or to disturb them such as kidney stones. These processes assisted the present-day composition of the outside mineral world.

Gypsum was the spark for this promenade through time. The corollary to geology was intended to stimulate a look behind the ramparts of time, to see how life co-shaped today's earth and hopefully triggers indirectly some ideas for the development of new materials or to copy some natural processes for the synthesis of materials, occasionally in situ (aragonite in shells) or preventing unwanted synthesis (weddelite in breast cancer). In Table 6.1, the minerals found in humans are listed, excerpted from Table 3 in a paper by Hazen et al. [232]. The list of minerals produced by biomineralization is much longer and interested readers are referred to the paper of Hazen and colleagues.

Calcite is volumetrically the most significant biomineral and thermodynamically the most stable. Its crystallographic structure is rhombohedral while aragonite is orthorhombic and vaterite hexagonal (simplified). Vaterite is the least stable, transforms to calcite in aqueous medium but can be stabilized by other metal ions as witnessed by its persistent presence in gallstones. A scientific novelty is the dramatic and sudden shift of calcite to aragonite in the late Paleozoic through the mid Jurassic some 300–150 million years ago. The phosphates serve as skeletal minerals. The organominerals weddelite and whewellite are observed in urinary sediments and, as mentioned, in breast tumors.

Table 6.1 Minerals found in humans

Name	Formula	Name	Formula
Aragonite	$CaCO_3$	Calcite	$CaCO_3$
Vaterite	$CaCO_3$		
Brushite	$Ca[PO_3(OH)].2H_2O$	Fluoapatite	$Ca_5(PO_4)_3F$
Hydroxylapatite	$Ca_5(PO_4)_3(OH)$	Monetite	$Ca[PO_3(OH)]$
Whitlockite	$Ca_{18}H_2(Mg,Fe)_2(PO_4)_{14}$		
Epsomite	$MgSO_4.7H_2O$	Gypsum	$CaSO_4.2H_2O$
Urea	$CO(NH_2)_2$	Weddelite	$CaC_2O_4.2H_2O$
Whewellite	$CaC_2O_4.H_2O$		

6.3 Thermoplastic Polymers

Although still widely used and cost effective, plaster is gradually replaced by other materials. The positive model is no longer produced by taking casts but the limb, be it the neck, the whole trunk or legs, is digitalized by scanning with an advanced laser system. Software allows image manipulation occasionally for anatomical correction of the *virtual limb*. Subsequently, computer-aided machining reproduces the limb in a polymer foam. An appropriately heated PE or PP sheet is closely fitted (vacuum) to the model to obtain the negative 'cast'. Biocompatibility constraints are relatively simple because these external supports are screened from direct contact with skin by underwear in cotton or other common tissues. More details on thermoplastic polymers are found in Chap. 11.

6.4 External Fixators

Complex fractures, fractures with large bone gaps, off-axis position and so on were difficult if not impossible to repair in the 1950s: lack of appropriate instruments, antibiotics, trained orthopedic surgeons. But Gavril Abramovich Ilizarov revolutionized the world of traumatology during those years (biography Sect. 6.7).

Ilizarov developed gradually the present-day instruments, two examples of which are shown in Fig. 6.3. Limb lengthening was not done, may be even not thought off in those days. He was doing research on stress–strain behavior of bone. The story goes that one of his patients was accidentally giving during fracture healing distraction instead of compression. Figure 6.3a makes the reader clear how that could have happened: by just turning the nuts in the wrong sense. Ilizarov discovered radiographically neoformation of bone in the fracture zone. He did not reject this peculiarity as a rare coincidence but, characteristic for the true scientist, draw the right conclusion and the principle of limb lengthening came into being.

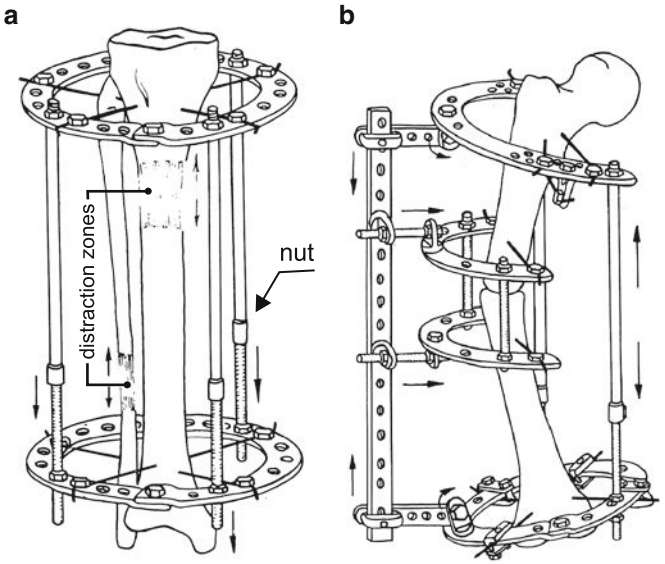

Fig. 6.3 Ilizarov techniques. Two examples: (**a**) use for lengthening of the tibia and fibula after compactotomy; (**b**) correction for off-axis and diaphyseal pseudoarthrosis (from the catalogue of Hospital & Medical Supplies)

The bone, broken by any external reason or broken on purpose before the start of lengthening or correction for off-axis growth or a burden of other reasons, is kept in position by pins, called Kirschner pins with diameter of 1.5–1.8 mm. The pins perforate skin and bone creating ample entry gates for infection. In limb lengthening, however, infection is unexpectedly rare according to the hospitals specialized in Ilizarov techniques that we asked for advice. Review reports, however, consider infection as devastating in trauma surgery and often leads to septic nonunion and chronic osteomyelitis.[2] Open fractures represent, almost by definition, the highest risk. The use of implants favors the risk. The formation of a biofilm seems to be the crucial step in the proliferation bacteria on the implant. The biofilm consists of cells and extra-cellular polysaccharide matrix and is handy for bacteria because it enables them to deceive the patients defence. The most common bacterial strains in bone and joint surgery are *Staphylococcus (S.) epidermidis* and *S. aureus*, both known as slime-producing bacteria; treatment is (increasingly?) difficult. Prophylaxis is in this instance crucial and it should start already in the operating room, followed by adequate systemic administration of antibiotics.[3] The extracellular polysaccharide substance is composed of a range of low and high molecular weight compounds such

[2] Osteomyelitis is an acute or chronic inflammatory process of bone, mostly an infection provoked by *Staphylococcus aureus*.

[3] Systemic: affecting the body as a whole. Example: through intravenous administration of antibiotics.

as the carbohydrates D-glucose, D-galactose, D-mannose, L-fucose, L-rhamnose and amino sugars, uronic acid and/or polymers like polyols, the whole forming a rewarding substrate for bacterial survival.

Complementary to systemic administration of antibiotics is the use of implants with bactericidal or bacteriostatic coatings. The coatings we met thus far pursued a different goal: corrosion protection, wear resistance, porosity for promoting ingrowth. The advantage of implants bearing bactericidal compounds was recognized since long and is since many years common practice in bone cements containing an antibiotic, often gentamicin. An excellent example of its efficiency is shown in a paper by Lucke and colleagues for fixation of infected tibia fractures with uncoated and gentamicin-coated Kirschner wires. Other bactericidal coatings contain chlorhexidine or chloroxylenol [236, 237]. Hereafter, we describe one out of a few alternatives namely a proposal for coating the surface with silver particles.

Silver as Filler or in Coatings

The antibacterial property of silver is well documented since many years. Already in the 1930s, Ernst Gräfenberg, a German obstetrician, found silver to be active against sperm and applied it in a intrauterine device (IUD).[4] It consisted of helical silk threads covered with fine silver wire and bent into a ring. It has a high affinity to S^{-2} and –SH groups (see K_{stab} in Table 4.2). The deposition of silver can follow different routes. Hardes and colleagues realized and implanted silver-coated megaprostheses (<very long hip stems) to prevent deep infection in orthopedic tumor surgery. These authors deposited galvanically a 10–15 μm thick silver layer on the Ti-Al-V stem; from the picture in Hardes' paper the coated surface area was estimated at about 30 cm^2. The stem was previously covered by a 0.2 μm gold layer to assure a sustained release of silver ions in the periprosthetic tissue (not well understood!). A cohort of 20 patients with different tumors was involved in this study. The authors focused on signs of systemic and local argyrosis, wound healing and neurological impairments.[5] The serum levels became enhanced from the preoperative 0.4 ppb to around 5 ppb but the periprosthetic tissue concentration could in some patients amount 1,600 ppb. From this study, the authors could conclude that no local or systemic side effects or toxicity could be shown by the silver release of their megaprostheses [238].

Another approach is followed by German groups in Giessen and Bremen. The challenging aspect of Ag particles is their antibacterial activity in vitro against *S.epidermidis* and *S.aureus* and, more important, Ag nanoparticles are exclusively effective against all strains including their methicillin-resistant variants (to which gentamicin is not effective). Bone cement (see for more details on poly-methylmetacrylate (PMMA) in Chap. 11) loaded with silver salts was unsuitable for all day

[4] Ernst Gräfenberg was a German-born medical doctor born in Adelsleben (Germany) 1881, moved to USA in 1937 and died in New York 1957.

[5] Argyrosis: blue or bluish-grey coloration of the eye by ingestion of colloidal silver or silver compounds.

clinical use but mixed with 1% *Nano Silver* it probably is. *NanoSilver* refers to particles of 5–50 nm with an active surface of 4 m^2/g and a porosity around 90% (0% in commercial silver powder). At the concentration of 1%, no bacterial growth is allowed (Fig. 5 of a paper by Alt et al. [239]).

For coatings an in situ deposition of a polymer-Ag composite was used [240]. Biocompatible, chemically inert, insoluble, mechanically and thermally stable films can be deposited on stainless steel and titanium Kirschner nails by plasma polymerization using as precursor hexamethyldisiloxane. The films consist of an SiO_x plasma polymer. Silver porous clusters, size of clusters around 10 nm, were formed using inert gas evaporation. They can be produced either by deposition on the bare metal (type A) followed by a plasma polymer layer, or embedded between two plasma polymer layers (type B). As shown in Fig. 6.4, a percolating path runs between the Ag islands. The polymer film on top of these islands makes contact with the metal surface in between the Ag nanoparticles assuring a well adhering coating.

The results are shown in Fig. 6.5 for 6 repetitions. The strain on duty for in vitro tests is *S.epidermidis*. Uncoated wires show uninhibited bacterial proliferation with negligible delay (vertical axis). Type A (columns 3 and 4) shows complete inhibition with only a small exception for Ti in column 4. The same story for Ti with coating B but B is ineffective on SS. It might be concluded that technique A exhibits promising bactericidal activity on both stainless steel and titanium. Why type B on SS is not effective remains unclear.

The discussion of bactericidal Ag coatings and a reference to Ag fillings is merely a random choice out of an abundant list of items in the literature. It is giving just a taste of what is going on in this part of the biomaterial world and what might be on the menu in the years to come. Moreover, the use of nanosilver particles as well as nanoparticles in general should be handled with care because they figure high on the list of the emerging new branch in toxicity testing. Histopathological examinations of rats exposed to inhalation of silver nanoparticles indicated dose-dependent increases in internal lesions. Target organs were considered to be lungs and liver [241].

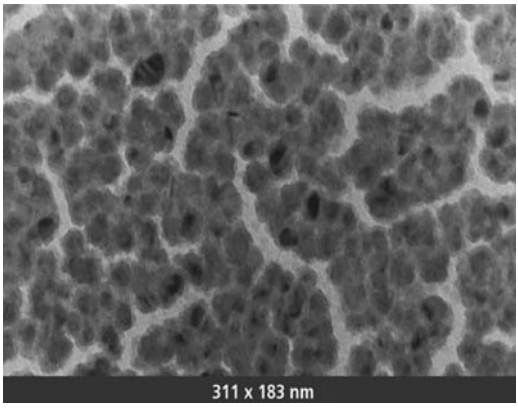

Fig. 6.4 Transmission electron microscopy of Ag clusters deposited on the metal surface (type A). From [240], by courtesy of Springer Verlag

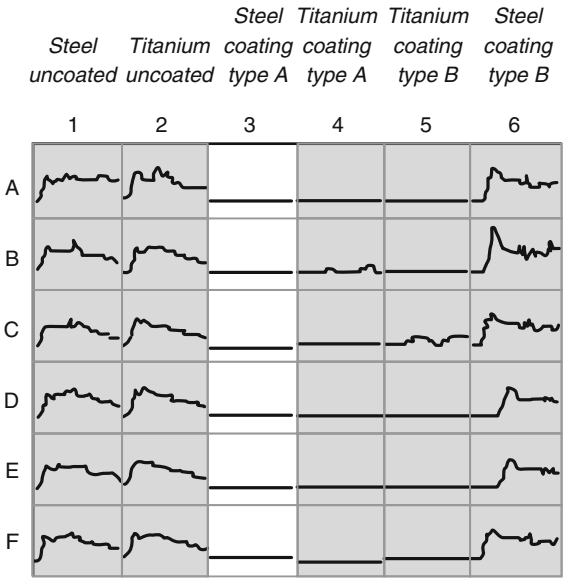

Fig. 6.5 Time-proliferation curves for 6 Kirschner wires (A–F) (diameter 2 mm, length 150 mm) in SS or Ti without coating and with coatings type A and B. From [240], by courtesy of Springer Verlag

6.5 Exploring the Future

In several places throughout the book, we tried to see in the crystal ball. Excellent alloys of mechanical and chemical high standard as well as improved design during the last six decades resulted in orthopedic devices with undeniably outstanding performance. Surface modifications, exception made for hydroxyapatite coatings, did contribute only marginally to the present success of these devices. Despite enormous research efforts over a wide field of potential candidate materials few found the way to successful commercial products. We saw in this chapter how Ilizarov's 'garage box' engineering became a booming practice in mainly three directions: fracture healing, shape corrections and limb lengthening. Improvements of the now traditional devices have reached an asymptotic regime. The knob, however, has been turned and the focus for the coming era will be on biomolecular interventions, what does not imply that all 'traditional' materials research is becoming obsolete.

For accelerated fracture healing, a long list of candidates, some of which already approved for clinical use, populate the biomedical journals: autologous blood concentrates including platelet-derived growth factor (PDGF); the angiogenic vascular endothelial growth factor (VEGF); recombinant human bone morphogenetic proteins (rhBMP), known as the most powerful osteoinductive factors; chrysalin, the synthetic peptide drug TP508; insulin-like growth-I (IGF-I); demineralized bone matrix retaining collagen and noncollagenous proteins. The latter are already

available for clinical use; BMP-7, BMP-2, rhBMP-2 are actively investigated (since at least three decades) with undeniable excellent promises but no real breakthrough.

Functionalizing Surfaces

A metal oxide film is screening the metal substrate from the outside world to prevent further oxidation. It is formed simply by exposure to air or is deliberately grown by chemical or electrochemical means. A beneficial osteoconductivity or simple biotolerance was a welcome bonus. Nanosilver coating was an example to assign an active function to the implant-tissue interface but one with only bactericidal capability. But there is more to come.

For orthotopic administration as wanted for intraosseous implants the growth factors need a carrier on the implant surface. Several authors studied the in vitro and in vivo release of IGF-I and human recombinant bone morphogenetic protein-2 (rhBMP-2) adsorbed on porous β-tricalcium phosphate as carrier. Dose-dependent osteoinduction, osteogenesis around the implant, densification of peri-implant trabeculae and increased resorption of the ceramic are firmly substantiated. A vast body of papers is published (see, for example, papers of Laffargue et al. [242, 243]). The study by these authors was performed on cylinders of the phosphate ceramic and not on implants coated with this porous ceramic; rabbits were used as animal model. An obvious alternative ceramic is calcium hydroxyapatite, although other porous resorbable substrates as used in drug delivery systems should not be excluded. Although coating technique by phosphates is established knowledge, growth factor-loaded hip, knee or osteosynthesis implants are not commercialized in as far as we know. A sound reason might be that BMPs behave somewhat strange. The choice of concentration is tricky business and too high a concentration has the inverse effect: osteoblast activity decreases (Private communication, H.F. Hildebrand and [243]).

Scaffolds

Different calcium phosphates passed already the scene in the literature. A relatively new proposal is published by Schek and colleagues [244, 245]. The objective was to make a biphasic scaffold for repairing osteochondral defects. A porous polylactic acid (PLA) is seeded by chondrocytes, the other phase is a hydroxyapatite (HA) with orthogonal pores which are seeded with fibroblasts infected by a BMP-7-expressing adenovirus. The two phases are separated by a thin film of polyglycolic acid (PGA). After implantation in a mouse model, the HAP side showed formation of bone, the PLA side a cartilaginous tissue. This composite scaffold is schematically represented in Fig. 6.6. The composite produced by Schek had a diameter 5 mm, a height of 6 mm and the pores were 800 or 300 μm wide. The results are encouraging but to our knowledge only tested on animals.

HA scaffolds are or can be applied to fill large bone gaps, while the HA matrix gradually disappears and is replaced by bone. For large scaffolds, angiogenesis is

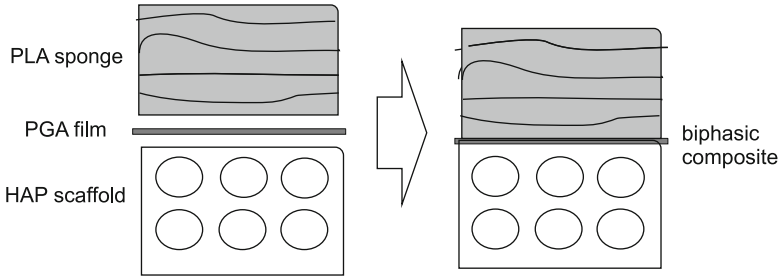

Fig. 6.6 The production of a biphasic scaffold: orthogonal pores of 800 or 300 μm wide in the HAP phase, layers of polylactic acid, separated from the HAP phase by a thin glycolic acid film

the limiting factor but it is known that VEGF is promoting angiogenesis and bone turnover. We do not know whether or not it has been integrated in commercially available implants. More about scaffolds are found in Chaps. 7 and 13.

Wood-Derived Hydroxyapatite Scaffolds

On page 101 and in Fig. 1.2, we made reference to wood as prosthesis material or as an example of design in nature conditioned by mechanical constraints (*tensegrity* model?).[6] On pages 10 and 143 and in Fig. 5.12, questions were raised whether or not pore or building block size distribution could contribute to improved biomimicking. In a way, these comments/propositions find an experimental synthesis in recent research by Tampieri and colleagues. These authors took *Nature as a source of inspiration for the development of hierarchically structured biomaterials* [246].

Taking total porosity and pore size distribution as criteria, pine wood and rattan were selected to produce *biomimetic hydroxyapatite bone scaffolds having highly organized micro- and macro-porosity*.[7] They have, respectively, a total porosity of 70 and 85%. Pine wood has large pores: 41% with a diameter of 80±45 μm; the large pores of rattan have diameters of 250±40 μm (Fig. 6.7a,b,d,e).

A scaffold was manufactured following the scheme represented in Fig. 6.8. The skeletal anisotropic (!) structure of the wood serves as template and is conserved after pyrolysis. The carbon skeleton is infiltrated with calcium, thermally transformed into CaC_2, oxidized to CaO, hydrothermally carbonated to $CaCO_3$ and finally phosphatized. Each step is thermodynamically documented and fully characterized by X-ray diffraction, infrared spectroscopy, scanning electron microscopy (SEM) and finally evaluated on porosity and mechanical properties. The compression strength of

[6] *Tensegrity* is a term coined by Buckminster Fuller (American Architect(1895–1983)) for structures, which borrow their stability from the way the members are organized rather than from the individual strength of the members.

[7] Rattan (Manau), or Rotan in Indonesian language, belongs to the botanical *ordo* of the Palmales and *family* of the *Palmae*. Mainly from South East Asia.

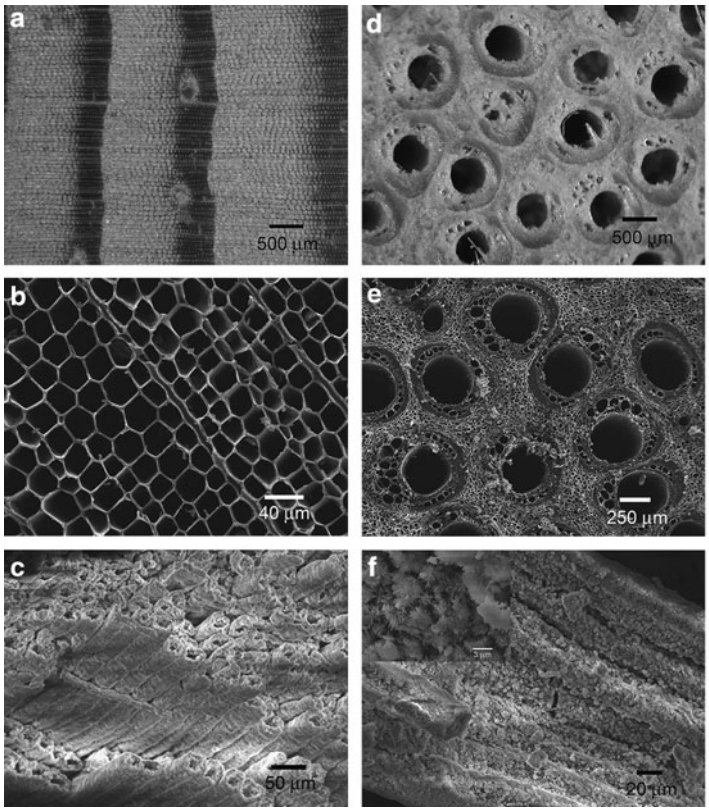

Fig. 6.7 SEM images of pine wood (**a**, **b**, **c**, **f**) and rattan (**d**, **e**): (**a**, **d**) native forms; (**b**, **e**) pyrolyzed; wood-derived hydroxyapatite: (**c**) parallel fastened hydroxyapatite microtubes; (**f**) needle-like hydroxyapatite nuclei grown on the microtube surface. Reproduced with permission of The Royal Society of Chemistry [246], Figs. 1(a, b, c, d) and 10

the pinewood scaffold, measured parallel to the channels ranges from 2.5 to 4 MPa, perpendicular to the channels 0.5–1 MPa. The pore size of the rattan-derived scaffold is 100–300 µm together with sizes ranging form 0.01 to 100 µm. Pinewood processing resulted in a bimorphic hydroxyapatite: ordered parallel microtubes 100–150 µm long and 15–30 µm wide with a hollow core and, as shown in the insert of f, needle-like nuclei grown crystals, typical aspect of a dissolution/precipitation crystallization process (Fig. 6.7). The pores were proved to have a high degree of interconnectivity.

The authors do not report any in vitro or in vivo or clinical testing. This fabrication technique, however, was discussed into some detail because it is a stimulating topic: using Nature as template. It is not unthinkable to use a plant structure, forced into a mechanically desired morphology during growth, as bone scaffold template. Following the same biomimicking philosophy, cell-produced aligned collagenous matrices have been proposed as scaffolding material to enhance ligament and tendon healing [247]. Phantasy, for the time being yes but part of a bioengineer's dream.

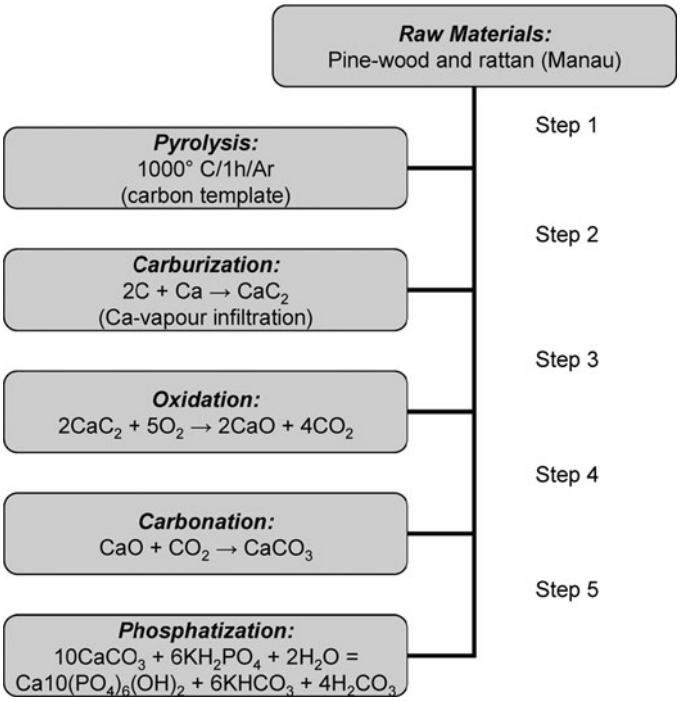

Fig. 6.8 A five-step processing scheme for transformation of pine wood or rattan to a porous hydroxyapatite scaffold. Reproduced with permission of The Royal Society of Chemistry [246]

6.6 Osteosynthesis

Broken legs, however, are not healed by speculation over the future but for the time being by decent plates and screws. Nothing special, in particular, has to be said about the basic materials because the classics dominate the field: stainless steel (316L) and titanium alloys (Ti6Al4V or Ti6Al7Nb). Fracture fixation demands mostly high strength alloys in cases as shown in Fig. 6.1 and even more for complex femur or tibia fractures. The classic alloys match perfectly the endo-prosthetic mechanical requirements and thus... end of the debate?

Nothing is less true. The reason we devote a section to osteosynthesis devices is that we want, once again, to point to possible failure of even the best material when used under wrong conditions. For many devices, the main progresses will be situated in design rather than in 'naked' materials properties. In Chap. 3, corrosion between screw head and osteosynthesis plate was cited as a location of fretting corrosion (see 149). In a device recently introduced by Zimmer, locking caps are used.[8] It allows to achieve angular stability of the screw and it meets simultaneously the

[8] Zimmer GmbH. Info: www.zimmer.com.

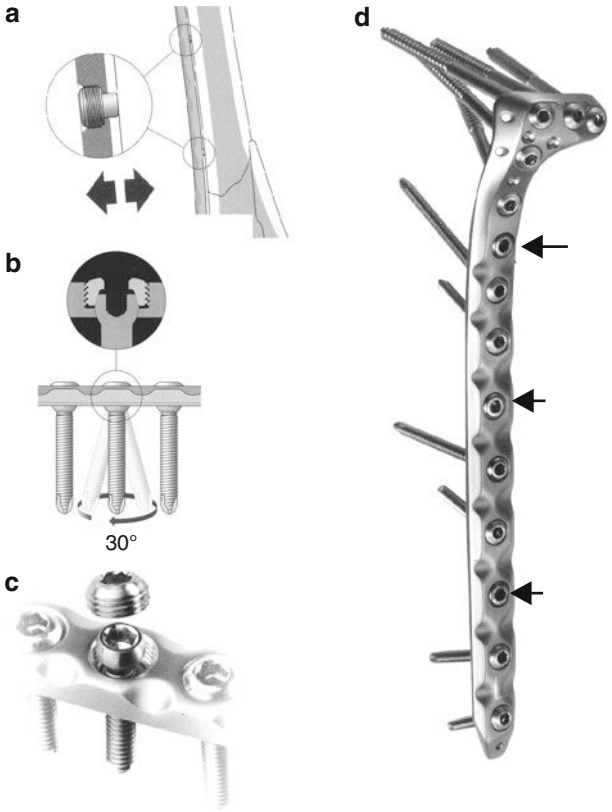

Fig. 6.9 Locking plate system for trauma surgery: (**a**) noncontact bridging; (**b**) screws can be placed at different angles; (**c**) angular stability achieved by using locking caps; (**d**) example of a NCB-PT Proximal Tibia plate. Arrows indicate the position of Noncontact Bridging screws. Reprinted from Zimmer, NCB®Polyaxial Locking Plate System (2008)

inconvenient consequence of fretting (b–d in Fig. 6.9). The alloy used is Ti6Al4V (ASTM F-136 or Protasul-64, the Zimmer Trade Name).

An inconvenience of plates is the possible damage of the periost and vascular trauma. A solution is to make the plate nonbridging by the use of spacers as shown in Fig. 6.9a. Another Swiss company tackled the problem years ago by their Limited Contact Plate (LCP) combining another two design peculiarities: limited contact and uniform bending and torsional stiffness. A plate of uniform section shows stress concentration at the screw holes, sites of corrosion and onset of fracture. Based on finite element analysis, a plate was produced with uniform stiffness over the whole length. Bending such a plate has a continuous curvature which improves fit to the contour of the bone and minimizes risk of fracture and corrosion (Fig. 6.10).

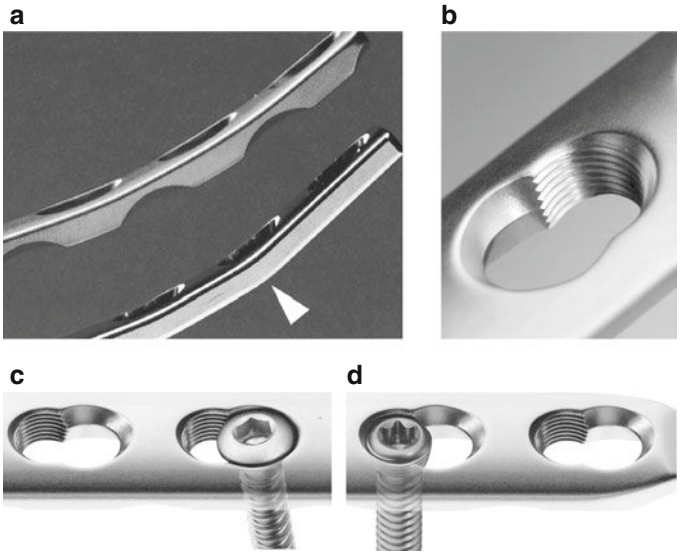

Fig. 6.10 Limited Contact Plate (LCP): (**a**) conventional plate (*bottom*), arrow points to spot of stress concentration; plate with uniform bending stiffness (*top*); (**b**) recent modification: combi hole: threaded for fixed angle or conventional; (**c**) with conventional screw; (**d**) with locking screw. Reprinted from Synthes, Locking Compression Plate, Instructions for Use (2007)

Outside the alloys just mentioned, Synthes uses also pure titanium with controlled concentrations of oxygen.[9]

To conclude: this chapter was a walk in the dark, exploring how fractures were, are and possibly will be healed, hereby taking also a couple of sideroads. We tried to make clear once again that materials properties and design constraints are intimately linked to achieve a successful end product. A next big leap in hard tissue implantology seems to be imminent but breakthroughs of the size brought about by Charnley or Ilizarov are not seen yet.

6.7 G.A. Ilizarov

In total hip arthroplasty, the bell name is Prof. Charnley (see Chap. 2). Another monument of orthopedic surgery is Gavril Abramovich Ilizarov.

Fiddler on the roof, a village in tsarist Russia in 1905 (musical from 1964 based on a book of Joseph Stein). It could well have been a scenery of the village Dagestan near Vitebsk (Russian Caucasus), where on June 15, 1921 Ilizarov was born as the oldest of eight children of a poor family. He could only start his school curriculum

[9] Synthes GmbH: www.synthes.com.

at the age of 11 but apparently caught up very quickly. In 1939, he was already accepted to Simpherol Medical School in the Crimea, where he graduated in 1944. Due to the turbulent situation created by the German invasion in Russia, the school had to move three times and settled finally in the Soviet middle east (Kzyl-Orda). After graduation, he was sent to a small Kurgan village Dolgovka in western Siberia where he started working as a young physician, the only one in an area of some thousands of square kilometer, without any previous practical training. Despite the primitive and harsh working conditions, he became a self-trained internist, surgeon, obstetrician, pediatrician and orthopedist!

His success fixed him up with a position as staff physician in the Hospital for War Invalids in Kurgan, a lucky coincidence after all. He became the one- or better two-eyed king in the land of the blinds. From the thousands of wounded veterans, a substantial number had osteomyelitis and other complications of gunshot fractures, all complications difficult to treat in the preantibiotic era. Again the primitive working conditions he was bound to forced him (*necessity, mother of invention!*) to develop a technique and device for repairing complex fractures and nonunions. He started with what was at hand: Kirschner bows and pins. Joining two bows together to form a ring and connecting two rings with metal rods he created a ring external fixator. It was patented as one of the world's first tension-wire skeletal fixators. During the 1950s, Ilizarov discovered that osteotomy which preserved a bone's periosteal and medullary blood supply, when combined with slow distraction, permitted bone lengthening without the need of a bone graft (see in Fig. 6.3a).

A long road of incomprehension, if not disapproval, for this provincial orthopedist and traumatologist by the Russian medical and state authorities was waiting him before he got the national recognition. This recognition came accidentally in 1967 when he succeeded to cure the open tibia fracture of Valery Brumel, the famed Soviet high-jumper. Operated 14 times unsuccessfully in Moscow, he was finally referred to Ilizarov who cured the fracture by his osteotomy and distraction technique. The athlete resumed jumping after surgery and this fact "catapulted" Ilizarov to national prominence. In the 1980s, he got the recognition he merited when his techniques penetrated the orthopedists' community worldwide. By 1992, his hospital got already 24 operating theaters manned by 350 orthopedic surgeons and a staff of 1,500 nurses! The seminal paper on limb lengthening by Ilizarov and Ledyaev was reprinted in *Clinical Orthopedics and Related Research*. It is introduced by a short biography of Ilizarov written by Vladimir Golykhovsky; the biographical notes above has been extracted from this text [248].

Chapter 7
Layer by Layer

The porous structure of Fig. 6.6 was produced by 3D printing. Shape and pore size were computationally designed. The printer deposited a layer of molten polysulfonamide (PSA) followed by deposition of a wax layer and this printing is repeated until the required scaffold size is obtained. Subsequently, the PSA is dissolved in acetone. The wax mold is further processed in different ways to produce scaffolds in polylactic acid and/or hydroxyapatite, however, restricted in size and not suited for metal structures.

But how to remedy an acetabular defect with massive bone loss shown in Fig. 7.1? After a first unsuccessful surgical intervention with a metal mesh to provide a backing for the cup, along which new bone could be formed, the reconstruction was mechanically inefficient. Without a good bone backing, the fixation screws of the metal net visible on the radiograph were useless.

Massive bone loss can be caused by arthrosis, removal of a malignant tumor or a complex fracture in the hip region and is commonly treated with a total hip prosthesis: a stem with spherical head in the proximal femur and an acetabular cup in the pelvis. Stems are available in all shapes and sizes but not so for the cup.

This chapter is devoted to new forming techniques that revolutionized the manufacturing of personalized prostheses. Rapid prototyping are known under the general term *Solid Free Form (SFF)* fabrication techniques. The very complex shape of this kind of implants cannot be manufactured by conventional techniques such as forging, casting or machining.

7.1 Computer-Aided Design

The solution is offered by a highly automated design and evaluation procedure to create an anatomically correct model of the impaired bone. The model is the approximate mirror image of the other hemi-pelvis if still intact or, if not, a best fitting mesh from a database. The images of both intact and impaired hemi-pelvis are extracted from Computed Tomography scans (CT). From a set of computed operations and after approval by the surgeon, a personalized hip implant is proposed. Shape, position of the cup, exact defect filling with, if desired, a 3D porous scaffold structure on

J.A. Helsen and Y. Missirlis, *Biomaterials*, Biological and Medical Physics, Biomedical Engineering, DOI 10.1007/978-3-642-12532-4_7,

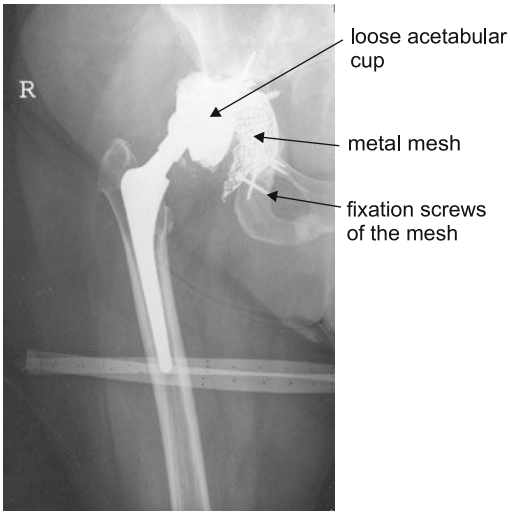

Fig. 7.1 Massive acetabular defect and failed acetabular cup

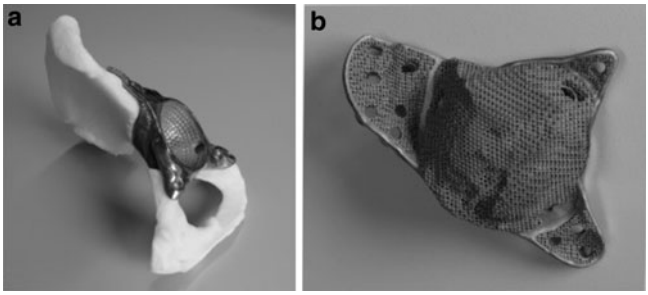

Fig. 7.2 Tri-flange acetabular cup produced by Electron Beam Melting (EBM). Photographed by courtesy of F. Gelaude

the back side to enable bone ingrowth, screw holes, etc. are all part of the details of the virtual device. Mechanical strength is derived from finite element analysis. The final step is the manufacturing of the device, called the *triflange acetabular cup*, by means of electron beam melting (EBM) of Ti6Al4V powder.[1] The housing for the head of the femoral component is the only mechanical post-EBM intervention needed (machining and polishing). The triflange cup implant is shown in Fig. 7.2, put at our disposition by F. Gelaude.[2]

The very simplified 'flow sheet' from examination of the patient's impaired hip to the customized prosthesis is the outcome of an intense collaboration between

[1] Manufactured by FIT (Fruth Innovative Technologien, Parsberg (Germany)).

[2] Mobelife n.v., Kapeldreef 60, BE-3001 Leuven (Belgium). CEO: Frederik Gelaude, email: Frederik.Gelaude@mobelife.be.

surgeons, computer specialists and biomechanical engineers. An alternative technique is provided by selective laser melting (SLM).[3]

Manufacturing of personalized prostheses as just discussed is the result of worldwide intense research programs. Referred to here is an example of a real case and a real custom-made device. The direct and indirect prehistory of the triflange acetabular cup can be found in papers by Gelaude, all containing an extended list of bibliographic references relevant to the subject [249–252].

The philosophy for rapid manufacturing always starts from a digitized model, one example was briefly discussed above. In the following sections, the technology of four different techniques will briefly be commented and illustrated with a few representative examples. The heart of the techniques is always a focused beam, either an electron or a laser beam, melting metal or ceramic powder or polymer powder, or polymerizing (and solidifying) liquid mono- or oligomers. The volume of the heated zone is constrained to micrometer-sized diameter and depth. Needed are (1) a digitalized size and shape of the device that has to be manufactured, (2) software that slices the digitalized device in thin xy-slices, and (3) a scanning focused beam (photons or electrons) that is copying and drawing the details of one xy-slice on the plane of the *Build* cylinder (covered by powder or by a liquid).

The advantages of all four techniques are:

- Unlimited geometric freedom.
- No tooling or set-up costs; cost-effective production of unique implants, instruments or small series.
- Fully digital production.
- Use of biocompatible alloys.
- Integration of osteoconductive structures.
- Patient-specific implant design, validation and production.

7.2 Electron Beam Melting

Machine Layout

Rapid Manufacturing of metal objects of any shape can be realized by use of Electron Beam Melting. Electrons are generated in the electron beam gun, accelerated (*Anod*) and electromagnetically focused (*Focus coil* as shown in Fig. 7.3).[4] Powder is spread over the *Building Table* and the electron beam melts a thin layer of metal powder, copying successively the slices of the digitalized object to be manufactured.

[3] LayerWise is one of the companies using SLM, located at Kapeldreef 60, BE-3001 Leuven, Belgium. E-mail: info@layerwise.com. Managing director: Peter Mercelis, email: Peter.Mercelis@layerwise.com.

[4] The machine *Arcam A*2 is produced by Arcam AB Krokslätts Fabriker 27A, 431 37 MLNDAL, Sweden.Website: www.arcam.com.

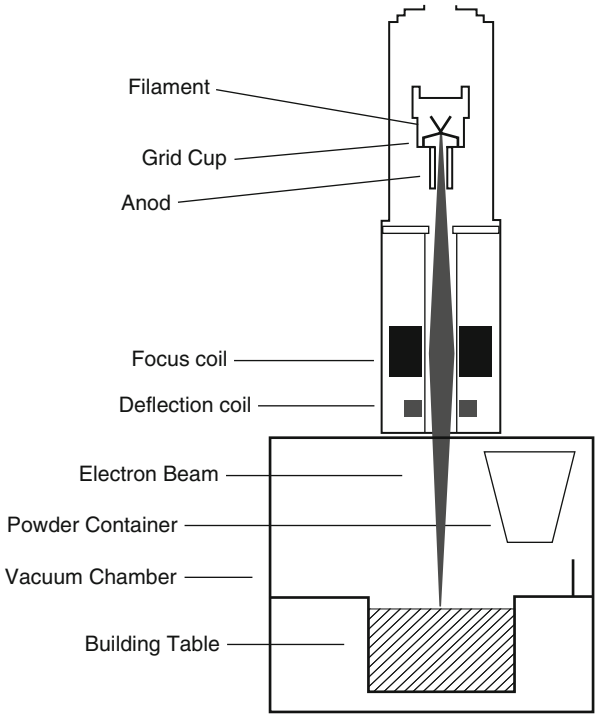

Fig. 7.3 Electron beam melting. Schematic layout of the Arcam A2 machine. By courtesy of Arcam

The layer in this technique is 0.05–0.2 mm thick. The control system allows for an extremely fast beam translation with no moving parts.

The scan speed of the electron beam is >1,000 m/s, its positioning accuracy is ±0.025 mm and the parts accuracy ±0.3 mm. The machine has a Powder Recovery System enabling 95% recovery of unmelted powder.

Performance

Two characteristics of this technique are:

- The high build temperature which provides good form stability and low residual stresses in the object.
- The vacuum melt process eliminates impurities.
- Very efficient use of material.

The released materials are different grades of Ti6Al4V and CoCr (ASTM F75). The microstructure of Ti6Al4V after EBM is shown in Fig. 7.4 and this alloy proves to exhibit mechanical properties in between a cast and wrought alloy (the properties

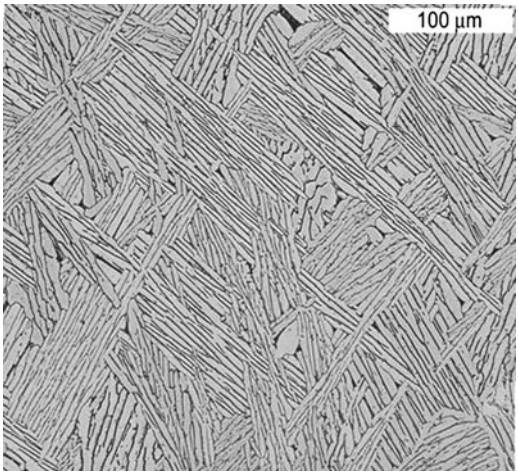

Fig. 7.4 Microstructure of Ti6Al4V after EBM. Courtesy of Arcam

Table 7.1 Mechanical properties of Ti6Al4V deposited by SLM compared to the same alloy conventionally drawn and annealed

	Layerwise	Reference
Accuracy[a] (µm)	±60	
Surface roughness (µm)	3–8[b]	
	25–50[c]	
Density kg/m[c]	4,420	4,430
Hardness (Vickers)	405	350
Tensile test		
E (GPa)	94	114
UTS (MPa)	1,250	1,035
YS 0.2% (MPa)	1,125	965
Elongation (%)	6	11
Bending		
E (GPa)	88	110
UTS (MPa)	2,000	1,900
YS (MPa)	1,900	1,500

[a] Dependent on part geometry.
[b] R_a: arithmetic average of vertical roughness (peak to valley).
[c] Average width of the valleys R_y.

should be comparable to those given in Table 7.1). It is fully dense. The triflange cup displayed in Fig. 7.2 has been manufactured by an Arcam A2 machine.

In a recent paper by Murr and colleagues, they reviewed the microstructure and mechanical behavior of devices of Ti6Al4V produced by EBM and SLM [253]. The authors found for their samples an increase of 50% in tensile strength with respect to wrought samples. The authors mentioned that one EBM machine is capable to produce about 4,000 custom knee implants/year. Adapting process parameters allows to produce a wide range of crystallographic phases and microstructures. Till proof of the opposite, the future looks rosy for these techniques.

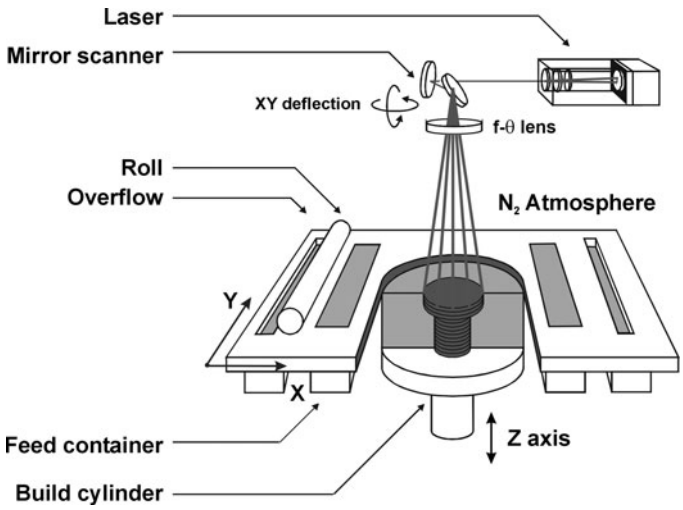

Fig. 7.5 Principle of Selective Laser beam Melting (SLM). Courtesy of Layerwise

7.3 Selective Laser Melting of Metal Powder

Selective laser melting (SLM) is closely related to selective laser with photosensitive monomers (e.g., acrylates) and known as SLA. It is discussed in Sect. 7.4.

Machine Layout

A plateau (*Build cylinder* in Fig. 7.5) is covered with a fine layer of metal, ceramic or polymer powder by the *Roll* rolling over the *Feed container*. Subsequently, the focused laser beam melts or sinters the powder. The xy position of the focused laser beam is determined by the *Mirror scanner*. The latter is computer monitored in such a way that one xy slice through the digitalized device is drawn on the plane of the *Build cylinder*.

After finishing the first slice, the *Build cylinder* is lowered by the thickness of one slice and the next slice is processed and so on till the whole device is manufactured (Layerwise!).

Performance

The accuracy of a finished product in Ti6Al4V is about 60 μm decreasing with the size of the object, a value which is comparable to conventional not-too-demanding machining. The density is almost 100%. The mechanical properties are often better

Fig. 7.6 Bridging of a pelvic discontinuity by a patient-specific implant: (**a**) as implanted, shown on the model of the patient's left pelvis; (**b**) backside of the porous structure. The device was implanted in June 2010. Courtesy of Mobelife NV (Leuven, Belgium). Case provided by dr.H.Delport (AZ, St.-Niklaas, Belgium)

than a conventional alloy (see Table 7.1). The following biocompatible alloys can be processed:

- Commercially pure titanium (ASTM grades 1, 2 and 5/23).
- Cobalt–chromium alloys.
- Niobium and tantalum (under study but with promising results already!).

Examples

Large bone defects created by accidents or tumor resection will not be restored in a natural way. Figure 7.6 tells a story of a complex acetabular revision using computer-aided planning similar to the tri-flange acetabular cup shown in Fig. 7.2. A 50 years old female patient developed a pseudotumor after Resurfacing Arthrolasty (resurfacing is discussed Sect. 4.6). Conventional revision failed and the patient developed a pelvic discontinuity. A patient-specific implant and guide was manufactured using computer-aided planning tools, following procedures similar to the ones described in the first section of the present chapter. A specialized implant manufacturer, Mobelife NV(Leuven, Belgium), made the implant in Ti6Al4V. Screw positions and lengths are preoperatively planned depending on bone quality of the patient, and transferred into surgery using jig guiding technology (Materialise NV, Leuven, Belgium) as shown in Fig. 7.6a. In Fig. 7.6b is shown the backside of the porous structure allowing for optimal fit and bone in-growth.

A comment and/or question should be added here about porosity. Often throughout this book, reference is made to a common aspect of biological 'fabrics': *fractality*. Would it add to the biological performance of some implants when pores had a fractal size distribution, say between 10 and 500 μm? Having seen the high flexibility of the present techniques manufacturing would not be the obstacle. The question might not be relevant for nonresorbable metal fabrics. However, it could be relevant for resorbable metal or polymer fabrics?

Fig. 7.7 Metal implant structure to support an entirely new set of dentures. Courtesy of Layerwise

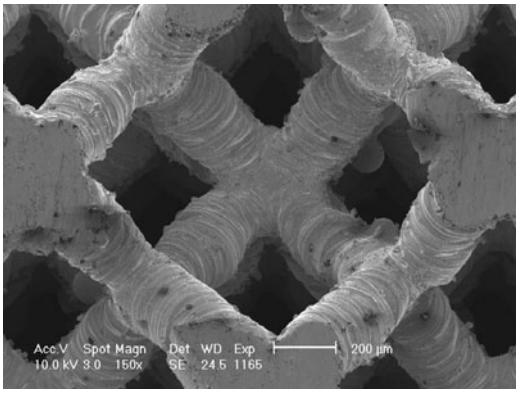

Fig. 7.8 Porous structure in tantalum with a pore size somewhat less than 1 mm and strut size of about 200 µm

A second example is the dental framework shown in Fig. 7.7: (a) the manufactured metal support, (b) the ceramic-coated implant, (c) the final result.

Recently, we successfully realized the manufacturing of tantalum porous structures. One example of a structure with cubic pores of 1×1×1 mm is shown in Fig. 7.8. The strut size is about 200 µm.

7.4 Stereolithography of Polymers

Machine Layout

The foregoing techniques started from solids either metals, ceramics or polymers. Objects are built up layer by layer by melting or sintering. A third technique, although chronologically the one it all started with, consists of curing or polymerizing a liquid monomer by a focused laser beam. The laser beam is scanning over the liquid surface curing a thin slice (Fig. 7.9). The scanning is monitored in a way similar to the two former techniques. After finishing one layer, the supporting platform is lowered to start curing the following slice. The monomers are a blend of epoxies and acrylates, whose composition is kept secret by the suppliers. Biocompatibility for surgical guides is not a problem but is not sufficient for endoprostheses.

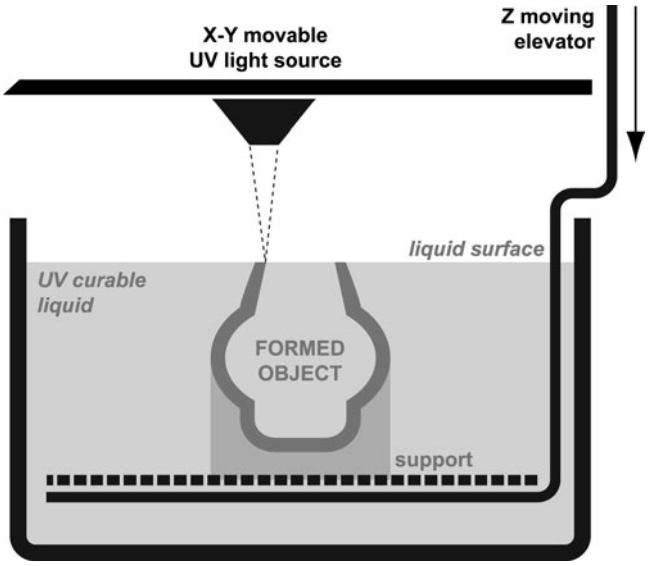

Fig. 7.9 Principle of stereolithography. Courtesy of Materialise NV

Performance

The layers are 0.1–0.2 mm thick. Curing is performed by a UV laser with $\lambda = 355$ nm. The XY precision of the manufactured pieces is 0.2 mm or 0.2% for large-scale objects and the pieces are dimensionally stable.

Alternatives

Juxtaposed to Stereolithography is Selective Laser Sintering (SLS). SLS is an alternative similar technique shown in Fig. 7.10. Polymer powder is spread in a thin layer over the central plateau (Z movable piston) and molten by an IR laser, scanning over the plateau following computer instructions as for the other techniques described above. Here too the technique does not allow to produce long-term endoprostheses. For long-term implants, the use of PEEK (PolyarylEtherEtherKetone) is under investigation but a biomedical grade is not yet available.

Based on what is actively looked for in the semiconductor industry (3D interconnect technology) an innovative suggestion would not be misplaced here. Why not coating polymer (PEEK?) porous structures by, say, tantalum in order to make the pores osteoconductive? One already succeeds in the semiconductor industry to apply a conductive and continuous layer in trenches with very high aspect ratios [254].

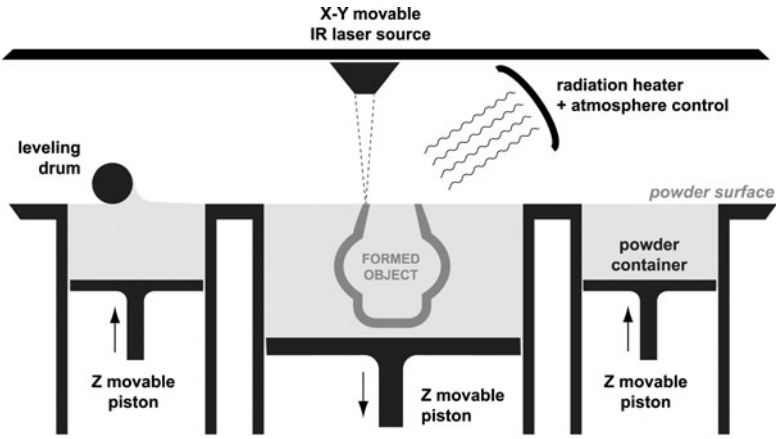

Fig. 7.10 Principle of Selective Laser Sintering. Courtesy of Materialise NV

For less complex shapes, Synthes delivers Patient Specific Implants (PSI) for replacement of bony voids in the cranial/craniofacial skeleton in CP Ti or in biocompatible PEEK (Peek Optima-LT).[5] The shape is determined based on CT scans. The PEEK implants are radiolucent, have bone-like stiffness and strength and are autoclavable. Titanium is radio-opaque. The implants are manufactured by machining.

Examples

A first example is a 3D model of the upper dental arch derived from medical tomography (CT or MR scans). Dental implants should be positioned at places where sufficient bone stock is present. Preoperative planning and exact drilling is a 'must' for obtaining the required stability of the implants. The model of Fig. 7.11 serves as drilling guide.

A second and extremely important example is the 3D skull model of Fig. 7.12. This hardcopy is produced by Rapid Prototyping (RP) techniques, in the present case by Stereolithography. Highlighted (red) is the position of a tumor. It is used to accurately plan and prepare for surgery. It also serves as an excellent presentation tool to discuss the treatment plan with the patient and the surgical team.

Dental guides will probably continue to be produced by this technique while orthopedic applications will be covered mainly by SLS and EBM.

[5] Synthes GmbH: www.synthes.com.

Fig. 7.11 A 3D model of the upper dental arch produced by stereolithography. Drilling guide for inserting dental implants. Courtesy of Materialise Dental (F. Maes)

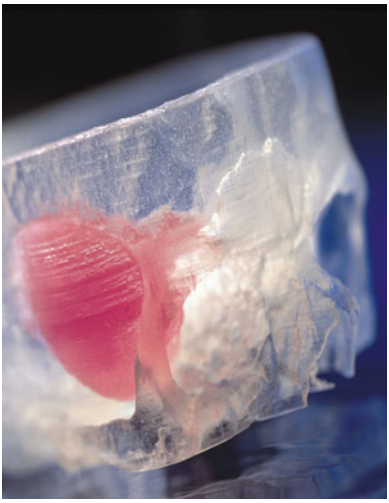

Fig. 7.12 3D Rapid Prototyping (RP) medical model produced from a CT scan by stereolithography. Highlighted (red) is the tumor to be removed. Courtesy of Materialise Dental (F. Maes)

7.5 Characterization of Porous Structures

Characterization of porous structures can be and is done by study of conventional stress–strain techniques. A more interesting and new approach is imaging the deformation under stress by X-ray microfocus computed tomography which supplies at worst qualitative and at best very acceptable quantitative information.

An experiment runs as follows: a sample is stressed (compression or tensile) in an *ad hoc* developed stress–strain device fitted to the CT instrument. At selected intervals, the compression stops and a CT scan is recorded consisting of a series of 2D images digitally combined into a 3D representation of the sample. The resolution of the various instruments are in the range of 10 μm for standard micro-CT, 1–2 μm for high resolution standard and synchrotron micro-CT and 0.4–0.6 μm for nano-CT. An 'ideal' sample is cancellous bone: 50–90% porosity, trabeculae thickness of 100–200 μm and a material-like bone with an optimal X-ray density. Individual trabeculae are perfectly visualized by standard micro-CT equipment with excellent

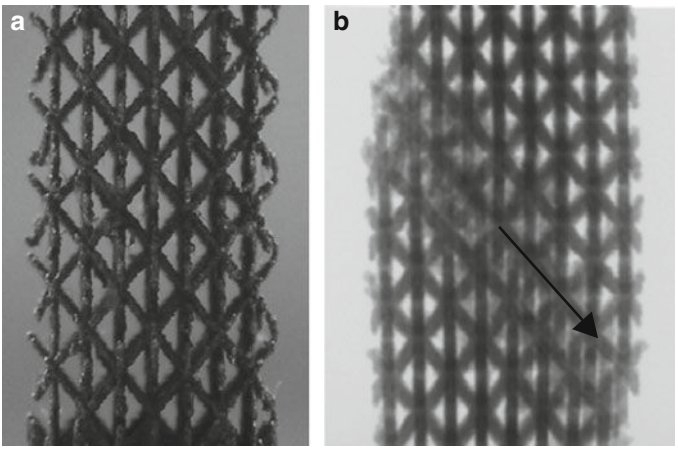

Fig. 7.13 CT image of a porous titanium structure recorded using a Philips HOMX 161 X-ray system with the AEA TOMOHwk CT-software. Courtesy of Prof. M. Wevers, KULeuven

match between CT-images and optical microscopy images. Herewith, a number of pitfalls for quantitative analysis are indicated: partial volume effect, radiation density, focal spot size of the X-ray source, architecture of the sample. High density metals as well as low density polymers lead to difficulties for the quantitative analysis. In Fig. 7.13, a porous titanium cylinder is shown before and after deformation. The sample is sheared along a direction indicated by the arrow. Innovative protocols are proposed to meet the various pitfalls for quantitative analysis [255]. Details of the protocols are beyond the scope of this section but a reference to this technique could not be omitted in a chapter in which the manufacturing of porous structures was not the only but the main subject.

7.6 Conclusion

The four techniques discussed here became in the last few years mature forming techniques for metals, ceramics and polymers. Rapid manufacturing of complex shapes as shown in Fig. 7.2 is not feasible by conventional forming techniques as casting, forging or machining.[6] The ever better-performing medical imaging techniques and their link to computer-aided design, evaluation and machining will shape the future of personalized prostheses, which will gain an increasing share in the prosthesis practice. The mechanical and chemical properties of the basic materials,

[6] The figures in this chapter were provided for our own convenience by companies in Leuven unless otherwise indicated. Worldwide, however, many other are active in this field and our selection was not intended to discriminate anybody whatsoever.

inorganic as well as organic, can be tailored for nearly optimal performance. Three progress steps to be expected in the next decade are:

- Personalized shape optimization (stress distribution, space filling, ...) exclusively made possible by the new forming technologies.
- The creation of interfaces with active physiological properties (anti-bacterial, osteoinduction and other stimulation effects).
- Increasing importance of tissue engineering (see Chap. 13).

For 'heavy duty' implants for hip and knee we expect that customized or personalized prostheses will offer the most direct and substantial advantages in the next decade... dare we say more than from surface engineering?

Chapter 8
Metal Implants Bound to Disappear

Since the dawn of the *Bronze Age* some ten thousand years ago our fellow ancestors started the extremely tedious pilgrimage to more efficient production processes of metals and to master composition, heat and mechanical treatments to get an appropriate ratio between mechanical properties and density or, within mechanical properties, between say fatigue strength and Young's modulus, fitting unconsciously the modified form of the term *biological performance*, all this of course without the slightest suspicion of what was going on at the atomic scale.[1] Gold was the almost exclusive metal to be found as native metal in nature. Silver or copper was exceptionally found in native form (silver was more expensive than gold in ancient Egypt). The straightforward explanation for this behavior is the high positive redox potential (see Table C.1), where gold occupies the very top position of the E_0 ranking. Gold, silver and copper figure in the same column of Mendelejev's wonderful periodic system (Table A.1). All three have an f.c.c. crystal structure and share a number of chemical and mechanical properties, e.g., workability intrinsically linked to its f.c.c. structure. Silver and copper are relatively easily reduced to metal and this is obviously the reason why the *Iron Age* follows the *Bronze Age* and not vice versa: iron is less easily reduced than copper. Native iron is only found in meteorites.

Cast iron (>3%C) is brittle. During the nineteenth century the carbon content was gradually lowered resulting in alloys combining good strength, ductility and machinability. This development is the culmination point of the *Iron Age*, embodied in thé icons of this age: Iron Bridge in Shropshire (England, 1781) and the *Eiffel tower* in Paris (1887–1889). The iron alloys with a carbon content $< 2\%$ are housed in the somewhat vague generic family named *steel*. But steel corrodes and the Eiffel tower needs 50–60 tonnes of paint every seven years to protect it from rust. This makes clear why the progressing steel industry was accompanied by an emerging new technology and science: *corrosion science*.

Covering unhealthy teeth by gold was good fashion for those who could pay for. Insertion of a gold foil in joints was practiced with good long-term success near the end of the nineteenth century. They were bound to stay in the body. Copper or bronze was used only for surgical instruments but not for implants. But things

[1] see Helsen and Breme, p. 25 [35].

J.A. Helsen and Y. Missirlis, *Biomaterials*, Biological and Medical Physics, Biomedical Engineering, DOI 10.1007/978-3-642-12532-4_8,

went wrong when, by the necessity of the time, surgeons used iron osteosynthesis devices in the 1st World War hospitals in Flanders Fields and Northern France. As a matter of fact, these implants were *soluble* (to some extent) and protective intrabody coatings were not available. The challenge of the pilgrims was the search for alloys for which *postconstruction*, in our case *postoperative*, corrosion protection was not needed or was a self-preserving process. Low carbon stainless steel, Co–Cr, Ti, Zr, Ta and Nb alloys form the club of alloys allowing to make for most permanent implants an acceptable choice: good biological performance, acceptable corrosion (or low dissolution) rate and low toxicity. But in this present chapter, we go again downhill: soluble but nontoxic metals!

Ungrateful as we are, we want to get rid of that piece of metal as soon as the implant's function becomes obsolete, say after healing of a fracture supported by an osteosynthesis plate. Moreover, we want it to be done without the burden of surgery. So, down to soluble metals.

8.1 Soluble Metals?

Gold blinks brightly at the top of Table C.1, other elements figure at the bottom of the table: Ti, Zr, ... all with E_0s far below the standard potential of the H^+/H_2 system. The latter metals are oxidized by ... water but once again, do not forget our warning about the constraints formulated earlier for the use of E_0s. Through a pleasant physicochemical accident, however, the vigorous reaction of these metals with oxygen or water created, in a self-preserving act, an almost impenetrable barrier to further oxidation. Not so for magnesium. If, however, the reactivity could be kept under control in one way or another, it will become a valuable candidate metal for a resorbable implant.

The idea of making resorbable implants was not born in a stubborn metallurgist's mind but first introduced in the 1970s by scientists using polymers with controlled dissolution rates: polylactides and polyglycolides. But metals have better mechanical properties and therefrom the present emerging research field on soluble metals. The iron implants of WWI were not suited because on the one hand they did not dissolve quick enough and on the other hand it was probably accompanied by an unwanted local acidification. So far only one element or major alloy element is a valuable candidate: magnesium.

Magnesium is the seventh most abundant element in earth's crust, about 23 $g\,kg^{-1}$, an essential and major constituent element of our body and nontoxic unless at unrealistic concentrations. But the problem for intrabody use emerges from its bottom position in the E_0 ranking and its nonprotective oxide layer. A quick look at the Pourbaix diagram of Fig. 8.1 tells us that the possible protection compound $Mg(OH)_2$ is far beyond the viable biological pH range. The electrochemical reaction sequence at the horizontal transition border between immunity and corrosion is:

$$Mg \rightarrow Mg^{2+} + e^- \text{(anodic)} \tag{8.1}$$

$$2H_2O + 2e^- \rightleftharpoons +2OH^- + H_2 \nearrow \text{(cathodic)} \tag{8.2}$$

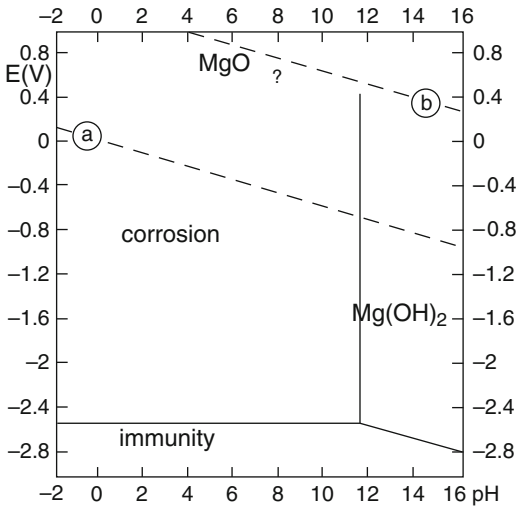

Fig. 8.1 Pourbaix diagram of Mg. Lines *a* and *b* delimit the stability domain of water. (Pourbaix, modified) [195]

followed by the precipitation of the hydroxyde:

$$Mg^{2+} + 2OH^- \Rightarrow Mg^{2+} + OH^-. \tag{8.3}$$

The overall chemical reaction may be written as:

$$Mg + 2H_2O \rightarrow Mg(OH)_2 + 1/2H_2 \nearrow . \tag{8.4}$$

The nascent hydrogen gas bubbles as a consequence of the cathodic reaction is not exactly what we want in our body, invoking the horror of deep-sea divers, the *caisson disease*.

For the electrochemical and chemical reactions above, we always should keep in mind that all ions are at least hydrated, if not present as complex with anions such as Cl^- or others, which changes the activity, shifts the reaction equilibria, and hence the Pourbaix diagram. The persistence of MgO in the presence of water is questionable: it is probably hydrated to $Mg(OH)_2$ which is more stable and does probably not contribute to slowing down corrosion... or is dissolved by complexation reactions exposing bare magnesium metal and enhancing corrosion. Recording the evolution rate of hydrogen is an easy way for monitoring corrosion in vitro. Dramatic differences in hydrogen evolution rates exist between Mg alloys as demonstrated by Fig. 8.2: from 0.008 to 26 ml cm^{-2}/day! An evolution rate of 0.01 ml cm^{-2}/day seems to be on the safe side, i.e., the evolved hydrogen can be evacuated safely through diffusion and the bloodstream without forming bubbles. So appropriate measures are vital to keep corrosion rate under control.

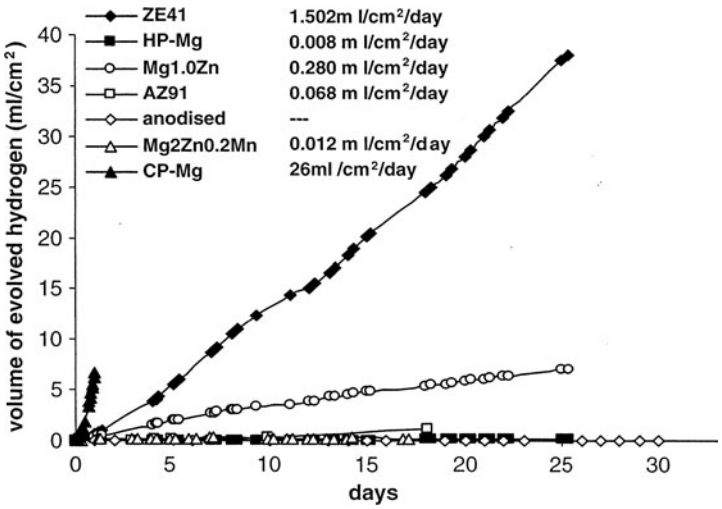

Fig. 8.2 Hydrogen evolution and the average rates of Mg and 4 alloys specimens immersed in SBF. Reprinted with permission of Elsevier from [256] Fig. 1

Figure 8.2 gives us immediate help in this respect:

- *Refining* as illustrated by the difference between CP and HP, commercially pure versus high purity Mg. Trace elements as Fe, Ni and Cu have harmful effects on corrosion resistance due to galvanic potential differences between the matrix and fine intermetallic phases rich in Fe, Ni or Cu.
- *Alloying* as well illustrated by the difference between Mg0.1Zn and Mg2Zn 0.2Mn.
- Surface treatment as illustrated for the anodized specimen.

A detailed study of the electrochemical behavior and surface characterization is performed by Hallopeau and colleagues on Mg and AZ91E alloy in a 0.5 M Na_2SO_4 solution. These experiments were not performed in conventional media for in vitro testing but anyway a few useful conclusions can be drawn from this investigation: (1) Al as alloying element blocks the dissolution (lower oxidation current density) but the effect disappears at higher current densities probably because of the formation of better soluble compounds and the increasing pH; (2) the dissolution is a multistep process of which (8.1) is the fast step and reaction (8.4) the slow one. The oxidation can efficiently be hindered by inhibitors such as CrO_4^{2-} and SiO_3^{2-}. Chromate seems to be the most efficient near neutral pH but is excluded for in vivo use because cancerogenous and the other is efficient only at high pH [257]. A similar study but including electrochemical impedance measurements was performed by Müller and colleagues on the alloys AZ31 and LAE442 in contact with phosphate buffer and albumin. The main conclusions are that LA442 (containing rare earths) is the more corrosion resistant alloy, albumin (and adsorption of other proteins?) act as corrosion inhibitors, partially also phosphates but chlorides favor dissolution and localized corrosion [258].

Table 8.1 Chemical composition relative to alloys on which biomedical data are reported in the literature. Composition in weight %; Mg is the balance; Cu, Ni in general <0.001%; << means <0.001; all values rounded to two decimals; open spaces: not known or not determined. Collation of data from [258, 261–263]

Alloy	Al	Zn	Si	Fe	Mn	Ca
Mg cp/cast	0.04	<0.01	0.05	<<	0.02	0.02
AZ91/cast	10.14	1.33	0.03	<<	0.01	<<
AZ91Fe0.03/cast	9.56	0.86	0.04	0.03	0.11	0.01
AZ91Fe0.05/cast	10.12	1.05	0.06	0.05	0.03	0.01
AZ91/50	9.93	0.84	0.08	<<	0.1	<<
AZ91/5	10.09	0.87	0.11	0.01	0.07	<<
AZ91/2.5	4.75	0.02	<<	<<	0.41	<<
AZ91E	8.22	0.65	0.01	<0.01	0.27	
AZ31	3.00	0.83	0.01	0.003	0.31	
MgCa5/cast	0.04	<<	<<	<<	0.01	4.75
Mg hp					<0.01	
Mg0.6Ca						0.6
Mg1.2Ca						1.2
Mg1.6Ca						1.6
Mg2.0Ca						2.0

Will a Ti coating, formed by ion plating on pure Mg bring relief from the problems? The authors of that proposal were seduced by the long and successful story of Ti as bioalloy and they succeeded in applying a coating which was homogeneously deposited, without pores, well adhering through an interdiffusion layer and a corrosion current one order of magnitude smaller than for pure Mg [259]. Congratulations but will we be waiting for *Godot* till we will see the first clinical results?

Two controlling mechanisms, coating and alloying, passed the review. Composition is the third foot to stand on. The composition of a set of different alloys is given in Table 8.1, collated only from papers discussing potential or actual biomedical applications. A short remark on manganese as alloying element may not be omitted. We referred to potential hazards of manganese in Chap. 4 and in stainless steels it may be present in higher concentrations than in the current Mg alloys? However, as the latter are *bound to dissolve*, more Mn may circulate in the body than with corrosion-resistant alloys. In a recent paper, it is reported that Mn in some proteins (Cu^{2+}- and Zn^{2+}-cupin A) Mn can replace irreversibly Cu^{2+} or Mn^{2+}. The experiments were performed with the cyanobacterium *Synechocystis* but the authors state in their conclusion: *One crucial consequence of nascent proteins having tight affinities for the wrong metals is a risk of metal associations with aberrant binding sites. Imperfect metal homeostasis, due to environmental or genetic factors, may allow accumulation of competitive metals in the wrong proteins, which could be pathological. There is a need to test whether this is one factor underlying links between copper and degenerative disorders, including Alzheimer's disease and Creutzfeld-Jacob disease* [260].

8.2 Prospecting for the Best

Better performance for lower weight was an industrial incentive to develop Mg alloys: with a density around 1,800 kg.m^{-3} and a YS of some 300 MPa the ratio of YS or UTS to ρ is positioned in between those for CoCr and Ti alloys (see Table 8.3). However, a 'best' alloy is not identified yet. In Table 8.2, we collected a set of data on the mechanical performance of potential biomedical candidate alloys. The table shows the highly diverging data, a demonstration of the high sensitivity to thermal and mechanical history and composition. Compare the data for YS and UTS of AZ91 (as cast) at the top of the table with those for the same type of alloy but reported by another author. Alternatives are Mg-Al-RE containing rare earths (Ce, Nd, ... with refined microstructure and improved strength) and Mg-Li-Al,RE alloys (LAE, WEL, LE).

The crystallographic structure of the pure metal is h.c.p. as the other elements in the same column of the periodic table. The matrix is mainly dendritic α-Mg with an eutectic β-phase consisting of the intermetallic compound $Mg_{17}Al_{12}$, plus a finely grained (1–5 μm) Mn-rich phase. UTS and grain size are strongly related, following

Table 8.2 Mechanical properties of Mg alloys: collation of data from [258, 261–263]

Alloy	E	YS	UTS	Elongation	Grain size
	GPa	MPa	MPa	%	μm
AZ91(as cast)		69	210	7	
AZ91(heat treated)		108	240	3	
AZ91(473)[a]		364	400	1.9	1.2
AZ91(623)[a]		277	325	7.1	15.6
AZ91(ECAE)[b]		277	318	2.5	1.0
Bending					
Mg cp	14		9.5		
Mg0.6Ca	15		143		
Mg1.2Ca	18		132		
Mg2.0	18		108		
Compression					
Mg cp	45	90	198		
Mg0.6Ca	402				
Mg1.2Ca	50	97	254		
Mg2.0Ca	59	73	233		
MgCa5			85		
AZ91Fe0.03		95	145		
AZ91Fe0.05		105	200		
AZ91/50[c]		218	315		
AZ91/5		215	315		
AZ91/2.5		130	235		

[a] Extruded at 473 or 623°C

[b] ECAE: Equal Channel Angular Extrusion, a large shear strain extrusion process. For more detail and the effect on grain size, see [264]

[c] AZ91 but in bars of 50, 5 or 2.5 mm diameter

Table 8.3 Physical properties of die-cast AZ91

	AZ91	PA6[a]	PLA[a]	CoCr	Ti6Al4V
E (GPa)	46	2.1	3.0		
YS (MPa)	160				
YS/ρ	88			58	205
UTS (MPa)	276	83	48		
UTS/ρ	152	73		93	220
Elongation (%)	6.5	300	2		
ρ (kg.m^{-3})[b]	1,820	1,130			

[a]Respectively polyamide and resorbable l-polylactic acid
[b]Multiplied by 10^3

the earlierly mentioned Hall & Petch equation. A consequence of a pure h.c.p. structure is poor formability (reduced number of slip planes!). Fortunately, the alloys are not single phase, which makes that the mechanical properties can be modified by heat treatments: the YS of AZ91 can roughly be doubled by heating (solving, re-precipitation, ...) and aging.

Fatigue stress to failure for AZ91D (die cast) is at best 80 MPa for 3×10^7 cycles but 50 MPa is about the lower limit. However, cracks can bring this limit further down. Cracks progress in general interdentritically but they often are initiated at contraction cavities formed during solidification. Let us notice here that substantial improvements are possible by techniques like equal channel angular pressing (ECAP) [265].

To be honest, our prospection is not very lucky thus far because of too much uncertainty and unpredictability. The mechanical properties will probably be manageable but the high concentration of aluminum and/or manganese should be a matter of great concern (see Chap. 4, [161]). Is there hope for better?

8.3 Hope?

When a metal solidifies from the melt, unavoidable temperature gradients create anisotropic grain growth. As an example, the macroscopically visible dendritic fingers of a section through a pure copper ingot is shown in Fig. 8.3, displayed here for the didactical quality of the image. Anisotropy means anisotropy in properties, most often an 'inconvenient truth'.

A solidifying alloy transforms into a number of allotropic forms, consequence of solubility, formation of intermetallic compounds, freezing-in metastable phases during nonequilibrium cooling and so on. In the simplified phase diagram of AZ91 of Fig. 8.4, four domains are defined:

- I: Melt, solution of all alloying elements.
- II: α phase, i.e., h.c.p. Mg with a small percentage of Al.
- III: α + liquid, where the liquid phase coexist with α.
- IV: $\alpha + \beta$ where β is the intermetallic phase $Mg_{17}Al_{12}$, the latter contains also some Zn, a result of nonequilibrium solidification.

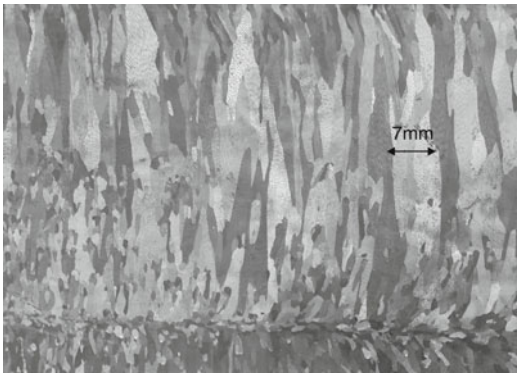

Fig. 8.3 Macroscopic section through a copper ingot. *Top of the figure*: external surface where cooling starts, *bottom*: center of the ingot where two cooling fronts meet

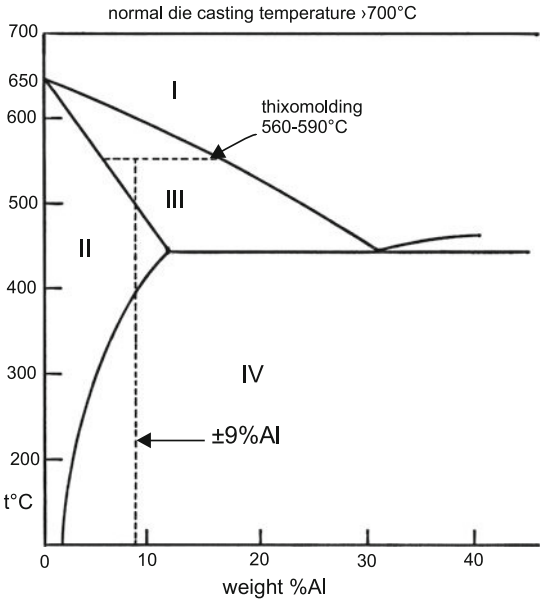

Fig. 8.4 Phase diagram of AZ91

The melt with a composition of about 16%Al segregates, when cooled below the solidus/liquidus temperature of 560–590°C, into solid α particles containing ~5%Al and a liquid solution. Further cooling brings us to the domain, where α and β coexist. The interesting thing is now that this domain is reached not by conventional cooling from the normal die casting temperature of $\geq$700°C but by injection at temperatures of 560–590°C into a mold. The technique is called here

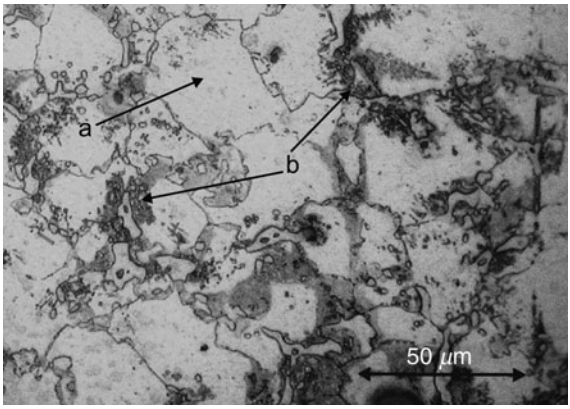

Fig. 8.5 Metallographic section of thixomolded AZ91, polished and etched (HF): (**a**) α-Mg, (**b**) $Mg_{17}Al_{12}$. Photo by P. Crabbé

thixomolding and is similar to the one used for injection molding of thermoplastic polymers. The term is derived from the Greek noun $\theta\acute{\iota}\xi o\varsigma$ meaning the action of touching, in particular meaning that the mixture flows easily on touching, here on molding. It is possibly an example of non-Newtonian viscosity (see Fig. 2.12 and Chap. 11), though we did not find reference to conventional experimental viscosity data to prove this hypothesis. The melt contains something like 30% solid but its fluidity is similar to a pure liquid. The dendritic structure is destroyed by the high shearing forces during injection. The background in Fig. 8.5 is the α, the islands are the intermetallic β-phase $Mg_{17}Al_{12}$. This phase is called a divorced eutectic because the eutectic structure appears as massive phases (islands) instead of the classic finely divided mixture of a normal eutectic. The equiaxed α grains are about 10–20 μm in diameter. An analysis by scanning electron microscopy (SEM-EDX) confirms the metallography: the energy dispersive X-ray spectra (EDS), intensity vs. energy, refer respectively to the matrix (α) and to the islands of $Mg_{17}Al_{12}$. The corresponding atomic concentration percentages are about (a) 92 for Mg and 85% for Al and (b) 69% for Mg and 31% for Al, the latter roughly corresponding to an atomic ratio of 17/12 (Fig.8.6).

The reliability of *thixomolded* parts seems now to be high, so time to summarize semifinal properties and advantages of Mg alloys.

The physical properties of AZ91D as collated in Table 8.3 compare favorably to a polyamide or to the Class l of resorbable polymers, the polylactides, or to the YS/ρ or UTS/ρ of CoCr and Ti6Al4V. Plenty of room for phantasy about potential applications. In Table 8.4, the composition of the main commercial alloys suitable for thixomolding and eye-catching features are given.

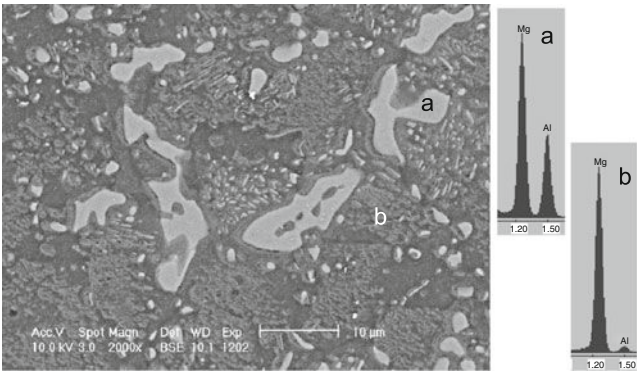

Fig. 8.6 SEM-EDS analysis of thixomolded AZ91: left the backscattered image, right the spectra of (**a**) the islands (and hardly visible fine dendrites) of $Mg_{17}Al_{12}$ and (**b**) the grey matrix of the α-phase. Photo by P. Crabbé

Table 8.4 Commercial Mg grades for thixomolding. Composition in weight %; Mg: balance; minor elements Si, Cu, Ni, Fe: <0.05%

Alloy	Al	Zn	Mn	Feature
AZ91D	8.5–9.5	0.45–0.90	0.17–0.40	High strength, good corrosion resistance
AM60B	5.6–6.4	≤0.20	0.25–0.50	Shock absorbing, high ductility
AM50A	4.5–5.3	≤0.20	0.28–0.50	Shock absorbing, high ductility
AS41B	3.7–4.8	≤0.10	0.35–0.60	

8.4 Mg Foams

Tantalum has a high density and is too heavy for bulky implants. Therefore, we paid much attention to its porous variant. Although Mg belongs to the lightest elements used for biomedical purposes, its porous variant also triggers our attention and, when oxidation rate could be kept under control, a route is opened to intriguing applications. An AZ91 foam with open cellular structure can be produced having a density of 50 $kg.m^{-3}$. A cubic meter of pure solid Mg weighs 1,740 kg!

The fabrication starts with a polyurethane foam. Plaster is poured into that foam. The polyurethane is removed by heating the plaster mold to 473°C. The resulting plaster mold is an open porous fabric. Subsequently, the molten Mg alloy is poured into the plaster mold either at atmospheric pressure or in vacuo and heated to 573°C. The plaster is removed by water jet. Pore sizes, estimated from a micrograph, range from less than a millimeter to a few millimeter and a wall thickness around 0.3 mm [266].

An interesting property of foams, which was not discussed in Chap. 5, is energy absorption during impact or loading. A look at the stress–strain behavior in compression will clarify why. In a typical stress–strain curve of foams (Fig. 8.7a), three particular zones can be defined:

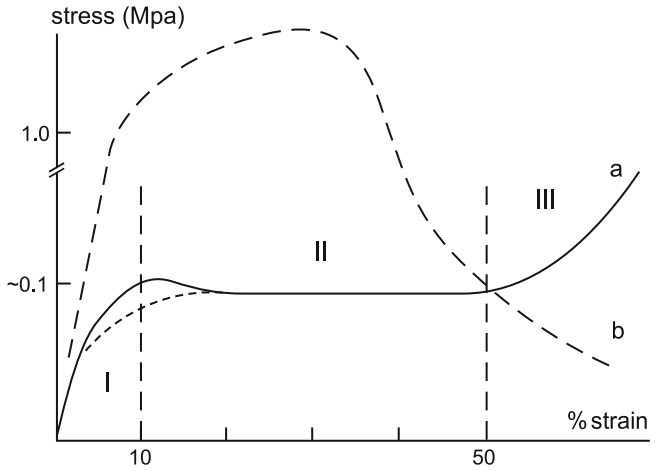

Fig. 8.7 Stress–strain behavior of foams. Notice that the scale of stress is different for curve b

- I: Elastic region: deformation of the pore walls below YS; for some configurations, the curve passes over a maximum before reaching region II. The higher that maximum, the higher the efficiency for coping with impact forces.
- II: A plateau of nearly constant flow stress and large strain (10–50%).
- III: Densification region with steep increase of flow stress: the plastic collapse occurs when the moment exerted by the compression force exceeds the plastic moment of the cell edges.

And exactly the plateau of superplasticity explains why in a relatively wide interval any increasing strain hardly entails increasing stress. The energy absorbed per unit volume in a given strain interval is equal to the area below the stress–strain curve (taking % compressive strain proportional to change in volume). The plateau length decreases on increasing density. The efficiency of the energy absorption is expressed as the ratio between the actual absorbed energy and the energy absorbed by an ideal plastic material of equal initial physical properties. The values indicated in Fig. 8.7 correspond to an AZ91 foam with $\rho = 50\,\mathrm{kg\,m^{-3}}$, an average cell diameter is not given by the authors. The stress–strain behavior of foams in tension is roughly similar to everyday ductile metals (curve b in Fig. 8.7).

For further reading: [267, 268].

8.5 In Vitro and In Vivo

A paper by López and colleagues on the behavior of Mg in SBF did not show but results that could be predicted without doing the effort of the experiment. They used highly polished 99.96% pure Mg samples, which were either used as such, heat treated at 345°C for 15 min, or soaked in 40 vol% HF for 30 min at 30°C; the treated samples were soaked in SBF at 30°C [269]. The authors report that the

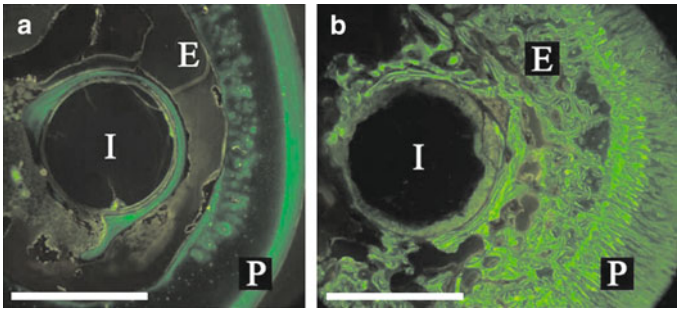

Fig. 8.8 Fluoroscopic images of cross-sections through a guinea pig femur: (**a**) implanted with PLA and (**b**) with a Mg rod. Bar = 1.5 mm; I = implant; P = periosteal and E = endosteal bone formation. Reprinted with permission of Elsevier from [270] Fig. 2

pH of the SBF increases as function of immersion time accompanied by a decrease in weight of the sample. We cite this paper as a paper reporting on a badly conceived experiment. The increase of pH of the (static) solution is simply predictable (see (8.1) and ff.). Moreover, such an experiment is irrelevant in a biomedical context: the body is a dynamic environment and homeostatic mechanisms are always active. Consequently, the measured corrosion cannot simulate the response in the body, be it alone the change in pH.[2]

Over to the better work. Witte and colleagues investigated the degradation at the bone–implant interface [270]. They implanted 4 different Mg alloys in the femora of guinea pigs and retrieved them after 6 and 18 weeks (Fig. 8.8). The polylactide SR-PLA96 served as control. On the negative side, we notice that gas bubbles accumulate after 2–3 weeks (although no adverse effects were seen after 18 weeks). Positive is (1) that LAE442 is degrading at a lower rate than AZ91 and AZ31 consistent with the results by Müller et al. referred to earlier, (2) the degraded implant was replaced by a conversion layer containing Ca and P while rare earth elements were distributed homogeneously in the corrosion layer but were not diffusing into the surrounding tissue, (3) new bone was formed in periosteal and endosteal areas. The authors conclude that *there is a strong rationale for magnesium as future implant material in bone surgery*.

8.6 Conclusion

The reader may be a little disappointed because this chapter is missing a happy end. The full history of magnesium and past trials to introduce this metal as implant material is comprehensively reviewed by Frank Witte [271]. History instructs us

[2] *Dynamic* and *homeostatic* are not contradictory terms: homeostasis can only be maintained by the dynamics of selective flow of products. Therefore, Y.Missirlis prefers the term homeodynamics. Homeostasis, however, emphasizes the conservative aim of the phenomenon.

that for apparently very promising materials the way to Tipperary is long, very long. Witte concludes his review by stating that no commercial implants are yet available and *researchers and clinicians should be warned from all the historical reports that Mg is a special lightweight metal that needs specific knowledge, careful professional handling and experience-based design to be a successful biomaterial*. Consequently, hallelujahs are not permitted yet.

Chapter 9
A 7,000 Year Old Story: Ceramics

Some six to seven thousand years ago, Chinese craftsmen managed to manufacture pottery by firing clay. Definitely not more than thousand years later, the Egyptians did the same (independently?). Throughout the successive millennia, both regions refined this art to dazzling heights. Faience was already invented in predynastic Egypt around 3000 B.C. and the potters wheel was introduced there around 2500 B.C. The start of the *ceramic industry* in the Neolithicum figures among the major stepping stones in the great adventure of human kind. Evermore since then and throughout the developing world ceramists manufactured art, objects for kitchen, religious (*ex votos*!) or medical purposes and today they still do the same.

9.1 Greek Pottery, a Useful Intermezzo?

The summit of Greek craftsmanship in ceramics was the invention around the seventh century of a technique to produce red pots with a black glaze decoration. We had to wait till the eighteenth century P.C.(8) to uncover the potter's secret. *Man does not discover, he uncovers* as Larry Hench used to say. For decoration the potters used a paste, obtained by concentrating a colloidal suspension of illitic clay low in calcium but rich in iron oxides-hydroxides. The suspension formed spontaneously in rain water. By this suspension technique, the right particle size was sequestered. Potash (K_2CO_3) was added as a flux responsible for what is called making the *black vitreous slip*. After decoration, the pots were fired in a single cycle beginning by heating the kiln to around $\sim$950°C with all kiln vents open. In this oxidizing atmosphere both pot and glaze (from the paint) become reddish brown (formation of hematite Fe_2O_3). The red color of fired clay is due to the presence of iron which is rather the rule than the exception: iron is after all the fourth most abundant element in earth's crust. Subsequently, the vents were closed and green wood was introduced in the kiln. In this reducing atmosphere (CO) hematite was reduced to a mixture of black wuestite (FeO) and magnetite (Fe_3O_4) while the temperature went down to <850°C. At this stage, the vents were re-opened and the pots turn again to orange-red except the black glaze because this is, say *oxygen tight* due to the vitrification of the illite, whereas the vase is porous.

J.A. Helsen and Y. Missirlis, *Biomaterials*, Biological and Medical Physics, Biomedical Engineering, DOI 10.1007/978-3-642-12532-4_9,

The Greek potters were not chemists, neither were bronze or steel makers metallurgists: science followed, not preceded technology. What are the physical and chemical foundations underlying Greek pottery manufacturing and what does it illustrate for or teach to twenty-first century people?

About silicates. An estimate of 59% of all minerals on earth are feldspars. Clay minerals were formed either at the site from the original feldspar like the very pure and white China clay (kaolinite), or at the spot, but moved by water, wind, glaciers, erosion like Attic clays. During their long voyage, they underwent particle size selection and collected impurities, impurities which affected the color of the fired clay and gave the Attic clay its unusual plasticity. The same clay sediments are exploited today (Amarousion near Athens).

About colloidal suspensions. The separation of the fine colloidal fraction by sedimentation of the suspension is the way it is still performed today. That the suspension was probably formed in rain water is not a marginal detail because rain water is *distilled water*: in tap water with calcium and other ions the suspension would have flocculated. The theory behind this point is part of the basic physical chemistry of colloidal dispersions.[1] This theory should be brought on the forefront. Many authors in current biomedical journals, who claim to publish innovative or novel production techniques for phosphate-based scaffolds, cements, etc. seem to have forgotten this – we cannot deny – rather aged but not fossilized science!

About glaze formation and fluxes. The hallmark of Attic pottery is the black and red stain. The addition of soda or potash lowers the melting temperature and probably the potters will have noticed the difference in behavior between both fluxes. Although both potassium and sodium are alkali metals, their chemical effect is substantially different. The black glaze has some metallic sheen due to a very particularity of clay. It consists of tiny platelets, around 0.6 or 1.0 nm thick and tens of nanometer wide, a genuine nanomaterial: remember *we only uncover*. When the decoration is applied these particles orient parallel to the substrate during drying and burnishing of the glaze and from there…

The most important group within clay minerals are the phyllosilicates (*φύλλον*: leaf or sheet). The main elements are Si and Al and minor elements such as Fe or Mg, Ca, Na, K either as substitutional or as interlayer exchangeable ions. The sheet of kaolinite is composed of two layers: (1) a layer with silicon in the center of a tetrahedron with 4 oxygen atoms on the apices, each tetrahedron shares two oxygens with the adjacent Si tetrahedron; (2) an octahedral layer with Al in the center and oxygens at the apices, both layers linked together by sharing apical oxygens. Other phyllosilicates have a tetrahedral layer on both sides of the octahedral layer (smectites, vermiculites). The fact that silicon tetrahedra share two oxygens makes that the basic chemical formula for silica is SiO_2 and not SiO_4. The tetrahedra might be stacked in a 3D crystalline array respecting the corner-to-corner

[1] A colloidal suspension or sol consists of a solid dispersed in a liquid and is one type of colloidal dispersion. A characteristic property is the homogeneous distribution of the particles and stability, i.e., nonsettling. Colloidal particles have a size ranging from >2 to <1,000 nm. Distinguished examples are printing ink, milk, clay suspensions…

rule. Cristobalite, an allotropic form of quartz (pure SiO_2) is an example. They can, however, be randomly stacked with some violation of the corner-to-corner rule by smuggling small cations into the array. The crystalline structure vanishes in this case and it becomes a *glass* endowed with very different properties. Outside its use as base mineral in ceramics, kaolinite is used in pharmaceutical products as filler and in the paper industry (glazed paper). Moreover, although unaware of the size of the basic particles, ceramists were true nanotechnologists!

About oxidation/reduction. Oxidation and reducing ... they did it without knowing that:

$$4Fe^{2+} + 3O_2 \rightarrow 2Fe_2O_3 \tag{9.1}$$

(reaction is not balanced and simplified by omission of anions and water) and

$$Fe_2O_3 + CO \rightarrow 2FeO + CO_2 \tag{9.2}$$

or

$$3Fe_2O_3 + CO \rightarrow 2Fe_3O_4 + CO_2 \tag{9.3}$$

and then again oxidized to Fe_2O_3 except for the glaze. Unless special effects are pursued (the glaze), iron is in its highest oxidation states. Part of the glamor of ceramics is their inertness, a consequence of the oxidation state of the elements present.

Was this introductory circuitous way irrelevant for the subject of the book? Presumably, the reader knows our answer: no. The ancient technological achievements were considered a convenient heading to introduce a few fundamental concepts helping to understand ceramics and... remaining is the fascinating high technical proficiency and standardization by these ancient manufacturers. Be it clear that ceramists or manufacturers of any other high quality product today need no less than high technical proficiency profile.

Further reading: [272–275].

9.2 Ceramics, Impossible to Define?

The term *ceramics* is derived from the Greek word κεραμε(ι)ος, *kéramos* or *kerameios* (of potter's earth or potter's clay) or *kerameía* (potter's craft). There is much uncertainty about its etymological root but a most attractive assumption is a Germanic and Baltic etymon *qer-* meaning to burn, to heat [276]. Respecting the etymological origin of the term an acceptable definition could be one according to which

> ceramics are nonmetallic inorganic materials shaped and consolidated at high temperature.

As technology evolves as well with respect to compounds as to shaping technology and modes of heat treatment, the term had to be accommodated to an increasingly broader range of materials. We want, however, to keep consolidation by heat a basic

aspect. In this sense, concrete is not a ceramic but objects of sintered alumina, carbides and nitrides are all at least partially crystalline.[2] Glass is consolidated by heat but is amorphous. A vitreous ceramic contains crystalline particles embedded in an amorphous matrix and combines the best of two worlds.[3] From the foregoing discussion, two generic classes emerge. They are kept together under the umbrella of *ceramics*, both having in common *consolidation by heat*. A third basket was added collecting mostly the same compounds but used in combination with a (metal) substrate:

- Ceramics: mainly compacted and sintered crystalline compounds but subdivided in *High performance* and *Low performance*
- Glasses and glass–ceramics (in-between-glasses and ceramics)
- ceramic/glass coatings

High performance stands here for what is known as *Technical Ceramics*, roughly subdivided in *Engineering Ceramics* and *Electro-ceramics* (piezo-, etc.). *Low performance* stands for the *Traditional Ceramics*, low strength and/or more recent types like soluble phosphate ceramics.

9.3 Ceramics

9.3.1 High Performance

High performance refers here to ceramics mainly used in joint replacements, where they are subjected to high compressive loads and wear. Throughout the earlier chapters, the *pros* and *cons* of metals in hard tissue replacement were discussed and the high standards, that are actually achieved, were highlighted. Arthroplasty is a unique clinical success story but what are the criteria for surgeons to select one device instead of another? A very distinct taste exists among surgeons of different countries as shown in Table 9.1 for wear couples and femoral ball head materials. In France, the surgeons seem to be more conservative and prefer conventional polyethylene but without pronounced preference for metal or ceramic heads. The crosslinked polyethylene is preferred in the USA combined with metal heads, while Korea seems to make the most advanced selection with an overwhelming preference for ceramic-on-ceramic couples. The other countries keep the middle between these two extremes. It is a divergence, which is wider than the documented success rates of the different devices and materials. Is it due to liability laws, reluctance toward innovation, lack of understanding or walking only on familiar routes?

[2] Notice that solidifying metallic alloys bear exciting similarities to the granular structure/texture of ceramics [277].

[3] *Glassy* and *vitreous* are synonyms.

Table 9.1 Choice of wear couples and femoral ball heads around the world

	A[a]	*B*	*C*	*D*	*E*	*F*
Wear couples (in %)						
CL-Polyethylene/metal	62	30	28	5	50	14
Conv-Polyethylene/metal	9	48	50	65	22	14
Metal/metal	21	6	10	5	8	2
Ceramic/ceramic	5	14	10	25	20	**70**
Other	3	2	2			
Femoral ball heads (in %)						
Metal	87	43	71	50	45	28
Ceramic	10	56	24	50	53	**72**
Other	3	1	5		2	

[a]A: USA; B: Germany, Austria, Switzerland; C: UK; D: France; E: Italy; F: Korea
CL-Polyethylene Crosslinked Polyethylene; *Conv-Polyethylene* Conventional Polyethylene; Metal-on-Metal; ceramic-on-ceramic; Other. Source: The Magazine of CeramTec AG, Med. Prod. Div. p. 5 of issue 1/2008

Alumina

Alumina, *la grande dame* of high performance ceramics, underwent quite a bit plastic surgery during her long years of active service. It is occurring in nature as corundum or gemstones such as sapphire, purple by the presence of vanadium, or ruby, red by the presence of chromium. Almost all alumina for industrial purposes, some 45 million tonnes a year, is preponderately extracted from bauxite, an ore containing some iron hydroxides/oxides, silica and clay minerals. Aluminum is purified by dissolving in sodium hydroxide (Bayer process) from which $Al(OH)_3$ is precipitated and transformed into alumina, Al_2O_3, by calcination.

Why so special? Aluminum is in Al_2O_3 in its highest oxidation state excluding further oxidation or electrochemical attack, the first *pro* and common characteristic of all oxygen-based ceramics: resistance to corrosion. By inspection of ion sizes, another set of characteristics is emerging: Al^{3+} and Si^{4+} with ionic radii of 0.051 and 0.042 nm, respectively, are small ions compared to oxygen the radius of which is 0.14 nm. This allows an economical use of space because the small cations find a cozy corner in between the oxygens. The crystallographic structure is shown in Appendix B, Fig. B.6. Follows a chain of consequences: dense packing implying high concentration of bonds which in turn implies high thermal energy to separate the atoms from one another, which is explaining the high melting temperatures... and its insolubility. The latter property makes it inert with respect to tissue. In joints, inertness and wear resistance is an absolute *pro*, but when used for a hip stem or dental implant, it is a *con* because it will not grow in and becomes surrounded by fibrous tissue. The issue of implant-tissue interaction can be summarized as follows:
toxic: the contacting tissues degenerate.
nontoxic and bioinert: formation of fibrous tissue (e.g., domain B in Fig. 9.14);
nontoxic and bioactive: interfacial bonding occurs (e.g., domains A and E in Fig. 9.14);

nontoxic and soluble: the material dissolves and is replaced by tissue (e.g., domain C in Fig. 9.14).

Hardness of ceramics is dictated by the partial covalency of the chemical bonds in Al_2O_3. Covalent bonds are stronger than metallic bonds where the atoms are held together by a 'sea' of electrons. Difference in electronegativity determines how the binding electrons are shared by the partners aluminum or silicon and oxygen.[4] So, strength is another *pro*. And by the way, none of the bonding electrons are in the conduction band, which makes most ceramics extremely good electrical insulators. Moreover, the bonds are directional and that makes slipping of one crystal plane over another unfavorable. Not so for metals for which malleability is intrinsically linked to the easy traveling of dislocations. Thus, ceramics are *brittle* which is mostly a *con*. It entails that shaping by techniques used for metals like forging are excluded. A real unpleasant consequence of brittleness is inadvertent fracturing at subcritical stress levels, which limits their use in bending. Crack propagation in alloys is mostly progressive but fast to catastrophical in ceramics.

A few words more about fracture. Fast fracture will occur *when in a material subjected to a tensile stress σ, a crack reaches some critical length a*. Tabulated values of fracture toughness are calculated by equation:

$$\sigma\sqrt{a}Y = \sqrt{EG_C} = K_C, \tag{9.4}$$

where E is the elasticity modulus, G_C the energy absorbed in making a unit area of crack, called *toughness*. Y is a critical flaw factor, equal to $\sqrt{\pi}$ for internal or volume defects and to $\sqrt{\pi/2}$ for surface defects. Both are material properties. High toughness means that it takes more energy to make a crack propagate. The left term is abbreviated by the symbol K_C and called *fracture toughness* (or K_{IC} when in the test mode the stress is perpendicular to the crack). The units are MPa $\mathrm{m}^{1/2}$ or MN $\mathrm{m}^{-3/2}$.

A design engineer aims to be able to calculate the survival probability of a ceramic object. For this purpose, he/she will not use Gaussian but *Weibull statistics*. In particular for Properties Tables of ceramics, the Weibull modulus is given, usually represented by the symbol m. Passing over the theory of this function, it suffices to mention that for engineering ceramics $m > 10$ and for metals $m \geq 100$. An example of its practical use in reliability testing is demonstrated in Fig. 9.1. We learn from this figure that the results are dependent on the mechanical solicitation mode: $m \simeq 24.8$, 25.4 and 22.3 and the characteristic strength 353, 386 and 339 MPa, respectively, for the test modes four-point-, three-point-flexure or uniform-pressure-on-disk method. From the constant Y in (9.4), it is clear that the shape of the test

[4] Electronegativity is a term introduced by Linus Pauling in his very famous book (first edition in 1939) *The Nature of the Chemical Bond*, third edn., Cornell University Press, Ithaca, NY, 1960 or recently revised editions. Ionicity of a bond is in most cases only partial. Alumina is ionic for 56% and zirconia for 67%. LiF is the prototype example of an ionic solid, diamond is the other covalent extreme.

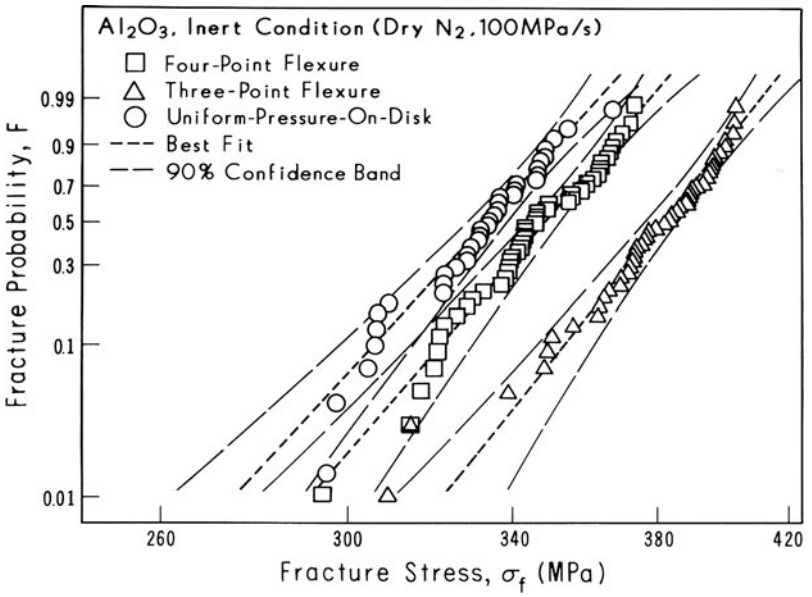

Fig. 9.1 Linearized Weibull plots of the fracture stresses measured in different test conditions in inert atmosphere. Reprinted with permission of ASTM from [279], Fig. 2

specimen affects the value of K_{IC} [36, 278, 279]. Life is not simple for ceramists! A setup for a 4-point bending test and ball head burst test is shown in Fig. 9.3.

The design engineer is even better served by the knowledge of the stress intensity factor, indicated in Fig. 9.2 by the log of crack propagation velocity extrapolated to log of $-\infty$. Below K_{I0} no crack propagation occurs. And there is more to learn from Fig. 9.2. It is a convincing illustration of the progress with respect to pure alumina. It is rendered possible by the combining different compounds into composites, compounds which compensate for each other's shortcomings.

Making ceramic objects. Basically, the procedure for obtaining a ceramic object did not change in the course of time. However for more complex systems such as BIOLOX®delta (see below), a more complex flow sheet as shown in Fig. 9.4 is followed.[5] The flow sheet is self-explaining.

Plastic surgery on alumina. A convincing result of surgery on alumina is illustrated in Table 9.2. Substantial improvement in bending strength and fracture toughness is attributed to a tailored evolution in composition and particle size. The ISO 6474-1 standard *Implants for surgery – Ceramic materials – Part 1: Ceramic materials based on high purity alumina* (or its ASTM equivalent F 603) was released in 1994. An ISO 6474-2 standard *Part-2: Composite materials based on a high*

[5] Our warm thanks to Dr.Meinhardt Kuntz, Bernard Masson and Dr.Thomas Pandorf (CeramTec, Medical Products) who provided in preview their paper *Current State of the Art of the Ceramic Composite Material BIOLOX®delta*. The authors permitted to use their data and comments.

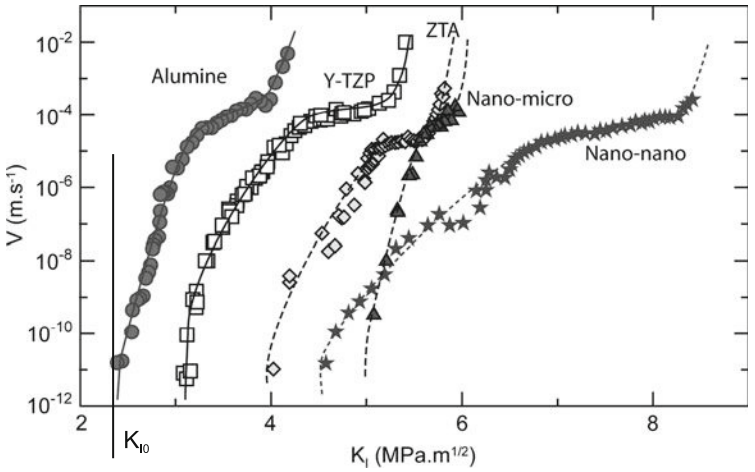

Fig. 9.2 Crack propagation resistance of alumina, 3Y-TZP, 12Ce-TZP, Mg-PSZ, A10Z0Y (Y-TZP with 10% zirconia), micro-nano-alumina-zirconia composite, Nano-nano-Ce-TZP-alumina composite. K_{I0} is the extrapolation to $-\infty$, the stress intensity factor below which no crack propagation occurs. Copyright Elsevier 2009: Fig. 2 in [280]

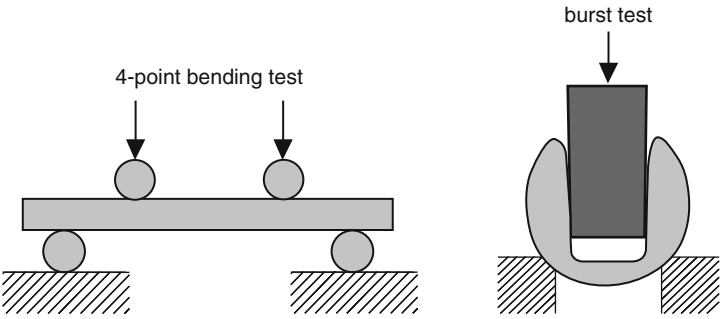

Fig. 9.3 4-Point bending and ball heads testing. By courtesy of CeramTec AG, Medical Products

purity alumina matrix with zirconia reinforcement will be released in 2009. The latter is defined such that a broad range of inorganic compositions are included and specifications for hydrothermal aging and radioactivity are added. Basic requirements are: $\geq$60 wt% alumina and $\geq$10 wt% zirconia, other ingredients are allowed. BIOLOX®delta is to be catalogued under the standard ISO 6474-2 but let it be clear, this standard is not exclusively designated for this product. Its anatomical study will reveal the reason for and result of the plastic intervention.

A composite ceramic. A *con* of ceramics is catastrophic fracture. The case shown in the left picture in Fig. 9.5 is an example of a fast fracture but the patient could still go on for a while. If that happened with a ceramic stem, it would have been really catastrophic. A remedy (but a rough one) is shown in the right picture: the ceramic insert is supported by a titanium cup. This *ensemble* is mounted in another titanium

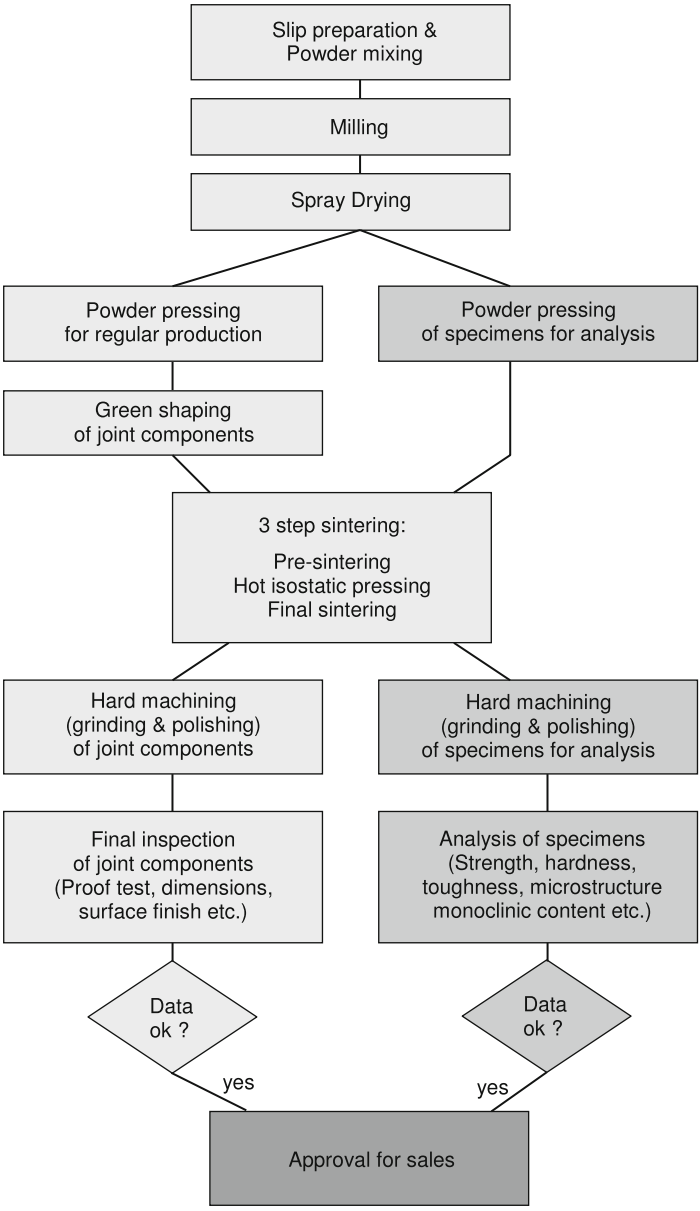

Fig. 9.4 Production scheme for BIOLOX®delta. By courtesy of CeramTec AG, Medical Products

cup, which is cemented in the reamed acetabulum. This design allowed to exchange the ceramic liner or insert in case of fracture without having to remove the cemented backing.

Ample stimulus exists to enhance fracture toughness. The first aim is thus to find a mechanism to stop propagation of cracks. Decreasing particle size of alumina

Table 9.2 Evolution of properties of alumina with respect to the ISO standard of 1994

	Units	ISO 6474-1	BIOLOX®	BIOLOX® forte	BIOLOX® delta
		Composition			
Al_2O_3	wt%	≥99.7	99.7	99.8	Balance
ZrO_2	wt%				24.0–25.5
$Y_2O_3+Cr_2O_3+SrO$	wt%				1.4–2.0
Other oxides	wt%				<0.22
MgO	wt%	≤0.2			
Monoclinic content	%				4.4
		Properties			
Density	kg/m^3	≥3,940	3,950	3,970	4,370
Grain size	μm	≤2.5	4	1.75	*0.54*
Hardness HV1	GPa	≥18	20	20	17.2
Compressive strength.	MPa	>4,000[a]			
Bending strength	MPa	≥500	500[c]	631[c]	*1,411*[c]
E modulus	GPa	≥380	410	407	385
K_{IC}	$MPa\,m^{1/2}$	≥2.5	3.0	3.2	*6.4*
Shear modulus	GPa	162[a]			
Weibull modulus		≥8			14.9
Cyclic fatigue limit		no failure at 200 MPa[b]			

[a] Data collected from [281].
[b] 200 MPa at the start of test, 150 MPa and no failure after 10^6 fatigue cycles [281].
[c] From 4-point bending test.

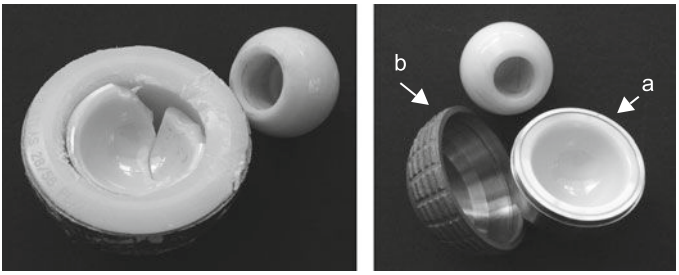

Fig. 9.5 *Left*: retrieved broken ceramic insert, supported by a polyethylene and metal backing. *Right*: ceramic liner backed (in case of revision) by a metal support (**a**). This ensemble is inserted in a cemented metal cup (**b**)

powder was one remedy: compare bending strength and K_{IC} of the ISO standard in Table 9.2 with the next three columns. A most intelligent approach, however, is the integration of a kind of *automatic feedback system*. It is based on the universal principal that nature always tends to minimize a system's internal energy. Once again *Water does not flow uphill*.

The anatomy of BIOLOX®delta is shown in Fig. 9.6: it consists of an alumina matrix as the major component, mixed with zirconia and platelets. Alumina is with

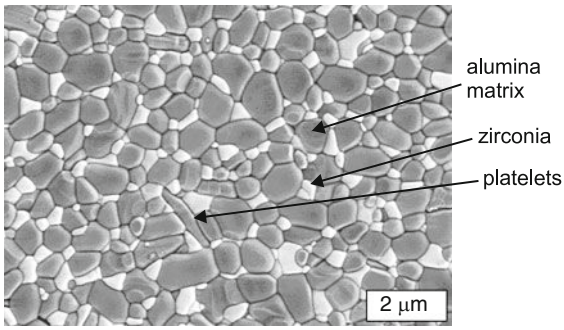

Fig. 9.6 Microstructure of a composite ceramic. By courtesy of CeramTec AG, Medical Products

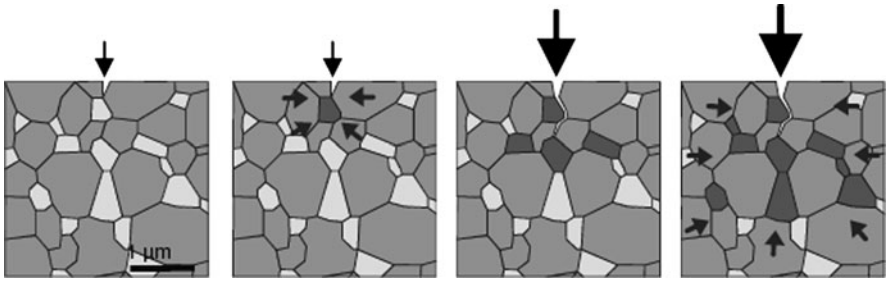

Fig. 9.7 Reinforcing mechanism in alumina–zirconia composite. *Grey*: alumina, *light grey*: tetragonal zirconia; *dark grey*: monoclinic zirconia. By courtesy of CeramTec AG, Medical Products

its 75wt% (80vol%) responsible for the order of magnitude of most of its properties. Grain size is not forgotten either (see Table 9.2 and length bar in Fig. 9.6). Platelets are the third salient aspect of its anatomy.

To explain how the feedback system is operating, we should read Fig. 9.7 from left to right. The high tensile stress at the crack tip triggers a phase transformation of tetragonal zirconia (light grey) to its monoclinic counterpart (dark grey). The accompanying volume expansion leads to compressive stresses which are blocking crack propagation. For more crystallographic details, see Appendix B. The complete story is beautifully described in a review paper by Hannink et al. [282].

Why is this happening? A quick look at Table 9.3 informs us that the monoclinic form is about 2.3% less dense, or occupies about 4% more volume. Tensile stresses (or reduced pressure) around the crack tip favor the transformation to the under this condition thermodynamically most stable monoclinic phase. A true automatic feedback system!

The presence, however, of tetragonal ZrO_2 is not obvious and needs to be stabilized. At a concentration of Y_2O_3 <2mol% in ZrO_2 at room temperature, the monoclinic phase is stable and the tetragonal phase is metastable. The strain energy produced by the stiff alumina matrix on the embedded *small* zirconia particles, however, retains the tetragonal phase. This mechanism is called *mechanical stabilization*. 'Small particles' is emphasized because size matters for a successful phase

Table 9.3 Main crystallographic phases of zirconia

Phase	Transformation temperature (°C)	Density (kg/m^{-3})
Monoclinic	1,000–2,000	5,560
Tetragonal	2,000–2,280	5,720
Cubic	>2,200 (for low Y_2O_3%)	6,090

competition interplay. The temperature shift in the phase diagram as function of Y_2O_3 doping is called *chemical stabilization*.

Y_2O_3 doping is not the end of the story. The ZrO_2 phase addition lowers hardness and wear resistance. For maintaining the right hardness chromium oxide is added, hence the pink color of the heads and acetabular insert. The addition of SrO to the ZrO_2(:Y_2O_3)-matrix results in the formation of platelets of about 3 μm in length and 0.8 μm wide (see Fig. 9.6). It improves fracture toughness but lowers hardness. The mix of compounds are undergoing following reactions during treatment (between brackets the volume percent in the end product):

$$2YCrO_3 \rightarrow Y_2O_3 + Cr_2O_3 \tag{9.5}$$

$$SrZrO_3 \rightarrow SrO + ZrO_2 \tag{9.6}$$

$$Al_2O_3 + Cr_2O_3 \rightarrow Al_2O_3 : Cr(80\%) \tag{9.7}$$

$$SrO + 6Al_2O_3 : Cr \rightarrow SrAl_{12-x}Cr_xO_{19}(3\%) \tag{9.8}$$

$$ZrO_2 + Y_2O_3 \rightarrow ZrO_2 : Y(17\%) \tag{9.9}$$

Al_2O_3:Cr and ZrO_2:Y stands for solid solutions of Cr and Y in the alumina and zirconia matrix, respectively. The platelets consist of the hexagonal ternary phase $SrAl_{12-x}Cr_xO_{19}$. There reinforcing action becomes efficient when they are formed in situ. This is feasible provided a correct processing procedure is followed. The advantage of the in situ formation is the excellent anchoring of the platelet to the matrix.

Cracks propagate from their nucleation site on by transmitting the stress, induced by the martensitic transformation, to next grain and so on, a typical nucleation and growth process. An obvious solution to enhance crack resistance could be a decrease in toughening particle concentration below a value where, say, one particle does not feel its next neighbor, i.e., lowering below the *percolation threshold*. Percolation is an important physical concept and part of the physics of phase transitions and scaling theory. For a short but excellent introduction to this theory, the book of Dietrich Stauffer is recommended literature [283]. An alumina toughened by a concentration of zirconia particles below the percolation threshold is reported to be under development (referred to as ZTA, zirconia-toughened alumina).

A major inconvenience is low temperature degradation (aging), a relevant issue for zirconia containing ceramics and provoking transformation of the tetragonal to monoclinic phase, an effect relatively fast at nonphysiological temperatures.

However, autoclaving the ceramic composite discussed above at 134°C in 2 bar steam for 10 h, the standard test procedure and corresponding to 4 yr in vivo, is reported to decrease only marginally the bending strength (4-point bending in Ringer's solution, cyclic load of 600 MPa, 5.10^6 cycles). The monoclinic phase content increased from 30 to 47% relative to the total volume of the material.

Wear. High performance ceramics are used exclusively in joint replacement and wear is an important issue. The wear volume is reported to decrease from 1.5 $mm^3/10^6$ cycles for the BIOLOX®forte variant to 0.2 mm^3 for BIOLOX®delta.

To conclude: The 'surgical' intervention on the manufacturing of alumina composites has been quite successful.

References: the already mentioned text by Kuntz, Masson and Pandorf (to be published in 2009, 3rd quarter [284]) and [285–287].

Zirconia

The herald of a new generation of ceramics, with superb mechanical properties and biocompatibility, was introduced in the 1980s. The superior resistance to fracture allowed the production of balls with a diameter of 22 mm, for alumina the lower limit of the diameter was 32 mm. The mechanism to stop crack propagation is the tetragonal to monoclinic phase transformation as explained above. Hundreds of thousands femoral heads were implanted till in 2001 like a bolt from the blue 400 balls, produced by Prozyr®, failed in a very short period of time. The high failure rate was found to be attributed to two particular batches produced after a modification in the processing technique (continuous furnace instead of batch processing), which resulted in a different microstructure. A poor resistance to low temperature degradation was the consequence of this. The orthopedic community overreacted and the market sale dropped between 2001 and 2002 by 90%, partly justified and partly not.

The mechanical properties of *Yttria-stabilized Tetragonal Zirconia Polycrystals* (Y-TZP according to ISO the standard 13356, revised in 2008) are collated in Table 9.4. The values in bold are those far superior to pure alumina (see Table 9.2). Bending strength and K_{IC} of BIOLOX®delta are somewhat lower than the best out of the three (Demarquest).

Who should hang for the Prozyr®disaster?

Out of the abundant (and confusing) literature, the following conclusions were distilled.

The damage nucleates on surface spots where tetragonal grains transform due to one or more coincidences, such as crystal orientation, residual stresses, grain size and shape, lower yttria content, presence of the cubic phase, or presence of alumina grains. The monoclinic volume expansion leads to microcracking which in turn creates an entrance path for water. The resulting swelling roughens the surface. Wear may lead to grain pull-out and formation of craters. Grain pull-out was anyway an old sore for biomedical ceramics since alumina started its career in implants. The free particles may get squeezed between the articulating surfaces and cause

Table 9.4 Properties of Y-TZP compared to ISO 13356 (data from Table III in [288])

	Units	ISO	Desmarquest[a]	Metoxit[b]	Kyocera[c]
Density	kg/m^3	≥6,000	>6,080	6,080	6,080
Grain size (av.)	μm	≤0.6	<0.5	0.4	0.2
Hardness HV1	GPa	n.s.[d]	n.s.	12	13
Bending strength	MPa	*>800*	*>1,500*	*1,200*	*1,200*
E modulus	GPa	n.s.	n.s.	210	210
K_{IC}	$MPa\,m^{1/2}$	n.s.	*8–10*	*8*	*5*

[a]J.M. Arnaud et al. in 30e Meeting de la Sociètè Orthopédique de l'Ouest, Pont l'Aubée (France, June 1997)
[b]W. Rieger, on p. 283 in *World Tribology Forum in Arthroplasty* (Hans Huber, Bern, 2001)
[c]H. Oonishi et al. on p. 7 in *Reliability and long-term results of ceramics in orthopedics* (Thieme, Stuttgart, 1999)
[d]n.s.: nonspecified

progressing third body wear. Immunological effects of wear debris will be discussed later. An interesting in depth analysis of a zirconia head broken 34 months after surgery is published by Piconi and colleagues with similar conclusions [288]. In a paper of 1999, Allain and colleagues reported a survivorship of eight years for only 63% of the total hip replacements they implanted using a zirconia head/polyethylene cup. Abundant osteolysis near the implantation site was observed, something they did not see for alumina heads. Consequently, they abandoned the use of zirconia heads [289]. The ceramics world, however, did not stop here. The company Mathys (Bettlach, Switzerland) uses for their heads and cups a composite, tradename *Ceramys*, which is, compared to BIOLOX®delta, positioned at the other end of the composition line. It consists of a nanocrystalline homogeneous dispersion of 20% alumina with 80% zirconia and no other elements involved. We are not aware of long-term studies about the use of this composite.

The Story Does not End Here

From foregoing discussion, it should be clear that ceramic composites and not the single oxide ceramics, pure Al_2O_3 or ZrO_2, are the future. A weak point of zirconia remains wear resistance. Figure 9.8 illustrates what is going on in the field of technical ceramics and the composite ZrO_2–WC–Al_2O_3 meets the weak wear resistance of zirconia and might find application in the biomedical field. The fracture toughness of ZrO_2–TiCN composites prepared from nanopowders is about $3.9\,MPa\,m^{1/2}$ and it has a Vicker's hardness of $HV_{10} = 1{,}630\,kg\,mm^{-2}$, and although not bad, the toughness is still lower than that of Y-TZP (Table 9.4). A ceramic with exquisite properties, probably to be situated in the upper right corner of Fig. 9.8 is silicon nitride Si_3N_4. It does not suffer from low temperature degradation (zero water absorption), is not sensitive to stress corrosion, is hard ($2{,}200\,kg\,mm^{-2}$ Knoop) and has high compressive strength (360–434 MPa) and excellent fracture toughness

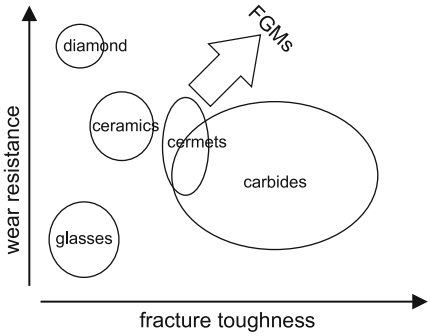

Fig. 9.8 Families of current technical ceramics. The hope is that functionally graded materials (FGMs) will perform better

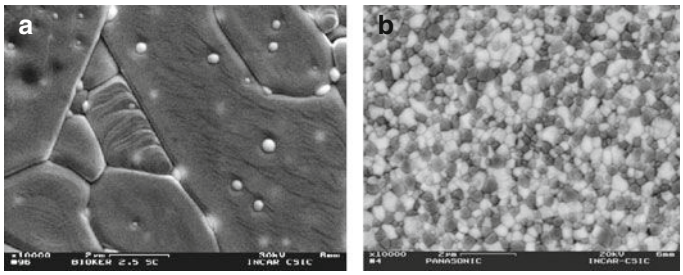

Fig. 9.9 SEM picture of a micro–nano composite (**a**) and a Nano–nano-composite (**b**). Scale: width of one picture is 12 μm. Copyright of Elsevier 2009: Fig. 3a and b in [280]

(K_{IC} of 5.0–8.0 MPa $m^{1/2}$) and wear resistance. Its biomedical compartment will probably be restrained to coatings because of its high production cost.

Still more candidates arise on the horizon: ceria (CeO_2) and magnesia (MgO) doped zirconia (Ce-TZP and Mg-PSZ), micro-nano and nano-nano Ce-TZP. All have superior fracture toughness as shown in Fig. 9.2 and, moreover, are less prone to degradation by water. CeO_2 doping decreases the number of oxygen vacancies, which are accepted to be responsible for diffusion of water into the lattice. Micro-nano means that nano-sized zirconia particles are dispersed in micro-sized alumina while nano-nano stands for an intimate mixture of nano-sized particles of both oxides. The small white dots in (a) of Fig. 9.9 are the nano-zirconia particles dispersed in micro-alumina grains. Important to remark here is that the concentration of zirconia particles should be below the percolation threshold. The black and white particles in (b) are the nano-alumina and nano-zirconia particles.

Examples are the micro-filled and micro-hybrid dental composites in Sect. 10.3.2.

An emerging new class of ceramics are *Functionally Graded Materials* (FGMs). In Chap. 5, we already encountered something of the kind: the in situ formed oxide on zirconium is a well adhering layer because of the gradient between external zirconia and zirconium substrate. FGMs are a step forward. A relatively easy processing from colloidal dispersions allows the production of a green near-net shape object. The aim is a smoother stress distribution between coating and substrate as shown in Fig. 9.10 and appropriate mechanical properties.

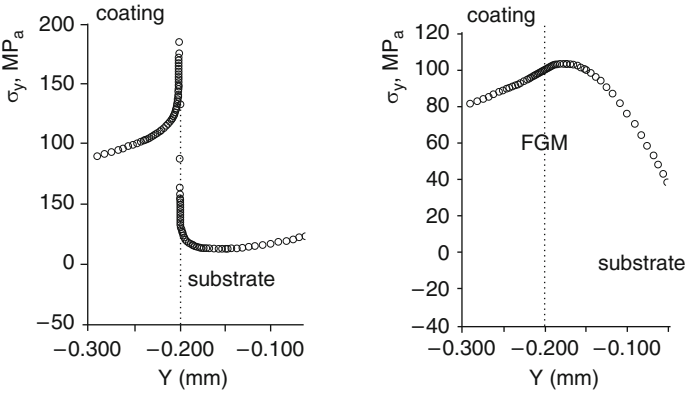

Fig. 9.10 Smooth stress distribution in FGMs. By courtesy of Prof. J. Vleugels, Department of MTM, KULeuven (Belgium)

The potential field of application is extremely wide but still hurdles have to be cleared before FGMs will become an established item. A taste of experimental performance is given in Fig. 9.11 for an Al_2O_3 disc with a ZrO_2 concentration profile (top left); the light grey spots in the micrographs (B,C,D) are zirconia; the survival probability S (Weibull plot) and biaxial stress for a pure alumina disc to the FGM disc are compared (bottom left). It may not look that spectacular but an increase in Weibull modulus from $m = 9 - 12$ is an encouraging result. The biaxial strength is spectacular.

An onset to a biomedical design in an FGM is the acetabular cup manufactured in near-net shape by *electrophoretic deposition*. A section through the cup (right) and the corresponding concentration profile (left) are shown in Fig. 9.12. The *green* cup was further processed by sintering, Hot Isostatic Pressing (HIPping) and finished by grinding [290, 291]. A product manufactured with an FGM is, as far as we are aware of, not on the market yet. What might be at the verge of success is a titanium or titanium alloy coated with (Ti,Al,Zr)nitride with a TiN as gradient interlayer. This is, however, not quite an innovation. Oxinium, the product discussed in Chap. 5, is in fact also a gradient material.

For more detailed reading: [280, 282, 292–294].

Squeaking Hips

A phenomenon that should not be forgotten is *squeaking*, audible noise mainly observed in younger, heavier or taller patients bearing a ceramic-on-ceramic hip joint. A number of surgical, patient and implant-related factors (malposition, age, activity, resonance) should combine to produce sound in the audible range. Although not completely cleared out, it is suggested that *squeaking is due to forced vibration with a frictional driving force and a dynamic response. The high levels of friction*

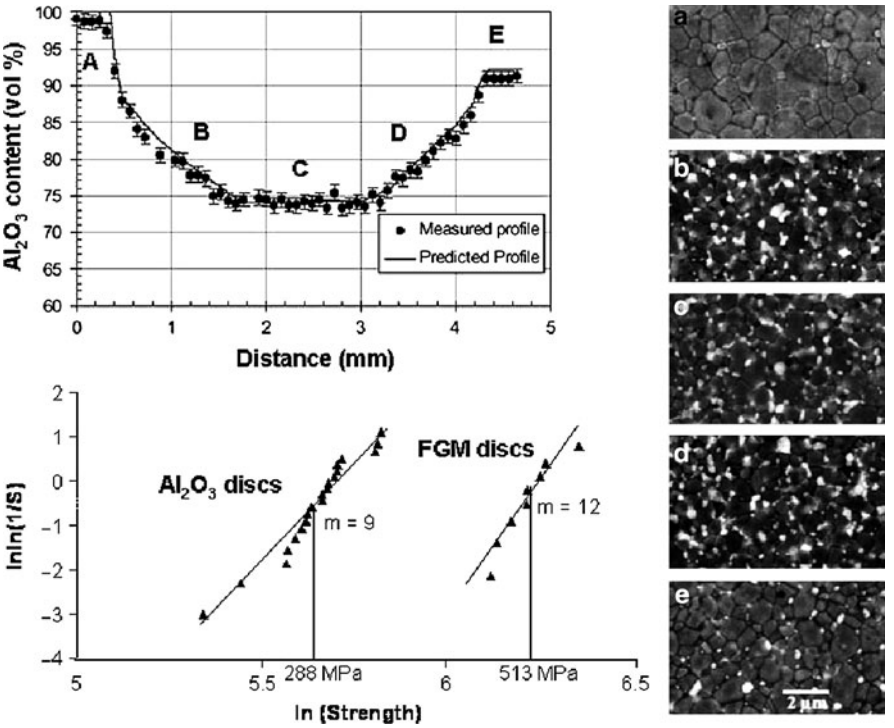

Fig. 9.11 Survival probability (Weibull plot) of a pure alumina disc and an FGM disc with the concentration profile (*top left*); micrographs illustrating the distribution of zirconia (*light grey spots*); the biaxial strength (*bottom left*). By courtesy of Prof. J. Vleugels

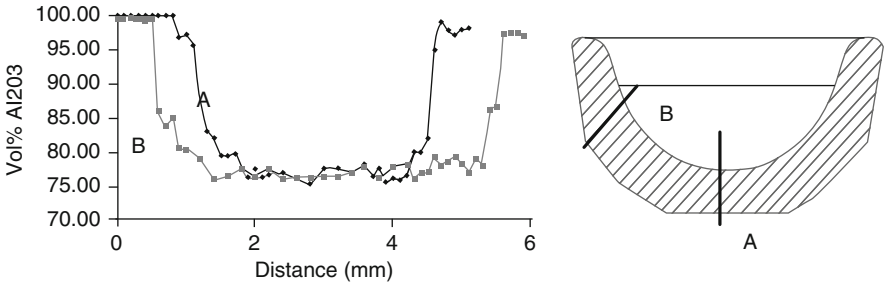

Fig. 9.12 Composition profile of an acetabular cup insert: volume $\%Al_2O_3$ vs. distance. Courtesy Prof. J. Vleugels

produced by hard-on-hard bearings, when there is a breakdown of fluid film lubrication, provide more energy to the system than can be dissipated in the usual way. Under the right conditions the metallic parts (titanium backing of the cup) amplify this vibratory driving force into an audible event. The text in italics is copied from a paper by Walter and colleagues [295]. Resonance of the titanium shells and femoral

components falls within the audible region (<15 kHz) and is probably the source of squeaking. The incidence is less clear but is estimated around 1% [296].

9.3.2 Low Performance

The mineral phase of bone, 60% by weight, consists preponderately of calcium hydroxyapatite (HA), stoichiometrically $Ca_{10}(PO_4)_6(OH)_2$. Other ions may partly substitute hydroxyl or phosphate groups (CO_3^{-2}, SiO_4^{-4}, Mg^{+2}, Sr^{+2}, Na^+ F^- and so on) and the 'biological' form is always a calcium-deficient HA. The ideal Ca/P ratio is 1.67; phosphates with ratios below 1/1 are not suitable for implantation. Stoichiometric HA can be sintered to ≥1,300°C without too much risk for phase transformation (possible formation of CaO or $Ca_3(PO_4)_2$). CaO is itself toxic but reacts to portlandite or carbonate. Because of its similarity to the mineral phase of bone, it was decades ago the obvious choice as biomedical ceramic. While alumina and zirconia are quoted as inert ceramics, HA is slightly soluble and therefore bioactive. The rate of dissolution depends on the degree of stoichiometry and the substitutional or interstitial elements. However, as it becomes clear by inspecting Table 9.5, hardness, compressive strength, bending strength and certainly fracture toughness K_{IC} are far below the requirements for joints or weight-bearing applications; as such it is quasi exclusively used as coating on a metal substrate (see Sect. 9.5). More about other phosphates are found in Chap. 10.

9.4 Glass and Glass–Ceramics

Alumina and zirconia consist of compacted and sintered more or less well ordered, i.e., crystallized particles. Near the other end of solid state order is the more or less chaotically organized glassy state. A typical glass former is silicon. As referred to Sect. 9.1, the small cations smuggled into the silica array are most commonly sodium and calcium (window glass; see [297]). A characteristic of amorphous

Table 9.5 Properties of dense hydroxyapatite (HA) ceramics compared to ISO 6474-1 for zirconia and Y-TZP (Metoxit, cfr. Table 9.4)

	Units	ISO	HA	Y-TZP
Density	kg/m^3		3,156	6,080
Hardness (HV)	GPa	≥18	5–8	12
Compressive strength	MPa	>4,000	100–900	
Bending strength	MPa	≥500	20–30	1,200
E modulus	GPa	≥380	70–120	210
K_{IC}	MPa $m^{1/2}$	≥2.5	∼1	8

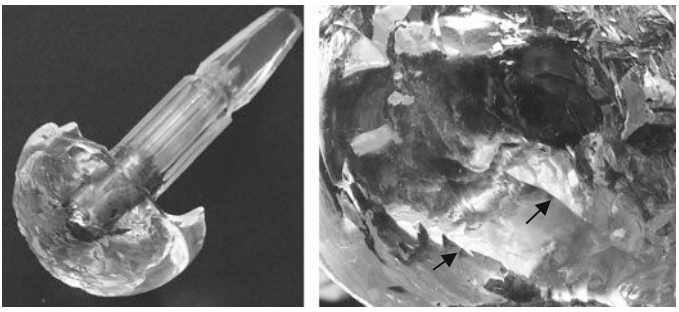

Fig. 9.13 Damaged ball head of the femoral component of an all glass hip prosthesis: salient aspect of broken glass surface. *Right*: detail; arrows point to conchoidal edges

materials is their conchoidal fracture with very sharp cutting edges.[6] Therefore, it was used for scalpels for surgery and cutting blades in microtomes. Amorphous silica occurs in nature as obsidian (volcanic glass) or flint (silex). It permitted Stone Age men to produce tools, a substantial achievement in the technological evolution of mankind. Less successful was its use in hip implants. The conchoidal character of fracture is nicely demonstrated by Fig. 9.13, conform with theory, nice for the physicist, however, not for the patient having implanted the hip prosthesis (left picture).

9.4.1 Bioactive Glasses

Ordinary glass is corroding in a wet environment and small surface defects determine and/or co-determine the fracture of glass. A consequence is that the strength depend on the size of the test specimen, similar to the behavior of high performance ceramics (Weibull statistics). And the same holds for bioactive glasses (BAG). On the one hand, the matching of E moduli of bone and BAG were an attractive mechanical feature (Table 9.6) but, on the other hand, all other properties are simply unsuitable for any load bearing application.

So, end of the story?

It all started in a most appealing way in the late 1960s, early 1970s. Why? It is easily explained in Fig. 9.14, where the dependence of interaction with tissue on composition is demonstrated. In the composition domain around E both bone and soft tissue bonding happens, while in A bonding to bone is stimulated. Thus, modulating composition allowed to tailor a material for a specific purpose. Moreover, the success was supported by a few spectacular results: a segmental bone replacement in a monkey made of 45S5 Bioglass®-ceramic was broken in the implant

[6] From κόγχη (greek) or *concha* (latin) mollusk shell.

Table 9.6 Mechanical properties of bioactive glasses (BAG) and glass–ceramics [298, 299]; juxtaposed the data for bone (from tables in Sect. 2.3)

	Units	BAG	BAG-cer	A-W	Bone
E	GPa	35	70–124	117	16
UTS	MPa	35–70	83	186	93
Bending strength	MPa	42–100	53–233		160*
K_{IC}	MPa $m^{1/2}$	0.5–0.8	0.9–2.95	2.6	1–12

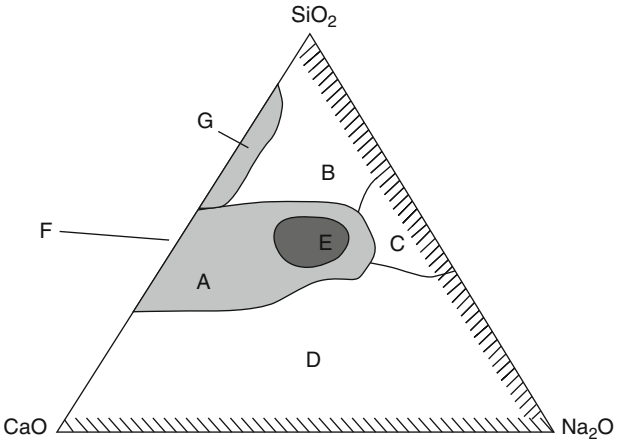

Fig. 9.14 Bioactivity vs. composition. (**a**) bone bonding; (**b**) bioinert; (**c**) resorbable; (**d**) unstable; (**e**) bonding to bone and soft tissue; (**f**) apatite/wollastonite glass–ceramic; (**g**) bioactive gels and glasses. By courtesy of Springer [40], Fig. 16.7

by impact-torsional loading but left the bond to bone intact; in another case the bond between an apatite/wollastonite glass–ceramic implant and bone proved to be stronger than both bone and ceramic [300, 301]! What could be wished more?

Series of BAGs were produced and patented and the best known is 45S5: 45 referring to the SiO_2 %w/w (S = networkformer) and the last figure to the molar ratio $R = CaO/P_2O_5$. A composition with $R < 5$ does not bond to bone. A substantial difference with window glass is the presence of P_2O_5, responsible for the formation of hydroxyapatite in the interface glass/tissue (Table 9.7) and mediator for bonding. The formation reaction is a high rate reaction which should lead to fast tissue bonding and therefore stabilizing the implant. Histologically, the formation is observed of osteoid, intermixed with collagen fibers, as a transit to mature mineralized bone. The surface layer consists of a poorly organized layer with complex composition but definitely responsible for the osteoconductivity, an essential characteristic of these materials (see Fig. 4.8). The thickness of the layer between mature tissue and substrate is influenced by the level of activity of the material, be it glass or any other substrate. Unfortunately, the mechanical properties do not allow the use of glasses as free-standing, load-bearing implants. The applications of BAGs are limited to fillers for large bone gaps (one trade name is Biogran in dentistry), the ossicular

Table 9.7 Composition in %(w/w) of a bioactive glass and a glass ceramic (data collected from [303–305]; GC = glass–ceramic)

	45S5 BAG	KG Cera G–C	MB GC G–C	A–W G–C
SiO_2	45	46.2	19–52	34.2
P_2O_5	6		4–24	16.3
CaO	24.5	20.2	9–3	44.9
CaF_2				0.5
$Ca(PO_3)_2$		25.5		
MgO		2.9	5–15	4.6
Na_2O	24.5	4.8	3–5	
K_2O		0.4	3–5	
Al_2O_3			12–33	

Fig. 9.15 Dissolution of bioactive glass grains (Biogran®) after two months of implantation in a beagle dog's jaw. Original magnification X100, Stevenel's blue and Von Giesen Picro-fuchsin stain. By courtesy of Prof. E. Schepers (UZ-KULeuven, Department of Dentistry)

chain in the middle ear and occasionally coatings (see Sect. 9.5). Another potential opening to application is the integration by ion-exchange of Ag^+. The authors report antibacterial activity at nontoxic levels and improvement of the bioactivity of the starting glass [302].

Before concluding the subject, still a pretty fact about the interaction between medium-sized BAG grains (300–350 μm) and bone. Figure 9.15 shows how, after 2 months of implantation in the lower jaw of beagle dogs, the particles are partly dissolved – big surprise – not starting at the surface but excavated!

One of those wonderful but capricious ways along which nature is acting! Six months later, bone formation is noticed inside the cavities [306, 307]. An example of a nontoxic and soluble product, which is gradually replaced by osseous tissue.

9.4.2 Glass–Ceramics

Glass–ceramics contain within the vitreous mass microcrystalline particles and differ as such from glass, which is structurally a homogeneous material. These

microcrystals are not added to but produced in the mass by spontaneous precipitation during firing or cooling. Glass is, as stated above, an amorphous material, which exhibits a *glass transition* and is as such a subset of the generic class of amorphous materials: all glasses are amorphous solids but not all amorphous materials are glasses.[7] It is not clear why certain chemical compositions spontaneously form glasses and other do not. Easy glass formers are the oxides SiO_2, GeO_2, As_2O_3 and P_2O_5. They form an infinite network with, by definition, no long-range periodicity. Addition of oxides such as Na_2O and CaO to SiO_2 is breaking up the continuous network and these oxides are called *network modifiers*. Not all compositions, however, give rise to stable vitreous end products. Slow cooling or programmed refiring along specific heat/time profiles allows a crystalline phase to precipitate. That is the way a first class of glass–ceramics form; properties and crystallite size are conditioned by the thermal history. The bioactive glass 45S5 (melting temperature 1,350°C) can be turned into a ceramic by refiring at 500°C. Another example is the ceramic formed by melting hydroxyapatite and glass (>50%SiO_2). After well-defined thermal conditioning (time, temperature), an apatite-wollastonite ceramic is formed with fairly improved mechanical properties (see Table 9.6). A second class are glasses transformed into glass–ceramics by loading with refractory oxides, nitrides, fibers and so on as nucleation sites for crystallization.

The output for clinical use remains restrained to a very few niches, to our opinion mainly due to deficient mechanical performance. Contrary to what one might think, it is not quite the end of the story. A total of 6,800 papers have been published since the beginning of the story. In the years 1988, 1998, 2005 and 2008, respectively, 102, 231, 481 and 635 papers were published, a pure logarithmic increase. Scientists' interest did not vanish through all those years and continue to believe in a potentially wider field of application! In a recent paper by Lao and colleagues, BAGs doped with strontium were evaluated in a fairly quantitative approach [308]. Strontium has a recognized beneficial effect on cell activity and bone remodeling. Moreover, there are still other candidate elements than strontium or other combinations to be looked at. The possibility for tailoring dissolution kinetics and other properties continues to be an appealing prospect. Whether or not the observed failings were the 'end of the story' demands a polychrome answer.

9.5 Coatings

Coating is or should be a win–win situation for both substrate and ceramic: the substrate wins by a more favorable interaction with tissue, occasionally corrosion protection, and the coating wins by the superior mechanical performance offered by the substrate, overcoming its own lack of strength.

[7] Notice that the 'science' of amorphous materials remains somewhat fuzzy. To learn more about the amorphous state, the book of Elliot is useful [229].

Hydroxyapatite

High mechanical stability is required for hip and knee prostheses. To impart stability to stem and cup, Prof. Charnley cemented femoral and acetabular parts by a PMMA cement (1960s!). Although this cement is immensely improved since Charnley's days (lower concentration of monomer), cementing is not without risk for the patient and remains a point of discussion as well as the cementless alternative. To impart 'biological' fixation, a common practice is coating the stem with a bioactive coating, almost exclusively HA. The coating is applied by the well-established technique of plasma-spraying. The plasma is energized in a stream of ionized argon (or mixtures with by passing through a high frequency coil 200–2,000 kHz. The core of the plasma is extremely hot: >10,000°C but with steep gradients to the cooler periphery. Most compounds will be decomposed at these temperatures were it not that the powder, fed to the Ar stream, is accelerated to nearly sonic velocities ($\sim$200 m s^{-1}). It reduces the residence time of the particles in the plasma to milliseconds, so that only partial melting takes place with relative small changes in composition. The substrate is moving in front of the torch to expose the area to be coated which at the same time reduces excessive heating of the substrate. Nevertheless, some changes take place. The coating becomes with respect to the original powder, partly amorphous and may contain other crystallographic phases (analysis by X-ray diffraction). HA coating by plasma spraying allows to keep composition, texture and structure under control and to obtain adhesion strengths of >80 MPa.

Many manufacturers coat only the proximal one third of the stem and the whole backside of the acetabular cup, while others coat the whole stem. The CORAIL total hip prosthesis (DePuy) is a particular successful example of the latter. The coating has a thickness of 150$\pm$40 μm, a porosity <10%, a crystallinity around 60% and an adhesion strength >35 MPa. Excellent overall survival rates were reported: 99.5% after 4.5 year, 95% after 10 year for the total hip replacement. For the stem only, however, a 0.977% survival rate after 10 year is reported. In general, it is accepted that a primary mechanical fixation is needed which is followed by a secondary, biological, one. The interface seems to act as an efficient barrier to wear debris, which is carried toward the pelvis and not into the interface. After all those years, HA is definitely proven not to be toxic and does not produce inflammatory reactions. Resorption happens, an unescapable consequence of (bio)activity. It has been observed that, where HA coating has disappeared, new bone in direct contact with the metal surface is formed without interposition of fibrous tissue [309, 310]. Tight mechanical fit remains a major issue when pursuing osseointegration.[8]

[8] For another support of the statement that a tight fit is maintaining the integrity of bone tissue, see Chap. 11 for a similar effect in the elastomer-coated prosthesis.

BAG Coatings

Due to the nature of their mechanical properties, BAGs need a strong backing. Several techniques have been proposed for the application of BAG coatings (hot dipping, electroforming, plasma spraying, you name it!). None has found its way to commercial products yet. The composition is more subtle than HA and the composition is subject to change during heating. It already starts at the production stage of the glass. For melting, the basic compounds inert crucibles (platina) are a must to avoid contamination during heating (1,300–1,450°C). Next, if plasma spraying is the coating technique of choice, a smooth feeding of the plasma torch needs a free-flowing powder. Preparing such a powder is another time consuming, costly and occasionally contaminating step with considerable loss of material (sequestration of the required particle size). Helsen and collaborators met these disadvantages by developing *Reactive Plasma Spraying*, the essence of which is the synthesis of the glass in the plasma itself. The production of the free-flowing powder happens, except the last step, at room temperature. It starts from base chemicals as calcium carbonate, tricalcium phosphate, sodium silicate. An aqueous slurry of appropriate composition (already corrected for losses during the residence in the plasma) is spray dried, cold isostatically pressed, broken, milled, sieved to separate the right fraction (40–70 μm) and finished with a thermal treatment at 950°C; the fraction outside the right size range is easily reprocessed. This production flow sheet is flexible and cost efficient. As proven by X-ray diffraction analysis, the coating consist of a true nonporous glass with homogeneous composition of thicknesses up to 50 μm. Adhesion strengths >84 MPa were routinely obtained; adhesion strength was tested by a newly developed technique for cylindrical specimens [141,142]. The excellent osteoconductivity was demonstrated in vivo by implantation in the jaw of beagle dogs and the result was already shown in Fig. 4.8. But even that cost-efficient process with excellent in vivo results could not seduce industry.

9.6 General Conclusion

This chapter opened by addressing the superior skills of ancient ceramists. The link to contemporary ceramics is surprisingly straightforward. For any practical purposes, despite our present day insight in the basic physical and chemical principles, technical proficiency is still the-stay-behind for a good ceramist... as catastrophically demonstrated by the Prozyr case. Where indicated, the micro- or nanostructural particularities leading to the actual performance of the selected ceramic products were analyzed.

One particular aspect of ceramics like barium titanate has not been addressed. The favorable promotion of osteogenesis by the combination of hydroxyapatite-barium titanate (piezoelectric) after implantation in jawbones of dogs was announced but it is not translated into a clinical application in humans in as far as we are aware of [311].

Nonmetallic, *inorganic* and *consolidated by heat* forms the backbone of our definition for *ceramics*, the latter part respecting the etymology of the term. Two generic classes were considered: crystalline and amorphous compounds. *Coatings*, the third class, consist of basically the same compounds but, because of their low fracture toughness, are used supported by a strong (metal) backing.

The mechanical properties are preponderating for high performance inert ceramics, while bioactivity is the dominating property of the lower strength ceramics. Hydroxyapatite was for the latter an obvious choice because of its widespread and successful use.

The compounds that were addressed represent only a selection of the best-performing ceramics. Sialons, nitrides and other advanced high performance ceramics with biomedical potential were not discussed. The palette of proposals is endless, and predicts whether a product will lead to a breakthrough is risky.

Despite the protracted absence of clinical success, bioactive glasses were discussed into some detail for, say, sentimental reasons as there are: the sparkling *entrée* on the biomedical scene so many years ago, the intriguing nonfading fascination to an increasing number of materials scientists, believing in their future success, and the exciting possibility to tailor their properties to specific applications.

Further reading: [299, 303, 312].

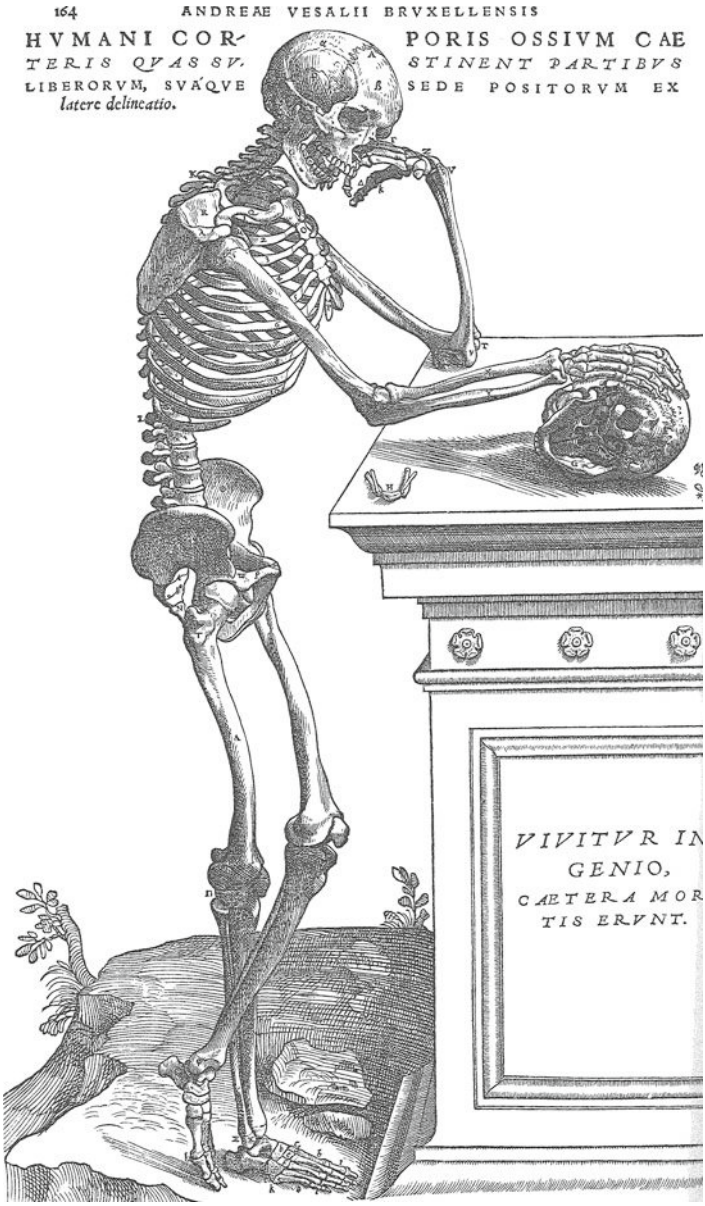

Andreae Vesalii: De humani corporis fabrica libri septem
Basileae: ex officina Joannis Oporini, 1543

What about better teeth?

Chapter 10
Dental Materials

Drilled molar crowns of adult persons were discovered in a Neolithic graveyard in Pakistan (Mehrgarh, Baluchistan) dating back 8,000 years. The practice is quoted as a type of *proto-dentistry*. Drilling was probably performed for therapeutic reasons (caries?) but trace of filling material was not detected. Anyway, one thing was clear: the drilling tool was a flint tip [313]. Flint is amorphous silica and at different instances we underlined the basic significance of amorphous materials for mankind. A tooth consists of an outer shiny part, *enamel*, the hardest substance in the human body and formed during childhood, and an inner much softer part *dentine*, continuously renewed like other bony tissue. The historical hierarchy of the two parts has an interesting consequence. Concentration and isotopic ratio of, for example, strontium in enamel is determined by childhood diet, while that of dentine is governed by the diet of the last few years, an archaeological clue for mobility studies of early men.

An exciting example of the use of this isotopic ratio conservatism is given by the identification of a recently found body of an unknown soldier killed during World War I in Flanders Fields. Based on the combination of DNA analysis and determination of the isotopic ratio of strontium in enamel, he was identified by a consortium of the Universities of Leuven, Oxford and Cranfield and Governmental Departments of Great Britain and Australia as Private Alan James Mather. The isotopic ratio of strontium in its enamel matched the geological characteristics of one region. DNA analysis of potential family members in that particular region confirmed the identification. The Australian Army reburied him with full military honors alongside his comrades in a Commonwealth War Graves Commission cemetery in Belgium on July 22, 2010.

Tooth degradation is a problem at all times. In a Gallo-Roman necropolis archaeologists discovered an iron implant, substituting the right second upper premolar of an adult man. The original tooth stood model for the implant: it fitted well the alveolar wall and was *osseointegrated*. As stressed in former chapter for hydroxyapatite-coated cementless prostheses, 'optimal fit' is the condition *sine qua non* prior to osseointegration [314]. Once more, *we do not discover but uncover!*

But before proceeding to the problems of today, mention should be made of the name of Professor Per-Ingvar Brånemark: born in Sweden in 1929, graduated as orthopedic surgeon at Lund University, started as an Associated Professor at Gothenburg University in 1960, where he was promoted to Professor of Anatomy

J.A. Helsen and Y. Missirlis, *Biomaterials*, Biological and Medical Physics, Biomedical Engineering, DOI 10.1007/978-3-642-12532-4_10,

in 1969. His research represents a key development in osseointegration. The history of this exciting *discipline* is extensively described by McClarence [315].

10.1 Difficulties to "Bridge"

The specifications of materials for support or substitution in and around the mouth are in some aspects similar to those needed in other hard tissue replacements. Specific challenges, however, exist. While endoprosthetic devices are exposed to the homeostatic (homeodynamic) conditions inside the body, materials exposed to food and drinks face more extreme conditions, to name only the subzero degree ice-cream or phosphoric acid present in Coca Cola (pH $\simeq$ 2). Oral problems to *bridge* – an appropriate term in this context – and practices are summarized in the panoramic radiograph of a patient's mouth shown in Fig. 10.1:

- Dental practices
  - No replacement but repair of a damaged surface by filling, conventionally, with amalgam, or today, by organic fillers (a).
  - Substituting a missing tooth by implantation (b).
  - Replacement of missing teeth by bridging between two healthy teeth (c).
  - Bridging a set of implants by bridges or overdentures.
- Problems faced
  - Toxicity and wear of amalgam.
  - Fatigue, strength, mechanical anchoring, improved anchoring by texturing the surface or promotion of ingrowth by bioactive coating of implants, veneering by ceramics or polymers of substructures of alloy or ceramics (cosmetic effects).
  - Idem but, additionally, adhesion of alloy (noble or other) to ceramic.
  - Chemical and electrochemical attack (galvanic couples).

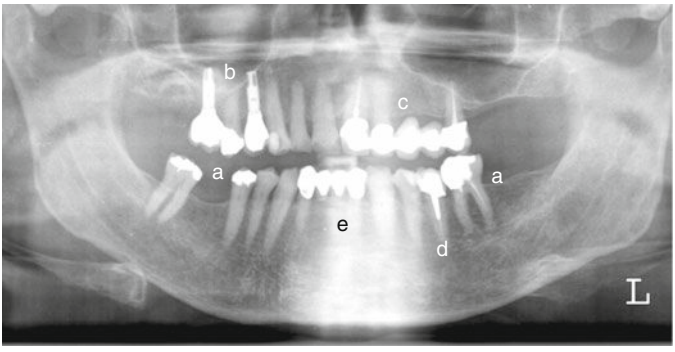

Fig. 10.1 Panoramic radiograph of mouth and jaws: (**a**) amalgam filling; gutta percha canal filling of left tooth, (**b**) Ti-implants (Brænemark), (**c**) AuPtPd-alloy+ceramic, low gold alloy posts, (**d**) post crown (AuPtPd+ceramic), (**e**) idem as c. Explanation see text

10.2 Amalgam

A Special Case

Amalgam entails the introduction of a special class of metals: *intermetallic compounds*. Intermetallic phases consist of two or more types of metal atoms. They are compounds in their own right, whose properties cannot be transformed continuously into those of their constituents by changes of composition alone, an aspect by which an intermetallic compound is distinguished from what currently is understood by the term *alloy*. They display distinct crystalline structures and form species separated by phase boundaries from their metallic components. An intermetallic or an intermetallic composite containing mercury is called *amalgam*. The word has an obscure and uncertain etymological origin, not something to worry the materials' scientist to whom amalgam remains an intriguing product.

Toxic?

In Chap. 4, the toxicity of mercury was abundantly illustrated starting with the historical sensitivity case of Alfred Stock. Mentioned were the three *amalgam wars* around 1840, 1930 and the present day one. The controversies are not less harsh today than hundred and fifty years ago. As usual, the prophets of doom appeal on *Dr.So-and-So* to support their prediction of an apocalyptic disaster.[1] It does not mean, however, that there is no reason for concern but despite all the age-old alarming voices, amalgam survived the former two wars. Will it survive the ongoing war?

Let us look at the facts.

The Facts

We are confronted with mercury as vapor Hg, Hg_2^{2+}, Hg^{2+}, oxides, chlorides (the sparsely soluble Hg_2Cl_2 or calomel and soluble $HgCl_2$), hydroxides and so on. Vapor or solid state oxidation and reactions may transform amalgam mercury into each of these chemical forms by reaction. The long residence time in the body is a consequence of the high affinity of mercury (1) to $-SH^-$ in cysteine and albumin, and (2), to its selenohydryl counterpart. The latter is a part of the important antioxidant *glutathione peroxidase* (see Chap. 4 and [316]). Another common and easily formed compound is monomethylmercury CH_3-Hg^+X^-, X^- being any anion. It is commonly abbreviated to methylmercury or MeHg. The highly covalent bond –C–Hg– is responsible for its stability. Inorganic mercury is less lipophilic than methylmercury and MeHg passes easily through cell membranes.

[1] See f.i. the Internet site 'The Mercury Amalgam scam: How Anti-Amalgamists Swindle People'.

Eley and Cox evaluated in the 1980s extensively in vivo effects of amalgam as well as alleged toxicity or hypersensitivity complaints by patients. Most striking is the accumulation of mercury in the renal cortex of guinea pigs bearing subcutaneously implanted amalgam powder releasing 22 μg Hg/day. Nutritional levels of selenium (0.2 μg/g/day) were sufficient to counteract toxic effects of released Hg. Patients show undoubtedly enhanced levels of Hg during insertion or removal of amalgam. According to these authors, none of the symptoms of the alleged cases of Hg toxicity and hypersensitivity did fit into any pattern of Hg toxicity [317–322]. More nuances, however, are found in a recent Swedish Report according to which evidence is yielded for side effects in the sensitive portion of the population [323]. The lowest exposure, in terms of urinary secretion, that has been found to give rise to a demonstrable toxic effect, is accepted to be 10–25 $\mu g\, l^{-1}$. The report concludes that amalgam is unsuitable for dental restoration but removal of existing fillings should not be an option. In an FDA Hearing, September 6–7, 2006, the same conclusions were drawn but it is admitted that further research is needed. Those who defend the use of amalgam, admit a potential but quantitatively minor risk. Moreover, amalgams are more cost-effective than the alternatives, composite resins, which are reported to incite also problems, the longevity is shorter and costs are finally higher. Mentioned is, for example, the Casa Pia study in 2006 which showed 'that after 5 years the need for additional restorative treatment was approximately 50% higher in the composite group'. Concluding in one direction or another is difficult: how to extrapolate animal experiments to risk for patients, how to detour selection (a problem of statistics: only failed restorations analyzed).

Basically, start and end products of amalgamation are:

$$Ag_3Sn[\gamma] + Hg \rightarrow Ag_2Hg_3[\gamma 1] + Sn_{7-8}Hg[\gamma 2] + Ag_3Sn[\gamma]. \qquad (10.1)$$

Stoichiometric coefficients were omitted, because of the complexity of reactions going on simultaneously and proceeding at different rates. Deficient corrosion resistance promotes $\gamma 2$ to the substance to be avoided. Its presence can be prevented by the addition Ag/Cu particles reducing the end product to the composite $\gamma 1 + Cu_6Sn_5[\eta']$ and is known as HCD $\gamma 2$-free amalgam. A second approach is the addition in the start mixture of $Cu_3Sn[\Sigma]$ resulting in the composite containing the phases $\gamma + \gamma 1 + \eta' + \Sigma$[unreacted] and known as HCSC $\gamma 2$-free amalgam. Typical compositions of alloy powders are 69/12/18/1 (Dispersalloy) and 59/28/13/0 (Tytin), respectively, for the elements Ag/Cu/Sn/Zn; the alloy powders are mixed with mercury, respectively, in a ratio (w/w) of 50/50 or 57.5/42.5. The alloy powders react to intermetallic compounds when dissolving in the liquid mercury. Diffusion is the main rate determining parameter.

Not being an alloy but an intermetallic is an important fact. From the definition of an intermetallic, it is evident that mercury will not display the characteristic of pure liquid mercury: its vapor pressure in amalgam is in the worst case lowered by a thousand times (Table 10.1). The emission from amalgam, experimentally measured and averaged over 24 h, is 0.048 $ng\, cm^2\, s^{-1}$, roughly 4×10^6 times less than for pure mercury.

Table 10.1 Vapor pressure of mercury pure and in amalgam. Partly collected from [324, 325]

	Pressure[a] Pa	Vapor density $\mu g/m^3$
Mercury (pure, 37°C)	2.2×10^{-1}	19
Amalgam		
– as formed	2.4×10^{-6} (8×10^{-7})	0.2 (6×10^{-2})
– abraded	1.0×10^{-4} (1.7×10^{-4})	8.0 (14)

[a]Data obtained by residual gas analysis or, between brackets, by quartz crystal microbalance.

Table 10.2 Mechanical properties of amalgam of γ, $\gamma 1$ and composite [325]

	γ	$\gamma 1$	Composite
Tensile strength (MPa)	170	14	55–69
Compressive strength (MPa)	520		385–440
Elongation (%)	<1		

Shaping is performed while malleable. Setting starts after a few minutes, continuing for days without reaching a true equilibrium state not even after many years. Amazing are the mechanical properties: a high discrepancy between tensile and compressive strengths. It is a composite keeping the middle between the stronger (main) component and the much softer one. Honestly, these properties are after all 'honorable'. The few data in Table 10.2 are reliable at least for the order of magnitude. Numerical data of mechanical properties for amalgam are widely diverging and the same holds for two other important aspects: dimensional changes during setting and wear. Ideally, the dimensional change should be slightly positive to realize a good mechanical fixation, neither too much because provoking damage and pain, nor too small because of bad mechanical anchoring. Part of these phenomena are understood crystallographically but the final result depends on, what we referred to in Chap. 9, the *technical proficiency* of the manufacturer.

According to the principles discussed in Chap. 3, the interface created between cavity wall and amalgam is asking for problems: the formation of an oxygen concentration cell. In general, no dramatic events are happening, a protective tin oxide film prevents rapid progress of corrosion. The anodic polarization curve of low-copper amalgam indicates a breakdown potential of −0.15 V vs. SCE. At potentials more positive than this one the protective oxide/hydroxide film breaks down and the first victim is the $\gamma 2$ phase, really unwelcome company. The high-copper amalgams do not show distinct breakdown potentials and are less prone to corrosion.

Presence of noble metals together with amalgam in the mouth is provoking galvanic corrosion. As explained in Chap. 3, the corrosion potential E_{corr} is a mixed potential of two or more interacting electrochemical couples. The formation of E_{corr} of two metals in permanent direct or low resistance contact is illustrated in Fig. 10.2, which is the semilogarithmic version of Fig. 3.6, called Evans diagram. E_{corr} stabilizes where anodic and cathodic currents intersect. A higher i_{corr} is recorded for M, an amalgam for instance, in contact with gold or platina. The situation is worsened by: the low counter concentration of the metal ions in saliva ($\leq 10^{-6}$M), the presence of complexing ions in saliva (Appendix D) and the often greater surface of the noble

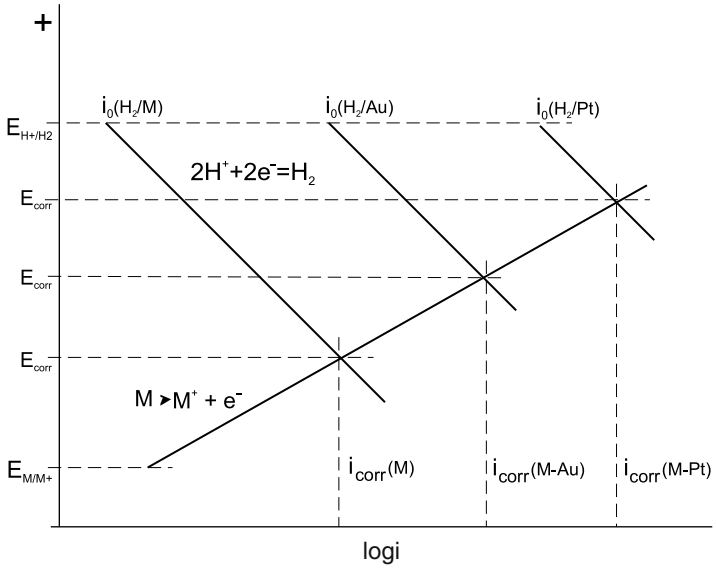

Fig. 10.2 Plot of corrosion potential versus for log (corrosion current) for amalgam-platina and amalgam-Au couples (not on scale)

cathode like Au or Pt (lower current density) versus the smaller anode of amalgam (higher current density). As a matter of fact, enhanced corrosion of amalgam in contact with gold has often been observed. However, contradicting the quotation *Ill fortune seldom comes alone*, a multitude of factors prevents catastrophical propagation of corrosion: small $i_0(O_2)$ of noble metals and consequent high polarization resistance, passivation and re-passivation rate, slow diffusion of oxygen the main oxidizing agent in saliva...

A last comment on Table 10.2. The ratio tensile/compressive strength of the composite is about 1/7, similar to concrete. Sections through amalgam and concrete are remarkably similar. Although the length scale is a thousand times smaller, the time scale is at least of the same order of magnitude. After one and a half century, millions of undeniably successful restorations have been performed but remain subject of acidulous debate. The debate itself, the scientific deficit on their use, their fascinating properties and introduction to intermetallics justified for us this seemingly disproportionately long section.

Further reading: [326, 327].

10.3 Composite Alternatives

Presumably, the last amalgam war will be lost while composite acrylic resins became mature alternatives. With respect to the original nonfilled acrylic resins, maturity was a matter of improved chemical, mechanical and esthetic properties.

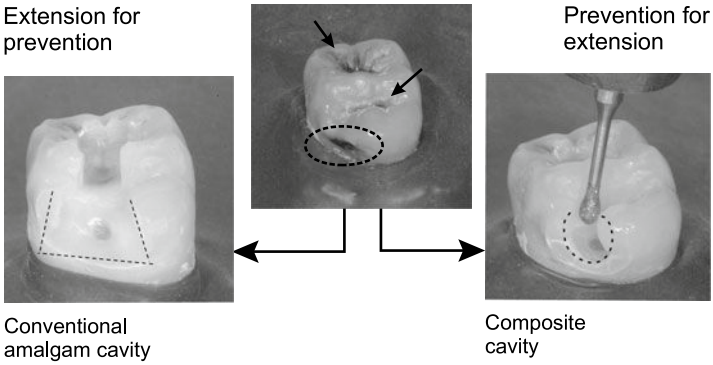

Fig. 10.3 *Center*: tooth with caries (*arrows, ellips*); *left*: preparing for amalgam filling; *right*: preparing for composite filling. By courtesy of K.L.Van Landuyt

The chemistry of polymer substitutes progressed since its first use in 1945. Amalgam is beaten by the war-winning products in three important battles: setting time, adhesion to dentin and enamel and esthetics. The rapid setting of amalgam necessitates overfilling the cavity and 'postsculpturing' by grinding to the right shape. Grinding is named as one of the causes of enhanced mercury contamination risk for the patient as well as for the dentist. No adhesive bonding between amalgam and dentin exists and fixation is realized by making mechanical retention points in the cavity walls: a tooth-unfriendly operation because more dentin has to be removed than just the necrotic part of the caries. Aesthetics, or rather the absence of it, does not need to be commented.

None of these drawbacks with polymer composites. Caries is restored consecutively by minimal (!) cavity preparation, application of adhesive on the cavity walls, filling with the restoration composite and polymerizing. In Fig. 10.3, both preparation techniques are compared. The adhesive is a polymer composite with low percentage of inorganic filler and with low viscosity (more solvent) to assure covalent bonding between adhesive and the dentin lining. The restoration composite with up to 87% inorganic fillers (see below) is wear resistant, has low shrinkage on polymerizing, has a high viscosity so that it is easily modeled to the right shape, has a well-sealed bond with the adhesive and is available in a wide palette of colors. Only when everything is in the right shape follows as last step the polymerizing by irradiation with light... whereupon the patient may walk out of the dentist's cabinet. No, that was a joke. Last corrections and polishing takes quite a bit more time than for amalgam which is one of the reasons why some practitioners prefer amalgam above composite for posterior restorations.

Not all but a whole series of both adhesives and restoration polymers have as repeating unit (<*mer*) acrylic [=CH–] or methacrylic [=C(CH_3)–] acid and its esters. An ester is formed by an acid catalyzed reaction of an organic acid [–COOH] with an alcohol [HO–R]:

$$H_2C = C(CH_3)–COOH + HO–R \rightleftharpoons H_2C = C(CH_3)–CO–O–R + H_2O \quad (10.2)$$

Although slowly, esters are susceptible to hydrolysis, the opposite reaction of esterification, which is one of the potential onsets of in vivo degradation. The ester name is formed by adding the suffix *-ate* to the root of the acid name and is preceded by the nomenclature name of the root of the alcohol molecule (ex.: *methyl*-alcohol): the ester of methacrylic acid with methanol is *methyl methacrylate*, commonly abbreviated as MMA. If the alcohol is *ethyleneglycol* [HO–CH_2–CH_2–OH], the ester is *2-hydroxyethyl methacrylate* [H_2C=C(CH_3)–CO–O–CH_2–CH_2–OH], abbreviated as HEMA. One end is [(CH_2)=C–] and the anchoring point for polymerization, the other end consists of polar groups. These compounds constitute a first group of participants. The common abbreviations of monomers listed in the documents of manufacturers of adhesives and restoration composites are collated in Table 10.3.

A second group, basic constituents of adhesives, consists of functional monomers whose function is:

Table 10.3 A list of methacrylate monomers used by manufacturers of adhesives and restoration composites: (*) those typically used in adhesives, † cross-linking monomers, ‡ cross-linking having also functional groups

Abbreviation	Nomenclature name
AMPS*	2-acrylamido-2-methyl-1-propanesulfonic acid
DEMA	decandiol dimethacrylate
di-hema P‡	di-HEMA phosphate
DMA	dimethacrylate
EAEPA*	ethyl2-[4-(dihydroxyphosphoryl)-2-oxalobutyl]acrylate
EGDMA	ethyleneglycol dimethacrylate
bis-EMA_6†	bisphenol A polyethylene glycol diether dimethacrylate
bis-GMA†	bisphenol A diglycydyl ether dimethacrylate
HEDMA	hydroethyl dimethacrylate
HEMA*	2-hydroxyethyl methacrylate
HEMA-P*	HEMA-phosphate
MA*	methacrylic acid
MAC-10*	11-mmemthacryloyloxy-1,1-undecanedicarboxylic acid
4-MET*	4-methacryloxyethyltrimellitic acid
10-MDP*	10-methacryloyloxydecyl dihydrogenphosphate
MDPB	methacryloylodecylpyridinium bromide
MMA*	methyl methacrylate
MMEP	mono-2-methacryloyloyethyl phthalate
5-NMSA*	N-methacryloyl-5-aminosalicylic acid
NPG-GMA*	N-phenylglycine glycidyl methacrylate
NTG-GMA*	N-tolylglycine-glycidyl methacrylate
PENTA*‡	dipentaerythritol pentacrylate monophosphate
Phenyl-P*	2-(methacrylaloyloxyethyl)phenyl hydrogenphosphate
TEGDMA†	triethyleneglycol dimethacrylate
UDMA†	urethane dimethacrylate

- *Wetting and diluting:* MMA, HEMA.
- *Wetting and demineralizing:* MA, sulfonic acid [–SO_3H] (AMPS), phosphate [–O–PO_3H] (Phenyl-P, HEMA-phosphate, 10-MDP), phosphonate [–PO_3H] (EAEPA, MAEPA), carboxyl [–COOH] (MA, 4-MET, 4-AET, MMEP, 5-NMSA);
- *Co-initiators:* tertiary amines [–N¡](NPG-GMA, NTG-GMA, DMAEMA);
- *Antibacterial fluoride:* [–F] or bromide [–Br] (MDPB).

The difference between a phosphonate and phosphate group is shown below in Fig. 10.7. EAEPA is the simplest representative of a monomer with phosphonate as functional group.

The purpose of a third group of monomers is *cross-linking*. They all have at least two end-standing methacryl groups. Its simplest member is EGDMA but PENTA as five $CH_2{=}CH_2(CH_3)$–CO– groups plus phosphate as functional group, say a true 'social networker'! The result after polymerization is a densely branched network held together by strong covalent bonds.

The presence of oxygen and nitrogen is allowing also hydrogen bonding. A hydrogen, bonded to a more electronegative atom like oxygen, nitrogen or fluorine, can be 'shared' with another electronegative atom [=N–H···O=C–]; one atom is the hydrogen bond acceptor, the other the donor. The sharing happens within a molecule (*intramolecular*) or between molecules (*intermolecular*). Intermolecular bonding is making the polymer network more rigid. The most exquisite example of hydrogen bonding happens in water [H–O–H· · ·O–H], increasing the boiling point of such a low mass molecule to an amazing 100°C! Example of a typical cross-linker is the double-headed 'Janus' molecule, *triethylene glycol dimethacrylate* (TEGDMA) as shown in Fig. 10.4.

The molecule has two end-standing methacrylate groups separated by three ethylene glycol units CH_2OH–CH_2OH.

A fourth group combines cross-linking capability with one or more functional groups. A simple representative of this group is di-HEMA phosphate with two polymerizing anchor groups (methacrylate) bound together by the functional phosphate group as shown in Fig. 10.5.

10.3.1 Adhesives

The key to a well-adhering restoration composite is the adhesive. The process consists of three distinct steps: conditioning of the cavity wall(1), covering the wall

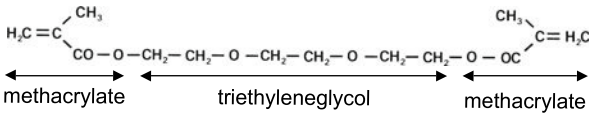

Fig. 10.4 The cross-linking molecule triethylene glycol dimethacrylate (TEGDMA)

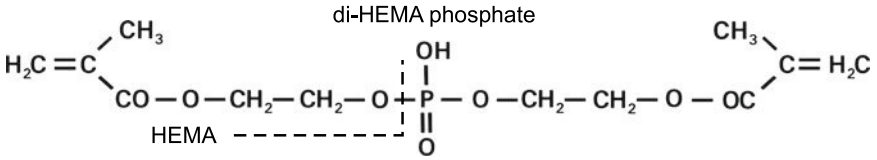

Fig. 10.5 The cross-linking molecule di-HEMA phosphate. 2-hydroxyethyl methacrylate (HEMA) is the part left of the dashed line and the right half substituted by hydrogen –H

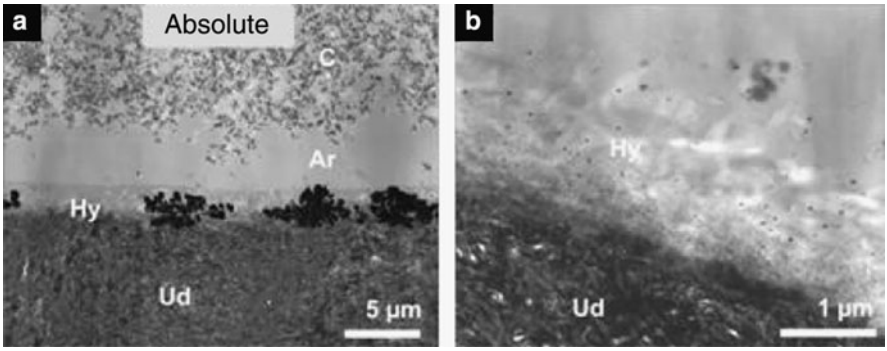

Fig. 10.6 TEM micrograph of a moderately strong self-etch-adhesive. *Left*: overview of a restorative composite (C) bonded to dentin (Ud: unaffected dentin) with as intermediates the hybrid layer (Hy) and the adhesive resin (Ar); (**b**) detail of the hybrid layer. The dark conglomerates in (**a**) result from silver infiltration but not discussed any further in the present context. The filler particles in C can be clearly distinguished. By courtesy of K.L. Van Landuyt [328]

with a hydrophilic monomer(2) with on top the adhesive(3). To make a long story short, we selected, out of a mishmash of possible procedures, one modern *self-etch adhesive*, a one-step procedure, combining the *surface conditioning* (the first step in 3-step procedures by etching with phosphoric acid), the *priming* (second step with monomethacrylate+initiator+inhibitor) and the *adhesive* (third step with a mixture of methacrylates, initiator, inhibitor and filler).

Etching demineralizes the surface by extraction of calcium from the mineral phase, mainly hydroxyapatite and carbonate and is freeing the collagen bundles of dentin (typically collagen type I). The hydrophilic monomers with viscosity similar to water act as wetting agents and diluting solvents (MMA, HEMA). They diffuse into the wetted zone to form a hybrid transition layer, clearly shown at low and high magnification in Fig. 10.6.

Derivatives of these basic components are monomers whose main function is demineralization. Another example is *10-methacryloylodecyl dihydrogeniumphosphate* (10-MDP) with at one end the methacryl group and at the other end a phosphate group as shown in Fig. 10.7.

The end groups in 10-MDP are separated by an alkyl chain of ten methyl groups, called *spacer groups*. Because spacers modify the interaction between the end groups and the flexibility of the molecule, they co-determine the over all properties of the monomer as well as of the polymer!

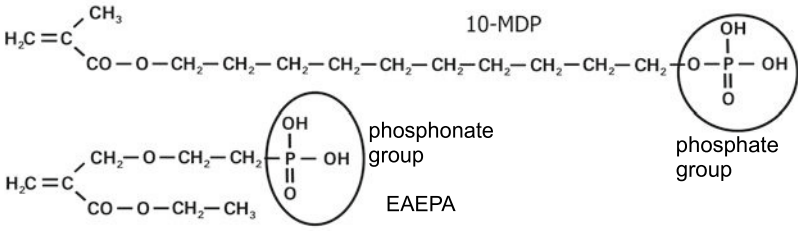

Fig. 10.7 Difference of phosphate and phosphonate end groups in 10-MDP and EAEPA

In situ Curing by Irradiation with Light

So far were presented the building stones but the crowning glory is polymerization, a process that can be performed chemically, the rule for bone cements and in dentistry where metal of ceramic parts prohibit the transmission of light (see Chap. 11). In most other cases, light curing is the usual practice. As said above, polymerization starts when the acryl monomer meets a molecule bearing a *radical*. The reaction is called *free radical* or *addition polymerization*.

A radical atom has an unpaired electron and is symbolized as [–C·]. The polymerization *propagates* because the unpaired electron is transferred to the central carbon atom of the acryl ester which in turn links by the same mechanism to another monomer. When two radicals meet, the propagation stops by a process called *termination by transfer* or *disproportionation*. The polymerization sequence for acrylic monomers is represented in Fig. 10.8. Termination happens randomly resulting in polymer chains with a distribution of chain lengths. Addition polymerization leads in general to more homogeneous chain lengths, hence with a narrower distribution than other mechanisms.

But what is the 'initiation rite' for the first radical?

Formation of a radical is not a spontaneous process, so we need a source of energy and an acceptor, named an *initiator*. For the time being, the main initiator candidate is *camphorquinone*; the energy source is visible light.

Initiation by this molecule is effective but at low rate. Therefore, booster molecules such as amines are added to accelerate the reaction. Examples are: *methylethylenediamine* (aliphatic) or *N-phenylglycine* (aromatic). The reactions are schematized in Fig. 10.8.[2] Irradiation is performed by halogen light filtered around a wavelength of 470 nm, a standard for that purpose although Light Emitting Diodes (LED), emitting a narrower wavelength band near 470 nm, will gradually substitute the halogen sources.

Camphorquinone is yellowish and is by some manufacturers partially substituted by *1-phenyl-1,2propanedione*. This initiator is only slightly yellow, which eases

[2] For an in-depth description of the mechanisms, see Jakubiak and colleagues [329].

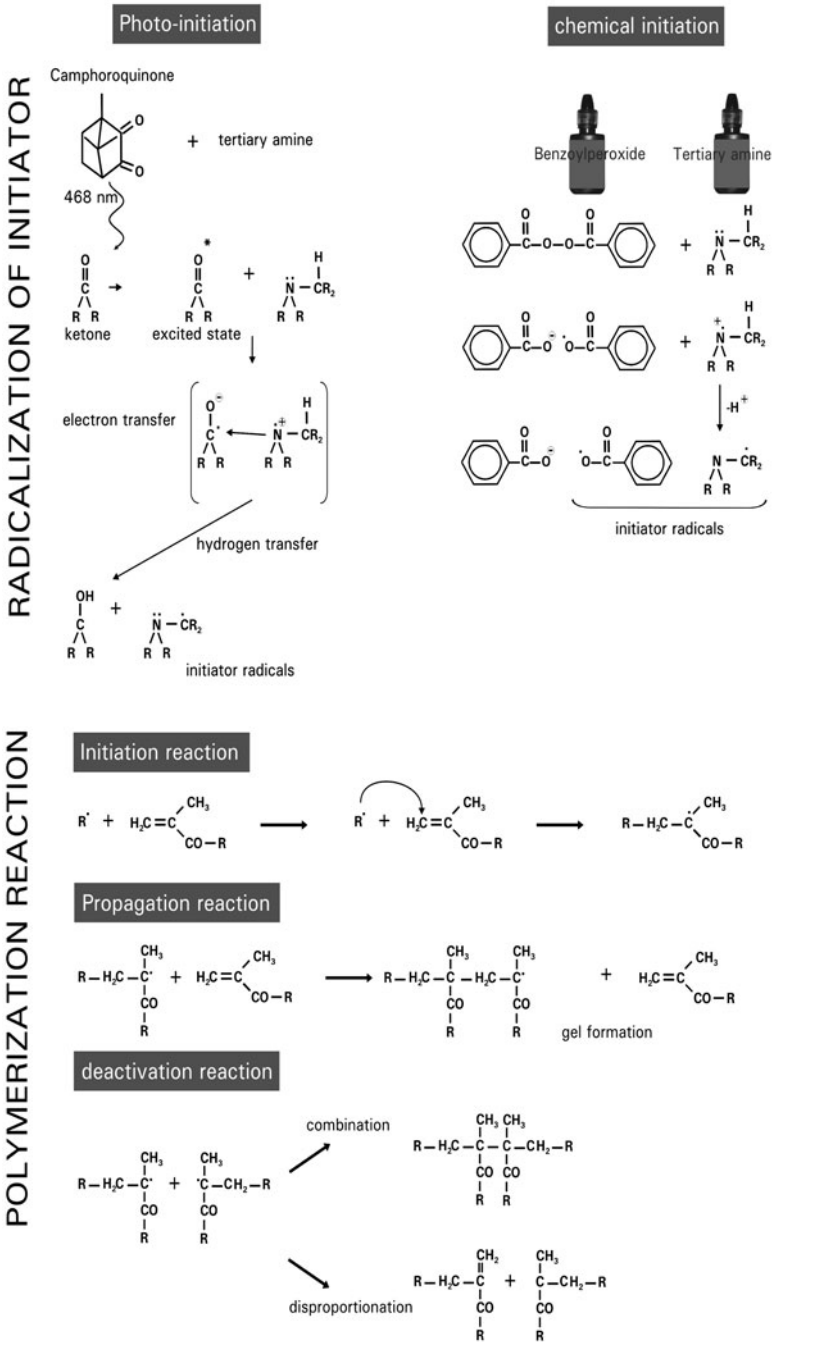

Fig. 10.8 Initiation by camphorquinone and teriary amines; a polymerization reaction scheme for methacrylates. Termination of the polymerization by combination (transfer) or disproportionation. The latter involves a hydrogen transfer leading to the formation of a saturated and an unsaturated chain. By courtesy of K.L. Van Landuyt [328]

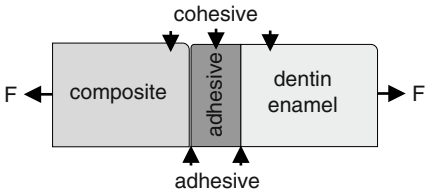

Fig. 10.9 Sites of potential failure in the system enamel or dentin-adhesive-composite resin

modern color matching of the restorative composite, yielding for the modern trend of bleaching.

Performance of Bonding

The mechanical performance of bonding can be determined using standard micro-tensile equipment. For excellent bonding, failure will happen cohesively in dentin (or enamel) or in the composite resin; the interfaces are the failure sites for less performing adhesives (Fig. 10.9). Typical bond strengths to enamel are 32 ± 8 MPa and 38 ± 8 MPa to dentin (for Optibond FL) but performance is widely differing from one manufacturer to another [328].

10.3.2 Restorative Composites

While the function of adhesive resins is to serve as 'go-between', the restorative counterpart faces mastication forces, severe temperature gradients and chemical aggression (ice-cream, coca-cola!) and should be color stable. The monomers cited in Table 10.3 form the backbone of the resin part but details 'making the difference' are not released by the manufacturers. New low-shrinkage composites are reported with zero water solubility, low water sorption, shrinkage $<1.3\%$ and $-C = C-$ conversion of $>70\%$.[3]

Resins

Ceramic Fillers

Mechanical properties of the resin were substantially improved by addition of a ceramic filler. Loading such a complex system is an example of a nonlinear dynamic

[3] See Dental Polymers Poster II of IADR/AADR/CADR 87th General Session and Exhibition, April 1–4, 2009.

Table 10.4 Composite micro-filled and micro-hybrid resins compared to PMMA, enamel and dentin

	Units	PMMA	μ-filled	μ-hybrid	E[a]	D[a]
			Filler			
Size	μm		0.01–0.12 0.02–0.75[b]	0.01–3.0		
Content	vol%		30–55	60–70		
			Mechanical properties			
Exp.coeff.	$°C.10^{-6}$		50–68	20–40		
Hardness[c]	$kg.mm^{-2}$		20–36	50–80	$\simeq$350	68
Tensile strength	MPa	70	225–300	200–350	384	294
Compressive strength	MPa	76	25–35	35–60	10	52
E	GPa	2.9–3.3	3–5	7–14	84	19
Shrinkage	%		2–3	1–1.7		
			Clinical properties			
Appearance			$\simeq$enamel	good gloss		
Polishable			high	good		

[a] E:enamel; D:dentin.
[b] Nanocomposite: particle size <0.03 μm. Allows more esthetic restorations.
[c] Knoop hardness.

system, where *the whole is more than the sum of its parts*, a paradigma of the physics of complex systems. No doubt that strength and modulus as shown in the general overview of Table 10.4 are satisfactory, but also fracture toughness K_{IC} increases from a mere 0.8–1.4 to 1.9 MPa $m^{1/2}$, respectively, for 0,28 and 53 vol% of filler. Notice that the degree of filling is preferentially expressed in vol%; weight percent is often misleading because properties of *Micro-filled resins* consist of ground polymer particles, inorganic filler particles either ytterbium trifluoride (YbF_3 with particle size of 40–200 nm) or zirconia (ZrO_2), titanium dioxide (TiO_2), silica (SiO_2) and a resin matrix filled with colloidal silica. *Micro-hybrid*, on the contrary, has a resin matrix filled with silica particles, occasionally down to nano-sized particles, and silane-coated silica or glass with more efficient bonding between matrix and particle.[4]

Wear is a multi-facetted phenomenon and difficult to put a number on. Decreasing the size of the filler particles improves wear resistance (what gives way to the use of nanoparticles) and, not immediately obvious, filler particles softer than enamel exhibits improved wear resistance. Energy generated during mastication is thought to be better dissipated over the resin volume by softer than by harder particles.

Obvious modern descendants of microhybrids and microfills are *nanohybrids* and *nanofills*. Nanohybrids are filled with combinations of silica and Ba–B–F–Al silicate

[4] Silane, the silicon equivalent of methane, is SiH_4 or more in general Si_nH_{2n+2}. The organosilanes are widely used in adhesive chemicals and surface modifiers.

glass, occasionally plus TiO_2, or silica with glass ceramic, or a prepolymer, silica and barium glass, all with particle size <100 nm. The presence of barium, titanium, zirconium or ytterbium renders the composite radiopaque. A nanofilled member of the family should be paid special attention, not because of any connection with the manufacturer but because part of the filler consists of a somewhat new class of particles: nanoclusters. A product that gets particularly high scores in many respects, has a total filler content 79 wt% or 59.5 vol%, subdivided in 8 wt% silica nanoparticles with a size range of 5–20 nm and 71 wt% zirconia/silica clusters 0.6–1.4 wt%. Silane-coated individual 50 nm silica particles are still dispersed in the resin matrix but accompanied by nanoclusters incorporating silica and zirconia nanoparticles, infiltrated and coated by silane. *Nanocluster* refers to the inclusion of nanoparticles but is in a certain sense a misnomer because the cluster itself is micrometer sized. The significantly increased biaxial flexural strength (∼180 MPa) and Weibull modulus (>10) is pointing to the fact that the clusters do not act as defect centers (crack initiators) but as said before, dissipate more efficiently the mastication energy.

All that Glitters Is not Gold

Is it nothing but peace in the postamalgam scenery? No. The greatest obstacle to absolute victory of composite fillings is the technique-sensitivity, it still remains the time-consuming procedure and clinical studies remain vague about the longevity of the fillings. The monomers exhibit systemic toxicity, although the incidence is low and the long-term effects are unknown.

The data of this section were preponderately collected from references [329–333] and in particular from the comprehensive text on adhesives by Kirsten Van Landuyt [328].

10.4 Orthodontics

Did the radiograph of Fig. 10.1 belong to a teenage girl with a nonstarlike set of teeth, orthodontic wiring would have been the prominent feature of the panorama. A wire is wrapped around the teeth bow and tightened to force teeth in the desired position. The allowed stress is constrained to a level by which the patient is still feeling comfortable. The stress decreases by gradual repositioning of the teeth and to continue repositioning, the wire has to be re-tightened, in case of, say, a stainless steel wire, after a relatively short period of time. That is easily understood by analyzing the stress–strain behavior of a steel wire, curve c in Fig. 10.10. The stress should of course remain below the yield stress provoking a strain <0.2%. Curve c represents the initial portion of a stress–strain curve for an ordinary steel. The energy stored is proportional (not equal) to the area enclosed by the curve and the boundaries of strain. Indeed not super that area as the reader will remark... but another

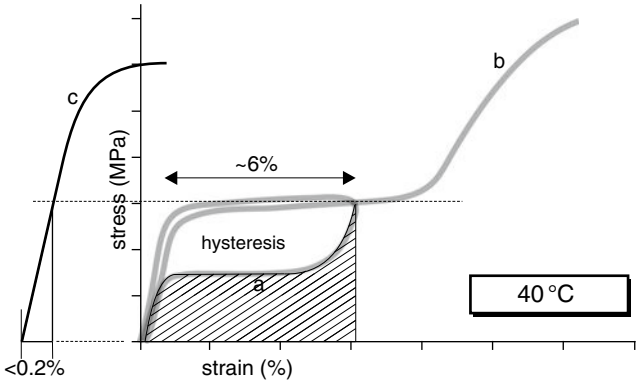

Fig. 10.10 Stress–strain behavior of nitinol with a pseudoelastic plateau over about 6% of strain (in bold registered curves). Curve c is shifted to the left for clarity

classmate of intermetallics is offering an intelligent medication, one endowed with three special properties *shape memory* effect, *superelasticity* and *high damping*.

Nitinol

The discussion hereafter will be limited to one member of the class: a *nickel-titanium intermetallic* (NiTi). Austenite, also called parent or β-phase, is undergoing a *displacive, shear-like transformation* to martensite either by cooling below a critical temperature or isothermally by applying stress (*stress-induced martensite* (SIM)). Displacive transformation is the key notion here. Atomic rearrangements over only interatomic distances are required for the austenite to martensite transition, which explains the high transformation rates. In diffusion-controlled transformations on the contrary, atoms have to travel over distances of $1–10^6$ interatomic spacings, which is considerably slowing down a transformation process. We met martensite transformation earlier in Chap. 2 and similar transformations for zirconia in Chap. 9. A most common composition is nickel 55 and titanium 45%w/w.

Back now to Fig. 10.10. If a NiTi wire is loaded with stress comparable to the steel wire, only a minimal increase of stress (upper branch of curve a) provokes an increase of strain in some cases to over 6%. Removal of stress makes the wire returning to zero strain (lower branch). In between loading and unloading a *hysteresis* is present, the area of which is proportional to dissipated energy. The area below the lower branch of the curve and the 0 to 6% strain boundary is proportional to the energy stored. This one is considerably greater than in the steel wire case, thus the efficient remedy to frequent re-tightening of archwires. Stress above the plateau value, when the parent phase is completely converted into martensite, follows a conventional stress–strain relationship till fracture (curve b). Reversible elastic deformation of the size shown in Fig. 10.10 is expected for polymers rather than for metals but both types of elasticity are basically different. The

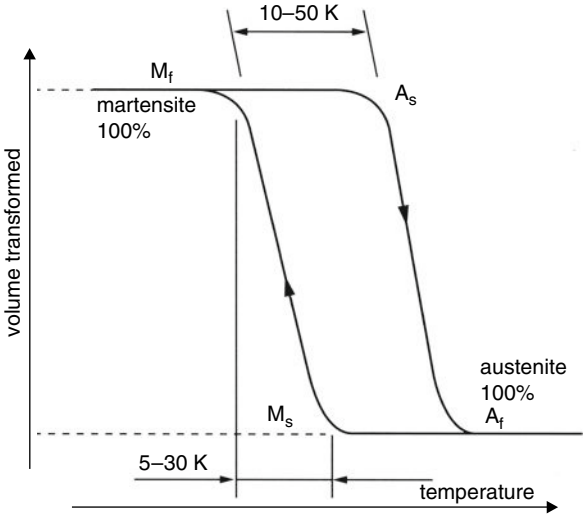

Fig. 10.11 Volume transformed of nitinol as function of temperature

apparent elasticity of NiTi is possible through crystallographic exchange between two phases of different volume for the same number of atoms. For this reason, the phenomenon is qualified by the term *pseudoelasticity*. Orthodontic wires are an obvious application of pseudoelasticitiy.

A few words about Shape Memory Effect (SME), another biomedically exploitable characteristic of a group qualified as Shape Memory Alloys (SMA). NiTi is a member of this group and till present the most widely used in biomedical devices. The martensite induction is activated by change of temperature as shown in Fig. 10.11. The transformation is characterized by four temperatures: M_s martensite start and M_f martensite finish temperature, A_s start of reverse transformation and A_f finish of reverse transformation of martensite. The temperatures at which it all happens for SM as well as for pseudoelastic behavior depend on composition and thermomechanical processing.

When a spring shaped wire is stretched at a temperature below M_f, it will return to its original shape when heated at a temperature above A_f but will not return to the stretched state when cooled below M_f: the *one-way SME*. With appropriate training, ignoring here the crystallographic background, two shapes can be memorized: one shape existing below M_f and the second above A_f. The process can be repeated indefinitely provided strain levels and temperatures are not exceeding certain limits (twice the pseudoelastic strain domain, some tens of degrees above A_f). NiTi staples for immobilizing bone fractures are a good example of a one-way SME. The staples remember the former closed shape and tighten at body temperature, thus compressing the matching parts of the fracture. Another orthodontic application is shown in Fig. 10.12, a spring which closes at body temperature.

Fig. 10.12 Body heat activated NiTi superelastic spring, exerting nearly constant force (Sentalloy, Dentsply Int.)

NiTi contains nickel and its presence always elicits suspicion. In a paper by Lijima et al., galvanic corrosion is described of the following couples: 304-NiTi, 304-Elgiloy, 304-β-Ti, Ti-NiTi, Ti-CoCr, Ti-304 and Ti-β-Ti [334,335]. A few conclusions of this work are worth to be reproduced here. The combinations of alloys were coupled in NaCl 0.9%. In all couples, the galvanic current decreased with time and becomes nearly constant after 24 h. The coupling SS304 with NiTi is unfavorable because the galvanic current density is 10 times higher than for other couples. An odd result is obtained for the couple Ti–NiTi. Initially, Ti was the anode and corroded but that reversed after 1 h or so and NiTi got corroded. At the start, the electrode potential of Ti was less than that of NiTi but that reversed after about 1 h: NiTi became the anode. An XPS study (X-ray Photo-electron Spectrometry) revealed that the subsurface layer of NiTi was rich in Ni and depleted in Ti. The growing oxide film needed Ti which diffused to the surface enriching the subsurface in nickel. These results may be somewhat premature and not the end of the discussion but clinicians should remain alert, when they treat patients sensitive to nickel. By the way, we never fully trusted NiTi in a biomedical environment.

We are not aware of biomedical devices in which damping, the third characteristic of SMAs, is the leading actor. However, it is something to keep in mind because the Specific Damping Capacity (SDC) of typical SMAs is in excess of 40% (percentage of energy dissipated as heat), a value close to hard rubber (application in scaffolds?).

An increasing number of medical devices are developed utilizing one- or two-way SME or pseudoelasticity in orthopedics, dentistry, vascular and prostatic stents, micro-actuators, etc. and instruments.

Nitinols are offered on the market in a range of mechanical properties, some are summarized in Table 10.5.

Other Alloys

Two classes of titanium alloys are used for archwires: NiTi discussed above and a β-titanium.

Beta-titanium. TMA (Ormco,Sybron) is β-titanium orthodontic alloy; some basic properties were shortly reviewed in Sect. 2.2.3. The major elements are molybdenum

Table 10.5 Some properties of NiTi SMA. Gathered from [336] and Johnson Matthey Medical

Property	Unit	Value
E (austenite)	GPa	∼90
YS (austenite)	MPa	195–690
YS (martensite)	MPa	70–140
UTS (martensite)	MPa	800–1,000
Fatigue strength ($N = 10^6$)	MPa	350
Hysteresis	°C	5–50
Maximum one-way memory	%	8
Normal two-way memory	%	1.2
Normal working stress	MPa	100–130
Superelastic strain	%	6–8
Superelastic energy storage	J g^{-1}	6.5
Maximum recovery stress	MPa	600–900
Work output	J g^{-1}	4
Corrosion resistance		Excellent
Biological compatibility		Excellent

Table 10.6 Flexural and tensile properties of β-Ti from 12 and SS archwires from 10 different manufacturers; averaged and rounded values

	Units	β-Ti	SS
Flexural E modulus	GPa	80	170
Tensile E modulus	GPa	70	170
YS	MPa	1,140	1,750
Spring back (YS/E)	$\times 10^{-3}$	13	10
UTS	MPa	1,150	2,060
Strain at fracture	%	3.5	2.0

(11.3%w/w), zirconium (6.6%), tin (4.3%) and titanium being the balance. Molybdenum stabilizes the β-phase, zirconium and tin increase strength and hardness without, however, allowing the formation of the embrittling ω-phase. A true particularity of the β-alloy is its unusual mix of a low E modulus centered around 65 MPa and high YS of about 200 MPa. That compares in particular for endoprosthetic use favorably with tempered stainless steel and CoCr with values centered around 200 GPa for E and >1,000 MPa for YS. Moreover, they are nickel-free, which is another attractive aspect of these alloys. See also the discussion in Sect. 2.2.3 of Chap. 2 on β-alloys and the formation of oxide layers [59]. In Table 10.6, a comparison is made of the flexural and tensile properties of two groups of wires from different manufacturers, 12 for β-Ti and 10 for SS. The intragroup variability is narrow, so the values, calculated from data of a paper by Verstrynge, were averaged and rounded [337].

The higher the ductility, the higher the allowed plastic deformation before fracture. Rematitan, a nitinol, showed the highest ductility with a strain at fracture of 5.2%. The YS is below average (848 MPa). The highest ranked strain at fracture

for SS wire is 3.7 for a YS of 1,556 MPa%. All surfaces after fracture showed the typical aspects of ductile fracture (see Chap. 2).

Stainless steel. Both 302 and 304 are used and are very similar. Properties and composition are tabulated in Tables 2.3 and 2.4. Most values in these tables refer to the annealed state. Archwires are tempered and have a YS > 1,000 MPa, even as high as 1,700 MPa. They represent the cheapest version of archwires. Here too we have to refer to caveat's formulated for these alloys in Chaps. 2 and 3. Daems et al. characterized a fairly large number of as-received and explanted archwires. Manufacturing processes introduced surface irregularities, which led to crevice corrosion. Moreover, surface stresses as a consequence of bending or grooves caused by orthodontic pliers as well as bracket-wire-contacting surfaces, wear and surfaces coated with plaque were potential nuclei of corrosion [338]. The importance of finish of a device with respect to corrosion or fracture (polishing, rounded corners; , . . .) is not different from what has been said about orthopedic implants.

Cobalt–chromium-nickel alloy. Elgiloy from the homonymic manufacturer Elgiloy Speciality Metals or Phynox (Matthey SA) seems to be the commonly used alloy. It is not liked for endoprosthetic uses because of its high nickel content but is otherwise a superalloy. The composition in %w/w from manufacturer's data (*Elgiloy) is: 19–21%Cr, 15–16Ni%, 15.8%Fe*, 6.5–7.5%Mo, 1.5–2.0%Mn, ∼1.2%Si, ∼0.15%C, ∼0.015%P and S and ∼0.001%Be (0.04%Be*), Co being the balance. The designation is CoCr20Ni16Mo7. It is an austenitic cobalt-based alloy that is strengthened by cold work and capable of hardening by aging. The properties of CoCr20Ni16Mo7 is extremely sensitive to its mechanical and thermal history. About 40% cold worked doubles the Vickers hardness (HV_1) from 200 to 400 MPa. The YS of 400 MPa increases to 1,000 MPa for a 20% cold worked sample. The difference between 20% cold worked and 20% cold worked + hardened (520°C, 3 h) is of the order of 100 MPa. The modification of properties by thermal aging is a result of the formation of intermetallic compounds. The manufacturers offer wires in different (color-coded) tempers: soft, ductile, semiresilient and resilient. A soft wire can be shaped and then heat-treated to provide the required resilience. It is nonmagnetic. The resistance to corrosion, superior to all other stainless steels, together with passivity in contact with tissue completes the picture of excellence. However, clinicians should remain aware of the risk of nickel allergy and a beryllium-free alloy might be the alloy of preference, because of the recognized mutagenicity and cancerogenicity of this element.

A short comment on the notion springback, a notion which is used in orthodontics. It is derived from known mechanical parameters discussed on many occasions throughout this book. The springback of an archwire is expressed as YS/E and ranges from 0.0045 to 0.0099 and represents the amount of elastic strain during unloading but only for alloys with a linear stress–strain behavior below YS (NiTi behave nonlinearly in this respect).

Further reading: [35, 333, 339].

10.5 Implants

The (Braenemark) implant in the radiograph of Fig. 10.1 is pure titanium or a titanium alloy (Ti6Al4V). Years ago, a hydroxyapatite-coated implant was the blessing from above for ingrowth but practice learned that good old titanium surfaces did the job just as well. Titanium and its alloys are no strangers and their properties were discussed in former chapters and they are not different in a dental context.

10.6 Ceramics

Good looking and latest fashion was not the first concern for endoprosthetic materials. Not so in dentistry. Gold crowns were a quality as well as a fashion product. Ceramic teeth with natural look, similar in color and luster to the remaining teeth are the rule nowadays. Will next fashion be patients asking colors adapted to their tatoos? Strength of a single tooth or bridges remain, however, the main concern for most people, a quality that is offered by fabrics in noble metals, CoCr alloys, metal supported ceramics or pure ceramics. The finishing touch is given by porcelain veneering the structure with luster, color and color gradient. The main heavy duty ceramics are alumina and zirconia and were under scrutiny in Chap. 9. Both are in use in dentistry but our attention in this section will be focused on the very successful zirconia. Although the pursuit of innovation is not ebbing away, exact fit, necessitating custom manufacturing, is becoming a major concern. Modern shaping techniques are offering economically feasible solutions, a taste of which was already presented in Chap. 7. In the short *slide show* of Fig. 10.13, key moments are presented of a zirconia bow manufacturing, bridging seven implants similar to those shown in Fig. 10.1.

(a) Abutments(1) are mounted on each oral implant and these are embedded in an acrylic replica(1) of the teeth, details of this technique being not relevant here.
(b) The outer dimension of the teeth on the replica is reduced as shown by the black space between acrylic replica(1) and original wax-up(2). This is done to give space to the finishing porcelain layer.
(c) The final acrylic replica. The surface is smoothed, an important action because sharp edges are potential onsets of fracture.
(d) The next step is digitalizing the replica by a precision measurement of the contours.
(e) The virtual blank of (c).
(f) The virtual blank is machined by CAD/CAM systems out of a Y-TZP bloc (remember from Chapter 9: Yttria-stabilized Tetragonal Zirconia Polycrystals). At least three varieties of Y-TZP are available with the same chemical composition but differing in strength and translucency, according to the powder type used and the production history. The blocs are presintered to allow easy machining (<green machining approach). An alternative is densifying the powder

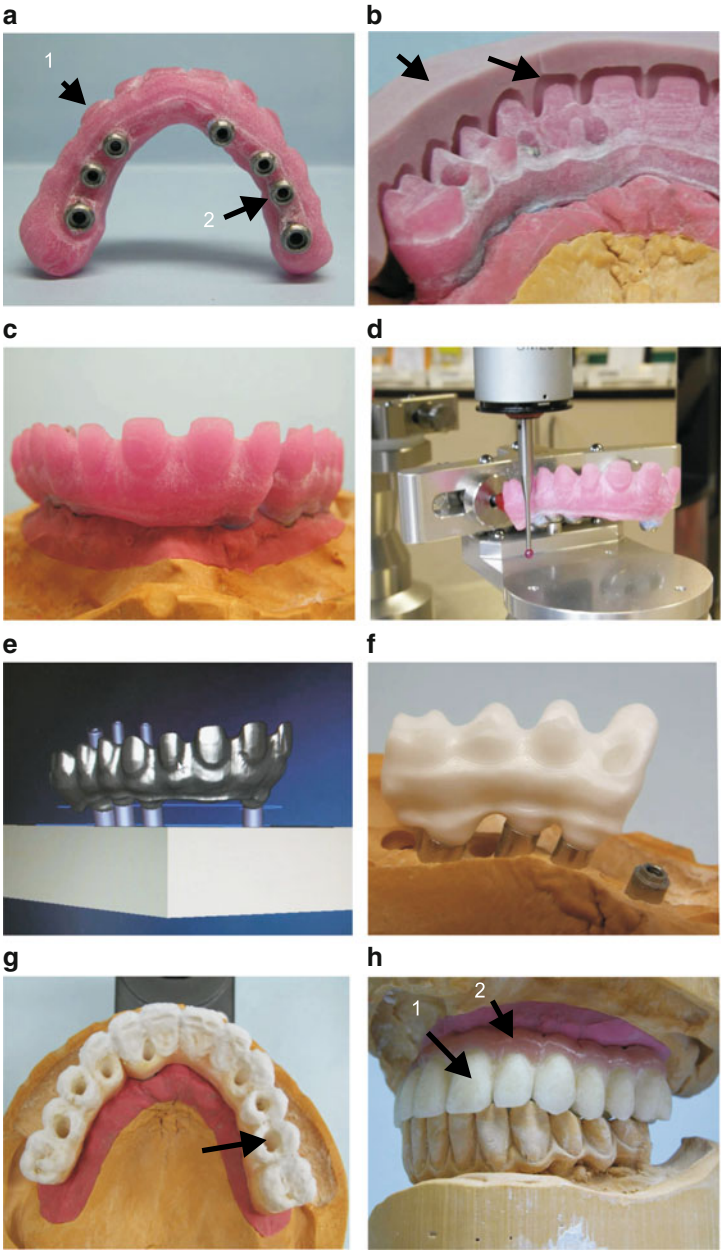

Fig. 10.13 Manufacturing process of ceramic fixed prosthesis (product: Nobel Biocare-Procera). For comments, see text. Courtesy: J.B. Beckers, UNI-DENT (Leuven, Belgium)

by hipping (Hot Isostatic Pressing), allowing to gain something like 20% in strength but is time consuming, more costly and more demanding of the milling instruments than green machining. After milling, it is sintered pressureless at temperatures of 1,350–1,500°C. The next processing step is the application of the porcelain layer. The two shoulders below the teeth are additional mechanical supports for the porcelain layer: they are stress borders to the mastication loads. A clue to the mechanical compatibility of porcelain layer and framework is a thermal expansion coefficient lower than the framework material. Ceramic materials do not like to be stressed: they have low tensile strengths.

(g) The finished bridge. Through the holes (arrow), the fixed prosthesis is secured by screws to the implants. The holes are filled with guttapercha and finished with a cosmetic composite.

(h) The porcelain is fashioning the zirconia into naturally looking teeth(1) with a gradient in color toward the mucosa(2). The contrast on the picture has been blown up for demonstrating the available color palette.

Mentioned sub(g) was gutta percha, one of the natural products, a polymer in this case, still in use in dentistry. It is produced from the milky colloidal suspension (latex) tapped from a tree Isonandra gutta (Family Sapotaceae, Order Ebenales). The main chemical component is trans-1,4-polyisoprene, is bioinert, resilient and thermoplastic. Natural rubber is a similar product, also produced from a milky colloidal suspension but tapped from Hevea brasiliensis (Family Euphorbiaceae, Order Euphorbiales) with main component cis-1,4-polyisoprene. Gutta percha is exclusively used to obturate root canals or as described in sub (c). After slight warming, it is applied by a sealer or, after warming to ca. 70°C, by injection depending on the manufacturer. The commercial product contains zinc oxide as filler (33–61.5%). Almost no allergic reactions on gutta percha are reported in the current literature.

10.7 Calcium Phosphates

Phosphates are, say, part of life and considering their 'spectrum' of solubilities and kinetics of consolidation, no wonder that phosphates were candidates for 'biocements': calciumphosphate cements (CPBCs). In Table 10.7 are summarized the biorelevant phosphates together with their specific Ca/P ratio, nomenclature name, mineral name and the logarithm of the thermodynamic solubility product K_{sp}. The ionic product *IP* of a supersaturated solution with ions suitable for precipitating, for example, HAP is calculated by equation:

$$IP = [\mathrm{Ca}^{2+}]^{10}[\mathrm{PO}_4^{3-}]^6[\mathrm{OH}^-]^2\gamma_1^2\gamma_2^{10}\gamma_3^6. \tag{10.3}$$

The molar concentrations are enclosed in square brackets and γ_n represents the activity coefficients. The equilibrium depends strongly on pH for at least two reasons: the presence of OH^- is one factor, and the other is PO_4^{3-}. The latter is the 'naked' anion of H_3PO_4 whose first acid function is strong, the second is weak

Table 10.7 Calcium phosphate phases. Data collated from [340, 341]

Notation	Formula	Ca/P	log K_{sp} mol L^{-1}
MCPM	$Ca(H_2PO_4)_2.H_2O$		
DCP	$CaHPO_4$	1	−6.9
DCPD	$CaHPO_4.2H_2O$	1	−6.6
OCP	$Ca_8(HPO_4)_2(PO_4).5H_2O$	1.33	−72.5
WH	$Ca(MgFe)_{10}(HPO_4)(HPO_4)_6$	1.43	−81.7
TCP	$Ca_3(PO_4)_2$	1.50	−28.6
OHA,HAP,HA	$Ca_{10}(PO_4)_6(OH)_2$	1.67	−117.1
DOHA	$Ca_{10-u}(HPO_4)_u(PO_4)_{6-u}(OH)_{2-u}$	(10−u)/6	−85.1

and the third is very weak. For all practical purposes, the concentrations of the ions figuring in the equations of thermodynamic constants should be corrected for all reactions compromising the active concentrations (protolysis, complex formation, activity coefficients...) as discussed at some length in the chapters on corrosion and toxicity (<*conditional constants*).

The notations used in Table 10.7 refer to:

- MCPM: monocalcium phosphate monohydrate.
- DCP(A): dicalcium orthophosphate (anhydrous); 'ortho-'because derived from a reaction of $Ca(OH)_2$ with orthophosphoric acid (IUPAC nomenclature). Mineral name: Monetite. Occurs in nature as a tan coating on a magnesium phosphate (newberyite).
- DCPD: idem but crystallized with 2 molecules of water.
- OCP*: octacalcium (ortho)phosphate.
- WH**: mineral name Whitlockite. Occurs in nature and is prominently present in lunar rocks.
- TCP: β-tricalcium (ortho)phosphate; α-tricalcium phosphate.
- HA(P): calcium hydroxyapatite. Trivial name.
- DOHA or (C)DHA: (calcium)-defective apatites, $0 \leq u \leq 2$. HAP as mineral or biomineral is almost never simply stoechiometric and/or well crystallized. OH^- may partially be substituted by fluor, carbonate or chloride, Ca^{2+} by Mg^{2+}.
- TTCP: tetracalcium phosphate.
- KCA:

*OCP is a somewhat elusive compound. It might be formed from precipitated amorphous calcium phosphate (Ca/P = 1.45) and may serve as template for the crystallization of HAP (a statement formulated many decades ago!). **An amorphous calcium phosphate (ACP) might be the precursor of DOHA and is considered as being WH with colloidal dimensions.

When *IP* of a supersaturated solution exceeds for a given compound, the conditional solubility product, which is as a matter of fact the equilibrium value of *IP*, the compound will start to precipitate, a due consequence of our thermodynamic slogan *water does not flow uphill*. The Gibbs-free energy difference $-\Delta G$ between solution and solid acts as the driving force:

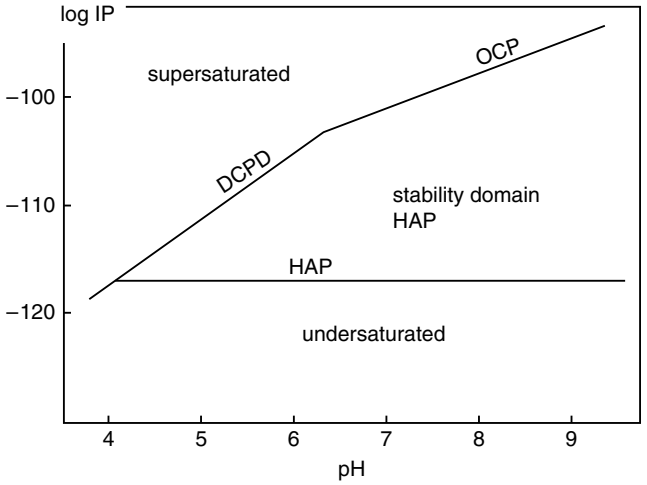

Fig. 10.14 Stability domain of HAP. Modified from [341]

$$-\Delta G \sim \log(IP/K_{sp}). \tag{10.4}$$

The reader will notice that this proportionality function is similar to the Nernst equation, where ΔE acts as the driving force in electrochemical reactions. The active concentration of PO_4^{-3} in solution is function of pH. Consequently, the chemical equilibrium between precipitate and solution will be pH dependent and we will be able to construct the plot of log *IP* versus pH shown in Fig. 10.14, a plot suspiciously similar to Fig. 3.4, the E-pH or Pourbaix diagram for chromium. The practical limitation on both plots are absolutely similar.

Considering the fairly large differences in K_{sol}, selective precipitation of the different phosphates should be a piece of cake. Unfortunately, it is not. Precipitation is a consecutive process of nucleation, kinetics of crystal growth, accompanied or disturbed by absorption and, at high supersaturation, polynucleation of other phases on the growing crystals. At pH = 7 and a ratio Ca/P equal to 1, the expected intermediates between ACP (or WH) and HAP is DCPD but experiment shows them to be OCP and DOHA. It is crystal clear that simulating the formation of a given phosphate is not simple business. Moreover, it is not impossible that more reliable solubility products will be obtained by a new and interesting determination technique promoted by Darvell and collaborators [342–344].

In order to be of any practical use, one should be able to master a number of specific material characteristics. Three applications are shortly discussed: cements, porous structures as drug carriers and scaffolding.

Bone cements. Four obvious characteristics for cements are setting time, temperature increase during setting, mechanical performance and biocompatibility. The interest in calcium phosphate cements (CPCs) started in the early 1980s [345]. In the subsequent years, setting time of CPCs could be tailored to practical clinical limits,

osteointegration was shown and, while PMMAs heated the surrounding tissues to 80°C or higher, CPCs did not. The linear setting shrinkage of PMMAs is around 1%, for CPCs it is 0%. Compressive strengths of 70 MPa could be obtained, quite sufficient for the aimed applications. Driessens and colleagues introduced the term *osteotransductivity* to describe the transformation, after the initial fast osteointegration, the slow resorption and gradual replacement of the CPC by new bone tissue.[5] We do not know whether the use of this term is continued, most authors we think use *osteoinductivity* to describe this process [346, 347].

The complexity of setting is nicely illustrated by real-time ATR-FTIR-monitoring of the setting reaction of an equimolar mixture of β-TCP and MCPM with citric acid as setting retardant [27].[6] The analysis provided evidence for the formation of an intermediate dicalcium phosphate-citrate complex. A time delay was indicated before the formation of DCP started, which was explained by the ability of citric acid to chelate calcium ions, remember our comments on factors limiting application of thermodynamic constants. At high levels of citric acid, significant levels of DCPA are formed which led to increased porosity and dramatic decline in strength. In order to see whether the kinetics for three different concentrations of citric acid shown in Fig. 3 of Hofmann's paper are equal, the IR-absorbance was also plotted versus reduced time, i.e., time t divided by $t_{1/2}$, the time after reaching half the maximum IR-absorbance. It allows a good visual observation of similarity or dissimilarity of processes performed under different experimental conditions. This often forgotten technique was already recommended in Chap. 1.

Drug carrier. Porosity of phosphate cements is compromising mechanical strength. A controllable porosity, however, is one of the distinguished characteristics needed for transport and slow release of drugs, an other being the harmless dissolution of the carrier in course of time. A wide range of products have been incorporated in porous phosphates ranging from antibiotics as gentamicin and vancomycin to bone morphogenetic proteins, most with success over time periods of days to months. But is a highly competitive area and we do not have any view on the winner. The porosity can theoretically be tailored based on the Higuchi equation describing the released amount M_t as function of effective diffusivity, the solubility C_s, C_d the concentration as function of time and ϵ the porosity:

$$M_t = [D_{\text{eff}} C_s (2C_d) - \epsilon C_x t]^{1/2} \tag{10.5}$$

Scaffolds. The burden of alternatives to phosphates are mentioned on different locations throughout the book. They will – although we are reluctant to advance a given position – presumably not be the winning item and will not be discussed any further.

Further reading: [340, 348, 349]

[5] Ferdinand Driessens passed away at age of 71 on March 30, 2008.

[6] Fourier-Transform-Infra-Red spectrometry equipped with an Attenuated-Total-Reflection attachment.

10.8 Postscript

Will a chapter on dental materials soon be obsolete?

In an article released on 4th August 2009 in Medicine News, Japanese scientists announced that they have grown new teeth in mice. They pretend that their *bioengineered tooth germ develops into a fully functioning tooth with sufficient hardness for mastication and a functional responsiveness to mechanical stress in the maxillofacial region*.[7] Indeed, regenerative therapy was and still is the wet dream of many scientists. It will definitely be the hot spot of clinical research in the twenty-first century. What is then the answer to the question? When the steam engine became perfect or the black and white or color films were perfect, we did not need them anymore, one kind of an answer.

We are not that pessimist and our answer is 'no' because experience learns us that many obstacles block the road before we will get germs for new teeth implanted.

The long discussion of amalgams is already justified and the introduction of polymer composites is a natural exit imposed by the cons of amalgams. Shape memory alloys do not need to be defended, phosphate cements on the contrary deserve more comments. The practical use of calcium phosphate cements is very limited, though potential applications are not to be excluded. The length of the contribution is justified by the active presence in all interphases between tissue and implants which are aiming to conduct or promote bone growth. Beyond doubt that it will go on for a while. A thirty-page long chapter is and cannot be a comprehensive text on dental materials. The selected subjects and the length of the discussion devoted to them were justified by – how else could it be – subjective criteria but they refer anyway to active research fields and/or to historically interesting (important?) areas. The reader will judge. When finally the book will be nothing but history, biomaterials will conserve a place in the collective memory of mankind.

[7] Tokyo University of Science and Organ Technologies Inc. Project leader: Takashi Tsuji. Homepage: http://www.tsuji-lab.com/.

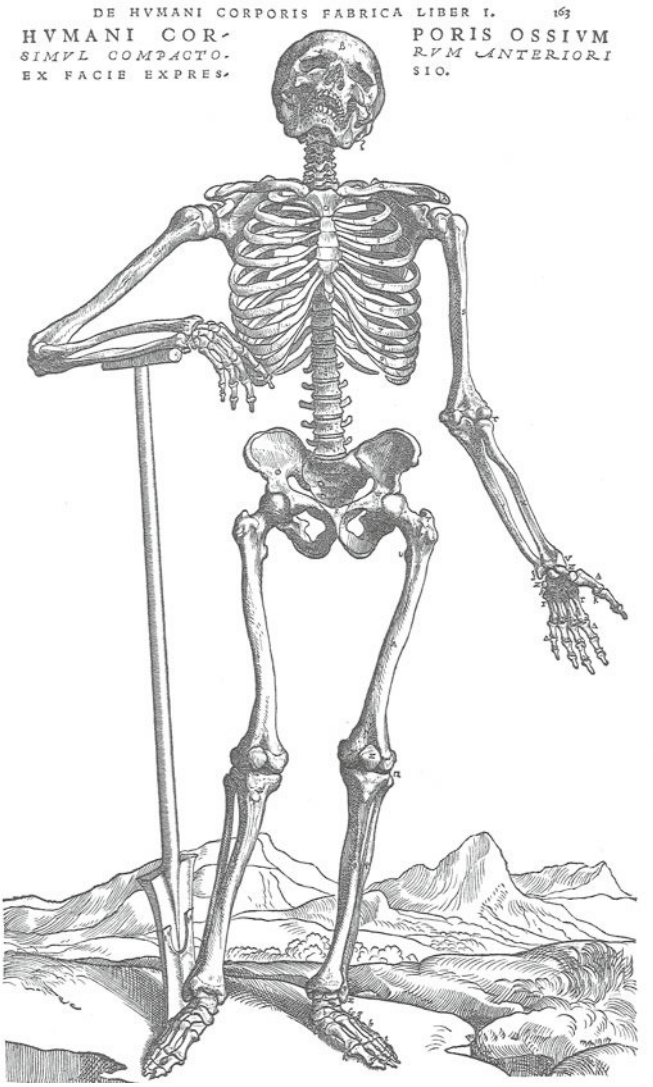

Andreae Vesalii: De humani corporis fabrica libri septem
Basileae: ex officina Joannis Oporini, 1543

A noble job...
creating a perfect prosthesis

Chapter 11
The Perfect Prosthesis?

In Chap. 2, we started with the case study of a cemented Charnley prosthesis, a superior design for it is still in use in only slightly modified form and served as template for numerous other designs. However, the stainless steel stem finally failed and even after substitution of the originally used alloy by other better-performing one as well as the introduction of a modular design, the prosthesis was not ideal yet, witness the abundance of numerous subsequent designs. Was the Charnley prosthesis after all not that ideal? A number of examples can be cited, where the femoral cortex is weakened by bone resorption, to be attributed to the phenomenon called *stress shielding*. The E-modulus of stainless steel is about twenty times higher than cortical bone and so is the ratio of stiffness between femur and prosthesis. Consequence is that stresses are unequally distributed over the femur walls, i.e., that *stress* on one part of the femur wall is *shielded* from expressing a similar stress on other parts of the femur wall (cortex, cortical bone).

By the patient's body weight, the prosthesis is tilted as shown in Fig. 11.1 (*varus* tilt) with the consequence that voids are created and a dynamic pressure difference is built up by which 'peri-joint' fluid, occasionally containing wear debris, is pumped into the void. The destructive action of wear debris is already discussed in Chaps. 2 and 4.

These facts must have been the concern of Robert Mathys Sr., when he developed his isoelastic design in the late 1960s (animal experiments [352]; in current human arthroplasty since 1977 [353], [354, pp. 591–596]).[1]

11.1 The Isoelastic Prosthesis

The outcome of the experimental campaign of Mathys was a modular prosthesis composed of a polyacetal body (stem), reinforced by a metal core (stainless steel 316L or Ti6Al4V) with tapered top, to which either a stainless steel, ceramic or

[1] Robert Mathys Foundation, CH-2544 Bettlach, Switzerland.

J.A. Helsen and Y. Missirlis, *Biomaterials*, Biological and Medical Physics, Biomedical Engineering, DOI 10.1007/978-3-642-12532-4_11,

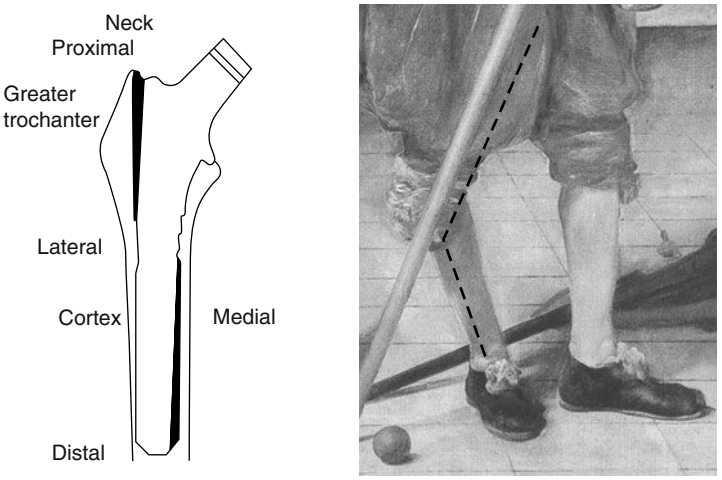

Fig. 11.1 *Left*: varus tilt of a stiff prosthesis: the shaded areas laterally at the proximal end and medially at the distal end [350, Fig. 5]. *Right*: the term *varus* tilt of the femur is nicely illustrated by the overstretched right knee (*dotted line*) shown in this cutout from a painting by De Silva *Don Juan d'Austria*, cited in [351, pp. 52–53]

CoCr alloy head can be fitted. The stem is endowed with an over all deformation behavior equal for all marketed stem lengths and of course similar to the one of bone. The required stiffness is obtained by adapting the depth of the longitudinal grooves in the core, i.e., adapting the effective section of the stem while maintaining the same overall shape of the metal core. The whole construction is illustrated in Fig. 11.2: force and bending moments, a section through an implant in situ and the external view. The bending moment is maximal at the site of the greater trochanter, the lower 2/3 has the lowest stiffness. The properties of the main alloys were reviewed in Chap. 2 making the choice of a titanium alloy obvious for the stem and for a head of CoCr. Ceramics are the subject of a separate chapter.

The head is articulating in a cup cemented or introduced cementless into the reamed acetabulum. The material, the use of which is surviving from Charnley's time till today, is polyethylene (PE), originally low density, nowadays always high density. However, it is increasingly substituted in modern designs by CoCr alloys or ceramics in various combinations: metal on metal, metal on ceramic, ceramic on ceramic. The cup is highly polished inside. The rear side can be bare PE or coated with calcium-hydroxyapatite (HAP) or titanium powder, backed by titanium gauze with on top plasma sprayed HAP, or supported by a titanium backing. The few examples of Fig. 11.3 are displayed as steppingstone to start the discussion on currently used and potentially future materials.

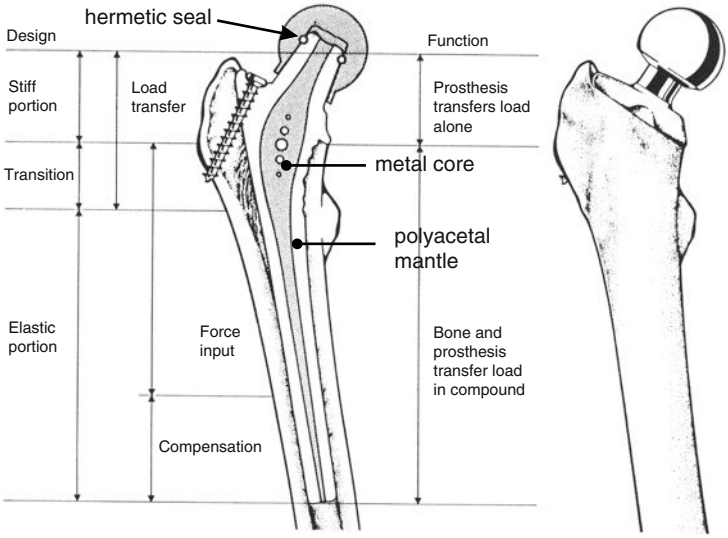

Fig. 11.2 Concept of the Isoelastic Hip Prosthesis [355]. Courtesy of Mathys AG Bettlach (Switzerland)

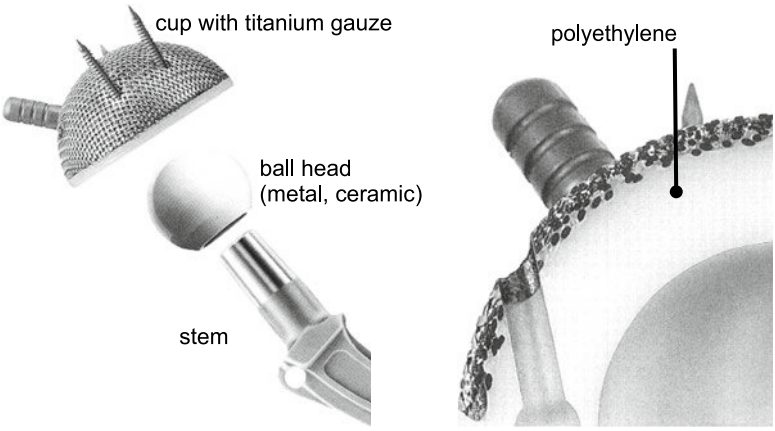

Fig. 11.3 *Left*: combination cup-head-stem. *Right*: section through a cup (Alpro, Sulzer)

11.2 Polymers for Implants

Polymers consist of chains of a repeating unit, a *mer*, which means part of a body, part of a larger unit or the like. Polymer synthesis is a randomized process delivering at the end of the line a soup of molecules with chain lengths more or less widely distributed (*molecular weight* and *distribution of molecular weight (MW)*). The *backbone* can be a rosary of carbon atoms or a sequence of some other elements

(–C–O–, –C–N–, –Si–O–, –P–N–) and, moreover, the backbone can be branched with side chains (*chemical structure*). The side chains can react with groups on adjacent chains called interchain links called *cross-linking* (already discussed in Chap. 10). If only carbon atoms are contained in the backbone, they are called *homochain* polymers, e.g., polyethylene, if other atoms are present in the sequence, they are called *heterochain* polymers, e.g., polyacetal. The chain may also consist of a sequence of more than one repeating unit. Chemical structure (repeating unit or units, end groups, branches, structural sequence) and molecular weight distribution are fundamental to all other properties of polymers.

During solidification, the chains staple with different degree of ordering, which means that the solid may become amorphous or partly *crystalline*. The chains, anisotropic by nature (length to diameter ratio), are not easily motivated to settle in military order and, in as far as we now, never do for a full 100%. The crystallite size is usually smaller than the length of a molecule, which is explained by *chain folding*. The rest of the solid remains a chaotically entangled network, cooked spaghetti at molecular scale!

Spaghetti is an exemplary model: the spaghetti snakes allow bending and axial torsion and... one cannot be moved without disturbing the neighboring one! In other words: before collective movement of chains is possible, an energy barrier has to be crossed (similar to the representation of collagen shown in Fig. 2.13). That brings us to a unique characteristic of polymers: they transform at a characteristic temperature domain below melting or decomposition temperature from a glassy state to highly viscous substance. This transformation is called *glass transition*. The phenomenon was first observed in ordinary window glass, therefrom the name. All solid organic and inorganic macromolecular compounds exhibit glass transition at some temperature on condition they contain amorphous regions. A higher concentration of low molecular weight molecules enhances the mobility of the long chains and these molecules act as *plasticizers*: they lower melting and glass temperatures, E moduli and their colligative properties. It perfectly illustrates why the distribution of molecular weight is basic to all mechanical and thermodynamic properties of polymers and why polymers are so an exquisite class of materials.

The height of the energy barrier inhibiting free chain movement can have different origins (in order of increasing strength): mechanical entanglement of long chains, attraction forces, hydrogen bonds, ionic bonds, covalent bonds. Hydrogen bonds are formed between hydrogen bonding donors: –O–H, –N–H, –S–H, –X–H (X: halogens), –C–H and –P–H, and bonding acceptors: oxygen from alcohols, aldehyde, ethers, esters, etc., nitrogen (amines, peptides, proteins, etc.), halogens, carbon (e.g., isonitriles or isocyanates). Hydrogen bonding is the preponderant player determining the strength of Brønsted acids.

Each term or keyword, emphasized in italics, is standing for a phenomenological characteristic property of the polymer. However, the terms *glass* and *amorphous* used thus far still need to be properly defined. We are not aware of any universal definitions of both terms but support those given by Elliott [229, p. 6]:

> Amorphous materials do not possess the long-range translational order (periodicity) characteristic of a crystal.

This definition renders the adjectives noncrystalline and amorphous synonyms. The definition is restricting amorphous to absence of long-range order, leaving to the reader the choice where to classify materials exhibiting short-range order. The definition of *glass* is also more restrictive than other common ones:

> A glass is an amorphous solid which exhibits a glass transition.

If a substance is fully crystalline, it melts and does not show glass transition. If the crystalline and amorphous regions are mixed, it will show both melt *and* glass transition. The subject was already opened in Chap. 9.

A clear and simple definition on condition we know what is meant by 'solid'. An arbitrary definition distinguishes solids from nonsolids in terms of viscosity: solids have a shear viscosity below $10^{13.6}\,\mathrm{N\,s\,m^{-2}}$, corresponding to a *relaxation time* of one day. Relaxation time, commonly designated by τ, is the time after which the stress is reduced by a factor $1/e = 1/2.718\ldots$. The time τ is zero for a Hookean body, an ideal spring: the deformation disappears immediately after removal of stress because stress and deformation are linearly related. Polymers, however, are not Hookean bodies and the relaxation time differs from zero.

Speaking about the relation between stress and deformation brings us to the last of important mechanical characteristics of a material: *creep*. It is defined as increase of deformation at constant stress and is characterized by a retardation time. All materials are subject to it. Metals and alloys creep at temperatures far above room temperature, but polymers creep at room temperature and deleteriously above the glass transition. Hereafter, the practical implication of these properties for a biomedical application will be illustrated for a number of specific polymers.

A more extended qualitative treatment of polymers, megamolecules as they are sometimes quoted, is given in the older but enjoyable book *Megamolecules* of Hans-Georg Elias [356]. For more advanced reading on structural properties, the book of Allen and Thomas may be recommended [38]. A comprehensive and excellent book on the basics of polymer science is written by Van Krevelen [357].

With foregoing and following discussion, we try to demonstrate the basic capabilities as well as the constraints of polymers. More than mechanical properties only count for a biomedical application but in load bearing applications they represent the *conditio sine qua non*. Items as toxicity, surface characteristics and so on are more difficult to treat in general terms but are highlighted for specific cases. The polymers in the next subsections are ordered according to increasing complexity and are relative to case studies treated thus far but are conceptually entangled with others in following chapters.

In the preceding paragraphs, we pointed to chemical composition of polymers determining what is called an *intrinsic property*. Degree of ordering (e.g., orientation) and its consequences, for instance for its mechanical behavior, is a *product property*. It is clear that product property is added to the intrinsic property during *processing*. These three facets are of course true for all materials but distinctively true for polymers.

Polyethylene

Polyethylene is a rather old polymer. It is discovered in 1932, produced since 1939 and used in those days mainly as garbage bags. It was a good dielectric insulator for high frequency, exactly what was needed for radar installations at the beginning of World War II. For *la petite histoire*, some historians say that the Battle of Britain was won by PE: no PE, no radar, without radar no early alert, without early alert no successful defense (story told in Elias' book [356, p. 85]).

Polyethylene has a zig–zag backbone of carbon atoms and the repeating unit is the ethyl group: and capped on both ends by a methylgroup $–CH_3$. It is called *polyethylene* because its synthesis starts from *ethylene* (or the scientific name recommended by IUPAC nomenclature *ethene*, and the polymer *polyethene*).[2]

The carbon atoms are linked in a happy marriage by covalent bonds with a bond length of 0.154 nm and a valence angle of 112°C. The theoretical modulus in chain direction is 340 GPa and 3 GPa perpendicular to it. The number of units n is distributed around 140 for low density, 18,000 for high density, and up to more than 70.000 for the ultra high molecular weight (UHMWPE). We skip a detailed discussion on the steric conformation because peer pressure of adjacent chains forces it to adopt the ordered *trans* conformation as illustrated in the figure.

In real-life, the chains in conventionally processed PE are not nicely aligned and a realistic E-modulus is <1 GPa. Alignment is present in the crystalline parts of the bulk for 50–70%. However, fibers with ultra-oriented chains reach moduli of over 100 GPa. Note that this is far superior to steel, definitely when the *specific modulus*, modulus divided by density, is considered. UHMWPE is the only one used in load-bearing applications, such as hip cups. It has a UTS of >200 MPa and an E-modulus >2 GPa. The crystallinity is >70%. It has a low glass transition temperature (-90°C) but behaves, nevertheless, as a solid at room temperature.

Polyethylene belong to the generic group of *polyolefins*, which can be processed by *injection molding*. The chain length of PE in its UHMWPE version is very long and the chains are intensely entangled which explains its resistance to flow or creep and the raise of the deformation temperature from 50°C of conventional PE to 115°C. For the very same reason, however, it cannot be shaped any longer by injection molding and must be machined. Hip cups are machined out of UHMWPE blocks. The metal or ceramic head of the prosthesis hinges in the cup and as already mentioned, resisting wear with great success: UHMWPE does but HMW variants do not. Figure 11.5 illustrates disastrous wear of a prosthesis head manufactured by Oscobal (Selzach, Switzerland; no longer active since 1999) with high density PE after an implantation period of a couple of years. This prosthesis was used in hemiarthroplasty, where only the femoral head is replaced and not the acetabulum. After early good results, most of the prostheses failed within 2 years. At reoperation a thick capsule was found, the stem always loose. Both the femur and the acetabulum were surrounded by necrotic-like tissue. Histology showed a massive

[2] International Union of Pure and Applied Chemistry.

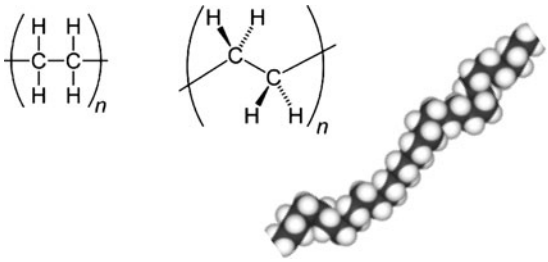

Fig. 11.4 *Left*: flat 2D representation of the repeating unit of polyethylene. *Center*: 3D representation; *arrow*: in front of paper plane, *dashed line*: back of the paper plane. *Right*: simulated polymer structure

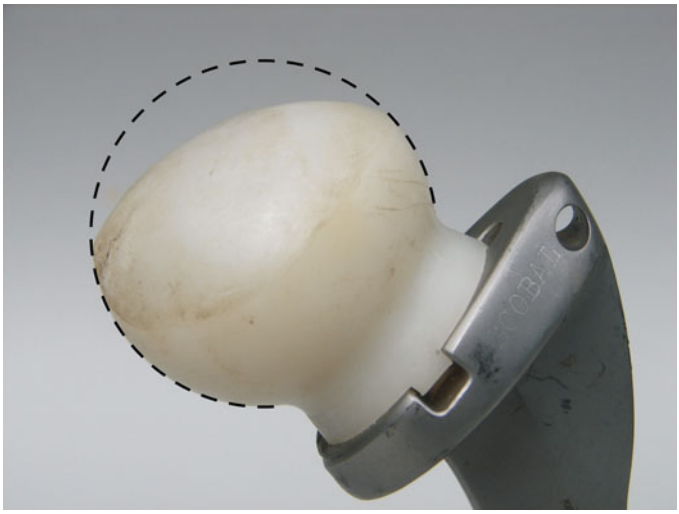

Fig. 11.5 Disastrous wear of a polyethylene prosthesis head after implantation of a couple years. The dashed line gives the original contour of the head. The prosthesis was a product of Oscobal (Selzach, Switzerland)

foreign body reaction with abundant giant cells and intra- and extracellular HDP particles [358]. The use of this prosthesis was a disaster. This case is an illustration of both the importance of MW on properties and the lack of sufficient mastering materials properties.

In Fig. 11.4, a simple linear nonbranched PE chain is represented but if it was nothing but that the polymer world would lack its wonderful flexibility. Chains in UHMWPE are less efficiently packed into a crystal structure, which results in lower density but is tougher and better wear resistant. High density is generated for a species with a low degree of branching and thus stronger intermolecular forces (*cross-linking*). In this way, the thermoplast can be turned into an elastomer (PEX)! While the polymerization of ordinary PE starts from pure ethylene, another set of properties can be generated by *copolymerization* with other short chain olefins such as I-butene, a process not yet mentioned thus far.

Polypropylene

The story is slightly different for polypropylene (or according to IUPAC *polypropene* is derived from the monomer *propene*). The monomeric unit is: $-(CH_3)CH-CH_2-$.

The backbone still is –C–C– but with methyl side groups, called *chain substituents*, $[-R]=[-CH_3]$. The methyl groups can be arranged all along one side of the chain (*isotactic*) (Fig. 11.6), or only the second methyl group reaches the same position as the first (*syndiotactic*).[3] The size of a methyl group is larger than the distance between one and the next third carbon, so the isotactic isomer is for steric reasons energetically less favorable. If the positions are random up and down of the backbone, the isomer is called *atactic*.

An interesting aspect is the helical structure of syndiotactic polypropylene. One turn in isotactic PP is made up by three successive units as shown in Fig. 11.7.

Left- and right-winding helices are present in equal amounts because R is symmetric. In other polymers where R is asymmetric, helices are forced into a left- or right-winding chain. Notice that the optical active biomolecules are all left-winding. The amino acids added to MEM solutions, listed in Appendix D, are all the L-forms (L-arginine, L-leucine, etc.). The influence of such a 3D conformation is reflected in the profile of mechanical properties : the theoretical E modulus is 50 GPa, while that of PE is 340 GPa! PE has a zig–zag chain, which is much harder to strain than a helix. The practical E modulus of PP is 1.1–1.6 GPa. To illustrate how extreme

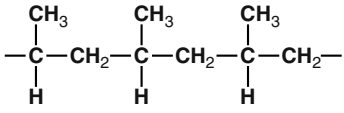

Fig. 11.6 Polypropylene

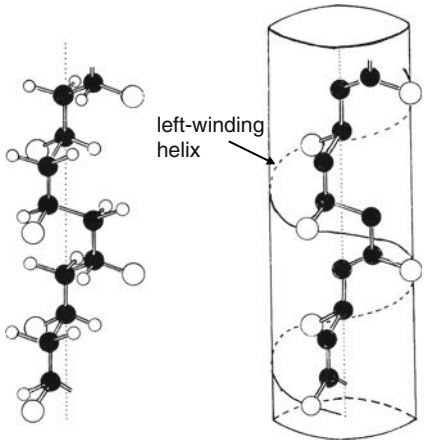

Fig. 11.7 Representation of the 3_l of isotactic polypropylene. White balls: H, small black balls: C, big white: CH_3. *Left*: spatial arrangement. *Right*: same chain but not showing the hydrogen atoms. The positions of the methyl groups correspond to a left winding helix. By courtesy of Springer [356, Fig. 22]

[3] The terms are derived from the Greek words: taktikos= ordered; isos= equal; syn= with, together; dio= two.

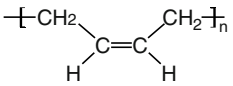

Fig. 11.8 Polybutadiene

effect of a different conformation on the properties of a polymer can be: the *trans*-isomer of polybutadiene (methylene groups sterically alternating up and down) is a hard semicrystalline material, while *cis*-polybutadiene (methylene groups on the same side)is a soft amorphous rubbery material! Its structure is illustrated in Fig. 11.8.

A paragraph about this important rubber: polybutadiene is one of the first types of synthetic rubber to be invented and is very similar to natural rubber, polyisoprene. A polymer chain is often a sequence of more than one *mer* as pointed out in the first paragraph of Sect. 11.2. A hard industrial version of it, SBS rubber, has a backbone chain made up of three segments. The first is a long chain of polystyrene, the middle a long chain of polybutadiene, and the last segment is another long section of polystyrene. It is a type of copolymer called a *block copolymer*.

Suffices further to say in quite general terms that side groups are not inhibiting crystallization, if they are orderly arranged: iso- and syndiotactic PP crystallizes, atactic does not. The crystallization degree of PP's is in the range of 50–70%. The glass transition temperature of isotactic PP is $-15°C$.

Polypropylene is thermoplastic and can be shaped by injection and by compression molding. The softening temperature is around $-160°C$ and as such, suited for medical use because it can be autoclaved. It has an excellent fatigue behavior. Chemically speaking, it shows high resistance to environmental stress cracking, a property that will be of particular importance for vascular materials as polyurethanes. Vascular materials are treated in Chap. 13. Copolymers do also exist. A randomly copolymerized PP helps in making them optically more transparent.

Polypropylene was discussed here to some extent because of its resemblance to polyethylene, because it allowed to introduce a few more aspects important for understanding properties and performance of polymers in general and because it is an integral part of a class of thermoplastic elastomers we introduce in Sect. 11.6. Moreover, long before the helical structure of DNA was proposed by Watson and Crick in 1953, H. Staudinger and H. Lohmann proposed and determined experimentally the single helix structure for polyethyleneoxide in 1932. C.W. Bunn proposed in 1942 a helix structure for isotactic polypropylene, which was experimentally confirmed by G. Natta and P. Corandini eleven years later.

Polyacetal

The two polymers discussed thus far cannot be quoted as high strength materials. For the stem of the isoelastic prosthesis, a material mechanically comparable to bone is needed. Polyacetal or polyoxymethylene (POM or Delrin, the tradename

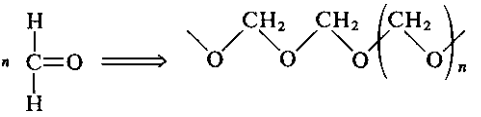

Fig. 11.9 Polyacetal or polyoxymethylene

of Dupont) is such one (Fig. 11.9). Its synthesis starts from formaldehyde and the resulting polymer has a backbone of alternating carbon and oxygen atoms.

It has an E-modulus around 3 GPa and a tensile strength around 70 MPa. Remember the values for UHMWPE with, respectively, 2.2 GPa and >27 MPa and for bone around 2 GPa and 150 MPa. In the isoelastic prosthesis design, the moduli are approximately equalized to bone by the metal core. Polyacetal has excellent fatigue properties and the design was fatigue tested under realistic loads up to 140.10^6 cycles. It is chemically very stable and has a very low absorption of water (0.25% after 24 h).

Polymethyl Methacrylate

The case discussed in Chap. 2 was a cemented prosthesis. The voids between femoral cortex and prosthesis stem were filled with a cement. It is basically a mixture of polymethyl methacrylate powder (PMMA); the *mer* is the monomer methyl methacrylate, which polymerizes in situ by a process called *addition polymerization* discussed also as substantial part of dental composites alternatives for amalgam in Chap.10 (Fig. 11.10).

The resulting polymer is amorphous, is optically transparent, has a high refraction index, is hard and brittle and suitable for a number of biomedical applications.

In Charnley's days, the cement contained higher concentrations of monomer than today with two major consequences: the polymerization reaction is an exothermal process and provoked an unacceptable temperature rise detrimental to bone; the monomer is toxic. These disadvantages are completely overcome nowadays. The cement is a complex mixture of monomer, PMMA powder, an initiator, a promotor of polymerization (or *curing*), a protector to prevent premature polymerization during mixing and a filler.

The polymerization is forced to progress by the formation of free *radicals*, for example by mixing with the initiator dibenzoyl peroxyde, giving the radical $C_6H_5\cdot$. The '·' stands for the unpaired electron, characteristic of a radical. This radical forms a radical with the monomer, which in turn attacks another monomer to form a dimer radical and so on. *N*,*N*-dimethyl-*p*-toluidine accelerates curing; hydroquinone is added to prevent premature curing by temperature or exposure to light. The result after curing is a compact solid of newly polymerized and already present solid PMMA. $BaSO_4$ may be added as filler and makes the cement radiopaque.

The commercial product is offered as a liquid: monomer, accelerator, retarder, and a solid powder: PMMA, methyl methacrylate-styrene copolymer, filler and initiator. They have to be mixed before use under well controlled conditions mainly to prevent the formation of pores. The latter affect substantially the mechanical properties. The required minimum compressive strength is 70 MPa and in practice up to 90 MPa can be obtained.

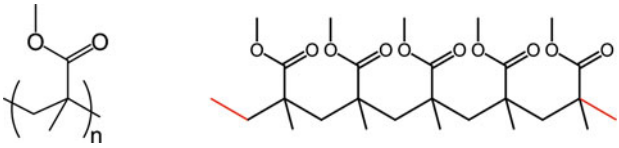

Fig. 11.10 *Left*: the repeating unit methylmethacrylate. *Right*: the polymer chain

11.3 Why Is a Polymer Like PMMA Transparent to Visible Light?

On preparing your pastis or ouzo the water you pour it in is getting cloudy, the mysterious 'mouche'. The optical transparency of PMMA was briefly mentioned above. It is not obvious for a material to be transparent but say for eye lenses, a relevant quality. The interaction of electromagnetic radiation with polymers will be briefly discussed.

X-rays. A radiographic image is based on subject contrast. The contrast increases with increasing difference in thickness, in density and atomic number. Less simple is the effect of the energy of the X-ray beam because the attenuation is a complex interplay of coherent scattering, photoelectric effect, Compton scattering and energy of the X-ray beam. Water, fat and many polymers do not differ much in these contrast producers and are not likely to be discriminated at least in a classical radiograph. If a PE acetabulum has no metal backing as in Fig. 11.3, it is hardly visible in a radiograph. To control position, migration and so on by the surgeon, PE acetabula without metal backing were made more visible by integrating a metal wire in the outer perimeter of the cup. For PMMA cement, the contrast problem is solved by adding a filler like $BaSO_4$ ($Z = 56$). The medical imaging world has been drastically changed of course by computed tomography, where more subtle differences can be detected than were classically obtainable.

If topographic information, for instance a measurement of the subsidence of a knee prosthesis, is important, the presence of some marker element is indicated with a higher atomic number than calcium ($Z = 20$). Small beads of tantalum ($Z = 73$) could be used as inserts [28, Chap. 6]. For the same (diagnostic) X-ray beam energy, the attenuation increases roughly with the third power of the atomic number: bone is most easily distinguished in ordinary radiographs because calcium has an atomic number and/or concentration exceeding all other elements, trace elements excepted, in the surrounding tissues. For tissues or complex bodies, the *effective atomic number* of the tissue can be taken into consideration: it is for compact bone ($Z_{\text{eff}} = 13.8$), while that for soft tissue is ($Z_{\text{eff}} = 7.4$). It makes that the probability for a photon to be absorbed by photoelectric interaction in bone is roughly 6.5 greater than for soft tissue of equal thickness. For more detailed reading, an abundant literature is available [359–361].

Optical wavelengths. Most polymers do not show specific absorption in the visible region of the spectrum and are therefore colorless. No color but often not

transparent or opaque. Why? *Refraction, absorption, reflection and scattering* are the most important optical properties in this respect. Absorption is a function of wavelength and groups like –C–H, –C–C–, –C=C–, –O–H, –N–H show specific absorption bands in the infrared (IR) part of the spectrum $\lambda > 1{,}000$ nm, not in the visible part of 350–770 nm. The specific IR-absorption bands are basic to identification and characterization of polymers but also to study microstructural details (configuration, conformation, chain order, crystallinity and so on). A comprehensive treatment of these aspects, beyond the scope of this book, can be found in *The vibrational spectroscopy of polymers* [362]. All media reflect or transmit light partly. *Transmittance* is the ratio between the intensity of incident light to light passing through; it is determined by reflection, absorption and scattering. If absorption and scattering can be neglected with respect to reflection, the material becomes *transparent*. *Opaque* are called materials with very low transmittance for most of the incident light scattered (*opalescence*). And to return to your ouzo: the opalescence is a result of spontaneous emulsification; the phenomenon is not mere a science *curiosum* but may occasionally lead to the production of drug-loaded nanoparticles [363, 364].

Light scattering is caused by optical nonhomogeneities in the medium with size of 100–1,000 nm, order of magnitude of optical wavelengths. The refractive index n, the quantitative expression of refraction ($n = 1$ for vacuum), is different for a crystalline and amorphous PE. Crystallites of the right size act as scatter centers and the polymer's appearance is whitish. On the contrary, PMMA is homogeneously amorphous, no scatter centers, and is transparent ($n = 1.490$; diamond: 2.417).

When a transparent material, *in casu* here a polymer, is anisotropic, it can be *birefringent*. Birefringent materials rotate the polarization plane of polarized light. *Birefringence* is defined as the difference in refractive index parallel and perpendicular to the plane of polarization: Anisotropy may originate in noncubic crystallinity but, as in polymers, may be induced by stretching and PMMA is an excellent example. This peculiarity allows to visualize stress distribution in 2D models of PMMA. The phenomenon is called *photoelasticity*. Its use for quantitative evaluation became somewhat obsolete and study of stress distribution is substituted by computer simulation (Finite Element Analysis).

11.4 Polyethyleneterephtalate

The list of polymers used as implant material is limited to those illustrating best (to our perception) the basics of this generic class of materials. Polyethyleneterephtalate (PET) and polyamides in next section may not be absent because they are backbone materials in Chaps. 12 and 13 dedicated to soft tissues. As can be understood from Fig. 11.11, ethyleneterephtalate is an aromatic ester. They find widespread application in surgical suture threads and in vascular surgery. Dacron® is a respected representative of this group. Although an ester, it is relatively well resistant to hydrolysis. Threads are manufactured by melt spinning, more bulky products can be made by injection molding.

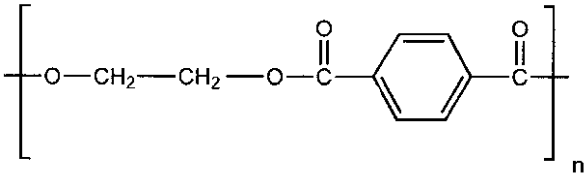

Fig. 11.11 Basic unit of polyethyleneterephtalate (PET). By courtesy of Springer Verlag [40, p. 168]

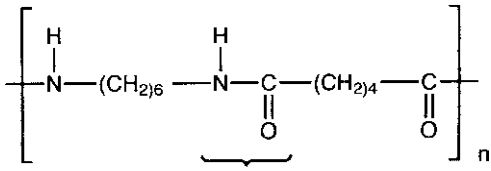

Fig. 11.12 Basic unit of polyamide; above the brace '{' the amide group. By courtesy of Springer Verlag [40, p. 173]

11.5 Polyamide

Polyamide was marketed as Nylon (PA 66) and Perlon (PA 6) since 1937. The fiber-forming abilities are excellent due to interchain hydrogen bonding, with its –N– and –C=O groups an obvious marriage, and a high degree of crystallinity increasing tensile strength in the fiber direction (Fig. 11.12). The $-(CH_2)_n-$ can be substituted by benzene C_6H_6 as in PET (Fig. 11.11). One variant is made by Dupont and known as Kevlar®. Its specific strength is five times that of steel. They exhibit good hemocompatibility. They are hygroscopic (water adsorption of 1–3.5%) and water molecules act as plasticizer.

11.6 Was the Isoelastic Concept a Good Idea?

Mid of the 1990s, the production and use of this prosthesis stopped. First generation implants were not that big a success (subsidence, slight varus tilt, stem and metallic head fracture due to imperfect design). These inconveniences were perfectly met by the subsequent improvements (longer stem, better initial fixation, larger neck shaft angle) and the results on cohorts of patients with third generation implants proved very satisfactory after two years follow-up [350]. Niinimki et al. reported in 1994 that only half of the 71 cases were satisfactory after 7 years follow-up [365]. Ali et al. report on 111 hips of patients from 30 to 70 years old after a follow-up time of 5–12 years and found an average Harris score of 80, a high incidence of lateral migration, 3 were revised for aseptic loosening, 6 radiographically loose and osteolysis noted around 2 hips. The authors continued to believe in the principle of isoelasticity but improvements in design and material of the femoral component are required [366].

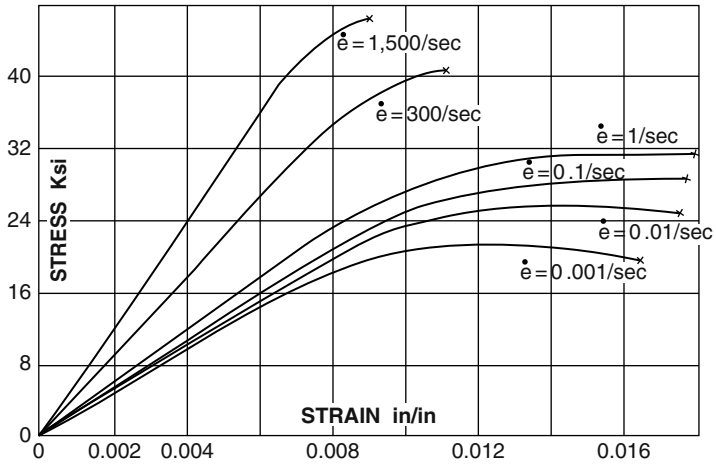

Fig. 11.13 Stress–strain curves with strain rate as parameter for human compact bone. Reprinted with permission of APS [368], Fig. 5

Anticipating the latter comment, the company Mathys introduced a new patent with basically the same design but, as stated in the abstract, *provided with an additional superficial layer made of a biocompatible material having thickness of less than 600* μm *and a higher surface hardness than the envelope* [367]. By *envelope* is meant the first nonmetallic layer enveloping the metal core and is intended to have an E modulus between 0.5 and 10 GPa.

Living tissues do not display Euclidean order (fortunately!) and linear behavior is not the rule. Tabulated mechanical properties have low precision and accuracy is for obvious reasons a question mark: almost no skeletal bone allows sampling of test specimens homogeneous over any meso- or macroscopical length scale. Values for E-modulus of the long bones center around 20 GPa, UTS around 140 MPa, compression strength around 150 MPa (see Appendix(zie app.eig. weefsels). However, let us set aside for a moment the absolute values and focus on what happens when stress–strain behavior is studied as function of strain rate. Remarkably, stress is already doubling, when the rate of deformation is enhanced from 0.01 to 300 s^{-1} as shown in Fig. 11.13; strain rate is the parameter in this figure. The value 0.01 s^{-1} corresponds to quasistatic loading. But is such a dramatic increase of strain rate for doubling stress biologically relevant?

For that purpose, it is instructive to follow the hip force pattern generated during walk. The hip contact forces were calculated from registered ground forces for a female test person (age 25 y, weight 59 kg) during normal walk. In Fig. 11.14 are displayed the vertical force component F_z is versus time t (left) and (right) the derivative $\mathrm{d}F/\mathrm{d}t$. In the onset of the step around $\sim$0.2 s the derivative peaks at 25.0 kN s^{-1}! The gait pattern and calculated contact forces are comparable to published by other authors [369, 370].

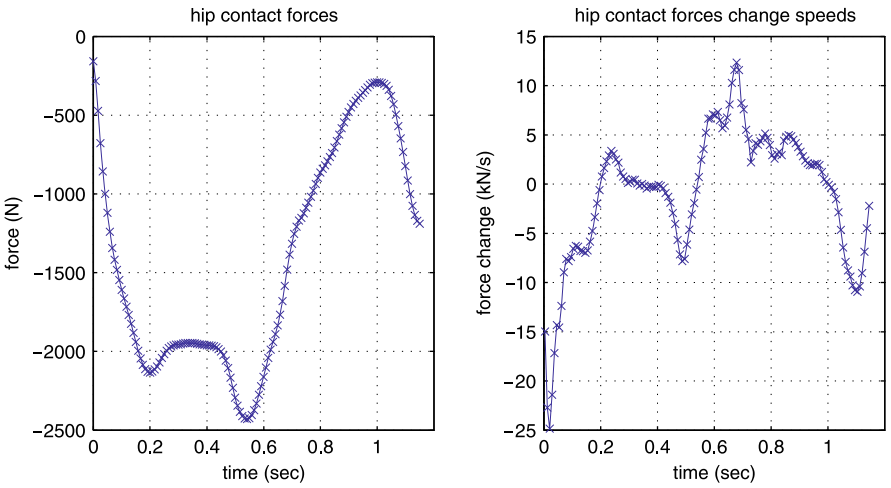

Fig. 11.14 Normal walk of female test person (59 kg): (*left*) the vertical component F_z in N vs. time in s of hip contact forces (Spaepen, Private communication, 2007). *Right*: the derivative of force with respect to time. Reprinted with permission of Prof. A. Spaepen (Dept. Kinesiology, KULeuven)

The transformation of data of Fig. 11.14 for $\mathrm{d}F/\mathrm{d}t$ to $\mathrm{d}\epsilon/\mathrm{d}t$ may look theoretically simple but in practice it is not. The transfer of force through a system of joint fluid (non-Newtonian), cartilage, cancellous bone (non-Hookean) to the cortex of the femur is complex. Detailed analysis is beyond the scope of the chapter but in a first approximation the following relation sounds reasonable: $\mathrm{d}F/\mathrm{d}t \sim k\mathrm{d}\epsilon/\mathrm{d}t$. The proportionality factor k is definitely not a constant but a complex function of the stress–strain behavior of the proximal femur *ensemble* and, as we do not know the mechanical characteristics of that *ensemble*, k cannot be calculated. Anyway, inspection of the first derivative given in Fig. 11.14 allows to accept that strain rate changes, as mentioned above for doubling the stress, are biologically sound or even common: from $\mathrm{d}F/\mathrm{d}t$ values passing through zero up to $25.000\,\mathrm{N}\,.\,\mathrm{s}^{-1}$ within a lapse of time less than 0.2 s should be a perturbation of comparable order of magnitude.

Conclusion of the foregoing discussion? A prosthesis to match the properties of the implant site is in urgent need of a material performing in a much more complex way than, say, a polyacetal can offer. Before proposing a remedy (Sect. 11.8), first something about dashpots, plungers and the world of Heraclitus.

11.7 Heraclitus, 2500 Years Old and Still Alive

Hitting billiard balls deform slightly during the impact. The deformation is immediately and entirely restored after that tiny moment the intimate contact lasts: billiard balls act as nearly ideally elastic bodies, *ideal spring*, and deform reversibly

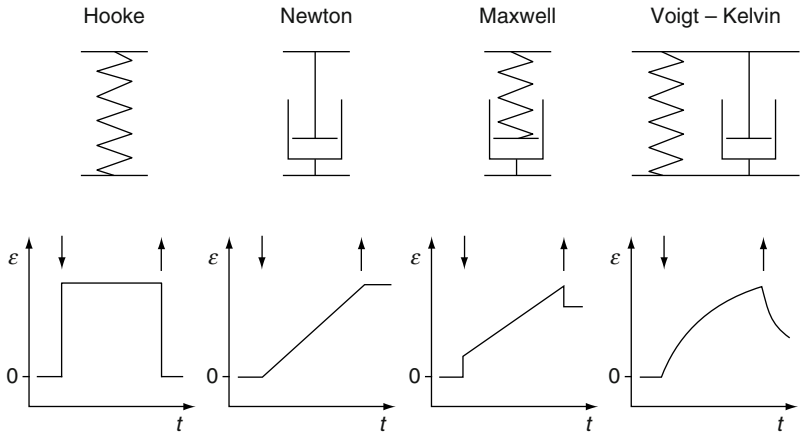

Fig. 11.15 Mechanical analogies for the stress–strain behavior of polymers: application of load indicated by ↓ or removal of load by ↑. Courtesy of Springer [356, Fig. 42]

with a linear *quasi time-independent* relationship between strain and stress. Hooke sketched that this situation already in the seventieth century as pointed out in Sect. 2.2. However, not all materials 'do it' reversibly like billiard balls and even, fanatics of perfection will say that in the limit solids act never at all neither as perfect springs nor simple dashpots: life, as we stated more than once, is never that simple. And he knew it 2500 years ago Heraclitus, with his fierce statement Πάντα ῥεῖ, *panta rei* or 'everything flows', rocks as well as whisky! Not an iota has to be changed of Heraclitus' statement, although he definitely was unable to measure it.[4] Whether we observe it macroscopically or not, it depends on the timescale and conditions such as temperature and pressure. An instructive number in this respect is the *relaxation time*: it is the time after which the stress is reduced to $1/2.718\ldots$ of the original value (one divided by Euler's number e). The timescale varies between extremely small to geological ones. The pictorial representations in Fig. 11.15 are four mechanical models used in the description of observed experimental facts. We start simply with an old acquaintance Hooke: the ideal spring with no time delay between applied force and resulting deformation or *mutatis mutandis*, when dimensionally normalized, stress and strain, is called a Hookean body. Stress or strain versus time will show a nice square wave in perfect time harmony with each other. When the second device, a *dashpot*, is filled with a fluid and a force is applied, viscous stresses are brought into play proportional to the *rate* of deformation. The property of possessing such stresses is called *viscosity* and fluids in which a simple proportionality exist between stress and rate of shear are quoted as a *Newtonian liquid*, a tribute to no less an old acquaintance Newton. When the load

[4] Saying attributed to Heraclitus by Aristoteles (*De Caelo*, 3,1.298) and by Simplicius' comments on Aristoteles (*Physica*, 8,8).

is dynamically applied, usually sinusoidally, the stress is exactly 90° out of phase with the strain. Spring and dashpot represent the mechanical analogues of the elastic and viscous properties of a fluid. . . Life, however, is lived in between springs and dashpots. Section 2.3.1 the flow of fluids is discussed at some length.

Two classics for simulating the viscoelastic character are presented in Fig. 11.15: the Maxwell body with both elements in series and both in parallel for the Voigt body. A sudden load causes a sudden initial deformation of the spring followed by a slow deformation of the dashpot of the Maxwell body. The spring retracts on removal of the load but the dashpot reaction lags behind the one of the spring. This phenomenon is called *relaxation*. A similar story can be told for a Voigt element. From these two simple but basic circuits, it is immediately obvious that their response to frequency will be a function of the relative weight of each component and of course, more complex situations require more complex circuits. Algorithms allow the numerical evaluation of these circuits.

For any practical purpose, the various components of the simulation circuit have to be allocated to some physical arrangement inside the intestines of the polymer. That only opens a door to a better understanding of stress–strain behavior, relaxation and so on. That is in turn the relay between a particular structure and processing. It is thus the stepping stone to an intelligent adaptation of the processing to fulfill the aspirations of the engineer and no less, the bioengineer! The main purpose of the qualitative story we told was to guide qualitatively the reader through one of the curly paths leading to *intelligent design*, obviously here a path slightly more down to earth than what creationists mean by it.

It is the absolute beauty of science that vibrating machine parts, electrical networks, electronic circuits and electrochemical interfaces use at least basically the same mathematical algorithms for their spectral analysis. Dashpot and ideal condenser, spring and ideal resistor are the obvious analogues. In Chap. 2, one reason for fracture of the prosthesis was corrosion and we commented briefly the electrochemical or galvanic origin of corrosion. Advanced electrochemical analysis of the interface of metals and alloys and the environment, occasionally the biological environment, appeals on electrochemical impedance spectroscopy. A reference work on the subject is the book *Impedance Spectroscopy* by Macdonald [371] or more compact in a chapter by J. Hubrecht in *Metals as Biomaterials* [35, Chap. 14].

11.8 We Shall Overcome . . . Do We?

If the considerations about the ultimate incongruity of the isoelastic concept are correct. . . is there a practical way to overcome them?

The metal stem was hyperelastic, the Mathys concept isoelastic but a few dreamers tried out a concept at the bottom of the elasticity line: they made the stem *hypoelastic*. How do this elastomer-coated prosthesis (ECP) looks like?

An alloy core was coated with a material by far less elastic than femoral bone or simply said: the stem was coated by an *elastomer*, a polymer with rubberlike

properties.[5] Dreamers, yes, but nevertheless they started from a compelling hypothesis in the pursuit of the ideal physiologic prosthesis and we will see if it paid off:

1. The elastomer mantle should meet at least partially the objections formulated in Sect. 11.6 with respect to the compression (or shear) behavior of polyacetal. The elastomer mantle acts as a mechanical buffer between bone and metal core. It should damp impacts during walking (dashpot function).
2. The mantle is custom made allowing the best press-fit and best apposition to bone, minimizing voids with subsequent elimination or at least reduction of formation of fibrous tissue.
3. The better press-fit immobilizes the interface between elastomer and inner femur wall. Ever present micro movements of the prosthesis stem with respect to the cortex wall provokes wear as is beautifully demonstrated by Figs. 2.4 and 5.1 (Chaps. 2 and 5). The micro-displacements are converted into shear deformation of the elastomer mantle.
4. The immobilized interface minimizes the production of wear debris.
5. The inner femur shaft is never smooth. Small protuberances give rise to stress concentration on these sites with two consequences: the metal prosthesis stem for cementless as well as for cemented ones is subject to wear on these spots (as beautifully illustrated in Chap. 2); point contacts are considered as 'the' or at least one of the sources of pain. The elastomer mantle is avoiding stress concentration by distributing stress over a wider area.
6. The elastomers should meet the general requirements with respect to fatigue and wear resistance, chemical stability, nontoxic, tolerated by bone tissue, *osteoconductive* or if at all possible, *osteoinductive*.

And it did not stop here: they also followed a rigorous research flow sheet. The figure is self-explaining and we will see how far the dreamers went on.

As ultimate goal these researchers definitely had in mind is a custom-made prosthesis, preoperatively planned based on a tomographic 3D-model and preoperatively manufactured. That was in the early 1990s but in those days it was still a bridge too far. The flow sheet is about that item a bit more modest. Since that time, however, the accuracy of tomography is substantially improved and in particular in Chap.7 a pandora box is opened with nothing but good spirits.

After dreaming of a new design, materials selection is the first challenge. The choice of a thermoplastic elastomer was dictated, outside mechanical and (bio) chemical requisites, by perioperative manufacturing constraints. Two classes of elastomers were considered: two thermoplastic polyolefins (TPO), Santoprene and Sarlink, and a thermoplastic polyurethane (TPU). The structure will be discussed in next section. Both can be obtained in various degrees of hardness, are thermoplastic, have excellent fatigue and wear resistance and are chemically stable. For practical reasons, availability and nonadhesive to the injection mould, Sarlink was most extensively tested. On the biochemical side, however, polyurethane has an

[5] The term rubber is merely used for a product based on natural latex. Elastomers is an appropriate name for synthetic rubbers.

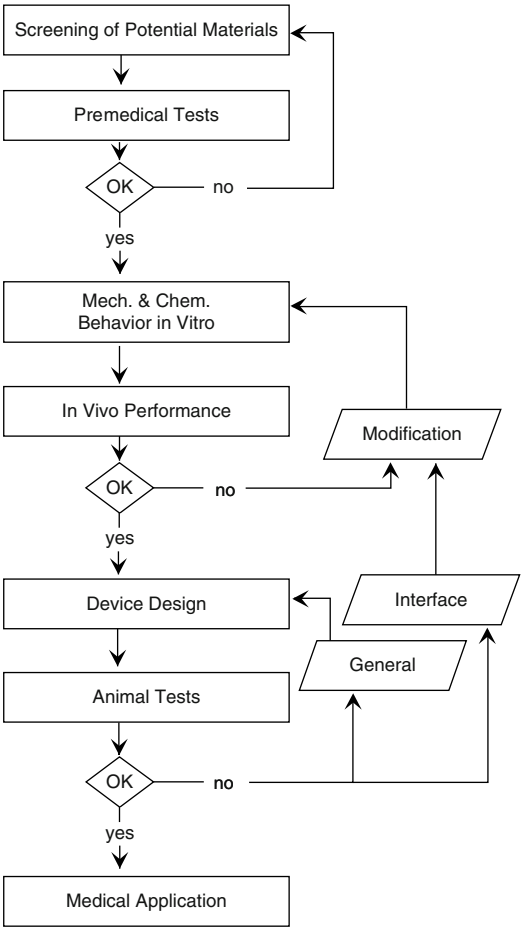

Fig. 11.16 Designing a hip prosthesis: a research flow sheet

established biomedical record. TPOs were relatively cheap but neither were they 'naturalized' citizen of biomaterials country nor did they have a long-term medical record, except only the animal experiments described by the designers of the hypoelastic model. Although TPUs are good candidates, TPOs were investigated more in depth for developing the elastomer coated hip prosthesis. In the context of this book, the case study *development of the hypoelastic hip stem* is taken as anchor illustration of the tedious experiments and evaluation procedures the development of a new product always is demanding, a promenade through dreamland. . . but here guided by the flow sheet of Fig. 11.16.

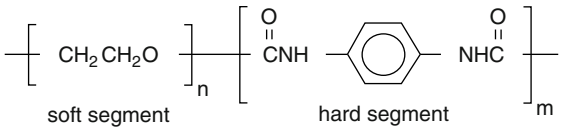

Fig. 11.17 Basic composition of polyurethanes with hard and soft segments

11.9 Thermoplastic Elastomers

11.9.1 Polyurethane

The basic unit of polyurethane consists of, as most technically used polymers, hard and soft segments as shown in Fig. 11.17. They need no special 'tricks' for being thermoplastic but, when shaped by injection molding, they have the unpleasant property to adhere to the injection molds; can be overcome but releasing agents anyway need special attention. Companies do not like to communicate about the content of their products. PUs are widely applied in the extremely important field of vascular surgery (see Chaps. 12 and 13). The major brands of commercially available biocompatible PUs are Biomer™, Cardiothane™, Pellethane™ and Tecoflex™. For the aimed application, Pellethane should be the most suitable (with respect to the range of available hardnesses).

11.9.2 Thermoplastic Polyolefins

TPOs are a magic mixture of three main components: the thermoplast polypropylene as matrix, dispersed in this matrix an EPDM rubber, thoroughly mixed under addition of a nonspecified mineral oil. EPDM is dominating the synthetic rubber market. It is a terpolymer consisting of copolymerized ethene [$CH_2{=}CH_2$], propene [$CH_2{=}CH{-}CH_3$], and a nonconjugated diene.[6] Santoprene and Sarlink are two TPOs, respectively, manufactured by Monsanto and DSM, the main difference being the degree of cross-linking (>95 and <95% respectively).

Premedical Tests, Assessment of Fatigue Damage, In Vivo Experiments

Premedical testing. A material which is intrinsically toxic is out of the question for biomedical use. Therefore, the designers looked first whether or not the TPO and

[6] The IUPAC names for ethylene and propylene are ethene and propene. *Nonconjugated* diene means that the two double bonds are separated by two or more single bonded carbons [$CH_2{=}CH{-}[{-}C{-}C{-}]_n{-}CH{=}CH_2$].

PU passed the examination imposed by the US Pharmacopeia Class VI of 1980 for being recognized as "medical grade" materials. These were:

1. Acute systemic toxicity
2. Hemolysis
3. Muscle implantation
4. Mutagenicity
5. Cell adhesion

The examination was a full success, hence followed the next 'go or no-go': performance under the expected mechanical constraints.

Fatigue. The interface of hip stems is mainly exposed to shear forces. For in vivo simulating of shear fatigue, samples were squeezed between a wedge-shaped steel anvil and a stamp, immersed in conventional simulated body fluid (SBF). The latter is a solution copying the ionic composition of body liquids, in particular of blood plasma. It is obvious that the composition should be adapted to the site in the body where the tested material is expected to function. In Appendix D, three groups of compositions are listed: SBF, artificial saliva and heart valves and grafts.

The anvil was sinusoidally loaded at a frequency of 3 Hz and applying shear stress cycled between 150 and 1,500 kPa. These conditions were derived from normalized theoretical and experimental data. Force and displacement of the anvil were sampled 64 times per cycle and the number of cycles was registered. This went on to over 3.10^6 cycles, a common number of cycles in fatigue testing. The loads exceeded three times the expected real life load and the number of load cycles corresponded to an estimated survival period of 5 years [372–374]. Figure 11.18 is an example of a fatigue set up with sample immersed in SBF (Hanks').

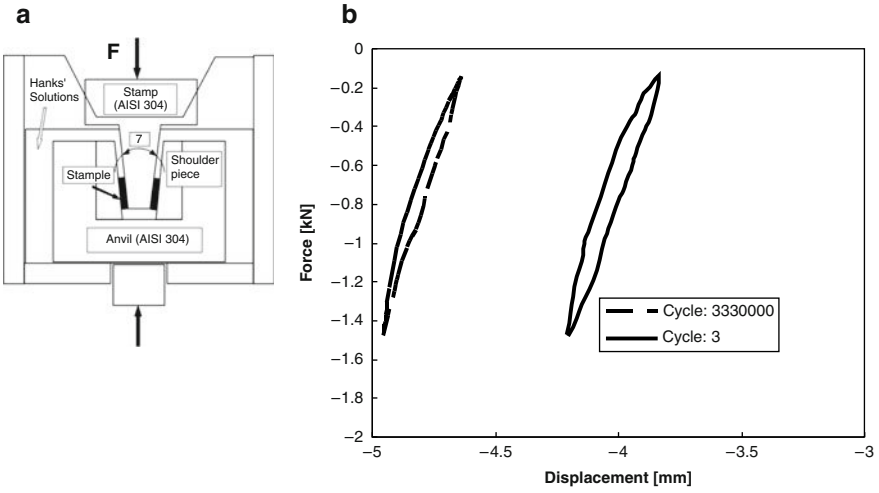

Fig. 11.18 Fatigue test of Sarlink (hardness Shore A 80). Conditions: sinusoidal force variation between 150 to 1,500 N, frequency of 3 Hz. (**a**) Experimental fatigue set up; (**b**) hysteresis curves as function of number of load cycles, up to 3.10^6 cycles. The shift of the curves on progressing number of load cycles is proportional to creep. Courtesy of S.Jaecques [375, Fig. 16, 16]

The plots of force-displacement data, after appropriate reduction to stress–strain data, result in a series of closed loop within the hysteresis curve. The surface within the hysteresis curve is proportional to the energy stored during compression. After a few thousands of cycles the creep reduces to low values and the stored energy decreased (decreasing area of the hysteresis curve) or in other words, the elastomer was tending toward ideal elasticity. All samples survived the fairly brutal tests but, however nice they might have looked, they were partly a blow for the aims of the noble dreamers who hoped to preserve viscoelastic behavior (shock attenuation). A polymer with fashionable viscoelastic characteristics ... was not within reach of the dreamers.

Although the test did not go on till complete destruction of the sample, the damage had anyway to be evaluated. Not a burden of proper tools exists for that aim. A true engineering evaluation was the evolution of stress–strain curves. The engineer needs it for prediction of the life expectancy of the material, if only mechanical parameters would be part of the game.

Evaluation of fatigue. Small cracks in elastomers close when shear or tensile forces disappear and become visually or even microscopically obscured. However, simple kinetics – remember what was said in Chap. 1! – may already help. Polymers, even the very hydrophobic ones, such as polyolefins, swell in contact with water or other solvents. The % of *swelling* of Sarlink 3–82 followed linear $\sqrt{t}$ kinetics (Fick's law) before fatigue and after fatigue but subdivided in two parts with different slope and in between a short transition zone. A faster diffusion is expected in cracks, even in micro-cracks, than in the bulk of the elastomer, after all not surprized to observe a more complex curve. The observation is instructive because the graph is warning that different things are happening as function of time and gives a hint to the probable mechanisms behind, in the present case a two-step diffusion. In the cracks first and second through the matrix, the latter following the swelling kinetics before fatigue. Optical or scanning electron microscopy are not adequate tools in this case because cracks in elastomers are nicely closed after removal of stress. Dynamic Mechanical Thermal Analysis (DMTA) indicates an increase of frequency at the maximum of the loss tangent which points to an apparent decrease in macroscopic dimensions, which in turn is explained by the existence of (micro-)cracks, a conclusion in line with the kinetics of swelling.

The modest although sizeable modification in properties could be sufficient for short-term practical purposes but the materials fanatics want to know what is going on. The damage can be studied by X-ray scattering Wide Angle (WAXS), Small Angle (SAXS), by Small Angle Neutron Scattering (SANS) or by Raman spectroscopy. In case of polypropylene, a much cheaper tool is available: Fourier Transform-Infra Red spectroscopy (FT-IR). PP is partially crystalline and shows in the IR-spectrum two pseudocrystalline peaks at 1168 and 974 cm^{-1}.[7] The absorbance ratio plotted vs. time in Fig. 11.19 refers to intra- and intermolecular changes of PP and in particular to the helicoidally ordered portion (see Sect. 11.2). The relaxing fatigued samples tend to higher crystallinity than the control (the small relaxation of the control is an artefact of sample preparation).

[7] The wavenumber for IR-spectra is normally given in cm^{-1} and not in MKS units m^{-1} or mm^{-1}.

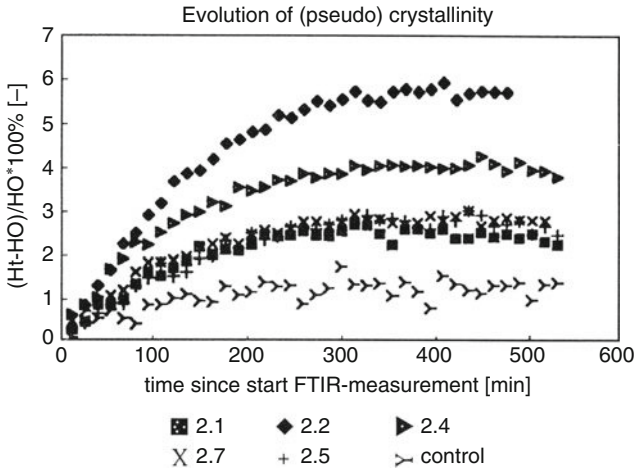

Fig. 11.19 Relaxation of the ratio of A_{1168}/A_{964} as a function of time since the end of the fatigue test. By courtesy of S. Jaecques [375, Fig. 48]

In vivo performance, device design, animal tests. The next step in the flow sheet of Fig. 11.16 is the in vivo performance, which was tested under static conditions by implantation of cylindric samples in the paravertebral muscle of guinea pigs and in the hind legs of dogs. The animals were kept under close veterinarian control and tissues surrounding the implants as well as of sensitive organs (liver, spleen, lungs, kidneys and local lymph nodes) were histologically evaluated *post mortem*. UHMWPE was used as control material. Without going into details, the histological study did not reveal any response more than generally accepted for bioinert material (like UHMWPE), which could be prohibitive to the next step: device design. Quantitative computed tomography (as described in Chap. 7) was not available yet. Prostheses were developed guided by Finite Element Analysis based on morphometric studies of dogs femora and implanted in dogs (German shepherds). Along with continuous veterinarian control, gait analysis did not indicate that the animals experienced much hinder of the implantation. The *postmortem* analysis of the explanted femora gave at least very encouraging results. Important in this stage of evaluation is the histological inspection of neoformation (osteoinduction) or osteoconduction of bone, amount and type of fibrous tissue, presence of necrosis, giant cells, . . . A pleasant observation was adaptation of the elastomer mantle to the rugosity to the cortex wall (was part of the hypothesis!). Figure 11.20 is giving a good summary of these conclusions. Tough not perfect – nothing is perfect in this world – it could be said that the hypothesis the authors started from, was not contradicted (negative appreciation) and for an acceptable part verified (positive appreciation).

At this point we have arrived near the bottom of the flowsheet and should give a feedback to improve the design on at least two-eye-catching features: more perfect shape fitting (quantitative tomography) and occasionally a surface treatment. Despite the very hydrophobic nature of the applied elastomer, histology

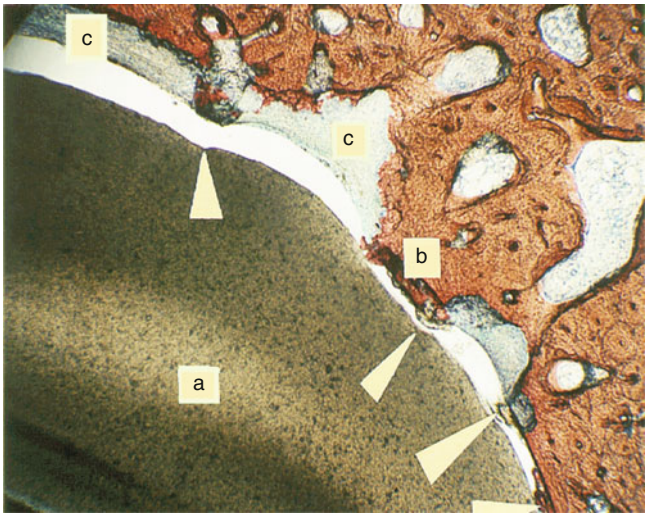

Fig. 11.20 Ground section embedded in PMMA. *Bottom left*: the metal core; (**a**) Sarlink; (**b**) mature bone; (**c**) fibrous tissue. The void space is a preparation artefact. The arrows indicate the spots where the coating has adapted its shape to protuberances of the cortex wall: spreading point stresses over a wider area. Courtesy of S. Jaecques [375, Fig. 135]

showed bone neoformation. It is not a dogma but, as often proposed on many occasions, shape is an important issue in hard tissue implantation and, honestly, surface modification was the little brother. Excuses, however, are the success of the hard tissue implants mainly as result of adequate shape and to a lesser extent of surface condition.

11.10 Conclusion

The intention of the last section was not a plea or defense of a given project but the project for testing the hypoelastic hypothesis was the tourist guide through dreamland. A promenade never pretends more than sketching the contours of the subject, comprehensive only in the description of the subjects' philosophy. It should create the taste for knowing more. Described were experiments, own, students' and Ph.D. work, used during lecturing and on congresses. Details are crystallized in papers [375–381]. Fear for legal liability aspects prevented commercial implementation so far. Another frustration of the authors of that project remains the creation of a viscoelastic coating meeting the ultimate goal of the 'perfect prosthesis'. something must be left to the next generation but that is not an excuse.

The perfect prosthesis is not a reality yet. Hopefully, the contours of what is needed to realize such a device was made sufficiently clear in Sect. 11.8. These points are as a matter of fact a summarizing conclusion of what has been said, discussed or criticized in former chapters.

Chapter 12
Heart Valve Substitutes

12.1 Introduction: Valve Explants

On 19/5/2005 a male patient, aged 44, underwent surgery for explanting his mitral bioprosthetic heart valve, which was malfunctioning, having become stenotic. The valve had remained in the patient's heart for 63 months. It was made out of bovine pericardium sheet, i.e., the membranous structure that envelopes the bovine heart, in the form of three cusps sewn on a low profile stent, produced from a polyacetal resin, while the sewing ring was coated with a carbofilm. Examination of the explant revealed ingrowth of vascularized tissue on the pericardial leaflets, as well as calcified areas in the leaflets. Furthermore, fibrotic tissue was present on the stent and the sewing ring. These alterations resulted in compromising the initial ideal matching of the cusps and the failure of the prosthesis. To state it in an other way: the failure of this prosthetic device was not due to material's failure but, rather, to harmful changes in the structure/architecture of the device, probably invoked by the interaction of the materials that the device was made of with the biological millieu of the patient, i.e., blood and surrounding cardiovascular tissues. Figure 12.1 shows a similar valve before implantation and after explantation. The failed explanted valve showed presence of vascularized tissue and calcified areas on pericardium leaflets. Abundant growth of fibrotic tissue on stent and sewing ring. Not perfect cusps matching.

On 20th December 2005, a female patient, aged 74, had her mitral monostrut tilting disc prosthesis explanted, after it being in place for 18 years. The clinical evidence necessitating the removal of this mechanical heart valve was severe stenosis. The materials used for this valve were graphite coated with pyrolytic carbon (for the disc), Haynes 25 (for the housing) and Teflon (for the sewing ring).[1]

All the materials of this explant were very well preserved, no macroscopic traces of wear were present. However, the device could not function properly because pannus had grown over the sewing ring on the outflow side of the valve, had extended onto the valve housing, therefore causing stenosis and hindrance of the proper movement of the tilting disc (see Fig. 12.2).[2]

[1] Haynes 25 is a Cobalt-based alloy, which includes Chromium, Tungsten and Nickel.

[2] Pannus, a term used to describe a flap of fibrous tissue, sometimes calcified, and vascularized.

J.A. Helsen and Y. Missirlis, *Biomaterials*, Biological and Medical Physics, Biomedical Engineering, DOI 10.1007/978-3-642-12532-4_12,

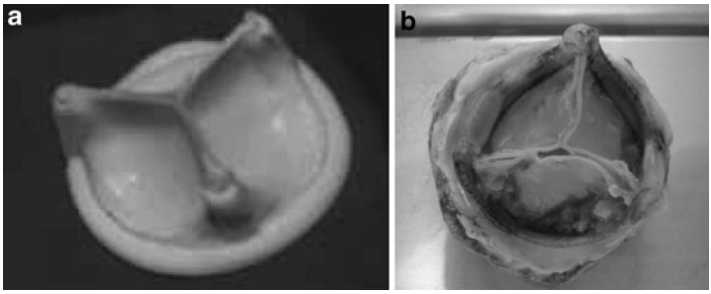

Fig. 12.1 Heart valve: (**a**) bovine pericardium valve before implantation; (**b**) failed explanted valve: presence of vascularized tissue and calcified areas on pericardium leaflets. From [382, 383]

Fig. 12.2 Explant monostrut tilting disc valve prosthesis. From [382]

Let us start, however, from the beginning. What are the heart valves and how they function, why they fail in their operation, why there is a need to replace failing valves and what kind of designs and materials are utilized for this purpose, and, very importantly, how the body reacts to the 'intruder'. The body does not like intruders, even if such intruders mean well: the body activates a long list of defence mechanisms against the intruders. Do we have the means to fool such defences?

12.2 The Natural Heart Valves

The four valves of the mammalian heart, the *aortic*, between the left ventricle and the aorta, the *mitral*, which is intracardial, i.e., between the left atrium and the left ventricle, the *pulmonary*, which separates the right ventricle from the pulmonary artery, and the *tricuspid*, also intracardiac, connecting the right atrium to the right ventricle perform their unique function of opening and closing, in response to pressure gradients, i.e., passively, 40,000,000 times each year throughout life, without stopping for maintenance or general repair.

A schematic of the valves in their anatomical position within the human heart is shown in Fig. 12.3. In diastole (left), the relaxing heart has its two atrioventricular

Fig. 12.3 A schematic of human heart valves in their anatomical position. *Left*: when the heart relaxes, the *aortic* and *pulmonary* valves are closed while the *mitral* and *tricuspid* are open. *Right*: when the ventricles contract: the opposite is true

valves open, and (right) the two valves which regulate the blood flow toward outside the ventricles closed. The opposite is true in systole (Fig. 12.3 [Right]) when the ventricles contract.

The two atrioventricular valves, the mitral and the tricuspid, are larger in cross-sectional area and consist of a number of *cusps, chordae tendinae* and *papillary muscles*. The cusps (three in the tricuspid and two main ones in the mitral valve) emanate from a mainly collagenous *annulus fibrosus* and are thin membranes consisting of collagen and elastin fibers embedded in a mucopolysaccharide matrix. The cusps move for opening or closing the valves on the action of the papillary muscles via the chordae tendinae.

The arterial or semilunar valves are quite different from the atrioventricular ones. They are totally passive (no direct muscle contraction involved) and the cups move to open or close the valves driven only by the pressure difference between the ventricles and the aorta or the pulmonary artery, respectively. The three cusps in each valve are also thin membranous structures consisting of collagen and elastin fibers embedded in a mucopolysaccharides matrix.

All vascular cusps are covered with endothelial cells, whose main role is to keep the flowing blood in its natural state, i.e., to prevent the underlying fibrous structures from interfering with thrombus formation mechanisms. Apart from the endothelial cells, few cells exist in the bulk of the cusps material, namely a few fibroblasts.

12.2.1 The Aortic Valve

Let us take the aortic valve as an example for further consideration. This particular valve consists of three anatomical entities, which function complimentarily.

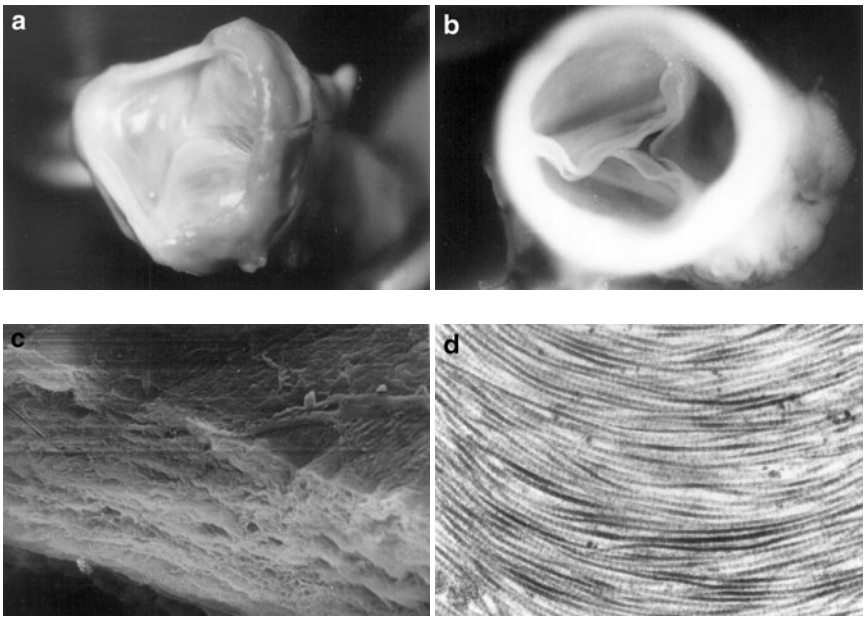

Fig. 12.4 A photograph of a relatively healthy human aortic valve is shown in (**a**), as seen from the ventricle's side under an aortic pressure of $P = 88$ mm Hg. The same valve is photographed from the aortic side at a pressure of $P \simeq 1$ mm Hg to show the waviness and coaptation of the 3 leaflets (**b**). SEM of a leaflet's cross-section (top layer is the ventricular side) at a magnification of 340x shows the multi-layered structure of the leaflet (**c**). A TEM (magnification 25000x) from the central part of the leaflet shows the directionality of the collagenous fibers (**d**)

They are the three *sinuses of valsalva,* the *aortic ring* (or annulus fibrosus) and the three valve *cusps* (or leaflets), as shown in Fig. 12.4. Each of these structures serves a partial but unique function, however, all three together are essential for the full operation of the aortic valve. The sinuses are three dilated pouches, much thinner than the arterial wall, of which are a continuation, and mainly utilized by the hemodynamics in their region to provide the heart muscle with blood, via the coronary arteries, and to aid the cusps in the closing process of the valve. The aortic ring (having a scalloped cross section) is a stiff collagenous structure which gives rise to the three cusps (which are thicker near the ring and thinner toward the center) and maintains the whole valve during systole and diastole in its anatomical position.

The three cusps are about equal in size, with an average thickness of 0.6 mm. Their area is such that, in the closed position they interrupt the blood flow completely, i.e., they cover a circular area of about 25 mm in diameter, and as they coapt together the thinnest part of the leaflets, from the ring toward the center (called lunulae) oppose each other and protrude in the aortic root.

As it was mentioned before, the composition of the leaflets is collagen and elastin, which form a multilayered and highly anisotropic and inhomogeneous structure (see Fig. 12.4c,d).

12.2.2 Aortic Valve Substitutes

There are several diseases, both congenital and acquired, that render the aortic valve incompetent. The clinical indicators which determine the decision for replacing a malfunctioning valve are not discussed here, as they are out of the scope of this textbook. We should bear in mind, however, that whatever the cause of disease, besides the valve, other structures may be adversely affected. That is to say that if the valve leaflets have been calcified probably the aorta is also calcified, meaning that an accommodation process has been going on for sometime and replacing the valve will leave the aorta still calcified, therefore stiffer, and that must be taken into consideration for choosing, for example, the proper valve substitute.

The last statement poses therefore the question: why are there different types of substitute aortic valves? How it all started? Which criteria are used for selecting one substitute valve over another? What is the role of the materials and/or the design in the overall performance of the valve in the recipient?

In the following, we shall attempt to address the above posed questions by focusing mainly on the biomaterials aspects associated with this particular situation.

Brief History and Development of Substitute Valves

The anatomy of the human heart valves was known at least since the Hellenistic times [384]. Leonardo da Vinci has produced remarkable human anatomical drawings, the valves also included [10]. A representative example of these drawings is depicted in Fig. 12.5. It was in 1931 that the topographic anatomy and histology of the valves of the human heart was described in a publication by Gross and Kugel [385]. However, it took another 25 years, i.e., until 1955 for heart valve replacement to be used clinically. Why this delay?

The reason was that to surgically operate on the heart, the heart itself could not operate as the pump of the blood circulation while at the same time the lungs could not serve their purpose for the gas exchanges of the blood elements. Therefore, an assist system to carry out these functions was necessary so that the surgeon could operate on the heart. The, so-called, heart–lung machine provided the solution to this problem. This *machine* receives the venous blood containing CO_2 just before entering the right heart, via a catheter. It pumps the blood through a *membrane oxygenator*, where gas exchange takes place, i.e., the CO_2 leaves the blood, while O_2 is loaded onto the blood by reacting with the protein *hemoglobin*. Then the oxygenated blood is pumped back to the patient's aorta. Figure 12.6 shows the first artificial oxygenator developed by the Gibbons.

The cardiac surgeon then, from the mid-1950s, could operate for a limited time on the heart. The time is limited by blood–material interaction and is discussed in Sect. 12.4. He could excise, for example, a malfunctioning valve and suture a substitute device in its place to perform the excised valve's function. What could such a device be?

Fig. 12.5 Leonardo da Vinci. The blood flow through the aorta (about 1513), brown ink on paper, The Royal Collection 2009, Her Majesty Queen Elizabeth II, RL 19082r. The explanatory superimposed signs (a–f) are after [10]. **a**: an aortic mould, **b**: experimental drawings to investigate "the true shape" of the valve, **c**: the right ventricle, **d**: the left ventricle with the aortic valve and vortices in the sinuses of Valsalva, **e**,**f**: texts describing the various drawings. (Q.II.10,r.) [386]

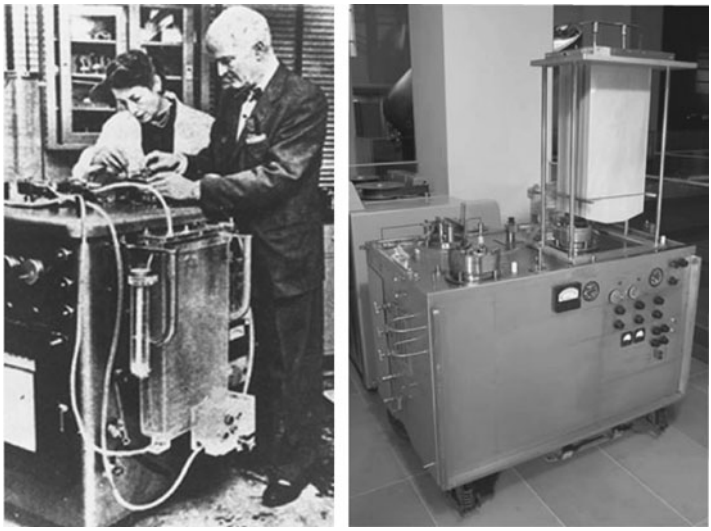

Fig. 12.6 Artificial oxygenator. Gibbon's heart–lung machine (1955)

One major stream of thinking is that if a system has been evolved through millions of years of trial and error, or adaptation, then it must have been optimized. Therefore, according to this way of thinking, if one has to replace a malfunctioning part of the system, one has to find an identical replacement or, if one has to design and produce this part *de novo*, one has to mimic as much as possible the "optimized," in our case natural, part.

Trileaflet Valve Substitutes

It is not surprising that the first attempts for substitute aortic and mitral valves were ready-made ones: either *homografts (allografts)* or *heterografts (xenografts)*.

An *homograft* is a valve taken from another human body cadaver. Several issues are relevant in this case: the health state of the donor valve, the time of valve collection after donor death, the means of *sterilization* and *preservation* until the time of operation, the surgical procedure for placement of the donor valve into the recipient's heart, availability and size-matching. While certain improvements in most of the parameters just mentioned have occurred in the last 30 years, such as *cryopreservation* which keeps the valve viable in a *valve bank*, and substituting not only the valve itself but the whole aortic root, their major drawback is still their limited availability. They are prescribed mainly for younger patients.

A xenograft was the answer to the availability problem. A xenograft is a preserved aortic valve removed from a killed animal (usually a pig, because the anatomy of the pig's heart is quite similar to that of the human, but also from elk, as they practice it in China) and mounted on a rigid or flexible cloth-covered frame.

Several preservation techniques have been developed and used, through these years, varying with respect to the chemical preservative (usually it is *glutaraldehyde*), the mechanical state of the animal valve during the chemical treatment, i.e., the process may be static or dynamic, low or high pressure, the processing time, etc. The xenografts are not viable valves and the action of the glutaraldehyde molecules, apart from preserving the tissue, is to crosslink the collagen fibers and therefore improve the mechanical function of the xenograft. Porcine xenograft aortic valves are widely used, especially for those patients for whom anticoagulation therapy is not recommended; however, their durability is limited due to, among other factors, the *calcification* of the tissue.

Instead of using naturally made valves from human or animal origin, another approach has been envisaged and materialized. First, as the human body has abundant membranous structures, why not harvest a small amount of such a membrane from the same patient who is to receive a valve. This is termed *autologous* tissue, and it has the obvious advantage of not evoking rejection reactions. It is cut into 3 pieces shaped after the patient's valve, which are then sutured on a clothed-covered frame or *stent* to make up a substitute bioprosthetic valve. Several attempts have been made along this thought and membranes such as the *dura mater*, the *peritoneum* and mostly the *fascia lata* (which surrounds skeletal muscles) have been tried. These valves have had limited use so far. One drawback seems to be that they are not on the *clinical shelf* ready to be used but they have to be constructed and placed on the patient almost at the same time. Along the same line, attempts have been made to use animal membranous tissue, especially *bovine pericardium*. As with other *bioprosthetic* valves, the latter have gone through various stages of improvement that had to do with the mounting stent (from rigid to flexible, from high profile to low profile, i.e., low overall height of the valve device), the glutaraldehyde preservation etc.

Some more considerations about animal-derived valves. Let us consider the two animal-derived valves and compare their similarities and differences. The porcine bioprosthesis (main trade names are Hancock, Carpentier–Edwards; see Fig. 12.7.) has an overall geometry (stereometry) designed by nature to serve the valvular function. In fact, this general shape is its major advantage, whereas the material properties of its tissue have been affected by the preservation technique. Some of these properties have been improved, in the sense of adapting them to human use while negative consequences may have resulted from the preservation (for instance, more prone to calcification) [387]. From the design point of view these valves may be thought of as designed by nature and technically modified. The bovine pericardium bioprosthesis (major trade names are Ionescu–Shiley and Carpentier–Edwards) has a similar geometry (tri-leaflet structure), however, the leaflets have been cut out of a nonvalvular tissue, they are equal in size, as opposed to nonequal size of natural valve leaflets, they are sutured on a frame, but as in the previous case the material properties of the tissue have been affected by the preservation technique. These valves are biologically derived but totally artificially designed (biomimetically).

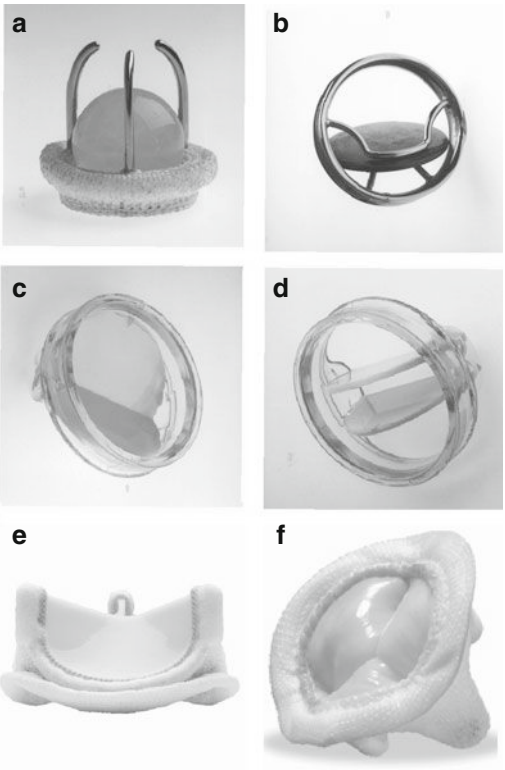

Fig. 12.7 Photographs of (**a**) ball valve (*upper left*), (**b**) disc valve, (**c, d**) model of St.Jude valve: open (*middle-left*), closed (middle-right), (**e**) Carpentier–Edwards PERIMOUNT Magna Aortic valve, (**f**) Hancock porcine bioprosthesis

At the same time that open heart surgery was made possible the plastics revolution was taking place. The ability of artificial polymeric materials to be processed in thin membranous films provoked the desire of the cardiac surgeons to use this easy-to-shape, flexible, overall 'manageable' material into forming a trileaflet artificial polymeric valve looking similar to the natural one. The general procedure was to select existing industrial polymers, known for their *strength*, flexibility and inertness, cast them (using appropriate stainless steel dies) as thin membranes that would approximate the shape and contour lines of the natural aortic valve leaflets in diastole and implant either single leaflets (in a few cases) or a total valve. *Polyurethane*, *Teflon*, *Silicone Rubber*, *Silastic*, *Ivalon* were all used in the early 1960s. The major problem associated with these early valves was their limited *durability*. In accelerated *pulse duplicator* (*mock circulation*) studies, as well as clinically, these valves failed quite early due to, among other factors, the *fatigue* and the subsequent rupture of the leaflets. How could this happen? Well, that is where *(bio)mechanics* come into the picture. That is where the necessity for an interdisciplinary approach to address

nonclassical topics in the sciences, in medicine, in engineering materialized in those days (1960s) and emerged as the discipline *biomedical engineering*.

The point in fact, in our case, is that it was not sufficient to reproduce artificially only the general shape and the overall operational mechanism of the valve using a thin, flexible, strong polymeric material. Careful histological examination of the natural aortic valve (Sect. 12.2.1) revealed a quite complicated structure of several *biopolymers*, at the same time being remodeled to a certain degree. Detailed mechanical testing of the leaflet tissue [388–390] furthermore produced evidence that the leaflets are mechanically *anisotropic*, inhomogeneous and that the opening and closing behavior of the valve depends on several factors, such as the dynamic pressure difference, the flow field in the vicinity, the mechanics of the aortic ring and the heart muscle. Consequently, if a homogeneous, *isotropic* flexible structure is constructed and put in operation, where the dynamics of the system required an *anisotropic* material, dysfunction leading to failure is not surprising. A corollary to such a conclusion, indeed an important one, is that eventually a candidate biomaterial to be used in a particular artificial organ should be evaluated not only as a 'material', i.e., physicochemical characterization, but in the environment of its designed use (in contact with blood, or bone etc.), the fluid or solid mechanics in the vicinity etc. We shall return to give a brief account of matters related to *soft tissue biomechanics* and *blood fluid mechanics* as they relate to the aortic valve.

Mechanical Valves

It was stated before that there may be other ways to design than simply copying Nature. Granted that (natural) optimization through evolution must have developed a reliable operating mechanism, invention is a major human (not limited only to humans!) exercise that has changed the course of humanity and the whole earth for that matter in unpredictable ways. The wheel is a relevant point. With reference to the development of substitute aortic valves, the problem was to develop a passive valve mechanism, i.e., opening and closing due to pressure difference driving forces. This artificial mechanism had to be contained within certain limits: to have a circular cross section 'seat' with diameter ranging from about 20–30 cm where, somehow, an occluding device could 'seat' and seal the passage or be lifted (and secured at a safe distance) to let the blood through. The first totally artificial (or mechanical as opposed to bioprosthetic) valve, which was successfully employed clinically and not having the trileaflet configuration was the *ball valve* (a well-known typical model is the *Starr-Edwards*). It consists of a spherical ball and an annular orifice, covered by a suturing ring. The ball is retained within a 3- or 4-legged cage arising from the ring (see Fig. 12.7a). The ball is made of *Silastic* (eventually problematic due to swelling, lipid adsorption, cracking etc.) or *stainless steel*, the annular ring and the cage were made of stainless steel and was bare or cloth-covered. There have been several versions of the original design.

Another family of mechanical valves are the single *disc valves*. A single thin disc, which is either hinged on the annular frame, or freely moving inside a wired cage or being restrained between two eccentrically situated support legs, is tilting up(down) to a certain angle (see Fig. 12.7b). The overall valve occupies less space than the ball valves, which is an advantage especially in the mitral position, and they are generally called also *low profile* valves. A typical representative is the *Björk-Shiley* one. The disc is made of either stainless steel or pyrolytic carbon. A modification of the single tilting disc low profile mechanical valve has been the development of the two tilting rigid semidisc valve, introduced as the *St Jude Medical*. In the open position the two semidiscs are in the vertical position with respect to the *annular ring, offering a minimum obstruction to the* blood flow and a mainly central flow. All the mechanical valves have the advantage of being quite durable due to the choice of materials (metals, ceramics). However, there are major disadvantages due to both the design and the materials used. These are: *nonphysiological blood flow* from the ventricle to the aorta and beyond; instead of central flow there is either peripheral flow or asymmetric one. Higher *pressure differences* exist in the full opened position, which in certain cases may overload dangerously the heart muscles. The existence of high shear stresses in the vicinity of the mechanical prosthesis and the mechanical interaction between the occluder (ball, disc, semidiscs) and the annular frame causes damage to the *red blood cells* (or *erythrocytes*) leading to *hemolysis*. Even if some designs lowered the hemolysis substantially the fact remains that erythrocytes are overstressed and strained leading to possibly adverse biological effects (such as release of substances, lower life span, etc.). A major drawback of all mechanical aortic valves is the risk of *thromboembolism*. This is due mainly to the materials used, with the overall geometry and the associated fluid flow behavior contributing toward thrombus formation. To reduce significantly thromboembolic risks, a life-time *anticoagulation* therapy is prescribed for the valve recipient. The mechanisms of thrombus generation by these valves will be discussed further in *blood–material interactions*. Problems of mechanical failure or *infection* have not as yet been eliminated either.

To recapitulate: Several designs and methodologies have been employed to develop heart valve substitutes. A brief outline of the first generation of such valves was presented including biologically derived or totally artificial devices. In all cases, there exist specific problems of durability, mechanical failure, calcification, thromboembolism, hemolysis and infection. The need to produce better substitute valves is everpresent. A general strategy to follow is to learn more about the mechanical properties of the natural valves and select accordingly treatments of biological tissues, or artificial materials that match those properties, if the aim is to develop a trileaflet valve. In addition, it is necessary to investigate the mechanisms of calcification, to design realistic experiments to assess the blood–material interactions. Furthermore, testing prototype new substitute valves in pulse duplicators and implanting them in appropriate animals will provide useful information before the preclinical and clinical trials begin. Therefore, a brief outline of the mechanical behavior of soft biological tissues, of the blood–material interactions and of the valve fluid mechanics is presented next.

12.3 Soft Tissue Biomechanics

Most soft biological tissues, including the heart valves, are composite structures consisting mainly of collagen fibers, elastin bands, mucopolysaccharides (or glucoseaminoglycans) and cells. Each tissue, and sometimes the same tissue at different anatomical positions is structured in a specific way underlying its ability to carry the anticipated dynamic loads during its operation. The simplest, and therefore the most frequently reported, experiment performed on soft tissues in vitro is the *uniaxial tensile* test. To perform such a test strips of tissue are cut out from an excised organ in standardized dimensions. Each strip is held by specialized grips, usually at 37°C and submerged in normal saline solution (0.9%) or kept wet in any case and is deformed at a constant rate along its main axis with simultaneous recording of the applied load and its dimensional changes. It is a property of the biological tissues to be *preconditioned*. That is before the tensile test is recorded a few cyclic tests up to a certain deformation should be performed to bring the tissue to a steady state. This state is determined when the area between the loading and unloading curves, being larger during the 1st cycle diminishes gradually until no more. The ensuing loading phase in depicted in Fig. 12.8a and b.

By defining stress (see also Chap. 1)

$$\sigma = \frac{F}{A}, \tag{12.1}$$

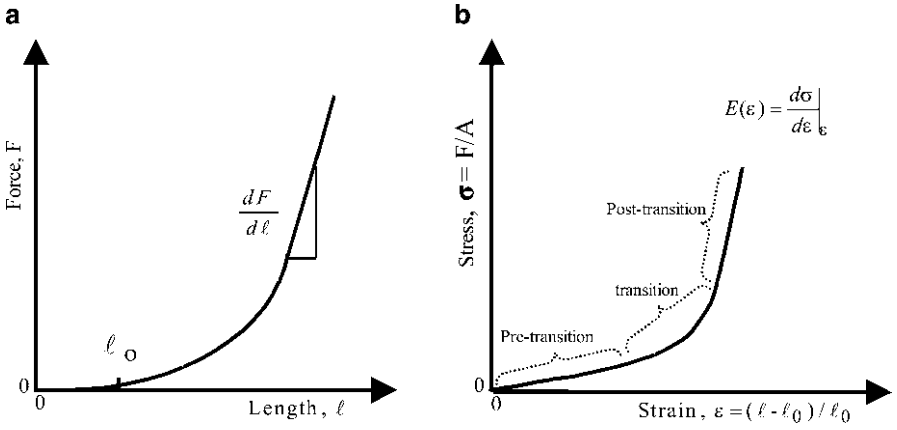

Fig. 12.8 (**a**) a typical uniaxial tensile test of a biological soft tissue strip, run at a constant strain rate, after preconditioning, shows the force-length relationship in the loading phase. (**b**) The stress–strain behavior of the same strip is derived from the force-length curve (A). Note that the elastic modulus of the tissue strip, $E = d\sigma/d\epsilon$, is a function of the strain, ϵ. The viscous effects are not considered. For simplicity, the nonlinear stress–strain curve is divided into 3 parts: the pretransition (approximately linear), the transition (non linear) and the post transition (approximately linear)

where A is the instantaneous cross-sectional area of the strip and assuming constant strip volume, V, during the test, i.e.,

$$V = A \cdot l = A_0 \cdot l_0 = const. \tag{12.2}$$

(l_0 is the zero stress length, l is the instantaneous length) the stress–strain curve (Fig. 12.8b) is obtained. Note that

$$\sigma = \frac{F}{A} = \frac{F(1+\epsilon)}{A_0}, \tag{12.3}$$

where $\epsilon = (l - l_0)/l_0$ is the engineering strain and the instantaneous elastic modulus

$$E(\epsilon) = \frac{\mathrm{d}\sigma}{\mathrm{d}\epsilon} = \frac{1+\epsilon}{A_0} \cdot \left(\frac{\mathrm{d}F}{\mathrm{d}l} \cdot l_0 + F \right) \tag{12.4}$$

This nonlinear behavior quite often is subdivided into 3 different phases (within the elastic region, before damage or nonreversible changes take place): the pretransition, the transition and the posttransition one. These phases correspond to the gradual recruitment of the structural components of the tissue as the load is applied. In pretransition, elastin is stretched while undulated collagen fibers do not pick up any load, they are straightened following the stretching of the elastin bands. During the transition, almost all collagen bundles are straight while in the posttransition the force is borne solely by collagen. The fact that the uniaxial tensile stress–strain behavior underlies the structural composition of the tissue (see legend of Fig. 12.9) is further demonstrated in Fig. 12.8, where strips cut at different directions from the same leaflet exhibit substantially varied elastic moduli. As the modulus was calculated at the posttransition phase of the stress–strain curve, where collagen fibers are loaded, the highest leaflet modulus is in the transverse direction; that is the direction that the vast majority of collagen fibers run (see Fig. 12.4). It is interesting to notice that the stress–strain behavior is substantially different from the simple basic relationship given in Fig. 1.6.

Several investigators have employed different approaches to relate the phenomenological mechanical behavior of soft biological tissues to its structure and constitutive equations have been proposed both for uniaxial and biaxial stress–strain relationships [390–393].

12.4 Blood-Material Interactions

As was stated earlier, one of the major drawbacks of the mechanical substitute heart valves is the need for permanent anticoagulation therapy to minimize the risk of thrombus formation. A brief outline of the events occurring during the interaction between an artificial device and the flowing blood is presented.

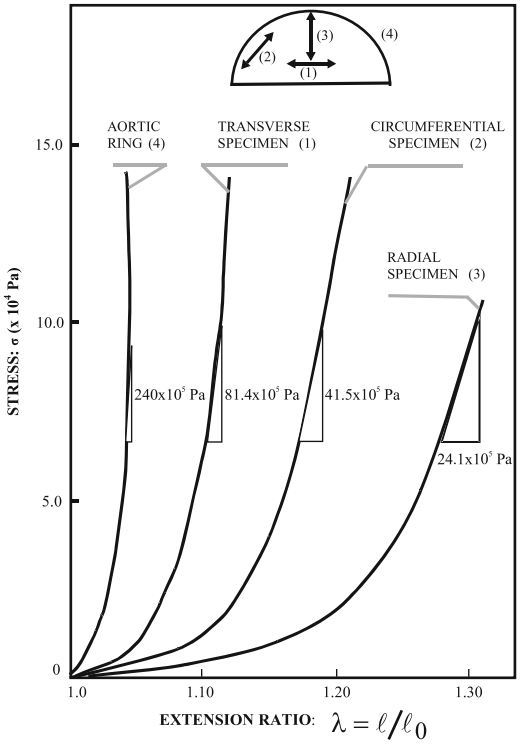

Fig. 12.9 The stress–strain ratio ($\sigma - \lambda$, where $\lambda = l/1_0$ and $\lambda = \epsilon + 1$) of three strips from the same aortic valve leaflet, cut in the directions shown in the schematic on the top of the diagram, as well as of a strip from the aortic ring are shown. The variation in the value of the posttransitory elastic modulus reflects the directional structural composition of the collagen in the valve. Data taken from Missirlis [388]

The natural reaction of the organism when a blood vessel is injured is to invoke the *hemostatic mechanism* to stop the loss of blood. This is materialized by a complex set of reactions involving cells and proteins of the blood and resulting in the formation of a *clot* or *thrombus*. The same process may be triggered if an artificial surface is presented to the blood stream. The rate of the processes and the amount of thrombus depend on the physicochemical character of the surface, the size of the device and the fluid mechanics of the region.

Blood is a complex tissue continuously circulating within the cardiovascular system, which consists of many kilometers of vessels varying in diameter from about 25 mm down to a few μm in the human body. As mentioned, the way these vessels are distributed is one of those magnificent examples of non-Euclidean order in Biology. It is done not necessarily for the sake of beauty but of efficiency (see page 8). At any moment, the average adult has about 5 l of blood with a continuous turnover of its components at different rates dependent on the particular demands. It consists of water, cells (erythrocytes, leukocytes, platelets), proteins, lipids, ions and other

transiently appearing molecules. The lining of the vessels consists of *endothelial cells*, which interact with the blood elements in such a way (for example by producing locally and diffusing into the blood stream certain constituents, if necessary) so as the blood is in a fluid state under normal physiological conditions. In that sense, the endothelial lining is considered as the perfect *nonthrombogenic* material. Blood has a pH = 7.40, a relative viscosity 2–4, relative density 1.05.

The *erythrocytes* are the most numerous cells in the blood. The average concentration is $5 \times 10^6\,\mathrm{ml}^{-1}$ and occupy on the average 40–45% of the total volume of blood (this value is also known at the *hematocrit*). Each erythrocyte, at rest, looks like a biconcave disc with central depressions on both sides, $2\,\mu\mathrm{m}$ thick, $8\,\mu\mathrm{m}$ in diameter, $90\,\mu\mathrm{m}^3$ in volume and $140\,\mu\mathrm{m}^2$ in surface area.[3] It is anucleated, consisting of an hyperelastic membrane (able to withstand uniaxial deformation of more than 100% elastically, but would rupture if its biaxial surface deformation, i.e., the increase in its surface area exceeded 4–5%) which contains a hemoglobin solution. In the context of erythrocyte-materials interactions, these cells do not adhere to surfaces, as for example platelets do. However, under certain stress conditions the erythrocytes may be damaged, their membrane may break with release of hemoglobin. Erythrocyte particles may then adhere to surfaces via their membrane glycoproteins. As erythrocytes contain significant amounts of *ADP*, which is a powerful *platelet aggregating* agent, even low-grade hemolysis may induce indirectly important blood (platelets)–material interactions. Another indirect way of influencing these interactions is through its flowing behavior. Because of their great numbers and their deformability, they collide during flow with platelets, leukocytes and proteins, driving them toward the surface. On the other hand, erythrocytes inhibit the *complement* activation in blood by binding and metabolizing the complement factor C3b.

The *leukocytes* (white blood cells) are nucleated cells. They are of various types and their size is from about $6\,\mu\mathrm{m}$ to more than $20\,\mu\mathrm{m}$ in diameter, their numbers in blood are between 5 and $10.10^3\,\mathrm{mm}^{-3}$. Many leukocytes leave the blood stream, when certain chemical messengers "inform" them, pass squeezing between endothelial cells and go to serve their purpose in inflammation, infection or wound healing situations. There are two classes of white cells: (a) the *granulocytes* or polymorphonuclear (PMN) ones, having inside them multilobe nuclei and granules and subdivided in *eosinophils*, *basophils*, and *neutrophils*. Neutrophils form the largest part of all leukocytes (60–70%). (b) *agranular* white cells which are either *monocytes* (mostly phagocytic) or *lymphocytes* (the second largest group, 20–30%, mostly involved in immunological reactions). The lifetime of leukocytes is from hours to days. In terms of leukocyte–materials interactions the mechanisms of their involvement are not very clear. However, it is known that they interact strongly

[3] On average, therefore, 25.10^9 erythrocytes circulate in the human blood stream. The life span of erythrocytes is approximately 120 days. Every second 3.10^6 erythrocytes are destroyed and replaced with new ones. Each erythrocyte has 300.10^6 molecules of hemoglobin, the protein that associates with 4 molecules of oxygen, O_2. Every time our heart beats, approximately 75 ml of blood is delivered to our body transferring $\sim 500.10^{15}$ molecules of bound O_2 to the tissues!

with the complement system as well as the coagulation and the fibrinolytic system. For example, stimulated monocytes express *tissue factor*, which can initiate the extrinsic coagulation cascade, while neutrophils may contribute to clot dissolution by releasing fibrinolytic enzymes (for example, elastase) [394].

Platelets (or thrombocytes) are the smallest class of blood cells. The nonactivated platelet is disc shaped, 2–4 μm in diameter, 10 μm^3 in volume. There are $2–4 \cdot 10^5$ platelets mm^{-3} in the human circulating blood. These cells are not nucleated but contain granules of certain substances in their cytoplasm and certain receptors in their membrane that make them very important for the process of arresting a bleeding by forming a platelet plug and catalyzing coagulation reactions. In particular, there are glycoproteins on the platelet membrane that are responsible for *platelet adhesion* (i.e., platelet adhering to a surface) or *platelet aggregation* (i.e., platelet adhering to another platelet). The phospholipids on the membrane accelerate coagulation reactions. Granules inside platelets contain the specific platelet proteins, *platelet factor 4* and *β-thromboglobulin*, proteins found in the plasma (*fibrinogen, albumin, fibronectin, factors V and VIII*), ADP, calcium ions, *serotonin* and lysing enzymes. Platelets are extremely sensitive cells and only a slight stimulation is sufficient to make them respond in different ways: they become sticky, they change shape with many pseudopods formed and they release different contents in response to different stimuli. In terms of their surface, interactions of great importance are the three processes: platelet adhesion, aggregation and activated release reaction.

If one separates the cells from the blood, the remaining fluid is called *plasma* (and if you still separate from plasma the fibrinogen you have a more clear solution, the *serum*). Plasma contains hundreds of proteins with a total mass of 70–80 $g\,l^{-1}$. In the following table (Table 12.1), the most important, as far as we know, proteins are listed, with their name, molecular weight and functional category they belong to.

To summarize: A brief summary of the blood constituents, cells and proteins, which participate in blood–material interactions was presented. The genetically programmed steady–state action of each blood element in the physiological (or even in certain stabilized pathological) range will be disrupted at the moment that the closed circulatory system is interfered with. When inserting a catheter, or lead the blood into extracorporeal circulation or fit the organism with a blood contacting artificial device, an alarm sounds and a series of actions by the blood elements start. The extent of blood element recruitment to deal with the new alarming situation, the race for the intrusion site, the competition or synergy of the various elements depend on the *material* surface they encounter and on the *device* as a structure.

The *material*, with biomolecules (such as albumin or heparin) grafted on its surface or not, should have the biomechanical properties necessary for the specific application and should be able to be processed to forms, shapes, and sizes appropriate to its final use. Of primary importance are of course its surface properties, as it is the surface that contacts the elements of blood and will interact dynamically with them. The surface properties are important for the initial contact with the blood so as to facilitate or hinder the initial chemical contact. Therefore *hydrophobicity* or *hydrophilicity*, *surface charge*, *polarity*, heterogeneity in the distribution of reactive chemical groups *(domains)*, *mobility* of the surface molecules, *smoothness*, etc. may

Table 12.1 Properties of plasma proteins

Name	Molecular Weight $\times 10^3$	Plasma concentration [μg/ml]
Intrinsic coagulation system		
Factor XII	80	30
Prekallikrein	80	50
HMW Kininogen	105	70
Factor XI	160	4
Factor IX	68	6
Factor VIII	265	0.1
VWF	$1–15 \cdot 10^3$	7
Extrinsic Coagulation system		
Factor VII	47	0.5
Tissue Factor	46	0
Common Pathway		
Factor X	56	10
Factor V	330	7
Factor II	72	100
Fibrinogen	340	2,500
Factor XIII	320	15
Complement Proteins (selected)		
C2	102	25
C4	200	600
C3	185	1,300
D	24	1
C5	190	70
C9	75	55
Cytokines		
Interleukin 1	13–17	
Interferon γ	20–25	
Immunoglobulins		
IgG	150	6–17,000
Fibrinolysis		
Plasminogen activator	69	
Albumin	66.5	35–45,000
Globulins		
Lipoproteins		
Protease inhibitors		

be important both initially and as they change with time, temperature, and evolving physicochemical environment.

The *device*, or the final product incorporating the biomaterial, should be used in the patient. It could be used for a relatively short time (minutes to hours), as with a catheter, a hemodialyzer, a blood oxygenator, or blood tubes used in extracorporeal devices, or it could be incorporated into the cardiovascular system permanently in the form of an artificial vessel, a heart valve, a left ventricular assist device, a total artificial heart, and in the future perhaps other artificial organs (lung, liver, etc.).

Thus, the flow conditions (shear rates, turbulence, secondary flows, etc.), duration of contact, size of the contact surface area, and actual placement site in the cardiovascular system are very important parameters to be considered, in addition to the surface finish due to fabrication and sterilization effects.

It is generally accepted that the first step of the interaction process between blood and artificial surfaces is the adsorption of plasma proteins. Subsequent events involve platelet and leukocyte adhesion and aggregation, and activation of the coagulation system, as well as the fibrinolysis and complement systems, resulting eventually in the formation of a *thrombus* on the artificial (e.g., polymer) surface. More specifically, the nature of the artificial surface, under specific hemodynamic conditions, may promote:

- Specific plasma protein *adsorption* with resultant activation, denaturation and/or desorption.
- Platelet *adhesion* and *activation* with release of active substances that are important in platelet *aggregation* leading to thrombus formation.
- Hemolysis.
- Leukocyte adhesion, *spreading* and activation, with further involvement of the inflammatory and complement systems.
- Interaction with other blood components, such as lipoproteins, trace plasma proteins, *inhibitors* of activated plasma proteins, and adhesive proteins (fibronectin, thrombospondin).

It should be noted that each of the above systems is quite complex in its own interaction with foreign surfaces and, as all the plasmic components, proteins and cells, interact among themselves, the complexity of the events becomes enormous. It should once more be emphasized that here we deal only with the complex interactions during the *initial events* at the *interface* and not the long-term effects at the site of implantation or elsewhere in the body.

It is almost axiomatic that when protein solutions are put into contact with solid surfaces, adsorption occurs. However as there are many different plasmic proteins with great variations in size, concentration, and purpose, it is logical to ask: What is the composition of the protein layer that is laid down on different surfaces in contact with blood? Is there a preference for specific proteins to be absorbed depending on the type of surface? Does the composition on a particular surface change as a function of time? And what happens to the proteins that get adsorbed: do they simply bind to the surface, do they undergo (after binding) different types of transformation, for example denaturation, changes in their biological activities... ?

Among the general conclusions that have come out of protein adsorption studies are the following [395]:

- Most proteins are adsorbed on most surfaces.
- The relative amounts of the different proteins vary from surface to surface.
- Many proteins (when whole blood is used) become degraded. This may be due to proteolytic enzymes derived from damaged cells.

- The Vroman effect is seen on most surfaces. This is the turnover at the same surface site of one protein by another as time progresses, which also may later be replaced by a third.
- Many proteins may be deposited at their own times (and conditions of flow) that have not yet been investigated.

Blood Coagulation and Fibrinolysis

When blood is exposed to damaged tissue or to an artificial surface, blood *coagulation* takes place, which comprises a series of consecutive enzymatic reactions (a cascade) that leads to the conversion of *fibrinogen* into a *fibrin clot*. Intimately associated with coagulation is the process of *fibrinolysis*, the enzymatic breakdown of fibrin (usually by *plasmin*). The dynamic steady state of coagulation and fibrinolysis maintains the patency of the circulatory system. Fibrin formation is a major contributor to thrombosis. There are two pathways for coagulation, which at a certain level merge into a common pathway.

The *intrinsic pathway* is triggered by collagen or other subendothelial components (or negatively charged surfaces) that on contacting factor XII activate it into factor XIIa. In this process, two other plasmatic components are involved as well, high molecular weight kininogen (HMWK) and kallikrein. Factor XIIa activates factor XI into XIa, which in turn, in the presence of Ca^{2+} activates factor IX into IXa. Then IXa in the presence of platelet membrane phospholipids, Ca^{2+}, and factor VIII converts factor X into Xa. This activated factor Xa, together with factor V and in the presence of Ca^{2+}, binds to platelet membrane phospholipids. The complex formed (sometimes referred as prothrombinase) catalyzes factor II (prothrombin) to *thrombin* (factor IIa). There are positive feedback mechanisms involving thrombin and the previous reactions, where factors V and VIII are involved.

The extrinsic pathway is triggered by tissue thromboplastin (made available either by subendothelium or by stimulated leukocytes, or by activated endothelial cells). Thromboplastin in the presence of Ca^{+2} complexes with factor VII to activate X into Xa. This is a point of convergence with the intrinsic pathway.

The generation of thrombin, therefore, is the key point of both coagulation pathways to make the final coagulation product, i.e., fibrin fibers. As it is the case in most situations, the process of activation of the circulating clotting factors has a counteraction. Indeed, there are a number of naturally occurring protease inhibitors, including antithrombin-III (AT-III). Deficiency of AT-III in a patient is associated with an increased risk of venous thrombosis.

Fibrinolysis also follows intrinsic or extrinsic pathways and depends on the plasma protein *plasminogen*.

In summary if an artificial or natural surface, negatively charged, comes in contact with blood, coagulation is initiated. This contact system of coagulation consists of four proteins: factors XII, XI, prekallikrein and HMWK. Activation of the contact system initiates the intrinsic and extrinsic coagulation pathways, intrinsic fibrinolysis, and the complement, kinin and renin–angiotension systems.

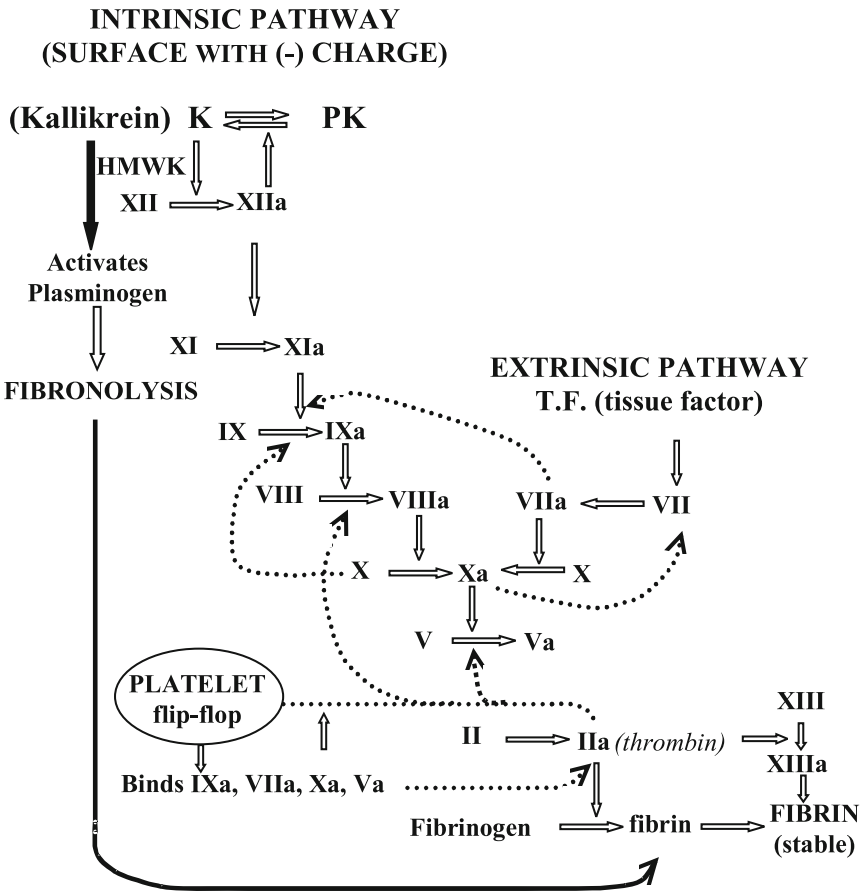

Fig. 12.10 The coagulation cascade involving the intrinsic, extrinsic and common pathways leading to the formation of fibrin

The plasma proteins involved in contact activation have been identified by studying the reaction in rare individuals with specific protein deficiencies. Figure 12.10 shows all the above cascading reactions in summary.

12.5 Anticoagulants

As the name implies, anticoagulants are chemical substances that, when present at a particular concentration in blood about to be coagulated either via the extrinsic or the intrinsic pathway, interfere with the coagulation process so that no clot is formed and the blood continues to be in the fluid state. In this way, thrombus formation is hindered, the risk of thromboembolism is minimized; however, the patient on

anticoagulants is at a high risk of bleeding, if vessel trauma occurs (for example, internal hemorrage in a car accident). Another class of chemicals may interfere with the role that platelets play in thrombus formation and they are termed *antiplatelet* drugs.

Heparin is one of the most important anticoagulants associated with artificial organs. Heparin is a *proteoglycan*, i.e., a combination of protein and polysaccharide. It has a linear polypeptide chain with linear polysaccharide side chains. As essential feature of a heparin molecule to act as anticoagulant is a pentasaccharide unit which has negatively charged roots such as –OH, –NH and especially $–SO_4$. Heparin is found in many mammals and commercially it is produced mainly from porcine mucosa and bovine lung. As a macromolecule has a range of molecular weights, from 1,700 to 30,000, the final manufactured product is provided usually as a heparin salt with Na^+.

The mechanism of its anticoagulant activity is catalytic. As you recall from the coagulation mechanisms, thrombin is the final factor (protease) that catalyzes the fibrinogen to fibrin polymerization reaction. This thrombin activity, however, is inhibited by serine protease inhibitors, which circulate in the blood plasma. One of those inhibitors is AT-III. It has been found that the rate of the thrombin–antithrombin reaction increases by 10^3 in the presence of heparin on whose molecule both the inhibitor AT-III and the protease (thrombin) bind. Actually when AT-III binds on to heparin, its conformation changes so that its reactive site is more accessible to thrombin. When the complex heparin-thrombin-AT III is formed, heparin is released from it.

Heparin molecules with molecular weight less than 3–4,000 do not exhibit this catalytic action. However, these lower M. W. heparin molecules catalyze the inhibition of the factor X_a by the AT-III. In fact, there is a growing interest in the use of low M.W. heparins in many clinical situations, such as after surgery, so as to reduce the risk of venous thromboembolism caused by the high doses of regular heparin.

There exist other protease inhibitors, such as *heparin cofactor II* whose action is catalyzed by heparin (which inhibitor predominates depends on the concentration of heparin, among other parameters). Heparin-like action is produced also by similar compounds, such as *heparin sulfate* and *dermatan sulfate*, which are found on the surface of many cells.

Similar anticoagulant activity by inactivating thrombin is achieved by *hirudin* which is secreted from the buccal glands of leeches. Hirudin has been manufactured synthetically as well.

Heparin is used clinically in extracorporeal blood handling devices, as in hemodialysis, in certain surgical interventions and as a surface attached substance in artificial organs that come into contact with blood. Because heparin cannot be absorbed through the gastrointestinal mucosa it is delivered intravenously. In situations, therefore, that chronic anticoagulation therapy is required, for example when a patient is fit with a mechanical heart valve, the anticoagulation drug cannot be heparin. In such cases, oral anticoagulants are prescribed. Many such oral anticoagulants have been synthesized as derivatives of the compound *4-hydroxy coumarin* (dicumarol, warfarin, etc.) [396]. Their mechanism of anticoagulation action is quite

complex but it suffices to say that they are antagonistic to vitamin K which in a certain form is necessary to activate the coagulation factors II, VII, IX and X.

Heparin is also used in vitro when blood is withdrawn from the body and collected in plastic bags for transfusion or retrieval of cellular or proteinous components by separation techniques, or in tubes for clinical analysis in hematological labs or to run experiments for blood–material interactions (if blood is placed in a glass tube it will clot in 4–8 min). Other anticoagulants used in vitro are the *ethylenediamintetraacetic acid (EDTA)* and the *trisodium citrate* which are chelating agents that bind Ca^{2+}. As it has been mentioned previously Ca^{2+} (along with phospholipids) accelerate many times the conversion reactions to produce the activated factors in the coagulation cascade. The difference between EDTA and citrate is that EDTA causes some injury to platelets so that their aggregation is prevented and therefore the blood sample drawn into EDTA can be used for platelet counting (carried usually in an electronic particle counter).

Depending on a particular test that should be carried out sometimes a mixture of anticoagulants may be used. It is also noted that apart from anticoagulants there exist *fibrinolytic* and *thrombolytic* (such as *plasminogen*, a_2*-antiplasmin*) drugs, as well as *antiplatelet* drugs, such as *aspirin*.

In summary it is noted that with regard to testing blood–material interactions, which are complex and involve many cells and proteins, care should be taken to use a particular anticoagulant, for a particular time, at a specific concentration.

Heparin is used in another way as well. Alone or in combination with albumin or urokinase is adsorbed/bound onto the surface of polymeric biomaterials in order to improve their hemocompatibility [397].

12.6 Blood Flow Through the Heart Valves

Certain serious problems and complications associated with the clinical use of artificial heart valves include thromboembolism, hemolysis, tissue overgrowth and damage to the endothelial tissue lining in the vicinity of the valves. These problems are directly related to the hemodynamics (fluid dynamics) in the valvular region [398]. Other associated problems such as tissue overgrowth, infection, tearing of sutures, valve failure due to material fatigue or chemical change are indirectly related to the fluid mechanics.

Knowledge, therefore, of the blood fluid mechanics in the vicinity of the natural valves, including the pressure difference across the valve, the velocity profile at the outflow, the development of disturbed flow regimes (flow separation, vortices, etc.) provide useful information in understanding the mechanisms of opening and closing of the valves.

In order to obtain such information in a healthy human subject or in an animal (in vivo) measuring probes and sensors should be inserted in the blood stream for accurate monitoring. Such a procedure is certainly impossible for healthy humans and quite cumbersome accompanied with adverse effects in the animals. Of course

some direct information has been obtained during diagnostic procedures but to be able to get large amounts of data, especially when a new artificial valve is to be evaluated, physical models simulating the relevant parts of the cardiovascular system have been built and fluid dynamical studies, experimental and computational, of valves are carried out [399].

As was described in Sect. 12.4, blood is a very complex fluid; actually it is a suspension of viscoelastic particles (cells) in a liquid (blood plasma). The description of flow of blood within the cardiovascular system is very complex, and it is beyond the scope of this textbook. However, a few remarks are necessary here to appreciate the reasons for this complexity and, at the same time, to be aware of the limitations present when using simplified expressions to ascertain the interactions between heart valve function and associated blood flow.

The basic relationship to describe the movement of a fluid inside a tube, i.e., to relate the velocity profile resulting from a pressure differential is the Navier–Stokes equation:

$$\rho \mathrm{d}U/\mathrm{d}t - \eta \Delta^2 U + gradP = O, \tag{12.5}$$

where ρ is the fluid's density, η fluid's viscosity, u the velocity vector and P the pressure.

If the following assumptions are made, namely: the vessel is cylindrical (circular cross section), the vessel walls are nondeformable, the flow is steady-state, and the flowing fluid has a constant viscosity, the Navier–Stokes equation is simplified and results in the velocity profile at any cross-section as follows:

$$U = (-\Delta P)R^2/4\eta L[1 - (r/R)^2], \tag{12.6}$$

where L is the length of the vessel and r the radius of the vessel having a value between 0 and R.

Integration of this equation over the cross-sectional area results in the volumetric flow rate

$$Q = \pi(\Delta P)R^4/8\eta L \tag{12.7}$$

If, next, the generated flow is not steady, but results as a consequence of a sinusoidal imposition of pressure, i.e., $\Delta P/L = A \sin \omega t + B \cos \omega t$, where A and B are constants ant ω is the frequency, the velocity profile is of exponential nature with respect to time and the space parameters are associated with Bessel functions.

If, further, it is assumed that the vessel wall is deformable, and its movement is linearly elastic, i.e., the material characteristics of the wall are explicitly characterized with a single parameter E, the elastic modulus, the resulting velocity profile, and the volumetric flow are of the form:

$$U = A \sinh(f(r)) + B \cosh(f(r)) \tag{12.8}$$

$$Q = C \sinh(f(r)) + D \cosh(f(r)). \tag{12.9}$$

It is apparent that as we add more realistic configurations to this set of assumptions, attempting to mimic the real system of blood flow through the cardiovascular

loop, the mathematics of the governing equations will become more complex, numerical methods have to be employed for the solution of the equations, and there are excellent references on computational fluid dynamics (CFD) dealing with this issue.

From a practical point of view with respect to evaluating the performance of heart valves, however, the situation is much simpler. What is considered important as far as the operating quality of a prosthetic heart valve is concerned is the relationship between the pressure drop across the valve, ΔP in mm Hg, and the mean systolic ejection flow rate, Q in ml s^{-1}.

In 1951, before the prosthetic valves entered the clinical scene, Gorlin and Gorlin published an article that contained the formula for the calculation of cardiac valvular orifices from flow and pressure-gradient data [400]. Actually, it was developed to assess the resistance to flow, as a natural valve developed stenosis leading to a higher pressure drop (gradient). The formula is as follows:

$$VA = Q/44.3C\sqrt{\Delta P}, \tag{12.10}$$

where VA is the valve orifice area (cm^2), Q the mean diastolic ejection flow (ml s^{-1}), C a factor depending on whether the valve is aortic ($C = 1$) or mitral ($C = 0.85$) and ΔP the mean diastolic gradient (mm Hg).

This formula, and many variations of it, has been used ever since either to assess the valvular function in vivo, or to evaluate the performance of prosthetic valves in vitro, i.e., in cardiovascular mock circulation systems.

Figure 12.11 shows a picture of such a mock circulation system, used for routine measurements of prosthetic heart valves and bloodpumps, developed at Missirlis's laboratory. Similar devices have been utilized at the Helmholtz Institute of the RWTH-Aachen (www.ame.hia.rwth-aachen.de).

12.7 Epilogue-Future

In a perspective note titled *The Development of Prosthetic Heart Valves – Lessons in Form and Function* the article starts as follows [401]:

> The 2007 Lasker Award for Clinical Medical Research, granted in mid-September to Albert Starr and Alain Carpentier, recognizes their extraordinary contributions to the development of the prosthetic heart valve, which represents a milestone in the journey toward the fabrication of synthetic living tissues and organ systems. The prosthetic heart valve was built on a foundation laid down during the first half of the twentieth century with the introduction of cardiac catheterization by Andr Cournand and Dickinson Richards, the development of innovative surgical techniques by Alfred Blalock, the invention of the heart-lung machine by John Gibbon, and the discovery of heparin by Jay McLean and dicumarol by Karl Paul Link. In the late 1950s, as clinical practice was being linked more closely to the surgical laboratory and collaborations were established with those working in the nascent field of biomedical engineering, new intellectual and technical frameworks were created for replacing dysfunctional organ components with biologic or synthetic prostheses.

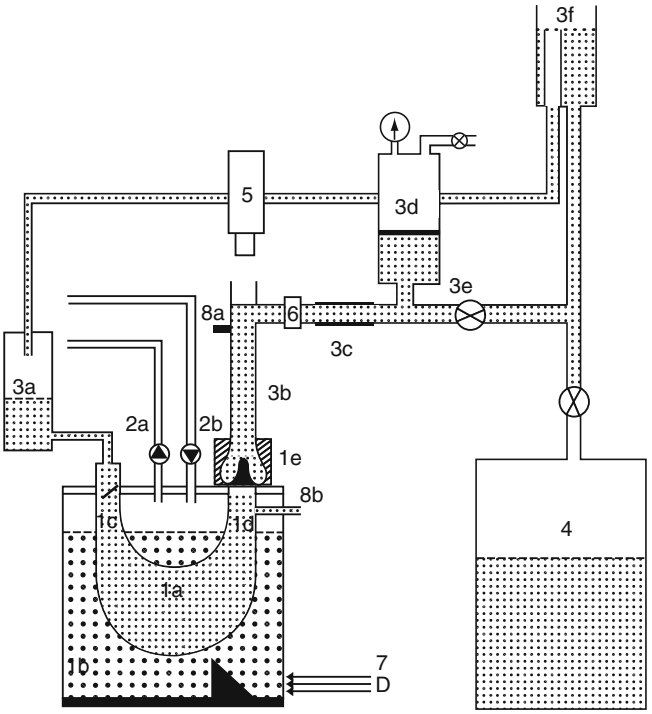

Fig. 12.11 Schematic diagram of a pulse duplicator system for fluid-dynamical testing of aortic heart valves. 1a: silicon rubber sack. 1b: rigid closed outer vessel. 1c: inlet valve (mitral position). 1d: valve under test (aortic position). 1e: rigid transparent model of aortic root, with three Valsalva sinuses at 120° between them. 2a and 2b: solenoid valves (inlet–outlet) for the compressed air. Simulation of left atrium (3a), ascending aorta (3b), aortic compliance (3c), variable peripheral compliance (3d), variable peripheral resistance (3e), overflow tank (3f). Reservoir (4), videocamera (5), electromagnetic flow probe (6) and back-light source with 45° mirror (7). (8a) and (8b) are pressure monitoring ports. Reprinted from D.Mavrilas (Ph.D. Thesis, University of Patras, Greece, 1991)

It concludes by stating that:

> Valve-replacement surgery has dramatically altered the natural history of valvular heart disease, affecting the lives of millions of patients. Limitations of the current technology will continue to drive the field toward new, minimally invasive and endovascular approaches for valve delivery. Valves that have the capacity for growth and self-repair, especially suited to the treatment of congenital heart disease, may be within reach through the application of tissue-engineering strategies.

In the following chapter, the concept of tissue engineering and regenerative medicine will be addressed with key example the vascular grafts and heart valves.

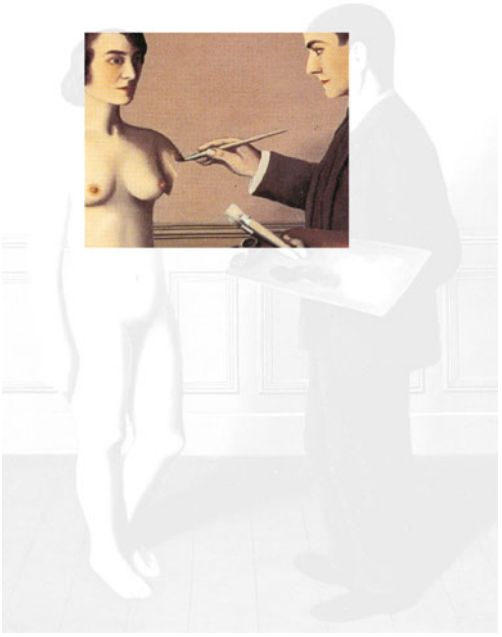

René Magritte (1898-1967)
La tentative de l'impossible (1928)

The ultimate dream of the bioengineer: makable human body parts or . . . just dream?

Chapter 13
Tissue Engineering: Regenerative Medicine

13.1 It Has Been Described Before!

The Greek poet Hesiod (Eighth century B.C.) has given us, in his Theogony, examples of interesting cross-breeding creatures, such as the Lernea Hydra, which was born as the third offspring of Echidna and Typhon. This Hydra was multiheaded and had the capacity of *immediate* regeneration of a severed head. Actually, according to the story, in the place of one cut head the regeneration produced two (a siamese analog?), and Heracles had to ask the help of Iolaos to stop the regeneration process by denaturing the biological molecules (severed necks) through the application of heat (Fig. 13.1).

Another, very prophetic, example of regeneration, described in the same text more than 2700 years ago, is presented as a mode of punishment: that of Prometheus being chained on a mountain rock and an eagle eating his liver every day, while it had to be regenerated within 24 h so that it could be eaten up again, and so on. Prometheus was punished by Dias, the king of gods in this way, because he had stolen the fire from Olympus and had given it to the mortal people. Nevertheless, it was again Heracles who saved Prometheus from his perpetual martyrdom.

Almost everyone is aware, and many people all over the world have observed that in various species of salamanders, after a limb is cut off, regeneration of that limb takes place. Recent studies have further revealed that a salamander can regenerate limbs, tail, jaws, ocular tissues, intestine and parts of the heart [402]. The mechanisms responsible for this great versatility in the regenerative ability of the blastemas of salamanders are under intense investigation, and in general, the regenerative properties of salamanders have been identified as autonomy, scaling, and plasticity.[1]

The regenerative ability of salamanders, and of other animal species, such as fish, echinoderms, etc. is currently under intense investigation, as, apart from its intrinsic interest in understanding the process at the molecular level, it may offer

[1] Blastema is a mass of undifferentiated cells, such as the mound of mesenchymal stem cells at the end of a limb stump, capable of growth and regeneration into an organized structure.

J.A. Helsen and Y. Missirlis, *Biomaterials*, Biological and Medical Physics, Biomedical Engineering, DOI 10.1007/978-3-642-12532-4_13,

Fig. 13.1 *Hercules killed Hydra together with Iolaos.* Painting by Sebald Beham (1500–1550). Heading of the painting: *Hercules una cum Iolao Hydram occidit 1545.* Private collection

important insights into the possibilities of regenerating a complex structure in adult vertebrates [403].

In the meantime, the medical needs of an ever increasing and aging population, along with the concomitant surge of all kinds of accidents, necessitating a greater supply of artificial organs or replacement tissues and organs, have prompted the emergence of a novel discipline aiming at achieving, at least partially, this aim. The name of this discipline is *Tissue Engineering*, one version of which is called *Regenerative Medicine*.

13.2 Basic Scheme of Tissue Engineering

Whereas the classical biomaterials science aims at developing biocompatible materials to be used in artificial organs, either as permanent replacement of malfunctioning organs or as temporary devices for supporting vital functions, a different strategy is employed in tissue engineering. In this case, the biomaterials used serve a different purpose, that of being the carrier of biological entities, i.e., cells and biomolecules at a targeted site in the body for the purpose of biomanufacturing a new tissue or organ. A classical textbook on this subject has already its 3rd edition [404].

The basic principle involved here is that the tissue or organ to be generated at a preselected site within the body will be the result of the manufacturing process of the right cells. Therefore, the right selection of cells is the crucial issue. An ever-expanding research effort is going on in the biology and biotechnology of *stem cells*, adult or embryonic, of *progenitor cells*, of the procurement site, of the methods of expansion, of desired differentiation, and, as far as we are here concerned, of the

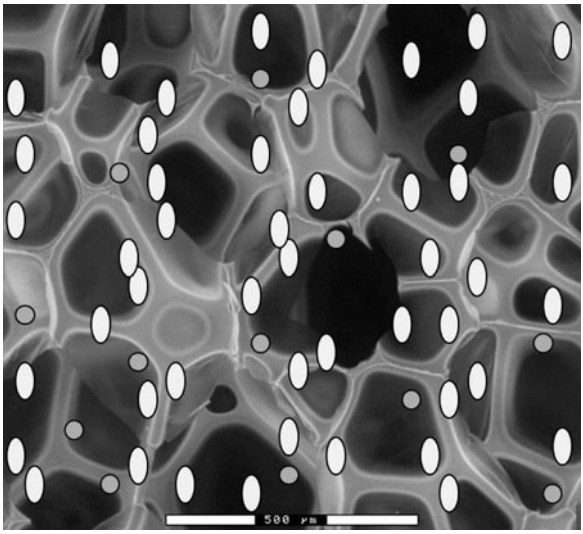

Fig. 13.2 The basic 3 units/materials for a tissue construct, a biodegradable scaffold (*light gray*), the tissue cells (*empty oval*), and the biomolecules (*circles*) acting as facilitators for the interaction of the scaffold with the cells. Adapted from http://vascuplug.teltow.gkss.de

delivery of these cells to the targeted area. An abundance of pertinent literature surveys is published [405, 406]. At the same time, as it happens so often when the initial enthusiasm overrides our better judgement, the need to better understand the process of angiogenesis, stem cell science, and the utilization of molecular biology and systems biology tools has emerged as mandatory for a deeper comprehension of tissue development and control [407].

A simplified scheme for tissue engineering, involving biomaterials, is the following: *(3D porous biomaterial scaffold) + (cells) + (growth factors) = (tissue construct)*. An example is shown in Fig. 13.2. This scheme implies that fully organized and mature tissues must be created *ex vivo*, outside the body. Subsequently, these tissues have to be transplanted and functionally integrated in the needed site. Such a strategy involves three great challenges: (1) generation of functional tissues, (2) transplantation in a manner that preserves their viability and function of the cells, and (3) biological and mechanical fixation and integration with surrounding tissue [405].

While a few cases involve thin tissue grafts, such as skin or corneal tissue, therefore not necessitating the existence within the graft of a vascular system for the transport of nutrients and products of metabolism, and cartilage is physiologically avascular, the majority of applications requires three-dimensional structures as well as a developed functioning vascular system for the survival of the graft.

Of course, the three key players in this story: scaffolds, cells, and biomolecules, are in a constant dialogue and interrelate to each other in particular ways for each specific tissue or organ. We shall briefly examine them separately, with emphasis on the scaffolds.

13.3 Scaffolds

Three-dimensional scaffolds with a specific interconnecting porosity are of crucial importance for the purpose of tissue generation and engineering. The mechanical properties of the construct, its shape and its material properties are designed such as to prevent an initial invasion of the surrounding tissues (if the scaffold is implanted for tissue generation in vivo) and to integrate with the rest of the tissues at the appropriate time. The internal surface of the scaffold provides the cells with the necessary space to migrate, to attach, to survive and proliferate, and eventually to differentiate into the needed cell phenotype. At the same time, the voids within the scaffold, due to their initial porosity and as a result of a desired degradation process, provide the space where new tissue formation and initial remodeling of such tissue as well as vascularization within this tissue occur.

A wide variety of materials and designs has already been available both for experimentation and in clinical use. We shall present here a brief summary of the key issues that relate to the design of a scaffold for a particular application. A recent review on the subject is available [408]. These issues are: material(s), porosity and architecture, surface chemistry and topography, mechanical properties, degradation kinetics, and fabrication techniques.

13.3.1 Materials

In a few cases, metals, such as titanium, tantalum and some alloys, have been used as scaffolds (see Chaps. 6, 7 and 8). These metallic scaffolds (except magnesium ones) and some ceramic ones do not degrade and remain permanently at the implant site. However, while their stability may provide durability in certain settings, there is an intrinsic disadvantage for their use. Their presence may stress shield the adjacent newly produced tissue which in turn may result in tissue loss, mechanical failure at the interface and, in case removal is deemed necessary due to infection for example, the whole implant, scaffold and newly formed tissue may be lost.

Tissue-derived materials such as allograft bone, skin, intestinal submucosa, xenogenic or allogenic heart valves, have also been used as scaffolds. All of them have to become decellularized and treated in a way, that only the matrix remains, thus creating an architecturally desirable porous structure for that particular situation. These scaffolds are essentially made of the *extracellular matrix* (ECM). However, some decellularized scaffolds implanted in humans demonstrated a strong inflammatory response and structural failure [409].

Natural biomaterials including collagen I, gelatine, silk protein (fibroin), fibrin, alginate, hyaluronan, chitosan (chitin), and extracellular matrix models (Matrigel), as well as plan-derived biopolymers, for example soy-based or starch-based, are utilized.

Synthetic water-insoluble polymers or copolymers are also used. Poly(L-lactic acid)(PLLA), poly(DL-lactic acid)(PDLLA), poly(lactic-co-glycolic acid)(PLGA),

polyglycolic acid(PGA), poly(caprolactone)(PCL), polytyrosine carbonates, poly (vinyl alcohol)(PVA), poly(ethylene oxide), or PEO-based materials are the major families already adapted or being further developed. Combinations of poly(ethylene glycol)fumarate, being hydrophilic, with polypropylene fumarate, or polycaprolactone fumarate, both being hydrophobic and with load bearing capacities, have been also utilized [410].

Especially for bone regeneration ceramics or mineral-based matrices are used as scaffolding materials: hydroxyapatite (HA), tricalcium phosphates, calcium sulfate are some examples. Due to intrinsic properties as brittleness and low resorption rates, they are combined with natural or synthetic polymers to produce polymer/ceramic nanocomposite scaffolds [411]. HA has been combined among others with PLA, PLGA, PCL, polyamide, polyethylene, gelatine, collagen, chitosan, PMMA.

All the above categories of materials are biodegradable and their degradation kinetics will be discussed in Sect. 13.3.5.

13.3.2 Porosity and Architecture

It is rather obvious that the bulk material(s) to be used as scaffold have to provide space for the biological entities, cells and biomolecules, to enter, colonize, travel, and occupy the interior of the 3D structure. Furthermore, they have to do their job, to create new tissue and new blood vessels, to receive nutrients and get rid of metabolic products, and eventually to connect to the rest of the healthy tissue of the organism.

The scaffold, therefore, must have an architecture that gives its structure the desired mechanical properties (see Sect. 13.3.4) and a porosity of particular size(s) with interconnectivity among the pores. Most scaffolds are designed so as their internal porous structure of voids are interconnected through channels between 10 and 1,000 μm. Actually, there is a hierarchical way of producing the void space from nanometer to millimeter scale with the scope of balancing the conflicting demands of their mechanical function (strength, more material) and the mass transport requirements (permeability, diffusion, etc.) [412].

The pore size for most bone ingrowth settings is between 150 and 500 μm [405]. The larger the pore size the deeper the penetration of the cells. However, a systematic study has not been reported so far.

The geometrical characteristics of the pores is also an important issue. Depending on the application and the structural stereometry of the physiological tissues as revealed, for example, by the inorganic structure of the trabecular bone or coral formations, and on the fabrication technique (see Sect. 13.3.6 as well as Chap. 7), many irregular, foamy creations have been used. Obviously, despite the positive and informative results originating from the experimental use of such designs, the nonreproducibility aspects of such formations cannot serve as a predicting cue for further development. The use of computational topology design and solid free-form(SFF) fabrication has made it possible to create scaffolds with controlled architecture [412]. This concept is extensively treated in Chap. 7 and is further illustrated in Fig. 13.3.

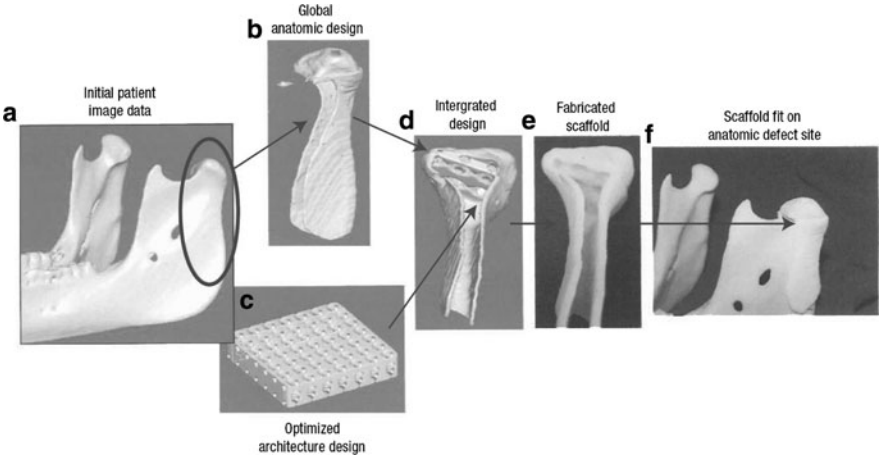

Fig. 13.3 Image-based procedure for integrating designed microstructure with anatomic shape. (**a**) A CT (as shown here) or MRI scan serves as starting point for designing scaffold exterior. (**b**) The scaffold exterior shape is created with additional features for surgical fixation. (**c**) Architecture image-design is created using CTD. (**d**) Global anatomic and architecture design are integrated using boolean image techniques. (**e**) SFF is used to fabricate design from degradable biomaterial, in this case SLS was used to fabricate a PCL scaffold (fabricated scaffold created by Suman Das). (**f**) Final fabricated scaffold fits well on the intended anatomic reconstruction site. Reprinted with permission from [412]. Copyright 2006 Nature Publishing Group

13.3.3 Scaffold Surface Chemistry and Topography

When the cells meet the scaffold surface and 'negotiate' with it by a cohort of interactions serving the cells' best interests, they never 'see' a pristine surface, i.e., one that has been formed during the fabrication of the scaffold. The material surface becomes coated with water molecules, ions, proteins, lipids, and the dynamics of the adsorbed molecules produce a 'new' surface that mediates the response of the cells (see also Sect. 12.5) for the plasma proteins interactions with materials. This means that the cell surface receptors will interact with whatever part/epitope of the particular protein(s) exposed at the exact time of their interaction.

The biological fluids, blood, saliva, spinal or synovial fluids, etc. contain a very large amount of different proteins, in different concentrations, and of varying importance in terms of their adsorption properties, whereas the cells themselves present hundreds of distinct membrane receptors. The cells, to perform their task (see also Sect. 13.4.1), have to attach themselves on a surface and, physiologically, this attachment involves specific interactions between the cell receptors and ligands presented in the extracellular matrix. Extensively studied are the interactions between fibronectin, a protein found in many extracellular matrices, one that likes to adhere better to hydrophilic than hydrophobic surfaces, and integrins [413]. Integrins are a family of cell receptors found in a variety of tissue cells. Based on this knowledge,

many attempts have been made to increase the interaction of cells with the scaffolds by precoating the scaffold surfaces with fibronectin or laminin.

The cells do not just probe the chemistry of an intended landing surface. There is plenty of evidence that the surface roughness, or topography, and in particular, nanostructural features (10–100 nm) influence the way that cells explore the attachment possibilities, for example by producing pseudopodia ([414, 415]). Nanotopography might influence the diffusion process of important biomolecules that may affect, in turn, the probing of the landscape by the cells. However, the mechanism(s) by which the cells "feel" the nanofeatures of surfaces is not clearly understood.

13.3.4 Mechanical Properties

There are at least three different aspects associated with the significance of the mechanical properties of the scaffolds, as they are related to the function of the cells and the new tissue being built. First, from the moment of implantation the scaffold must be integrated mechanically to the tissue/organ environment, i.e., it must stay in place, bear the recurring loads, adapt to the deformations and fluid shear stresses. In certain cases, it has to be fixed with internal fixation techniques (see Fig. 13.5). Second, the scaffold should operate at the implantation site in a way such as to provide the appropriate mechanical signals to the attached complexes of protein–cells in order for the cells to produce the expected extracellular material. Furthermore, the mechanical cues from the dynamical behavior of the scaffold should act as attractive signals for the desired flowing cells to become attached to the available scaffold surface. Third, and this is related and amplified in the next subchapter, as the scaffold degrades with time, its remaining mechanical properties (moduli of elasticity, strength, toughness, etc.) in association with the mechanical properties of the newly formed tissue should create the right mechanical environment for the continuation of the regeneration process.

These mechanical requirements are desired of course, but little is known about the time-dependent parameters (cellular interpretation of mechanical signals, degradation kinetics in vivo, as well as of other biological reactions, such as inflammatory responses, which are not dealt here) of the multiplex dynamic environment, which is created during and after the implantation, involving also the wound healing process. This is one of the main reasons why so many different materials, designs, and processes are found in the literature: lack of detailed knowledge leads to the trial-and-error approach. Nevertheless, the effort is continuing, and some aspects of the particular problem, that of how the architectural structure of the scaffold at all levels, from the nano- to the macroscopic one, modulates the material properties of the scaffold bulk materials is gaining both experimental and computational attention [412].

13.3.5 Degradation Kinetics

There are several issues concerning the fate of the scaffold within the body. Apart from the rate that it loses its mechanical properties, as mentioned earlier, the rate of chemical degradation, usually by hydrolysis, determines the nature and the concentration of the degradation products that initially are produced within the construct environment. These products will be further degraded or removed from the site. Both initial degradation material and further broken down to lower molecular weight entities influence directly the behavior of the cells (possible toxicity), or indirectly, by effecting the local acidity (pH and ionic strength). These effects depend on the concentration of the degradation products and the rate of their clearance from the site.

In vitro experiments to study the degradation phenomenon under various environments, most notably under dynamic loading conditions in simulated body fluid (SBF), have resulted in information on the relationship of mass loss and molecular weight decrease as a function of time, and on the possible mechanism of degradation [416, 417]. However, in recent years, it has become more evident that, even in controlled conditions, the mechanical (due to fatigue damage for example) and chemical degradation of the same polymer can vary substantially between species, individuals, anatomic locations, and clinical settings [405].

When polyesters, such as polylactides and polyglycolides, and their copolymers, having been used extensively in many applications: bioresorbable sutures and surgical meshes, osteosynthetic screws and plates, experimental scaffolds, degrade, they produce eventually lactic acid and glycolic acid. These materials are the final metabolic products in physiological metabolic pathways, therefore harmless for the organism, as long as their concentration is within certain limits. However, if the degradation of a scaffold produces at a certain time a high concentration of, say, lactic acid, that would create a profound decrease in pH with concomitant deleterious effects to the cells in the neighborhood. A linguistic 'play with a word' might be appropriate here: in the Greek language *pharmako* means medicinal drug and *pharmaki* means poison! The same chemical could be a drug or poison depending on the concentration!

The blending of gelatin with chitosan to form scaffolds showed, upon degradation in the presence or absence of lysozymes, an effect on both the amount of degradation and the pH decrease, when compared with pure chitosan scaffolds [418]. Other examples of naturally derived scaffolds, such as ECM scaffolds derived from porcine urinary bladder, or liver, when degraded by acid, resulting in low-molecular-weight peptides, demonstrated an important antibacterial activity against clinical strains of *Staphylococcus aureus* and *Escherichia coli*. These results, in combination with reported resistance of biological scaffolds composed of ECM to deliberate bacterial contamination in preclinical studies in vivo, might suggest that several different low-molecular-weight peptides with antibacterial activity exist within ECM [419].

Of particular significance is the case of scaffold matrices loaded with particular biomolecules, and designed in such a way that they release their biomolecules for

an intended biological purpose upon matrix degradation. Examples of this type of application will be dealt with Sect. 13.4.1.

13.3.6 Fabrication Techniques

Knowledge from physical chemistry, materials science, process engineering, laser technology and recent innovative technological techniques has been used for the construction of scaffolds. Traditional methods of fabricating scaffolds include *solvent-casting and particulate (salt or ice crystals)-leaching, gas foaming, thermally induced phase separation (TIPS), fiber meshes/fiber bonding, melt moulding, emulsion freeze drying, solution casting and freeze drying*. These methods create isotropically distributed voids and connecting pores, much like in a sponge, but have been largely unsuccessful in controlling the internal architecture to a high degree of accuracy or homogeneity [405, 420].

Currently, rapid prototyping techniques or SFF fabrication technologies are used with the aim of creating scaffolds with identical internal architectures so as to facilitate the mechanobiological characteristics of the construct. These technologies include stereolithography, selective laser sintering, fused deposition modeling and three-dimensional printing (see Chap. 7 and [412, 420]). Representative examples of both traditional and solid free-form (SFF) fabrication techniques are shown in Figs. 13.4 and 13.5, respectively.

In attempting to mimic the ECM, composed largely of collagen fibers in the range of 50–500 nm in diameter, considerable effort has been devoted in producing

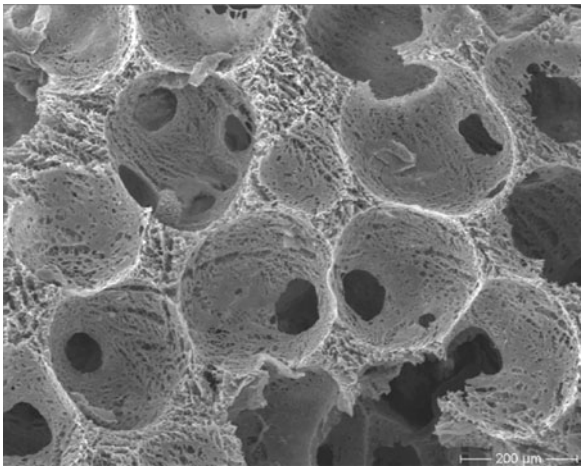

Fig. 13.4 SEM photograph of a poly-lactic-glycolic acid copolymer foamy scaffold with almost spherical pores, 280–315 µm in diameter, produced by leaching of paraffin spheres. Smaller surface and porosity features can also be seen. Adapted from http://vascuplug.teltow.gkss.de

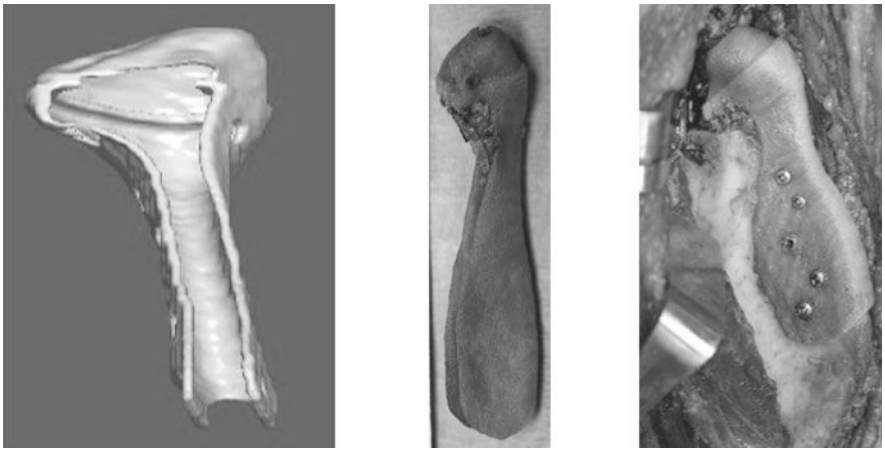

Fig. 13.5 A designer scaffold, made from a minipig computer tomography(CT) scan providing the data for the fabrication of the polycaprolactone (PCL) scaffold (see also Fig. 15.3). Implantation of the scaffold to replace the minipig's condyle (shown at the picture at right) has been secured by screwing it to place. Adapted from http://www.mem.drexel.edu/biomanufacturing. Reprinted with permission from Nature Publishing Group

nanofibrous scaffolds for tissue engineering. The methods used are (a) *electrospinning*, where an electric field is used to draw a polymer solution from an orifice to a spinning collector, producing fibers with diameters in the range of nanometers to micrometers, (b) *molecular self-assembly*, in which supramolecular architectures are formed, utilizing noncovalent bonding, electrostatic, and hydrophobic interactions [421], and (c) *specific TIPS technique*, comprising polymer dissolution, phase separation and gelation, solvent extraction, freezing, and freeze-drying under vacuum [411]. The fiber assemblies, produced by these techniques, should subsequently be treated with particulate leaching or other porogenic techniques for the formation of the necessary interconnecting pores.

As probably expected, combination of fabrication techniques are also used to create either polymeric-ceramic nanocomposite scaffolds, for example by soaking a prefabricated polymer scaffold in SBF in order to allow nanoscale apatite crystals to grow onto its pore surfaces [411], or by using a layer-by-layer self-assembly technique, to deposit gelatine on polylactide nanofibers, or combining 3D fiber depositing (periodical macrofibers) with electrospinning (microfibers), each type of fibers serving a complementary purpose [411, 422].

Some protocols on specific scaffold fabrication technologies can be found in a recent publication [423].

13.4 Biomolecules and Cells

13.4.1 Biomolecules

Having the desired scaffold is a prerequisite for placing it in the right biological environment, either in a bioreactor or directly at the implantation site. The various features of the exposed surfaces of the scaffold material will attract the necessary biomolecules which will serve as cues/signals for the attachment, migration, proliferation, and desired differentiation of (usually) tissue progenitor cells as needed.

In some cases, especially in scaffolds produced as gels, the various biomolecules are incorporated in the scaffold material during the fabrication process, and they are designed to be exposed at the surface or released from the scaffold, as it is degraded.

A third option is a combination of all necessary ingredients, i.e., scaffold materials, biomolecules, and cells, being delivered to the implantation site at once. As an example, an injectable, in situ hardening calcium phosphate cement(CPC) composite scaffold, made from tetracalcium phosphate [TTCP: $Ca_4(PO_4)_2O$] and di-calcium phosphate (DCPA: $CaHPO_4$), incorporating a fast dissolving mannitol porogen and slow dissolving chitosan fibers, for the creation of a time-dependent in situ porosity, is the first ingredient. The second ingredient was a model protein (protein A) for the 2 intended growth factors to be used clinically, i.e., bone morphogenetic protein-2 (BMP-2), and transforming growth factor-β (TGF-β). The kinetics of availability of protein A from the mixture of CPC and chitosan were found similar to reported in the literature kinetics of BMP release from similar mixtures. The third ingredient cells, had to be delivered within the whole scaffold and to be protected initially, during the setting/hardening of the CPC-chitosan cement. Alginate was used as an encapsulating gel to protect the cells. The alginate hydrogel beads served three functions: (1) as a vehicle to deliver cells and nutrients into CPC-chitosan and CPC-chitosan-mesh composites; (2) to protect the cells from environmental changes during cement setting; and (3) to generate a porous structure in CPC via subsequent degradation of the hydrogel beads [424].

Main issues involving biomolecules in the tissue engineering context relate to (1) which biomolecule(s) for a particular application, (2) how it is delivered/presented to the appropriate cells, and (3) what are the kinetics of release and availability, when the delivery to the site is through nanoparticles.

Locally delivered growth factors, such as BMPs, fibroblast growth factor-2 (FGF-2), and vascular endothelial growth factor (VEGF) can target specific cells. These molecules and other small bioactive peptides may be presented to the cells by covalent linking to the surface, thus providing more control over their conformation and their release rate, or, especially many soluble proteins, are encapsulated in a variety of bioresorbable micro- or nanoparticles (liposomes, alginates, PLLA, PLGA, silk fibroin...) or conjugated to gold nanoparticles and leach out of the particles in the immediate neighborhood of cells, within the pores of the scaffold. Alternatively, proteins can be bound to the surfaces by nonspecific surface

interactions, via dip-coating or lyophilization, as it is the case with two clinically used products for improving bone healing (Infuse; Medtronic Sofamor Danek, Memphis, Tennessee, delivering BMP-2, and OP-1 Device; Stryker Biotech, Hopkinton, Massachusetts, delivering BMP-7) [405].

In those cases that is necessary to deliver the biomolecules encapsulated, either for initial protection from enzymatic attack or for controlling their release into the scaffold milieu the encapsulated material plays an important role as well. A recent study showed important differences over spatial and temporal controlled delivery of two recombinant human growth factors, bone morphogenetic protein 2 (rhBMP-2) and insulin-like growth factor I (rhIGF-I), from PLGA vs silk fibroin microspheres incorporated within an alginate gel, thus influencing the differentiation of human mesenchymal stem cells (hMSCs) [425].

When bioinert surfaces of scaffolds are grafted with bioactive peptides, or other pertinent biomolecules, cell recruitment from a pool of cells can be controlled. The peptide REDV interacts with endothelial cells but not platelets, fibroblasts, or smooth-muscle cells, whereas the peptide KRSR, which interacts with osteoblasts but not fibroblasts [426]. This approach becomes important when different cells have to cohabit a particular space to generate specific tissue (such as bone) and the appropriate vasculature for the metabolic support of the newly formed tissue.

Combination of different biological factors are also being tried, including growth factors, drugs and genes [411, 427].

13.4.2 Cells

In a recent editorial, on the origins of the terms *Tissue Engineering* and '*Regenerative Medicine*' [428], reference is made to one of the pioneering attempts in tissue engineering of a 'living skin equivalent' published in *Science*, in 1981 by Eugene Bell, utilizing collagen (as scaffold) and fibroblasts, as the appropriate 'living' cells.

The choice of tissue-specific, fully differentiated cells, from the donor, to be used as the tissue generators within predetermined favorable conditions, appropriate scaffolds and growth factors in vitro, or delivery of cell suspensions at the intended site in vivo, is laden, however, with inherent limitations. Such cells, for example keratinocytes and dermal fibroblasts, have very limited ability for self-regeneration, and this accounts for the eventual failure of an initially promising engrafment of a skin autograft [429].

What was the reason, however, that some dermal autografts exhibited varying degrees of successful engrafment? A plausible explanation has to do with the presence or absence, within the cell suspension employed, of stem or progenitor cells. The long-term success of a skin graft depends on the appropriate rate of replenishment of stem cells in the graft.

The question therefore arises: what are the stem cells? and why are they important? The stem cells are distinguished from all other cell types by two characteristics. First, they are unspecialized cells capable of renewing themselves through

cell division, sometimes after long periods of inactivity. Second, under certain physiologic or experimental conditions, they can be induced to become tissue- or organ-specific cells with special functions. Detailed information on stem cells, on the difference between embryonic and adult (or somatic) stem cells, on their potential therapeutic possibilities, etc. can be found on the webpage http://stemcells.nih.gov/info/basics.

Stem cells are present in all adult tissues and are critical to tissue health, maintenance, and response to injury or disease throughout life [405].

13.5 Tissue Engineered Heart Valves

In Chap. 12, the subject of clinically available heart valve substitutes has been dealt with, covering many aspects on materials, function, and interactions with the surrounding living host tissues. It was emphasized that several critical problems, associated with either the mechanical or the tissue valves exist, such as the need for continuous anticoagulation therapy, calcification and tissue overgrowth, infection and immunological reactions against the foreign materials, and possible thromboembolisms. For these reasons, with the early encouraging results of tissue engineering applications, such as the skin, the setting was ready for research into applying tissue engineering principles to develop viable, heart valve substitutes with a thrombo-resistant surface and a viable interstitium with repair, remodeling and growth capabilities. If the results of such research efforts were successful, it would benefit immeasurably the pediatric patient in need for valve replacement, as it is obvious that the valve has to grow in harmony with the rest of the organism.

As it was mentioned earlier (Sect. 13.4), there are two major strategies in tissue engineering: one involves the generation of the replacement tissue ex vivo, while the other utilizes the direct implantation of appropriate scaffolds/matrices at the pertinent site for potential cell ingrowth and remodeling in vivo. Matrices used for the latter approach included de-cellularized tissues derived from pericardium or valves or small intestine submucosa, fibrin gels, or biodegradable synthetic polymers, such as PGA, PLA, polyhydroxyalkanoates (P3HB). Despite the fact that such scaffolds, when implanted in humans, showed growth of host cells and no calcification, they exhibited a strong inflammatory response, resulting in their structural failure [430].

The in vitro attempts for tissue engineering heart valves follow the classical paradigm presented in Sect. 13.2. Namely, autologous cells are harvested from the patient and are cultured/expanded in vitro. Afterward, when a sufficient number of cells are available, these cells are seeded onto appropriate biodegradable heart valve scaffolds. The third stage, before implantation, is the placement of the seeded scaffolds in a bioreactor with operating conditions such as to enable tissue formation and maturation.

Therefore, in order for the whole operation to be successful, one has to choose the right autologous cells, the appropriate scaffold and the optimal bioreactor operating conditions. Different sources of cells have been used by various investigators. We

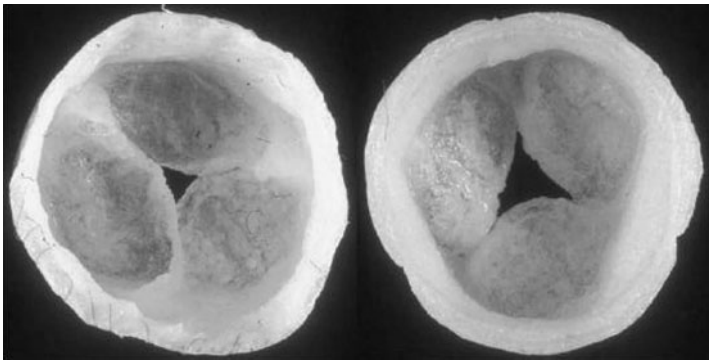

Fig. 13.6 Photographs of a tissue-engineered heart valve after 14 days conditioning in a bioreactor (view from ventricular and aortic side). reprinted with permission from S.P. Hoerstrup et al., *Functional Living Trileaflet Heartvalves Grown In Vitro* [Circulation, 102:III-44-III49,200]. 2000 American Heart Association, Inc

have to bear in mind that the thin living leaflets of a valve need two different types of cells: fibroblasts, which are responsible for the production and maintenance of the leaflet matrix (collagen, elastin, mucopolysaccharides), and endothelial cells, which cover the whole leaflet surface and provide for the hemocompatibility. For human applications, cells have been derived from the vasculature, from bone marrow, from blood, from umbilical cord, and from chorionic villi, although other sources, such as skin have also been used [430]. Figure 13.6 shows a picture of a tissue engineered heart valve.

It has been reported, however, that the valvular interstitial cells (VICs, mainly fibroblasts) have a complex phenotype, and that the quality of the remodeled valvular extracellular matrix (ECM) depends on the VIC viability, function and adaptation. The nonviable VICs are deleterious! VICs are often damaged during processing of tissue valve substitutes [431].

13.6 Vascular Grafts

In a recent, rather provocative but insightful, paper, our attention is brought to the fact that synthetic vascular grafts are used in clinical practice for almost half a century with mixed success [432]. *Mixed* refers in this particular case to the fact that large diameter prostheses, used in aortic and iliac surgery, have performed impressively well, whereas smaller diameter grafts usually fail.

Let us start, however, by stating the problem and the available solutions. Vascular diseases, both at the heart and in the arterial tree (periphery), are very common among most of the people, as they grow older. The most common vascular disease is atherosclerosis, meaning hardening of the arteries, through the accumulation of fatty deposits, cholesterol crystals and calcium salts on the inner lining of the vessel.

When the accumulation reaches a critical point, the regional hemodynamics become highly disturbed and may lead to thromboembolic events, or organ failure and death. Another, less common but serious nevertheless, situation arises when the wall of the artery becomes thinner, due to trauma, or genetic conditions or other medical reasons, the vessel bulges (aneurysm), and is prone to rupture, leading to internal bleeding that most often leads to death.

In both situations, the diseased part of the aortic vessel needs medical intervention. Depending on the severity of the disease, the site, the vessel diameter, and on a host of other medical indices, the treatment may be one of the following:

1. Surgical excision of the diseased part and replacing it by suturing an autologous part of a vein or artery, also surgically excised.
2. Replacement of the excised diseased part by suturing a synthetic vascular graft.
3. Nonsurgical intervention, by placing a stent intraluminously to the atherosclerotic site, using a catheter, and letting the self-expansion of the stent restore the blood flow by opening the lumen.
4. In specific cases, especially in abdominal aortic aneurysms, a stent-graft is utilized. A stent-graft is a synthetic graft, as in case 2, supported at the outside with a metal mesh.

In this section, we shall review the biomaterials aspects of the cases 2 and 3, as well as the current research on developing tissue engineered vessel grafts. One more note: the surgical treatment involving the first two cases, 1 and 2 is also called bypass surgery.

13.6.1 Synthetic Vascular Grafts

Several polymeric materials have been tested for manufacturing vascular grafts. The ones most currently in use are from polyethylene terephthalate (known as Dacron), expanded PolyTetraFluorEthylene (ePTFE), and Polyurethanes (PU) [433].

Polyethylene terephthalate $[O–C=O–C–C_6H_6–O–C=O–CH_2–CH2–]_n$ is a polyester in the form of filaments, which may be either woven or knitted into vascular grafts. The woven grafts have small pores, while the knitted ones, formed by the velour technique (looping fibers together) have larger pores. The large pores facilitate and promote tissue ingrowth, and the whole structure is more compliant, but there is a price to pay: due to the pore size leakage may be a serious problem, especially at high pressure sites, and for this reason it is necessary to *preclot* prior to use the knitted Dacron grafts with albumin, gelatine or even blood to prevent seepage. While the biological coating may degrade over 2–3 months Dacron itself is nonbiodegradable. Dacron is highly crystalline, has a tensile strength of 170–180 MPa and a tensile modulus of 14 GPa. It is used mainly as aortic and large diameter peripheral bypass grafts. A photograph of a Dacron graft with a main large arterial part leading to two ‘daughter’ iliac arteries, smaller in diameter is shown in

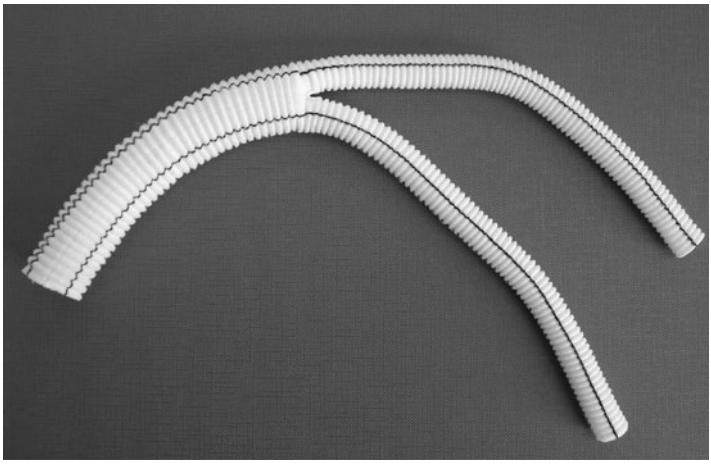

Fig. 13.7 A photograph of a bifurcating Dacron vascular graft. The structure is corrugated to allow for expansion when placed in vivo. The black line is for X-ray identification

Fig. 13.7. To improve its resistance to infections, silver-coated polyester grafts have also been employed.

Polytetrafluoroethylene $[–(CF_2\text{-}CF_2)–]_n$, PTFE or Teflon, becomes of a more microporous nature (standard pore size is 30 μm) by extrusion and sintering to form the so-called expanded PTFE (ePTFE). ePTFE is also nonbiodegradable, with an electronegative luminar surface that renders it antithrombotic. The electronegativity, and thus the improvement of its antithrombotic properties, especially an antiplatelet effect, is enhanced further by carbon-coating, or heparin attachment (see Chap. 12). Heparin can either impregnate the ePTFE grafts, or be bound covalently, to provide a controlled release, or to be attached to fibrin glue on the grafts. Teflon is also highly crystalline (>90%) but less stiff than Dacron, having a tensile strength of 14 MPa and a tensile modulus of 0.5 GPa. It is widely used as lower limb bypass grafts.

Polyurethanes $[–NH–O–C{=}O–R–]_n$ contain urethane groups –NH–CO–O– and depending on the composition of their hard and soft segments exhibit tensile strengths from 20 to 90 MPa (much more compliant than either Dacron or Teflon), while their tensile modulus ranges from 5 to 1,150 MPa. Both polyester urethanes and polyether urethanes have been shown to degrade in vivo, this fact being a major disadvantage to this otherwise promising biomaterial. A newer version of PU was based on carbonate linkages, having, that is, no ester linkages that have been prone to oxidation. A poly(carbonate-urea)urethane (Cardiotech®) was found to be resistant to hydrolytic and oxidative stresses [434].

Apart from the above-mentioned three categories of stable, nonbiodegradable (at least with the intention of being so) polymeric materials, another class of materials, which are intended to degrade in the human body has been used for vascular grafts. The rate of degradation of such biodegradable polymers depends on several

parameters, the porosity being an important one. The tacit implication in this situation is, of course, that the biodegradable grafts will be replaced by ingrowing tissue in such a way as to balance the loss (due to degradation) of the polymeric material by replacement of the appropriate tissue that the organism, through the pertinent cells will provide. It is important that during this remodeling process the overall mechanical properties of the construct will remain patent, and no aneurism will develop. Polymers that are used in this mode are the polylactic acid (PLA), the polyglycolic acid (PGA), the polyhydroxyalkanoate (PHA), and polydioxanone (PDS). These biodegradable polymers have been used in single component grafts, but improved function has been demonstrated with the synergistic effect of at least two of them, such as PLA-PGA mixes (see Sect. 13.3).

Summarizing the above, and without presenting clinical data, which can be found in [432, 433], it suffices to say that the synthetic polymers with or without surface modifications perform rather satisfactorily as replacement grafts for higher diameter vessels (>5–6 mm), and more so at high flow rates regimes [432, 433]. For small diameter synthetic vascular grafts (<5 mm), and especially at locations of low blood flow rates and high resistances the patency is very poor. Strategies to increase the patency, either by using various protein coatings to minimize blood–material interactions, or by seeding their lumen with endothelial-like cells to create a 'living' hemocompatible lining have shown some improvement, however problems with chronic inflammation and bacterial colonization still persist.

13.6.2 Stents

In a recent editorial addressing the best possible choice between a bypass graft (for the particular medical case, not a synthetic but an autologous vessel), involving surgery, and percutaneous coronary intervention with stents the conclusion was that a multicenter, randomized, and structured in such a way as to have as criterion the patient's survival is still needed, despite the plethora of similar trials that have been published [435]. It is out of the scope of this section to discuss the clinical decisions related to whether a graft is a priority over a stent to be placed by a cardiologist or a radiologist etc. Instead, here, we shall review the materials and the evolving trends of stenting, as such an intervention has become standard for both the coronary and the peripheral artery diseases.

A stent is a hollow cylindrical device made of interconnected struts of various designs and thicknesses, whose purpose is to be inserted into vascular lesion sites following transluminal angioplasty, expand in situ and stay in place to inhibit vessel restenosis. A characteristic design is shown in Fig. 13.8. The first generation were metallic stents and their development followed arguments related to stent design, including assessment of different materials and surface modifications. In later years, the introduction of drug eluting stents (DES) and the associated pharmacology shifted the interest to pharmacodynamics, while problems of late stent thrombosis seems to be an increased risk of DES. Currently, there is a big research effort going

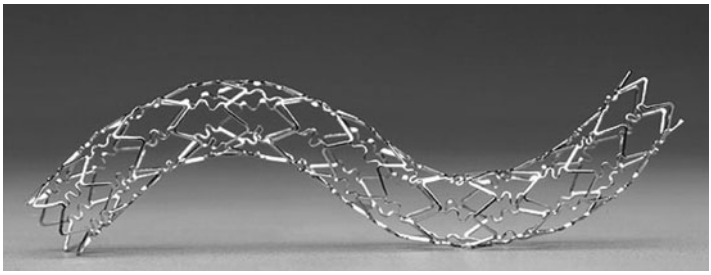

Fig. 13.8 A photograph of a metallic stent

on at many levels, including development of stent materials and nonpharmacological coatings, and technologies to deliver large biopharmaceuticals, especially from cardiovascular stents [436, 437].

The technical, preclinical, and clinical requirements for placing, securing and monitoring the stent in its place had all to be taken into consideration for selection of material and design characteristics. The first self-expanding stents were reported in 1986 by the name Wallstent®. Cobalt–chromium alloys have been used because their high elastic modulus enabled the process of self-expansion of the structure. Other alloys such as the L605 (Co-20Cr-15W-10Ni), MP35N (Co-20Cr-35Ni-10Mo) have entered the scene, through the balloon-expanding process. Their higher strength enabled the construction of thinner struts, which cause less trauma and therefore reduce the restenosis rate. They are radioopaque allowing X-ray monitoring and not at least, have improved corrosion resistance. In addition to these alloys and to stainless steel (316L), many efforts to reduce the strut thickness and improve the radiopacity by adding, for example, platina are in progress. Other alternatives are the use of composite structures: a marketed example is the TriMaxx®** stent which is comprised of a thin layer of tantalum sandwiched between two layers of 316L stainless steel. Furthermore, knitted wire and helical wound wire structures of tantalum have been made into stents, and niobium, as well as nickel-free steels have also been tried.

Mechanical characteristics of present day materials set a limit on further reduction of struts' thickness. The continuous need for improvement of the bare metallic stents forces researchers to deal with the surface properties to improve the compatibility with the vascular environment and to decrease restenosis of the lumen. This cannot be reduced below a certain limit. In an effort to reduce metal ion release, especially nickel and molybdenum, employment of carbon coatings was investigated. Diamond-like carbon (DLC), pyrolytic carbon, fluorine-doped DLC, even silicon carbide have been utilized as coatings. Some authors by-passed the problem of coating adherence by ion implantation of carbon. While short-term effects showed an improvement, i.e., lower restenosis rates compared to bare stents, longer term results were not encouraging [436]. Other coatings include titanium-nitride-oxide coating (physical vapor deposition of titanium in an oxygen–nitrogen gas

mixture) or iridium oxide (reactive sputtering of iridium in an oxygen atmosphere on the substrate).

Another class of stents is the drug delivery ones, the DES. The need to locally and temporally deliver anti-restenotic agents arose from the failure of the use of systemic drug administration, as shown by clinical trials, or the limitations of the catheter-based drug delivery devices which addressed only the aspect of 'locally' but not the controlled release over time [437]. The basic idea was to coat the metallic stent with a synthetic polymer, or a hydrogel, or a polysaccharide, in which a bioactive agent would be loaded. Many variants of this concept have been clinically employed. The Cypher®stent has three different layers. The first one applied to the stent surface is the poly(p-xylelene), or parylene polymer, the second is a mixture of polyethylene-co-vinyl acetate and poly-n-butyl methacrylate which contains the drug Sirolimus, and the top layer is the same mixture, without the drug, to control the drug elution rate. The Taxus®stent has a single polymer/drug layer: the triblock copolymer poly(styrene-b-isobutylene-b-styrene) loaded with the drug Palitaxel. The permanent presence of synthetic polymers, however, might be the reason for risks of late stent thrombosis. This has led other developers into utilizing biodegradable polymers, such as the already mentioned PLA, PGA, or PLGA as drug-carrying coatings, or to pursue the concept of loading the drugs without any intermediary polymeric surface. Nanoporous aluminium oxide thin layers over stainless steel stents loaded with drugs, microtextured through a basic grit blasting process, stainless steel stents which have to be loaded with the drug just prior to implantation of the stent, or hydroxyapatite porous coatings are being tried as polymer-free DES. Another interesting technology for polymer-free DES is the one demonstrated by the stent CoStar®. Reservoirs for the storage and elution of the drugs are formed within the stent struts by laser cuts, while a biodegradable polymeric capping layer is placed over the drug.

Finally, the concept of using totally biodegradable stents presents some interesting ideas. The most obvious choice is the use of PLLA, and indeed there are reports of PLLA stents loaded with drugs in clinical trials. Magnesium alloys, such as the AE21 (containing $2 < 5\%$ rear earths) have been tried, while iron stents (positive aspects of corrosion!) have been tried in animal studies [438]. For the *pros* and *cons* of magnesium alloys, the reader is referred back to Chap. 8.

13.6.3 Tissue Engineered Blood Vessels

It was 1986 when the first completely biological tissue-engineered vascular graft was produced by Weinberg and Bell [439]. It was made from animal collagen gels and bovine vascular cells. It failed, however, in vivo due in part to its insufficient mechanical properties. Since then the research effort has continued and at least two different approaches have been pursued. One is using the traditional tissue engineering approach involving appropriate scaffolds, cells and biomolecules, as described

earlier in this chapter, and another one, which completely avoids the scaffolding material.

The last method has been pursued by the group of Nicolas L'Heureux in Canada. One of the hypotheses that drove their work was that the absence of any synthetic material or even exogenous biological material would preclude foreign body reactions, limit graft infection, and allow for complete graft integration [440]. They isolated and cultured three types of human cells: umbilical vein endothelial, umbilical vein vascular smooth muscle cells (SMC), and skin fibroblasts. They cultured the SMC and the fibroblasts to produce sheets of extracellular matrix (ECM) incorporating cells, which could be peeled off the culture flasks. They utilized a cylindrical perforated inert mandrel with an external diameter of 3 mm on which first they slipped an acellular inner membrane made from a fibroblast sheet, followed by an SMC sheet rolled around the first membrane, and finally a fibroblast sheet rolled around the second sheet. The whole process was carried out inside a bioreactor and a maturation period of at least 8 weeks was necessary. Then the mandrel was removed and the layered cylindrical construct was seeded with the endothelial cells. The construction of the engineered graft, excluding the process for decellularization of the inner membrane, and the expansion of the cells in culture, required at least 3 months! Structurally and mechanically, the tissue engineered vessel showed very good similarities to human arterial tissue and preliminary data from grafting it to animals (dogs) were promising. However, the cell source and the dynamics of the created construct will need a lot of research before its clinical implementation [440].

The classical tissue engineering approach will be demonstrated with two examples. Both start from the hypothesis that the development of the arterial vessel should be facilitated by the application of physiological mechanical stimuli on the vascular cells in the culturing system. The Langer group used polyglycolic acid (PGA) mesh scaffolds which were sewn into tubular form [441]. The surface of the fibers was partially hydrolyzed to increase its hydrophilicity and serum proteins adsorption for an improved cell attachment. SMCs were isolated from bovine aortic tissue and formed a smooth luminar surface after being cultured for 8 weeks in a bioreactor under conditions of pulsatile radial stress. Then, bovine aortic endothelial cells were introduced into the lumen of the vessel, allowed to adhere for 90 min, and continued to develop into an endothelial layer for the next 3 days with luminal flow rates to correspond to a preselected shear stress. Assessment of the mechanical properties of the constructed vessel, of phenotypical expressions of both type of cells, and histological observations were promising and led the group to proceed to animal experiments. Both bovine constructs and autologous ones were implanted in appropriate positions in Yucatan miniature swine provided several clues for further research, emphasizing the important effects of pulsatile culture conditions.

The Hoerstrup group put emphasis also on the pulse duplicator system in which the vascular construct would grow [442]. They utilized a composite scaffold made from nonwoven PGA mesh coated with a thin layer of poly-4-hydroxybutyrate (P4HB). P4HB is a biologically derived (from bacteria) rapidly absorbable, strong, pliable and thermoplastic biopolymer. The tubular scaffolds were made using a heat application welding technique, facilitated by the properties of P4HB, with internal

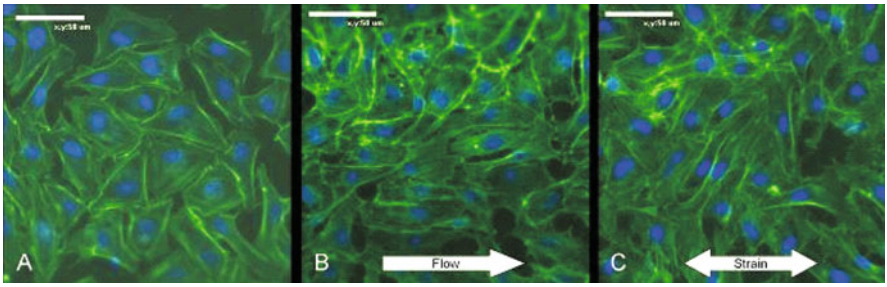

Fig. 13.9 Confocal images of BCE-HT+ endothelial cells stained with Phalloidin-FITC (green)/DAPI(blue). 100.000 cells cm^{-2} are seeded at the lumen of the tube as it rotates (9 rph) (**a**). Seven hours after seeding, a mechanical stimulus is superimposed. (**b**) flow of the feeding medium (wall shear stress 5 dyn cm^{-2} for 2 h). (**c**) 10Magnification 60×

diameter of 5 mm and lengths of 4 cm. The cell source was the ovine carotid artery. Myofibroblasts were seeded onto the inner surface of the scaffolds and cultured statically for 4 days, followed by the seeding of the endothelial cells. Afterward, the whole system was transferred into a bioreactor and grown under gradually increasing flow and pressure conditions for up to 28 days. The resulting constructs showed a well-organized layered tissue formation with acceptable mechanical properties, however, lacking a complete confluence of the endothelial cells, therefore concluding that further optimization of the in vitro conditions with regard to growth factors and pressure loading conditions are necessary.

As a concluding statement for this section, let us remind ourselves, once more, that even a seemingly simple structure compared to more complex vascular vessel, is the product of a long and multiparametered evolution, and that many details of its development and function are not fully known. The need therefore of more detailed basic research in the physiology and function, say for example of endothelial cells in response to specific environmental stimuli in in vitro conditions, is rather obvious. As an example of the strategy just mentioned, the Missirlis lab has designed and developed a modular bioreactor [443]. It provides seeding of endothelial cells inside the lumen of polymeric vessels covered with specific ECM, under rotating conditions and subsequent imposition of a combination of mechanical stimuli including pressure, shear rate, substrate stretching, torsion, and gravitational gradient.

The response of the cells to each and in combination of these stimuli in terms of morphology, structure of cytoskeleton components (F-actin, tubulin), and expression of genes for specific proteins that control cell–cell interactions (ZO-1, VE-cadherin), cell–substrate interactions (integrins), and inflammation (E-selectin), is to be evaluated. Figure 13.9 shows some preliminary results on the influence of specific separate imposition of either flow (shear stress) or substrate stretching on cultured endothelial cells. Observe the tendency of the cells to streamline themselves with the direction of flow, but move toward right angles in response to the substrate stretching.

Chapter 14
Water

> Of the four elements water is the second least heavy and the second in respect of mobility. It is never at rest until it unites with its maritime element, where, when not disturbed by the winds it establishes itself and remains with its surface equidistant from the center of the world. It is the increase and humour of all vital bodies. Without it nothing retains its first form. It unites and augments bodies by its increase. Nothing lighter than itself can penetrate it without violence. It readily raises itself by heat in thin vapor through the air. Heat sets it in movement, cold causes it to freeze, immobility corrupts it.
>
> Leonardo Da Vinci (Keele [10, p.24-25])

Da Vinci, Aristoteles and not less our present-day community continues to be touched, fascinated, enjoyed by that tiny molecule *water* or is concerned by it but why, it is so 'tiny' a molecule after all? Being a beginning research assistant in the early 1960s, the first author was witnessing a scientific storm, which seven or eight years later proved to be a storm in a tea-cup only. Russian scientists noticed that pure water enclosed in quartz capillaries had a higher viscosity and a lowered freezing point (Fedyakin, Deryagin [444]). The U.S. Bureau of Standards approved the experiments, herewith giving birth to a new form of water, polymerized water, officially crowned under the name *polywater*. But fear all over the place: contact of a tiny drop of polywater could turn all water into a viscous soup making all life on earth impossible! Serious doubts, however, about these experiments raised immediately and the famous polywater in capillaries was found to be a colloidal silicate sol, silicate dissolved from inefficiently cleaned walls [445]. People acquainted with adsorbed water on clay surfaces were neither fearing a catastrophe nor surprised by the final outcome. An aqueous suspension of 0.1% montmorillonite can under the right conditions (monodisperse) be turned into a viscous gel, demonstrating a distance effect of more than a few water layers! In Chap. 9, the important interplay was already underlined between clays[1] or other colloids, water and its cationic or anionic concentrations. And there is more to learn about phyllosilicates and water.

But has it all anything to do with biomaterials? Do not stop reading here, the link to biomaterials follows below.

[1] Clay refers to layered silicates subdivided kaolinites, smectites (f.ex. montomirllonite), vermiculites, illites, micas and chlorites. For more details see for example Meunier [273].

J.A. Helsen and Y. Missirlis, *Biomaterials*, Biological and Medical Physics, Biomedical Engineering, DOI 10.1007/978-3-642-12532-4_14,

14.1 Origin of Life

Passing over the crystallographic details, many clays exhibit a cation or anion exchange capacity due to imperfect intracrystal charge balance, one out of many examples of order–disorder effects making life on earth possible. The exchangeable ions are located in the interlayer space. A montmorillonite, for example, with Ca^{2+} as charge compensating cation on its surface, forms discrete hydratation levels of 1, 2, or 3 layers of water, increasing the layer-to-layer distance from 0.96 to, respectively, 1.23, 1.45, and 1.67 nm. When saturated with Na^{+}, the hydratation level can go to infinity, i.e., to the formation of a stable $\pm$ monodisperse suspension. The absolute particularity of the lower hydratation levels is the behavior of water, results which are the outcome of a long research history [446–450]. Water is highly dissociated and the surface exhibits a Brønsted acidity comparable to 1% sulfuric acid dissolved in acetic acid [451, 452]. Montmorillonite behaves in this state of hydratation as a solid acid. Its use as cracking catalyst many years ago was based on this property. Moreover, clay minerals may have interfered in the prebiotic world as an adsorbent for simple organic molecules formed in that period and subsequently or simultaneously as catalysts in the formation processes of oligomers out of these simple molecules. Short peptides are relatively easily formed from glycine ($HOOC–(CH_2)_2–NH_2$), alanine ($CH_3–CH(NH_2)–COOH$) or others, in presence of kaolinite or montmorillonite when exposed to heating-drying-wetting cycles, conditions that exist today and existed presumably also in prebiotic times [453]. The yields are not spectacular after, in human terms, a feasible number of cycles. If, however, these peptides are considered as building blocks for larger biopolymers and cycling was happening over geological time spans, an enticing hypothesis promotes water and clay minerals to co-authors in the drama of the origin of life. The experiments with clay were preceded by the well-known experiments of Miller with electric discharges in a supposedly primitive atmosphere, experiments which are continued till today by other authors [454, 455].

It is beyond the scope of the book to tackle paradigms like *replication first* or *metabolism first* and life did certainly not start right at the surface of kaolinite. Added here should be, before concluding this paragraph, a word about the physicochemical constraints within which life could take a start. The conventional ones are time, temperature, pressure, presence of water, basic inorganic molecules and a constant flow of utilizable energy. The latter point is a matter of thermodynamics. The second law, often referred to in this book, imposes that heat cannot be used as energy source for the formation of increasingly complex molecules (remember: *water does not flow uphill!*); solar energy is an obvious source. Another, often unrecognized, item is the reversibility of most chemical reactions. Why are the early synthesized oligomers not immediately hydrolyzed? A mechanism is compulsory to sustain synthesis for a sufficiently long period of time, to prevent hydrolysis and to collect a stock of prebiological molecules to bring about ultimately the first living organisms. As Mulkidjanian and Galperin express it: *the chemical composition of living beings is (should be) more conservative than the chemical composition of the*

environment [456]. As was already said, life has to sheat nature! And here we are possibly confronted with the active role of clays in these processes.

A first corollary to phyllosilicates, in particular smectites, is the very high specific surfaces (from tens to some 800 $m^2\ g^{-1}$) and, by adsorbing the oligomers, they could serve as 'deep freeze' for the synthesized oligomers hindering the reverse reaction. A second possible corollary to clays is a reaction called *Salt-Induced Peptide Formation* (SIPF). By Monte Carlo simulations and *ab initio* calculations, it was assumed that in NaCl solutions of >3 M the Na^+ ions had a dehydrating effect because the high concentration of salt provoked a deficit of water molecules to fill the first coordination shell of the sodium ions. In forming the peptide linkage from glycine, alanine and so on, a water molecule has to be removed which was a welcome guest for Na^+, herewith shifting the equilibrium in the direction of the peptide (see for similar effects Sect. 4.2 and the comments on oxidation-reduction potentials in Sect. 3.2). These findings were experimentally verified as were the very early experiments of Lahav but here by cycling between high and low concentrations; Cu^{2+} seemed to be the more efficient cation. The same type of experiments in presence of clays, SIPF is considered the rate determining step; the yields in particular for larger oligomers were better but Cu^{2+}-saturated clays did not perform better than, for example, Ca^{2+} saturated ones [457]. Rode and colleagues attribute the better yield to both conservation of the oligomers by adsorption and/or bringing two monomers in a suitable position [458]. Would it be worth a trial by confronting our assumption on catalysis by the enhanced acidity with Rode's view. For further reading on the subject, the book by Herdewijn and Kisakürek is recommended literature [459].

14.2 The Water Molecule

The subject is, compared to usual texts on biomaterials, apparently not an issue. Lazy as we are, water, or 'aq', was not figuring in the reactions in the text (unless as reaction product), not meaning that we forgot it! Nevertheless, it is a ligand and as such in competition with other ligands. Competition entails active participation in reaction equilibria. Reading Philip Ball's review in *Nature* and comparing this to the excellent comprehensive book on structure and properties of water by Eisenberg and Kauzmann, the progress of our knowledge on water is rather marginal [460, 461]. The basic structure of Fig. 14.1 of some 50 years ago still stands upright, even estimation of number of nearest neighbors (3.5 with respect to 4), of life time of 'broken' hydrogen bonds (with in those days much less performing instruments), thermodynamic properties, etc. did not change substantially. The vibrationally averaged structure, as suggested by Bernal in 1964, is still valid and accounted also for the density maximum of water at 4°C: *the linked, four-coordinated molecules form, instead of an ordered lattice as in ices, an irregular network of rings* [461, p.170]. This statement seems justified by a confrontation of Bernal's proposition with the proposition of structures given in Figs. 5.1, 5.2 and 5.3 by Lee and colleagues [462].

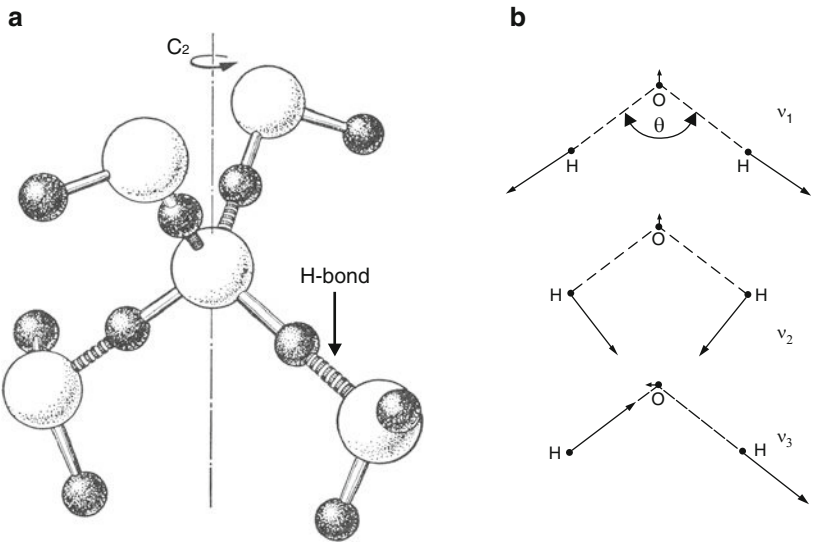

Fig. 14.1 (**a**) Tetrahedral hydrogen-bonded structure, containing five water molecules. (**b**) Fundamental vibration modes of the water molecule. The undistorted angle θ is 104.52°. Numerical values in Table 14.1. The tetrahedral structure model is reprinted with permission Oxford University Press [461, Fig. 4.25]

Table 14.1 Normal vibrations of water, deuterium oxide and hydrogen-deuterium oxide: modes and corresponding wavenumbers (cm^{-1})

Mode	Mode name	H_2O	D_2O	HDO
ν_1	Symmetric stretching[a]	3,657	2,671	2,727
ν_2	Deformation	1,595	1,178	1,402
ν_3	Asymmetric stretching	3,756	2,788	3,707

[a] Sensitive to molecular environment

It is beyond the intention of this chapter to give an integrated view on water (if possible at all!), its structure and function in biomaterials and their interface to tissues. The following paragraphs put the spotlight on only a very few unique aspects, see them as stimuli to keep our mind alert on the omnipresence of water and to share the fascination for this simple molecule. And by the way no effort seems to be too big: groups of the European Synchrotron Radiation Facility in Grenoble and at other synchrotron facilities throughout the world are involved in programs to decipher the *enigma* code of water.[2]

Vibrational Modes

Lithium has two stable isotopes ^{6}Li and ^{7}Li and are available at reasonable prices; they allow to perform some intelligent discriminative chemistry and analysis by

[2] Read for instance Number 49 (2009) of ESRF news with the front page title: *Making water crystal clear*, although crystal clear is somewhat a premature statement.

atomic absorption spectrophotometry. Hydrogen has the lucky advantage to have an obese isotope partner with the double of its own mass: deuterium. So great a difference in mass must have a considerable effect on the vibration frequency: the vibrational frequency depends on the masses of the atoms (as well as on the geometry of the molecule). Hence, substituting –H for –D shifts considerably the position of the absorption bands in the infrared spectrum. That gives the scientist access to some intelligent discriminative chemistry. Biological systems are unthinkable without water but likewise without organic molecules. The stretching bands of water interfere with the stretching bands of $–CH_3$, $–CH_2$, aromatic –CH or –NH; substitution in water of –H– by –D moves the water bands away from this interference. Similar shifts can, of course, be performed the other way round by substituting hydrogen by deuterium in the organic chain: –CH–→–CD– or R–OH→R–OD.

Another lucky coincidence is that all absorption bands of water are infrared active, but – often fortunately – weakly active in Raman.[3] Combined with the weak Raman activity of glass on the one hand and the use of visible laser excitation on the other, a wide range of materials can be analyzed in presence of water by Raman spectroscopy, when the sample needs to be contained in glass cells. Surfaces and/or restrained volumes (micro-IR or micro-Raman) can be observed in the infrared and Raman domain without need for high vacuum, an intrinsic disadvantage of techniques as Scanning Electron Microscopy (SEM), X-ray Photoelectron Spectroscopy (XPS), or Secondary Ion Mass Spectroscopy (SIMS).

Unusual Proton and Hydroxyl Mobility

Is it *the unbearable lightness of its being* that makes a proton such a fast runner, or does not run at all, or is it H_3O^+ that moves, or the cluster or hydrated complex $H_9O_4^+$ or $H_5O_2^+$ or what else?

Remark that, contra-intuitively, the apparent proton mobility is much higher in ice than in liquid, which is attributed to 'imperfect' hydrogen bonding in the liquid. Nothing but odds with water!

The experimental value of the proton's mobility is roughly seven times higher than other monovalent cations ($Li^+ \ldots$) (Table 14.2). Boring because also this behavior is still, although with nuances, explained by a model going back to Grotthuss 200 years ago.[4] Nuances, yes, because they temper somewhat our pessimism on the progress of the knowledge on water! The mechanism for proton and hydroxyl transfer is shown in Fig. 14.2 and the conclusion is obvious: both ions do

[3] Vibrations are active in infrared when there is a change in dipole moment during vibration, while a vibration is active in Raman when there is a change in polarizability during the vibration. The –C–H stretching is active in both IR and Raman, while for instance diamond in only Raman active. If more reading on these techniques is wanted, see [362, 463–466].

[4] Seminal paper on the subject by *de Grotthuss C.J.T.* in Ann. Chim., **58**, 54-73: *Sur la décomposition de l'eau et des corps qu'elle tient en dissolution á l'aide de l'électricité galvanique*, currently referred to in many textbooks [461, 467].

Table 14.2 Approximate mobilities of the proton (or hydronium H_3O^+), deuteron (or deuteronium D_3O^+), monovalent cations and OH^-. Collated from [98, 461]

Ion	Water	Mobility $cm^2\ s^{-1}\ V{-}1$
M^+	H_2O_{liq}	$\sim 5.10^{-4}$
H^+	H_2O_{liq}	$\sim 36.10{-}4$
M^+	H_2O_{ice}	$\ll 10^{-8}$
H^+	H_2O_{ice}	$10^{-7} - 1$
D^+	D_2O_{liq}	$\sim 25.10^{-4}$
OH^-	H_2O_{liq}	$\sim 20.10^{-4}$

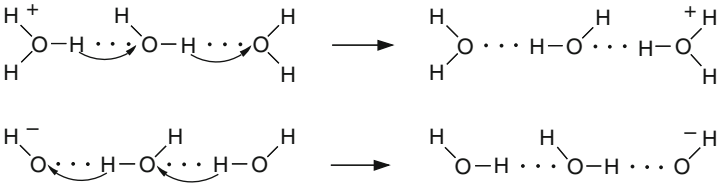

Fig. 14.2 Mobility of H^+ and OH^-

not move as such but a *cooperative transfer* in ensembles of three or more molecules explains (?) the high mobility.

Wetting of Biomaterial Surfaces

Our pessimism about progress was a provoking statement and is not paying tribute to the high quality scientists involved in the painstaking unravelment of the interaction of water molecules with surfaces. A book, edited by Morra and recommended literature because it advertises the unsolved aspects of the role of water in biomaterials, is comprehensive in the sense that the substantial part of the theoretical field and the practical relation to surface wetting is passing the review; the state-of-the-art, however, does not offer yet an off-the-shelf-receipt on how to reshuffle a surface for a dedicated application. It does offer a perspective view on foundation of the subject. Studies on solvation interactions of protein adsorption to biomaterials at the water–solid interface are highly relevant to understand and consequently to try developing surfaces that do or do not adsorb proteins. A typical field of application is the adsorption of proteins on biomaterials in contact with blood where adsorption has mostly undesirable consequences (artificial arteries, heart valves, stents, sensors, contact lenses).

Protein adsorption on surfaces has to do everything with water. Let us try to schematize (extremely simplified!) what is or could be going on in the interaction of proteins with hydrophilic and hydrophobic surfaces. The distinction between both is currently based on the measurement of the contact angle of a water droplet (or other liquids) on the surface. The work of adhesion W_{adh} is:

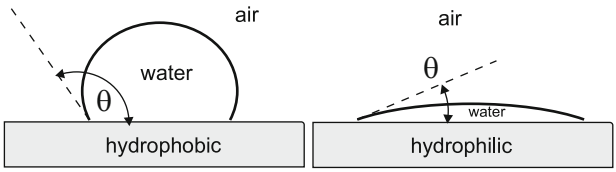

Fig. 14.3 A droplet of water on a hydrophobic and a hydrophilic substrate

Table 14.3 Keyword summary of the interaction water–protein surface

Surface	H_2O	Protein ads.	Hydration interaction	Cont. angle
Hydrophilic	H-bonded to surface	Poor	Hydrophilic repulsion	$<15°$
Grayzone				
Hydrophobic	not H-bonded to surface	∼Strong	Hydrophobic attraction	$>65°$

$$W_{\text{adh}} = \gamma_{\text{sa}} + \gamma_{\text{la}} - \gamma_{sl}. \tag{14.1}$$

Applied to the situation sketched in Fig. 14.3, the subscripts *la*, *sl* and *sa* refer, respectively, to liquid–air, solid–liquid and solid–air interfaces.

Rewritten in experimental quantities (under interface equilibrium condition, i.e., the Young-Dupré equation):

$$\gamma_{\text{sa}} = \gamma_{sl} + \gamma_{\text{la}}(\cos\theta). \tag{14.2}$$

The simple equation is, say, a practical help but, considering that the adhesion forces are a partition between dispersion forces and acid–base interactions, the relationship is much more complicated.[5] Let us try anyway to give some clarification at the hand of Table 14.3. Water is hydrogen bonded to a hydrophilic surface and is restricted in motion by the ± ordered structure. A hydrated protein molecule approaching the solvated surface has to disrupt the water structure before it can dehydrate the surface and settle. Whether settling will happen or not, is a matter of energy loss or gain, entropy increase or decrease with respect to the starting situation. Mostly, the situation is negative and the interaction will be repulsive.

On the contrary, water is not hydrogen-bonded to hydrophobic surfaces. The self-cohesive forces exceed surface attraction forces and the water molecules facing the solid surface are more ordered than in the bulk. The interaction becomes attractive and consequently, protein adsorption will be favored. Hydrophobic interactions are mostly the dominant forces for protein adsorption and the water structure is the major player in protein adsorption.

[5] It is impossible to go into detail of this equation within the present context but a full treatment is given by Van Oss, Chaudhury and Good [468].

Despite the gaps in the theory, material scientists cannot wait till everything is crystal clear and they practice surface modification in prevention of protein adsorption. Grafting oligomers or polymers on the surface is a feasible technique. Pluronics® is an example of a commercial coating. It consists of triblock copolymers polyethylene oxide-polypropylene oxide-polyethylene oxide (PEO-PPO-PEO). The density of the film (surface coverage) seems to be the predominant factor for success.

Not any detail has been given about the thermodynamical contributions (Gibbs-free energy, enthalpy and entropy changes) or acid–base properties at the interface. This section is nothing but a glimpse of what is going on in the field and it could not be more because a *handbook theory* is not yet at hand. In Sect. 11.9, we were wondering why our elastomer coating was behaving much better than expected from its hydrophobic character and why it is adsorbing a few percent of water. Study of the hydrophobic interaction may be the lead to an understanding of this phenomenon.

Super-Hydrophilic Surfaces

An extreme hydrophobic case is teflon-water with a contact angle of $\theta = 180°$. At the other end of the line, extreme hydrophilicity, are surfaces grafted by water-soluble long polymer chains such as polyethylene glycol (PEG). Hydrophilic surfaces are subdivided in:

- *Clear* because of sharp/rigid boundary: ionic for surfaces decorated with $–COO^-$ or nonionic with –OH decoration.
- *Super-hydrophilic* with a diffuse boundary, absence of a driving force for protein adsorption (zero interfacial free energy).

Theoretically, those super-hydrophilic surfaces should be anti-fouling (no deposit of cells or proteins). They can easily be produced (grafting, physical adsorption, etc.). Sepharose is, for example, a hydrogel with low cross-linking degree and adsorbs proteins only in marginal quantities... all appealing properties for scientists interested in blood compatible materials. But reality appeared to be less attractive. Blood platelet adhesion decreases with the water content of the hydrogel but increases steeply after passing through a minimum. So, blood compatibility is poor. Moreover, another unexpected effect was happening: most testing is performed for relatively short periods of time but time, as we stressed repeatedly in former chapters, is an important parameter. And indeed, superhydrophilic surfaces produce thrombi after an uncontrollable period of time.

Superhydrophilic surfaces are slippery and listed applications making use of this property are guide wires, catheters, endoscopes or contact lenses, a potentially more successful area because of restrained contact times. All these applications concern contact with soft tissue.

Other candidate molecules for enhancing hydrophilicity are polysaccharides: inositol, the natural polymer alginate, heparin (widely used in blood contacting devices), hyaluronan (eye surgery) [469]. They all merit attention but the main

purpose of this chapter was to incite interest in the often forgotten partner, a material we cannot manipulate but one which is inevitably interfering with all materials we want to shape to our convenience.

14.3 Conclusion

Considering its molecular weight, water should boil at −90°C; compare it with HCl which is boiling at −65°C. But water does not behave so. Becoming less dense below +4°C is another anomaly. Fortunately should we say, because without that density maximum, life on earth would be heavily compromised. Ice would sink to the bottom, making the survival of higher order life in seas and ponds very unlikely.

Clays and water are intimate *compagnons de route* involved in the emergence of life on earth: catalyzing the formation of peptides and, by adsorbing them on the surface, preserving the newly formed peptides from prompt hydrolysis, the 'deep freeze' function as we called it. And everything is linked to everything. The catalysis by clays is due to interaction of the exchangeable cations on their surface with adsorbed water, turning the clay into a solid acid catalyst. The position of the exchangeable cations, which are in general essential plant nutrient elements as sodium, potassium, calcium and so on, protect these cations from being eluted by the first heavy rain, as would be the case, when soils consisted of nothing but quartz sand. Were clay and water *compagnons de route* during the emergence of life, their ion exchange capacity makes them companions for sustaining life on earth. Is not that beautiful!

The interaction of water with hydrophilic or hydrophobic surfaces is for a substantial part undoubtedly responsible for their behavior as a biomaterial. Understanding these interactions remains difficult. However large-scale the research effort has been, *there is no means of systematically categorising or naming different surfaces based on measurable wetting properties* as Vogler concludes its chapter on wetting biomaterials surfaces [470]. A crushing statement, so a *handbook* version on the theory of water and surfaces is clearly not yet for tomorrow.

And by the way... this chapter has been written when the Olympic Winter Games were going on in Vancouver. Skating is a nice present of water physics: a special surface layer reduces the friction coefficient to such an extent that 75% of the skater's energy spending is due to air resistance and only 25% to the contact of skates with ice.

Chapter 15
Closing Dinner Speech

The round-up is the task of the closing dinner speaker. Supposed he is honest, and why should not he, his retrospection will start considering negative sides of the past two weeks, fourteen chapters long, and he will end throwing some flowers to the organizers. In the present case however, we will leave the negative considerations to the *dear colleagues* and omit the flowers.

No, the text was/is neither perfect nor comprehensive for the subject.

What was absent: separate chapters or sections on noble metals, ophthalmological applications, cochlear implants, burn dressings, resorbable polymers, ionomer cements, nanomaterials, chitosan, drug delivery materials, natural polymers, coatings and other kinds of surface modification, sterilization, materials for soft tissue implants other than for cardiac or vascular implants... Although not present in separate sections, most items are interwoven within subjects as, say, dental nano-hybrids, oxidized zirconium, and so on. Cellular response of hard tissue is underrepresented but we focused on the importance of close fit as one of the major facets of the success story that hard tissue implantation certainly is. Some sections may look too long with respect to their actual importance; an example of such a section is amalgam. The reason or excuse was our fascination by a material that should not have been used taking into account the recognized toxicity of mercury and with low profile mechanical properties. The astonishing number of amalgam fillings that have been performed over almost two centuries without dramatic failures, were unbelievably successful. A historical record may be said! Moreover, it was an introduction to intermetallic compounds. The contrast with the cited catastrophy of Prozyr® or the emerging problems with articular resurfacing cannot be greater, despite the enormous baggage of documented research and biomechanical experience preceding the clinical introduction of these techniques.

The former considerations justified the chosen mainframe for this project: to bring a mixture of historical and philosophical retrospection, the classics of metals, polymers and ceramics, a few currently active and new fields such as resorbable metals or rapid manufacturing techniques and apposition of two successful implantation areas in hard and soft tissue (including tissueengineering).

The last chapter, which after all could have been the first one, was handling the *matrix* offering the starting conditions for life and one all biomaterials are in contact with: water. The descriptive term *matrix* is used here in its full etymological

J.A. Helsen and Y. Missirlis, *Biomaterials*, Biological and Medical Physics, Biomedical Engineering, DOI 10.1007/978-3-642-12532-4_15,

meaning! It was reserved as the last item because *water is just there*, the physics not well understood and manipulation hardly possible, one, however, that cannot not be bypassed but whose presence is often ignored. . . and of course, because it is by its etheric nature pure fascination. With this romantic note, we conclude by wishing you, dear reader, instructive and pleasant reading.

Appendix A
Physical Data

In Table A.1, the atomic number, name, and symbol of the elements of the periodic system, i.e., the family tree of elements are given together with the common oxidation numbers. The noble gases are omitted in this table because none are ionized under ordinary conditions. The trans-uranium elements (atomic numbers >92) are of no relevance in the context of this book and are omitted. In the following table, the elements are arranged in groups (columns) 1 (IA) to 13 (VIIIA) and periods 1–7 (rows). On top of the element symbol, the atomic number is given, below the symbol the atomic mass. The atomic masses are determined for a natural mixture of isotopes and the basic reference mass is 1/12th of carbon isotope C^{12} with mass 12.0000. In green are given the basic constituting elements of life, in red the essential elements, in gray the main elements present in biomedical alloys.

The periodic ordering as shown was discovered in 1869 independently by Meyer (Breslau and Tübingen, 1830–1895) and Mendeleev (St.Petersburg, 1834–1907). It was not merely a historical *curiosum* but was a basic milestone in the development of chemistry. The unraveling of the electronic structure of atoms in the twentieth century provided the physical rationale. We emphasized in Chap. 4 the importance of coordination chemistry of transition metals (period 4 and groups IB to VIIIB). The ability to form complexes is explained by the structure of 3d orbitals. Periodicity of various other properties can be demonstrated in the same way: ionization potentials, covalent radii, metallic radii, formation of oxides, ... For further reading the book 'Chemical Periodicity' and the following edition 'Inorganic Chemistry' by Sanderson is refreshing reading [191, 471]. When ingested, cesium circulates in the body like sodium; strontium is integrated in bone like calcium because of their chemical similarity. This explains the intrinsic danger of radioactive fall-out containing considerable concentrations of the isotopes Cs^{137} and Sr^{90}, both β emittors with a radiation half-life of about 30 year.

Notice that those chemical elements that are physiologically essential for the living body, as well as elements that are biomedically relevant in implantology, are clustered together in a relatively small domain of the periodic table. A challenging observation.

J.A. Helsen and Y. Missirlis, *Biomaterials*, Biological and Medical Physics, Biomedical Engineering, DOI 10.1007/978-3-642-12532-4,

Table A.1 Atomic number(a), element name(b), element symbol(c) and common oxidation states(d)

a	b	c	d	a	b	c	d	a	b	c	d
1	hydrogen	H	+1	3	lithium	Li	+1	4	beryllium	Be	+2
5	boron	B	+3	6	carbon	C	−4,+2,+4	7	nitrogen	N	−(3,2,1),+1
8	oxygen	O	−2	9	fluorine	F	−1	11	sodium	Na	+1
12	magnesium	Mg	+2	13	aluminum	Al	+3	14	silicon	Si	−4,+2,+4
15	phosphorus	P	−3,+3,+5	16	sulfur	S	−2,+4,+6	17	chlorine	Cl	−1,+1,+3,+5,+7
19	potassium	K	+1	20	calcium	Ca	+	21	scandium	Sc	+3
22	titanium	Ti	+2,+3,+4	23	vanadium	V	+2,+3,+4,+5	24	chromium	Cr	+2,+3,+6
25	manganese	Mn	+2,+3,+4,+7	26	iron	Fe	+2,+3	27	cobalt	Co	+2,+3
28	nickel	Ni	+2	29	copper	Cu	+1,+2	30	zinc	Zn	+2
31	gallium	Ga	+3	32	germanium	Ge	−4,+2,+4	33	arsenic	As	−3,+3,+5
34	selenium	Se	−2,+4,+5	35	bromine	Br	−1,+1,+6	37	rubidium	Rb	+1
38	strontium	Sr	+2	39	yttrium	Y	+3	40	zirconium	Zr	+4
41	niobium	Nb	+3,+5	42	molybdenum	Mo	+3,+6	43	technetium	Tc	+4,+6,+7
44	ruthenium	Ru	+3	45	rhodium	Rh	+3	46	palladium	Pd	+2,+4
47	silver	Ag	1+	48	cadmium	Cd	+2	49	indium	In	+3
50	tin	Sn	+2,+4	51	antimony	Sb	−3,+3,+5	52	tellurium	Te	−2,+4,+6
53	iodine	I	−1,+1,+5,+7	55	cesium	Cs	+1	56	barium	Ba	+2
57	lanthanum	La	+3	58	cerium	Ce	+3,+4	59	praesodymium	Pr	+3
60	neodymium	Nd	+3	61	promethium	Pm	+3	62	samarium	Sm	+2,+3
63	europium	Eu	+2,+3	64	gadolinium	Gd	+3	65	terbium	Tb	+3
66	dysprosium	Dy	+3	67	holmium	Ho	+3	68	erbium	Er	+3
69	thulium	Tm	+3	70	ytterbium	Yb	+2,+3	71	lutetium	Lu	+3
72	hafnium	Hf	+4	73	tantalum	Ta	+5	74	tungsten	W	+6
75	rhenium	Re	+4,+6,+7	76	osmium	Os	+3,+4	77	iridium	Ir	+3,+4
78	platinum	Pt	+2,+4	79	gold	Au	+1,+3	80	mercury	Hg	+1,+2
81	thallium	Tl	+1,+3	82	lead	Pb	+2,+4	83	bismuth	Bi	+3,+5
84	polonium	Po	+2,+4	85	astatine	At		87	francium	Fr	+1
88	radium	Ra	+2	89	actinium	Ac	+3	90	thorium	Th	+4
91	proactinium	Pa	+4,+5	92	uranium	U	+3,+4,+5,+6				

Table A.2 Periodic table of elements. *Columns*: groups, *rows*: periods. In the element boxes are given: atomic number, element symbol, atomic mass: (red) essential elements; (green) basic biochemical elements; (shaded) most common elements present in implants

Periodic table of elements

	1	2	3	4	5	6	7	8	9	10	11	12	13	14	15	16	17	18
	IA	IIA	IIIB	IVB	VB	VIB	VIIB	VIIIB			IB	IIB	IIIA	IVA	VA	VIA	VIIA	VIIIA
1	1 H 1,01																	2 He 4,00
2	3 Li 6,94	4 Be 9,01											5 B 10,81	6 C 12,01	7 N 14,01	8 O 16,00	9 F 19,00	10 Ne 20,18
3	11 Na 22,99	12 Mg 24,31											13 Al 26,98	14 Si 28,09	15 P 30,97	16 S 32,06	17 Cl 35,45	18 Ar 39,95
4	19 K 39,10	20 Ca 40,08	21 Sc 44,96	22 Ti 47,90	23 V 50,94	24 Cr 52,00	25 Mn 54,94	26 Fe 55,85	27 Co 58,93	28 Ni 58,71	29 Cu 63,55	30 Zn 65,38	31 Ga 69,72	32 Ge 72,59	33 As 74,92	34 Se 78,96	35 Br 79,90	36 Kr 83,80
5	37 Rb 85,47	38 Sr 87,62	39 Y 88,91	40 Zr 91,22	41 Nb 92,91	42 Mo 95,94	43 Tc (98)	44 Ru 101,07	45 Rh 102,91	46 Pd 106,4	47 Ag 107,87	48 Cd 112,40	49 In 114,82	50 Sn 118,69	51 Sb 121,75	52 Te 127,60	53 I 126,90	54 Xe 131,30
6	55 Cs 132,91	56 Ba 137,34	57 La* 138,91	72 Hf 178,49	73 Ta 180,95	74 W 183,85	75 Re 186,21	76 Os 190,2	77 Ir 192,22	78 Pt 195,09	79 Au 196,97	80 Hg 200,59	81 Tl 204,37	82 Pb 207,2	83 Bi 208,96	84 Po (209)	85 At (210)	86 Rn (222)
7	87 Fr (223)	88 Ra 226,03	89 Ac (227)	90 Th 232.04	91 Pa 231.04	92 U 238.03												

*	58 Ce 140,11	59 Pr 140,91	60 Nd 144,24	61 Pm (145)	62 Sm 150,36	63 Eu 151,96	64 Gd 157,25	65 Tb 158,92	66 Dy 162,50	67 Ho 164,93	68 Er 167,26	69 Tm 168,93	70 Yb 173,04	71 Lu 174,97

Table A.3 Multiples and submultiples of SI units

Value	Name	Symbol
10^{12}	tera	T
10^{9}	giga	G
10^{6}	mega	M
10^{3}	kilo	k
10^{-3}	milli	m
10^{-6}	micro	μ
10^{-9}	nano	n
10^{-12}	pico	p
10^{-15}	femto	f
10^{-18}	atto	a

Table A.4 Conversion factors

Property	Dimensions	SI unit	Conversion factor[a]
Length	[L]	m	$1\,\text{ft} = 3.048 \times 10^{-1}\,\text{m}$
		(meter)	$1\,\text{in} = 2.54 \times 10^{-2}\,\text{m}$
			1 ft = 3.048 × 10−1 m
Mass	[M]	kg	$1\,\text{lb} = 4.5359 \times 10^{-1}\,\text{kg}$
		(kilogram)	
Force	$[\text{MLT}^{-2}]$	$\text{N} = \text{kgm/s}^2$	1 lbf = 4.44822 N
		(newton)	1 kgf = 9.80665 N
Pressure	$[\text{ML}^{-1}\text{T}^{-2}]$	$\text{Pa} = \text{N/m}^2$	$1\,\text{atmosphere} = 1.013 \times 10^{5}\,\text{Pa}$
(stress)		(pascal)	$1\,\text{lbf/in}^2 = 6.89476 \times 10^{3}\,\text{Pa}$
			$1\,\text{bar} = 10^{5}\,\text{Pa}$
			1 mm Hg = 9.80665 kPa
Energy	$[\text{ML}^{2}\text{T}^{-2}]$	J = Nm	1 cal = 4.1868 J
(work, heat)		(joule)	$1\,\text{eV} = 1.6021 \times 10^{-19}\,\text{J}$
Temperature		t(°C) (Celsius)	
		T(°K) (Kelvin)	T(°K) = t(°C) + 273.16
		t(°F) (Fahrenheit)	t(°F) = 9/5t(°C) + 32

[a]English units: *inch*: in or inch; *foot*: ft; *pound*: lb

Table A.5 Physical constants

Constant	Symbol	Value
Universal gas constant	R	$8.3143\,\text{Jmole}^{-1}\,\text{K}^{-1}$
Avogadro's number	N	$6.02252 \times 10^{-23}\,\text{mole}^{-1}$
R/N	k	$1.38054 \times 10^{-23}\,\text{JK}^{-1}$
Planck's constant	h	$6.6256 \times 10^{-34}\,\text{Js}$
Faraday	F	$9.6487 \times 10^{4}\,\text{Cmole}^{-1}$
Charge of the electron	e	$1.6021 \times 10^{-19}\,\text{C}$
Molar volume at STP		$2.2414 \times 10^{-2}\,\text{m}^3\,\text{mole}^{-1}$
Velocity of light	c	$2.997925 \times 10^{8}\,\text{ms}^{-1}$

Appendix B
Crystallographic Structures

Why is a particular crystallographic form favored by a particular set conditions? The structure with the lowest free energy content is favored as dictated by the second law of thermodynamics (Chap. 3). The reader not acquainted with that universal physical principle is wished pleasant reading of Atkins' book [472]. *Thermodynamically favored* does not mean that structure will be formed, because it might not have the time to do so (see the discussion on SS 316L 2.2.1). A nice introduction to the importance of understanding structure can be read in a paper by Galasso [473].

B.1 Crystal Systems

Crystal lattices are to be thought of as a periodic skeleton of imaginary points which has a fixed relation in space to the atoms of a crystal. For convenience, space is divided by three set of planes, the planes in each set being parallel and equally spaced. This division produces a set of cells, unit cells, each identical in size, shape and orientation to its neighbors. A cell is described by three crystallographic axes a, b, and c and the angles between them α, β, and γ as shown in Fig. B.1. Seven basic or primitive systems are derived from this set as shown in Table B.1.

B.1.1 Unit Cells

Three common structures appearing in Chap. 2 are body-centered cubic (b.c.c.), face-centered cubic (f.c.c.), and hexagonal close-packed (h.c.p.). The characteristic crystallographic *unit cells* are represented in Fig. B.2. The arrows point to atoms transforming a simple cubic unit cell into the less 'primitive' body-centered one, etc. Important to notice, however, is that *unit cells* do not exist as isolated items: they are a mental reduction, chosen for convenience and to conform to the symmetry elements of a lattice, which is the three-dimensional infinite stapling of unit cells ('infinite', an ellipsis referring to the size of the unit cell with respective to a macroscopic object).

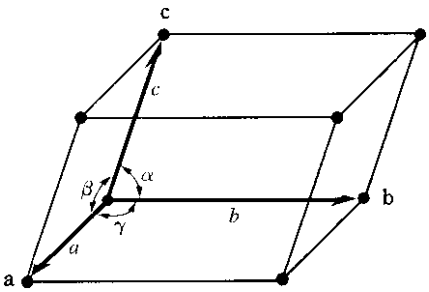

Fig. B.1 Basic crystal systems

Table B.1 The seven basic (primitive) crystallographic systems

System	Axial lengths and angles
Cubic	Three equal axes at right angles $a = b = c, \alpha = \beta = \gamma = 90°$
Tetragonal	Three equal axes at right angles, two equal $a = b \neq c, \alpha = \beta = \gamma = 90°$
Orthorhombic	Three unequal axes at right angles $a \neq b \neq c, \alpha = \beta = \gamma = 90°$
Rhombohedral	Three equal axes, equally inclined $a = b = c, \alpha = \beta = \gamma \neq 90°$
Hexagonal	Two equal coplanar axes at 120°, third axis at right angles $a = b \neq c, \alpha = \beta = 90°, \gamma = 120°$
Monoclinic	Three unequal axes, one pair not at right angles $a \neq b \neq c, \alpha = \gamma = 90° \neq \beta$
Triclinic	Three unequal axes, unequally inclined and none at right angles $a \neq b \neq c, \alpha \neq \beta \neq \gamma \neq 90°$

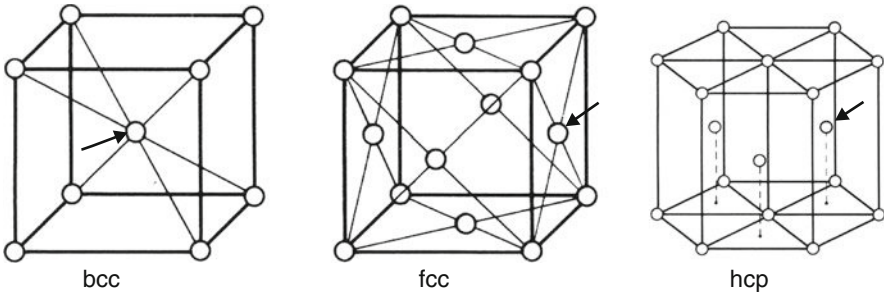

Fig. B.2 From left to right: unit cells of body-centered cubic, face-centered cubic, and hexagonal close-packed

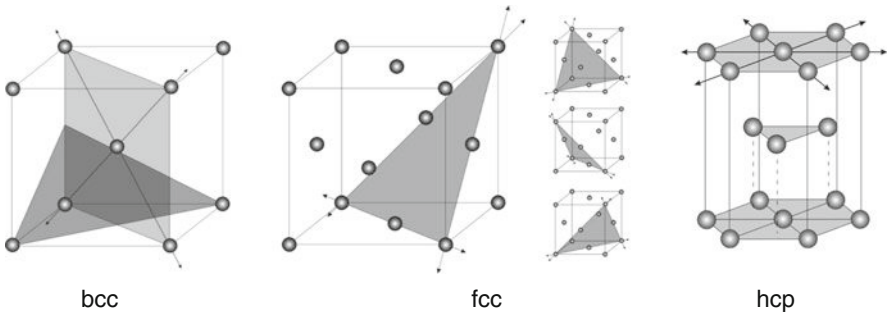

Fig. B.3 The unit cells b.c.c., f.c.c. and h.c.p. with their slip planes (gray). Three equivalent slip planes are represented for a f.c.c. cell. By courtesy of Prof. em. E. Aernoudt (MTM-KULeuven)

These typical structures were referred to when talking of Fe, Cr, Mo, Ta or Nb (b.c.c.), Ni, Al or Au (f.c.c.), Mg, Zr or Ti (h.c.p.).

B.1.2 Slip Planes

Crystals of, say, a pure metal, are irreversibly deformed by stress levels, much lower than the theoretical strength of the crystal and not along any random crystallographic direction. It happens, for example, along the widely spaced crystal plane [111] in f.c.c. crystals, a plane with a particularly high density of atoms per unit area. Let us call them *slip planes*. Card players like well slipping cards! Interesting observation but next paragraph tells us more about the consequences.

B.1.3 Dislocations

As often said throughout the text, nothing is (fortunately!) perfect in this world and crystals are not an exception on this rule. Imperfections or *dislocations* as they are named, are absolute fanatic hikers with a strong preference for slip planes, preferring paved paths frenetically avoiding Sahara sands. Herewith is explained why copper or iron can be drawn to wire or gold hammered to extremely thin sheet at stresses far below theoretical stresses. One type of dislocation is shown in Fig. B.4 but many other forms do exist. The study of dislocations started with the easier access to transmission electron microscopy (TEM) in the postsecond war years. It was a matter of spatial resolution, dislocation lines have nanometer-sized widths. And there are quite a few of those tiny lines in engineering alloys: a sugar-cube-sized piece contains about 10^5 km of dislocation line!

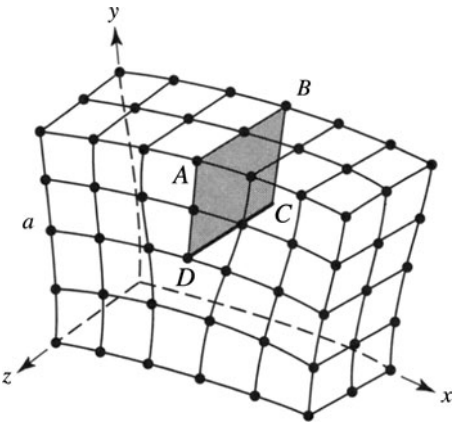

Fig. B.4 3D representation of an edge dislocation: an extra 'half plane' of atoms is added to the lattice

B.1.4 Diffusionless or Displacive Transformation

Usually transformation of one structure to another needs transport of atoms by diffusion what means transport 'long distance transport' of atoms. Exceptionally, it can be performed by a displacive mechanism. If iron is cooled below 914°C, it transforms from f.c.c., stable above that temperature, to b.c.c., thermodynamically stable below that temperature, without transport by diffusion. The phenomenon is illustrated in Fig. B.5 for iron, but similar processes take place for smart materials such as shape memory alloys, the use of which is illustrated in Chap. 10 or in some ceramics. In Fig. B.5, all corner points are occupied by iron atoms. Shown are two adjacent f.c.c. cells of austenite which make a distorted b.c.c. cell. The black balls highlight the body-centered tetragonal unit cell (another representation of austenite, the relation between both being called the Bain Correspondence). The encircled atom of the f.c.c. lattice (a) becomes the body-centered atom in the distorted b.c.c. lattice (b). When subjected to Bain strain, it becomes an undistorted b.c.c. cell of martensite (c). Herewith, it is clear that the transformation was performed by displacement of atoms over subcellular distances.

B.2 Ceramics

In crystals not composed of like atoms, the primitive crystallographic structures of Fig. B.2 are not part of the game as witnessed by the two examples of so-called ionic ceramics (differences in electronegativity) shown in Fig. B.6. Zirconia has an f.c.c. packing with the O^{2-} ions in the tetrahedral holes. Gray-colored zirconium ions form the corners of a tetrahedron with an oxygen ion at the center. Since there are

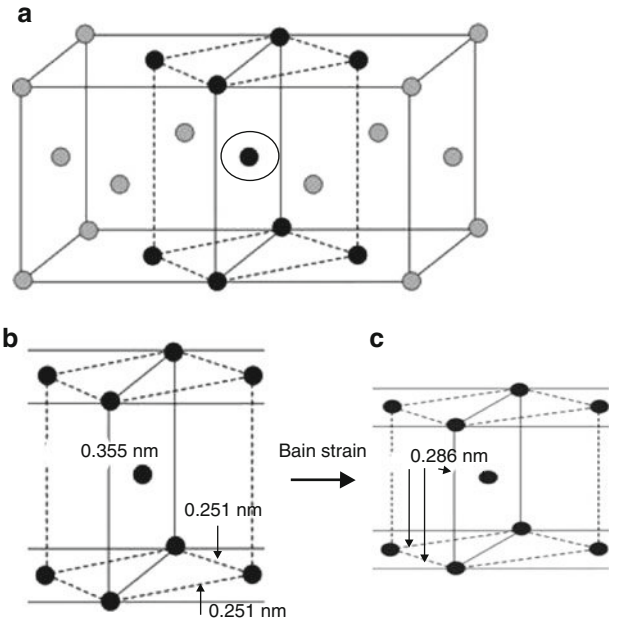

Fig. B.5 Austenite–martensite transformation. Explanation see text. By courtesy of Prof. em. E. Aernoudt

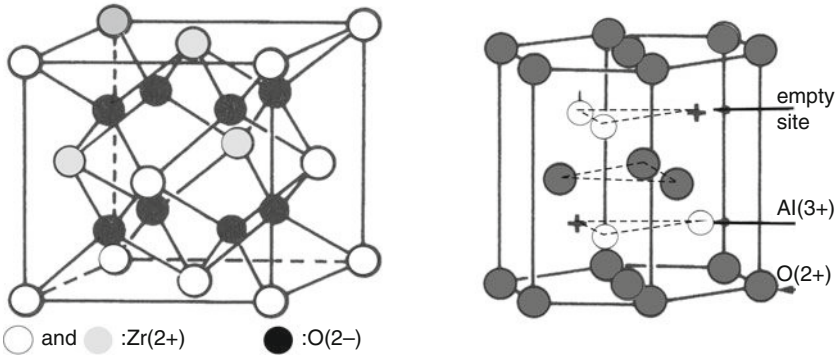

Fig. B.6 Crystallographic structure of (*left*) zirconia: f.c.c. packing of Zr with O in the tetrahedral holes; (*right*) alumina: h.c.p. packing of oxygen ions with Al^{3+} only in two-thirds of the octahedral holes (charge balance)

two tetrahedral holes for each atom of the f.c.c. structure, the formula is ZrO_2. In alumina, the oxygen atoms are hexagonally close-packed. The hexagonal structure has one octahedral hole and two tetrahedral holes per atom with Al^{3+} put into the octahedral interstices and each surrounded by six O^{2-} ions. In order to balance the charges only two thirds of the sites are filled and the formula works out at Al_2O_3.

Appendix C
Electrochemical Series

C.1 Equilibrium Electrochemical Series

The electrochemical series are set up by measuring series of metals and alloys with respect to a second electrode, a standard *nonpolarizable electrode*, *in casu* the standard or normal hydrogen electrode (SHE or NHE) or, for practical purposes, the standard calomel electrode (SCE). The characteristic of a nonpolarizable electrode is that its potential is not perturbed by small currents imposed by the measurement circuit itself (i.e., the power consumption, however small, of the voltmeter) or in other words, that the internal impedance of the electrode tends to zero. The reference half-cell in Fig. C.1 consists of a platina rod along which hydrogen gas at 1 atm is allowed to bubble (the gas adsorbs on the surface of Pt) and which is immersed in a solution of hydrogen ion with *activity* $a_{H+} = 1$.

The potential of the couple $H^+/\frac{1}{2}H_2$, toward the solution is arbitrarily taken to be zero when $a_{H+} = 1$ (cf. reaction in Table C.1). In practice, an SCE is mostly used. The electrode is always an integrated design containing the KCl bridge and the mercury/calomel electrode ($Hg/\frac{1}{2}Hg_2Cl_2$). Its potential with respect to the NHE is $+0.2681$ V and this potential is to be added to the potential measured to obtain the standard electrode potential. The other half cell, i.e., the left half of the corrosion cell of Fig. C.1, consists of a rod of the metal M to be measured immersed in a solution with $a_{M^{n+}} = 1$. For E_0 measurement, this activity should be 1.

The *activity* of an ion or *active concentration* at a given temperature is defined as the concentration (normal, molar or molal) multiplied by an activity coefficient. Although often taken to be the concentration, pH is equal to $-\log a_{H+}$, the activity of the hydrated hydrogen ion.

The activity coefficient corrects concentration for 'nonideal' behavior (compare to pressure-volume relationship for ideal and real gases) and is a function of physical interaction on the single hydrated ion by the solution; it can be calculated from the ionic strength: $I = 1/2 \sum_{i=1}^{i} c_i z_i^2$ with c the concentration (molar or molal) and z the valence of the ion. The reference state for solutions is *infinite concentration where* $f \rightarrow 1$. It is an integral part of the physical theory of solutions.

The total concentration of an ion in solution is also compromised by chemical reactions forming insoluble compounds or by complex-forming agents further

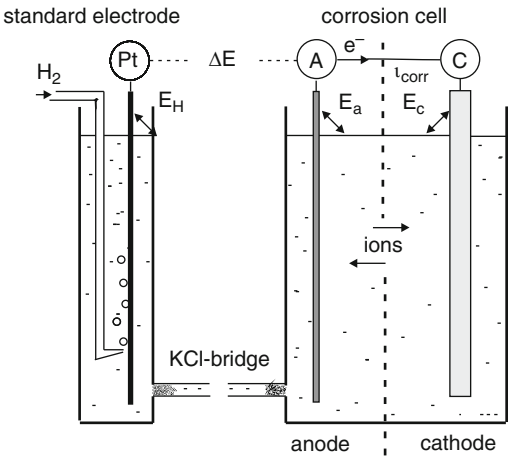

Fig. C.1 Electrochemical cell. *Left*: standard hydrogen electrode (solution with $a_{H+}) = 1$. *Right*: corrosion cell. The left half cell, if used as a separate unit, is a setup for measuring electrode potentials. In that case, the solution contains a specified activity of the metal ion of the electrode

reducing the effective concentration of the hydrated ion in solution but that is a chemical interaction. The concentration of the different ionic species in the log-term is extracted from the stability equation of the complex, in its simplest form equation (3.2). Subsequently the activities can be calculated.

For further reading, the textbook of Bockris and Reddy may be advised [98]. Within this book also references to textbook by Kortüm in which a particularly clear treatise is given on the basics of the physical chemistry of solutions. The treatment of electrode processes, electronic conductor and interphase region, called in modern electrochemistry *Electrodics*, is dated but it is great reading for those interested in the evolution of electrochemical concepts [97]. It represents the closure of the potential dominated era.

Standard Electrochemical Potentials

Standard electrochemical potentials for a selected number of electrochemical reactions are collected in Table C.1.

Anodic Back EMFs

These more realistic potentials were determined under constant current in equine serum; data collected in Table C.2. The weight loss was measured after immersion for 30 days at 37°C. Metals with ABE>568 mV show no loss of weight.

Table C.1 Electrochemical series of a selected number of elements. The IUPAC sign convention is followed

Electrochemical reaction	E_0 (in V vs. SHE)
$Au^{3+} + 3e^- \rightleftharpoons Au$	+1.50
$O_2 + 4H^+ + 4e^- \rightleftharpoons 2H_2O$	+1.2
$Pt^{2+} + 2e^- \rightleftharpoons Pt$	+1.20
$Ag^+ + e^- \rightleftharpoons Ag$	+0.80
$\frac{1}{2}Hg_2^{+2} + e^- \rightleftharpoons Hg$	+0.79
$Cu^{2+} + 2e^- \rightleftharpoons Cu$	+0.34
$H^+ + e^- \rightleftharpoons \frac{1}{2}H_2$	0.00
$Ni^{2+} + 2e^- \rightleftharpoons Ni$	−0.23
$Co^{2+} + 2e^- \rightleftharpoons Co$	−0.28
$Fe^{2+} + 2e^- \rightleftharpoons Fe$	−0.44
$Cr^{3+} + 3e^- \rightleftharpoons Cr$	−0.74
$V(II) + 2e^- \rightleftharpoons V$	−1.18
$Al_{3+} 3e^- \rightleftharpoons Al$	−1.66
$Ti^{3+} 3e^- \rightleftharpoons Ti$	−1.80
$Mg^{2+} + 2e^- \rightleftharpoons Mg$	−2.36
$Nb_2O_5 + 10H^+ + 10e^- \rightleftharpoons 2Nb + 5H_2O$	−0.65
$Ta_2O_5 + 10H^+ + 10e^- \rightleftharpoons 2Nb + 5H_2O$	−0.81
$TiO_2 + 4H^+ + 4e^- \rightleftharpoons Ti + 2H_2O$	−0.86
$ZrO_2 + 4H^+ + 4e^- \rightleftharpoons Zr + 2H_2O$	−1.43

Table C.2 Electrochemical series of alloys as determined by Clarke et al. [86]. Potentials determined in equine serum, normalized to the NHE; for loss of weight see text; (–) no data given

Alloy/element	Identification	AHE mV	Loss of weight mg/mm^2
Titanium		3768	–
Platina		1718	nil
Cr–Ni–Mo	Langalloy 5R	1143	–
Cr–Co–Mo	Vitallium	918	nil
18Cr–8Ni–3.25Mo	768		nil
Zirconium		588	nil

Table C.3 Pitting potential of metallic biomaterials in Hank's solution and re-passivating time in 0.9% NaCl (pH = 7.4). Reproduced from Breme [90]

Alloy	E_{pitt}	Re-passivation time (ms)			
		t_e		$t_{0.05}$	
	V	−0.5 V	+0.5V	−0.5 V	$+0.5V$
FeCrNiMo(316L)	0.2–0.3	>72,000	35	≫72,000	>6,000
CoCr (cast)	+0.42	44.4	36	≫6,000	>6,000
CoNiCr (worked)	+0.42	35.5	41	>6,000	5,300
TiAl6V4	+2.0	37	41	43.4	45.8
cp-Ti	+2.4	43	44.4	47.4	49
cp-Ta	+2.25	41	40	43	45
cp-Nb	+2.5	47.6	43.1	47	85

C.2 Pitting Potentials and Re-passivating Time

E_{pitt} or E_{crit} (see Fig. 3.7) is the potential at which the oxide layer is pierced, t_e time taken to restore an oxide layer and $t_{0.05}$ time taken by the oxide to grow to 5% of its final thickness; data collected in Table C.3.

Appendix D
Simulated Body Fluids

Numerous sets of solutions are used for in vitro testing of biomaterials. They simulate at least partially the composition of human body fluids: isotonic (same osmotic pressure as the body fluid the tested materials are expected to be in contact with), similar inorganic composition supplemented with some organic compounds and buffered at an adequate pH. Commonly used solutions are Hanks' and Ringer but in Table D.2 a recent versions are given. These solutions also serve to grow hydroxyapatite on substrates. In Table D.1, a summary of the prominent reactions involved in aqueous solution together with their equilibrium constants; the $-\log K_{sp}$ (sp: solubility product) of HA and $CaCO_3$ are, respectively, 117.0 and 8.6 [341, 474]. For more reliable data on solubility products, see Sect. 10.7. For oral materials, a simulation solution of saliva is used: it contains compounds that are not occurring in plasma or occur only at very low levels (Table D.3). Notice that the pH range of saliva is below intrabody values. A last example are solutions used for testing artificial heart valves (Table D.4). Minimum Essential Media (MEM) are very distinct from the SBFs because they contain various combinations of the amino acids: L-arginine, L-cystine, L-glutamine, L-histidine, L-leucine, L-isoleucine, L-methionine, L-tyrosine, and L-valine, considered essential to allow growth of cells for which the original Dulbecco version was intended to. Dulbecco's Eagle Medium (MEM) has about 28 different commercialized compositions for dedicated applications (ex.:Sigma Aldrich).

Table D.1 Main reactions of carbonate and phosphate; −log of the equilibrium constants are added in [−]. Data extracted from [340, 341, 474]

$H_2CO_3 \rightleftharpoons H^+ + HCO_3^-$ [6.31]	(D.1)
$HCO_3^- \rightleftharpoons H^+ + CO_3^{2-}$ [10.25]	(D.2)
$Ca^{2+} + HCO_3^- \rightleftharpoons CaHCO_3^-$ [−1.16]	(D.3)
$Ca^{2+} + CO_3^{2-} \rightleftharpoons CaCO_3$ [−3.38]	(D.4)
$H_3PO_4 \rightleftharpoons H^+ + H_2PO_4^-$ [2.20]	(D.5)
$H_2PO_4^- \rightleftharpoons H^+ + HPO_4^{2-}$ [7.19]	(D.6)
$HPO_4^{2-} \rightleftharpoons H^+ + PO_4^{3-}$ [12.19]	(D.7)
$Ca^{2+} + 2H_2PO_4^{3-} \rightleftharpoons CaH_2PO_4^+$ [−0.91]	(D.8)
$Ca^{2+} + HPO_4^{2-} \rightleftharpoons CaHPO_4$ [−2.39]	(D.9)

Table D.2 Nominal ion concentrations compared to human blood plasma in analytical concentration and the concentration of the dissociated ions. Strong electolytes (Na^+ etc.) are fully dissociated. Concentrations in mMol. c-SBF is the conventional composition, m-SBF the modified version and equal to plasma except for HCO_3^-. Data extracted from [474]

Ion	Blood plasma		c-SBF	m-SBF
	Total	Dissociated		
Na^+	142.0	142.0	142.0	142.0
K^+	5.0	5.0	5.0	5.0
Mg^2+	1.5	1.0	1.5	1.5
Ca^{2+}	2.5	1.3	2.5	2.5
Cl^-	103.0	103.0	147.8	103.0
HCO_3^-	27.0	27.0	4.2	10.0
HPO_4^{2-}	1.0	1.0	1.0	1.0
SO_4^{2-}	0.5	0.5	0.5	0.5

Table D.3 Average composition of saliva. Concentration in mM

Compound	Symbol	Concentration
Chloride	Cl^-	25
Bicarbonate	HCO_3^-	10
Phosphate	$-PO_4^{3-}$	5
Ammonia	NH_3	4
Urea	$CO(NH_2)_2$	∼3
Cyanide	$-CN^-$	0.001
Thiocyanate	$SCN\_$	2
Sulfhydryl	SH^-	0.07
Sodium	Na^+	20
Potassium	K^+	20
Calcium	Ca^{2+}	2
proteins		∼3
pH range		4–7.5

Table D.4 Fluid media for testing artificial heart valves and vascular grafts

The artificial valves/grafts are usually tested in pulse duplicators having as the liquid medium mainly one of the four alternatives:

1. Normal saline: 0.91% NaCl. Osmality: 300 mosmł$^{-1}$.
2. Normal saline + pleuracol V-10 to increase the viscosity to the viscosity of blood 4.10^{-3} Pa s (or 4 cp in non SI-units; w/specific gravity = 1.0).
3. Various mixtures of distilled water and glycerol for matching the solution to the viscosity of blood ∼ 4.10^{-3} Pa s.
4. Various polymeric solutions (polyacrylamid or Xanthan gum) may be used to explore the effect of non-Newtonian behavior on the mechanisms of opening and closing the valve.

The biologically derived valves/grafts are being tested in: Dulbecco's modified Eagle medium, supplemented w/sodium bicarbonate, L-glutamin, calf serum (10%) and antibiotics. In addition, Dextran is added to increase the viscosity to ∼ 4.10^{-3} Pa s.

References

1. R.H. March, *Physics for Poets* (McGraw-Hill, New York, 1970)
2. A. Vesalius, *De humani corporis fabrica libri septem.* (Ex officina Joannis Oporini, Basileae, Basel, 1543)
3. H. Glockner, *Die Europäische Philosophie* (Reclam, Stuttgart, 1958)
4. Hippocrates, *Epidemics I*, *The Loeb Classical Library, No.147*, vol. 1 (Harvard University Press, Cambridge, MA, 1984)
5. J. Black, *Biological Performance of Materials*, 2nd edn. (Marcel Dekker, New York, 1992)
6. D. Williams, Medical Device Technology pp. 8–11 (1994)
7. B. Di Ventura, C. Lemerle, K. Michalodimitrakis, L. Serrano, Nature **443**, 527 (2006)
8. G. Harveius, *De motu cordis et sanguinis in animalibus, Anatomica Exercitatio* (Ex officina Ioannis Maire, Lugduni Batavorum, 1539)
9. J.A. Borelli, *Die Bewegiung der Mengeringhausen* (Akademische Verlagsgeselschaft M.B.H., Leipzig, 1927)
10. K. Keele, *Leonardo da Vinci on movement of the heart and blood* (Harvey and Blythe, London, 1952)
11. D.W. Thompson, *On Growth and Form* (Dover Publications, New York, 1992). Unaltered republication of the work published by Cambridge, University Press, 1942
12. V. Smil, Nature **403**, 597 (2000)
13. M. Kleiber, *The fire of life* (Wiley, London, 1961)
14. G. West, J. Brown, B. Enquist, Science **276**, 122 (1997)
15. M. Schroeder, *Fractals, Chaos, Power Laws* (W.H. Freeman, New York, 1991)
16. C. McGowan, *Diatoms to dinosaurs: the size and scale of living things* (Island Press, Washington DC, 1994)
17. C. Mattheck, *Design in der Natur* (Rombach, Leipzig, 1993)
18. T. McMahon, Science **179**, 1201 (1973)
19. T. McMahon, Sci. Am. **233**, 93 (1975)
20. T. McMahon, R. Kronauer, J. Theor. Biol. **59**, 443 (1976)
21. C. Briand, S. Campion, D. Dzambo, K. Wilson, Am. J. Bot. **86**(12), 1677 (1999)
22. C.A. Darveau, R. Suarez, R. Andrews, P. Hochachka, Nature **417**, 166 (2002)
23. P. Reich, M. Tjoelker, J.L. Machado, J. Oleksyn, Nature **439**, 457 (2006)
24. B.B. Mandelbrot, *The Fractal Geometry of Nature* (W.H. Freeman, New York, 1983)
25. B. Ambati et al., Nature **443**, 993 (2006)
26. G. van Belle, *Statistical Rules of Thumb* (Wiley-Interscience, USA, 2002)
27. M. Hofmann, A. Young, U. Gbureck, S. Nazhat, J. Barralet, J. Mater. Chem. **16**(31), 3199 (2006)
28. L. Labey, Fixation strength and stability of tibial components of knee prostheses. Ph.D.thesis, University of Leuven, Faculty of Engineering, Department of Mechanics, Division of Biomechanics, Celestijnenlaan 200A, BE-3001 Leuven, Belgium (2003)
29. M.G. Li, K.G. Nilsson, J. Arthroplasty **15**, 744 (2000)

30. J.T. Schantz, A. Brandwood, D. Hutmacher, H. Khor, K. Bittner, J. Mater. Sci. Mater. Med. **16**, 807 (2005)
31. I. Manjubala, A. Woesz, C. Pilz, M. Rumpler, N. Fratzl-Zelman, P. Roschger, J. Stampfl, P. Fratzl, J. Mater. Sci. Mater. Med. **16**, 1111 (2005)
32. R. Mellaerts, C. Aerts, J. Van Humbeeck, P. Augustijns, G. Van den Mooter, J. Martens, Chem. Commun. 1375–1377 (2007)
33. T. Vicsek, *Fluctuations and Scaling in Biology* (Oxford University Press, Oxford, 2001)
34. F. Anscombe, Am. Stat. **27**(1), 17 (1973)
35. J. Helsen, H. Breme (eds.), *Metals as Biomaterials* (Wiley, Chichester, 1998)
36. M. Ashby, D. Jones, *Engineering Materials 1 and 2* (Butterworth-Heinemann, Oxford, 1998)
37. S. Timoshenko, *History of Strength of Materials* (General Publishing Company, Toronto, 1983)
38. S. Allen, E. Thomas, *The Structure of Materials* (Wiley, New York, 1999)
39. M. French, *Invention and Evolution* (Press Syndicate of the University of Cambridge, Cambridge, 1993)
40. E. Wintermantel, S.W. Ha, *Biocompatible Werkstoffe und Bauweizen* (Springer, Berlin, 1996)
41. G. Bergmann, F. Graichen, A. Rohlmann, Clin. Orthop. **335**, 190 (1997)
42. G. Bergmann, G. Deuretzbacher, M. Heller, F. Graichen, A. Rohlmann, J. Strauss, G. Duda, J. Biomech. **34**, 859 (2001)
43. M. Heller, L. Dürselen, M. Pohl, L. Claes, N. Haas, G. Duda, J. Biomech. **34**, 883 (2001)
44. M. Morlock, E. Schneider, A. Blum, M. Vollmer, G. Bergmann, V. Müller, M. Honl, J. Biomech. **34**, 873 (2001)
45. J.P. Simon, J. Orthop. Trauma **10**(7), 515 (1996)
46. G. Bergmann, F. Graichen, A. Rohlmann, J. Biomech. **26**, 969 (1993)
47. G. Bergmann, F. Graichen, A. Rohlmann, J. Biomech. **28**, 535 (1995)
48. A. Dowson, V. Wright (eds.), *Introduction to the Bio-mechanics of Joints and Joint Replacement* (Mechanical Engineering Publications, London, 1981)
49. J. Black, *Biological Performance of Materials*, third edn. (Marcel Dekker, New York, 1999)
50. T. Anderson, *Fracture Mehanics. Fundamentals and Applications*, 2nd edn. (CRC Press, London, 1995)
51. J. Black, *Biological Performance of Materials*, second edn. (Marcel Dekker, New York, 1992)
52. P. Williams, R. Warwick, M. Dyson, L. Bannister (eds.), *Gray's Anatomy*, 37th edn. (Churchill Livingstone, Edingburgh, 1989)
53. B. Verlinden, I. Smajdar, R. Doherty, *Thermo-mechanical Processing of Metallic Materials*. Pergamon Materials Series (Elsevier, New York, 2007)
54. R. Honeycombe, H. Bhadeshia, *Steels. Microstructure and Properties*, 2nd edn. (Edward Arnold, London, 1995)
55. D. Scharnweber, in *Metals as Biomaterials*, chap. 4, ed. by J. Helsen, H. Breme (Wiley, New York, 1998), pp. 101–151
56. P. Pedeferri, *Drawings on Titanium* (Cooperative libraria universitaria de politecnico, Milano, 1981)
57. P. Pedeferri, *Colors on Titanium* (Cooperative libraria universitaria de politecnico, Milano, 1982)
58. P. Pedeferri, *Movements on Titanium* (Cooperative libraria universitaria de politecnico, Milano, 1984)
59. D. Velten, K. Schenk-Meuser, V. Biehl, H. Duschner, J. Breme, Z. Metallkunde. **94**(6), 667 (2003)
60. M. Semlitsch, F. Staub, H. Weber, Biomed. Tech. **30**(12), 334 (1985)
61. M. Ashby, Acta Metall. **37**, 1273 (1989)
62. N. Waterman, M. Ashby (eds.), *Elsevier Materials Selector* (Elsevier Applied Science, London, 1991)
63. H.E. Boyer (ed.), *Atlas of Fatigue Curves* (ASM, Materials Park, OH, 1986)

64. A.K. Mishra, J. Davidson, R. Poggie, P. Kovacs, T. Fitzgerald, Mechanical and tribological properties and biocompatibility of diffusion hardened Ti-13Nb-13Zr - a new titanium alloy for surgical implants, in *Medical Applications of Titanium and Its Alloys: The Material and Biological Issues* (American Society for Testing and Materials, West Conshohocken, 1996), pp. 96–113. ASTM STP 1272
65. J. Helsen, Implantaten: materialen en hun mechanische eigenschappen, in *Handboek Orale Implantaten*, vol. A.6 (Bohn Stafleu Van Loghum, Houten, 2000), pp. 1–27. ISBN 90 650 2 675 4
66. R. Boyer, G. Welsch, E. Collings (eds.), *Materials Properties Handbook of Titanium Alloys* (ASM, The Materials Information Society, Materials Park, Ohio, 1994)
67. J. Mewis, A. Spaull, J. Helsen, Nature **253**, 618 (1975)
68. J. Helsen, L. De Groot, Trends Analyt. Chem. **1**, 259 (1982)
69. E. Solomon, R. Schmidt, P. Adragna, *Human Anatomy and Physiology*, second edn. (Saunders College Publishing, Philadelphia, 1990)
70. F. Evans, *Mechanical Properties of Bone* (Charles C Thomas, Springfield, Illinois, 1973)
71. D. Martin, P. Mayes, V. Rodwell, *Harper's Review of Biochemistry*, 18th edn. (Lange Medical Publications, Los Altos, CA, 1981)
72. J. Park, R. Lakes, *Biomaterials. An Introduction*, 2nd edn. (Plenum Press, New York, 1992)
73. J. Kärrholm, G. Garellich, P. Herberts, The Swedish Hip Arthroplasty Register. Annual Report 2005, www.jru.orthop.gu.se (2005)
74. P. Gebuhr, K. Stentzer, F. Thomsen, N. Levi, Acta Orthop. Belg. **66/65**(5), 472 (2000)
75. D. Markel, D. Hoard, C. Porretta, J. South. Orthop. Assoc. **10**(4), 202 (2001)
76. K. Abdel-Kader, J. Arthroplasty **15**, 205 (2000)
77. P. Herberts, L. Ahnfelt, H. Malchau, Clin. Orthop. **249**, 48 (1989)
78. H. Malchau, P. Herberts, G. Garellick, P. Söderman, T. Eisler, Prognosis of Total Hip Replacement, www.jru.orthop.gu.se (2002)
79. J. Kärrholm, G. Garellich, H. Lindahl, P. Herberts. Improved Analyses in the Swedish Hip Arthroplasty Register, www.jru.orthop.gu.se (2007)
80. B. Wroblewski, P.D. Diney, P.A. Fleming, Acta Orthop. **78**(2), 206 (2007)
81. J. Charnley, Lancet **277**(7187), 1129 (1961)
82. B. Wroblewski, Rheumatology **41**, 824 (2002)
83. J. Gilbert, C. Buckley, J. Jacobs, K. Bertin, M. Zernich, J. Bone Joint Surg. **76-A**(1), 110 (1994)
84. J. Collier, V. Surprenant, R. Jensen, M. Mayor, H. Surprenant, J. Bone Joint Surg. **74-B**(4), 511 (1992)
85. M. Scanziani, M. Hässer, Nature **461**, 930 (2009)
86. E. Clarke, J. Hickman, J. Bone Joint Surg. **35B**(3), 467 (1953)
87. H. Takayanagi, S. Kim, K. Matsuo, H. Suzuki, T. Suzuki, K. Sato, T. Yokochi, H. Oda, K. Nakamura, N. Ida, E. Wagner, T. Taniguchi, Nature **416**, 744 (2002)
88. J. Dumbleton, J. Black, *An Introduction to Orthopedic Materials* (Charles C Thomas, Springfield, IL, USA, 1975)
89. M. Barbosa (ed.), Biomaterials Degradation, *European Materials Research Society Monographs*, vol. 1 (North-Holland, Amsterdam, 1991)
90. J. Breme, Erzmetall **48**(4), 249 (1995)
91. Y. Yan, A. Neville, D. Dowson, J. Phys. D Appl. Phys. **39**(15), 3206 (2006)
92. J. Dobbelaar, J. de WIT, J. Electrochem. Soc. **137**(7), 2038 (1990)
93. R. Revie, H. Uhlig, *Corrosion and Corrosion Control. An Introduction to Corrosion Science and Engineering*, 4th edn. (Wiley Interscience, New York, 2008)
94. H. Hildebrand, P. Laffargue, A. Duquennoy, H. Mestdagh, Int. J. Risk Safety Med. **8**, 125 (1996)
95. A. Hodgson, S. Mischler, B. Von Rechenberg, S. Virtanen, Proc. Inst. Mech. Eng. H **221**, 291 (2007)
96. A. Hodgson, S. Kurz, S. Virtanen, V. Fervel, C.O. Olsson, S. Mischler, Electrochim. Acta **49**, 2167 (2004)

97. G. Kortüm, J. Bockris, *Textbook of Electrochemistry*, vols. 1 and 2 (Elsevier, New York, 1951)
98. J. Bockris, A. Reddy, *Modern Electrochemistry*, 3rd edn. (Plenum, New York, 1977)
99. D. Pletcher, F.C. Walsh, *Industrial Electrochemistry*, 2nd edn. (Chapman and Hall, London, 1990)
100. S. Lampman (ed.), *ASM Handbook on Fatigue and Failure*, vol. 19 (ASM International, Materials Park, Ohio, 1996)
101. B. Bhushan, *Introduction to Tribology* (Wiley, New York, 2002)
102. A. Fischer, J. Phys. D Appl. Phys. **39**(15), 1 (2006)
103. M. Huq, C. Butaye, J.P. Celis, J. Mater. Res. **15**(7), 1591 (2000)
104. A. Vieira, A. Ribeiro, L. Rocha, J.P. Celis, Wear **261**, 994 (2006)
105. J. Feeney, M. Blackburn, in *The theory of Stress Corrosion Cracking in Alloys*, ed. by J. Scully (NATO Scientific Affairs, Brussels, 1971), pp. 355–398
106. K. Lucas, A. Buchanan, J. Lemons, J. Biomed. Mater. Res. **15**, 731 (1981)
107. C. Griffin, A. Buchanan, J. Lemons, J. Biomed. Mater. Res. **17**, 489 (1983)
108. N. Thompson, R. Buchanan, J. Lemons, J. Biomed. Mater. Res. **13**, 35 (1979)
109. M. Barbosa, J. Scully, Corrosion Sci. **22**(11), 1025 (1982)
110. P. Jemmely, S. Mischler, D. Landolt, Wear **237**, 63 (2000)
111. S. Watson, F. Friedersdorf, B. Madsen, S. Cramer, Wear **181–183**, 476 (1995)
112. F. Renner, A. Stierle, H. Dosch, D. Kolb, T.L. Lee, J. Zegenhagen, Nature **439**, 707 (2006)
113. E. Wiberg, Chem. Ber. **83**(6), XIX (1950)
114. E. Mellon, J. Chem. Educ. **54**(4), 211 (1977)
115. Martin, Essential Elements, in *Toxicity of Inorganic Compounds* (Marcel Dekker, New York, 1988), p. 12
116. F. Sunderman, Nickel, in *Handbook on Toxicity of Inorganic Compounds* (Marcel Dekker, New York, 1988), pp. 454–468
117. K. Van Dyck, H. Robberecht, R. Van Cauwenbergh, H. Deelstra, Eur. Food. Res. Technol. **210**, 77 (1999)
118. E. Carlisle, Science **197**, 279 (1970)
119. K. Konhauser, E. Pecoits, S. Lalonde, D. Papineau, E. Nisbet, M. Barley, N. Arndt, K. Zahnle, B. Kamber, Nature **458**, 750 (2009)
120. L. Alderighi, P. Gans, A. Ienco, D. Peters, A. Sabatini, A. Vacca, Coord. Chem. Rev. **184**, 311 (1999)
121. A. Ringbom, *Complexation in Analytical Chemistry* (Wiley, New York, 1963)
122. A. Ringbom, *Les Complexes en Chimie Analytique* (Dunod, Paris, 1967)
123. A. Sigel, H. Sigel, R. Sigel (eds.), *Metal Ions in Biological Systems* (Marcel Dekker, New York, 1995)
124. G. Scharzenbach, H. Flaschka, *Complexometric Titrations*, 5th edn. (Methuen, London, 1969)
125. M. Margoshes, B. Valle, J. Am. Chem. Soc. **79**, 4813–4814 (1957)
126. M. Cherian, Metallothionein and its interaction with metals, in *Toxicology of Metals* (Springer, Berlin, 1995), pp. 121–137
127. D. Dawson, N. Ballatori, Membrane transporters as sites of action and routes of entry for toxic metals, in *Toxicology of Metals* (Springer, Berlin, 1995), pp. 53–76
128. M. Pauwels, J. Van Weyenbergh, A. Soumillon, P. Proost, M. De Ley, Eur. J. Biochem. **220**, 105 (1994)
129. N. Vandeghinste, P. Proost, M. De Ley, Cell. Mol. Biol. **46**(2), 419 (2000)
130. M. Rahman, M. De Ley, Cell. Biol. Toxicol. **24**, 19 (2008)
131. J. Novotny, M. Green, R. Boston (eds.), *Mathematical Modeling in Nutrition and the Health Sciences*. Advances in Experimental Medicine and Biology, vol. 537 (Kluwer Academic/Plenum Publishers, New York, 2003)
132. J. Gabrielsson, D. Weiner, *Pharmacokinetic and Pharmacodynamic Data Analysis: Concepts and Applications*, 4th edn. (J Gabrielsson and Swedish Pharmamceutical Society, Swedish Pharmaceutical Press, Stockholm, Sweden, 2000)
133. R. De Woskin, C. Thompson, Regul. Toxicol. Pharmacol. **51**, 66 (2008)

134. J. Ross, W. Slooff, Basisdocument Cadmium. Publikatiereeks Milieubeheer Rapport nr.4, Directoraat-Generaal Milieubeheer, Rijksinstituut voor Volksgezondheid en Milieuhygiene, Bilthoven (1990)
135. M. Rowland, T. Tozer, *Clinical Pharmacokinetics: Concepts and Applications*, 3rd edn. (Williams and Wilkins, Baltimore, 1995)
136. N. Shock, *Mortality and Measurement of Aging* (American Institute of Biological Sciences, Waverly Press, Baltimore, 1960), chap. 2, pp. 14–30
137. R. Arking, *Biology of Aging*, 2nd edn. (Sinauer Associates, Sunderland, 1998)
138. J. Brookbank, *The Biology of Aging* (Harper and Row, New York, 1990)
139. L. Pelletier, P. Druet, Immunotoxicology of metals, in *Metal Ions In Biological Systems* (Marcel Dekker, New York, 1995), pp. 77–92
140. B. Ratner, A. Hoffman, F. Schoen, J. Lemons (eds.), *Biomaterials Science*, 2nd edn. (Academic Press, Amsterdam, 1996)
141. J. Helsen, J. Proost, J. Schrooten, G. Timmermans, E. Brauns, J. Vanderstraeten, J. Eur. Ceram. Soc. **17**, 147 (1997)
142. J. Schrooten, J. Helsen, Biomaterials **21**, 1461 (2000)
143. N. Hallab, K. Merritt, J. Jacobs, J. Bone Joint Surg. **83-A**(3), 428 (2001)
144. F. Leynadier, F. Langlais, Total hip arthroplasties and allergy to metals, in *Biocompatibility of Co-Cr-Ni Alloys*. NATO ASI Series A: Life Sciences, vol. 158 (Plenum Press, New York, 1988), pp. 193–200
145. D. Tilsley, H. Rotstein, Contact Derm. **6**, 175 (1980)
146. A. Cvetkovic, Nature **466**, 779 (2010)
147. J. Helsen, B. Bloch, Acta Orthop. Belg. **43**, 62 (1977)
148. U. Hillen, M. Haude, R. Erbel, M. Goos, Contact Derm. **47**, 353 (2002)
149. S. Brown, L. Farnsworth, K. Merritt, T. Crowe, J. Biomed. Mater. Res. **22**, 321 (1986)
150. F. Sunderman, Carcinogenic risks of Metal Implants and Prostheses, in *Biocompatibility of Co-Cr-Ni Alloys*. NATO ASI Series A: Life Sciences, vol. 158 (Plenum Press, New York, 1988), pp. 11–19
151. C. Alexander, Am. J. Med. **53**, 395 (1972)
152. P. Roy, J. Bonenfant, L. Turcot, Am. J. Clin. Pathol. **50**(2), 234 (1968)
153. Angerer J., R. Heinrich, Cobalt, in *Handbook on Toxicity of Inorganic Compounds* (Marcel Dekker, New York, 1988), pp. 251–264
154. J. Bassham, A. Benson, L. Kay, A. Harris, T. Wilson, M. Calvin, J. Am. Chem. Soc. **76**, 1760 (1954)
155. E. Stiefel, The biogeochemistry of molybdenum and tungsten, in *Metal Ions in Biological Systems: Molybdenum and tungsten: their roles in bioligical processes*, vol. 39, chap. 1 (Marcel Dekker, New York, 2002), pp. 2–29
156. S. Malcolmson, S. Meek, E. Sattely, R. Schrock, A. Hoveyda, Nature **456**, 933 (2008)
157. K. Thompson, K. Scott, J. Turnlund, J. Appl. Physiol. **81**, 1404 (1996)
158. M. Cantone1, D. De Bartolo, A. Giussani, A. Ottolenghi, L. Pirola, C. Hansen, P. Roth, E. Werner, Appl. Radiat. Isot. **48**, 333 (1997)
159. F. Lagarde, M. Leroy, Metabolism and toxicity of tungsten in humans and animals, in *Metal Ions in Biological Systems: Molybdenum and Tungsten: Their Roles in Biological Processes*, vol. 39, chap. 22 (Marcel Dekker, New York, 2002), pp. 741–759
160. A. Alfrey, J. Mishell, J. Burks, S. Contiguglia, H. Rudolph, E. Lewin, J. Holmes, Trans. Am. Soc. Artif. Intern. Organs **18**, 257 (1972)
161. A. Wing, F. Brunner, H. Brynger, C. Chantler, R. Donderwolcke, H. Gurland, C. Jacobs, P. Kramer, N. Selwood, Lancet 90–192 (July 26, 1980)
162. E. Jeffery, Biochemical mechanisms of aluminum toxicity, in *Toxicology of Metals* (Springer, Berlin, 1995), pp. 139–161
163. A. Prescott, New Sci. 58–62 (21 January, 1989)
164. F. Kemper, Erzmetall **40**(10), 542 (1987)
165. L. Zhou, D. Eylon, G. Lütjering, C. Ouchi (eds.) *Tissue reactions and biological effects in patients with total joint prostheses from Ti-Base alloys*. Proceedings of the Xi'an International Titanium Conference, (XITC'98), vol. 2 (Intern. Acad. Publishers, Beijing, China, 1999)

166. J. Li, G. Ekberg, D. Crans, Y. Shechter, Biochemistry **35**, 8314 (1996)
167. A. Chandra, R. Ghosh, A. Chatterjee, Toxicol. Mech. Methods **17**, 175 (2007)
168. K. Kobayashi, S. Himeno, M. Satoh, Toxicology **228**, 162 (2006)
169. B. Mukherjee, B. Patra, S. Malapratra, P. Banerjee, A. Tiwari, M. Chatterjee, Toxicol. Lett. **150**, 135 (2004)
170. S. Glyn-Jones, H. Pandit, Y.M. Kwon, H. Doll, H. Gill, D. Murray, J. Bone Joint Surg. **91-B**(12), 1566 (2009)
171. D. Langton, A. Sprowson, R. Joyce, M. Reed, I. Carluke, P. Partington, A. Nargol, J. Bone Joint Surg. **91-B**(10), 1287 (2009)
172. D. Langton, S. Jameson, R. Joyce, N. Hallab, S. Natu, A. Nargol, J. Bone Joint Surg. **91-B**(1), 38 (2010)
173. W. Brodner, P. Bitzan, V. Meisinger, A. Kaider, F. Gottsauner-Wolf, R. Kotz, J. Bone Joint Surg. Am. **85-A**, 2168 (2003)
174. H.G. Willert, G. Buchhorn, A. Fayyazi, R. Flury, M. Windler, G. Köster, C. Lohmann, J. Bone Joint Surg. **87-A**, 28 (2005)
175. A. Davies, H.G. Willert, P. Campbell, I. Learmonth, C. Case, J. Bone Joint Surg. **87-A**, 18 (2005)
176. Y.S. Park, Y.W. Moon, L.S.-J., J.M. Yang, G. Ahn, Y.L. Choi, J. Bone Joint Surg. Am **8-A**, 1515 (2005)
177. P. Korovessis, G. Petsinis, M. Repanti, T. Repanti, J. Bone Joint Surg. **88-A**(6), 1183–1191 (2006)
178. A. Hart, T. Hester, K. Sinclair, J. Powell, A. Goodship, L. Pele, N. Fersht, J. Skinner, J. Bone Joint Surg. **88-B**(4), 449 (2006)
179. D. Langton, S. Jameson, R. Joyce, J. Webb, A. Nargol, J. Bone Joint Surg. **90-B**(9), 1143 (2008)
180. S. Kawanishi, Role of active oxygen species in metal-induced DNA damage, in *Toxicology of Metals* (Springer, Berlin, 1995), pp. 349–371
181. M. Andersen, D. Krewski, Toxicol. Sci. **107**(2), 324 (2009)
182. J. Campain, Metals and inorganic compounds, in *Physiologically Based Pharmacokinetic Modeling. Science and Applications* (Wiley-Interscience, Hoboken, 2005), pp. 239–270
183. J.P. Simon, Restoration of bone stock with impacted cancellous allografts and cement in revision of the femoral compontent in total hip arthroplasty. Ph.D. thesis, Department Orthopedic Surgery, University Hospital Pellenberg, Catholic University of Leuven, 1994
184. M. Ashby, Acta Metall. **37**(5), 1273 (1989)
185. D. Jihua, A note on the theory and applications of traditional Chinese medicine in orthopedics, in *China's New Achievements in Orthopedic Surgery* (New World Press, Bejing, 1993), pp. 157–159
186. E. Ezerietis, K. Gross, J. Vētra, in *Northsea Biomaterials 1998*. European Society for Biomaterials (Dutch Society for Biomaterials, 1998), p. 190
187. G. Hunter, J. Dickinson, B. Herb, R. Graham, J. ASTM Int. **2**(7) (2005)
188. G. Hunter, J. Dickinson, B. Herb, R. Graham, in *Titanium, Niobium, Zirconium and Tantalum for Medical and Surgical Applications*, ed. by L. Zardiackas, M. Kraay, H. Freese, ASTM STP 1471 (American Society for Testing Materials, West Conshohocken, PA, 2006), pp. 16–29
189. M. Weeks, *Discovery of the elements*, 7th edn. (J. Chem. Educ., 1978)
190. K. Purcell, J. Kotz, *Inorganic Chemistry* (Holt-Saunders International Editions, 1997)
191. R. Sanderson, *Inorganic Chemistry* (Reinhold Publishing Corporation, New York, 1967)
192. R. Webster, Zirconium and Hafnium, in *Metals Handbook*, vol. 2, 10th edn., (ASM International, Materials Park, OH, 1990), pp. 661–669
193. J. Hanchar, W. van Westrenen, Elements **3**(February), 37 (2007)
194. L. Hobbs, V. Rosen, S. Mangin, M. Treska, G. Hunter, Int. J. Appl. Ceram. Technol. **2**(3), 221 (2005)
195. M. Pourbaix, N. de Zoubov, J. Van Muylder, *Atlas d'Equilibres Electrochimiques* (Gauthier-Villars & C^{ie}, Paris, 1963)
196. A. Mamun, R. Schennach, J. Parga, M. Mollah, M. Hossain, D. Cocke, Electrochim. Acta **46**, 3343 (2001)

197. J. Davidson, C. Asgian, A. Mishra, P. Kovacs, Zirconia ZrO_2-coated zirconium-2.5Nb alloy for prosthetic knee bearing applications, in *Bioceramics*, vol. 5 (World Scientific, Singapore, 1992), pp. 389–401
198. G. Hunter, W. Jones, M. Spector, Oxidized Zirconium, in *Total Knee Arthroplasty* (Springer, Berlin, 2005), pp. 370–377
199. N. Sheth, P. Lementowski, G. Hunter, J. Garino, J. Surg. Orthop. Adv. **17**(1), 17 (2008)
200. M. Ries, A. Salehi, K. Widding, G. Hunter, J. Bone Joint Surg. **84-A** (Suppl.2), 129 (2002)
201. A. Kace, J. Hermida, C. Colwell, D. D'Lima, Clin. Orthop. Relat. Res. **428**, 120 (2004)
202. S. White, L. Whiteside, D. McCarthy, M. Anthony, R. Poggie, Clin. Orthop. Relat. Res. (309), 176 (1994)
203. R. Laskin, Clin. Orhtop. Relat. Res. (416), 191 (2003)
204. P. Lewis, C. Moore, M. Olsen, E. Schemitsch, J. Waddell, Orthopedics **31**(12S), 109 (2008)
205. J. Masonis, M. Kuremsky, S. Odum, B. Springer, Am. Acad. Orthop. Surg. Annu. Meet. Proc. **9**, 481 (2008)
206. C. Bragdon, K. Wannomae, A. Lozynsky, B. Micheli, H. Malchau, Trans. Orthop. Res. Soc. **34**, 2337 (2009)
207. S. Nasser, M. Mott, P. Wooley, Am. Acad. Orthop. Surg. Annu. Meet. Proc. **8**, 437 (2007)
208. J. Helsen, K. Dessein, L. Froyen, K. Cauwels, C. Pypen, H. Plenk, in *13th European Conference on Biomaterials, Göteborg, 4-7 september*. (European Society for Biomaterials, Göteborg 970825, Sweden, 1997), p. 41
209. F. Sisco, E. Epremian, *Columbium and Tantalum* (Wiley, New York, 1963)
210. E. Colin, in *Niobium, Proceedings of the international syplosium*, ed. by H. Stuart (The Metallugical Society of AIME, New York, 1984), p. 243
211. K. Matucha, Structure and properties of nonferrous alloys, in *Materials Science and Technology, a comprehensive treatment*, vol. 8 (UCH Publishers, New York, 1996)
212. H.J. Rätzer-Scheibe, H. Buhl, in *Titanium Science and Technology*, vol. 4, ed. by G. Lütjering, U. Zwicker, W. Bunk (Deutsche Gesellschaft für Metallkunde e.V., Adebauerallee 21, D-6370 Oberuresel1, 1985), pp. 2641–2648
213. L. Gypen, Mechanische eigenschappen en corrosiegedrag van substitutionele tantaallegeringen. Ph.D. thesis, Department of Metallurgy and Materials Engineering, KULeuven, 1979
214. J. Breme, H.J. Schmid, Criteria for the Bioinertness of Metals for Osseo-Integrated Implants, in *Osseo-Integrated Implants* (CRC Press, Boca Raton, 2000), pp. 31–79
215. N. Oliveira, S. Biaggio, R. Rocha-Filho, N. Bocchi, J. Biomed. Mater. Res. A **74A**, 397 (2005)
216. C. Pypen, K. Dessein, J. Helsen, M. Gomes, H. Leenders, J. de Bruijn, J. Mater. Sci. Mater. Med. **9**(12), 761 (1998)
217. C. Pypen, H. Leenders, M. Gomes, R. Dekkers, J. Helsen, H. Plenk, J. de Bruijn, in *Society for Biomaterials, 25th Annual Meeting, Providence*, ed. by M. LaBerge, C. Agrawal. (Society for Biomaterials, Minneapolis, MN, 1999), p. 588
218. G. Burke, Can. Med. Assoc. J. **43**(2), 125 (1940)
219. K. Plenk, G. Pfiuger, S. Schider, The current use of uncemented tantalum and niobium femoral endoprostheses, in *The Cementless Fixation of Hip Endoprostheses* (Springer, Berlin, 1984), p. 174
220. S. Hacking, J. Bobyn, K.K. Toh, M. Tanzer, J. Krygier, J. Biomed. Mater. Res. **52**, 631 (2000)
221. L. Zardiackas, D. Parsell, L. Dillon, D. Mitchell, L. Nunnery, R. Poggie, J. Biomed. Mater. Res. **58**, 180 (2001)
222. B. Levine, C. Della Valle, J. Jacobs, J. Am. Acad. Orthop. Surg. **14**(12), 646 (2006)
223. J. Bobyn, K.K. Toh, S. Hacking, M. Tanzer, J. Krygier, J. Arthroplasty **14**(3), 347 (1999)
224. J. Bobyn, G. Stackpool, S. Hacking, M. Tanzer, J. Krygier, J. Bone Joint Surg. **81-B**(5), 907 (1999)
225. D. Hofmann, J.Y. Suh, A. Wiest, G. Duan, M.L. Lind, M. Demetriou, W. Johnson, Nature **451**, 1085 (2008)
226. K. Jin, J. Löffler, Appl. Phys. Lett. **86**, 241909 (2005)
227. S. Buzzi, K. Jin, P. Uggowitzer, S. Tosatti, I. Gerber, J. Löffler, Intermetallics **14**, 729 (2006)

228. Q. Jiang, X. Nie, Y. Li, Y. Jin, Z. Chang, X. Huang, J. Jiang, J. Alloys Compd. **443**, 191 (2007)
229. S. Elliott, *Physics of Amorphous Materials*, second edn. (Longman Scientific and Technical, Essex, 1990)
230. C. Janot, *Quasicrystals, A Primer*, 2nd edn. Monographs on the Physics and Chemistry of Materials (Clarendon Press, Oxford, 1998)
231. J.M. Dubois, *Useful Quasicrystals* (World Scientific, Singapore, 2005)
232. R. Hazen, D. Papineau, W. Bleeker, R. Downs, J. Ferry, T. McCoy, D. Sverjensky, H. Yang, Am. Mineral. **93**, 1693 (2008)
233. S. Weiner, Y. Talmon, W. Traub, Int. J. Biol. Macromol. **5**, 325 (1983)
234. P. Fratzl, N. Fratzl-Zelman, K. Klaushofer, G. Vogl, K. Koller, Calcif. Tissue Int. **48**, 407 (1991)
235. J. Colantonio, J. Vermot, D. Wu, A. Langenbacher, S. Fraser, J.N. Chen, Nature **457**, 205 (2009)
236. M. Lucke, G. Schmidmaier, S. Sadoni, B. Wildemann, R. Schiller, N. Haas, M. Raschke, Bone **32**, 521 (2003)
237. R. Darouiche, J. Farmer, C. Chaput, M. Mansouri, G. Saleh, G. Landon, J. Bone Joint Surg. **80**, 1336 (1998)
238. J. Hardes, H. Ahrens, C. Gebert, A. Streitbuerger, H. Buerger, M. Erren, A. Gunsel, C. Wedemeyer, G. Saxler, W. Winkelmann, G. Gosheger, Biomaterials **28**, 2869 (2007)
239. V. Alt, T. Bechert, P. Steinrücke, M. Wagener, P. Seidel, E. Dingeldein, E. Domann, R. Schnettler, J. Biomater **25**, 4383 (2004)
240. V. Alt, M. Wagner, D. Salz, T. Bechert, P. Steinrücke, R. Schnettler, Plasma polymer - high-porosity silver composite coating for infection prophylaxis in intramedullary nailing, in *Practice of Intramedullary Locked Nails* (Springer, Berlin, 2006), pp. 297–303
241. J. Sung, J. Ji, J. Park, J. Yoon, D. Kim, K. Jeon, M. Song, J. Jeong, B. Han, J. Han, Y. Chung, H. Chang, J. Lee, M. Cho, B. Kelman, I. Yu, Toxicol. Sci. **108**(2), 452 (2009)
242. P. Laffargue, P. Fialdes, P. Frayssinet, M. Rtaimate, H. Hildebrand, J. Biomed. Mater. Res. **49**, 415 (2000)
243. P. Laffargue, H. Hildebrand, M. Rtaimate, P. Frayssinet, J. Amoureux, X. Marchandise, Bone **25**(2), 555 (1999)
244. R. Schek, J. Taboas, S. Segvich, S. Hollister, P. Krebsbach, Tissue Eng. **10**(9/10), 1376 (2004)
245. J. Taboas, R. Maddox, P. Krebsbach, S. Hollister, Biomaterials **24**, 181 (2003)
246. A. Tampieri, S. Sprio, A. Ruffini, G. Celotti, I. Lesci, N. Roveri, J. Mater. Chem. **19**, 4973 (2009)
247. H.C. Wang, F. Jia, T. Gilbert, S.Y. Woo, J. Biomech. **36**, 97 (2003)
248. G. Ilizarov, V. Ledyaev, Clin. Orthop. Relat. Res. (280), 7 (1992)
249. F. Gelaude, P. Broos, M. Mulier, B. Vandenbroucke, J.P. Kruth, B. Lauwers, J. Vander Sloten, in *Proceedings of the International Society for Computer Assisted Orthopedic Surgery* (CAOS 2007, Heidelberg, Germany, 2007)
250. F. Gelaude, T. Clijmans, P. Broos, B. Lauwers, J. Vander Sloten, Comput. Aided Surg. **12**(5), 286 (2007)
251. F. Gelaude, Comput. Methods Biomech. Biomed. Engin. **9**(1), 65 (2006)
252. F. Gelaude, J. Vander Sloten, B. Lauwers, Comput. Aided Surg. **13**(4), 188 (2008)
253. L. Murr, S. Quinones, S. Gaytan, M. Lopez, A. Rodela, E. Martinez, D. Hernandez, E. Martinez, F. Medina, R. Wicker, J. Mech. Behav. Biomed. Mater. **2**, 20–32 (2009)
254. O. Lühn, C. Van Hoof, W. Ruythooren, J.P. Celis, Microelectron. Eng. **85**, 1947 (2008)
255. G. Kerckhofs, J. Schrooten, T. Van Cleynenbreugel, S. Lomov, M. Wevers, Rev. Sci. Instrum. **79**, 0137111 (2008)
256. G. Song, Corrosion Sci. **49**, 1696 (2007)
257. X. Hallopeau, T. Beldjoudi, C. Fiaud, in *Proceedings of the Third International Magnesium Conference* The Institute of Metals, London, 1996, ed. by G. Lorimer, pp. 713–725
258. C. Müller, R. Koch, G. Deinzer, in *Magnesium Alloys and their Applications*, ed. by K. Kainer (Wiley-VCH, Weinheim, 2000), pp. 457–462

259. E. Zhang, L. Xy, K. Yang, Scr. Mater. **53**, 523 (2005)
260. S. Tottey, K. Waldron, S. Firbank, B. Reale, C. Bessant, K. Sato, T. Cheek, J. Gray, M. Banfield, C. Dennison, N. Robinson, Nature **455**, 1138 (2008)
261. H. Vojtích, H. Èíová, K. Volenec, Metall. Mater. **44**(4), 211 (2006)
262. Y. Wan, G. Xiong, H. Luo, F. He, Y. Huang, X. Zhou, Mater. Des. **29**, 2034 (2008)
263. H. Haferkamp, V. Kaese, M. Niemeyer, K. Philipp, P.t. Thai, B. Heublein, R. Rohde, Implantate - ein Neues Anwendungsfeld für Magnesiumlegierungen, in *Magnesium Taschenbuch* (Aluminium Verlag, Düsseldorf, 2000), pp. 669–677
264. K. Máthis, J. Gubicza, N. Nam, J. Alloys Compd. **394**, 194 (2005)
265. L. Vuong, L. Jiang, J. Jonas, S. Godet, B. Verlinden, P. Van Houtte, Can. Metall. Q. **47**(4), 437 (2008)
266. Y. Yamada, K. Shimojima, J. Mater. Sci. Lett. **18**, 1477 (1999)
267. H.P. Degischer, B. Kriszt (eds.), *Handbook of Cellular Materials* (Wiley-VCH, Weinheim, 2002)
268. K. Kainer (ed.), *Magnesium Alloys and their Applications* (Wiley-VCH, Weinheim, 2000)
269. H. López, D. Cortés, S. Escobedo, D. Mantovani, Key Eng. Mater. **309–311**, 453 (2006)
270. F. Witte, V. Kaese, H. Haferkamp, E. Switzer, A. Meyer-Lindenberg, H. Wirth, C.J. an Windhagen, Biomaterials **26**, 3557 (2005)
271. F. Witte, Acta Biomater.**6**, 1680 (2010)
272. J. Noble, *The Techniques of Painted Attic Pottery* (Faber, London, 1966)
273. A. Meunier, *Argiles* (Contemporary Publishing International, Paris, 2003)
274. C. Weaver, L. Pollard, *The Chemistry of Clay Minerals* (Elsevier, Amsterdam, 1973)
275. Y. Maniatis, M. Tite, in *Thera and the Aegean World I* (Thera Foundation, Santorini, Greece, 1978), pp. 483–492
276. H. Frisk, *Griechisches Etymologisches Wörterbuch*, vol. I, 2nd edn. (Carl Winter Universitätsverlag, Heidelberg, 1973)
277. C. Martin, Nature **445**, 34 (2007)
278. H. Scholten, L. Dortmans, G. de With, Application of mixed-mode fracture criteria for weakest-link failure prediction for ceramic materials, in *Life Prediction Methodologies and Data for Ceramic Materials*, STP 1201 (ASTM, Philadelphia, 1994), pp. 192–206
279. L.Y. Chao, D. Shetty, Time-dependent strength degradation and reliability of an alumina ceramic subjected to biaxial flexure, in *Life Prediction Methodologies and Data for Ceramic Materials*, STP 1201 (ASTM, Philadelphia, 1994), pp. 228–249
280. J. Chevalier, L. Gremillard, J. Eur. Ceram. Soc. **29**, 1245 (2009)
281. P. Auerkari, Mechanical and physical properties of engineering alumina ceramics. Research Notes 1792. Technical report, Technical Research Centre of Finland (1996)
282. R. Hannink, P. Kelly, B. Muddle, J. Am. Ceram. Soc. **83**(3), 461 (2000)
283. D. Stauffer, *Introduction to Percolation Theory* (Taylor and Francis, London, 1985)
284. M. Kuntz, B. Masson, T. Pandorf, Current State of the Art of the Ceramic Composite Material BIOLOX® delta, in *Strength of Materials* Materials Science and Technologies Binding (Nova Science Publishers, 2009). To be published in 2009; ISBN: 978-1-60741-500-8
285. R. Hannink, P. Kelly, B. Muddle, J. Am. Ceram. Soc. **83**(3), 461 (2000)
286. W. Burger, Keramische Zeitschrift **50**(11), 18 (1998)
287. W. Burger, Keramische Zeitschrift **49**(12), 1067 (1997)
288. C. Piconi, G. Maccaraud, L. Pilloni, W. Burger, F. Muratori, H. Richter, J. Mater. Sci. Mater. Med. **17**, 289 (2006)
289. J. Allain, S. Le Mouel, D. Goutallier, M. Voisin, J. Bone Joint Surg. **81-B**(5), 835 (1999)
290. G. Anné, S. Hecht-Mijic, H. Richter, O. Van der Biest, J. Vleugels, Scr. Mater. **54**, 2053 (2006)
291. G. Anné, Electrophoretic deposition as a near net schaping technique for functionally graded biomaterials. Ph.D. thesis, Department of Metallurgy and Materials Engineering, K.U.Leuven (2005). UDC 62-039.1
292. J. Chevalier, S. Grandjean, M. Kuntz, G. Pezzotti, Biomaterials **30**, 5279 (2009)
293. J. Chevalier, L. Gremillard, S. Deville, Annu. Rev. Mater. Res **37**, 1 (2007)

294. A. De Aza, J. Chevalier, G. Fantozzi, M. Schehl, R. Torrecillas, Biomaterials **23**, 937 (2002)
295. W. Walter, T. Waters, M. Gillies, S. Donohoo, S. Kurtz, A. Ranawat, W. Hozack, M. Tuke, J. Bone Joint Surg. Am. **90**, 102 (2008)
296. C. Jarrett, A. Ranawat, M. Bruzzone, Y. Blum, J. Rodriguez, C. Ranawat, J. Bone Joint Surg. Am. **91**, 1344 (2009)
297. P. Gaskell, M. Eckersley, A. Barnes, P. Chieux, Nature **350**, 675 (1991)
298. J. Schrooten, Ontwikkeling en evaluatie van een ti6al4v-oraal implantaat met een bioactieve glasdeklaag. Ph.D. thesis, Department of Metallurgy and Materials Engineering, K.U.Leuven, Belgium (1999)
299. A. Ravaglioli, A. Krajewski, *Bioceramics* (Chapman & Hall, London, 1992)
300. L. Hench, R. Splinter, W. Allen, T. Greenlee, J. Biomed. mater. Res. Symp. **2**, 117 (1971)
301. L. Hench, J. Am. Ceram. Soc. **74**(7), 1487 (1991)
302. E. Verne, S. Di Nunzio, M. Bosetti, P. Appendino, C. Brovarone, G. Maina, M. Cannas, Biomaterials **26**, 5111 (2005)
303. L. Hench, S. Best, Ceramics, Glasses, and Glass-Ceramics, in *Biomaterials Science*, 2nd edn. (Academic Press, Amsterdam, 1996), pp. 153–170
304. L. Hench, O. Andersson, Bioactive glasses, in *An Introduction to Bioceramics*. Advanced Series in Ceramics, vol. 1 (World Scientific, Singapore, 1993), pp. 41–62
305. U. Gross, C. Müller-Mai, C. Voigt, Ceravital® bioactive glass-ceramics, in *An Introduction to Bioceramics*. *Advanced Series in Ceramics*, vol. 1 (World Scientific, Singapore, 1993), pp. 105–123
306. E. Schepers, P. Ducheyne, J.Oral Rehabilitation **24**, 171 (1997)
307. A. Huygh, E. Schepers, L. Barbier, P. Ducheyne, J. Mater. Sci. Mater. Med. **13**, 315 (2002)
308. J. Lao, J. Nedelec, E. Jallot, J. Mater. Chem. **19**(19), 2940 (2009)
309. J. Vidalain, Eur. J. Orthop. Surg. Traumatol. **9**, 87 (1999)
310. J. Vidalain, Interact. Surg. **2**, 206 (2007)
311. F. Jianqing, Y. Huipin, Z. Xingdong, Biomaterials **18**, 1531 (1997)
312. L. Hench, J. Wilson (eds.), *An Introduction to Bioceramics*. Advanced Series in Ceramics (World Scientific, Singapore, 1993)
313. A. Coppa, L. Bondioli, A. Cucina, D. Frayers, C. Jarrige, J.F. Jarrige, G. Quivron, M. Rossi, M. Vidale, R. Macchiarelli, Nature **440**, 755 (2006)
314. E. Crubézy, P. Murail, L. Girard, J.P. Bernadou, Nature **391**, 29 (1998)
315. McClarence, E., *Close to the Edge* (Quintessence, London, 2003)
316. M. Molin, S. Marklund, M. Bergman, E. Stenman, Scand. J. Dent. Res. **95**, 328 (1987)
317. S. Cox, B. Eley, Br. J. exp. Pathol. **67**, 925 (1986)
318. B. Eley, S. Cox, Br. J. exp. Pathol. **67**, 937 (1986)
319. S. Cox, B. Eley, Arch. oral Biol. **32**(4), 257 (1987)
320. S. Cox, B. Eley, Biomaterials **8**, 296 (1987)
321. B. Eley, S. Cox, J. Dent. **16**, 90 (1988)
322. B. Eley, S. Cox, Biomaterials **9**, 339 (1988)
323. M. Berlin, Mercury in dental-filling materials - an updated risk analysis in environmental medical terms. Report, The Dental Material Commission - Care and Consideration, Kv. Spektern, SE-103 33 Stockholm, Sweden (2003)
324. M. Wieliczka, P. Spencer, C. Moffitt, E. Wagner, A. Wandera, Dent. Mater. **12**(3), 179 (1996)
325. R. Waterstrat, T. Okabe, *Dental Amalgam*, vol. 2, chap. 27, (Wiley, Chichester, 1995) pp. 575–601
326. G. Schmalz, Arenholt-Bindslev, *Biokompatibilität zahnartzlicher Werkstoffe* (Elsevier, München, 2005)
327. A. Schuurs, C. Davidson, *Amalgaam: de feiten* (STI, Nijmegen, 1995)
328. K. Van Landuyt, Optimization of the chemical composition of dental adhesives. Ph.D. thesis, School voor Tandheelkunde, Mondziekten en Kaakchirurgie, K.U.Leuven, Dept.Tandheelkunde, Kapucijnenvoer 7, 3000 Leuven, Belgium (2008)
329. J. Jakubiak, X. Allonas, J. Fouassier, A. Sionkowska, E. Andrzejewska, L. Linden, J. Rabek, Polymer **44**(18), 5219 (2003)

330. A. Curtis, W. Palin, G. Fleming, A. Shortall, P. Marquis, Dent. Mater. **25**, 188 (2009)
331. N. Krämer, C. Reinelt, G. Richter, A. Petschelt, R. Frankenberger, Dent. Mater. **25**, 750 (2009)
332. R. Moraes, L. Gonçalves, A. Lancellotti, S. Consani, L. Correr-Sobrinho, M. Sinhoretti, Oper. Dent. **34-5**, 551 (2009)
333. W. O'Brien (ed.), *Dental Materials and Their Selection*, 4th edn. (Quintessence, Chicago, 2008)
334. M. Lijima, K. Endo, T. Yuasa, H. Ohno, K. Hayashi, M. Kakizaki, I. Mizoguchi, Angle Orthod. **76**(4), 705 (2006)
335. S. Shabalovskaya, H. Tian, J. Anderegg, D. Schryvers, W. Carroll, J. Van Humbeeck, Biomaterials **30**, 468 (2009)
336. J. Van Humbeeck, R. Stalmans, P. Besselink, in *Metals as Biomaterials*, chap. 3, ed. by J. Helsen, H. Breme (Wiley, Chichester, 1998), pp. 73–100
337. A. Verstrynge, J. Van Humbeeck, G. Willems, Am. J. Orthod. Dentofacial Orthop. **130**(4), 460 (2006)
338. J. Daems, J.P. Celis, G. Willems, Eur. J. Orthod. **31**, X (2009)
339. J. Westbrook, R. Fleischer (eds.), *Intermetallic Compounds: Principles and Practice*, vols. 1 and 2 (Wiley, Chichester, 1995)
340. G. Nancollas, R. Tang, in *Materials in Clinical Applications VI*, ed. by P. Vincenzini, R. Barbucci. Advances in Science and Technology, 41 (Techna Srl, Faenza, 2003), pp. 249–258
341. F. Driessens, R. Verbeeck, in *Biominerals*, chap. 3, ed. by F. Driessens, R. Verbeeck (CRC Press, Boca Raton, Florida, 1990), pp. 37–59
342. Z.F. Chen, B. Darvell, V.H. Leung, Arch. Oral Biol. **49**, 359 (2004)
343. H.B. Pan, B. Darvell, Arch. Oral Biol. **52**, 618 (2007)
344. H.B. Pan, B. Darvell, Arch. Oral Biol. **54**, 671 (2009)
345. W. Brown, L. Chow, J. Dent. Res. **62**, 672 (1983)
346. F. Driessens, J. Planell, M. Boltong, I. Khairoun, M. Ginebra, Proc. Inst. Mech. Eng. H **212**, 427 (1998)
347. F. Driessens, M. Boltong, Key Eng. Mater. **254-256**, 161 (2004)
348. A. Sigel, H. Sigel, R. Sigel (eds.), *Biomineralization. From Nature to Application*. Metal Ions in Life Sciences, vol. 4 (Wiley, Chichester, 2008)
349. S. Mann, J. Webb, R. Williams (eds.), *Biomineralization* (VCH Verlagsgesellschaft mbH, Weinheim Germany, 1989)
350. T. Andrew, J. Flanagan, M. Gerundini, R. Bombelli, Clin. Orthop. **206**, 127 (1986)
351. J. Dequeker, *De kunstenaar en de dokter. Anders kijken naar schilderijen* (Davidsfonds NV, Blijde Inkomststraat, Belgium, 2006)
352. G. Maistrelli, V. Fornasier, A. Binnington, K. McKenzie, V. Sessa, I. Harrington, J. Bone Joint Surg. **73-B**(1), 35 (1991)
353. C. Von Hasselbach, R. Bombelli, OP-J. **6**(2), 29 (1990)
354. R. Mathys, *Hüftkopfnekrose* (Springer, Berlin, 1991)
355. R. Mathys, R. Bombelli, G. Horne, R. Mathys, *Isoelastic Hip Prostheses. Manual of Surgical and Operative Techniques* (Hogrefe and Huber, Seattle, 1992)
356. H.G. Elias, *Megamolecules* (Springer, Berlin, 1987)
357. D. Van Krevelen, P. Hoftyzer, *Properties of Polymers*, 2nd edn. (Elsevier, Amsterdam, 1976)
358. C.H. Hybbinette, Arch. Orthop. Trauma. Surg. **104**, 28 (1985)
359. T. Curry, J. Dowdey, R.J. Murry, *Christensen's Physics of Diagnostic Radiology*, 4th edn. (Lea and Febiger, Philadelphia, 1990)
360. R.A. Novellin, *Squire's Fundamentals of Radiology*, sixth edn. (Harvard University Press, Cambridge, England, 2004)
361. S. White, M. Paraoh, *Oral Radiography. Principles and Interpretation*, fifth edn. (Mosby, St.Louis, Missouri, 2004)
362. D. Bower, W. Maddams, *The Vibrational Spectroscopy of Polymers* (Cambridge University Press, Cambridge, 1989)
363. E. Scholten, E. van der Linden, H. This, Langmuir **24**, 1701 (2008)

364. E.M. Rozenbauer, K. Landfester, A. Musyanovych, Langmuir **25**(20), 12084 (2009)
365. T. Niinimäki, J. Puranen, P. Jalovaara, J. Bone Joint Surg. **76-B**(3), 413 (1994)
366. S.M. Ali, A. Kumar, Int. Orthop. **26**, 243 (2002)
367. R. Mathys, R. Mathys, B. Gasser, Shaft for an articulation endoprosthesis. U.S. Patent 5,571,202, 1996
368. J. McElhaney, J. Appl. Physiol. **21**, 1231 (1966)
369. B. Stansfield, A. Nicol, J. Paul, I. Kelly, F. Graichen, G. Bergmann, J. Biomech. **36**, 929 (2003)
370. G. Bergmann, G. Deuretzbacher, M. Heller, F. Graichen, A. Rohlmann, J. Strauss, G. Duda, J. Biomech. **34**, 859 (2001)
371. J. Macdonald, *Impedance Spectroscopy* (Wiley, New York, 1987)
372. G. Bergmann, J. Siraky, A. Rohlmann, J. Biomech. **17**, 907 (1984)
373. G. Bergmann, A. Rohlmann, G. Graichen, Z. Orthop. **127**, 672 (1989)
374. G. Bergmann, A. Rohlmann, F. Graichen, in *Clinical Implant Materials*. Advances in Biomaterials, vol. 9, ed. by G. Heimke, I. Soltsz, A. Lee (Elsevier, Amsterdam, 1990), pp. 639–644
375. S. Jaecques, Development of an elastomer coated hip prosthesis stem and study of the fatigue properties of a thermoplastic elastomer. Ph.D. thesis, Department of Metalllurgy and Materials Engineering, Catholic University of Leuven, Leuven, Belgium, Department MTM, Kasteelpark Arenberg 44, BE-3001 Leuven, Belgium (1995)
376. J. Helsen, S. Jaecques, Rec. Res. Dev. Polym Sci. **1**, 9 (1996)
377. S. Jaecques, J. Helsen, J. Teixeira, J. Appl. Polym Sci. **61**, 819 (1996)
378. S. Jaecques, J. Helsen, J.P. Simon, D. Mattheeuws, J. Mater. Sci. Mater. Med. **6**, 685 (1995)
379. J. Helsen, S. Jaecques, J.P. Simon, D. Mattheeuws, Polym. Polym. Compos. **2**(6), 399A (1994)
380. J. Helsen, S. Jaecques, J. Van Humbeeck, J.P. Simon, J. Mater. Sci. Mater. Med. **4**, 471 (1993)
381. S. Jaecques, J. Helsen, M. Mulier, D. Mattheeuws, Vet. Comp. Orthop. Traumatol. **11**, 29 (1998)
382. E. Vieira, E. Dall'Agnol, S. Mansur, R. Mazza, M. Pinotti, D. Braile, Revista Bras. Eng. bioméd. **15**, 63 (1999)
383. COST Action 537 publication of report of WG2, March 2007. Technical Report, European Commision (2007)
384. B. Farrington, *Greek Science* (Penguin Books, Baltimore, 1966)
385. L. Gross, M. Kugel, Am. J. Pathol. **7**, 445 (1931)
386. B. Boon, Neth Heart J. **17**(12), 496 (2009)
387. Y. Missirlis, M. Chong, J. Bioeng. **2**, 287 (1978)
388. Y. Missirlis, In-vitro studies of human aortic valve mechanics. Ph.D. Thesis, Rice University, Houston, Texas, 1973
389. A. van Steenhoven, The closing behavior of the aortic valve. Ph.D. Thesis, T.U. Eindhoven, The Netherlands, 1979
390. A. Sauren, The mechanical behavior of the aortic valve. Ph.D. Thesis, T.U. Eindhoven, The Netherlands, 1981
391. L. Lake, C. Armeniades, Trans. Am. Soc. Artif. Organs **18**, 202 (1972)
392. Y. Fung, Am. J. Physiol. **213**(6), 1532 (1967)
393. Y. Lanir, J. Biomech. **12**, 423 (1979)
394. S. Hanson, L. Harker, *Biomaterials Science* (Academic, San Diego, 1996). Blood coagulation and blood-material interactions
395. Y. Missirlis, W. Lemm, *Modern aspects of protein adsorption on Biomaterials* (Kluwer, Dordrecht, 1991)
396. P. Majerus, G. Broze, J. Miletich, D. Tollefsen, in *The pharmacological basis of therapeutics*, ed. by A. Gilman (Pergamon, New York, 1990), pp. 1311–1331
397. G. Michanetzis, N. Katsala, Y. Missirlis, Biomaterials **24**(4), 677 (2003)
398. A. Yoganathan, Y.R. Woo, F. Williams, *Advances in Cardiac Valves* (Yorke Medical Books, 1983), vol. 1, In vitro hydrodynamic characteristics of the St.Jude bileaflet aortic prosthesis, p. 123

399. A. Yoganathan, F. Sotiropoulos, *Business Briefing:US Cardiology*, pp. 1–5 (2004)
400. R. Gorlin, S. Gorlin, I. Am. Heart J. **41**(1), 1 (1951)
401. E. Chaikof, N. Engl. J. Med. **357**, 1368 (2007)
402. J. Brockes, A. Kumar, Science **310**, 1919 (2005)
403. A. Kumar, J. Godwin, P. Gates, A. Garza-Garcia, J. Brockes, Science **318**, 772 (2007)
404. R. Lanza, R. Langer, J. Vacanti, *Principles of Tissue Engineering*, 3rd edn. (Academic, 2007)
405. G. Muschler, C. Nakamoto, L. Griffith, J. Bone Joint Surg. **86-A**, 1541 (2004)
406. G. Vunjak-Novakovic, R. Freshney (eds.), *Culture of Cells for Tissue Engineering* (Wiley-Liss, Hoboken, NJ, 2006)
407. P. Johnson, A. Mikos, J. Fisher, J. Jansen, Tissue Eng. **13**, 2827 (2007)
408. P. Ma, J. Elisseeff (eds.), *Scaffolding in Tissue Engineering* (CRC, Taylor and Francis Group, Boca Raton, Florida, 2005)
409. P. Simon, M. Kasimir, G. Seebacher, G. Weigel, R. Ullrich, U. Salzer-Muhar, E. Rieder, E. Wolner, Eur. J. Cardiothorac Surg. **23**, 1002 (2003)
410. S. Wang, L. Lu, M. Yaszemski. Hydrophilic/Hydrophobic Polymer Networks Based on Poly(Caprolactone Fumarate), Poly(Ethylene Glycol Fumarate), and Copolymers Thereoff. Patent WO/2006/118987
411. I. Smith, X. Liu, L. Smith, P. Ma, WIREs Nanomed. Nanotechnol. **1**, 226 (2009)
412. S. Hollister, Nat. Mater. **4**, 518 (2005)
413. S. Johansson, G. Svineng, K. Wennerberg, A. Armulik, L. Lohikangas, Front. Biosci. **2**, 126 (1997)
414. D. Deligianni, N. Katsala, P. Koutsoukos, Y. Missirlis, Biomaterials **22**(1), 87 (2000)
415. A. Curtis, N. Gadegaard, M.J. Dalby, M. Riehle, C.D. Wilkinson, G. Aitchison, IEEE Trans. Nanobioscience **3**(1), 61 (2004)
416. M. Dauner, H. Planck, L. Caramaro, Y. Missirlis, E. Panagiotopoulos, J. Mat. Sci. Mater. Med. **9**, 173 (1998)
417. A. Oyane, H.M. Kim, T. Furuya, T. Kokubo, T. Miyazaki, T. Nakamura, J. Biomed. Mater. Res. **65A**, 188 (2003)
418. Y. Huang, S. Onyeri, M. Siewe, A. Moshfeghian, S. Madihally, Biomaterials **26**(36), 7616 (2005)
419. E. Brennan, J. Reing, D. Chew, J. Myers-Irvin, E. Young, S. Badylak, Tissue Eng. **12**(10), 2949 (2006)
420. C. Buckley, K.U. O'Kelly, *Topics in Bio-Mechanical Engineering* (Trinity Centre for Bio-engineering & National Centre for Biomedical Engineering Science, Dublin, 2004), Regular Scaffold Fabrication Techniques for Investigations in Tissue Engineering, pp. 147–166
421. S.G. Zang, Nat Biotechnol. **21**(10), 1171 (2003)
422. L. Moroni, R. Schotel, D. Hamaan, J. de Wijn, C. van Blitterswijk, Adv. Funct. Mater. **18**, 53 (2008)
423. G. Khang, M. Kim, H. Lee (eds.), *A Manual for Biomaterials/Scaffold Fabrication Technology* (World Scientific, New Jersey, 2007)
424. H. Hu, M. Weir, C. Simon, Jr., Dent. Mater. **24**(9), 1212 (2008)
425. X. Wang, E. Wenk, X. Zhang, L. Meinel, G. Vunjak-Novakovic, D. Kaplan, J. Control. Release **134**(2), 81 (2009)
426. J. West, in *Biopolymer Methods in Tissue Engineering*, ed. by A. Hollander, P. Hatton (Humana, Totowa, NJ, 2004), pp. 113–121
427. H. Storrie, D. Mooney, Adv. Drug Deliv. Rev. **58**(4), 500 (2006)
428. M. Lysaght, J. Crager, Tissue Engin. A **15**(7), 1449 (2009)
429. P. Bianco, P. Robey, Nature **414**, 118 (2001)
430. D. Schmidt, S. Hoerstrup, Swiss Med. Wkly **135**, 618 (2005)
431. F. Schoen, J. Heart Valve Dis. **8**, 350 (1999)
432. P. Zilla, D. Bezuidenhout, P. Human, Biomaterials **28**, 5009 (2007)
433. R. Kannan, H. Salacinski, P. Butler, G. Hamilton, Seifalian, J. Biomed. Mater. Res. B Appl. Biomater. **74B**, 570 (2005)
434. H. Salacinski, M. Odlyha, G. Hamilton, A. Seifalian, Biomaterials **23**, 2231 (2002)

435. R. Shemin, Circulation **118**, 2326 (2008)
436. B. O'Brien, W. Carroll, Acta Biomater. **5**, 945 (2009)
437. H. Takahashi, D. Letourner, D. Grainger, Biomacromolecules **8**(11), 3281 (2007)
438. M. Peuster, C. Hesse, T. Schloo, C. Fink, P. Beerbaum, C. Von Schnakenburg, Biomaterials **27**, 4955 (2006)
439. C. Weinberg, E. Bell, Science **231**, 397 (1986)
440. N. L'Heureux, S. Paquet, R. Labbe, L. Germain, F. Auger, FASEB J. **12**, 47 (1998)
441. L. Niklason, J. Gao, W. Abbott, K. Hirschi, S. Houser, R. Marini, R. Langer, Science **284**, 489 (1999)
442. S. Hoerstrup, G. Zuend, R. Sodian, A. Schnell, J. Gruenenfelder, M. Turina, Eur. J. Cardio-Thoracic Surg. **20**, 164 (2001)
443. G. Michanetzis, N. Katsala, Y. Missirlis, Biomaterials **24**(4), 677 (2003)
444. B. Derjaguin, Disc. Faraday Soc. **42**, 109 (1966)
445. W. Bascom, E. Brooks, B. Worthington, Nature **228**, 1290 (1970)
446. R. Calvet, J. Chaussidon, P. Cloos, C. De Kimpe, J. Fripiat, M. Gastuche, J. Helsen, A. Jelli, A. Léonard, G. Poncelet, J. Uytterhoeven, Bull. Groupe français. Argiles **XV**, 59 (1963)
447. J. Fripiat, J. Helsen, L. Vielvoye, Bull. Groupe franç. Argiles **XV**(10), 3 (1971)
448. J. Fripiat, A. Jelli, G. Poncelet, J. André, J. Phys. Chem. **69**, 2185 (1965)
449. J. Fripiat, J. Helsen, *Clays & Clay Minerals* (Pergamon, Oxford & New York, 1966), Proceedings of the 14th National Conference on Clays and Clay Minerals, Berkeley, California Kinetics of Decomposition of Cobalt Coordination Complexes on Montmorillonite Surfaces, pp. 163–179
450. B. Theng, *The Chemistry of Clay-Organic Reactions* (Adam Hilger, London, 1974)
451. J. Helsen, Bull. Groupe français Argiles **XXII**, 139 (1972)
452. J. Helsen, J. Chem. Educ. **59**, 1063 (1982)
453. N. Lahav, D. White, S. Chang, Science **201**, 67 (1978)
454. K. Plankensteiner, H. Reiner, B. Schranz, B. Rode, Angew. Chem. Int. Ed. **43**, 1886 (2004)
455. S. Miller, Science **117**, 528 (1953)
456. A. Mulkidjanian, M. Galperin, in *Origin of Life. Chemical Approach*, ed. by P. Herdewijn, M. Kisakürek (Wiley, Weinheim, 2008), pp. 81–93
457. J. Budjak, H. Slosiarikova, N. Texter, M. Schwendinger, B. Rode, Monatshefte für Chemie **125**, 1033 (1994)
458. B. Rode, D. fitz, T. Jakschitz, in *Origin of Life. Chemical Approach*, ed. by P. Herdewijn, M. Kisakürek (Wiley, Weinheim, 2008), pp. 185–213
459. P. Herdewijn, M. Kisakürek (eds.), *Origin of Life. Chemical Approach* (Wiley, Weinheim, 2008)
460. P. Ball, Chem. Rev. **108**(1), 74 (2008)
461. D. Eisenberg, W. Kauzmann, *The Structure and Properties of Water* (Oxford University Press, London W.1, 1969)
462. J. Lee, T. Li, K. Park, in *Water in Biomaterials Surface Science*, ed. by M. Morra (Wiley, Chichester, 2001), pp. 127–146
463. J. Laserna (ed.), *Modern Techniques in Raman Spectroscopy* (Wiley, Chichester, 1996)
464. J. Grasselli, B. Bulkin (eds.), *Analytical Raman Specgroscopy* (Wiley, New York, 1991)
465. T. Wall, D. Hornig, J. Chem. Phys. **43**(6), 2079 (1965)
466. Y. Rezus, H. Bakker, Phys. Rev. Lett. **99**, 148301 (2007)
467. H. Finston, A. Rychtman, *A New View of Current Acid-Base Theories* (Wiley, New York, 1982)
468. C. Van Oss, M. Chaudhury, R. Good, Chem. Rev. **88**, 927 (1988)
469. M. Morra (ed.), *Water in Biomaterials Surface Science* (Wiley, Chichester, 2001)
470. E. Vogler, in *Water in Biomaterials Surface Science*, ed. by M. Morra (Wiley, Chichester, 2001), pp. 269–290
471. R. Sanderson, *Chemical Periodicity* (Reinhold Publishing, New York, 1960)
472. P. Atkins, *The second law* (Scientific American Books, New York, 1984)
473. F. Galasso, J. Chem. Ed. **70**(4), 287 (1993)
474. A. Oyane, H.M. Kim, T. Furuya, T. Kobubo, T. Miyazaki, J. Biomed. Res. **65A**, 188 (2003)

Index